Development of New Catalysts and Concepts for Enantioselective Synthesis of Amines and Alcohols

Author: Erika Marina Vieira

Boston College

The Graduate School of Arts and Sciences

Department of Chemistry

DEVELOPMENT OF NEW CATALYSTS AND CONCEPTS FOR ENANTIOSELECTIVE SYNTHESIS OF AMINES AND ALCOHOLS

A dissertation by

ERIKA M. VIEIRA

Submitted in partial fulfillment of the requirements
For the degree of
Doctor of Philosophy

August 2013

in loving memory of

Maria Amelia and Alfredo Cardoso

Acknowledgements

My tenure at Boston College has been characterized by an intense and incredible degree of personal and professional development, most profoundly influenced and shaped by Professor Amir Hoveyda. It is in part due to my immense good fortune that I had the opportunity to learn and grow under his attentive tutelage. It was through his unwavering support and encouragement that I was able to mature as a scientist, scholar, educator, and leader. I am most grateful for the rigorous education, thank you, Amir.

My remarkably good fortune does not end there; I was also most privileged to have had amazing colleagues of whose actions and words I often imitated, and in whose seemingly infinite knowledge I would bask. I must acknowledge the endless patience with which Dr. Laura Wieland Brown coached my early months in Amir's research group as I fearfully entered the world of methodology. After which, the guidance of Dr. Pamela Lombardi, Dr. Tricia May-Dracka, Dr. Adil Zhugralin, and Dr. Kang Sang Lee, among others, ensured my success. More importantly, the relationships forged through my years at Boston College, which are too many to list here, have cemented as close friendships and I most fortunate to have met, befriended, and worked with these extraordinary individuals. I will miss all of our lunch dates (Thai food and sushi!), long talks, coffee and ice cream breaks, nights out, happy hours, movie filming, summer group outings, and in-lab hijinks. Thank you for the memories, I am happy I have many of these recorded!

I am also most fortunate that I was given the opportunity to work on engaging research projects that seemed to provide an endless amount of questions to investigate. I must acknowledge the tremendous efforts put forward by my colleagues that has both contributed to the work outlined in this dissertation, and will surely continue to influence

future discoveries. Studies directed by Dr. Fredrik Haeffner and Nicholas Mszar have enhanced my own understanding of the NHC–Cu-catalyzed processes described in Chapters 2 and 3, while Daniel Silverio, Dr. Tatiana Pilyugina, and Dr. Sebastian Torker were instrumental in the discovery of the boron-based catalyst and elucidation of its mechanism discussed in Chapter 4. I am grateful for their significant input during my own tenure and I look forward to what their future endeavors hold.

I want to recognize the proofreaders of this document who have undoubtedly improved its content. I am grateful for Benz Radomkit, Nicholas Mszar, Hao Wu, Kevin McGrath, and Daniel Silverio for their insights, as well as, Professors Amir Hoveyda, Marc Snapper, and Shih-Yuan Liu for their remarks and for serving as members of my doctoral committee.

Finally, it is with the most sincere gratitude that I acknowledge my family's contribution to the completion of this thesis. I know that I was a constant presence in their thoughts, prayers, and well wishes. The immeasurable love and support from my parents, Ana and Manuel, is a perpetual source of comfort, the foundation of my well-being, and the reason for my success. My husband David, of course, is most deserving of a great deal of praise for his daily encouragement and reassuring words; I would be lost without his love.

muito obrigada

DEVELOPMENT OF NEW CATALYSTS AND CONCEPTS FOR ENANTIOSELECTIVE SYNTHESIS OF AMINES AND ALCOHOLS

Erika Marina Vieira

Thesis Advisor : *Amir H. Hoveyda*

Abstract

■ Chapter 1

Ag-Catalyzed Enantioselective Vinylogous Mannich Reactions of Ketoimines

Few catalytic methods have been reported for the enantioselective synthesis of *N*-substituted quaternary carbon stereogenic centers, typically the low reactivity of the electrophilic partner cannot be overcome. Herein, a silver-based catalyst is described which promotes highly site-, diastereo-, and enantioselective additions of siloxyfurans to ansidine-derived ketoimino esters. Mechanistic investigations, undertaken to elucidate the nature of the active silver–phosphine complex, supported the proposed origin for the *anti*-selective Mannich-type additions.

Wieland, L. C.; Vieira, E. M.; Snapper, M. L.; Hoveyda, A. H. "Ag-Catalyzed Diastereo- and Enantioselective Vinylogous Mannich Reactions of α–Ketoimine Esters. Development of a Method and Investigation of its Mechanism" *J. Am. Chem. Soc.* **2009**, *131*, 570–576.

■ Chapter 2

New Catalysts for the Enantioselective Cu-Catalyzed Additions of Allyl Groups to Phosphinoylaldimines

The deficiencies in modern organic synthesis regarding the preparation of chiral molecules bearing amines, despite their incredible significance, are addressed. The

development of *a new method and catalyst* for the preparation of enantiomerically enriched allyl-substituted α-chiral amines is described. Copper based catalysts bearing chiral C_1-symmetric *N*-heterocyclic carbenes promote reactions between diphenylphosphinoyl aldimines and allyl boronic acid pinacol ester affording the homoallylic amines with high levels of efficiency and selectivity. Furthermore, the mechanistic rationale describing the selectivity patterns of the designed catalysts is analyzed.

Vieira, E. M.; Snapper, M. L.; Hoveyda, A. H. "Enantioselective Synthesis of Homoallylic Amines through Reactions of (Pinacolato)allylborons with Aryl-, Heteroaryl-, Alkyl-, or Alkene-Substituted Aldimines Catalyzed by Chiral C1-Symmetric NHC–Cu Complexes" *J. Am. Chem. Soc.* **2011**, *133,* 3332–3335.

■ Chapter 3

NHC–Cu-Catalyzed Enantioselective Propargyl Group Additions to Phosphinoylaldimines

The copper complex of a chiral *N*-heterocyclic carbene is found to be uniquely effective at promoting highly selective reactions of a commercially available allenylboron reagent and diphenylphosphinoyl aldimines. The enantiomerically enriched homopropargylic amines are exclusively afforded within an hour in the presence of as low as 0.25 mol % catalyst. The utility of the method is further demonstrated through the elaboration of the appended alkyne to difficult-to-access functionalities, highlighted by the synthesis of a key fragment for the preparation of the aza-epothilones, macrocyclic lactams which exhibit acute cytotoxicity.

Vieira, E. M.; Haeffner, F.; Snapper, M. L.; Hoveyda, A. H. "A Robust, Efficient, and Highly Enantioselective Method for Synthesis of Homopropargyl Amines" *Angew. Chem. Int. Ed.,* **2012**, *51*, 6618–6621.

■ Chapter 4

Metal-Free Catalysts for Enantioselective Synthesis of Allenic Carbinols

A metal-free catalyst, unique in structure and mechanism, is developed to address the remaining deficiencies in allyl addition chemistry, an area dominated by metal catalysis. The key organizational and enabling feature of the catalyst is a proton, a simple point charge which affects the facility of the C–C bond formation through electrostatic interactions. The unique α-selectivity delivered by the boron-based catalyst, a product of a catalytic cycle characterized by two γ-selective allyl transfer processes, allows for the unprecedented synthesis of enantiopure allenyl-substituted tertiary alcohols. Moreover, the described transfomations can be performed in a matter of minutes with <0.5 mol % catalyst.

Silverio, D. L.; Torker, S.; Pilyugina, T.; Vieira, E. M.; Haeffner, F.; Snapper, M. L.; Hoveyda, A. H. "Simple Organic Molecules as Catalysts for Enantioselective Synthesis of Amines and Alcohols" Nature **2013**, *494*, 216–221.

Table of Contents

■ Chapter 3

NHC–Cu-Catalyzed Enantioselective Propargyl Group Additions to Phosphinoylaldimines

■ Chapter 4

Metal-Free Catalysts for Enantioselective Synthesis of Allenic Carbinols

Chapter One

Ag-Catalyzed Enantioselective Vinylogous Mannich Reactions of Ketoimines

1.1 Introduction

Chiral amines have proven efficacious as both powerful pharmacophores and as components in chiral catalysts. Their ubiquity in the fields of medicinal chemistry[1] and asymmetric catalysis[2] may be unsurprising as they possess a wealth of structural information augmented by their propensity to participate in metal chelation or in H-bonding. Despite the overwhelming demand for rapid access to *N*-substituted stereogenic centers, discovery of methods for their enantioselective synthesis has far lagged behind those that produce the corresponding alcohols.[3] The principal reason behind this discrepancy is the reduced reactivity of amine precursors. Enantioselective nucleophilic hydride or carbanion additions to carbonyls and imines represent the most practical and widely used disconnections to afford various chiral alcohols and amines. In comparison to carbonyls, however, the unsaturation of imines is much less polarized[4] and therefore the weaker dipole moment of the C=N double bond ultimately corresponds to a dramatic

[1] (a) "Analysis of the Reactions Used for the Preparation of Drug Candidate Molecules," Carey, J. S.; Laffan, D.; Thomson, C.; Williams, M. T. *Org. Biomol. Chem.* **2006**, *4*, 2337–2347. (b) "Chiral Amine Synthesis – Recent Developments and Trends for Enamide Reduction, Reductive Amination, and Imine Reduction," Nugent, T. C.; El-Shazly, M. *Adv. Synth. Catal.* **2010**, *352*, 753–819. (c) Chiral Amine Synthesis (Ed.: T. C. Nugent), Wiley-VCH, Weinheim, **2010**.

[2] For reviews, see: (a) "Chiral Tertiary Diamines in Asymmetric Synthesis," Kizirian, J-C. *Chem. Rev.* **2008**, *108*, 140–205. (b) "Nitrogen-Containing Ligands for Asymmetric Homogeneous and Heterogeneous Catalysis," Fache, F.; Schulz, E.; Tommasino, L.; Lemair, M. *Chem. Rev.* **2000**, *100*, 2159–2231.

[3] "Additions of Organometallic Reagents to C=N Bonds: Reactivity and Selectivity," Bloch, R. *Chem. Rev.* **1998**, *98*, 1407–1438.

[4] The difference in electronegativities of O and N account for the disparity in the polarizations of the C=X bonds (on the Pauling scale, O = 3.44, N = 3.04, and C = 2.55).

reduction of the electrophilicity of the prochiral carbon.

Besides the inherent lower reactivity, further challenges are uniquely associated with reactions of imines (Scheme 1.1): 1) Unlike carbonyls, imines have a third substituent, often a protecting or activating group, and as such controlling the geometry of the unsaturation (*E*/*Z*) can prove problematic. Further complications include low barriers to *E*/*Z* isomerization in solution and the potential for the isomeric forms to lead

Scheme 1.1 Challenges in Enantioselective Synthesis of 2° and 3° Carbamines and Biologically Relevant Molecules Bearing the Latter Moiety

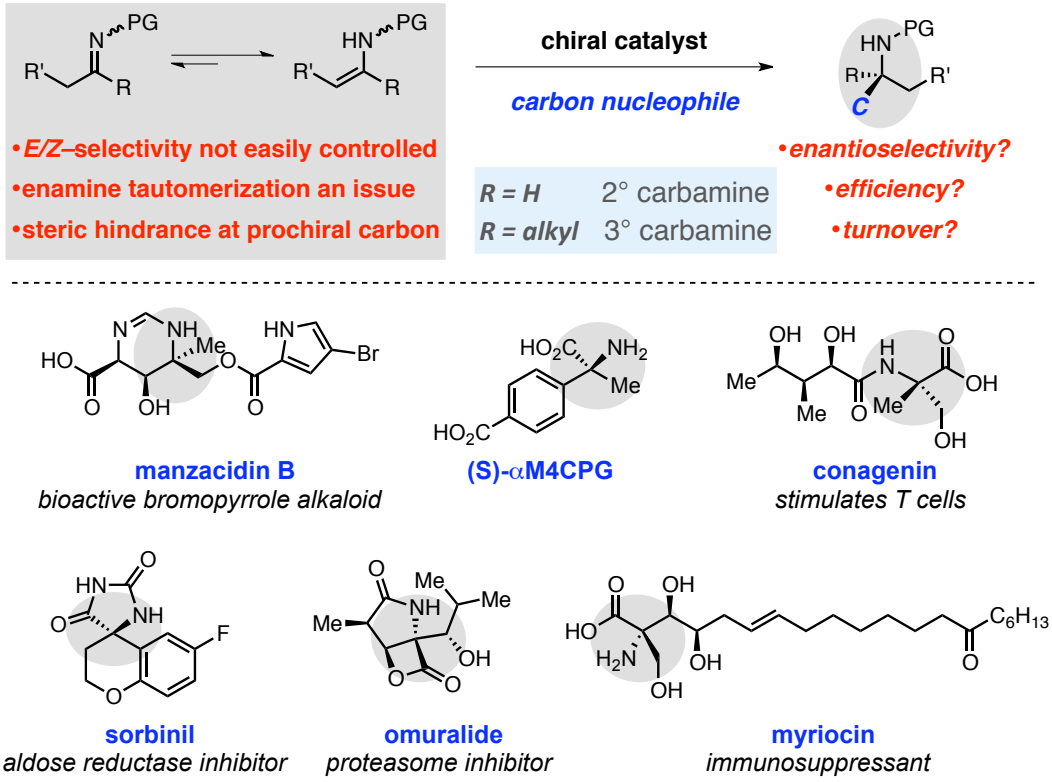

to opposite enantiomers of the addition products in catalyst-controlled transformations. 2) The inherent third substituent also results in increased steric hindrance at the prochiral carbon, a challenge that is exasperated in reactions of ketoimines to afford tertiary carbamines. 3) Imines with an α-proton are prone to rapid tautomerization, establishing

an equilibrium in which the imine isomer is unfavored; on the other hand, the keto tautomer of enolizable ketones and aldehydes is often lower in energy, such that the enol isomers are present in only small concentrations. Population of the nucleophilic enamine tautomer not only depletes the electrophilic reaction partner, but can also lead to undesired side processes. Discovery of practical and reliable methods for the preparation of enantiomerically pure secondary and tertiary carbamines requires the identification of selective and powerful catalysts that overcome the aforementioned obstacles with a high degree of efficiency.

1.2 Background

Despite the challenges outlined, significant advances have been made over the last two decades in the catalytic synthesis of α-chiral amines. Much of this progress, however, has involved reactions of imines derived from aldehydes for the formation of secondary carbamines,[5] while the corresponding reactions to prepare tertiary carbamines remain, in comparison, much less developed. Additionally, the strategies that have dominated the field involve methods of reduction, either hydrogenations or hydride additions, protocols that are inapplicable for the generation of tertiary carbamines. With the lack of catalytic methods, industrial synthesis of *N*-substituted quaternary stereogenic centers continues to rely on chemoenzymatic and classical racemate resolution, or diastereoselective techniques.[6] Moreover, quaternary α–amino acids and their

[5] For comprehensive reviews, see: (a) "Catalytic Enantioselective Addition to Imines," Kobayashi, S.; Ishitani, H. *Chem. Rev.* **1999**, *99*, 1069–1094. (b) "Recent Developments in Asymmetric Catalytic Addition to C=N bonds," Friestad, G. K.; Mathies, A. K. *Tetrahedron*, **2007**, *63*, 2541–2569. (c) "Catalytic Enantioselective Formation of C–C Bonds by Addition to Imines and Hydrazones: A Ten-Year Update," Kobayashi, S.; Mori, Y.; Fossey, J. S.; Salter, M. M. *Chem. Rev.* **2011**, *111*, 2626–2704.
[6] (a) "Industrial Methods for the Production of Optically Active Intermediates," Breuer, M.; Ditrich, K.; Habicher, T.; Hauer, B.; Keßeler, M.; Stürmer, R.; Zelinski, T. *Angew. Chem., Int. Ed.* **2004**, *43*, 788–824. (b)"Asymmetric Synthesis of Active Pharmaceutical Ingredients," Farina, V.; Reeves, J. T.; Senanayake C.

derivatives,[7] a particularly important class of tertiary carbamines, are embedded in the structures of a number of biologically significant molecules (Scheme 1.1). Although pioneering examples of catalytic enantioselective additions of cyanide (Strecker reactions)[8], alkyl[9], aryl[10], allyl[11], and alkynyl[12] groups to ketone-based imines have been disclosed, these reports provide entry to tertiary carbimines of only specific substitution patterns, very few of which represent the class of quaternary α or β–amino acids. The lack of efficient and general access to *N*-substituted quaternary stereogenic centers has resulted in their curtailed use as advanced building blocks in favor of the more accessible

---

H.; Song, J. J. *Chem. Rev.* **2006**, *106*, 4537–4558. (b) Process Chemistry in the Pharmaceutical Industry Volume 2: Challenges in an Ever Changing Climate (Ed.: T. C. Nugent),Wiley-VCH, Weinheim, **2008.** For a review on the most commonly used chiral auxillary for amine synthesis, see: (c) "Synthesis and Applications of *tert*-Butanesulfinamide," Robak, M. T.; Herbage, M. A.; Ellman, J. A. *Chem Rev.* **2010**, *110*, 3600–3740.

[7] For reviews on the stereoselective synthesis of quaternary α-amino acids see: (a)."Enantio- and Diastereoselective Construction of α,α-Disubstituted α-Amino Acids for the Synthesis of Biologically Active Compounds," Ohfune, Y.; Shinada, T. *Eur. J. Org. Chem.* **2005**, 5127-5143. (b) "Recent Progress on the Stereoselective Synthesis of Acyclic Quaternary α-Amino Acids," Cativiela, C.; Díaz-de-Villegas, M. D. *Tetrahedron: Asymmetry* **2007**, *18*, 569-623.

[8] For examples, see: (a) "Structure-Based Analysis and Optimization of a Highly Enantioselective Catalyst for the Strecker Reaction,' *J. Am. Chem. Soc.* **2002**, *124*, 10012–10014. (b) "Catalytic Enantioselective Strecker Reaction of Ketoimines," Masumoto, S.; Usuda, H.; Suzuki, M.; Kanai, M.; Shibasaki, M. *J. Am. Chem. Soc.* **2003**, *125*, 5634–5635. (c) "Asymmetric Activation of *tropos* 2,2'-Biphenol with Cinchonine Generates an Effective Catalyst for the Asymmetric Strecker Reaction of *N*-Tosyl-Protected Aldimines and Ketoimines," Wang, J.; Hu, X.; Gou, S.; Huang, X.; Liu, X.; Feng, X. *Angew. Chem. Int. Ed.* **2007**, *46*, 8468–8470.

[9] (a) "Catalytic Asymmetric Synthesis of α,α,α-Trifluoromethylamines by the Copper-Catalyzed Nucleophilic Addition of Diorganozinc Reagents to Imines," Lauzon, C.; Charette, A. B. *Org. Lett.* **2006**, *8*, 2743–2745. (b) "Catalytic Asymmetric Alkylations of Ketoimines. Enatioselective Synthesis of *N*-Substituted Quaternary Carbon Stereogenic Centers by Zr-Catalyzed Additions of Dialkylzinc Reagents to Aryl-, Alkyl-, and Trifluoroalkyl-Substituted Ketoimines," Fu, P.; Snapper, M. L.; Hoveyda, A. H. *J. Am. Chem. Soc.* **2008**, *130*, 5530–5541.

[10] (a) "Rhodium-Catalyzed Asymmetric Arylation of *N*-Tosyl Ketimines," Shintani, R.; Takeda, M.; Tsuji, T.; Hayashi, T. *J. Am. Chem. Soc.* **2010**, *132*, 13168–13169. (b) "Asymmetric Synthesis of (Triaryl)methylamines by Rhodium-Catalyzed Addition of Arylboroxines to Cyclic *N*-Sulfonyl Ketimines," Nishimura, T.; Noishiki, A.; Tsui, G. C.; Hayashi, T. *J. Am. Chem. Soc.* **2012**, *134*, 5056–5059

[11] (a) "Catalytic Enantioselective Allylation of Ketoimines," Wada, R.; Shibuguchi, T.; Makino, S.; Oisaki, K.; Kanai, M.; Shibasaki, M.; *J. Am. Chem. Soc.* **2006**, *128*, 7687–7691. (b) "Enantioselective Rhodium-Catalyzed Nucleophilic Allylation of Cyclic Imines with Allylboron Reagents," Luo, Y.; Hepburn, H. B.; Chotsaeng, N.; Lam, H. W. *Angew. Chem., Int. Ed.* **2012**, *51*, 8309–8313.

[12] (a) "Highly Enantioselective Zinc/BINOL-Catalyzed Alkynylation of α-Ketoimine Ester: A New Entry to Optically Active Quaternary α-CF_3 α amino acids," Huang, G.; Yang, J.; Zhang, X. *Chem. Commun.* **2011**, *47*, 5587–5589. (b) "Direct Catalytic Asymmetric Alkynlation of Ketoimines," Yin, L.; Otsuka, Y.; Takada, H.; Mouri, S.; Yazaki, R.; Kumagai, N.; Shibasaki, M. *Org. Lett.* **2013**, *15*, 698–701.

amines residing within tertiary centers.

The Mannich reaction, the addition of an enolate equivalent to an imine or iminium salt, has proven of particular consequence in regards to enantioselective synthesis of β–amino carbonyls. Enantiospecific Mannich processes,[13] more so than additions of other carbanion equivalents, offer the opportunity to access chiral amines of increased molecular complexity; introduction of substitution at both the α and β

Scheme 1.2 Diastereoselective Approach to Mannich Reactions of Ketoimines

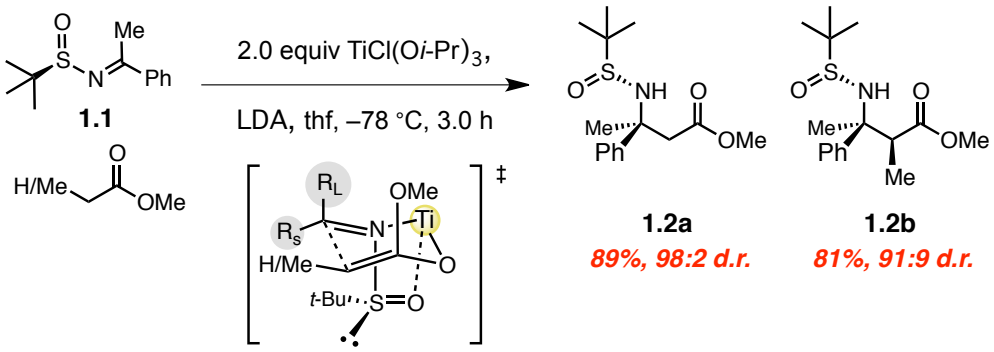

positions can be achieved through selection of the appropriately substituted enolate nucleophile and aldimine or ketoimine partner. For example, a broad range of substitution patterns are attained in the highly diastereoselective transformations of *tert*-butanesulfinyl imine **1.1**.[14] Additions of the titanium enolates, derived from either methyl acetate or ethyl propionate, afford the corresponding β–amino esters **1.2a** and **1.2b** in 89% and 81% yields respectively (Scheme 1.2). The enantiotopic faces of the

[13] For reviews, see: (a) "Modern Variants of the Mannich Reaction," Arend, M.; Westermann, B.; Risch, N. *Angew. Chem., Int. Ed.* **1998**, *37*, 1044–1070. (b) "The Direct Catalytic Asymmetric Mannich Reaction," Córdova, A. *Acc. Chem. Res.* **2004**, *37*, 102–112. (c) "Catalytic Enantioselective Cross-Mannich Reaction of Aldehydes," Marques, M. M. B. *Angew. Chem., Int. Ed.* **2006**, *45*, 348–352. (d) "Organocatalysed Asymmetric Mannich Reactions," Verkade, J. M. M.; van Hemert, L. J. C.; Quaedflieg, P. J. L. M.; Rutjes, F. P. J. T. *Chem. Soc. Rev.* **2008**, *37*, 29–41. (e) "Organocatalytic Asymmetric Mannich Reactions: New Methodology, Catalyst Design, and Synthetic Applications," Ting, A.; Schaus, S. E. *Eur. J. Org. Chem.* **2007**, 5797–5815.

[14] "Asymmetric Synthesis of β–Amino Acid Derivatives Incorporating a Broad Range of Substitution Patterns by Enolate Additions to *tert*-Butanesulfinyl Imines," Tang, T. P.; Ellman, J. A. *J. Org. Chem.* **2002**, *67*, 7819–7832.

chiral imine can be effectively differentiated through a closed chelated six-membered transition state; for this reason, ketoimines that bear substituents with significant size disparity can participate in additions that produce tertiary carbamines with the high diastereocontrol typically observed with aldimines (R_s = Me vs. H).

The enantiotopic faces of achiral hydrazone **1.3** can also be effectively differentiated, however, in this case, through *in situ* complexation with a stoichiometric strained silane Lewis acid **1.5** (Scheme 1.3).[15] The Mannich process with silyl ketene acetal **1.4** efficiently and selectively produces β,β–dialkyl–β–hydrazidoesters **1.6a–b** in

Scheme 1.3 Mannich Reactions of Ketone-derived Hydrazones Promoted by Chiral Lewis Acidic Silicon-Based Reagents

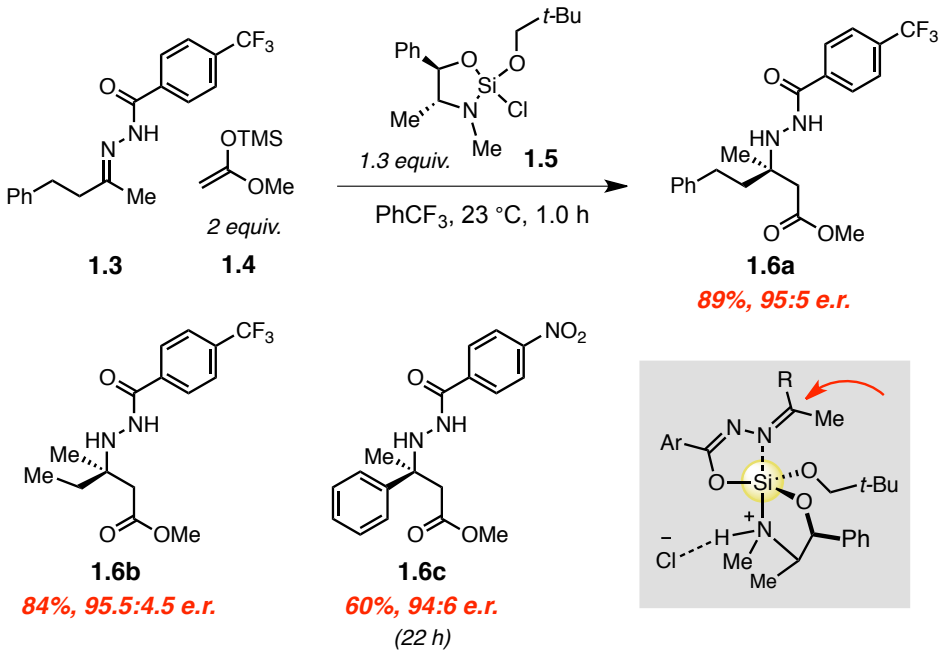

84–89% yield and in 95:5 e.r. (reactions complete within in an hour), however, hydrazones bearing larger alkyl or aryl substituents react with a significantly slower rate

[15] "A New Silicon Lewis Acid for Highly Enantioselective Mannich Reactions of Aliphatic Ketone-Derived Hydrazones," Notte, G. T.; Leighton, J. L. *J. Am. Chem. Soc.* **2008**, *130*, 6676–6677.

(22 hours required for 60% yield of **1.6c**). The two diastereoselective approaches to tertiary carbamines discussed make use of highly electron-withdrawing groups in combination with strong Lewis acids to render the C=N double bond more electrophilic.

In the first example of Mannich reactions of ketoimines reported to employ a catalytic source of chirality, relied on a similar activation strategy of imine partners. Many of the challenges previously discussed for nucleophilic additions to ketoimines are addressed with the design of α–ketoimino ester **1.7** (Scheme 1.4): all three of the C=N

Scheme 1.4 Zn-pybox Catalyzed Mannich Reactions of α–Ketoimino Ester **1.7**

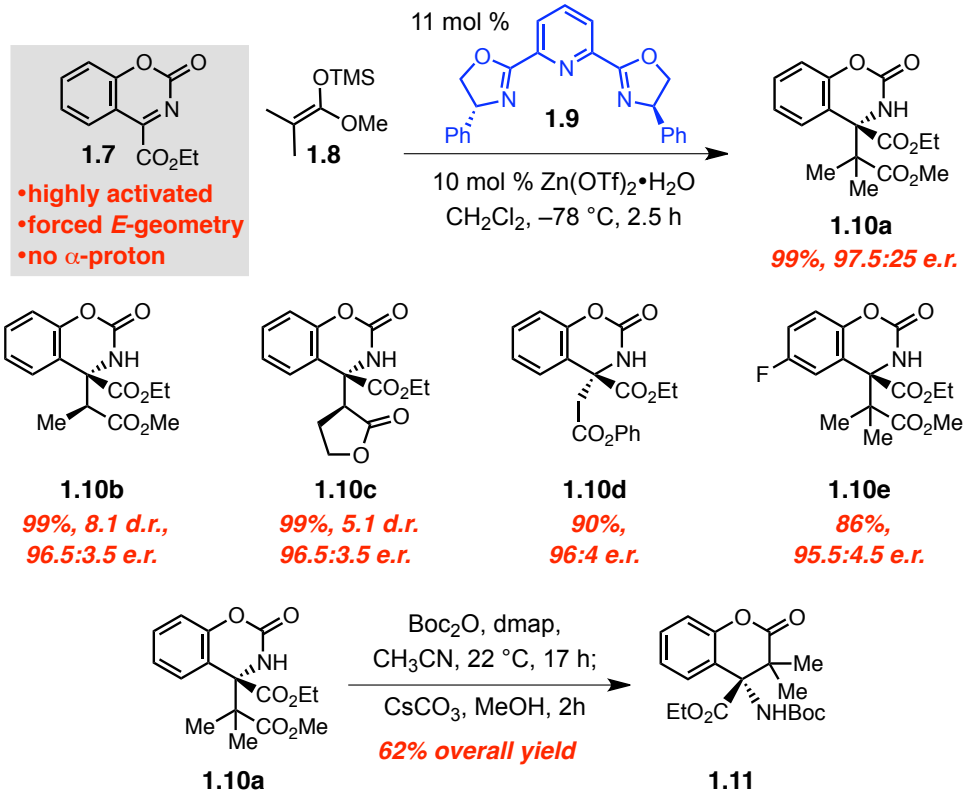

double bond substituents are electron-withdrawing, amplifying the electron deficiency at the prochiral carbon, and the cyclic nature of the anchored protecting group enforces a single planar *E*–conformation. A Lewis acidic Zn-pybox complex coordinates the bidentate ketoimine and promotes addition of various silyl ketene acetals to afford

β–aminoesters **1.10a–e** in >86% yield and >95.5:4.5 e.r., with mono-substitution on the

Scheme 1.5 Direct Mannich Reactions of α–Ketoimino Ester **1.7** Catalyzed by a Nucleophilic Secondary Diamine

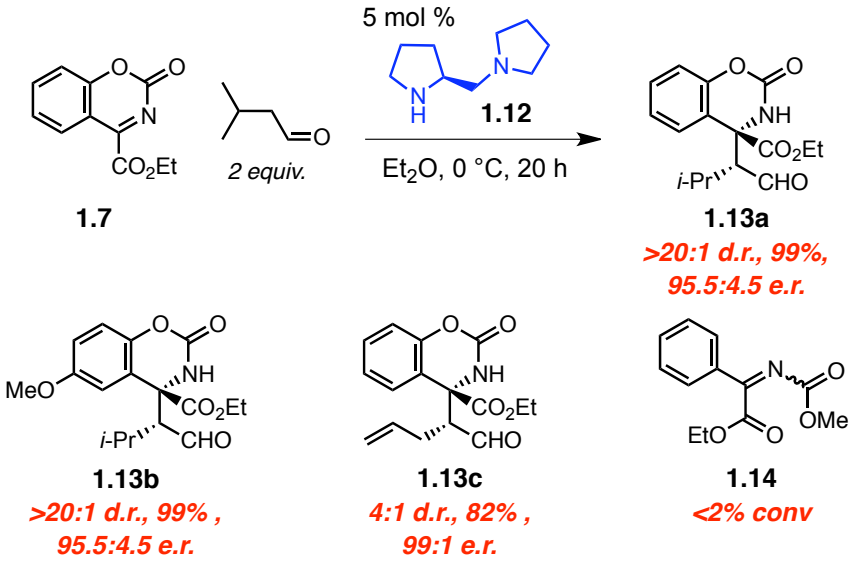

silyl-based nucleophiles resulting in preferential generation of the *anti*–diastereomers with selectivity levels between 5 and 8:1.[16] A two-step procedure is used to deprotect the amine from the anchored carbamate to afford amide-substituted chromanone **1.11** in 62% overall yield. Due to the high activity of engineered iminoester **1.7**, it was utilized to examine direct Mannich reactions[17], and consequently, likely a result of the induced ring strain, cyclic carbamate **1.7** proved a competent electrophile in contrast to its non-anchored analogue (<2% conversion with **1.14**, Scheme 1.5). In the presence of proline-derived **1.12** and enolizable aldehydes, the corresponding enamine can perform stereoselective additions affording Mannich bases **1.13a–c** in 4–>20:1 d.r., >82% yield,

[16] "The First Catalytic Highly Enantioselective Alkylation of Ketimines–A Novel Approach to Optically Active Quaternary α-Amino Acids," Saaby, S.; Nakama, K.; Lie, M. A.; Hazell, R. G.; Jørgensen, K. A. *Chem. Eur. J.* **2003**, *9*, 6145–6154.

[17] "Direct Organocatalytic Mannich Reactions of Ketimines: An Approach to Optically Active Quaternary α-Amino Acid Derivatives," Zhuang, W.; Saaby, S.; Jørgensen, K. A. *Angew. Chem. Int. Ed.* **2004**, *43*, 4476–4478.

and >95.5:4.5 e.r. (Scheme 1.5). The breadth of the catalytic enantioselective reactions described is, however, limited by the requisite *ortho*-phenoxy substitution of the derived *N*-substituted quaternary stereogenic centers.

In 2007, Shibasaki and coworkers reported a more general approach for the preparation of β–disubstituted-β–amino carbonyls.[18] Aryl-substituted diarylphosphinoyl ketoimines **1.15** react with silyl ketene acetal **1.16** in the presence of a chiral phosphine–Cu complex to afford the corresponding quaternary Mannich bases **1.18a–d** in 61–81% yield and >95.5:4.5 e.r. (Scheme 1.6). Efficiency of the transformation is greatly improved with the introduction of $(EtO)_2Si(OAc)_2$; the turnover-limiting step is presumed to be restoration of an active Cu-based catalyst[19] from the intermediate Cu–amide and, as

Scheme 1.6 Phosphine–Cu-Catalyzed Mannich Additions to Aryl-Substituted Phosphinoyl Ketoimines **1.15**

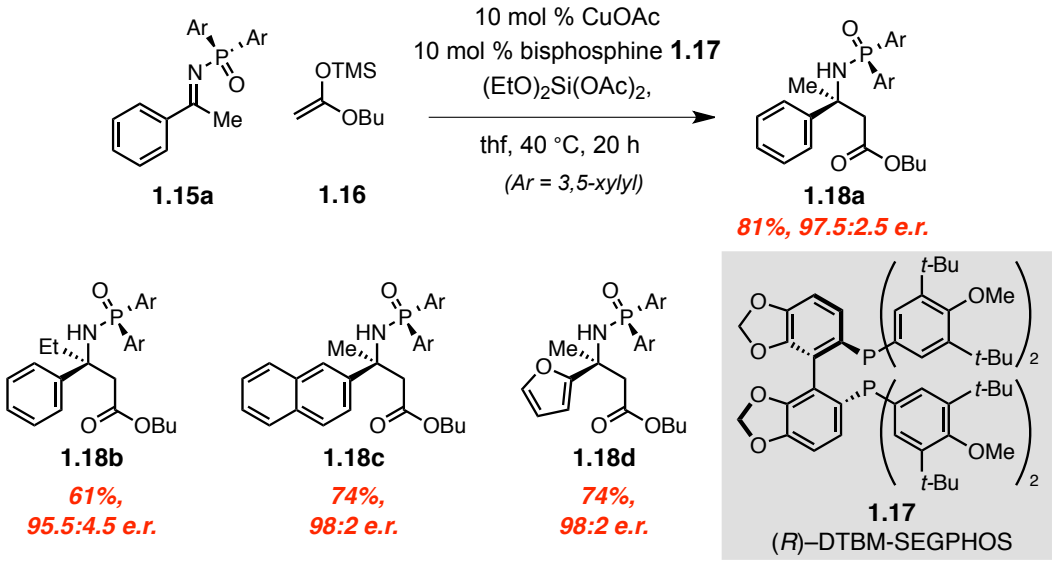

[18] "Catalytic Enantioselective Mannich-type Reactions of Ketoimines," Suto, Y.; Kanai, M.; Shibasaki, M. *J. Am. Chem. Soc.* **2007**, *129*, 500–501.

[19] In related aldol reactions of ketones promoted by a CuF-Taniaphos complex, after Cu-enolate addition, regeneration of the active catalyst from the intermediate Cu-aldolates was found to be turnover-limiting. Highly electrophilic silicon species were identified as additives to facilitate product release, for more

such, an electrophilic silicon species was found to be required for efficient product release/CuOAc regeneration. Extending the scope to generate β–dialkyl-β–amino carbonyls, however, proved to be complicated by competitive enamine isomerization,

Scheme 1.7 Optimized Conditions for Phosphine–Cu-Catalyzed Mannich Additions to Aliphatic Ketoimines

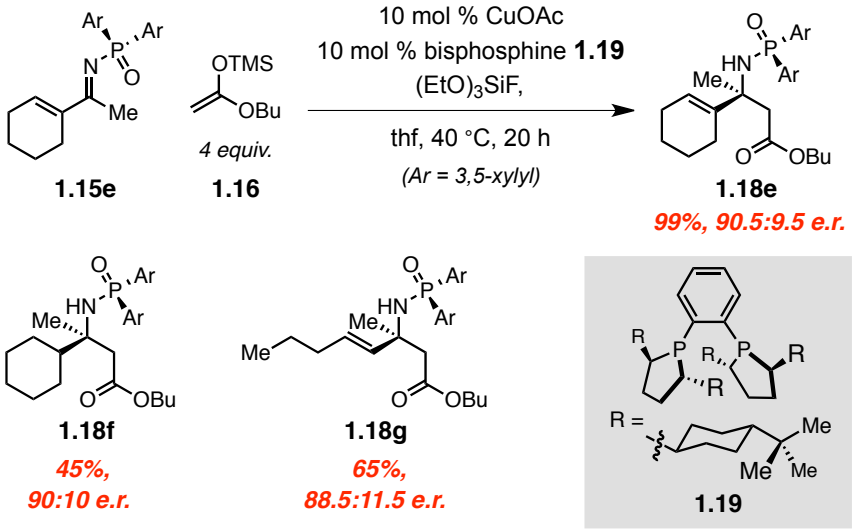

resulting in diminished yields using the conditions described in Scheme 1.6 (27% yield of **1.18e**, data not shown). This undesired pathway can be sufficiently suppressed in the presence of four equivalents of the silyl-based nucleophile, the Cu-complex derived from DuPHOS derivative **1.19**, and an equivalent of $(EtO)_3SiF$, such that Mannich adducts **1.18e–g** can be obtained in 45–99% yields and >88.5:11.5 e.r. (Scheme 1.7).

1.3 Ag-Catalyzed Mannich Additions Employing Amino Acid-Based Ligands

The critical developments described in employing chiral auxiliaries and chiral catalysts notwithstanding, major limitations in the generality of the transformations to

---

details, see: "Catalytic Enantioselective Aldol Reaction to Ketones," Oisaki, K.; Zhao, D.; Kanai, M.; Shibasaki, M. *J. Am. Chem. Soc.* **2006**, *128*, 7164–7165.

provide enantiomerically pure tertiary carbamines, particularly those related to the synthesis of α or β–amino acids, persist. Our interest in amino acid-based ligands for enantioselective catalysis,[20] particularly Ag–phosphine complexes developed for various transformations of aldimines, led us to pursue the development of more practical and general silver-catalyzed transformations for the synthesis of the corresponding *N*-substituted quaternary stereogenic centers.

The complex of silver acetate and phosphine **1.21a** was found to promote highly efficient and stereoselective transformations of *ortho*-anisidyl aldimines **1.20** with preformed silyl-based nucleophiles to generate various secondary carbamines (Scheme 1.8); for example, Mannich reactions using silyl enol ethers and silyl ketene acetals afford the β–amino ketones **1.22a–c**[21] and esters **1.22d–e**[22] in the presence of 3–5 mol % of the silver-based catalyst. Moreover, the same class of anisidyl aldimines participates in cycloadditions with the Danishefsky diene providing access to enantiomerically enriched piperidinones **1.22f–g** in excellent yields.[23]

Catalytic enantioselective vinylogous Mannich (EVM) reaction of arylimine **1.20**

---

[20] For selected examples, see: (a) "Discovery of Chiral Catalysts through Ligand Diversity: Ti-Catalyzed Enantioselective Addition of TMSCN to *meso* Epoxides," Cole, B. M.; Shimizu, K. D.; Krueger, C. A.; Harrity, J. P. A.; Snapper, M. L.; Hoveyda, A. H. *Angew. Chem. Int. Ed. Engl.* **1996**, *35*, 1668–1671. (b) "Ti-Catalyzed Enantioselective Addition of Cyanide to Imines. A Practical Synthesis of Optically Pure α-Amino Acids," Krueger, C. A.; Kuntz, K. W.; Dzierba, C. D.; Wirschun, W. G.; Gleason, J. D.; Snapper, M. L.; Hoveyda, A. H. *J. Am. Chem. Soc.* **1999**, *121*, 4284–4285. (c) "Modular Peptide-Based Phosphine Ligands in Asymmetric Catalysis: Efficient and Enantioselective Cu-Catalyzed Conjugate Additions to Five-, Six-, and Seven-Membered Cyclic Enones," Degrado, S. J.; Mizutani, H.; Hoveyda, A. H. *J. Am. Chem. Soc.* **2001**, *123*, 755–756. (d) "Asymmetric Synthesis of Acyclic Amines through Zr- and Hf-Catalyzed Enantioselective Alkylzinc Reagents to Imines," Akullian, L. C.; Porter, J. R.; Traverse, J. F.; Snapper, M. L.; Hoveyda, A. H. *Adv. Synth. Catal.* **2005**, *347*, 417–425.

[21] "Ag-Catalyzed Asymmetric Mannich Reactions of Enol Ethers with Aryl, Alkyl, Alkenyl, and Alkynyl Imines," Josephsohn, N. S.; Snapper, M. L.; Hoveyda, A. H. *J. Am. Chem. Soc.* **2004**, *126*, 3734–3735.

[22] "Practical and Highly Enantioselective Synthesis of *β*–Alkynyl-*β*–amino Esters through Ag-Catalyzed Asymmetric Mannich Reactions of Silylketene Acetals and Alkynyl Imines," Josephsohn, N. S.; Carswell, E. L.; Snapper, M. L.; Hoveyda, A. H. *Org. Lett.* **2005**, *7*, 2711–2713.

[23] "Efficient and Practical Ag-Catalyzed Cycloadditions between Arylimines and the Danishefsky Diene," Josephsohn, N. S.; Snapper, M. L.; Hoveyda, A. H. *J. Am. Chem. Soc.* **2003**, *125*, 4018–4019.

Scheme 1.8 Enantioselective Reactions of Aldimines Catalyzed by the Ag Complex of Amino Acid-Based Phosphine **1.21a**

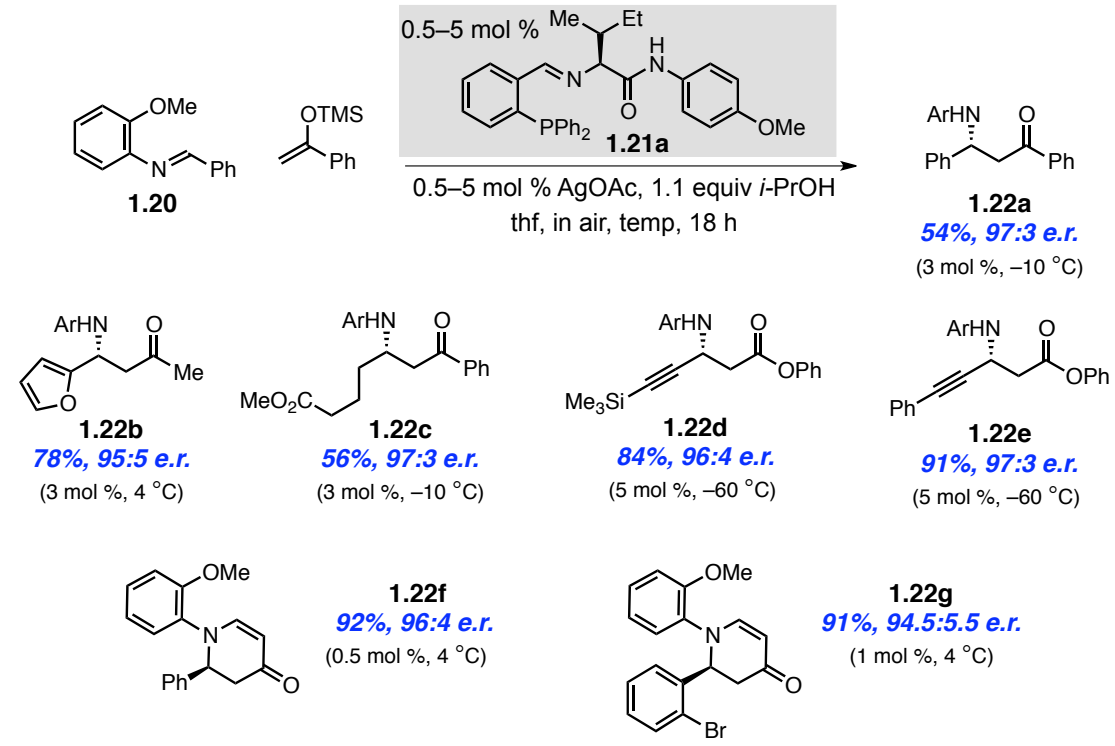

with 2-siloxyfuran **1.23** proceeds to install two contiguous stereocenters with complete diastereoselection (Scheme 1.9).[24] While unsubstituted and 4–Me-substituted siloxyfurans lead to the *anti*-butenolides,[25] 3–Me-substitution results in a reversal of selectivity to yield the *syn*-isomer **1.24e**. Discussion regarding this reversal in the approach of the nucleophile is pertinent to the mechanistic studies on a related class of silver-catalyzed vinylogous Mannich reactions that will be discussed in greater detail in Section **1.5** of this chapter.

There are several noteworthy points in regards to the utility of the silver-catalyzed

[24] "A Highly Efficient and Practical Method for Catalytic Asymmetric Vinylogous Mannich (AVM) Reactions," Carswell, E. L.; Snapper, M. L.; Hoveyda, A. H. *Angew. Chem., Int. Ed.* **2006**, *45*, 7230–7233.
[25] The diastereomers are termed *syn* or *anti* in this chapter on this basis of the relative stereochemistry of the N and O substituents.

Scheme 1.9 Enantioselective Vinylogous Mannich Reactions of Aldimine **1.20** Catalyzed by the Ag Complex of Amino Acid-Based Phosphines

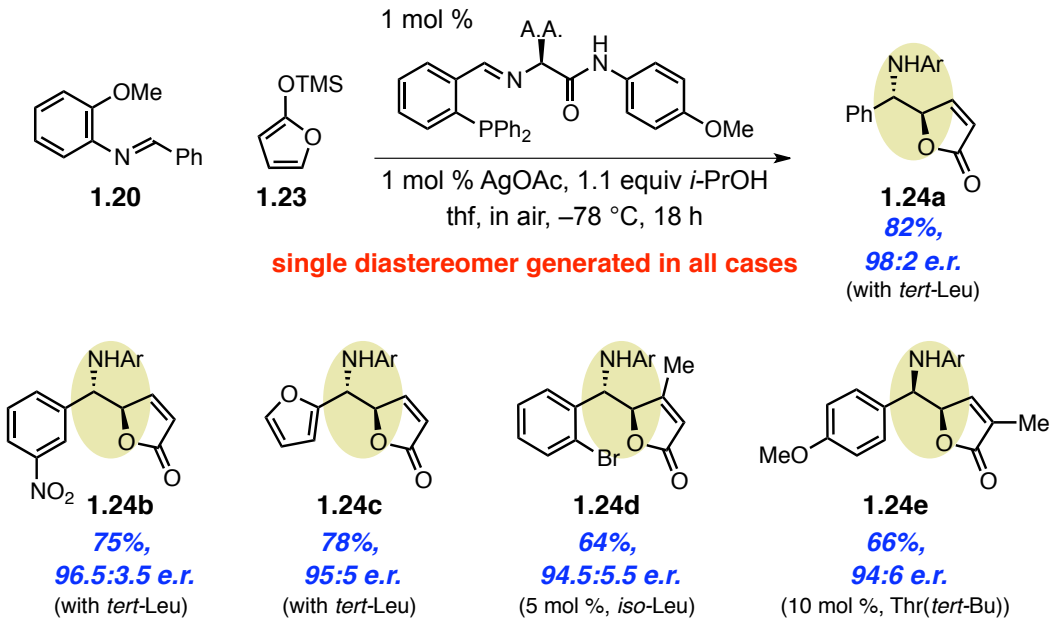

transformations described above: 1) Reactions promoted by the phosphine-based silver acetate complexes are practical, robust, and tolerant of air and moisture. 2) The presence of the *ortho*-anisidine protecting group on the imine is often required for both reactivity and enantioselectivity; we presume that bidentate chelation with the Lewis acidic silver center results in both its activation towards nucleophilic additions and to enhance stereodifferentiation of the enantiotopic faces. 3) The Lewis basicity of the *C*-terminus amide of the amino acid-based ligand has been shown to be critical to obtain high levels of reactivity and selectivity.[26] We have postulated that this class of ligands has bifunctional behavior:[27] in the case of reactions involving silyl-based nucleophiles, the

[26] For screening data related to this observation, see: refs 22 and 23. For a previous mechanistic study on related Ti-catalyzed Strecker reaction, see: "Mechanism of Enantioselective Ti-Catalyzed Strecker Reaction: Peptide-Based Metal Complexes as Bifunctional Catalysts," Josephsohn, N. S.; Kuntz, K. W.; Snapper, M. L.; Hoveyda, A. H. *J. Am. Chem. Soc.* **2001**, *123*, 11594–11599.

[27] For selected examples, see: (a) "Bifunctional Asymmetric Catalysis: A Tandem Nucleophile/Lewis Acid Promoted Synthesis of *β*-Lactams," France, S.; Wack, H.; Hafez, A. M.; Taggi, A. E.; Witsil, D. R.; Lectka, T. *Org. Lett.* **2002**, *4*, 1603–1605. (b) Shibasaki, M.; Kanai, M. (2006) "Chiral Bifunctional

Lewis basic amide can coordinate the silicon atom inducing activation,[28] while the Schiff base at the *N*-terminus houses the Lewis acidic metal. 4) Of the classes of silicon-based nucleophiles examined, siloxyfurans, which react in a vinylogous manner through the γ–position, offer the highest levels of reactivity, such that the transformations depicted in Scheme 1.9 can be performed at –78 °C with high efficiency.

There are several reasons that account for the elevated nucleophilicity of 2-siloxyfuran **1.23**. First, the HOMOs of silyl ketene acetals are raised in comparison to those of their enol ether counterparts, in part due to the filled-filled orbital interactions between the π bond and the lone pairs on the adjacent oxygen atom. Secondly, enol silanes react with electrophiles in a two-step manner in which, first, the electrons of the

Figure 1.1 Relative Nucleophilicities of Various Silyl Enol Ethers and the Corresponding Silyl Ketene Acetals

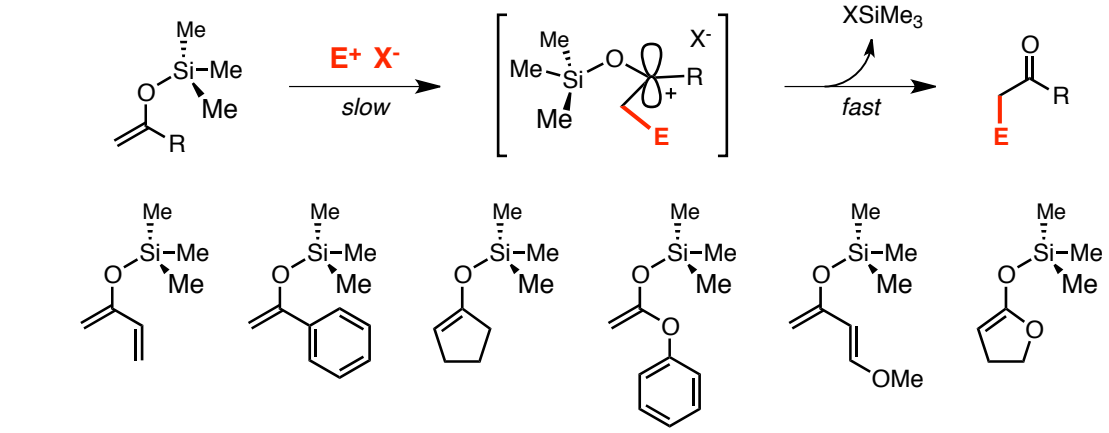

Acid/Base Catalysts" in *New Frontiers in Asymmetric Catalysis* (eds Mikami, M. and Lautens, M.), John Wiley & Sons, Inc., Hoboken, NJ. (c) "Recent Progress in Asymmetric Bifunctional Catalysis Using Multimetallic Systems," Shibasaki, M.; Kanai, M.; Matsunaga, S.; Kumagai, N. *Acc. Chem. Res.* **2009**, *42*, 1117–1127.

[28] For an excellent review regarding the theory and utility of Lewis base activation of Lewis acids, particularly with respect to Si-containing molecules, see: "Lewis Base Catalysis in Organic Synthesis," Denmark, S. E.; Beutner, G. L. *Angew. Chem., Int. Ed.* **2008**, *47*, 1560–1638.

olefin react with the electrophile and then, the resultant stabilized carbocation collapses to afford the carbonyl products (Figure 1.1). The rate at which silyl-based nucleophiles trap an electrophile can be correlated with their capacity to stabilize the developing δ^+ positive charge;[29] for example, although phenyl-substituted silyl enol ether reacts an order of magnitude faster than then dienyl silane (benzylic vs. allylic carbocation formation), the corresponding phenoxyvinylsilane is 50 times more reactive. The trend in which the oxygen-substituted variants react at faster rates is both due to the higher HOMO coefficients at the reacting carbons, as well as the ability for the lone pairs of the oxygen to hyperconjugate with the empty p orbital of the incipient carbocation.

Siloxyfuran **1.23** belongs to a class of vinylogous[30] nucleophiles in which the nucleophilicity of the enol silane can be extended through a conjugated π–system. Whereas Li enolate **1.25** reacts at the C_2 position affording products of α-addition, the

Figure 1.2 HOMO Coefficients of Vinylogous Nucleophiles

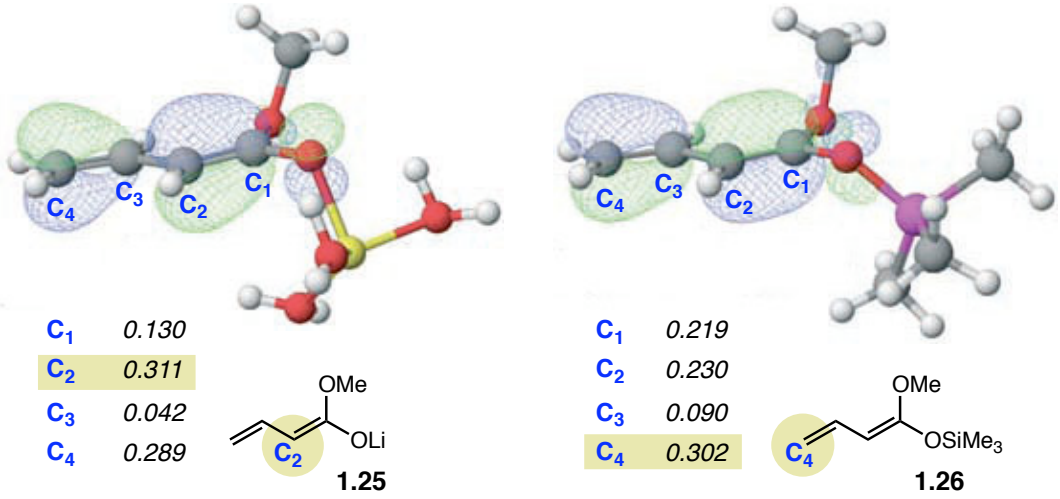

[29] "Determination of the Nucleophilicities of Silyl and Alkyl Enol Ethers," Burfeindt, J.; Patz, M.; Müller, M.; Mayr, H.; *J. Am. Chem. Soc.* **1998**, *120*, 3629–3634.

[30] (a) "The Principle of Vinylogy," Krishnamurthy, S. *J. Chem. Educ.* **1982**, *59*, 543–547. For a review outlining the utility of vinylogous nucleophiles in the context of aldol and Mannich reactions, see and references cited therein: "The Vinylogous Aldol and Related Addition Reactions: Ten Years of Progress," Casiraghi, G.; Battistini, L.; Curti, C.; Rassu, G.; Zanardi, F. *Chem. Rev.* **2011**, *111*, 3076–3154.

corresponding silyl ketene acetal **1.26** preferentially reacts through C_4.[31] Due to the high degree of electron density of both silyl and metallodienolates their reactions are mainly governed by electrostatic interactions and thus electron density calculations are useful predictive models for their behaviors (Figure 1.2). In concurrence with acyclic silyl ketene acetal **1.26**, siloxyfuran **1.23** reacts with complete γ-selectivity; C–C bond formation through C_4 is electronically and sterically preferred as it is a more electron rich and less hindered site than C_2.[32] It is the inherent high nucleophilicity and site-selectivity of siloxyfuran **1.23** that led us to select it as a partner for reactions of notoriously unreactive ketone-derived imines.

1.3a Investigations into Ag-Catalyzed Mannich Additions to Ketoimines

Initial investigations of the promotion of reaction between anisidine-protected α-ketoiminoester **1.27** and siloxyfuran **1.23** were undertaken employing the optimal silver-

Scheme 1.10 Enantioselective and *syn*-Selective Ag-Catalyzed Vinylogous Mannich Reactions of α-Ketoiminoester **1.27**

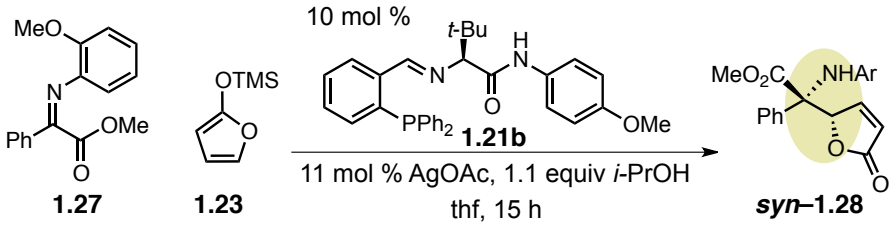

[31] For a discussion regarding the utility of vinylogous nucleophiles in aldol processes and the electronic and steric factors that govern their reactions, see: "Catalytic, Enantioselective, Vinylogous Aldol Reactions," Denmark, S. E.; Heemstra, J. R. Jr.; Beutner, G. L. *Angew. Chem., Int. Ed.* **2005**, *44*, 4682–4698.

[32] Steric contributions can play an important role in site-selectivity, in some cases overriding the electronic preferences. For instance, silyl ketene acetals with substitution at C_4 result in competitive additions through C_2. See the review in ref 28 for more details.

based catalyst discovered for related reactions of aldehyde-derived analogs (Scheme 1.10). Exclusive *syn*-addition of the butenolide moiety was observed affording *syn*–**1.28** in 68% conversion and 63.5:3.5 e.r. (lowering the temperature resulted in similar levels of enantioselectivity and diminished reactivities). Surprisingly, the opposite sense of addition is obtained in comparison to previous studies with anisidyl aldimines. Although incremental improvements could be rendered through modification of the catalyst and the conditions, ultimately lack of activity remained the challenge.[33]

In an attempt to increase the electron defficiency at the prochiral carbon of the ketoimine substrate, the electron rich *ortho*-anisidine protecting group was altered to affect the electronic distribution (Scheme 1.11). Introduction of an inductively

Scheme 1.11 Effects of the Electronic Parameters of the *N*-Aryl Group on the Reactivity and Selectivity of EVM

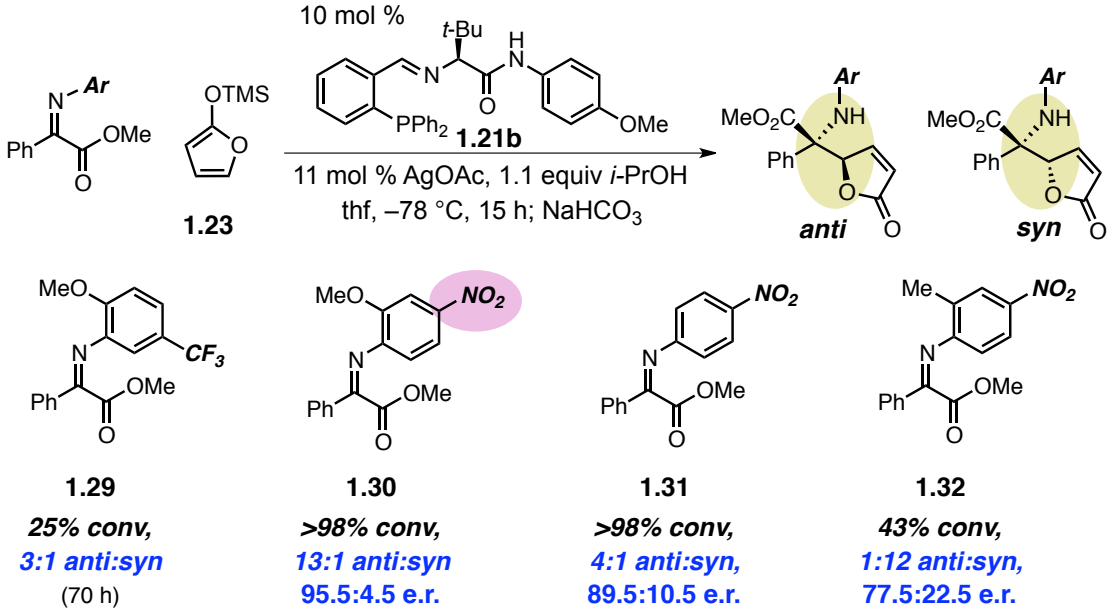

[33] "Silver-catalyzed Vinylogous Mannich-type Reactions of alpha-Ketoimine Esters with Siloxyfurans," in *Catalytic Enantioselective Synthesis of O- and N-Substituted Quaternary Carbon Stereogenic Centers*, Wieland, L. C., Ph. D. (Boston College, 2008).

withdrawing CF_3 group in **1.29** allows the alkylation to occur at –78 °C, albeit with only 25% conversion after 70 hours. Gratifyingly, a nitro group *para* to the imine proves significantly more efficacious at increasing the δ^+ at the reacting carbon; *para*-nitro containing **1.30** and **1.31** allow for high efficiency of the Mannich process, however, as previously noted, the *ortho*-methoxy unit of **1.30** is required for high diastereo- (13:1 vs 4:1 *anti*:*syn*) and enantioselectivity (95.5:4.5 vs 89.5:10.5 e.r.).[34] EVM of ketoimine **1.32**, bearing a 2-methyl-4-nitrophenyl group, stands to further corroborate the role in chelation of the anisidine group; 43% conversion to a 12:1 mixture of stereoisomers, in favor of the *syn* isomer, is obtained with moderate enantioselectivity. As will be discussed in a later section, the *syn* and *anti* approaches of the furan result from competitive pathways

Figure 1.3 Dependence of Selectivity and Yield of the EVM on Temperature

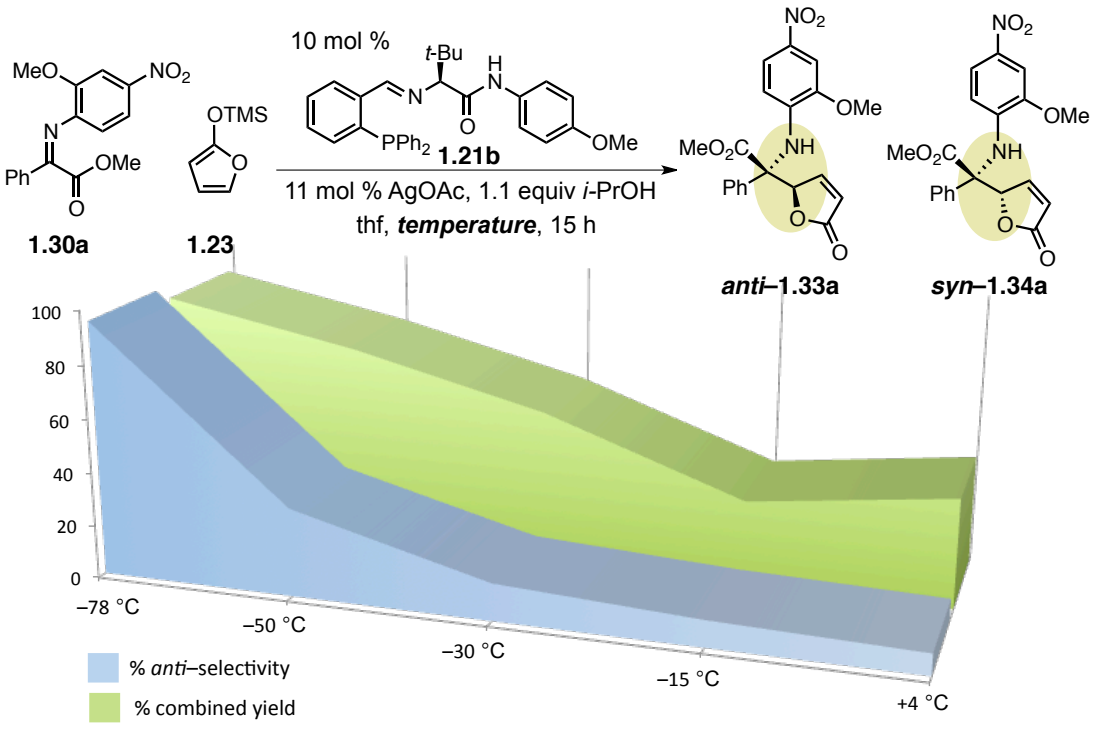

[34] The *ortho*-methoxy group is postulated to be necessary for bidentate chelation to the Lewis acidic silver center, this tight binding likely results in improved enantiodifferentiation in the nucleophilic addition; see ref 22 for similar observations.

dictated by the binding mode of the substrate. Although the *para*-nitro substituted anisidine in **1.30** provides sufficient activity along with high *anti*- and enantioselectivity *when the reaction is performed at –78 °C*, an interesting trend is observed at higher temperatures (Figure 1.3). At warmer temperatures, the EVM process loses the high diastereoselectivity and the isolated yields of the Mannich bases are significantly diminished. The cause of the decreasing yields was readily identified upon closer inspection of the reaction outcome.

Unreacted siloxyfuran **1.23**[35] is capable of competitively reacting with the γ-butenolides of the Mannich adducts **1.33** and **1.34** at higher temperatures, thus reducing the yields of the desired products. Further studies of this adventitious pathway revealed the Michael addition process to be silver-catalyzed (equation 1). When isolated *anti*-**1.33a** is subjected to siloxyfuran **1.23** under the EVM conditions, 44% conversion to bislactone **1.35** is observed (after 15 hours at –78 °C). The Michael addition, which generates an additional two contiguous stereocenters to those already set, does not occur in the absence of the silver catalyst and also appears to be fairly diastereoselective (two of the possible four diastereomers are formed in a 73:27 mixture). To diminish the formation of byproduct **1.35** and obtain improved yields of the Mannich products, a

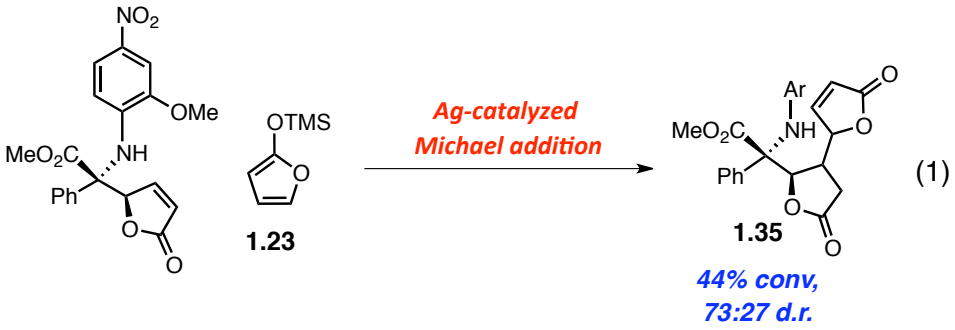

(1)

[35] Optimization of the reaction conditions had identified the requirement of 2.1 equivalents of 2-siloxyfuran **1.23** for high efficiency (1.05 equivalents results in 68% conversion and 2:1 *anti*:*syn* d.r.). See ref 30 for more details.

procedure to ensure complete protodesilylation of the unreacted siloxyfuran at –78 °C was instilled. Rather than the addition of a saturated aqueous solution of sodium bicarbonate to terminate the reaction, two equivalents of acetic acid in methanol were found to be more effective at quenching the reactive reagent.[36] Although an appropriate solution had elucidated the temperature dependence on isolated yield, there was no justification ascribed to the loss of *anti*-selectivity and preferential *syn*-approach at temperatures above –78 °C (Figure 1.3).

As demonstrated in Table 1.1, using conditions that were identified to provide highly diastereoselective and enantioselective Mannich-type additions, a variety of aryl- and heteroaromatic ketoimines participate in the EVM process to afford *anti*–**1.33a–k** in >66:34 d.r. and >90:10 e.r. The EVM process tolerates the presence of a number of functional groups appended in the *meta* or *para* positions with little effect on diastereo- or enantioselectivities. Notably, the presence of a potential secondary chelation site in 2-furyl-substituted **1.30j**, in addition to the *N*,*O*-bidentate coordination afforded by the *N*-aryl protecting group, results in disruption of the diastereocontrol (only 1:1–3:1 *anti*:*syn* d.r.), evidence suggestive of the impact that the mode of substrate coordination can have on the approach of the nucleophile. Once the chelating group is placed more remotely from the imine nitrogen, as in 3-thiophenyl **1.30k**, the high *anti*-selectivity is restored as it is less likely to compete for binding with the silver center. Additionally, the silver-catalyzed EVM reaction is amenable to gram-scale operations; the transformation can be

[36] The primary reason for the ineffectiveness of quenching a reaction at –78 °C with an aqueous solution is that it immediately freezes, and for this reason, protonation of the siloxyfuran actually occurs at much higher temperatures as the solution thaws. Acetic acid in methanol simply can homogeneously react at the desired temperature ensuring complete protodesilylation.

promoted with 10 mol % of less expensive valine-derived **1.21c**[37] to afford an 84% yield of *anti*–**1.33a** in 93:7 e.r. (equation 2, vs. 95.5:4.5 e.r. with *tert*-leucine based phosphine **1.21b** in Table 1.1). This catalytic protocol also allows access to the primary amine

Table 1.1 Ag-Catalyzed EVM of Aryl- and Heteroaromatic Substituted Ketoimino α-esters **1.30a–k**

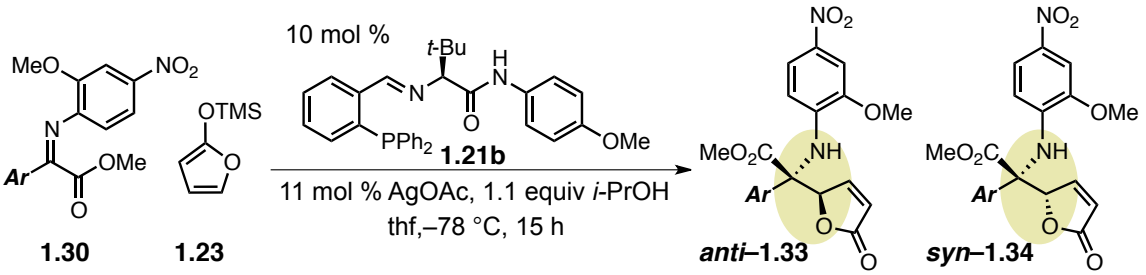

			aq $NaHCO_3$, –78 °C to 22 °C			AcOH in MeOH, –78 °C, 3 h		
entry	***Ar***		d.r.[a] *anti:syn*	yield[b] **1.33** (%)	e.r.[c] **1.33**	d.r.[a] *anti:syn*	yield[b] **1.33** (%)	e.r.[c] **1.33**
1	C_6H_5	**1.30a**	93:7	72	95.5:4.5	95:5	88	96:4
2	*m*-$OMeC_6H_4$	**1.30b**	80:20	76	93:7	95:5	95	96.5:3.5
3	*m*-ClC_6H_4	**1.30c**	75:25	51	90.5:9.5	92:8	72	93.5:6.5
4	*p*-ClC_6H_4	**1.30d**	-	-	-	>98:<2	80	97.5:2.5
5	*p*-BrC_6H_4	**1.30e**	88:12	78	96:4	96:4	80	96:4
6	*p*-IC_6H_4	**1.30f**	86:14	62	95:5	>98:<2	81	96.5:3.5
7	*p*-*t*-BuC_6H_4	**1.30g**	75:25	68	93:7	89:11	77	95:5
8	*p*-$CF_3C_6H_4$	**1.30h**	89:11	67	95.5:4.5	97:3	87	97:3
9	2-naphthyl	**1.30i**	93:7	68	95:5	>98:<2	81	95:5
10	2-furyl	**1.30j**	50:50	39	90:10	66:34	60	90:10
11	3-thiophenyl	**1.30k**	67:33	-	-	94:6	70	96:4

[a]Determined by analysis of 400 MHz ^{1}H NMR spectra of unpurified reaction mixtures; [b]Isolated yields of purified ***anti*–1.33**; >98% conversion in all cases. [c]Enantiomer ratio values were determined by HPLC analysis.

[37] The non-proteogenic amino acid L-*tert*-Leucine, required for the synthesis of optimal ligand **1.21b**, is 44 times more expensive than abundant naturally-occurring L-valine (price comparison is based on Aldrich catalogue, 2013).

employing a two-step oxidative removal of the *N*-aryl group (Scheme 1.12). It is, fortuitously, the presence of the *para*-nitro group, which was initially installed to enhance

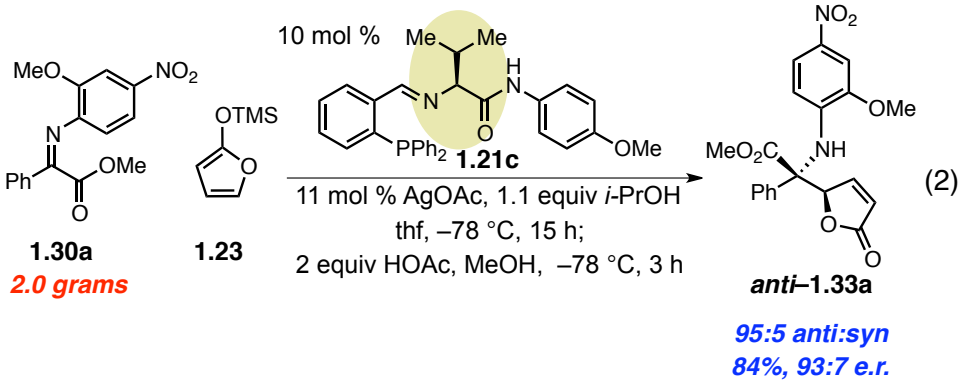

reactivity, that also provides a handle for deprotection. The nitro group can be reduced to afford the derived aniline **1.36a**, providing a competent nucleophile to effectively react with phenyl iodoacetate. Attempts at oxidative cleavage of the parent aniline **1.33a** are unproductive; the secondary amine on the quaternary carbon is too encumbered and is not sufficiently nucleophilic for effective reaction with oxidants. The primary aniline **1.36a** is oxidized to an azabenzoquinone intermediate, which is subsequently hydrolyzed under acidic conditions to generate the desired primary amine **1.37** in 81% overall yield.

Scheme 1.12 Oxidative Removal of the *N*-Aryl Unit to Afford Amine **1.37**

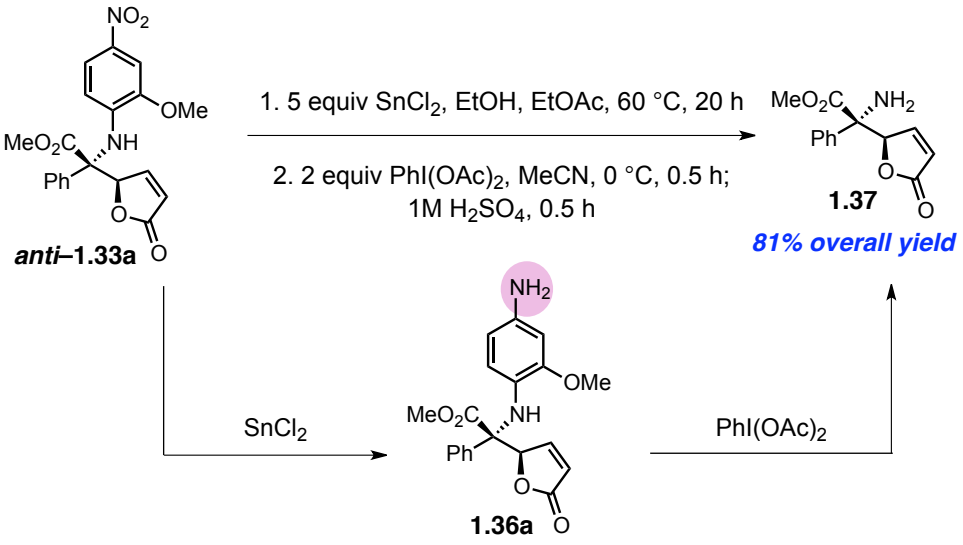

Several interesting conclusions can be reached from the studies that were undertaken to examine the generality of the EVM reaction: 1) As expected, the ineffectual quench with the saturated aqueous solution of sodium bicarbonate results in diminished isolated yields with increased amounts of Michael addition byproducts. Improved yields (60–95%, Table 1.1) of the *anti* adducts are obtained when acetic acid serves as a homogeneous protic source. 2) Unexpectedly and curiously, use of acetic acid also results in improved diastereoselectivities of the transformations in Table 1.1. For example, *anti*–**1.33f** can be obtained as a single diastereomer in 81% yield, whereas it had been obtained as an 86:14 mixture of isomers when an aqueous solution of sodium bicarbonate was used as quench. 3) A complete reversal of diastereoselectivity is observed with arylketoimines bearing *ortho*-substitution, such that, under the same reaction conditions, butenolide addition occurs from the opposite trajectory (Figure 1.4). Moreover, addition of encumbered 4–Me substituted siloxyfuran results in an 89% yield

Figure 1.4 The Correlation Between Sterically-Encumbered Substrates and *Syn*-Selectivity in the EVM Reaction

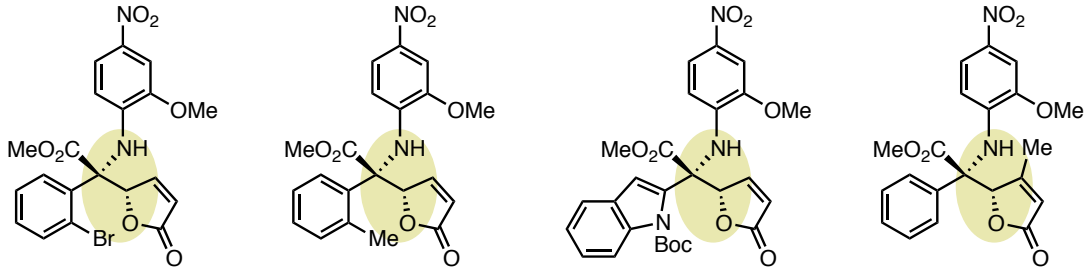

***syn*–1.34l**
>20:1 syn
87%, 66:34 e.r.

***syn*–1.34m**
>20:1 syn
89%, 70:30 e.r.

***syn*–1.34n**
>20:1 syn
80%, 70:30 e.r.

***syn*–1.38**
20:1 syn:anti
89%, 75:25 e.r.

of *syn*–**1.38**. Notably, only moderate levels of enantioselectivity are typically obtained for all of the *syn* isomers (66:34–75:25 e.r.). The cause of competitive *syn* addition as a function of temperature, its correlation to quench procedure, as well as its dependency on

the identity of the ketoimine partner hence became subject of mechanistic inquiry.

1.4 Mechanistic Investigations

There emerged two distinct rationales for the dependence of diastereoselectivity on temperature (92% *syn*-addition at 4 °C vs. 93% *anti*-selectivity at –78 °C, see Figure 1.3). It is possible that the variance in temperature has a significant effect on the relative energies of the isomeric transition states of the stereochemistry-determining step (i.e., at 4 °C, the transition state involving *syn*-approach of the enol silane would be lower in energy than that leading to *anti*-addition). An equally plausible scenario involves alterations to the structure of the chiral Ag–phosphine complex as a function of temperature; discrete identities of the chiral complex can result in divergent behavior in the EVM reaction, including the identity of the stereochemical defining step. We sought additional insight to distinguish between these two mechanistic pictures and began with studies aimed at indentification of the active chiral catalyst.

Since the chiral catalyst employed in the *anti*-selective EVM reactions is prepared *in situ* from equimolar parts silver acetate and phosphine **1.21b**, the efficiency and lability of their complexation was not well established. Studies aimed at elucidation of the structure of the active complex, in particular as a function of temperature, were initiated with solution infrared spectroscopic studies of a 1:1 mixture of silver acetate and phosphine **1.21b** performed using a ReactIR™ instrument. Measurements of the infrared spectra at variable temperatures revealed that the intensity and frequencies of the absorption bands fluctuated as a function of temperature (Figure 1.5). The temperature-dependent variance observed through infrared spectroscopy suggests that the nature and

Figure 1.5 ReactIR Study of the AgOAc-Phosphine **1.21b** Complex at Various Temperatures

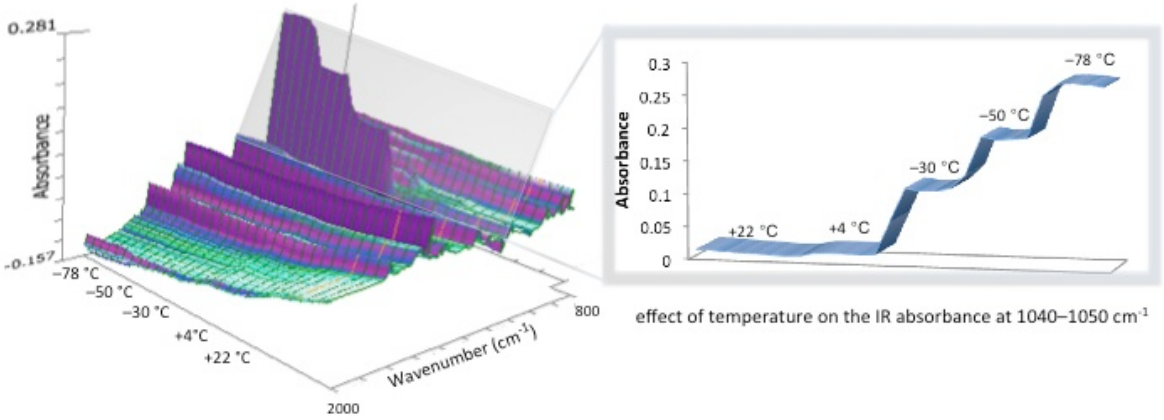

identity of the chiral Ag–phosphine catalyst may be more complex than anticipated. In order to interpret this apparent fluxional behavior, we undertook the isolation and characterization of the resultant complex in order to obtain further spectroscopic evidence of its behavior in solution and at variable temperatures.

Towards this objective, an air stable complex was generated through reaction of one equivalent each of silver acetate and phosphine **1.21b** (Figure 1.6).[38] Surprisingly, crystals produced from a saturated thf/petroleum ether solution of complex **1.39** are confirmed by X-ray crystallographic analysis to be 2:1 phosphine **1.21b**:AgOAc

Figure 1.6 Synthesis of Air Stable Pre-Complexed Ag-Based Catalyst **1.39**

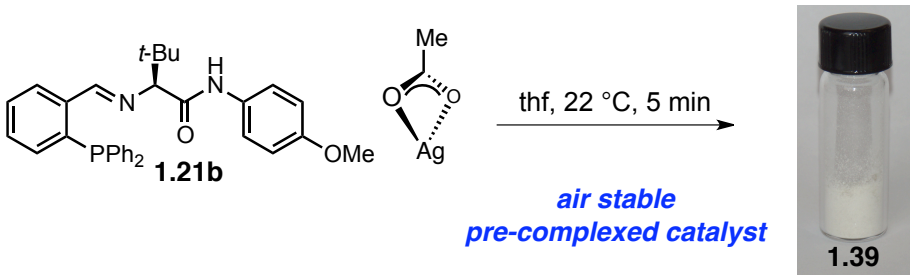

[38] After the silver salt and phosphine were allowed to premix in tetrahydrofuran for five minutes, the solution was filtered through a short pad of Celite® to remove any undissolved material. White solid **1.39**, which can be stored in air for years with no decomposition, is afforded upon concentration.

Figure 1.7 X-Ray Crystal Structure of Isolated Bisphosphine–Ag Complex **1.40**

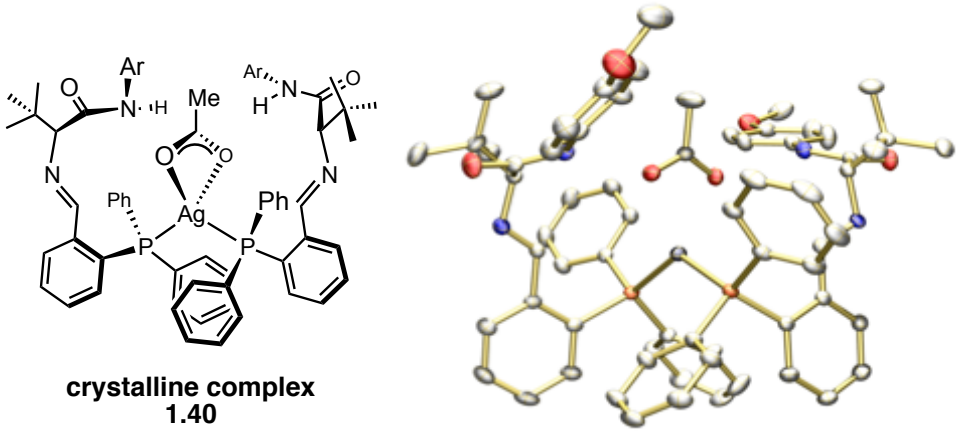

complex **1.40** (Figure 1.7).[39] The isolated and characterized bisphosphine **1.40**, however, proves to be an inefficient and *syn*-selective EVM catalyst (Scheme 1.4). In the presence of 5 mol % of the encumbered bisphosphine, 30–70% conversion to ≥95% *syn*–**1.34a** in 71:29–78:22 e.r. is obtained (Scheme 1.14); besides the added hindrance (vs. the theorized active 1:1 complex), coordination of two phosphines likely reduces the Lewis acidity at the silver center, disfavoring ketoimine coordination and engendering minimal

Scheme 1.14 EVM Activity of Bisphosphine–Ag Complex **1.40**

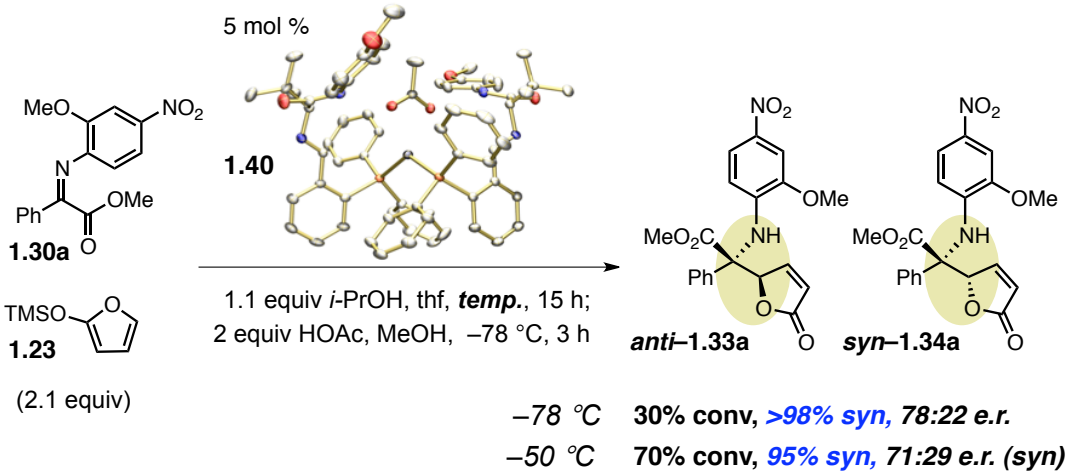

[39] The crystalline complex **1.40** is also air stable and can be isolated in 77% yield, see Experimentals for details.

activation once bound. Since 2:1 phosphine:AgOAc complex **1.40** selectively provides the *syn*-isomer, it is not the species that promotes highly *anti*- and enantioselective EVM of ketoiminoester **1.30**. However, in the presence of the air stable pre-complexed Ag–phosphine catalyst **1.39,** additions of siloxyfuran are promoted with nearly identical

Scheme 1.15 EVM Activity of Isolated Pre-Complexed–Ag Complex **1.39**

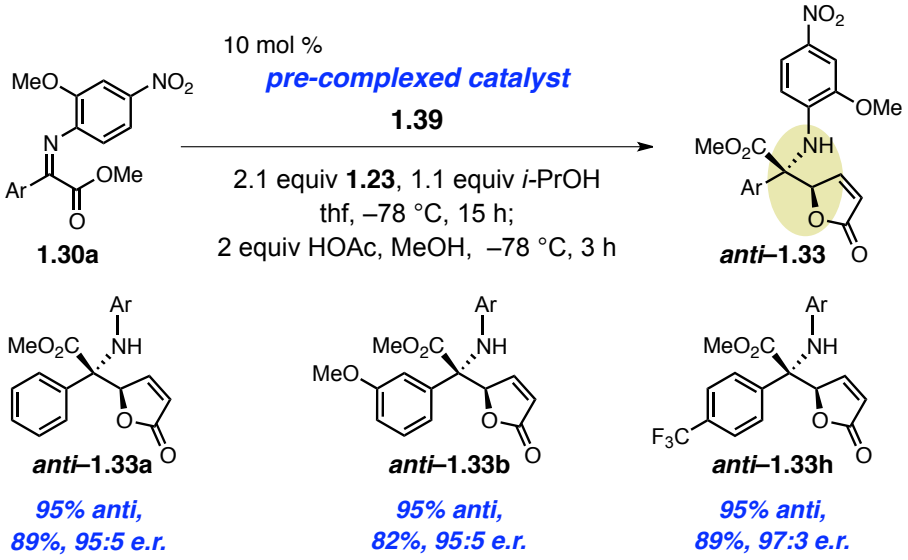

levels of reactivity and selectivity afforded with *in situ* generation of the catalyst; reactions of aryl-substituted ketoiminoesters afford *anti*–**1.33a**, **b**, and **h** with 95% *anti*-selectivity in >95:5 e.r. and in >82% yield (compare results in Table 1.1 with those in Scheme 1.15).[40]

The disparity in reactivity of the isolated Ag–phosphine complexes was perplexing, particularly given that the two silver-based catalysts appeared to be identical using multinuclear (400 MHz ^{1}H, 162 MHz ^{31}P, and 100 MHz ^{13}C NMR in d_8-

[40] The identity of the pre-complexed catalyst **1.39**, an air stable white solid, was unclear at this point; by ^{1}H NMR analysis, it seemed to only differ from the crystalline 2:1 phosphine:AgOAc complex **1.40** in ratio of the acetate to phosphine (i.e., where **1.40** was 1:2 by integration, **1.39** was 2:3). It was this assumed 2:3 AgOAc:phosphine **1.21b** by which catalyst loading was calculated.

tetrahydrofuran at 22 ºC) spectroscopic analysis.[41] However, when the same spectroscopic characterization of powdered complex **1.39** and crystalline bisphosphine **1.40** was attempted at –78 °C, the temperature at which EVM reactions are performed,

Figure 1.8 Variable Temperature 400 MHz ^{1}H NMR Study of Ag-Complex **1.39**

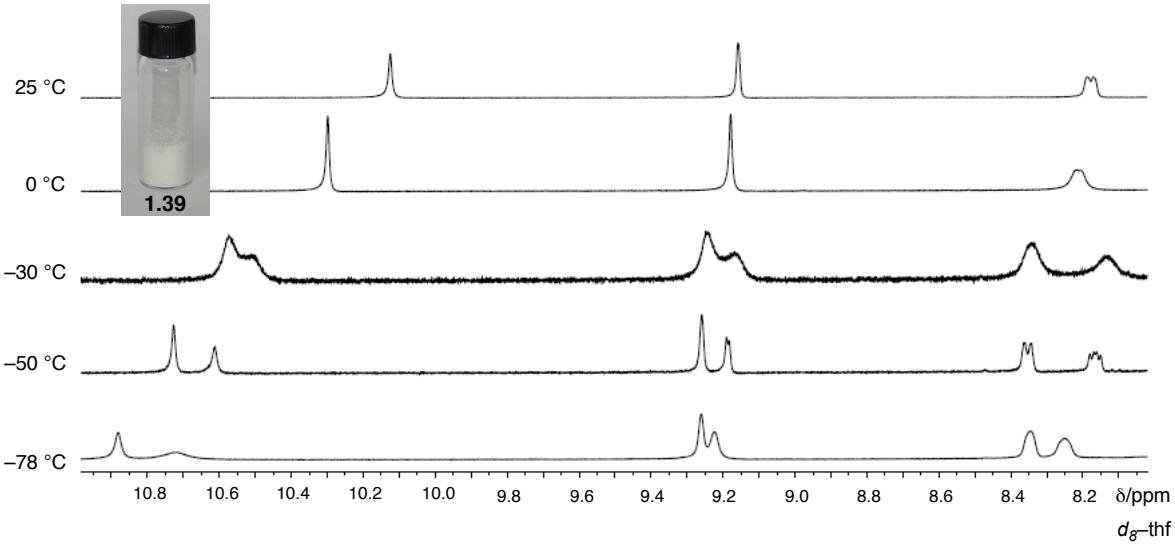

Figure 1.9 Variable Temperature 400 MHz ^{1}H NMR Study of Ag-Complex **1.40**

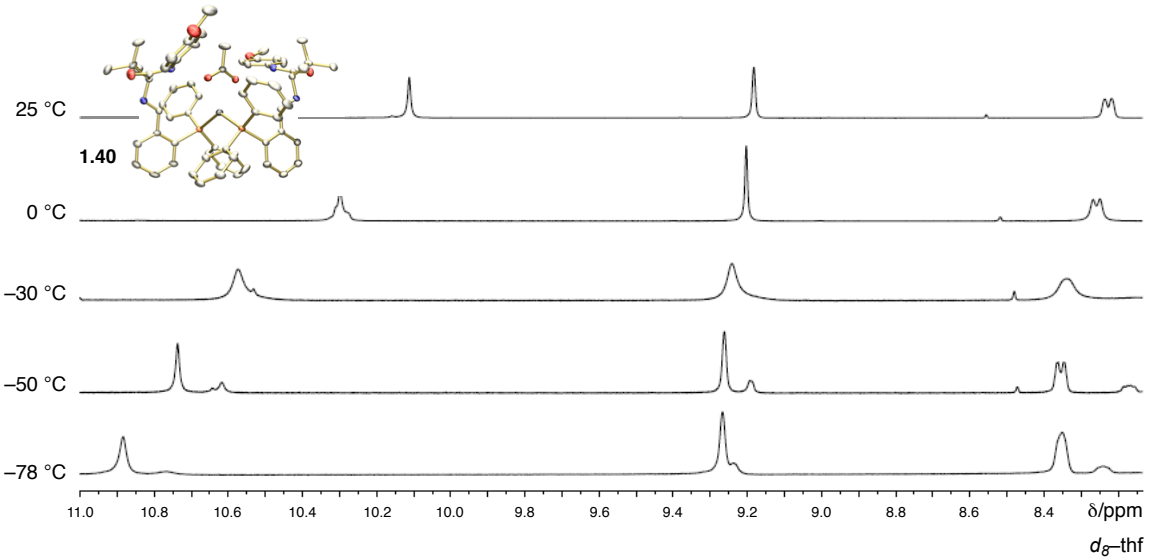

[41] Spectroscopically, *at 25 °C*, the complexes are indistinguishable, with exception of the difference in acetate integration mentioned in ref 37, e.g., see ^{1}H NMR data in Figure 1.7 and 1.8. ^{13}C and ^{31}P NMR data is not shown.

the distinction between the two complexes became evident. Variable temperature ^{1}H NMR analysis reveals that both complexes are, in actuality, mixtures of two distinct species, albeit in differing proportions (nearly a 1:1 ratio for complex **1.39**, and a 5:1 ratio for bisphosphine **1.40** by integration, compare Figures 1.8 and 1.9). At ambient temperature, the two species present in solution rapidly interconvert such that their signals coalesce and only their averaged chemical shifts are observed; for example, the coalesced signal for the amide proton of the two species begins to decelerate enough such that the two components can be differentiated at temperatures lower than –30 °C, and at –78 °C, two downfield-shifted amide proton chemical shifts at δ 10.78 and δ 10.87 ppm, corresponding to the two components, can be distinguished.[42] The observed decoalescence suggests that the identities of the two components are such that they can readily interconvert and rapidly establish an equilibrium in solution. Moreover, the relationship between temperature and the diastereoselectivity of the Mannich process (reversal of *anti* to *syn*-selectivity with higher temperatures, see Figure 1.3) may be correlated to the temperature-dependent nature of the dynamic exchange process elucidated by the NMR studies.

A similar analysis of the 162 MHz ^{31}P NMR spectra of the isolated Ag-complexes **1.39** and **1.40** at 25 °C resulted in a broadened solitary singlet, consistent with the averaged ^{1}H NMR spectra at 25 °C (Figure 1.10); evaluation of the two samples at –78 °C, where the rapid exchange has slowed, reveals two pairs of doublets[43] that occur

---

[42] It is important to note that upon warming the NMR sample that has decoalesced at –78 °C, the signals will recoalesce when warmed back to 25 °C to obtain the same averaged chemical shifts.

[43] A pair of doublets is expected since Ag has two magnetic isotopes found in nearly equal abundance: ^{107}Ag (48.161%) and ^{109}Ag (51.839%). For a related study on solution structure determination of tris and tetraphosphine–Ag complexes using ^{31}P NMR analysis, see: "Solution Structure and Kinetic Study of Metal–Phosphine and –Phosphite Complexes. I. The Silver (I) System," Muetterties, E. L.; Alegranti, C. W. *J. Am. Chem. Soc.* **1972**, *94*, 6386–6391. For a comprehensive review of the use of ^{31}P NMR for structure elucidation of metal complexes, see: "Applications of P–31 NMR to the Study of Metal–

in the same ratios that were observed for the two aforementioned amide proton signals. The measured J_{Ag-P} values, represented in Figure 1.10, are indicative of the structures of the two components: the major species present in solution of bisphosphine **1.40** is, as expected, consistent with a P–Ag–P complex (J_{Ag-P} = 413 and 477 Hz),[44] while the minor component corresponds to a pair of doublets with significantly larger J_{Ag-P} values (662

Figure 1.10 Variable Temperature 162 MHz ^{31}P NMR Study of Ag–Phosphine Complexes **1.39** and **1.40**

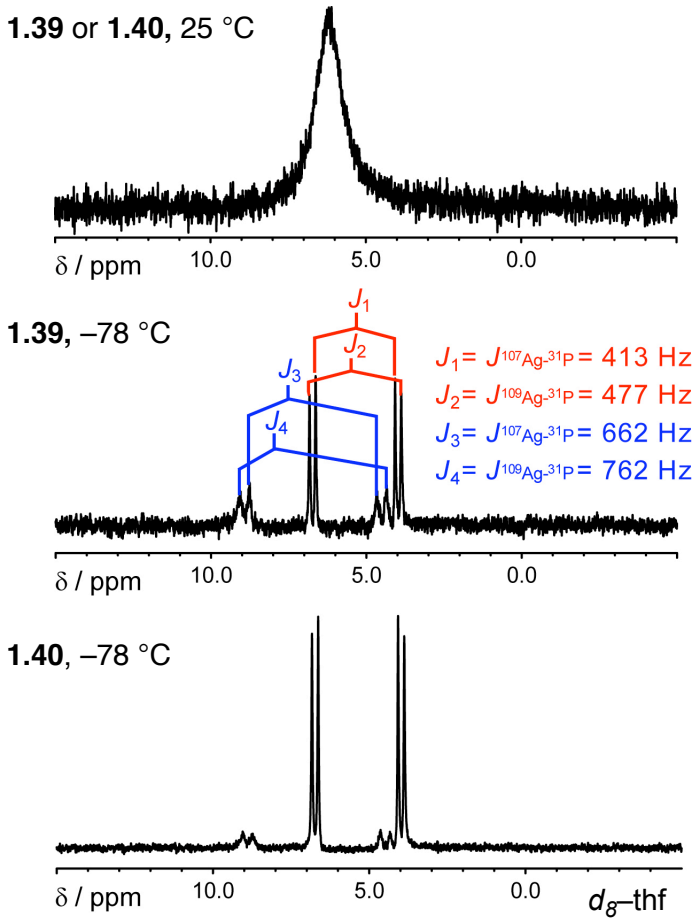

Phosphorous Bonding," Pidcock, A. In *Catalytic Aspects of Metal Phosphine Complexes*, Alyea, E. C.; Meek, D. W., Eds.; American Chemical Society: Washington, DC, **1982**; ACS Symp. Ser. No. 196, 1–21.

[44] Similar J_{Ag-P} values of 498 and 433 Hz are observed for dppf–AgOAc, see: "Mechanism of Silver(I)-Catalyzed Mukaiyama Aldol Reaction: Active Species in Solution in $AgPF_6$–(*S*)-BINAP versus AgOAc–(*S*)-BINAP Systems," Ohkouchi, M.; Masui, D.; Yamaguchi, M.; Yamagishi, T. *J. Mol. Catal. A* **2001**, *170*, 1–16.

and 762 Hz), suggestive of a monophosphine ligated Ag complex such as **1.41**.[45] The presence, of an albeit small concentration, of a 1:1 Ag–phosphine complex in the sample of the pure crystalline bisphosphine signifies the facility of ligand dissociation in solution, such that an equilibrium may be established between the mono- and

Scheme 1.16 Equilibrium Established in Solution of Mono- and Bisphosphine Ag-Complexes **1.41** and **1.40**

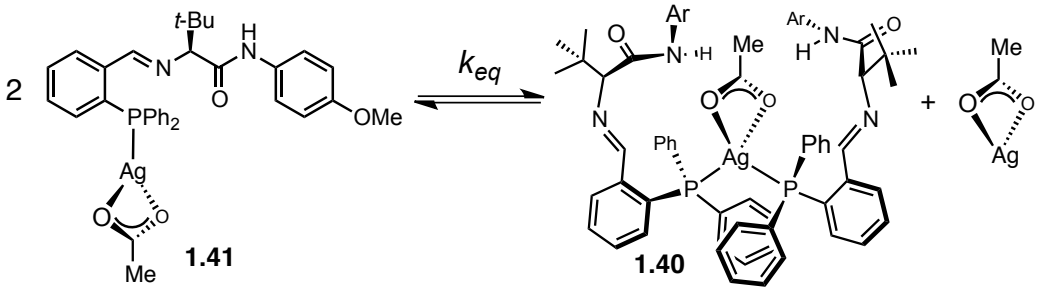

bisphosphines (Scheme 1.16). The more sterically accessible, and hence more active, 1:1 Ag–phosphine species **1.41** is present in much higher concentration in the highly *anti*- and enantioselective pre-complexed catalyst **1.39**,[46] we thus propose that monophosphine **1.41** is the catalytically active species at –78 °C. In reactions with bisphosphine **1.40**, the small percentage of the 1:1 complex fails to prevail, and as such the sluggish bisphosphine promotes a *syn*-selective EVM process.[47]

If the complexation that leads to the catalytically active 1:1 Ag–phosphine

[45] Consistent J_{Ag-P} values of 725 and 635 Hz are observed for a rare two-coordinate monophosphine–AgOAc complex [(*t*-Bu_3P)–AgOAc]. See: "Tri-*tert*-butylphosphine Complexes of Silver (I). Preparation, Characterization, and Spectral Studies," Goel, R. G.; Pilon, P. *Inorg. Chem.* **1978**, *17*, 2876–2879.

[46] When the integrations (by ^{1}H and ^{31}P NMR) are adjusted for the number of proposed chiral phosphines present on the two components, the ratios of **1.41:1.40** is 2:1 (not 1:1) for complex **1.39**, and actually 1:10 (not 1:5) for bisphosphine **1.40**, see discussion of variable temperature ^{1}NMR analysis.

[47] Reactions with lower than 10 mol % of the *in situ* generated 1:1 phosphine:AgOAc complex are less efficient and stereoselective, these results are consistent with the *syn*-selectivity observed with reactions performed with bisphosphine **1.40.** For example, with 3 mol % loading of *in situ* generated catalyst, only 29% conversion is afforded after 15 h of a 1:10 *anti*–**1.33a**:*syn*–**1.34a** with 58:42 e.r., while 5 mol % of bisphosphine **1.40** corresponds to the presence of only ~0.5 mol % of the 1:1 species.

complex **1.41** species is a dynamic process governed by the formula in Scheme 1.16, then addition of silver acetate should shift the equilibrium in favor of the monomeric species. In fact, when the sample of bisphosphine, which exists in solution as a 10:1 ratio in favor of the bisphosphine, is treated with silver acetate,[48] there is a significant adjustment in favor of the monomeric species (almost 2:1 monomer **1.41**: bisphosphine **1.40**; compare spectra of **1.40** and **1.40** + AgOAc in Figure 1.11). Interestingly, addition

Figure 1.11 Amounts of Active Species **1.41** in Various Preparations of the Ag-Based Catalyst Analyzed by ^{1}H NMR Spectroscopy at –78 °C

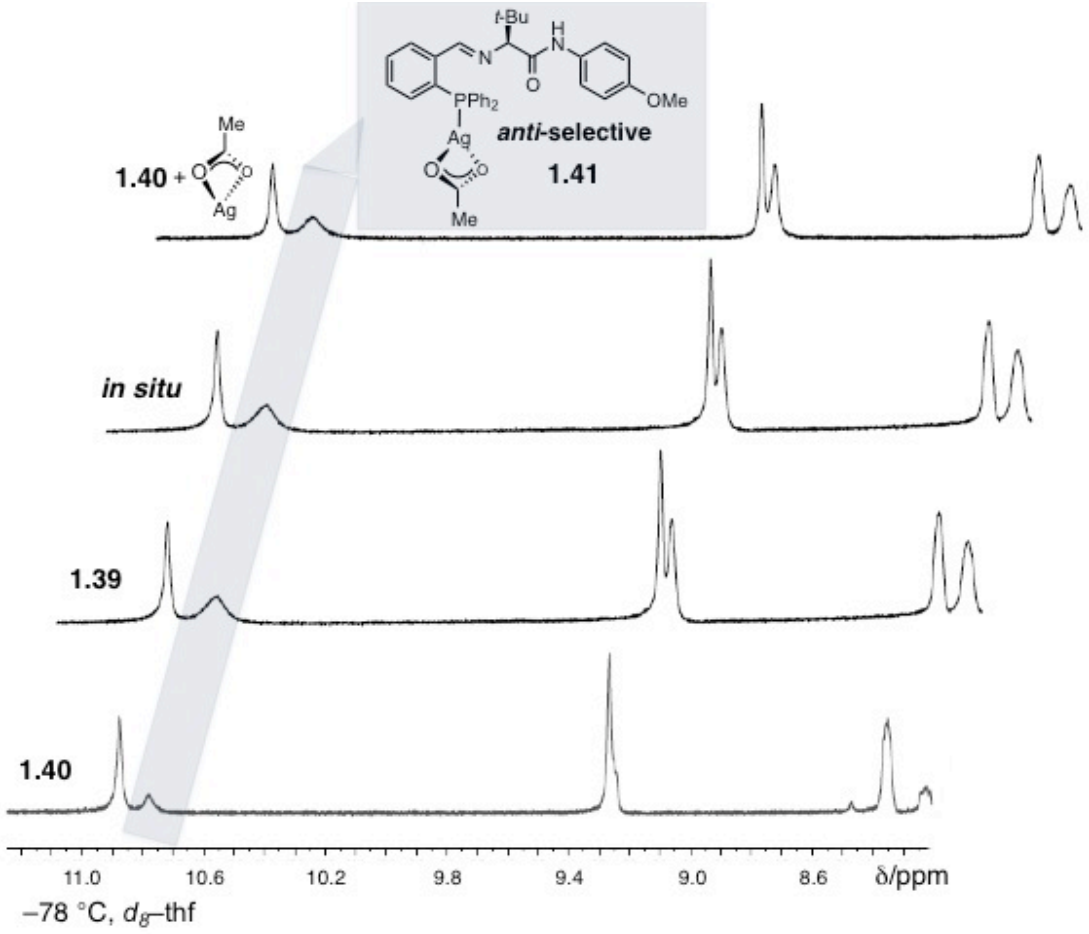

[48] The exact amount of AgOAc added is ambiguous due to the insolubility of the metal salt in the tetrahydrofuran solution at ambient or lower temperatures.

of more silver salt does not alter the equilibrium any further, likely due to the insolubility of the salt in tetrahydrofuran.[49] Both the pre-complexed catalyst **1.39** and the catalyst generated *in situ* (10 mol % **1.21b** and 11 mol % silver acetate) are similarly characterized by this upper limit of a 2:1 ratio of mono to bisphosphine (Figure 1.11).

Based on the spectroscopic evidence of this capacity to shift the equilibrium, equation 3 demonstrates that the high efficiencies, *anti*- and enantioselectivities of the EVM process can be restored with 5 mol% crystalline bisphosphine **1.40** *in the presence of an additional 6 mol % silver acetate* (such that the loading totals 10 mol % **1.21b** and 11 mol % silver acetate). This is particularly striking when noting that 5 mol % bisphosphine **1.40** alone yields *syn*-selective and inefficient transformations (30% conversion, >98% *syn*-selectivity, 78:22 e.r., Scheme 1.14). The observation that the present class of catalytic Mannich transformations proceed with reliably high stereocontrol with the presence of a slight excess of silver acetate (11 mol % to 10 mol % phosphine), is likely due to the higher concentration of the more reactive monomeric species generated in solution at –78 °C.

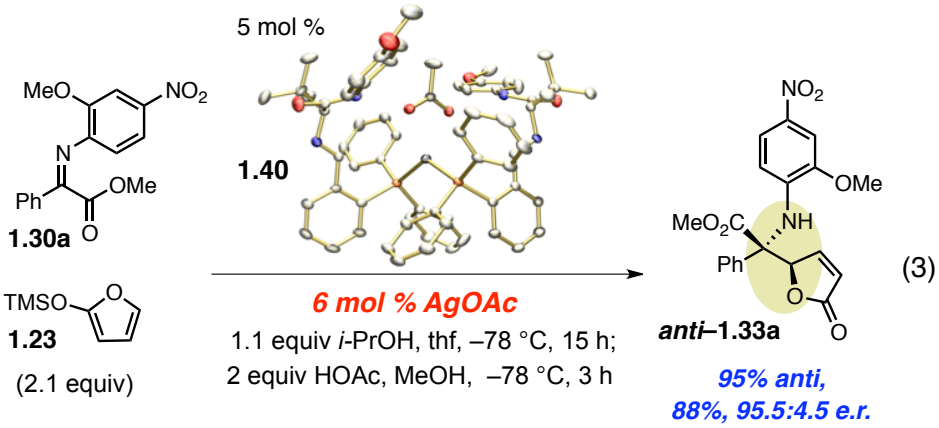

[49] However, addition of enough phosphine **1.21b** will result in complete preference for the bisphosphine **1.40**, with little detection of the monophosphine by spectroscopic analysis at –78 °C.

1.5 Mechanistic Proposal

The proposed mechanism[50] for enantioselective additions of siloxyfuran **1.23** to ketoiminoesters begins with coordination to active Ag (I) cationic species **I** (Figure 1.12). Coordination of the enol silane to the Lewis basic amide results in raising the energy of the HOMO of the vinylogous nucleophile[51]. Concomitant bidentate chelation of the *para*-nitroanisidyl ketoimine to the cationic silver center, such that the larger aryl group can be

Figure 1.12 Proposed Catalytic Cycle for EVM of Ketoiminoesters

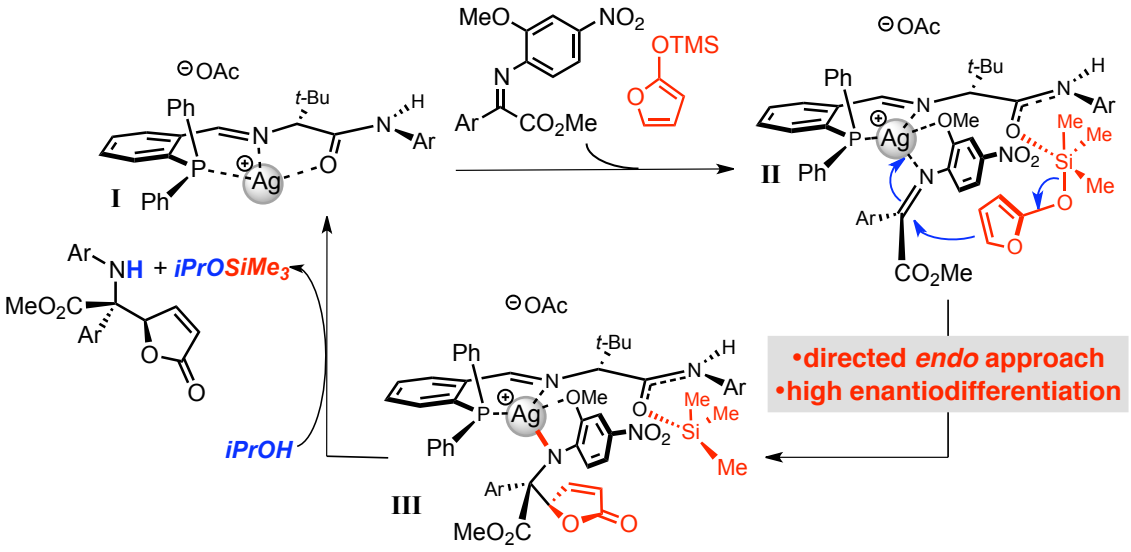

positioned *trans* to the incoming siloxyfuran, leads to activation of the prochiral carbon in transition state **II**. The required presence of an *ortho*-methoxy substituent for high activity and stereoselectivity supports the importance of the bidentate chelation mode for inducing the high degree of organization of catalyst–substrate complex **II**. Directed addition, a product of the bifunctional catalyst, affords *anti*-addition through the *endo*

[50] "Ag-Catalyzed Diastereo- and Enantioselective Vinylogous Mannich Reactions of α-Ketoimine Esters. Development of a Method and Investigation of its Mechanism," Wieland, L. C.; Vieira, E. M.; Snapper, M. L.; Hoveyda, A. H. *J. Am. Chem. Soc.* **2009**, *131*, 570–576.
[51] For a review describing the reactivity of organosilicon compounds at various hypervalent states and their utility in C–C bond-forming processes, see: "Hypervalent Silicon as a Reactive Site in Selective Bond-Forming Processes," Rendler, S.; Oestreich, *Synthesis*, **2005**, *11*, 1727–1747.

approach and high enantiodifferentiation of the prochiral faces of the bound imine.[52] Furthermore, the catalyst-directed reaction results in silylation of the active catalyst and formation of a Ag–N bond in intermediate **III**. A protic additive, isopropanol, is a key ingredient in promoting turnover from silylated **III** to regenerate monophosphine **I**; the product-catalyst complex is released through protonation of the bound-aniline and nucleophilic desilylation of the silylated amide. The critical function of protic sources in catalytic cycles, particularly for the acceleration of typically reluctant product release/catalyst regeneration steps, will be a key theme in forthcoming chapters.

Similar to mechanistic proposals to account for the reversal in diastereoselectivity in related Mannich additions to anisidyl aldimines,[23] *syn*-selective Mannich additions to ketoiminoesters likely proceed through a non-directed *exo* approach, an approach that also suffers from minimal differentiation of the prochiral faces of the Ag-bound imine (Figure 1.13). There are steric limitations induced by tightly organized *endo* approach **III**, such that *exo* catalyst-substrate complex **IV** is preferred when the produced imine or

Figure 1.13 Competing Transition State Model to Account for *Syn*-Selectivity in Certain Mannich Additions

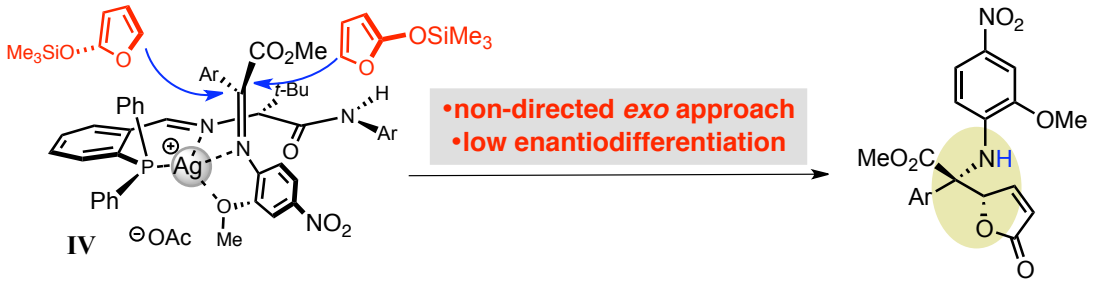

furan binding pockets of **III** are sterically inaccessible. Thus, additions to ketoimines bearing sterically encumbered *ortho*-substituted aryl groups or additions of 4–methyl

[52] Addition through transition state **II**, accounts for the absolute sense of enantioinduction; the stereochemical outcome was confirmed by X-ray crystal structure of reduced aniline **1.36d**.

substituted siloxyfuran preferably undergo EVM reactions through sterically attainable and lower energy *exo* transition state **IV** (see *syn*-selective EVM additions in Figure 1.4). Moderate enantioselectivities (<75:25 e.r.) are obtained in all of the *syn*-selective processes since there is minimal steric differentiation governing the approaches shown in **IV** (i.e., one approach is partially blocked by the triarylphosphine, while the other is hindered by the backbone *tert*-butyl group). Besides the presence of *syn*-selective bisphosphine in solution, which may be more active at higher temperatures, the 1:1 Ag–phosphine complex may also alter its stereochemical preference at higher temperatures, such that an *exo* approach can be favored at temperatures above –78 °C.

1.6 Conclusions

We have developed, for the first time, a catalytic enantioselective Mannich reaction of vinylogous nucleophiles with ketoiminoesters, to set two contiguous stereogenic centers, with high efficiency, site-, diastereo-, and enantioselectivities.[53] The products are members of an important class of *N*-substituted quaternary stereogenic centers and are amenable to provide access to various quaternary amino acids and substituted heterocycles.[53] The silver-catalyzed process involves a commercially available metal salt and nucleophile as well as an easily prepared amino-acid based ligand. The well established lack of activity of ketoimines, a hurdle that has severely limited the

[53] Since the publication of this research, two additional accounts of Cu-catalyzed vinylogous Mannich-type reactions of phosphinoyl ketomines have been reported. Use of the phosphinoyl group as the activator eliminates the requisite for an α-acyloxy group as an imine substituent; ketoimines derived from acetophenone can participate in Mukaiyama-type or direct Mannich additions to afford tertiary carbimines bearing a γ-butenolide moiety. (a) "Cinchona Alkaloid Amide/Copper(II) Catalyzed Diastereo- and Enantioselective Vinylogous Mannich Reactions of Ketimines with Siloxyfurans," Hayashi, M.; Sano, M.; Funahashi, Y.; Nakamura, S. *Angew. Chem., Int. Ed.* **2013**, *52*, 5557–5560. (b) "Direct Catalytic Asymmetric Vinylogous Mannich-Type Reaction of γ-Butenolides with Ketimines," Yin, L.; Takada, H.; Kumagai, N.; Shibasaki, M. *Angew. Chem., Int. Ed.* **2013**, *52*, 7310–7313.

availibility of reactions with this class of electrophile, was overcome employing modifications that led to electronic enhancement of reactivity.

A 1:1 Ag–phosphine complex was found to effectively promote high levels of stereocontrol observed in the EVM. A competing bisphosphine complex that is formed in solution is *syn*-selective, leading to diminution of stereoselectivity in certain cases. Mechanistic studies elucidated the factors, including temperature, catalyst composition, and catalyst concentration, that affect the stereochemical outcome of this class of Mannich additions.

1.7 Experimentals

General. Infrared (IR) spectra are recorded on a Perkin Elmer 781 spectrophotometer, ν_{max} in cm^{-1}. Bands are characterized as broad (br), strong (s), medium (m) or weak (w). ^{1}H NMR spectra are recorded on a Varian Unity INOVA 400 (400 MHz) spectrometer. Chemical shifts are reported in ppm from tetramethylsilane with the solvent resonance resulting from incomplete deuteration as the internal standard ($CDCl_3$: δ 7.26). Data are reported as follows: chemical shift, integration, multiplicity (s = singlet, d = doublet, t = triplet, q = quartet, br = broad, m = multiplet), and coupling constants. ^{13}C NMR spectra are recorded on a Varian Unity INOVA 400 (100 MHz) with complete proton decoupling. Chemical shifts are reported in ppm from tetramethylsilane with the solvent resonance as the internal standard ($CDCl_3$: δ 77.16 ppm). ^{31}P NMR spectra are recorded on a Varian Unity INOVA 400 (162 MHz) with complete proton decoupling. Chemical shifts are reported in ppm referenced using an external standard (H_3PO_4: δ 0.00 ppm). Enantiomeric ratios (e.r.) were determined by analytical liquid chromatography (HPLC) on a Shimadzu chromatograph (Chiral Technologies Chiralpak AS (4.6 x 250 mm),

Chiral Technologies Chiralcel OD (4.6 x 250 mm), Chiral Technologies Chiralcel OJ (4.6 x 250 mm), or Chiral Technologies Chiralpak AD (4.6 x 250 mm)) in comparison with authentic racemic materials. High-resolution mass spectrometry is performed on a Micromass LCT ESI-MS (positive mode) at the Mass Spectrometry Facility (Boston College). Specific rotations were measured on a Rudolph Research Analytical Autopol IV polarimeter.

Unless otherwise stated, all reactions are conducted under an inert atmosphere of nitrogen and carried out with distilled and degassed solvents. Tetrahydrofuran is purified by distillation from sodium benzophenone ketal immediately prior to use. All work-up and purification procedures are carried out with reagent grade solvents in air. All solvents are purchased from Doe and Ingalls. 2-(Trimethylsilyloxy)furan **1.23** and AgOAc were purchased from Aldrich and used as received. α-Ketoesters were purchased from commercial sources or synthesized from commercially available starting materials through known methods.[54] The corresponding ketoimines are synthesized using known methods.[55] EDC•HCl, HOBt•H_2O, trifluroacetic acid, *para*-anisidine, Boc-protected amino acids, and 2-(diphenylphosphino)benzaldehyde are purchased from commercial sources and used without further purification. Phosphino amino-acid based ligands **1.21b** and **1.21c** were prepared as previously reported.[56]

---

[54] (a) "(Cyanomethylene)phosphoranes as Novel Carbonyl 1,1-Dipole Synthons: An Efficient Synthesis of α-Keto Acids, Esters, and Amides," Wasserman, H. H.; Ho, W-B. *J. Org. Chem.* **1994**, *59*, 4364–4366. (b) "A General and Straightforward Approach to α,ω-Ketoesters," Babudri, F.; Fiandanese, V.; Marchese, G.; Punzi, A. *Tetrahedron* **1996**, *52*, 13513–13520. (c) "A Selective Method for the Preparation of Aliphatic Methyl Esters in the Presence of Aromatic Carboxylic Acids," Rodriguez, A.; Nomen, M.; Spur, B. W.; Godfroid, J. J. *Tetrahedron Lett*, **1998**, *39*, 8563–8566. (d) "A Mild, Rapisd, and Convenient Esterification of α-Keto Acids," Domagala, J. M. *Tetrahedron Lett*. **1980**, *21*, 4997–5000.

[55] (a) "Efficient Synthesis of 1-Azadienes Dervied from α-Aminoesters. Regioselective Preparation of α-Dehydroamino Acids, Vinylglycines, and α-Amino Acids," Palacios, F.; Vicario, J.; Aparicio, D. *J. Org. Chem.* **2006**, 71, 7690–7696. (b) "Tandem *N*-Alkylation–*C*-Allylation Reaction of a-Imino Esters with Organoaluminums and Allyltributyltin,"Niwa, Y.; Shimizu, M. *J. Am. Chem. Soc.* **2003**, *125*, 3720–3721.

[56] "A Highly Efficient and Practical Method for Catalytic Asymmetric Vinylogous Mannich (AVM) Reactions," Carswell, E. L.; Snapper, M. L.; Hoveyda, A. H. *Angew. Chem., Int. Ed.* **2006**, *45*, 7230–7233.

■ ***Analytical Data for α-ketoimine substrates* 1.30*:***

Methyl 2-((2-methoxy-4-nitrophenyl)imino)-2-phenylacetate (**1.30a**): 10:1 mixture of *E*/*Z* isomers. mp = 106–107 °C. IR (neat): 3101 (w), 3008 (w), 2945 (w), 2911 (w), 2865 (w, br), 2835 (w), 1729 (s), 1623 (s), 1585 (s), 1514 (s), 1484 (m), 1451 (m), 1409 (m), 1350 (s), 1336 (m), 1303 (s), 1260 (s), 1231 (s), 1181 (m), 1096 (m), 1020 (m), 1007 (m), 797 (m), 687 (m) cm^{-1}. ^{1}H NMR (400 MHz, $CDCl_3$, major isomer): δ 7.90 (2H, d, *J* = 7.3 Hz), 7.85 (1H, dd, *J* = 8.8, 2.2 Hz), 7.77 (1H, d, *J* = 2.2 Hz), 7.55 (1 H, t, *J* = 7.3 Hz), 7.48 (2H, t, *J* = 7.3 Hz), 6.89 (1H, d, *J* = 8.4 Hz), 3.89 (3H, s), 3.66 (3H, s). ^{13}C NMR (100 MHz, $CDCl_3$): δ 164.1, 161.8, 150.1, 145.9, 145.6, 133.3, 132.8, 129.1, 128.8, 119.5, 117.0, 106.7, 56.5, 52.4. HRMS Calcd for $C_{16}H_{15}N_2O_5$ $[M + H]^+$: 315.09810; Found: 315.09849.

Methyl 2-((2-methoxy-4-nitrophenyl)imino)-2-(3-methoxyphenyl)acetate (**1.30b**): 5:1 mixture of *E*/*Z* isomers. mp = 104–105 °C. IR (neat): 3084 (w, br), 3008 (w, br), 2957 (w, br), 2839 (w, br), 1742 (s), 1641 (m), 1585 (m), 1523 (s), 1354 (s), 1320 (m), 1253 (s), 1096 (m), 1028 (m), 796 (m), 670 (m) cm^{-1}. ^{1}H NMR (400 MHz, $CDCl_3$, major isomer): δ 7.86 (1H, dd, *J* = 8.4, 2.0 Hz), 7.77 (1H, d, *J* = 2.0 Hz), 7.51 (1H, s), 7.38 (2 H, d, *J* = 4.8 Hz), 7.13-7.08 (1H, m), 6.90 (1H, d, *J* = 8.4 Hz), 3.91 (3H, s), 3.87 (3H, s), 3.66 (3H, s). ^{13}C NMR (100 MHz, $CDCl_3$): δ 164.0, 161.7, 160.2, 150.1, 145.9, 145.6, 134.6, 130.0, 121.7, 119.5, 119.3, 117.0, 112.8, 106.7, 56.5, 55.7, 52.4. HRMS Calcd for $C_{17}H_{17}N_2O_6$ $[M + H]^+$: 345.10866; Found: 345.10892.

Methyl 2-(3-chlorophenyl)-2-((2-methoxy-4-nitrophenyl)imino)acetate (**1.30c**): 13:1 mixture of *E*/*Z* isomers. mp = 106–108 °C. IR (neat): 3111 (w, br), 3015 (w), 2955 (w),

2843 (w), 1725 (s), 1615 (s), 1579 (s), 1507 (s), 1487 (m), 1450 (m), 1412 (m), 1342 (s), 1318 (s), 1276 (m), 1250 (s), 1223 (s), 1175 (s), 1091 (m), 1024 (s), 938 (m), 866 (m), 830 (m), 794 (m), 714 (m), 682 (m), 665 (m) cm^{-1}. ^{1}H NMR (400 MHz, $CDCl_3$, major isomer): δ 7.94 (1H, s), 7.87 (1H, dd, *J* = 8.4, 2.2 Hz), 7.78 (1H, d, *J* = 2.2 Hz), 7.74 (1 H, d, *J* = 7.7 Hz), 7.53 (1H, d, *J* = 8.4 Hz), 7.42 (1H, t, *J* = 8.4 Hz), 6.89 (1H, d, *J* = 8.4 Hz), 3.91 (3H, s), 3.67 (3H, s). ^{13}C NMR (100 MHz, $CDCl_3$): δ 163.5, 160.4, 150.0, 145.8, 145.4, 135.3, 135.1, 132.7, 130.3, 128.6, 127.1, 119.4, 117.0, 106.7, 56.5, 52.6. HRMS Calcd for $C_{16}H_{14}ClN_2O_5$ $[M + H]^+$: 349.05912; Found: 349.05871.

Methyl 2-(4-chlorophenyl)-2-((2-methoxy-4-nitrophenyl)imino)acetate (**1.30d**): 11:1 mixture of *E*/*Z* isomers. mp = 132–134 °C. IR (neat): 3354 (w), 3091 (w), 3009 (w), 2957 (w), 2835 (w, br), 1734 (s), 1629 (s), 1581 (s), 1507 (s), 1493 (m), 1461 (m), 1405 (m), 1339 (s), 1310 (m), 1253 (m), 1224 (s), 1176 (m), 1090 (s), 1029 (m), 1008 (m), 858 (m), 842 (m), 796 (m), 766 (m), 744 (m), 727 (m), 671 (m) cm^{-1}. ^{1}H NMR (400 MHz, $CDCl_3$, major isomer): δ 7.85–7.77 (4H, m), 7.44 (2H, d, *J* = 8.4 Hz), 6.88 (1 H, d, *J* = 8.4 Hz), 3.89 (3H, s), 3.66 (3H, s). ^{13}C NMR (100 MHz, $CDCl_3$): δ 163.6, 160.6, 149.9, 145.7, 145.6, 132.32, 132.26, 130.2, 127.7, 119.4, 117.0, 106.7, 56.5, 52.5. HRMS Calcd for $C_{16}H_{14}ClN_2O_5$ $[M + H]^+$: 349.05912; Found: 349.05911.

Methyl 2-(4-bromophenyl)-2-((2-methoxy-4-nitrophenyl)imino)acetate (**1.30e**): 10:1 mixture of *E*/*Z* isomers. mp = 154–155 °C. IR (neat): 3352 (w), 3088 (w), 3007 (w), 2971 (w), 2834 (w), 2657 (w, br), 1732 (s), 1626 (s), 1581 (s), 1566 (m), 1505 (s), 1489 (m), 1462 (m), 1400 (m), 1309 (s), 1253 (m), 1224 (s), 1176 (m), 1123 (m), 1091 (m), 1069 (m), 1028 (m), 1005 (m), 859 (m), 687 (m) cm^{-1}. ^{1}H NMR (400 MHz, $CDCl_3$, major

isomer): δ 7.86 (1H, dd, *J* = 8.4, 2.2 Hz), 7.78–7.76 (3H, m), 7.63 (2H, d, *J* = 8.8 Hz), 6.88 (1H, d, *J* = 8.4 Hz), 3.90 (3H, s), 3.66 (3H, s). ^{13}C NMR (100 MHz, $CDCl_3$): δ 163.6, 160.5, 150.0, 145.7, 145.6, 139.1, 131.9, 130.2, 129.3, 119.4, 117.0, 106.7, 56.5, 52.6. HRMS Calcd for $C_{16}H_{14}BrN_2O_5$ $[M + H]^+$: 393.00861; Found: 393.00875.

Methyl 2-(4-iodophenyl)-2-((2-methoxy-4-nitrophenyl)imino)acetate (1.30f): 10:1 mixture of *E*/*Z* isomers. mp = 166–169 °C. IR (neat): 3070 (w), 3004 (w), 2959 (w), 2915 (w), 2833 (w, br), 2655 (w), 1730 (s), 1624 (m), 1579 (m), 1504 (s), 1487 (m), 1462 (m), 1395 (m), 1309 (s), 1251 (m), 1223 (s), 1175 (s), 1123 (m), 1092 (m), 1056 (m), 1026 (m), 1001 (s), 859 (m), 841 (m), 829 (m), 794 (m), 743 (m), 721 (m) cm^{-1}. ^{1}H NMR (400 MHz, $CDCl_3$, major isomer): δ 7.88–7.84 (3H, m), 7.78 (1H, d, *J* = 2.2 Hz), 7.62 (2H, d, *J* = 8.4 Hz), 6.88 (1 H, d, *J* = 8.4 Hz), 3.90 (3H, s), 3.66 (3H, s). ^{13}C NMR (100 MHz, $CDCl_3$): δ 163.6, 160.9, 150.0, 145.7, 145.6, 138.3, 132.9, 130.2, 119.4, 117.0, 106.8, 100.2, 56.5, 52.5. HRMS Calcd for $C_{16}H_{14}IN_2O_5$ $[M + H]^+$: 440.99474; Found: 440.99559.

Methyl 2-(4-(*tert*-butyl)phenyl)-2-((2-methoxy-4-nitrophenyl)imino)acetate (1.30g): 10:1 mixture of *E*/*Z* isomers. mp = 148–151 °C. IR (neat): 3101 (w), 3006 (w, br), 2866 (w), 2835 (w), 1730 (s), 1601 (m), 1578 (m), 1561 (m), 1488 (s), 1410 (m), 1312 (s), 1231 (m), 1191(m), 1173 (m), 1128 (m), 1091 (m), 1022 (m), 1005 (m), 873 (m), 843 (m), 793 (m), 736 (m), 536 (m) cm^{-1}. ^{1}H NMR (400 MHz, $CDCl_3$, major isomer): δ 7.87–7.77 (4H, m), 7.51 (2H, d, *J* = 8.1 Hz), 6.88 (1H, d, *J* = 8.4 Hz), 3.90 (3H, s), 3.66 (3H, s), 1.35 (9H, s). ^{13}C NMR (100 MHz, $CDCl_3$): δ 164.2, 161.6, 156.6, 150.2, 146.2, 145.4,

130.6, 128.7, 126.1, 119.5, 117.0, 106.7, 56.5, 52.3, 35.3, 31.3. HRMS Calcd for $C_{20}H_{23}N_2O_5$ $[M + H]^+$: 371.16070; Found: 371.16194.

Methyl 2-((2-methoxy-4-nitrophenyl)imino)-2-(4-(trifluoromethyl)phenyl)acetate (**1.30h**): 11:1 mixture of *E*/*Z* isomers. mp = 128–130 °C. IR (neat): 3118(w), 3012 (w), 2958 (w), 2839 (w), 2653 (w, br), 2514 (w), 1742 (s), 1641 (s), 1582 (s), 1523 (s), 1489 (m), 1464 (m), 1417 (m), 1328 (s), 1316 (m), 1256 (s), 1223 (s), 1181 (m), 1131 (m), 1067 (m), 1028 (m), 1007 (m), 910 (m), 873 (m), 856 (m), 801 (m), 742 (m) cm^{-1}. ^1H NMR (400 MHz, $CDCl_3$, major isomer): δ 8.02 (2H, d, *J* = 8.4 Hz), 7.86 (1H, dd, *J* = 8.4, 2.0 Hz), 7.78 (1H, d, *J* = 2.0 Hz), 7.73 (2H, d, *J* = 8.4 Hz), 6.90 (1H, d, *J* = 8.4 Hz), 3.90 (3H, s), 3.69 (3H, s). ^{13}C NMR (100 MHz, $CDCl_3$): δ 163.3, 160.4, 149.8, 145.9, 145.3, 136.6, 133.5 (q, *J* = 32.6 Hz), 129.2, 125.9 (q, *J* = 3.8 Hz), 123.9 (q, *J* = 217 Hz), 119.4, 117.0, 106.8, 56.5, 52.6. HRMS Calcd for $C_{17}H_{14}F_3N_2O_5$ $[M + H]^+$: 383.08548; Found: 383.08515.

Methyl 2-((2-methoxy-4-nitrophenyl)imino)-2-(naphthalen-2-yl)acetate (**1.30i**): 20:1 mixture of *E*/*Z* isomers. mp = 128–129 °C. IR (neat): 3109 (w), 3063 (w), 3017 (w), 2953 (w), 2854 (w, br), 2839 (w), 1742 (s), 1619 (s), 1582 (s), 1518 (s), 1493 (m), 1468 (m), 1412 (m), 1350 (s), 1312 (m), 1257 (s), 1223 (m), 1168 (m), 1126 (m), 1096 (m), 1033 (m), 1016 (m), 868 (m), 797 (m), 733 (m) cm^{-1}. ^1H NMR (400 MHz, $CDCl_3$, major isomer): δ 8.25 (1H, s), 8.12 (1H, dd, *J* = 8.6, 1.4 Hz), 7.94–7.87 (4H, m), 7.80 (1H, d, *J* = 2.0 Hz), 7.61–7.53 (2H, m), 6.95 (1H, d, *J* = 8.4 Hz), 3.91 (3H, s), 3.72 (3H, s). ^{13}C NMR (100 MHz, $CDCl_3$): δ 164.2, 161.8, 150.2, 146.1, 145.6, 135.5, 132.9, 130.8, 129.5,

129.1, 128.7, 128.1, 127.2, 124.1, 119.5, 117.0, 106.8, 56.5, 52.5. HRMS Calcd for $C_{20}H_{17}N_2O_5$ $[M + H]^+$: 365.11375; Found: 365.11481.

Methyl 2-(furan-2-yl)-2-((2-methoxy-4-nitrophenyl)imino)acetate (1.30j): 2.5:1 mixture of *E*/*Z* isomers. mp = 98–100 °C. IR (neat): 3147 (w), 3118 (w), 2953 (w), 2835 (w), 1742 (s), 1628 (m), 1518 (s), 1472 (s), 1354 (s), 1337 (s), 1257 (s), 1239 (m), 1096 (m), 1045 (s), 1016 (m), 1155 (m), 805 (m), 762 (m) cm^{-1}. ^1H NMR (400 MHz, $CDCl_3$, mixture of isomers): δ 7.84–7.81 (1 + [0.4]H, m), [7.72 (0.4H, s)], 7.71 (1H, m), 7.65 (1H, s), [7.28 (0.4H, s)], 7.12 (1H, d, *J* = 3.2 Hz), [7.03 (0.4H, d, *J* = 2.2 Hz)], 6.92 (1H, d, *J* = 8.8 Hz), [6.86 (0.4H, d, *J* = 8.4 Hz)], 6.56 (1H, t, *J* = 1.6 Hz), [6.41 (0.4H, s)], [3.97 (1.2H, s)], 3.84 (3H, s), [3.75 (1.2H, s)], 3.65 (3H, s). ^{13}C NMR (100 MHz, $CDCl_3$, mixture of isomers): δ [163.7], 161.8, 150.2, 149.5, 149.2, [148.6], [147.9], 147.5, [146.8], [146.5], [145.9], 145.4, 145.3, [145.1], [120.6], 120.3, 119.3, [118.8], [117.2], 117.1, 112.9, [112.5], 106.6, [106.6], 56.4, [56.4], [53.7], 52.7. HRMS Calcd for $C_{14}H_{13}N_2O_6$ $[M + H]^+$: 305.07736; Found: 305.07696.

Methyl 2-((2-methoxy-4-nitrophenyl)imino)-2-(thiophen-3-yl)acetate (1.30k): 8:1 mixture of *E*/*Z* isomers. mp = 153–154 °C. IR (neat): 3085 (w), 2960 (w), 2916 (w), 2848 (w), 1734 (s), 1617 (s), 1581 (m), 1511 (s), 1486 (m), 1465 (m), 1406 (m), 1345 (s), 1288 (m), 1226 (s), 1170 (s), 1125 (m), 1091 (m), 1023 (s), 860 (m), 803 (m), 731 (m), 687 (m) cm^{-1}. ^1H NMR (400 MHz, $CDCl_3$, major isomer): δ 7.96 (1H, s), 7.86 (1H, dd, *J* = 8.4, 2.2 Hz), 7.77 (1H, d, *J* = 2.2 Hz), 7.69 (1H, d, *J* = 4.8 Hz), 7.42–7.38 (1H, m), 6.90 (1H, d, *J* = 8.8 Hz), 3.89 (3H, s), 3.65 (3H, s). ^{13}C NMR (100 MHz, $CDCl_3$): δ 163.5,

156.0, 149.7, 145.9, 145.4, 137.3, 131.8, 127.1, 127.0, 119.8, 117.1, 106.7, 56.4, 52.5. HRMS Calcd for $C_{14}H_{13}N_2O_5S$ $[M + H]^+$: 321.05452; Found: 321.05540.

Methyl 2-(2-bromophenyl)-2-((2-methoxy-4-nitrophenyl)imino)acetate (**1.30l**): 5:1 mixture of *E*/*Z* isomers. mp = 102–106 °C. IR (neat): 3097 (w), 3012 (w), 2953 (w), 2939 (w), 1738 (s), 1653 (m), 1581 (m), 1518 (s), 1489 (m), 1463 (m), 1409 (m), 1354 (s), 1253 (s), 1215 (m), 1092 (m), 1058 (m), 1025 (m), 915 (m), 860 (m), 810 (m), 742 (m), 645 (m) cm^{-1}. ^1H NMR (400 MHz, $CDCl_3$, major isomer): δ 7.77 (1H, dd, *J* = 8.8, 2.4 Hz), 7.63 (1H, d, *J* = 2.4 Hz), 7.53 (1H, dd, *J* = 8.0, 1.6 Hz), 7.21–7.13 (2H, m), 6.93 (1H, dd, *J* = 7.2, 2.0 Hz), 6.81 (1H, d, *J* = 8.4 Hz), 3.97 (3H, s), 3.84 (3H, s). ^{13}C NMR (100 MHz, $CDCl_3$): δ 163.2, 162.4, (161.5), (161.2), 149.0, (148.3), 145.9, (145.4), 144.1, (137.2), 135.2, (133.3), 132.8, (132.4), (132.0), 131.5, 129.2, (128.0), 127.4, (122.3), 121.4, 119.4, (117.2), 116.8, (106.8), 106.7, (56.5), 56.3, 53.9, (53.0). HRMS Calcd for $C_{16}H_{14}N_2O_5Br$ $[M + H]^+$: 393.00861; Found: 393.01005.

■ ***Representative experimental procedure for gram-scale Ag-catalyzed vinylogous addition of silyl enol ether* 1.23 *to an α-ketoimino ester:*** A flame-dried 100 mL round bottom flask was charged with AgOAc (117 mg, 0.700 mmol), phosphine **1.21b** (320 mg, 0.636 mmol), and **1.30a** (2.00 g, 6.36 mmol). The flask was sealed with a septum and purged with an atmosphere of dry N_2. Freshly distilled tetrahydrofuran was added (64 mL) through a syringe, followed by *iso*-propanol (487 μL, 0.636 mmol), and the resulting homogenous yellow solution was allowed to cool to –78 °C (dry ice/acetone) with stirring. 2-Trimethylsiloxyfuran **1.23** (2.66 mL, 13.4 mmol) was added, and the resulting solution was kept at –78 °C for 15 hours before addition of acetic acid (765 μL, 13.4

mmol) in methanol (10 mL). The resulting solution was allowed to stir at –78 °C for an additional three hours, after which it was allowed to warm to 22 °C. A saturated aqueous solution of $NaHCO_3$ was added, after which the aqueous layer was washed with EtOAc (3 x 100 mL), dried over $MgSO_4$, and the volatiles were removed *in vacuo*. The unpurified residue (typically yellow oil) was obtained as a 20:1 mixture of *anti*–**1.33a**:*syn*–**1.34a** (determined by analysis of the ^{1}H NMR spectra of the crude reaction mixture), which can be separated by silica gel chromatography (3:1 petroleum ether:EtOAc) to furnish pure *anti*–**1.33a** as a yellow solid (2.24 g, 5.62 mmol, 88% yield, 96:4 e.r.), which was recrystallized from methanol to afford *anti*–**1.33a** (yellow crystals) in >99:1 e.r. (1.53 g, 3.84 mmol, 68% yield).

■ ***Analytical Data for the Products of Ag-catalyzed Enantioselective Vinylogous Mannich-type Reactions with α-Ketoiminoesters*** **(***anti*–**1.33a–k)*:***

(*S*)–Methyl 2-((2-methoxy-4-nitrophenyl)amino)-2-((*R*)-5-oxo-2,5-dihydrofuran-2-yl)-2-phenylacetate (*anti*–**1.33a**): IR (neat): 3396 (w, br), 1791 (m), 1766 (s), 1595 (m), 1532 (m), 1501 (m), 1338 (m), 1293 (s), 1256 (m), 1231 (m), 1092 (m), 734 (m) cm^{-1}. ^{1}H NMR (400 MHz, $CDCl_3$): δ 7.62 (1H, d, *J* = 2.4 Hz), 7.52 (1H, ddd, *J* = 6.8, 2.4, 0.4 Hz), 7.50 (1H, dd, *J* = 5.8, 1.6 Hz), 7.46–7.39 (5 H, m), 6.21 (1H, br s), 6.11 (1H, dd, *J* = 2.0, 1.6 Hz), 6.04 (1H, dd, *J* = 5.6, 2.0 Hz), 5.84 (1H, d, *J* = 8.8 Hz), 3.98 (3H, s), 3.80 (3H, s). ^{13}C NMR (100 MHz, $CDCl_3$): δ 171.6, 170.6, 152.4, 146.4, 140.6, 138.7, 133.5, 129.7, 129.6, 127.0, 124.0, 118.1, 111.4, 105.1, 84.7, 68.6, 56.4, 54.1. HRMS Calcd for $C_{20}H_{18}N_2O_7$ [M + H]$^+$: 399.11923; Found: 399.11946. $[\alpha]^{26}_D$ = +165.45 (*c* = 1.00, $CHCl_3$) for a sample with 96:4 e.r.. The enantiomeric purity of this compound was determined by HPLC analysis in comparison with authentic racemic material (Chiralcel OD, 80:20

hexanes:*i*-PrOH, 1.0 mL/min, 254 nm): t_R of *anti*–**1.33a**: 16 min (major) and 24 min (minor); t_R of *syn*–**1.34a**: 19 min and 21 min.

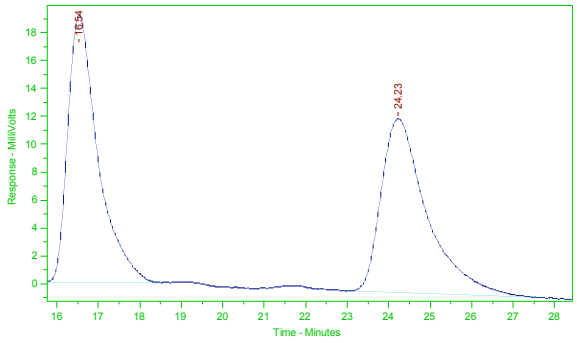

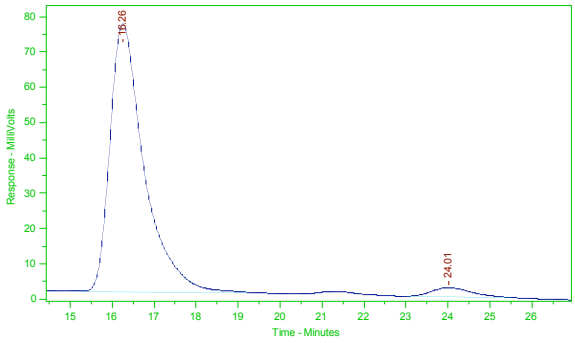

Peak #	Ret. Time	Area	Area %
1	16.5	967379	50.226
2	24.2	958669	49.774

Peak #	Ret. Time	Area	Area %
1	16.3	4274050	96.33
2	24.0	162829	3.67

anti–**1.33a** *after one recrystallization*

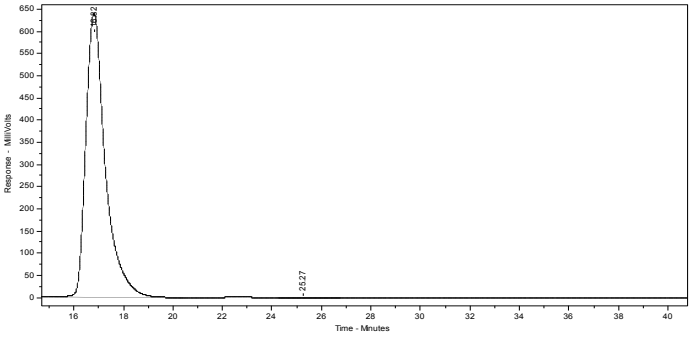

Peak #	Ret. Time	Area	Area %
1	16.8	35044100	99.858
2	25.3	49883	0.142

(*S*)–Methyl 2-((2-methoxy-4-nitrophenyl)amino)-2-((*S*)-5-oxo-2,5-dihydrofuran-2-yl)-2-phenylacetate (*syn*–**1.34a**): IR (neat): 3390 (w, br), 3100 (w, br), 2961 (w, br), 1791 (m), 1766 (s), 1596 (m), 1527 (m), 1501 (m), 1338 (m), 1294 (s), 1262 (m), 1161 (m), 1098 (m), 733 (m) cm^{-1}. ^1H NMR (400 MHz, $CDCl_3$): δ 7.61 (1H, d, J = 2.4 Hz), 7.53–7.50 (2H, m), 7.49 (1H, dd, J = 9.2, 2.4 Hz), 7.41–7.39 (3H, m), 7.30 (1H, dd, J = 6.0, 1.6 Hz), 6.26 (1H, br s), 6.17 (1H, dd, J = 6.0, 2.0 Hz), 6.05 (1H, d, J = 9.2 Hz), 5.93

(1H, dd, J = 1.8, 1.8 Hz), 3.89 (3H, s), 3.77 (3H, s). ^{13}C NMR (100 MHz, $CDCl_3$): δ 171.5, 170.2, 152.4, 146.4, 140.5, 138.8, 134.0, 129.54, 129.49, 127.6, 123.9, 118.3, 112.6, 104.9, 85.9, 69.2, 56.4, 54.0. HRMS Calcd for $C_{20}H_{18}N_2O_7Na$ $[M + Na]^+$: 421.1012; Found: 421.1009. $[\alpha]^{26}_D$ = +35.0 (c = 1.00, $CHCl_3$) for a sample with 87.5:12.5 e.r.. The enantiomeric purity of the compound is determined by chiral HPLC analysis in comparison with authentic racemic material (Chiralcel OD, 80:20 hexanes:*i*-PrOH, 1.0 mL/min, 254 nm): t_R of *syn*–**1.34a**: 19 min (major) and 21 min (minor).

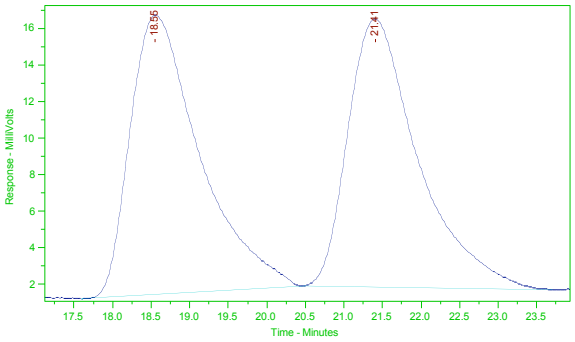

Peak #	Ret. Time	Area	Area %
1	18.6	960705	50.794
2	21.4	930684	49.206

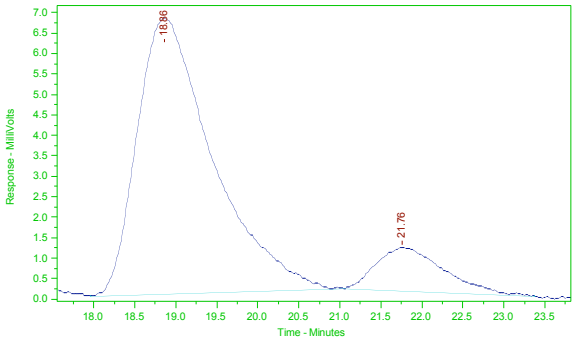

Peak #	Ret. Time	Area	Area %
1	18.9	432036	87.415
2	21.8	62198	12.585

racemic *anti*–**1.33a** and *syn*–**1.34a**

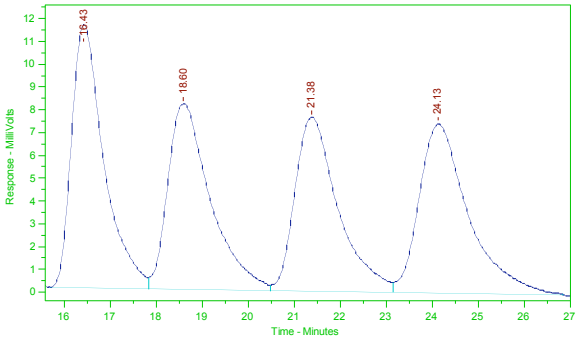

Peak #	Ret. Time	Area	Area %
1	16.4	565621	26.445
2	18.6	525228	24.557
3	21.4	498033	23.285
4	24.1	549947	25.713

(*S*)–Methyl 2-((2-methoxy-4-nitrophenyl)amino)-2-(3-methoxyphenyl)-2-((*R*)-5-oxo-2,5-dihydrofuran-2-yl)acetate (*anti*–**1.33b**)**:** IR (neat): 3389 (w, br), 3096 (w, br), 2954 (w, br), 2835 (w, br), 1795 (m), 1758 (s), 1596 (s), 1521 (s), 1503 (m), 1334 (m), 1303 (s), 1260 (m), 1228 (m), 1153 (w), 1098 (m), 1029 (w), 736 (w), 662 (w) cm^{-1}. ^1H NMR (400 MHz, $CDCl_3$): δ 7.61 (1H, d, *J* = 2.2 Hz), 7.53 (1H, dd, *J* = 8.8, 2.4 Hz), 7.50 (1H, dd, *J* = 5.7, 1.7 Hz), 7.34 (1H, t, *J* = 7.9 Hz), 7.02 (1H, ddd, *J* = 7.7, 1.1, 0.7 Hz), 6.98 (1H, t, *J* = 2.2 Hz), 6.93 (1H, ddd, *J* = 8.3, 2.5, 0.7 Hz), 6.19 (1H, br s), 6.10 (1H, t, *J* = 1.8 Hz), 6.03 (1H, dd, *J* = 5.9, 2.2 Hz), 5.86 (1H, d, *J* = 8.8 Hz), 3.98 (3H, s), 3.80 (3H, s), 3.77 (3H, s). ^{13}C NMR (100 MHz, $CDCl_3$): δ 171.6, 170.5, 160.5, 152.4, 146.4, 140.7, 138.7, 135.2, 130.8, 123.9, 119.0, 118.1, 114.3, 113.5, 111.4, 105.1, 84.7, 68.5, 56.5, 55.6, 54.1. HRMS Calcd for $C_{21}H_{21}N_2O_8$ $[M + H]^+$: 429.1297; Found: 429.1302. $[\alpha]^{23}_D$ = +75.3 (*c* = 1.00, $CHCl_3$) for a sample with 96.5:3.5 e.r.. The enantiomeric purity of the compound was determined by HPLC analysis in comparison with authentic racemic material (Chiracel OD, 80:20 hexanes:*i*-PrOH, 1.0 mL/min, 254 nm): t_R of *anti*–**1.33b**: 19 min (major) and 30 min (minor); t_R of *syn*–**1.34b:** 22 min (major) and 28 min (minor).

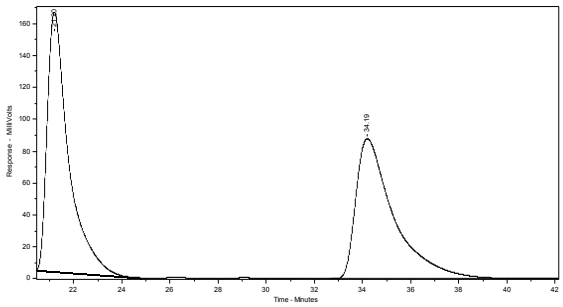

Peak #	Ret. Time	Area	Area %
1	21.2	9968915	50.844
2	34.2	9638127	49.156

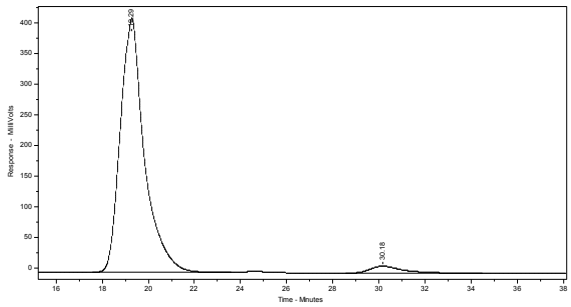

Peak #	Ret. Time	Area	Area %
1	19.3	29958420	96.254
2	30.2	1165924	3.746

(*S*)–Methyl 2-(3-chlorophenyl)-2-((2-methoxy-4-nitrophenyl)amino)-2-((*R*)-5-oxo-2,5-dihydrofuran-2-yl)acetate (*anti*–**1.33c**): IR (neat): 3383 (w, br), 3100 (w, br), 3018 (w, br), 2955 (w, br), 2943 (w, br), 2848 (w, br), 1784 (s), 1759 (s), 1590 (s), 1527 (s), 1507 (m), 1338 (m), 1239 (s), 1256 (m), 1231 (m), 1092 (m), 1029 (w) cm^{-1}. ^{1}H NMR (400 MHz, $CDCl_3$): δ 7.65 (1H, d, *J* = 2.6 Hz), 7.56 (1H, dd, *J* = 9.2, 2.6 Hz), 7.52–7.50 (1H, m), 7.46 (1H, dd, *J* = 5.9, 1.5 Hz), 7.41–7.33 (3H, m), 6.18 (1H, br s), 6.10 (1H, dd, *J* = 5.7, 1.8 Hz), 6.01 (1H, t, *J* = 1.8 Hz), 5.85 (1H, d, *J* = 9.2 Hz), 4.00 (3H, s), 3.80 (3H, s). ^{13}C NMR (100 MHz, $CDCl_3$): δ 171.3, 170.0, 152.0, 146.5, 140.1, 139.0, 135.70, 135.67, 130.8, 129.9, 127.5, 125.5, 124.3, 118.0, 111.4, 105.2, 84.4, 68.3, 56.5, 54.3. HRMS Calcd for $C_{20}H_{17}N_2O_7ClNa$ $[M + Na]^+$: 455.0609; Found: 455.0622. $[\alpha]^{25}_D$ = +106.65 (*c* = 1.00, $CHCl_3$) for a sample with 96:4 e.r.. The enantiomeric purity of the compound was determined by HPLC analysis in comparison with authentic racemic material (Chiralcel OD, 90:10 hexanes:*i*-PrOH, 1.0 mL/min, 254 nm): t_R of *anti*–**1.33c**: 42 min (major) and 80 min (minor); t_R of *syn*–**1.34c**: 46 min (major) and 66 min (minor).

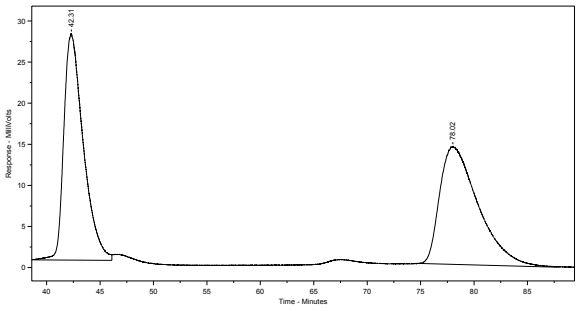

Peak #	Ret. Time	Area	Area %
1	42.3	3496745	49.405
2	78.0	3581021	50.595

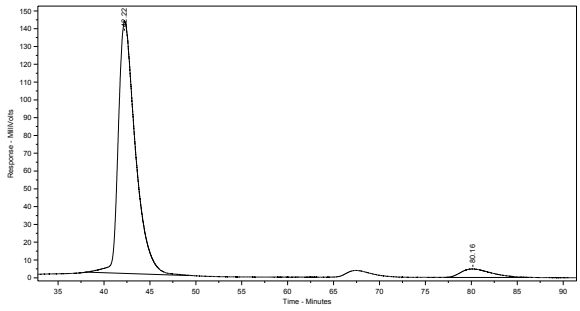

Peak #	Ret. Time	Area	Area %
1	42.2	18325730	94.174
2	80.2	1133718	5.826

(*S*)–Methyl 2-(4-chlorophenyl)-2-((2-methoxy-4-nitrophenyl)amino)-2-((R)-5-oxo-2,5-dihydrofuran-2-yl)acetate (*anti*–**1.33d**): IR (neat): 3381(w, br), 3094 (w, br), 2953

(w, br), 2846 (w, br), 1787 (m), 1754 (m), 1592 (m), 1523 (m), 1493 (m), 1324 (m), 1292 (s), 1228 (m), 1093 (m), 1026 (m), 816 (m), 796 (m), 744 (m) cm^{-1}. ^1H NMR (400 MHz, $CDCl_3$): δ 7.63 (1H, d, *J* = 2.6 Hz), 7.56–7.53 (1H, dd, *J* = 8.8, 2.6 Hz), 7.47–7.45 (1H, dd, *J* = 5.9, 1.5 Hz), 7.43–7.36 (4 H, m), 6.18 (1H, br s), 6.09–6.07 (1H, dd, *J* = 5.9, 1.8 Hz), 6.01 (1H, t, *J* = 1.8 Hz), 5.86 (1H, d, *J* = 8.8 Hz), 3.99 (3H, s), 3.79 (3H, s). ^{13}C NMR (100 MHz, $CDCl_3$): δ 171.6, 170.4, 152.3, 146.7, 140.3, 139.2, 136.0, 132.2, 130.0, 129.0, 124.5, 118.3, 111.7, 105.4, 84.6, 68.5, 56.7, 54.4. HRMS Calcd for $C_{20}H_{18}N_2O_7Cl$ $[M + H]^+$: 433.08025; Found: 433.07983. $[\alpha]^{25}_D$ = +67.6 (*c* = 1.00, $CHCl_3$) for a sample with 98:2 e.r.. The enantiomeric purity of the compound was determined by HPLC analysis in comparison with authentic racemic material (Chiralcel OD, 80:20 hexanes:*i*-PrOH, 1.0 mL/min, 254 nm): t_R of *anti*–**1.33d**: 18 min (major) and 39 min (minor); t_R of *syn*–**1.34d**: 24 min and 28 min.

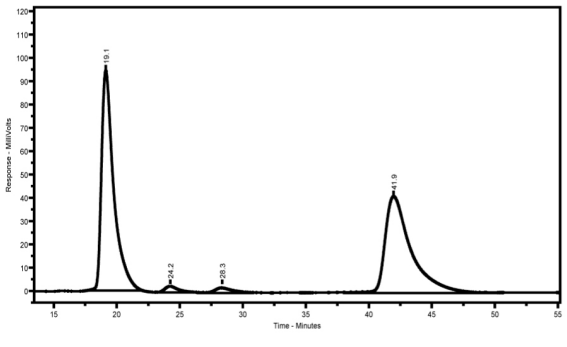

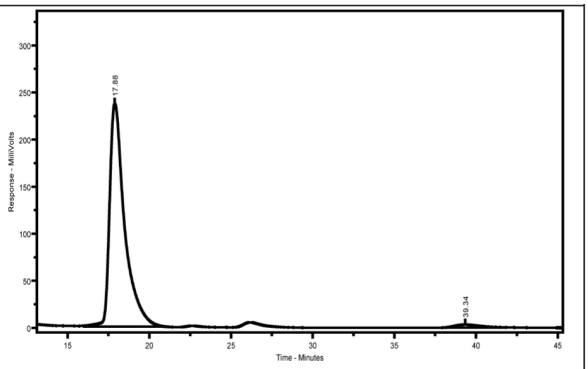

Peak #	Ret. Time	Area	Area %
1	19.1	6256026	50.467
2	24.2	180286	1.07
3	28.3	171191	1.381
4	41.9	578826	46.698

Peak #	Ret. Time	Area	Area %
1	17.88	15232200	97.901
2	39.34	326651	2.099

(*S*)–Methyl 2-(4-bromophenyl)-2-((2-methoxy-4-nitrophenyl)amino)-2-((*R*)-5-oxo-2,5-dihydrofuran-2-yl)acetate (*anti*–**1.33e**): IR (neat): 3386 (w, br), 3094 (w, br), 3019

(w, br), 2926 (w, br), 2846 (w, br), 1791 (m), 1753 (m), 1591 (m), 1523 (m), 1505 (m), 1338 (m), 1288 (s), 1232 (m), 1095 (m), 741 (m) cm^{-1}. ^1H NMR (400 MHz, $CDCl_3$): δ 7.63 (1H, d, *J* = 2.6 Hz), 7.56–7.52 (3H, m), 7.46 (1H, dd, *J* = 5.9, 1.5 Hz), 7.35 (2H, ddd, *J* = 9.2, 2.3, 2.3 Hz), 6.17 (1H, br s), 6.08 (1H, dd, *J* = 5.8, 1.8 Hz), 6.00 (1H, t, *J* = 1.8 Hz), 5.86 (1H, d, *J* = 9.2 Hz), 3.99 (3H, s), 3.79 (3H, s). ^{13}C NMR (100 MHz, $CDCl_3$): δ 171.3, 170.1, 152.1, 146.5, 140.1, 139.0, 132.8, 132.5, 129.0, 124.3, 124.0, 118.1, 111.5, 105.2, 84.3, 68.3, 56.5, 54.2. HRMS Calcd for $C_{20}H_{17}N_2O_7BrNa$ $[M + Na]^+$: 499.0117; Found: 499.0121. $[\alpha]^{26}_D$ = +67.8 (*c* = 1.00, $CHCl_3$) for a sample with 97:3 e.r.. The enantiomeric purity of the compound was determined by HPLC analysis in comparison with authentic racemic material (Chiracel OD, 80:20 hexanes:*i*-PrOH, 1.0 mL/min, 254 nm): t_R of *anti*–**1.33e**: 21 min (major) and 58 min (minor).

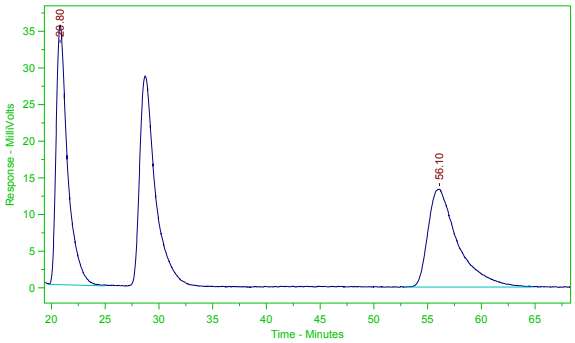

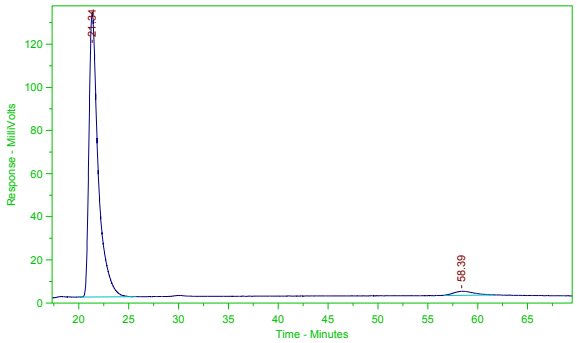

Peak #	Ret. Time	Area	Area %
1	20.8	2641062	50.596
2	56.1	2578827	49.404

Peak #	Ret. Time	Area	Area %
1	21.3	8461288	96.822
2	58.4	277741	3.178

peak at 28 min is racemic syn–**1.34e**

(*S*)-Methyl 2-(4-iodophenyl)-2-((2-methoxy-4-nitrophenyl)amino)-2-((*R*)-5-oxo-2,5-dihydrofuran-2-yl)acetate (*anti*–**1.33f**): IR (neat): 3387 (w, br), 1789 (m), 1758 (s), 1593 (m), 1526 (m), 1295 (s), 1231 (m), 1096 (m), 1028 (m), 746 (m) cm^{-1}. ^1H NMR (400 MHz, $CDCl_3$): δ 7.73 (2H, ddd, *J* = 8.8, 2.2, 2.2 Hz), 7.63 (1H, d, *J* = 2.6 Hz), 7.55

(1H, dd, *J* = 8.8, 2.6 Hz), 7.45 (1H, dd, *J* = 5.8, 1.5 Hz), 7.21 (2H, ddd, *J* = 8.4, 2.2, 2.2 Hz), 6.16 (1H, br s), 6.08 (1H, dd, *J* = 5.9, 2.2 Hz), 6.00 (1H, dd, *J* = 1.8, 1.8 Hz), 5.86 (1H, d, *J* = 8.8 Hz), 3.98 (3H, s), 3.78 (3H, s). ^{13}C NMR (100 MHz, $CDCl_3$): δ 171.3, 170.1, 152.1, 146.5, 140.1, 138.9, 138.7, 133.2, 129.1, 124.3, 118.1, 111.5, 105.2, 95.8, 84.3, 68.4, 56.5, 54.2. HRMS Calcd for $C_{20}H_{18}N_2O_7I$ $[M + H]^+$: 525.01587; Found: 525.01710. $[\alpha]^{24}_D$ = +69.9 (*c* = 1.00, $CHCl_3$) for a sample with 97:3 e.r.. The enantiomeric purity of the compound was determined by HPLC analysis in comparison with authentic racemic material (Chiralcel OD, 80:20 hexanes:*i*-PrOH, 1.0 mL/min, 254 nm): t_R of *anti*–**1.33f**: 26 min (major) and 89 min (minor); t_R of *syn*–**1.34f**: 33 min and 39 min.

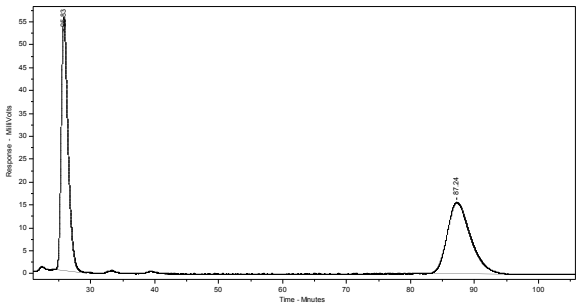

Peak #	Ret. Time	Area	Area %
1	25.8	4071878	50.713
2	87.2	3957386	49.287

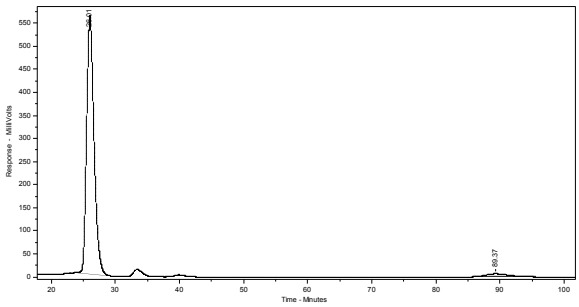

Peak #	Ret. Time	Area	Area %
1	26.0	45087000	96.968
2	89.4	1409877	3.032

(*S*)–Methyl 2-(4-(*tert*-butyl)phenyl)-2-((2-methoxy-4-nitrophenyl)amino)-2-((*R*)-5-oxo-2,5-dihydrofuran-2-yl)acetate (*anti*–**1.33g**): IR (neat): 3387 (w, br), 3099 (w, br), 3019 (w, br), 2961 (w, br), 2870 (w, br), 1788 (m), 1755 (m), 1592 (m), 1526 (m), 1504 (m), 1321 (m), 1292 (s), 1229 (m), 1093 (m), 1026 (m), 817 (m), 797 (m), 744 (s) cm^{-1}. ^{1}H NMR (400 MHz, $CDCl_3$): δ 7.61 (1H, d, *J* = 2.2 Hz), 7.54 (1H, dd, *J* = 8.8, 2.2 Hz), 7.48 (1H, dd, *J* = 5.9, 1.8 Hz), 7.43–7.33 (4 H, m), 6.15 (1H, br s), 6.11 (1H, t, *J* = 1.8

Hz), 6.03 (1H, dd, J = 5.9, 2.2 Hz), 5.86 (1H, d, J = 9.2 Hz), 3.97 (3H, s), 3.79 (3H, s), 1.31 (9H, s). ^{13}C NMR (100 MHz, $CDCl_3$): δ 171.7, 170.8, 152.8, 152.5, 146.4, 140.8, 138.6, 130.4, 126.62, 126.58, 124.0, 118.1, 111.4, 105.1, 84.9, 68.4, 56.5, 54.0, 34.9, 31.4. HRMS Calcd for $C_{24}H_{27}N_2O_7$ $[M + H]^+$: 455.18183; Found: 455.18032. $[\alpha]^{23}_D$ = +90.6 (c = 0.500, $CHCl_3$) for a sample with 95:5 e.r.. The enantiomeric purity of the compound was determined by HPLC analysis in comparison with authentic racemic material (Chiralcel OD, 80:20 hexanes:*i*-PrOH, 1.0 mL/min, 254 nm): t_R of *anti*–**1.33g**: 12 min (major) and 27 min (minor); t_R of *syn*–**1.34g**: 15 min and 17 min.

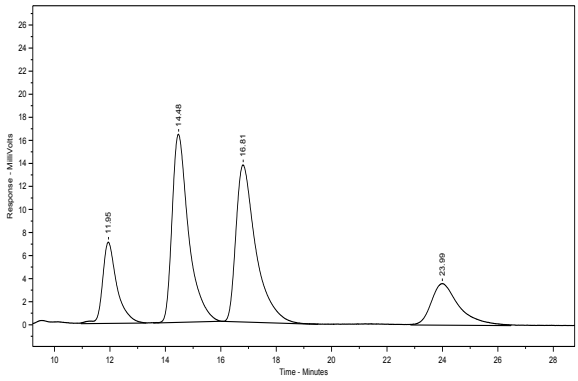

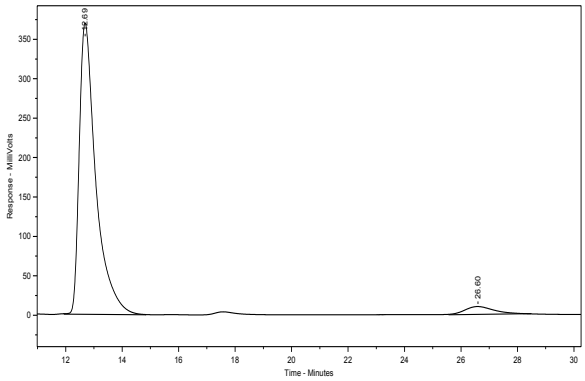

Peak #	Ret. Time	Area	Area %	Peak #	Ret. Time	Area	Area %
1	11.9	253446	13.634	1	12.7	14923210	94.871
2	14.5	674813	36.301	2	26.6	806859	5.129
3	16.8	679463	36.551				
4	24.0	251214	13.514				

(*S*)–Methyl 2-((2-methoxy-4-nitrophenyl)amino)-2-((*R*)-5-oxo-2,5-dihydrofuran-2-yl)-2-(4-(trifluoromethyl)phenyl)acetate (***anti*–1.34h**): IR (neat): 3389 (w, br), 3106 (w, br), 2986 (w, br), 2873 (w, br), 1791 (m), 1759 (m), 1589 (m), 1527 (m), 1508 (m), 1325 (s), 1294 (s), 1256 (m), 1237 (m), 1167 (m), 1130 (m), 1099 (m) cm^{-1}. ^{1}H NMR (400 MHz, $CDCl_3$): δ 7.67–7.63 (5H, m), 7.53 (1H, dd, J = 8.8, 2.4 Hz), 7.46 (1H, dd, J

= 5.8, 1.8 Hz), 6.24 (1H, br s), 6.10 (1H, dd, *J* = 6.0, 2.0 Hz), 6.03 (1H, t, *J* = 1.8 Hz), 5.82 (1H, d, *J* = 9.2 Hz), 4.00 (3H, s), 3.80 (3H, s). ^{13}C NMR (100 MHz, $CDCl_3$): δ 171.2, 169.9, 151.9, 146.5, 139.9, 139.1, 137.6, 131.8 (q, *J* = 33.0 Hz), 128.0, 126.5 (q, *J* = 3.8 Hz), 125.4 (q, *J* = 202 Hz), 124.4, 118.1, 111.3, 105.3, 84.2, 68.5, 56.5, 54.3. HRMS Calcd for $C_{21}H_{17}N_2O_7F_3Na$ $[M + Na]^+$: 489.0886; Found: 489.0882. $[\alpha]^{25}_D$ = +43.5 (*c* = 0.630, $CHCl_3$) for a sample with 95.5:4.5 e.r.. The enantiomeric purity of the compound was determined by HPLC analysis in comparison with authentic racemic material (Chiralcel OD, 80:20 hexanes:*i*-PrOH, 1.0 mL/min, 254 nm): t_R of *anti*–**1.33h**: 15 min (major) and 30 min (minor).

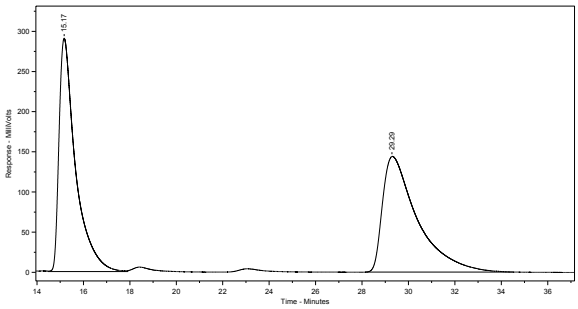

Peak #	Ret. Time	Area	Area %
1	15.2	14290790	48.836
2	29.3	14971950	51.164

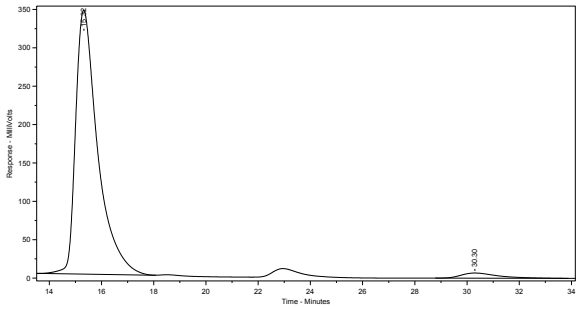

Peak #	Ret. Time	Area	Area %
1	15.3	20258000	96.862
2	30.3	656256	3.138

(*S*)–Methyl 2-((2-methoxy-4-nitrophenyl)amino)-2-(naphthalen-2-yl)-2-((*R*)-5-oxo-2,5-dihydrofuran-2-yl)acetate (*anti*–**1.33i**): IR (neat): 3382 (w, br), 3102 (w, br), 2953 (w, br), 1788 (m), 1759 (s), 1587 (s), 1527 (m), 1331 (m), 1301 (s), 1230 (m), 1093 (m) cm^{-1}. ^{1}H NMR (400 MHz, $CDCl_3$): δ 8.04 (1H, d, *J* = 2.2 Hz), 7.89–7.85 (2H, m), 7.85 (1H, d, *J* = 8.4 Hz), 7.62 (1H, d, *J* = 2.6 Hz), 7.58–7.54 (3H, m), 7.44 (2H, ddd, *J* = 10.4, 6.0, 2.0 Hz), 6.33 (1H, br s), 6.24 (1H, dd, *J* = 1.8, 1.8 Hz), 6.05 (1H, dd, *J* = 5.6, 2.0 Hz), 5.85 (1H, d, *J* = 8.8 Hz), 4.01 (3H, s), 3.80 (3H, s). ^{13}C NMR (100 MHz, $CDCl_3$):

δ 171.6, 170.6, 152.3, 146.5, 140.7, 138.7, 133.5, 133.4, 131.2, 129.7, 128.7, 128.0, 127.7, 127.3, 126.7, 124.1, 124.0, 118.1, 111.5, 105.1, 84.9, 68.8, 56.5, 54.2. HRMS Calcd for $C_{24}H_{20}N_2O_7Na$ $[M + Na]^+$: 471.1168; Found: 471.1164. $[\alpha]^{26}_D$ = +114.7 (*c* = 1.00, $CHCl_3$) for a sample with 95:5 e.r.. The enantiomeric purity of the compound is determined by HPLC analysis in comparison with authentic racemic material (Chiralcel OD, 80:20 hexanes:*i*-PrOH, 1.0 mL/min, 254 nm): t_R of *anti*–**1.33i**: 39 min (major) and 183 min (minor); t_R of *syn*–**1.34i**: 52 min and 64 min.

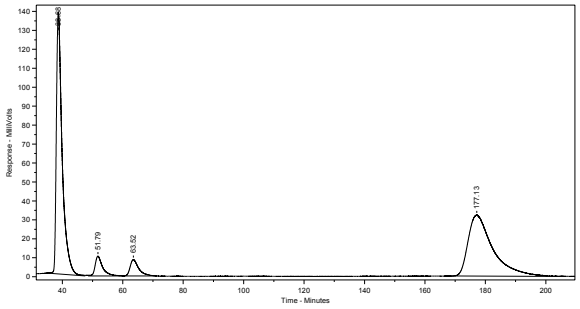

Peak #	Ret. Time	Area	Area %
1	38.7	18403890	45.821
2	51.8	1812002	4.511
3	63.5	1719289	4.281
4	177.1	18229490	45.387

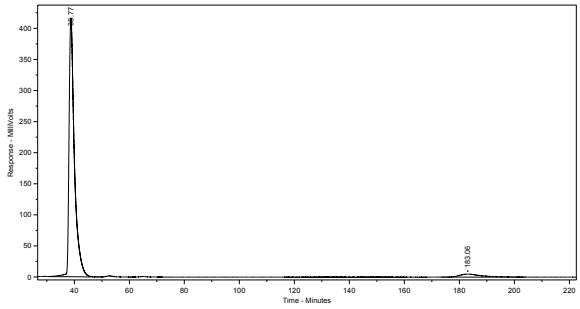

Peak #	Ret. Time	Area	Area %
1	38.8	56347020	95.269
2	183.1	2798026	4.731

(*R*)–Methyl 2-(furan-2-yl)-2-((2-methoxy-4-nitrophenyl)amino)-2-((*R*)-5-oxo-2,5-dihydrofuran-2-yl)acetate (***anti*–1.33j**): IR (neat): 3392 (w, br), 3101 (w), 2949 (w), 1793 (m), 1759 (m), 1594 (s), 1527 (m), 1502 (m), 1337 (m), 1294 (s), 1257 (m), 1159 (m), 1105 (m), 1025 (m), 910 (m), 881 (m), 797 (m), 750 (m) cm^{-1}. ^1H NMR (400 MHz, $CDCl_3$): δ 7.63–7.60 (2H, m), 7.58 (1H, dd, *J* = 6.0, 1.6 Hz), 7.45 (1H, dd, *J* = 2.0, 0.80 Hz), 6.58 (1H, dd, *J* = 3.2, 0.40 Hz), 6.46 (1H, dd, *J* = 3.2, 2.0 Hz), 6.13 (1H, br s), 6.11 (1H, dd, *J* = 5.6, 2.0 Hz), 5.96 (1H, dd, *J* = 1.8, 1.8 Hz), 5.89 (1H, d, *J* = 9.6 Hz), 3.96 (3H, s), 3.85 (3H, s). ^{13}C NMR (100 MHz, $CDCl_3$): δ 171.5, 168.8, 152.2, 146.8, 146.5,

143.7, 140.6, 139.0, 124.0, 118.4, 111.6, 111.0, 109.8, 105.1, 84.2, 65.1, 56.5, 54.4. HRMS Calcd for $C_{18}H_{16}N_2O_8Na$ $[M + Na]^+$: 411.0804; Found: 411.0797. $[\alpha]^{24}_D$ = +139.98 (*c* = 0.230, $CHCl_3$) for a sample with 93:7 e.r.. The enantiomeric purity of the compound was determined by HPLC analysis in comparison with authentic racemic material (Chiralcel OD, 80:20 hexanes:*i*-PrOH, 1.0 mL/min, 254 nm): t_R of *anti*–**1.33j**: 17 min (major) and 24 min (minor).

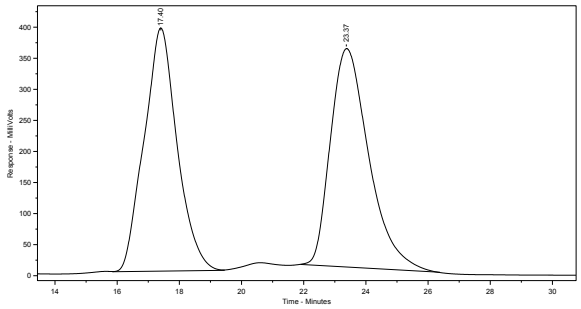

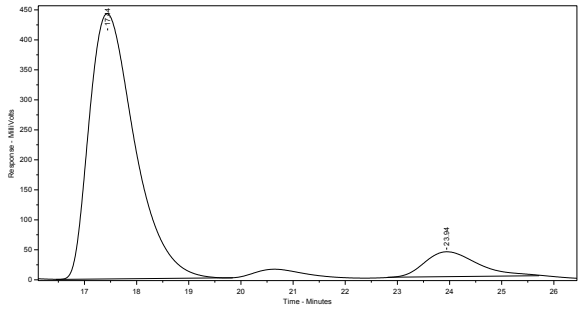

Peak #	Ret. Time	Area	Area %
1	17.4	28905790	48.901
2	23.4	30205150	51.099

Peak #	Ret. Time	Area	Area %
1	17.4	26744090	90.121
2	23.9	2931802	9.879

peak at 21 min is racemic syn–**1.33j**

(*S*)–Methyl 2-((2-methoxy-4-nitrophenyl)amino)-2-((*R*)-5-oxo-2,5-dihydrofuran-2-yl)-2-(thiophen-3-yl)acetate (*anti*–**1.33k**): IR (neat): 3384(w, br), 3104 (w, br), 2926 (w), 2852 (w), 1789 (m), 1732 (s), 1592 (s), 1525 (m), 1505 (m), 1323 (m), 1292 (s), 1229 (s), 1155 (m), 1095 (m), 1043 (m), 1026 (m), 890 (m), 798 (m), 745 (m) cm^{-1}. ^1H NMR (400 MHz, $CDCl_3$, major isomer): δ 7.63 (1H, d, *J* = 2.2 Hz), 7.58 (1H, m), 7.54 (1H, dd, *J* = 2.9, 1.5 Hz), 7.44 (1 H, dd, *J* = 5.9, 1.5 Hz), 7.35 (1H, dd, *J* = 5.1, 2.9 Hz), 7.04 (1H, dd, *J* = 5.1, 1.5 Hz), 6.13 (1H, dd, *J* = 5.8, 2.2 Hz), 6.03 (1H, s), 5.95 (1H, d, *J* = 8.8 Hz), 5.88 (1H, t, *J* = 2.2 Hz), 3.97 (3H, s), 3.80 (3H, s). ^{13}C NMR (100 MHz, $CDCl_3$): δ 171.4, 170.2, 152.2, 146.3, 140.6, 138.9, 134.6, 127.4, 126.8, 124.8, 124.0,

118.1, 111.0, 105.1, 85.0, 66.4, 56.4, 54.0. HRMS Calcd for $C_{18}H_{17}N_2O_7S$ $[M + H]^+$: 405.07565; Found: 405.07530. $[\alpha]^{23}_D$ = +107.9 (*c* = 1.00, $CHCl_3$) for a sample with 96:4 e.r.. The enantiomeric purity of the compound is determined by HPLC analysis in comparison with authentic racemic material (Chiralcel OD, 80:20 hexanes:*i*-PrOH, 1.0 mL/min, 254 nm): t_R of *anti*–**1.33k**: 18 min (major) and 29 min (minor); t_R of *syn*–**1.34k**: 24 and 26 min.

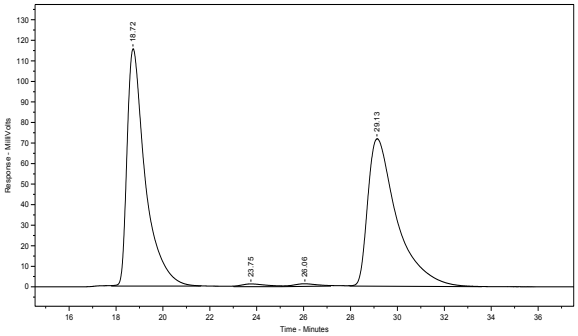

Peak #	Ret. Time	Area	Area %
1	18.7	6209680	49.379
2	23.7	99198	0.789
3	26.1	94179	0.749
4	29.1	6172575	49.084

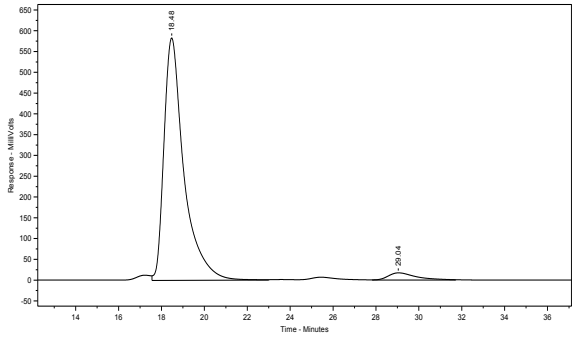

Peak #	Ret. Time	Area	Area %
1	18.5	37587020	96.053
2	29.0	1544582	3.947

(*S*)–Methyl 2-(2-bromophenyl)-2-((2-methoxy-4-nitrophenyl)amino)-2-((*S*)-5-oxo-2,5-dihydrofuran-2-yl)acetate (*syn*–**1.34l**): IR (neat): 3365 (w, br), 3083 (w), 2953 (w), 2833 (w), 1787 (m), 1760 (m), 1744 (m), 1592 (m), 1526 (m), 1503 (m), 1476 (m), 1439 (m), 1333 (m), 1292 (s), 1257 (m), 1228 (m), 1197 (m), 1159 (m), 1100 (m), 1029 (m), 889 (m), 823 (m), 800 (m), 746 (m) cm^{-1}. ^1H NMR (400 MHz, $CDCl_3$): δ 8.03 (1H, dd, *J* = 8.4, 1.6 Hz), 7.56 (1H, d, *J* = 2.8 Hz), 7.52–7.41 (3H, m), 7.34 (1H, dd, *J* = 6.0, 1.6 Hz), 7.25 (1H, dt, *J* = 7.6, 1.6 Hz), 6.44 (1H, br s), 6.29 (1H, dd, *J* = 4.0, 1.6 Hz), 6.18 (1H, d, *J* = 9.2 Hz), 6.11 (1H, t, *J* =1.6 Hz), 3.94 (3H, s), 3.86 (3H, s). ^{13}C NMR (100 MHz, $CDCl_3$): δ 171.0, 170.5, 151.9, 146.6, 140.2, 138.7, 135.2, 134.4, 131.7, 130.7,

128.0, 124.7, 123.0, 118.2, 111.5, 104.9, 84.4, 70.3, 56.4, 54.6. HRMS Calcd for $C_{20}H_{18}N_2O_7Br$ $[M + H]^+$: 477.0219; Found: 411.0793. $[\alpha]^{24}_D = -25.11$ (c = 1.00, $CHCl_3$) for a sample with 66:34 e.r.. The enantiomeric purity of the compound is determined by by HPLC analysis in comparison with authentic racemic material (Chiralcel OD, 90:10 hexanes:*i*-PrOH, 0.7 mL/min, 254 nm): t_R of *syn*–**1.34l**: 69 min (major) and 78 min (minor).

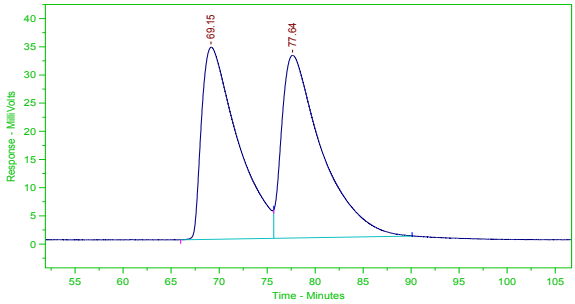

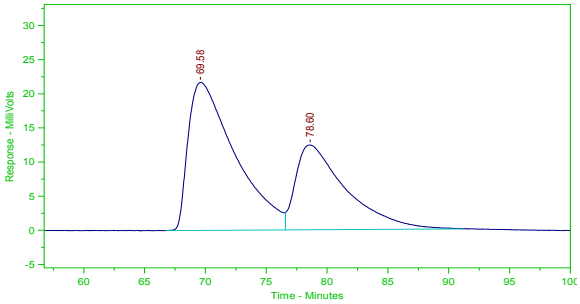

Peak #	Ret. Time	Area	Area %
1	69.1	8933499	48.769
2	77.6	9384385	51.231

Peak #	Ret. Time	Area	Area %
1	69.6	5831568	62.215
2	78.6	3541722	37.785

■ ***Experimental procedure for $SnCl_2$-mediated reduction of*** *anti*–**1.33a** ***followed by PhI(OAc)$_2$-mediated deprotection*****:** A 50 mL round bottom flask was charged with EVM product *anti*–**1.33a** (200 mg, 0.502 mmol), $SnCl_2$ (476 mg, 2.51 mmol), and ethanol (10.0 mL). The round bottom flask was fitted with a reflux condensor, and the mixture was allowed to warm to 65 °C with stirring. The resulting homogeneous solution was kept at 65 °C for 15 hours before careful addition of a saturated aqueous solution of $NaHCO_3$. The aqueous layer was washed with EtOAc (3 x 50 mL). The organic layers were combined, dried over $MgSO_4$, and the volatiles were removed *in vacuo*. The residue was redissolved in EtOAc and the solution was passed through a plug of SiO_2

(EtOAc). The volatiles were again removed *in vacuo*, and the resulting brown oil residue was analyzed by ^{1}H NMR spectroscopy. The residue was dissolved in MeCN (5.00 mL). The resulting homogeneous solution was allowed to cool to 0 °C with stirring. $PhI(OAc)_2$ (322 mg, 1.00 mmol) was added as a solid, and the homogeneous mixture was kept at 0 °C for 30 min before addition of 1M aqueous solution of H_2SO_4 (10.0 equiv, 5.00 mL). The aqueous layer was washed with dichloromethane (3 x 5 mL). The organic layers were combined and set aside. The aqueous layer was basified (pH = 10) by dropwise addition of a saturated aqueous solution of Na_2CO_3, and was subsequently washed with dichloromethane (6 x 5 mL). The organic layers were combined, dried over $MgSO_4$, and the volatiles were removed *in vacuo*. The dark brown oil was purified by silica gel chromatography (2:1 petroleum ether:EtOAc) to deliver **1.37** as an off-white oil (100 mg, 0.404 mmol, 81% yield over two steps).

(*S*)–Methyl 2-amino-2-((*R*)-5-oxo-2,5-dihydrofuran-2-yl)-2-phenylacetate (**1.37**): IR (neat): 3384 (w), 3321 (w), 2953 (w), 2924 (w), 1784 (m), 1759 (s), 1734 (m), 1601 (m), 1489 (m), 145 (s), 1434 (m), 1244 (m), 1144 (m), 1096 (m), 1050 (m), 1024 (m), 890 (m), 834 (m), 704 (m) cm^{-1}. ^{1}H NMR (400 MHz, $CDCl_3$): δ 7.61–7.59 (2H, m), 7.44–7.36 (3H, m), 6.97 (1H, dd, *J* = 5.8, 1.4 Hz), 6.14 (1H, dd, *J* = 6.0, 2.0 Hz), 5.89 (1H, dd, *J* = 2.0, 1.6 Hz), 3.82 (3H, s), 1.89 (2H, br s). ^{13}C NMR (100 MHz, $CDCl_3$): δ 173.2, 172.8, 153.4, 137.1, 129.3, 129.2, 125.7, 123.5 86.7, 65.2, 53.6. HRMS Calcd for $C_{13}H_{14}NO_4$ [M + H]$^+$: 248.09228; Found: 248.09293. $[\alpha]^{26}_D$ = +94.5 (*c* = 0.733, $CDCl_3$) for a sample with >99:1 e.r..

***Experimental procedure for $SnCl_2$-mediated reduction of anti–*1.33a:** A 100 mL round bottom flask was charged with *anti*–**1.33a** (398 mg, 1.00 mmol), $SnCl_2$ (1.14 g, 6.00

mmol), and ethanol (20.0 mL). The round bottom flask was fitted with a reflux condensor, and the mixture was allowed to warm to 65 °C with stirring. The resulting homogeneous solution was kept at 65 °C for 15 hours before careful addition of a saturated aqueous solution of $NaHCO_3$. The aqueous layer was washed with EtOAc (3 x 100 mL). The organic layers were combined, dried over $MgSO_4$, and the volatiles were removed *in vacuo*. The dark brown oil residue was purified by silica gel chromatography (1:1 petroleum ether:EtOAc) to afford **1.36a** as an off-white solid (285 mg, 0.771 mmol, 77% yield).

(*S*)–Methyl 2-((4-amino-2-methoxyphenyl)amino)-2-((*R*)-5-oxo-2,5-dihydrofuran-2-yl)-2-phenylacetate (**1.36a**): IR (neat): 3445 (w), 3356 (w), 2951 (w), 1785 (w), 1735 (s), 1616 (m), 1592 (m), 1512 (s), 1458 (m), 1429 (m), 1283 (m), 1238 (s), 1199 (s), 1166 (m), 1095 (m), 1061 (m), 1031 (m), 1004 (m), 948 (m), 906 (m), 836 (m), 826 (m), 795 (m), 725 (s), 696 (s), 612 (m) cm^{-1}. ^1H NMR (400 MHz, $CDCl_3$): δ 7.50 (2H, dd, *J* = 8.0, 1.5 Hz), 7.46 (1H, dd, *J* = 5.8, 1.5 Hz), 7.36–7.29 (3H, m), 6.19 (1H, d, *J* = 2.2 Hz), 5.98 (1H, d, *J* = 4.8 Hz), 5.96 (1H, d, *J* = 1.8 Hz), 5.90 (1H, dd, *J* = 8.4, 2.6 Hz), 5.83 (1H, dd, *J* = 5.9, 2.2 Hz), 5.10 (1H, br s), 3.76 (3H, s), 3.69 (3H, s), 3.37 (2H, br s). ^{13}C NMR (100 MHz, $CDCl_3$): δ 172.6, 172.2, 154.1, 150.1, 140.2, 136.5, 128.9, 128.8, 127.6, 126.2, 122.3, 117.4, 106.8, 99.8, 84.5, 69.9, 55.8, 53.4. HRMS Calcd for $C_{20}H_{21}N_2O_5$ [M + H]$^+$: 369.14505; Found: 369.14474. $[\alpha]^{25}_D$ = +76.25 (*c* = 1.00, $CHCl_3$) for a sample with >99:1 e.r..

(*S*)–Methyl 2-((4-amino-2-methoxyphenyl)amino)-2-(4-chlorophenyl)-2-((*R*)-5-oxo-2,5-dihydrofuran-2-yl)acetate (**1.36d**): IR (neat): 3444 (w, br), 3363 (w, br), 3098 (w, br), 3010 (w, br), 2850 (w, br), 2846 (w, br), 1763 (m), 1737 (m), 1515 (m), 1523 (m),

1463 (m), 1250 (s), 1201 (m), 1090 (m), 1026 (m), 947 (m), 892 (m), 821 (m) cm^{-1}. ^1H NMR (400 MHz, $CDCl_3$): δ 7.54–7.50 (2H, m), 7.45 (1H, dd, *J* = 5.9, 1.8 Hz), 7.35–7.32 (2 H, m), 6.23 (1H, d, *J* = 2.2 Hz), 6.01–5.94 (3H, m), 5.90 (1H, t, *J* = 1.8 Hz), 5.10 (1H, br s), 3.82 (3H, s), 3.72 (3H, s), 3.38 (2H, br s). ^{13}C NMR (100 MHz, $CDCl_3$): δ 172.2, 171.5, 153.6, 150.0, 140.1, 135.0, 134.6, 129.3, 128.9, 125.6, 122.7, 117.5, 106.8, 99.6, 84.2, 69.3, 55.7, 53.4. HRMS Calcd for $C_{20}H_{20}N_2O_5Cl$ $[M + H]^+$: 403.10607; Found: 403.10422. $[\alpha]^{23}_D$ = +41.8 (*c* = 0.500, $CHCl_3$) for a sample with >99:1 e.r.. The enantiomeric purity of the compound was determined by HPLC analysis in comparison with authentic racemic material (Chiralcel OJ, 70:30 hexanes:*i*-PrOH, 1.0 mL/min, 254 nm): t_R of **1.36d**: 40.0 min (major) and 79.9 min (minor).

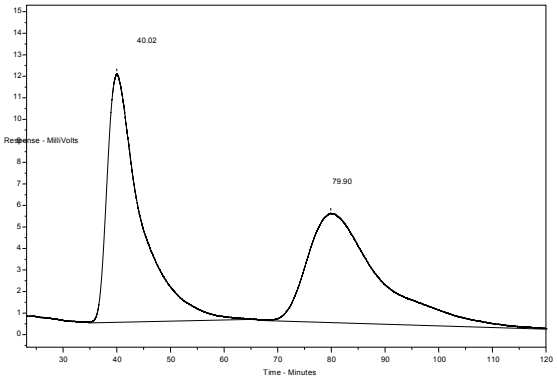

Peak #	Ret. Time	Area	Area %
1	40.0	4940318	51.877
2	79.9	4582752	48.123

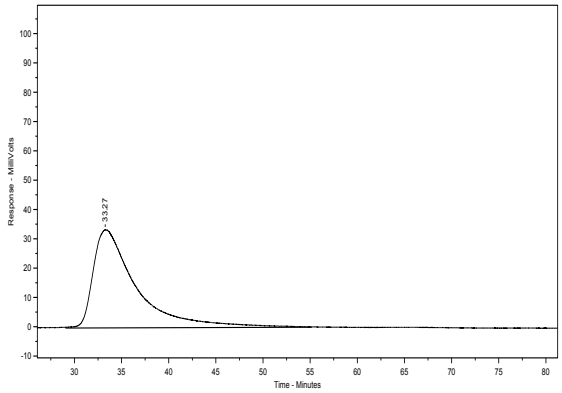

Peak #	Ret. Time	Area	Area %
1	40.1	12910630	100.000

***Experimental procedure for PhI(OAc)$_2$ mediated deprotection of aniline* 1.36a:** A 13x100 mm test tube was charged with aniline **1.36a** (36.8 mg, 0.100 mmol) and acetonitrile (1.00 mL). The resulting homogeneous solution was allowed to cool to 0 °C with stirring. $PhI(OAc)_2$ (64.4 mg, 0.200 mmol) was added as a solid, and the resulting homogeneous solution was kept at 0 °C for 30 min before addition of 1M aqueous

solution of H_2SO_4 (10.0 equiv, 1.00 mL). The aqueous layer was washed with dichloromethane (3 x 2 mL). The organic layers were combined and set aside. The aqueous layer was basified (pH = 10) by dropwise addition of a saturated aqueous solution of Na_2CO_3, and was subsequently washed with dichloromethane (6 x 2 mL). The organic layers were combined, dried over $MgSO_4$, and the volatiles were removed *in vacuo*. The resulting brown oil residue was purified by silica gel chromatography (2:1 petroleum ether:EtOAc) to furnish **1.37** as an off-white oil (21.0 mg, 0.0849 mmol, 85% yield).

***Experimental procedure for synthesis of Ag-based bisphosphine complex* 1.40:** A 50 mL round bottom flask was charged with phosphine **1.21b** (203 mg, 0.400 mmol), AgOAc (66.8 mg, 0.400 mmol), and tetrahydrofuran (5.0 mL). The mixture was allowed to stir at 22 °C for 5 min, and was then filtered through a pad of Celite® into a vial. Petroleum ether was added dropwise to the resulting homogeneous solution until the solution became slightly cloudy. At this point, tetrahydrofuran was added dropwise until the solution was again clear, and the vial was sealed and stored in the dark for 12 hours. The resulting colorless crystals of complex **1.40** were isolated through filtration (193 mg, 0.153 mmol, 77% yield). mp = 128–132 °C. IR (neat): 3249 (w), 3057 (w), 2954 (m), 2865 (w), 1687 (m), 1627 (w), 1545 (m), 1508 (s), 1479 (m), 1460 (m), 1436 (m), 1409 (m), 1292 (m), 1236 (s), 1160 (s), 1097 (m), 1068 (m), 1031 (m), 826 (s), 798 (m), 756 (s) 690 (s), 505 (s) cm^{-1}. ^1H NMR (400 MHz, $CDCl_3$): δ 10.03 (1H, br s), 9.12 (1H, br s), 8.20 (1H, d, *J* = 6.0 Hz), 7.59–7.47 (5H, m), 7.42–7.20 (7H, m), 7.14 (2H, t, *J* = 7.6 Hz), 6.89 (1H, t, *J* = 7.6 Hz), 6.79 (2H, ddd, *J* = 9.2, 3.2, 2.2 Hz), 3.79 (1H, br s), 3.69 (3H, s), 2.08 (1.5H, s, *AgOAc*), 0.73 (9H, s). ^{13}C NMR (100 MHz, $CDCl_3$): δ 187.7, 178.0,

167.9, 160.3, 160.2, 155.7, 138.8, 138.7, 135.0, 134.8, 134.3, 134.1, 133.3, 132.8, 132.5, 132.2, 131.0, 130.7, 130.5, 130.4, 130.3, 129.6, 129.3, 129.2, 129.16, 129.1, 120.7, 113.4, 82.5, 54.7, 34.9, 26.3. HRMS Calcd for 1:2 Ag–phosphine complex **1.40**: $C_{64}H_{66}AgN_4O_4P_2$ $[M - OAc]^+$: 1123.3610; Found: 1123.3625. $[\alpha]^{23}_D$ = –54.3 (*c* = 1.00, $CHCl_3$).

Experimental procedure for synthesis of pre-complexed Ag–phosphine catalyst **1.39**: A 50 mL round bottom flask was charged with phosphine **1.21b** (200 mg, 0.393 mmol), AgOAc (65.6 mg, 0.393 mmol), and tetrahydrofuran (5.0 mL). The mixture was allowed to stir at 22 °C for 5 min, and was subsequently filtered through a pad of Celite®. Volatiles were removed *in vacuo* to yield 258.5 mg of a white powder. mp = 148-153 °C. IR (neat): 3119 (w), 2951 (w), 2833 (w), 1648 (w), 1545 (m), 1509 (s), 1478 (m), 1462 (m), 1435 (m), 1400 (m), 1362 (m), 1234 (s), 1163 (m), 1095 (m), 1032 (m), 828 (m), 744 (m), 693 (s), 658 (s), 484 (s) cm^{-1}. ^1H NMR (400 MHz, $CDCl_3$): δ 10.14 (1H, br s), 9.17 (1H, br s), 8.18 (1H, d, *J* = 6.4 Hz), 7.57–7.55 (3H, m), 7.50 (2H, dd, *J* = 7.4, 3.6 Hz), 7,41–7.27 (7H, m), 7.19 (2H, t, *J* = 6.6 Hz), 6.86 (1H, t, *J* = 8.2 Hz), 6.72 (2H, d, *J* = 8.8 Hz), 3.93 (1H, br s), 3.69 (3H, s), 2.03 (2H, s, *AgOAc*), 0.72 (9H, s). ^{13}C NMR (100 MHz, $CDCl_3$): δ 178.0, 168.0, 160.3, 160.1, 155.7, 138.7, 138.67, 135.1, 134.9, 134.4, 134.2, 133.3, 132.9, 132.4, 132.45, 132.2, 131.8, 130.9, 130.8, 130.6, 130.5, 129.8, 129.4, 129.3, 129.15, 120.8, 113.4, 82.3, 54.7, 34.9, 26.4, 23.0. HRMS Calcd for 1:1 Ag–phosphine complex: $C_{32}H_{33}AgN_2O_2P$ $[M - OAc]^+$: 615.1331; Found: 615.1327. $[\alpha]^{23}_D$ = –69.25 (*c* = 1.00, $CHCl_3$).

***X-ray crystal structure of* 1.36d:**

Please note that the absolute and relative stereochemistry of the major product enantiomers formed in the enantioselective vinylogous Mannich reactions are inferred from that obtained through the X-ray crystal structure of aniline-containing Mannich base **1.36d** described below:

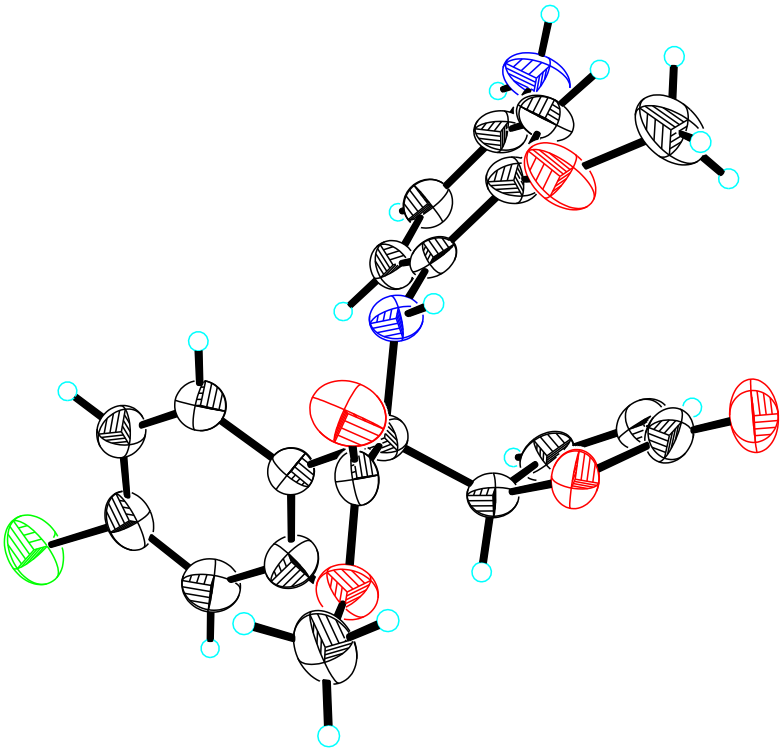

Table 1. Crystal data and structure refinement for **1.36d**

Identification code	emv01	
Empirical formula	$C_{20}H_{19}ClN_2O_5$	
Formula weight	402.82	
Temperature	193(2) K	
Wavelength	0.71073 Å	
Crystal system	Orthorhombic	
Space group	P2(1)2(1)2(1)	
Unit cell dimensions	a = 8.8375(16) Å	a= 90°.

	b = 11.630(2) Å	b= 90°.
	c = 18.584(3) Å	g = 90°.
Volume	1910.2(6) $Å^3$	
Z	4	
Density (calculated)	1.401 mg/m^3	
Absorption coefficient	0.235 mm^{-1}	
F(000)	840	
Crystal size	0.1 x 0.1 x 0.05 mm^3	
Theta range for data collection	2.07 to 28.31°.	
Index ranges	-11<=h<=10, -11<=k<=15, -24<=l<=18	
Reflections collected	14569	
Independent reflections	4754 [R(int) = 0.0728]	
Completeness to theta = 28.31°	100.0 %	
Absorption correction	Empirical	
Max. and min. transmission	none and none	
Refinement method	Full-matrix least-squares on F^2	
Data / restraints / parameters	4754 / 0 / 329	
Goodness-of-fit on F^2	0.995	
Final R indices [I>2sigma(I)]	R1 = 0.0615, wR2 = 0.1043	
R indices (all data)	R1 = 0.1139, wR2 = 0.1226	
Absolute structure parameter	0.05(9)	
Largest diff. peak and hole	0.247 and -0.171 $e.Å^{-3}$	

Table 2. Atomic coordinates (x 10^4) and equivalent isotropic displacement parameters ($Å^2$x 10^3). U(eq) is defined as one third of the trace of the orthogonalized U^{ij} tensor

	x	y	z	U(eq)
Cl(1)	-66(1)	2810(1)	119(1)	70(1)
O(2)	6754(2)	5252(2)	2680(1)	41(1)

O(5)	3296(3)	5135(2)	2927(1)	46(1)
O(4)	3827(3)	6925(2)	2592(1)	56(1)
C(9)	5920(4)	4578(3)	2162(2)	38(1)
N(2)	5285(3)	6322(2)	1433(1)	36(1)
C(15)	3491(3)	4680(3)	1411(2)	33(1)
C(8)	4672(3)	5354(3)	1836(2)	33(1)
O(3)	9175(3)	5670(3)	2898(2)	65(1)
C(13)	3873(3)	5914(3)	2491(2)	35(1)
C(10)	7112(4)	4125(3)	1672(2)	42(1)
C(12)	8272(4)	5191(3)	2528(2)	46(1)
C(3)	6020(4)	5485(3)	255(2)	38(1)
C(20)	2579(4)	5263(3)	916(2)	42(1)
C(4)	6281(3)	6185(3)	841(2)	33(1)
O(1)	7816(3)	7506(2)	1442(1)	63(1)
C(6)	8558(5)	6842(3)	255(2)	50(1)
C(17)	2152(4)	2940(3)	1109(2)	50(1)
C(1)	8281(4)	6123(3)	-332(2)	43(1)
C(16)	3237(4)	3522(3)	1500(2)	45(1)
C(18)	1313(4)	3529(3)	618(2)	46(1)
C(5)	7588(4)	6862(3)	831(2)	42(1)
C(19)	1511(4)	4688(4)	516(2)	44(1)
C(14)	2593(5)	5574(5)	3577(2)	57(1)
C(11)	8438(4)	4475(3)	1895(2)	48(1)
C(2)	7014(4)	5451(3)	-320(2)	40(1)
N(1)	9333(4)	6057(4)	-887(2)	64(1)
C(7)	9313(6)	7873(5)	1603(3)	73(2)

***X-Ray crystal structure of bisphosphine Ag complex* 1.40:**

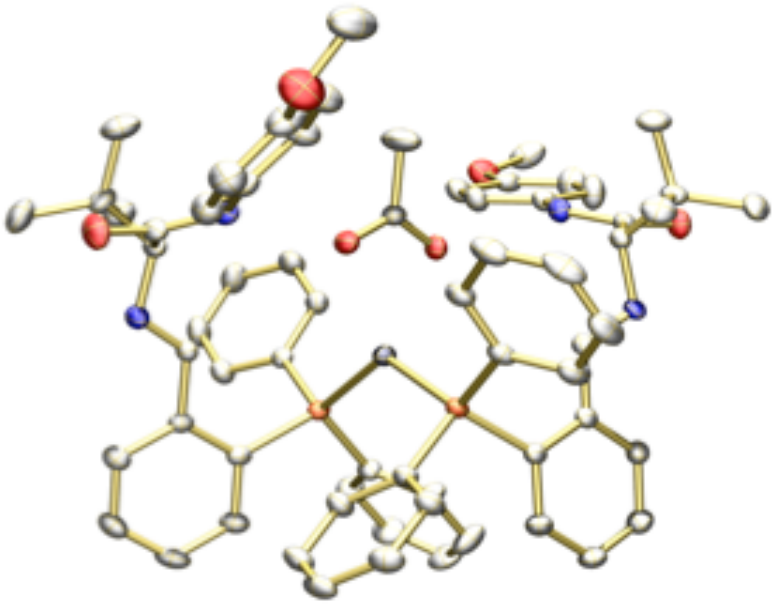

Table 1. Crystal data and structure refinement for AgOAc–**1.21b** complex **1.40**.

Identification code	bc106	
Empirical formula	$C_{70}H_{79}AgN_4O_7P_2$	
Formula weight	1258.18	
Temperature	193(2) K	
Wavelength	0.71073 Å	
Crystal system	Orthorhombic	
Space group	P2(1)2(1)2(1)	
Unit cell dimensions	a = 17.451(4) Å	a= 90°.
	b = 17.675(5) Å	b= 90°.
	c = 21.505(6) Å	g = 90°.
Volume	6633(3) $Å^3$	
Z	4	
Density (calculated)	1.260 Mg/m^3	
Absorption coefficient	0.406 mm^{-1}	
F(000)	2640	

Crystal size	0.12 x 0.10 x 0.10 mm^3
Theta range for data collection	1.49 to 25.00°.
Index ranges	-14<=h<=20, -18<=k<=21, -25<=l<=25
Reflections collected	42921
Independent reflections	11670 [R(int) = 0.0218]
Completeness to theta = 25.00°	100.0 %
Absorption correction	Empirical
Max. and min. transmission	0.9605 and 0.9528
Refinement method	Full-matrix least-squares on F^2
Data / restraints / parameters	11670 / 2 / 740
Goodness-of-fit on F^2	1.029
Final R indices [I>2sigma(I)]	R1 = 0.0316, wR2 = 0.0861
R indices (all data)	R1 = 0.0352, wR2 = 0.0895
Absolute structure parameter	-0.024(14)
Largest diff. peak and hole	0.936 and -0.350 e.$Å^{-3}$

Table 2. Atomic coordinates (x 10^4) and equivalent isotropic displacement parameters ($Å^2$x 10^3). U(eq) is defined as one third of the trace of the orthogonalized U^{ij} tensor

	x	y	z	U(eq)
Ag(1)	2286(1)	3664(1)	502(1)	32(1)
P(1)	1851(1)	2422(1)	838(1)	30(1)
P(2)	2558(1)	4084(1)	-551(1)	30(1)
O(1)	1963(1)	4614(1)	1264(1)	41(1)
O(2)	3193(1)	4342(1)	1256(1)	39(1)
O(3)	5525(1)	3198(1)	2099(1)	49(1)
O(4)	6799(2)	6206(2)	619(1)	66(1)
O(5)	-586(1)	5670(2)	933(1)	60(1)
O(6)	-1202(2)	4128(2)	3532(2)	80(1)

N(1)	4078(1)	2416(1)	1734(1)	33(1)
N(2)	4783(2)	4140(1)	1702(1)	39(1)
N(3)	574(1)	5452(2)	-70(1)	41(1)
N(4)	393(1)	5097(2)	1447(1)	40(1)
C(1)	2630(2)	4683(2)	1479(1)	37(1)
C(2)	2762(3)	5181(3)	2039(2)	86(2)
C(3)	2605(2)	1741(2)	655(1)	35(1)
C(4)	3338(2)	1822(2)	921(1)	34(1)
C(5)	3934(2)	1351(2)	725(1)	43(1)
C(6)	3812(2)	810(2)	270(2)	58(1)
C(7)	3098(2)	724(2)	17(2)	57(1)
C(8)	2495(2)	1187(2)	202(2)	47(1)
C(9)	3489(2)	2412(2)	1387(1)	31(1)
C(10)	4143(2)	3060(2)	2154(1)	33(1)
C(11)	4899(2)	3467(2)	1991(1)	35(1)
C(12)	4086(2)	2829(2)	2846(1)	39(1)
C(13)	3281(2)	2521(2)	2948(2)	55(1)
C(14)	4667(2)	2243(2)	3041(2)	52(1)
C(15)	4188(2)	3557(2)	3228(2)	59(1)
C(16)	5341(2)	4630(2)	1444(1)	40(1)
C(17)	5081(2)	5220(2)	1083(2)	46(1)
C(18)	5581(2)	5726(2)	813(2)	52(1)
C(19)	6355(2)	5658(2)	909(2)	47(1)
C(20)	6624(2)	5082(2)	1251(2)	63(1)
C(21)	6127(2)	4556(2)	1527(2)	64(1)
C(22)	7586(2)	6248(2)	773(2)	70(1)
C(23)	1603(2)	2256(2)	1649(1)	36(1)
C(24)	1721(2)	1563(2)	1931(2)	49(1)
C(25)	1472(2)	1456(2)	2542(2)	62(1)
C(26)	1120(2)	2025(3)	2858(2)	64(1)
C(27)	1000(2)	2714(3)	2579(2)	61(1)

C(28)	1254(2)	2836(2)	1977(2)	44(1)
C(29)	1020(2)	2075(2)	420(1)	35(1)
C(30)	842(2)	2404(2)	-152(1)	43(1)
C(31)	230(2)	2143(2)	-497(2)	53(1)
C(32)	-218(2)	1565(2)	-273(2)	49(1)
C(33)	-47(2)	1236(2)	284(2)	49(1)
C(34)	564(2)	1486(2)	638(2)	44(1)
C(35)	1692(2)	4137(2)	-1031(1)	32(1)
C(36)	1083(2)	4614(2)	-856(1)	31(1)
C(37)	441(2)	4671(2)	-1243(1)	40(1)
C(38)	390(2)	4236(2)	-1773(2)	46(1)
C(39)	964(2)	3732(2)	-1922(2)	50(1)
C(40)	1619(2)	3691(2)	-1559(1)	42(1)
C(41)	1113(2)	5043(2)	-268(1)	31(1)
C(42)	708(2)	5810(2)	530(2)	39(1)
C(43)	99(2)	5519(2)	982(2)	41(1)
C(44)	735(2)	6683(2)	478(2)	50(1)
C(45)	818(3)	7007(2)	1131(2)	70(1)
C(46)	37(3)	6998(2)	144(2)	73(1)
C(47)	1459(2)	6893(2)	110(2)	61(1)
C(48)	-9(2)	4836(2)	1977(2)	41(1)
C(49)	355(2)	4830(2)	2539(2)	56(1)
C(50)	-15(3)	4601(2)	3080(2)	63(1)
C(51)	-770(2)	4362(2)	3040(2)	57(1)
C(52)	-1130(2)	4344(2)	2470(2)	61(1)
C(53)	-764(2)	4585(2)	1945(2)	54(1)
C(54)	-902(4)	4230(3)	4120(2)	87(2)
C(55)	3205(2)	3482(2)	-996(1)	39(1)
C(56)	3590(2)	3728(2)	-1516(2)	50(1)
C(57)	4075(2)	3246(2)	-1839(2)	62(1)
C(58)	4165(3)	2522(2)	-1649(2)	68(1)

C(59)	3800(3)	2269(2)	-1129(2)	71(1)
C(60)	3310(2)	2742(2)	-800(2)	54(1)
C(61)	2956(2)	5042(2)	-623(1)	31(1)
C(62)	2806(2)	5503(2)	-1125(2)	43(1)
C(63)	3113(2)	6221(2)	-1153(2)	55(1)
C(64)	3570(2)	6478(2)	-673(2)	59(1)
C(65)	3718(2)	6031(2)	-172(2)	53(1)
C(66)	3411(2)	5306(2)	-146(2)	40(1)
O(1S)	6925(8)	3438(7)	3279(7)	314(6)
C(1S)	6727(6)	4760(5)	3235(4)	159(3)
C(2S)	6705(7)	4140(6)	3731(5)	198(5)
C(3S)	6820(9)	2876(8)	3890(6)	245(6)
C(4S)	6947(10)	2135(9)	3497(8)	299(8)

Table 3. Selected bond lengths [Å] and angles [°]

Ag(1)-O(1)	2.413(2)	Ag(1)-P(2)	2.4306(9)
Ag(1)-P(1)	2.4328(9)	Ag(1)-O(2)	2.562(2)
P(1)-C(29)	1.813(3)	P(1)-C(23)	1.820(3)
P(1)-C(3)	1.826(3)	P(2)-C(55)	1.824(3)
P(2)-C(35)	1.831(3)	P(2)-C(61)	1.836(3)

O(1)-Ag(1)-P(2)	117.79(6)	O(1)-Ag(1)-P(1)	110.69(6)
P(2)-Ag(1)-P(1)	127.81(2)	O(1)-Ag(1)-O(2)	52.37(7)
P(2)-Ag(1)-O(2)	109.06(5)	P(1)-Ag(1)-O(2)	115.26(5)
C(23)-P(1)-C(3)	105.75(13)	C(29)-P(1)-Ag(1)	114.08(10)
C(23)-P(1)-Ag(1)	120.28(10)	C(3)-P(1)-Ag(1)	107.81(10)
C(35)-P(2)-C(61)	102.55(12)	C(55)-P(2)-Ag(1)	115.58(10)
C(35)-P(2)-Ag(1)	112.35(9)	C(61)-P(2)-Ag(1)	115.72(9)
C(1)-O(1)-Ag(1)	95.73(17)	C(1)-O(2)-Ag(1)	88.98(17)

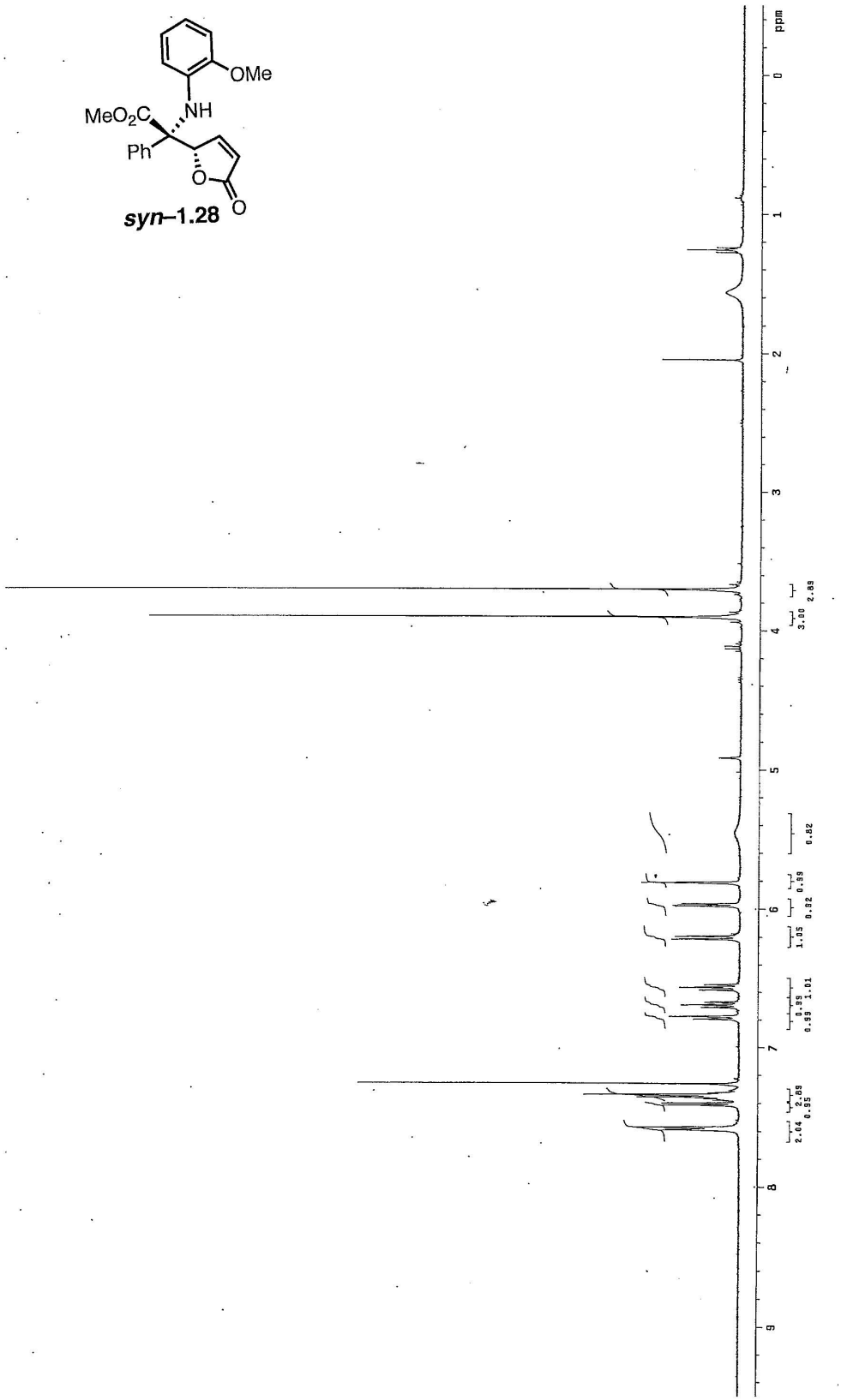
OMe
NH
MeO2C
Ph
O
O
syn–1.28
ppm
0
1
2
3
4
5
6
7
8
9
3.00
2.89
0.82
0.99
0.82
1.05
0.99
1.01
2.04
2.89
0.95

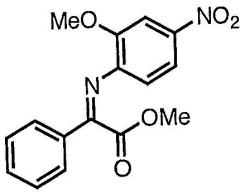

1.30a

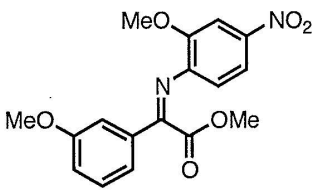

1.30b

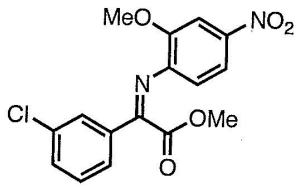

1.30c

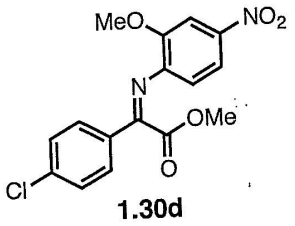

1.30d

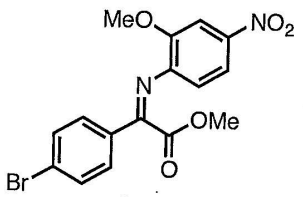

1.30e

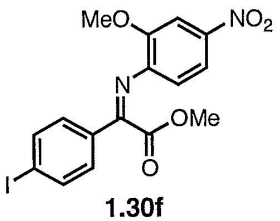

1.30f

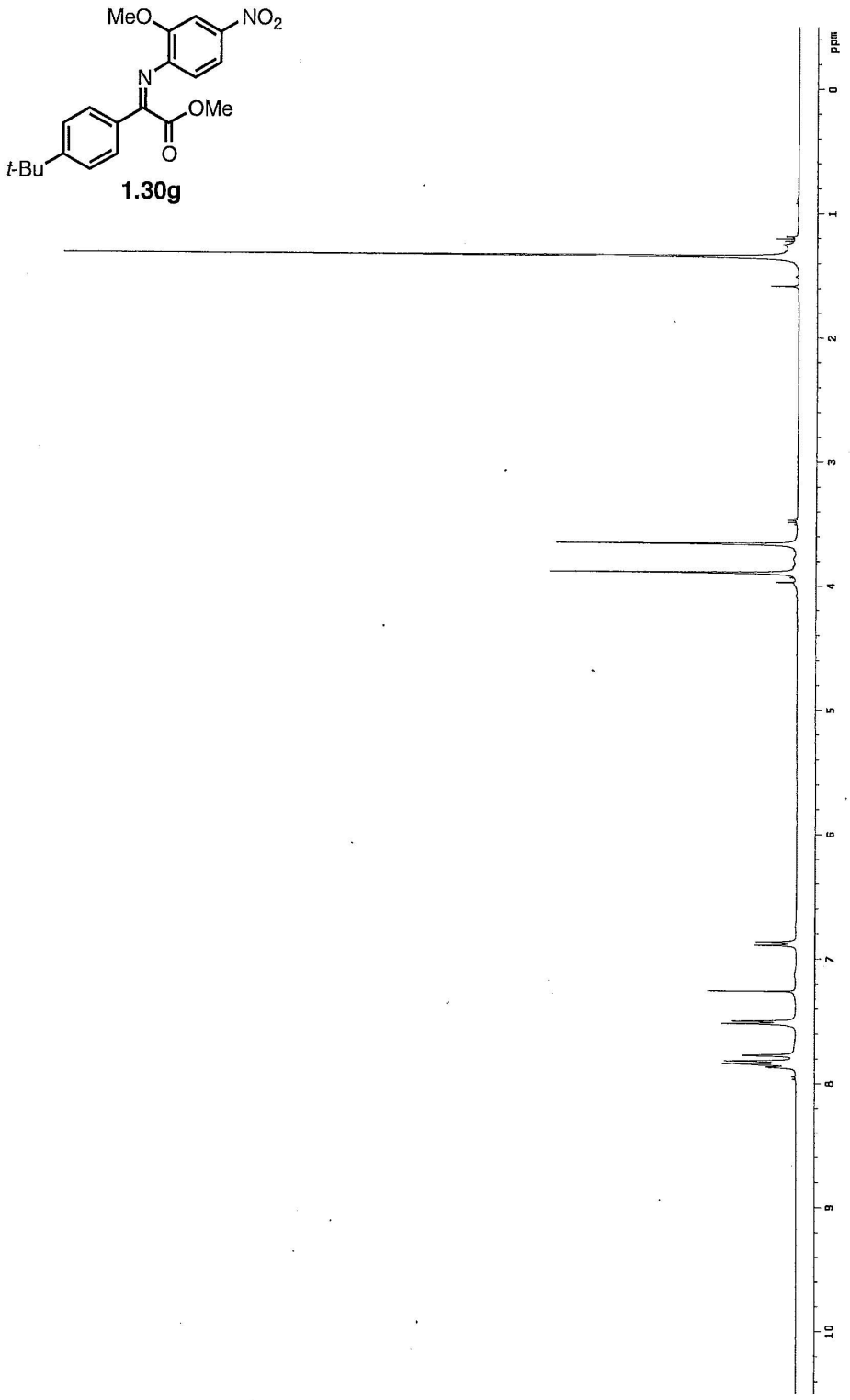
MeO
NO2
N
OMe
O
t-Bu
1.30g
ppm

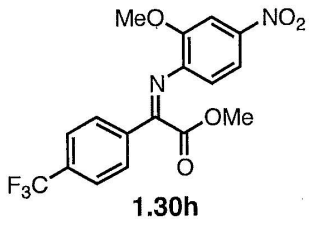

1.30h

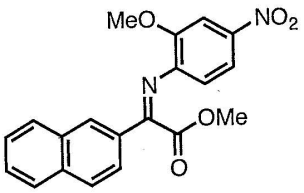

1.30i

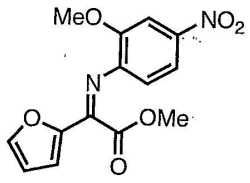

1.30j

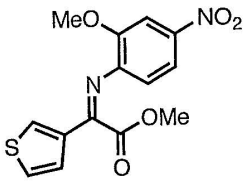

1.30k

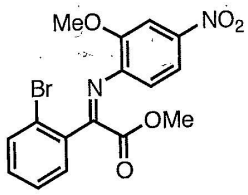
MeO
NO2
Br
N
OMe
O

1.30l

ppm
0
1
2
3
4
5
6
7
8
9
2.92
0.79
0.71
0.23
1.17
0.89
0.28
0.23
1.14
0.26
1.98
1.19
1.00

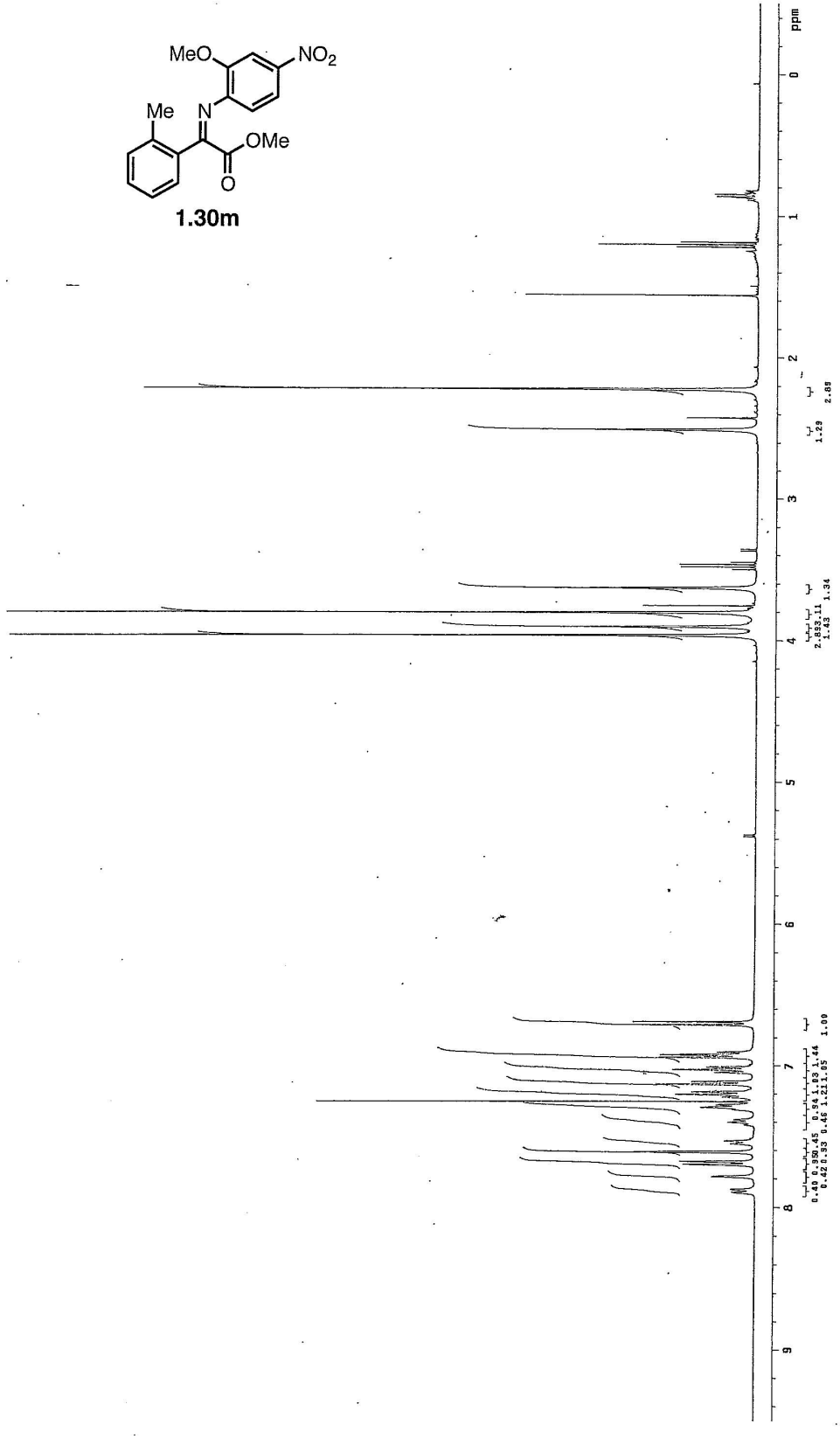
MeO
NO2
Me
N
OMe
O
1.30m
ppm

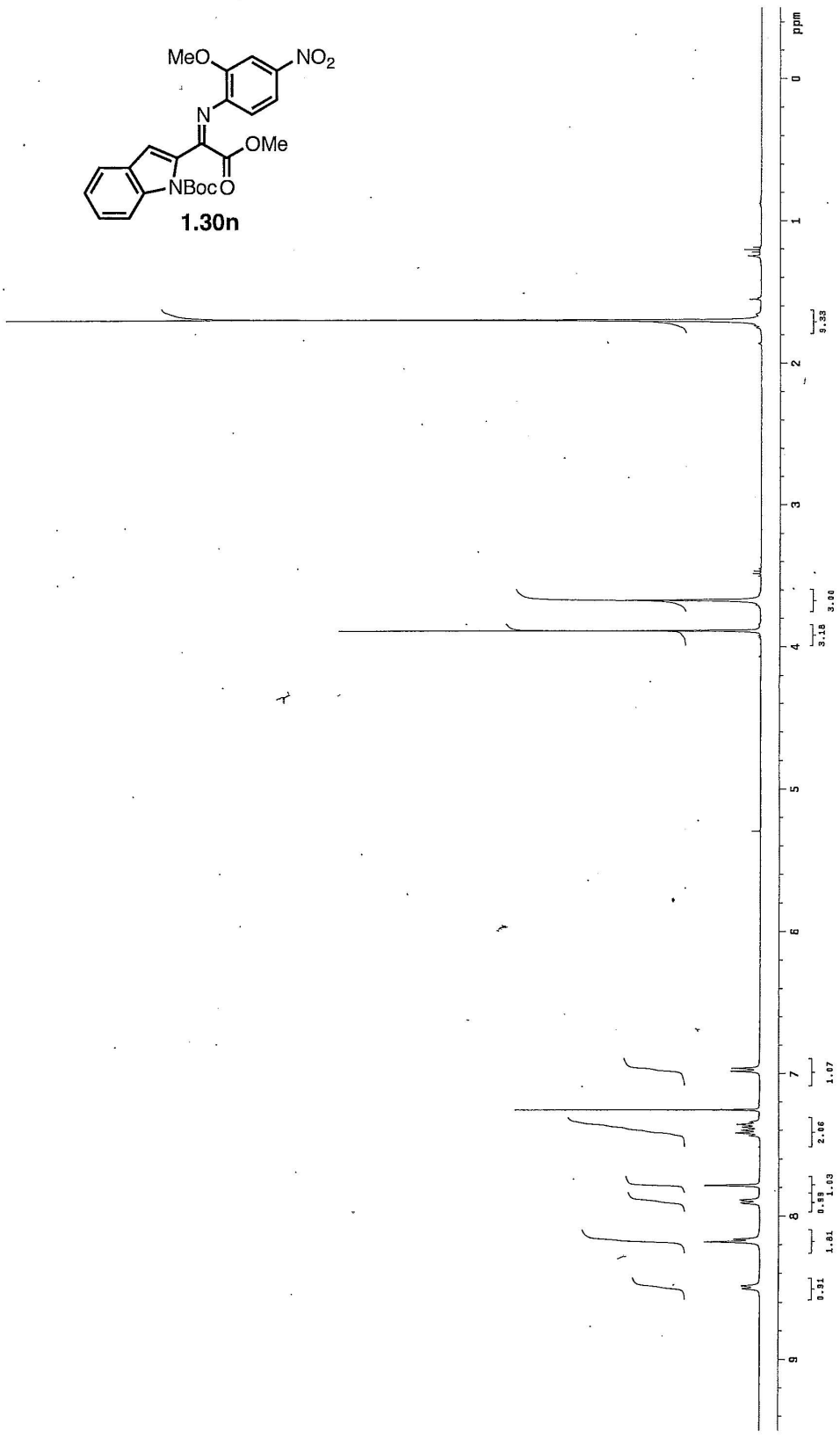
MeO
NO2
N
OMe
NBoc
O
1.30n
ppm
0
1
2
3
4
5
6
7
8
9
9.33
3.00
3.18
1.07
2.06
0.98
1.03
1.01
0.91

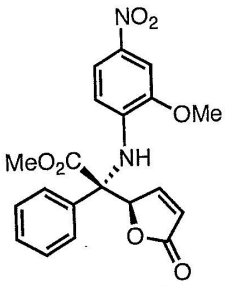

***anti*–1.33a**

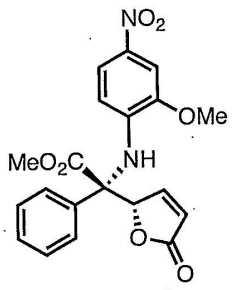

***syn*–1.34a**

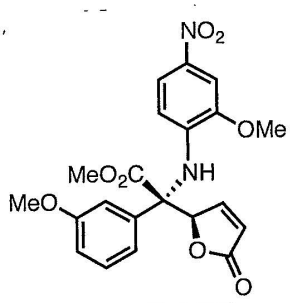

***anti*–1.33b**

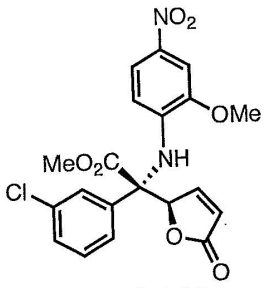

***anti*–1.33c**

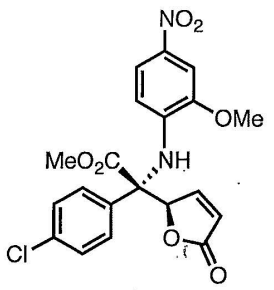

***anti*–1.33d**

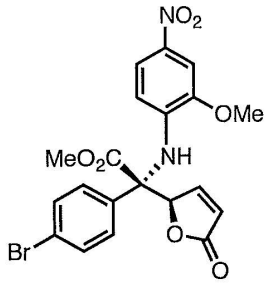

***anti*–1.33e**

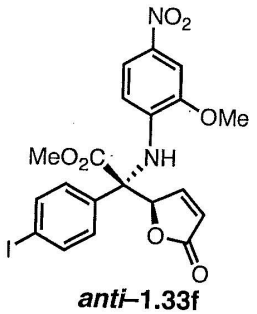

***anti*–1.33f**

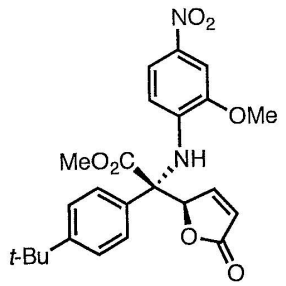

***anti*–1.33g**

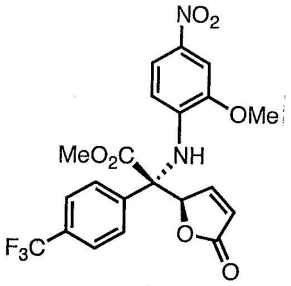

***anti*–1.33h**

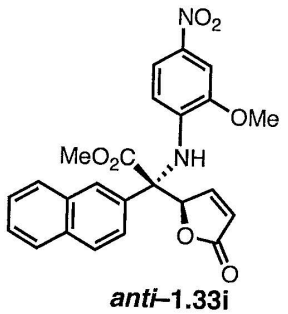

***anti*–1.33i**

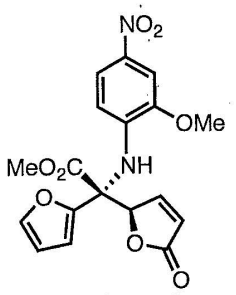

***anti*–1.33j**

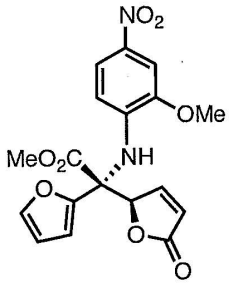

***syn*–1.34j**

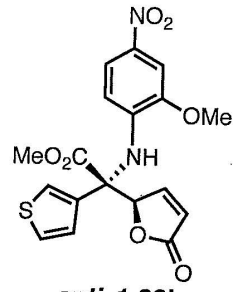

***anti*–1.33k**

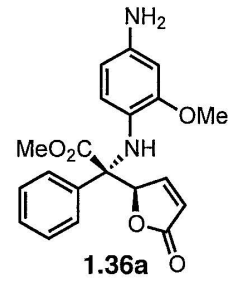

1.36a

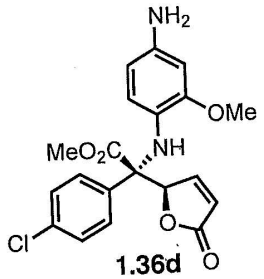

1.36d

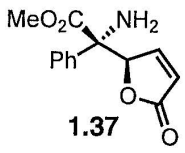

1.37

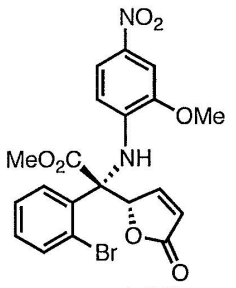
NO2
OMe
MeO2C
NH
Br
O
O

***syn*–1.34l**

ppm
0
1
2
3
4
5
6
7
8
9
2.97
1.05
1.08 1.05
1.01 1.05
3.38 1.46
1.07 1.04
1.07

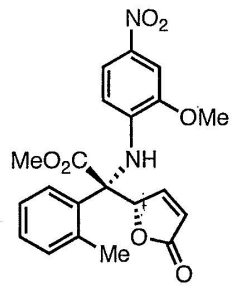
NO2
OMe
MeO2C
NH
Me
O
O

***syn*–1.34m**

ppm
0
1
2
3
4
5
6
7
8
9
2.91
2.98
3.06
0.22
1.05
1.03
1.14
1.00
2.03
0.96
2.02
1.03

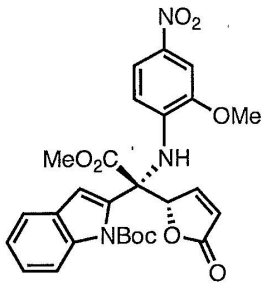
NO2
OMe
MeO2C
NH
NBoc
O
O

***syn*–1.34n**

ppm
0
1
2
3
4
5
6
7
8
9
8.25
2.75
2.95
1.00
1.01
1.09
0.97
1.09
0.82
1.03
1.16
1.15
1.83

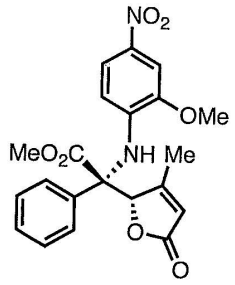
NO2
OMe
MeO2C
NH
Me
O
O

***syn*–1.38**

ppm
0
1
2
3
4
5
6
7
8
9
2.92
3.02
0.92
1.00
0.98
0.97
1.06
1.00
2.01

400 MHz ^{1}H NMR spectrum (22 °C, d_8–thf) of crystalline bisphosphine 1.40

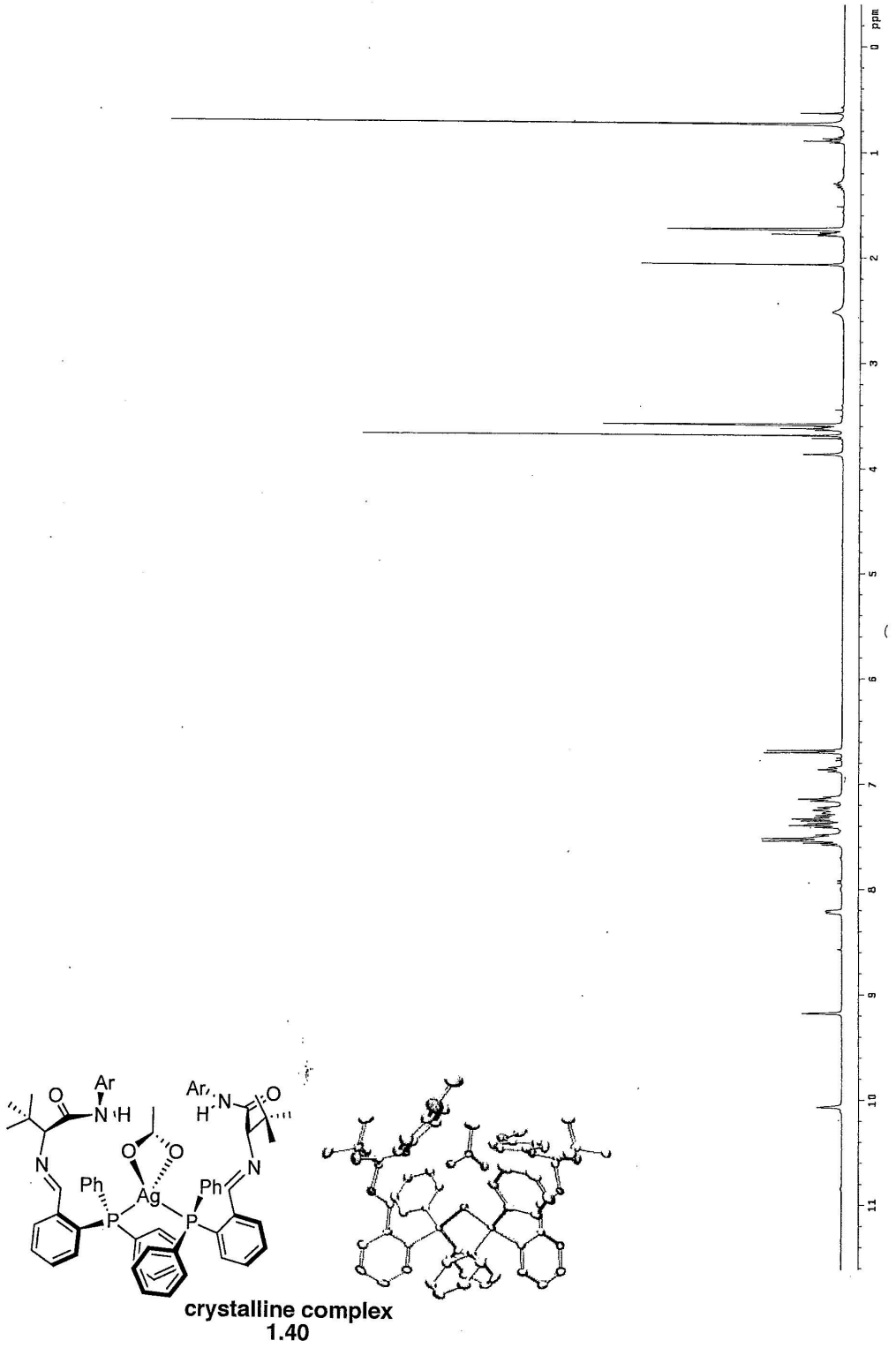

crystalline complex
1.40

100 MHz ^{13}C NMR spectrum (22 °C, d_8–thf) of crystalline bisphosphine 1.40

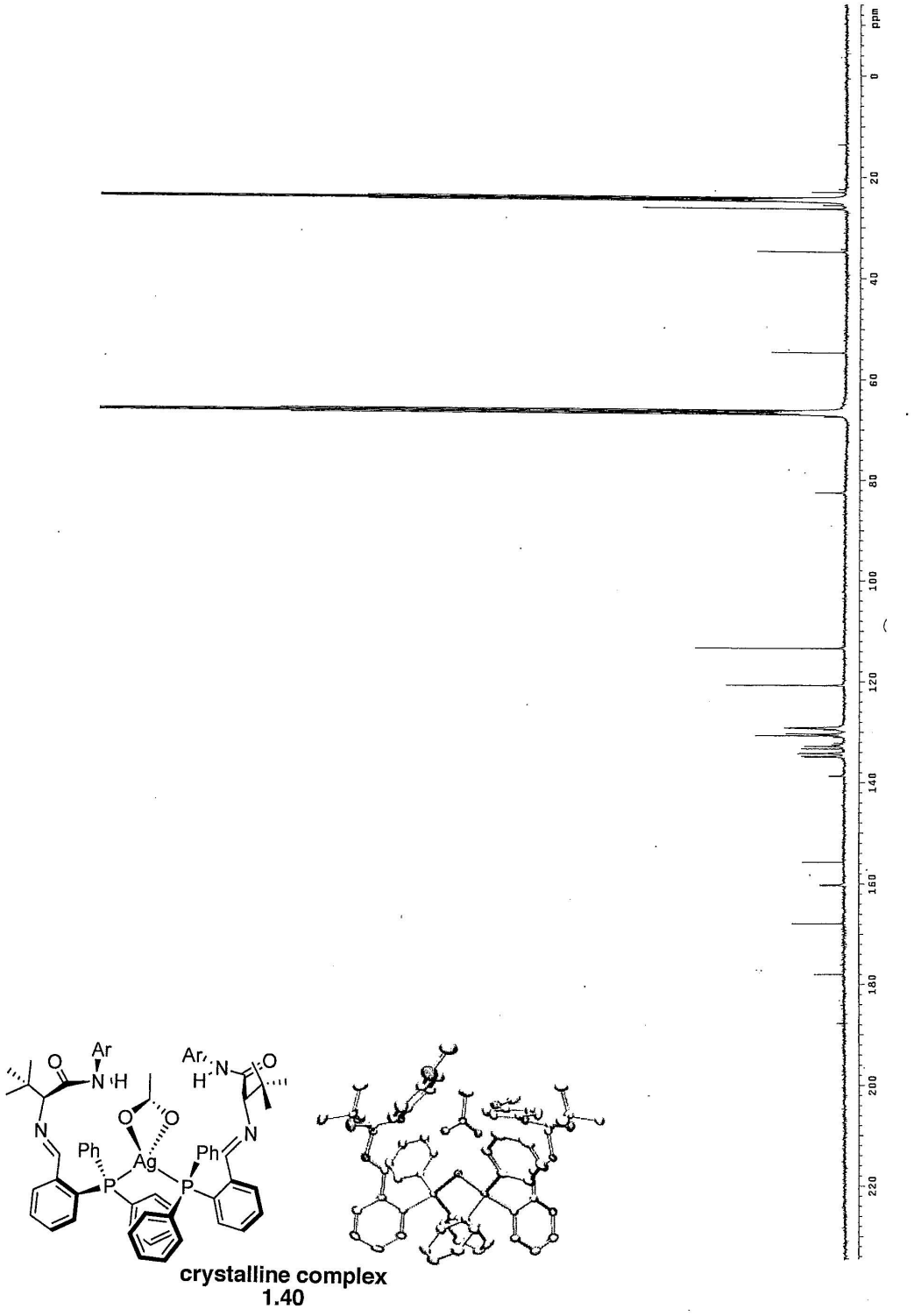

crystalline complex
1.40

400 MHz ^{1}H NMR spectrum (22 °C, d_8–thf) of precomplexed catalyst 1.39

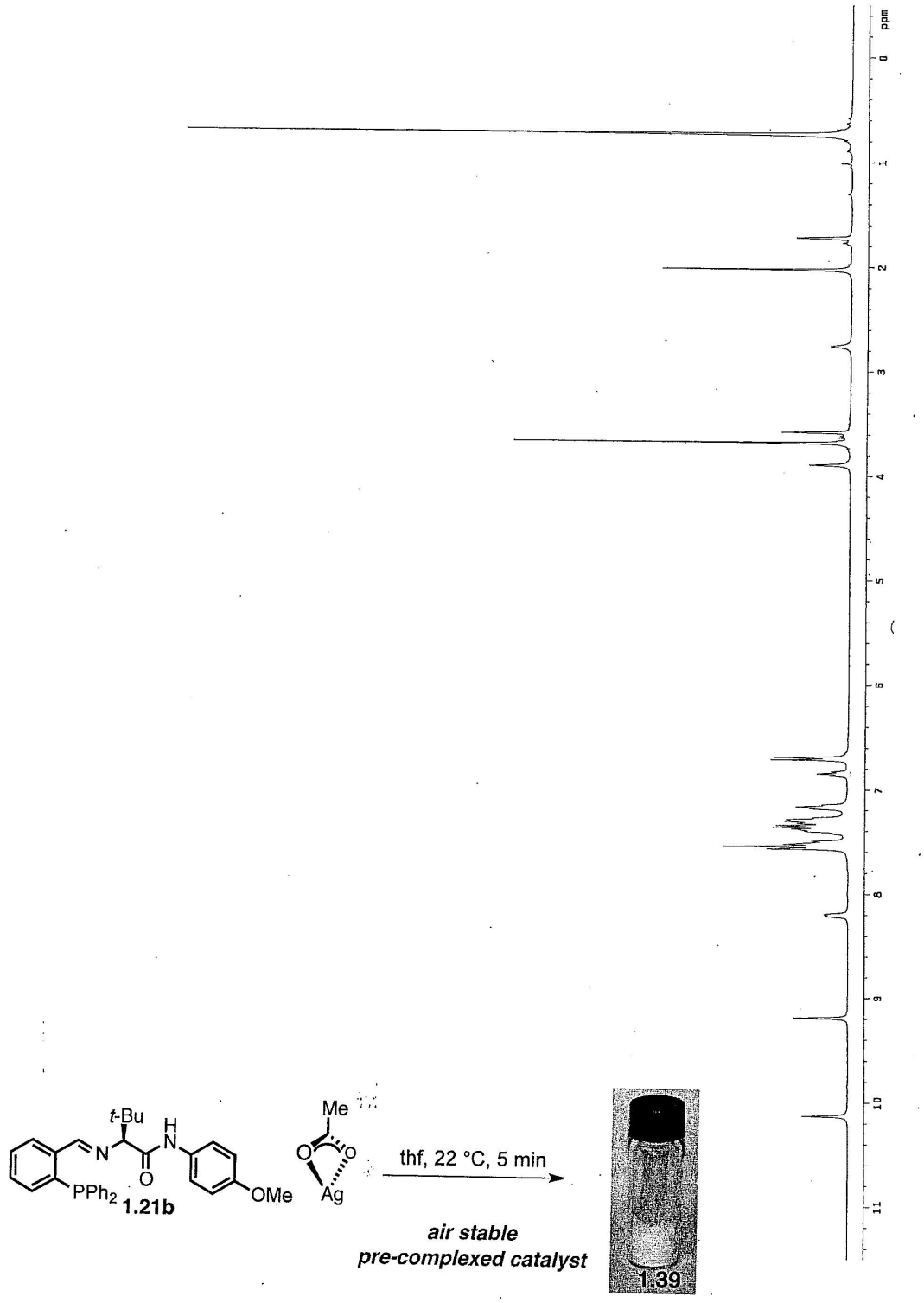

100 MHz ^{13}C NMR spectrum (22 °C, d_8–thf) of precomplexed catalyst 1.39

400 MHz ^{1}H NMR spectrum (VT, d_8–thf) of bisphosphine 1.40

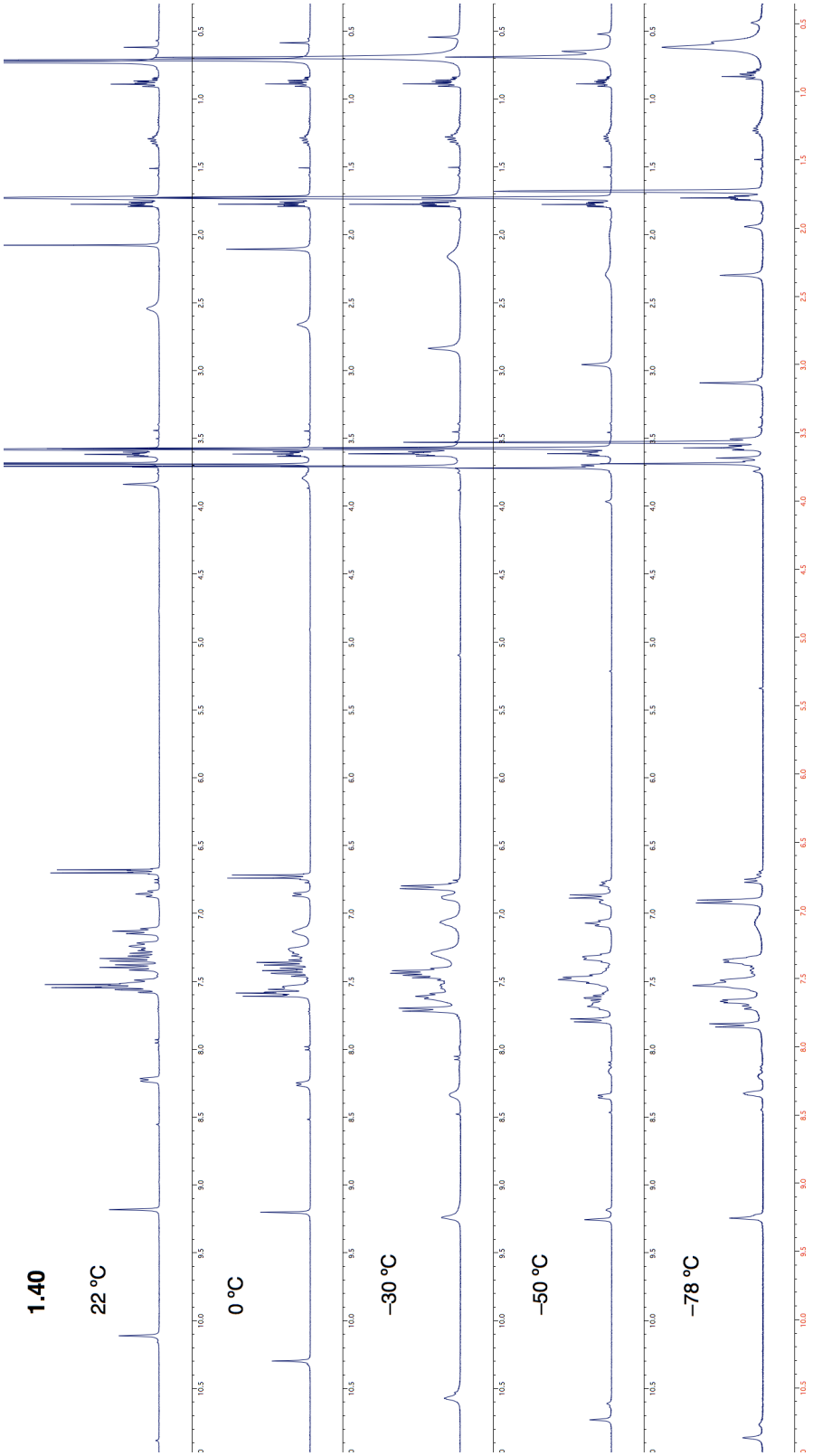

162 MHz ^{31}P NMR spectrum (VT, d_8–thf) of bisphosphine 1.40

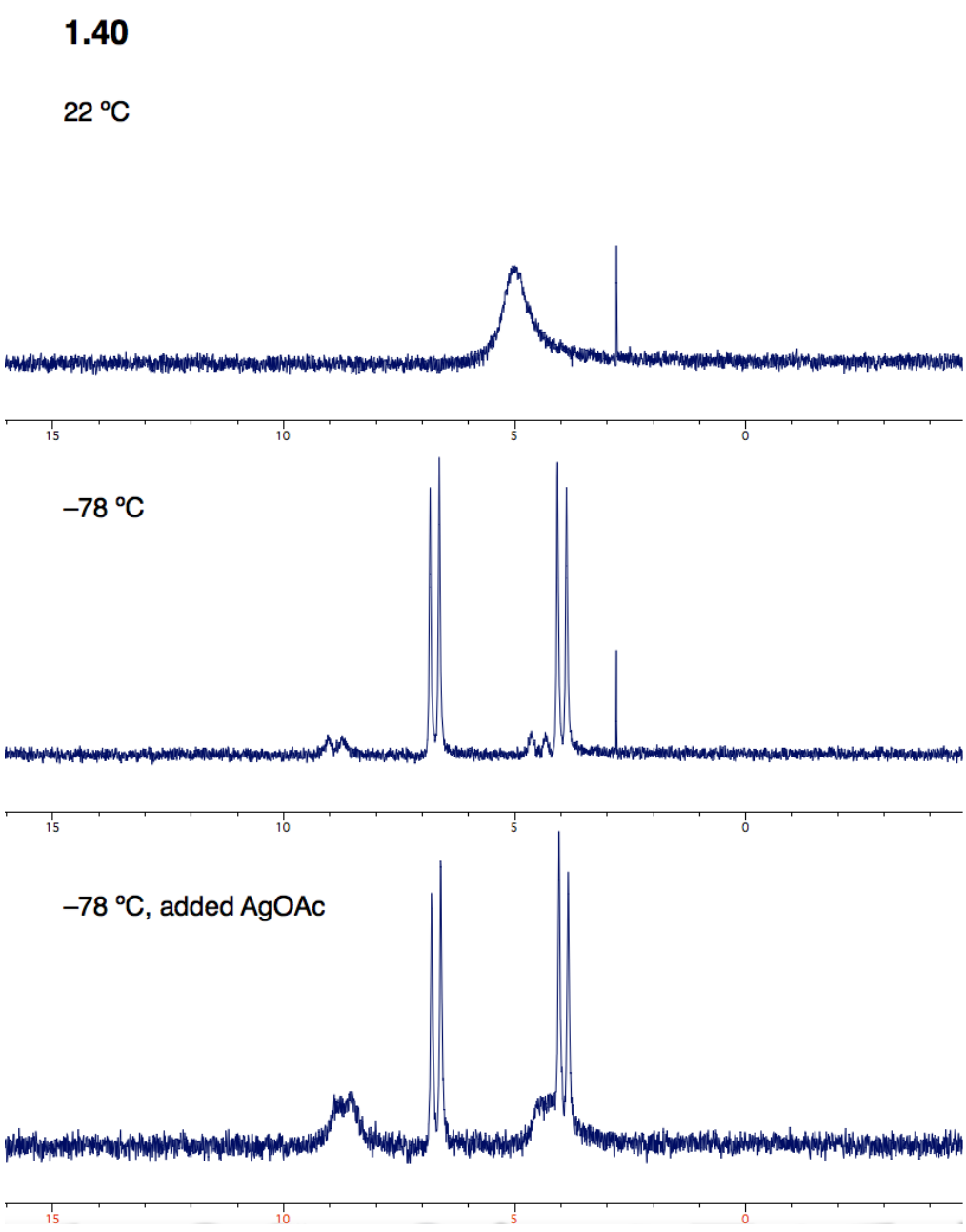

400 MHz ^{1}H NMR spectrum (VT, d_8–thf) of precomplexed catalyst 1.39

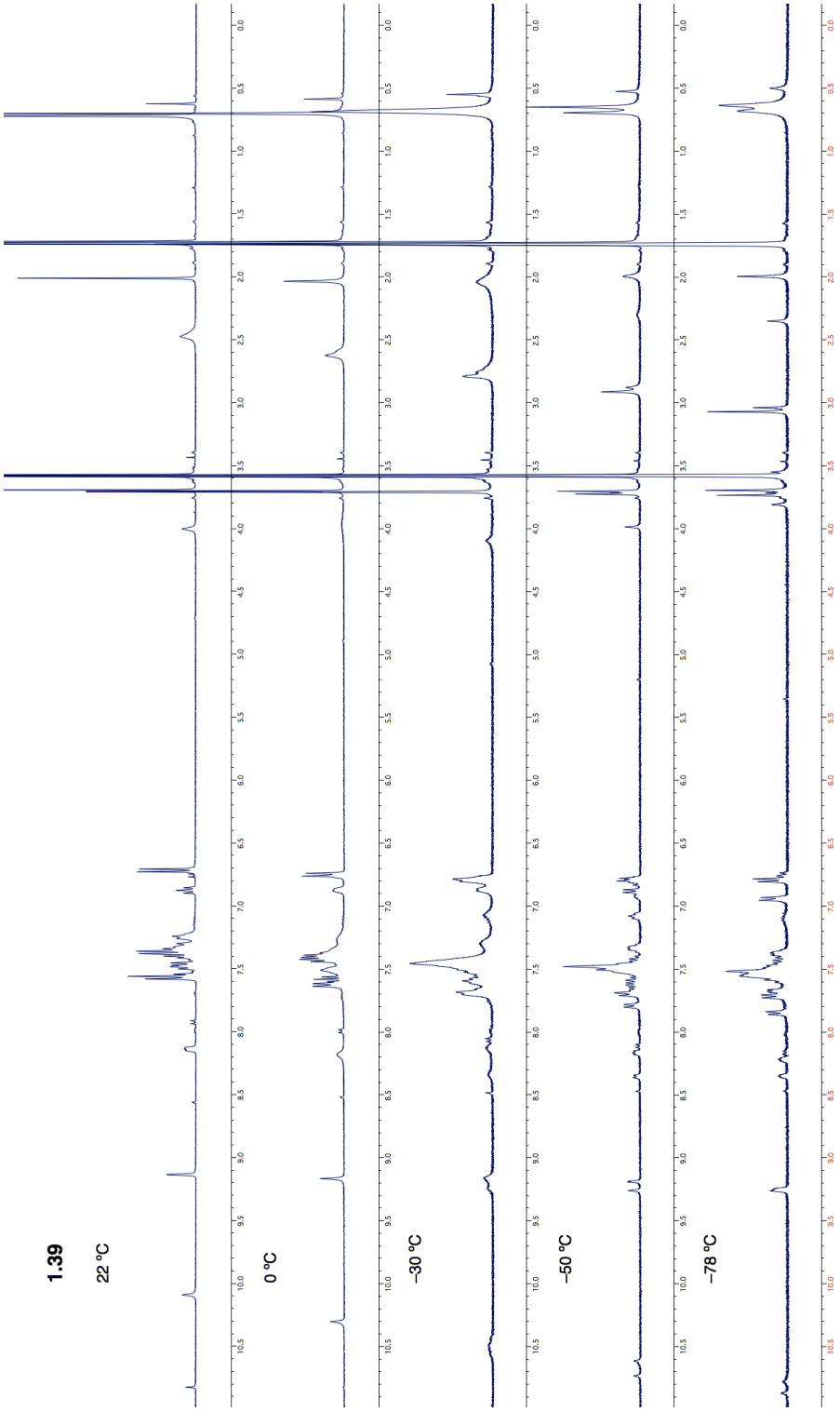

162 MHz ^{31}P NMR spectrum (VT, d_8–thf) of bisphosphine 1.39

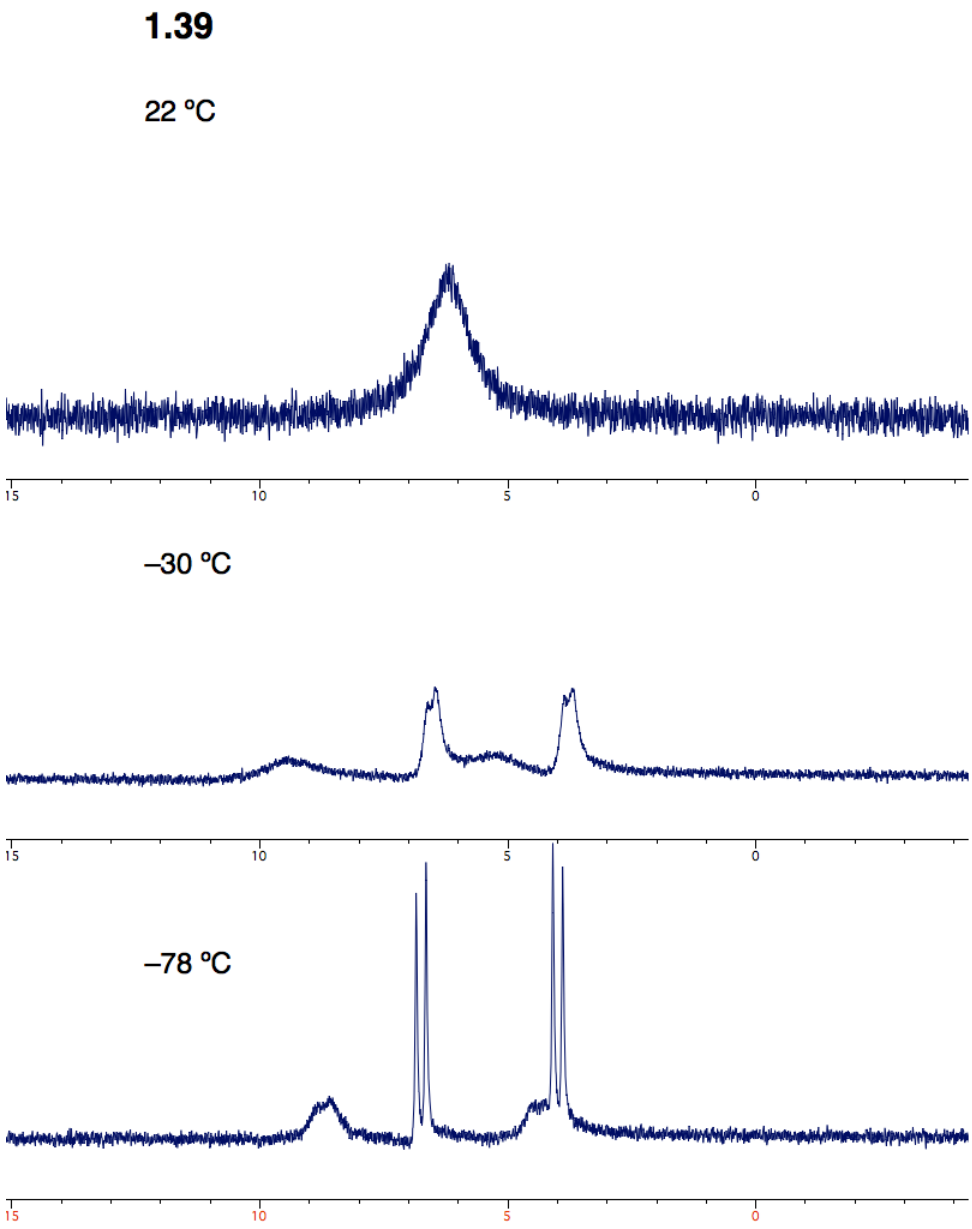

Chapter Two

New Catalysts for the Enantioselective Cu-Catalyzed Additions of Allyl Groups to Phosphinoylaldimines

2.1 Introduction

The prevalence of amines in nature is in part due to their unmatched capacity to engage in intra- and intermolecular interactions, features paramount to establishing effective molecular recognition[1] and the diverse array of structural scaffolds in biology. Successfully developed pharmaceuticals (e.g., Zoloft, a serotonin transporter inhibitor for depression, and Chantix, a nicotinic receptor agonist for smoking cessation) are often decorated with amines, amides and heterocycles in an effort to mimic and disrupt

Scheme 2.1 Pharmaceuticals Mimic the Interactions of Biologically Active Amines

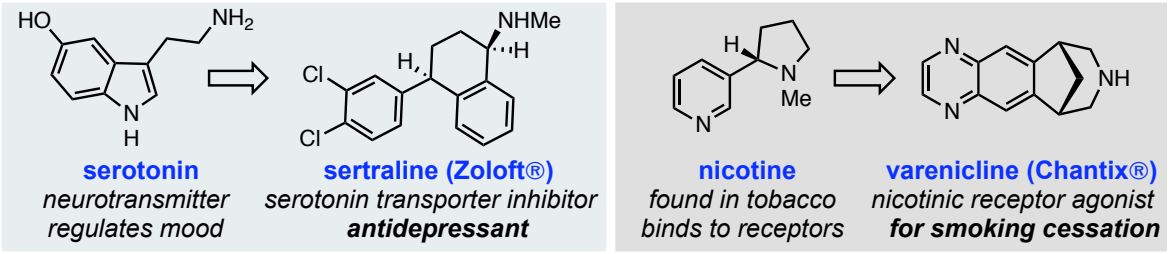

the site-specific native interactions that naturally occurring amines (e.g., serotonin and nicotine) establish with proteins (Scheme 2.1). Moreover, it is becoming increasingly vital to incorporate high degrees of saturation into drug candidates, structural complexity

[1] "A Medicinal Chemist's Guide to Molecular Interactions," Bissantz, C.; Kuhn, B.; Stahl, M. *J. Med. Chem.* **2010**, *53*, 5061–5084.

that often better and more selectively complements the spatial requirements that govern protein interactions.[2] Thus, creating avenues to efficiently synthesize amines with diverse substitution and functionality, particularly those residing within stereogenic carbon-based centers, would aid the discovery of novel therapeutics. In this regard, allyl-substituted α-chiral amines comprise a class of exceptionally valuable *N*-substituted building blocks.[3] Enantiopure homoallylic amines are motifs that not only exist within the structures of a

Scheme 2.2 Accessing Enantiomerically Enriched Homoallylic Amines and the Bioactive Targets in which They Reside

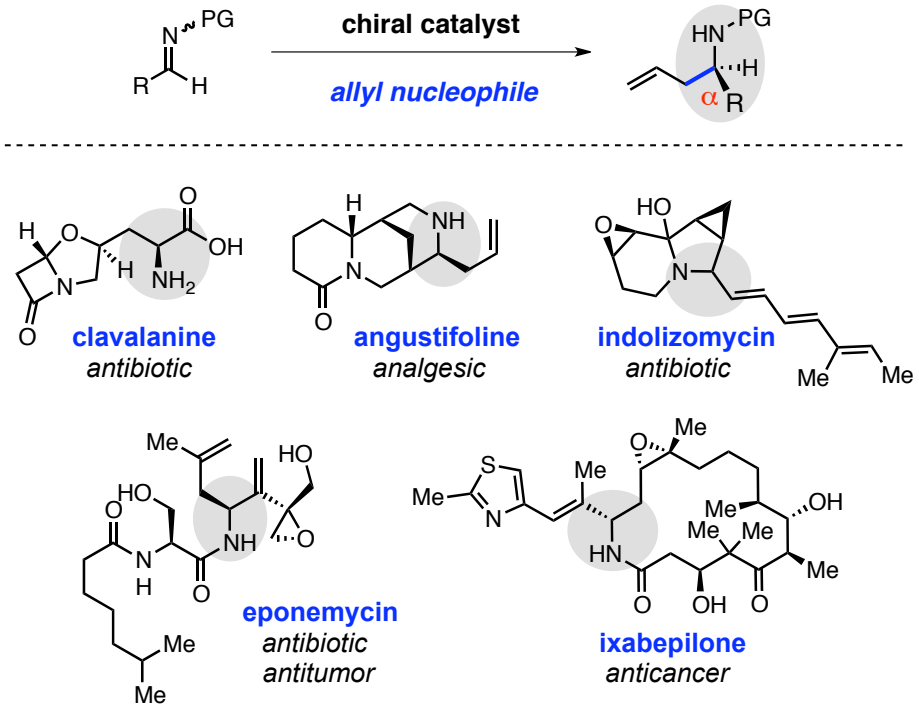

[2] (a) "Escape from Flatland: Increasing Saturation as an Approach to Improving Clinical Success," Lovering, F.; Bikker, J.; Humblet, C. *J. Med. Chem.* **2009**, *52*, 6752–6756. (b) "Escape from Flatland 2: Complexity and Promiscuity," Lovering, F. *Med. Chem. Commun.* **2013**, *4*, 515–519.

[3] For reviews regarding the utility of homoallylic amines in synthesis, see: (a) "Recent Advancements in the Homoallylamine Chemistry," Puentes, C. O.; Kouznetsov, V. *J. Heterocyclic Chem.* **2002**, *39*, 595–614. (b) "Asymmetric Addition of Allylic Nucleophiles to Imino Compounds," Ding, H.; Friestad, G. K. *Synthesis* **2005**, *17*, 2815–2829.

number of biologically active alkaloids such as analgesic angustifoline[4] and antibiotic eponemycin,[5] but are also amenable to synthetic diversification to allow access to antibiotics clavalanine[6] and indolizomycin,[7] as well as anticancer agent ixabepilone[8] (Scheme 2.2)[9].

Synthesis of optically active α-allyl-substituted carbamines can be achieved through nucleophilic addition of an allyl moiety to imines (Scheme 2.2),[10] a C–C bond-generating process that can be rendered diastereo- or enantioselective.[11] There are several

---

[4] "The Isolation and Characterisation of the Alkaloids of *ormosia jamaicensis* Urb." Hassall, C. H.; Wilson, E. M. *J. Chem. Soc.* **1964**, 2657–2663.

[5] "The Total Synthesis of Eponemycin," Schmidt, U.; Schmidt, J. *Synthesis,* **1994***,* 300–304.

[6] "A New Approach to Clavalanine β-Lactam Antibiotic: Transformation of Chiral α-Furfuryl Amide into the δ–Hydroxyl-α-amino Lactones via Asymmetrical Dihydroxylation," Liao, L-X.; Zhou, W-S. *Tetrahedron Lett.* **1996**, *37*, 6371–6374.

[7] "The Total Synthesis of *dl*–Indolizomycin," Kim, G.; Chu-Moyer, M. Y.; Danishefsky, S. J. *J. Am. Chem. Soc.* **1990,** *112*, 2003–2005.

[8] (a) "A Novel Application of a Pd(0)-Catalyzed Nucleophilic Substitution Reaction to the Regio- and Stereoselective Synthesis of Lactam Analogues of the Epothilone Natural Products," Borzilleri, R. M.; Zheng, X.; Schmidt, R. J.; Johnson, J. A.; Kim, S-H.; DiMarco, J. D.; Fairchild, C. R.; Gougoutas, J. Z.; Lee, F. Y. F.; Long, B. H.; Vite, G. D. *J. Am. Chem. Soc.* **2000**, *122*, 8890–8897. (b) "On the Interactivity of Complex Synthesis and Tumor Pharmacology in the Drug Discovery Process: Total Synthesis and Comparative in Vivo Evaluations of the 15-Aza Epothilones,"Stachel, S. J.; Lee, C. B.; Spassova, M.; Chappell, M. D.; Bornmann, W. G.; Danishefsky, S. J.; Chou, T-C.; Guan. Y. *J. Org. Chem.* **2001**, *66*, 4369–4378.

[9] For selected syntheses of natural products that have employed the intermediacy of a homoallylic amine (not pictured in Scheme 2.2), see: (a) "One-Pot Hydrogenation Conditions for a Sequental Process to (+)-Monomorine," Kim, G.; Jung, S-d.; Lee, E-j.; Kim, N. *J. Org. Chem.* **2003**, *68*, 5395–538. (b) "Concise Enantiospecific Synthesis of (+)-Calvine," Dewi-Wulfing, Gebauer, J.; Blechert, S. *Synlett*, **2006**, *3*, 487–489. (c) "Formal Total Synthesis of (–)-Emetine Using Catalytic Asymmetric Allylation of Cyclic Imines as a Key Step," Itoh, T.; Miyazaki, M.; Fukuoka, H.; Nagata, K.; Ohsawa, A. *Org. Lett.* **2006**, *8,* 1295–1297. (d) "Total Synthesis of (–)-Leuconicine A and B," Sirasani, G.; Andrade, R. B. *Org. Lett.* **2011**, *13*, 4736–4737.

[10] See Section 1.1 of Chapter 1 for discussion regarding the challenges associated with nucleophilic additions to imines versus the corresponding carbonyl-containing compounds.

[11] For recent reviews that highlight the research that has addressed this disconnection to access enantiomerically enriched homoallylic amines, see: (a) "Recent Developments in Asymmetric Catalytic Addition to C=N Bonds," Friestad, G. K.; Mathies, A. K. *Tetrahedron*, **2007**, *63*, 2541–2569. (b) "Allylation of Imines and Their Derivatives with Organoboron Reagents: Stereocontrolled Synthesis of Homoallylic Amines," Ramadhar, T. R.; Batey, A. R. *Synthesis*, **2011**, *9*, 1321–1346. (c) "Catalytic Enantioselective Allylation of Carbonyl Compounds and Imines," Yus, M.; González-Gómez, J. C.; Foubelo, F. *Chem. Rev.* **2011**, *111*, 7774–7854. (d) "Catalytic Enantioselective Formation of C–C Bonds by Addition to Imines and Hydazones: A Ten Year Update," Kobayashi, S.; Mori, Y.; Fossey, J. S.; Salter, M. M. *Chem. Rev.* **2011**, *111*, 2626–2704. (e) "Diastereoselective Allylation of Carbonyl Compounds and Imines: Application to the Synthesis of Natural Products," Yus, M.; González-Gómez, J. C.; Foubelo, F. *Chem. Rev.* **2013**, *113*, 5595–5698.

factors that rationalize the wealth of research dedicated to the study of stereospecific reactions of allylic metals: 1) Allylic metals are generally more reactive than other nonstabilized organometallic reagents, however, depending on the metal selected, a wide range of reactivities and differing regioselectivity (S_E2 or S_E2') can be observed. 2) Excellent diastereo- and, occasionally enantiocontrol, are feasible in 1,2-additions of allyl groups to carbonyls and imines. The Lewis acidic metal center can chelate the electrophile to organize a six-membered transition state for C–C bond formation; the close proximity of the reacting partners in the chair-like arrangement can aid in the transfer of stereochemical information in the generation of the new stereogenic center (whether by a chiral catalyst or chiral modifier on either reagent). Stereocontrolled additions of substituted allylic metals, whether cyclic or acyclic modes prevail, reliably provide molecules bearing two contiguous stereocenters of predictable stereochemistry, a distinguishing feature that has prompted the aldol and related Mannich transformations to be among the most powerful C–C bond forming reactions in organic synthesis.[12] 3) The three-carbon homologation to the carbon framework produces amines (or alcohols) bearing latent functionality in the appended olefin; various synthetic operations can manipulate the unsaturation for elaboration to diverse *N*-substituted molecules.

2.2 Background

Over the last three decades, a number of methodologies have arisen to provide entry to enantioenriched homoallylic amines.[13] The first class of approaches involves

---

[12] For reviews regarding stereocontrol in reactions with allylic metals, see: (a) "Acyclic Stereocontrol via Allylic Organometallic Compounds," Yamamoto, Y. *Acc. Chem. Res.* **1987**, *20*, 243–249. (b) "Addition of Organometallic Reagents to Imines Bearing Stereogenic *N*-Substituents. Stereochemical Models Explaining the 1,3-Asymmetric Induction," Alvaro, G.; Savoia, D. *Synlett* **2002**, 651–673.

[13] Although a majority of the approached involve enantioselective additions of allyl nucleophiles (to be discussed), a recently disclosed catalytic enantioselective Aza-Cope rearrangement strategy provides a unique disconnection, see: (a) "Catalytic Asymmetric Aminoallylation of Aldehydes: A Catalytic

additions of allyl nucleophiles to imine electrophiles where either of these two reacting partners are covalently fitted with a chiral modifier (Figure 2.1). Strategies that involve the use of chiral allyl nucleophiles include enantiopure allylboron[14] or allylsilane reagents[15,16] developed to react with achiral imines (or carbonyls) with excellent levels of diastereocontrol. Stereochemically pure allylic alcohols have also been recently shown to

---

Enantioselective Aza-Cope Rearrangement," Rueping, M.; Antonchick, A. P. *Angew. Chem., Int. Ed.* **2008**, *47*, 10090–10093. (b) "Direct Catalytic Asymmetric Aminoallylation of Aldehydes: Synergism of Chiral and Nonchiral Brønsted Acids," Ren, H.; Wulff, W. D. *J. Am. Chem. Soc.* **2011**, *133*, 5656–5659. (c) "Total Synthesis of Sedum Alkaloids via Catalyst Controlled aza-Cope Rearrangement and Hydroformylation with Formaldehyde," Ren, H.; Wulff, W. D. *Org. Lett.* **2013**, *15*, 242–245.

[14] For diastereoselective approaches that employ enantiomerically pure allylboron compounds, see: For a recent review, see: (a) "Recent Developments in the Chiral Synthesis of Homoallylic Amines via Organoboranes," Ramachandran, P. V.; Burghardt, T. E. *Pure. Appl. Chem.* **2006**, *78*, 1397–1406. For specific examples, see: (b) "Enantioselective Synthesis of Homoallylamines by Nucleophilic Addition of Chirally Modified Allylboron Reagents to Imines," Itsuno, S.; Watanabe, K.; Ito, K.; El-Shehawy, A. A.; Sarhan, A. A. *Angew. Chem., Int. Ed. Engl.* **1997**, *36*, 109–110. (c) "Highly Diastereoselective and Enantioselective Preparation of Homoallylic Amines: Application for the Synthesis of β-Amino Acids and γ-Lactams," Ramachandran, P. V.; Burghardt, T. E. *Chem. Eur. J.* **2005**, *11*, 4387–4395. (d) "Asymmetric Allylboration of Cyclic Imines and Applications to Alkaloid Synthesis," Wu, T. R.; Chong, J. M. *J. Am. Chem. Soc.* **2006**, *128*, 9646–9647. (e) "Asymmetric Synthesis with the Robust and Versatile 10-Substituted 9-Borabicyclo[3.3.2]decanes: Homoallylic Amines from Aldimines," Hernandez, E.; Canales, E.; Gonzalez, E.; Soderquist, J. A. *Pure. Appl. Chem.* **2006**, *78*, 1389–1395. (f) "Convenient Synthesis of Stable Aldimine–Borane Complexes, Chiral δ-Amino Alcohols, and γ-Substituted GABA Analogues from Nitriles," Ramachandran, P. V.; Biswas, D. *Org. Lett.* **2007,** *9*, 3025–3027.

[15] For diastereoselective methods that make use of enantiomerically pure allylsilanes, see: (a) "Direct Amino-Crotylsilylation of Achiral Acetals and Aldehydes: Asymmetric Synthesis of Homoallylic Amines and Functionalized Pyrrolidines," Panek, J. S.; Jain, N. F. *J. Org. Chem.* **1994**, *59*, 2674–2675. (b) "Asymmetric Synthesis of Homoallylic Amines and Functionalized Pyrrolidines via Direct Amino-Crotylation of In Situ Generated Imines," Schaus, J. V.; Jain, N.; Panek, J. S. *Tetrahedron* **2000**, *56*, 10263–10274. Employing a chiral strained silacycle, see: (c) "Phenol-Directed Allylation of Aldimines and Ketimines," Rabbat, P. M. A.; Valdez, S. C.; Leighton, J. L. *Org. Lett.* **2006,** *8*, 6119–6121. (d) "Enantioselective Imidazole-Directed Allylation of Aldimines and Ketimines," Perl, N. R.; Leighton, J. L. *Org. Lett.* **2007,** *9*, 3699–3701. (e) "Allylsilane–Vinylarene Cross-Metathesis Enables a Powerful Approach to Enantioselective Imine Allylation," Huber, J. D.; Perl, N. R.; Leighton, J. L. *Angew. Chem., Int. Ed.* **2008**, *47*, 3037–3039. (f) "Asymmetric Allylation, Crotylation, and Cinnamylation of *N*-Heteroaryl Hydrazones," Feske, M. I.; Santanilla, A. B.; Leighton, J. L. *Org. Lett.* **2010,** *12*, 688–691.

[16] For use of stoichiometric coordinating catalysts to generate an *in situ* chiral allylating reagent with allyltricholorsilanes, see: (a) "Chiral Sulfoxides as Neutral Coordinate-Organocatalysts in Asymmetric Allylation of *N*-Acylhydrazones Using Allyltrichlorosilanes," Kobayashi, S.; Ogawa, C.; Konishi, H.; Sugiura, M. *J. Am. Chem. Soc.* **2003**, *125*, 6610–6611. (b) "Stereospecific, Enantioselective Allylation of α-Hydrazono Esters by Using Allyltrichlorosilanes with BINAP Dioxides as Neutral-Coordinate Organocatalysts," Ogawa, C.; Sugiura, M.; Kobayashi, S. *Angew. Chem., Int. Ed.* **2004**, *43*, 6491–6493.

serve as chiral allyl sources in titanium-mediated reductive couplings with imines with excellent transfer of stereochemistry.[17]

Successful stereoselective synthesis of homoallylic amines has also been achieved through reactions of achiral allyl nucleophiles coupled with imines bearing a chiral *N*-substituent (Figure 2.1): examples include chiral *N*-acyl hydrazones,[18] various amino

Figure 2.1 Diastereoselective Allyl Addition Approaches Involving Stoichiometric Chiral Sources on Either Reacting Partner

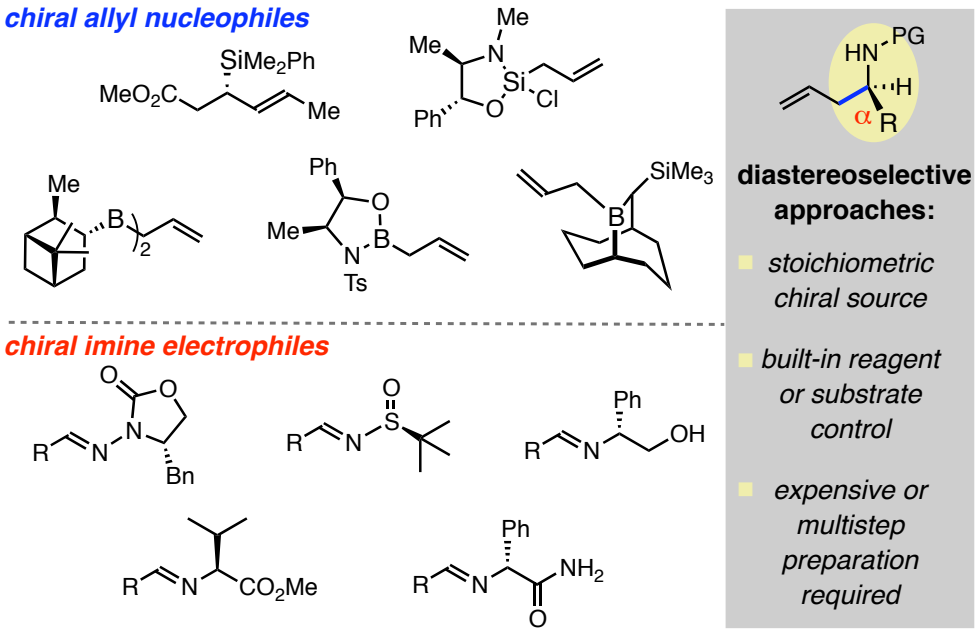

[17] For the reductive couplings of stereochemically-defined allylic alcohols with imines, see: (a) "Complex Allylation by the Direct Cross-Coupling of Imines with Unactivated Allylic Alcohols," Takahashi, M.; McLaughlin, M.; Micalizio, G. C. *Angew. Chem., Int. Ed.* **2009**, *48*, 3648–3652. (b) "Stereoselective Cross-Coupling between Allylic Alcohols and Aldimines," Lysenko, I. L.; Lee, H. G.; Cha, J. K. *Org. Lett.* **2009,** *11*, 3132–3134. (c) "Preparation of Stereodefined Homoallylic Amines from the Reductive Cross-Coupling of Allylic Alchols with Imines," Chen, M. Z.; McLaughlin, M.; Takahashi, M.; Tarselli, M. A.; Yang, D.; Umemura, S.; Micalizio, G. C. *J. Org. Chem.* **2010**, *75*, 8048–8059.

[18] For examples employing chiral *N*-acylhydrazones, see: (a) "Dual Activation in Asymmetric Allylsilane Addition to Chiral *N*-Acylhydrazones: Method Development, Mechanistic Studies, and Elaboration of Homoallylic Amine Adducts," Friestad, G. K.; Korapala, C. S.; Ding, H. *J. Org. Chem.* **2006**, *71*, 281–289. (b) "Asymmetric Synthesis of Aminochromanes via Intramolecular Indium-Mediated Allylation of Chiral Hydrazones," Samanta, D.; Kargbo, R. B.; Cook, G. R. *J. Org. Chem.* **2009**, *74*, 7183–7186.

acid-derived variants,[19] and *N-tert*-butanesulfinyl imines.[20] The latter auxiliary approach, developed by Ellman and coworkers, provides a highly robust, general, and reliably diastereoselective method for the preparation of a vast range of α-chiral *N-tert*-butanesulfinamides, readily converted to the amines with simple acid hydrolysis. However, this strategy, as with all diastereoselective approaches discussed, suffer from one or more of the inherent drawbacks associated with the use of a stoichiometric quantity of a chiral source: 1) In many cases, the pre-functionalized chiral reagents require multi-step preparation. 2) The built-in diastereocontrol can be substrate-dependent; different chiral modifiers may need to be developed for substrates bearing less-differentiating substitution patterns. 3) The chiral source employed may be too expensive to be a practical solution for large scale applications, especially if it cannot be recovered and recycled, or is recovered in poor yields.

---

[19] For imines that have been derived from amino acids and derivatives thereof, see: (a) "Asymmetric Synthesis of C-Aliphatic Homoallylic Amines and Biologically Important Cyclohexenylamine Analogues," Lee, C-L. K.; Ling, H. Y.; Loh, T-P. *J. Org. Chem.* **2004**, *69*, 7787–7789. (b) "Synthesis of Enantiopure 1-Aryl-1-butylamines and 1-Aryl-3-butenylamines by Diastereoselective Addition of Allylzinc Bromide to Imines Derived from (*R*)–Phenylglycine Amide," Dalmolen, J.; van der Sluis, M.; Nieuwenhuijzen, J. W.; Meetsma, A.; de Lange, B.; Kaptein, B.; Kellogg, R. M.; Broxterman, Q. B. *Eur. J. Org. Chem.* **2004**, 1544–1557. (c) "Indium-Mediated Asymmetric Barbier-Type Allylation of Aldimines in Alcoholic Solvents: Synthesis of Optically Active Homoallylic Amines," Vilaivan, T.; Winotapan, C.; Banphavichit, V.; Shinada, T.; Ohfune, Y. *J. Org. Chem.* **2005**, *70*, 3464–3471. (d) "Diastereoselective Access to Enantiomerically Pure *cis*-2,3-Disubstituted Pyrrolidines," Delaye, P-O.; Pradhan, T. K.; Lambert, E.; Vasse, J-L.; Szymoniak, J. *Eur. J. Org. Chem.* **2010**, 3395–3406. (e) "Switching Regioselectivity in the Allylation of Imines by N-Side Chain Tuning," Delaye, P-O.; Vasse, J-L.; Szymoniak, J. *Org. Lett.* **2012**, *14*, 3004–3007. For the use of an *in situ* generated chiral *N*-acyliminium ion, see: "Expedient Synthesis of Chiral Homoallylamines via *N*,*O*–Acetal TMS Ethers and Its Application," Suh, Y-G.; Jang, J.; Yun, H.; Han, S. M.; Shin, D.; Jung, J-K.; Jung, J-W. *Org. Lett.*, **2011,** *13*, 5920–5923.

[20] For examples that employ *N-tert*-butanesulfinyl imines developed by Ellman, see: (a) "Asymmetric Synthesis of Chiral Amines by Highly Diastereoselective 1,2-Additions of Organometallic Reagents to *N-tert*-Butanesulfinyl Imines," Cogan, D. A.; Liu, G.; Ellman, J. *Tetrahedron* **1999**, *55*, 8883–8904. (b) "Room-Temperature Highly Diastereoselective Zn–Mediated Allylation of Chiral *N-tert*-Butanesulfinyl Imines: Remarkable Reaction Condition Controlled Stereoselectivity Reversal," Sun, X-W.; Xu, M-H.; Lin, G-Q. *Org. Lett.* **2006**, *8*, 4979–4982. (c) "Asymmetric Synthesis of Homoallylic Amines Bearing Adjacent Stereogenic Centers by Addition of Substituted Allylic Zinc Reagents to *N-tert*-Butanesulfinylimines," Reddy, L. R.; Hu, B.; Prashad, M.; Prasad, K. *Org. Lett.* **2008**, *10*, 3109–3112. (d) "Stereoselective α-Aminoallylation of Aldehydes with Chiral *tert*-Butanesulfinamides and Allyl Bromides," González-Gómez, J. C.; Medjahdi, M.; Foubelo, F.; Yus, M. *J. Org. Chem.* **2010**, *75*, 6308–6311.

In this context, *catalytic enantioselective* methods for the addition of allyl groups to imines offer several intrinsic advantages: 1) An effective chiral catalyst allows generation of large quantities of enantiopure high value molecules with the investment of a small quantity of chiral material (i.e., 5 mol % loading can afford up to 20 times the amount of desired product). 2) Reactions are under catalyst controlled selectivity profiles, and not restricted to substrate-control. The sense of addition is enforced by the structure of the catalyst and, as such, is not necessarily dictated by the size differential of the substituents on the reaction partners. 3) Simple, easily accessible achiral imines and allyl nucleophiles can be combined in the presence of a catalyst to generate high worth stereochemically-defined amine building blocks in one step.

The earliest examples of catalytic enantioselective approaches for the synthesis of homoallylic amines involved copper-catalyzed ene reactions of α-imino esters,[21] transformations specific to the formation of 2-substituted homoallylic α-amino acid derivatives, as well as, palladium-catalyzed additions of allyltributyltin to a larger subclass of benzyl-protected imines.[22] Yamamoto describes a transmetalation event between an allylstannane and β-pinene-derived bis-π-allylpalladium complex **2.1**, which, upon imine coordination, transfers an allyl unit through a cyclic transition state (Scheme

---

[21] For catalytic enantioselective ene reactions of imines to afford allyl-substituted amino acid derivatives, see: (a) "Catalytic Enantioselective Ene Reactions of Imines: A Simple Approach for the Formation of Optically Active α-Amino Acids," Yao, S.; Fang, X.; Jørgensen, K. A. *Chem. Commun.* **1998**, 2547–2548. (b) "A Novel Synthesis of α -Amino Acid Derivatives through Catalytic, Enantioselective Ene Reactions of α-Imino Esters," Drury, W. J., III; Ferraris, D.; Cox, C.; Young, B.; Lectka, T. *J. Am. Chem. Soc.* **1998**, *120*, 11006–11007.

[22] (a) "Catalytic Asymmetric Allylation of Imines via Chiral Bis-π-allylpalladium Complexes," Nakamura, H.; Nakamura, K.; Yamamoto, Y. *J. Am. Chem. Soc.* **1998**, *120*, 4242–4243. (b) "Chiral Bis-π-allylpalladium Complex Catalyzed Asymmetric Allylation of Imines: Enhancement of the Enantioselectivity and Chemical Yield in the Presence of Water," Fernandes, R. A.; Stimac, A.; Yamamoto, Y. *J. Am. Chem. Soc.* **2003**, *125*, 14133–14139. For similar reactions with allylsilanes, see: (c) "Chiral π-Allylpalladium-Catalyzed Asymmetric Allylation of Imines: Replacement of Allylstannanes by Allylsilanes," Nakamura, K.; Nakamura, H.; Yamamoto, Y. *J. Org. Chem.* **1999**, *64*, 2614–2615. (d) "The First Catalytic Asymmetric Allylation of Imines with the Tetraallylsilane–TBAF–MeOH System, Using the Chiral Bis-π-allylpalladium Complex," Fernandes, R. A.; Yamamoto, Y. *J. Org. Chem.* **2004**, *69*, 735–738.

2.2). Despite the significant advance represented by this strategy, several weaknesses can be identified. Long reaction times are often needed for effective transformations, lower

Scheme 2.2 Chiral Bis-π-allylpalladium Catalyzed Allyl Additions to Imines

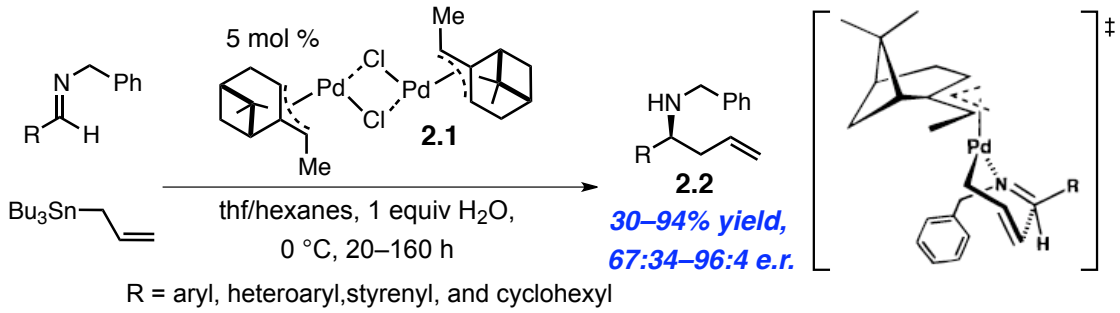

R = aryl, heteroaryl,styrenyl, and cyclohexyl

selectivity levels are afforded with aliphatic imines and imines with electron-rich substituents, and chemoselective cleavage of the benzyl protecting group of **2.2** can pose a significant challenge (especially when R = aryl or heteroaryl, examples in which the resultant amines are doubly benzylic). Several other chiral copper, zirconium, and palladium based catalysts were reported to react with allylstannanes to provide improved results for the synthesis of homoallylic amines,[23] however, subsequent investigations moved towards less toxic and environmentally benign sources for allyl nucleophiles including silicon, indium, and boron.

Subsequent studies involving silyl-based allyl donors were marked by low reactivity.[24] Imine reaction partners are limited to α-hydrazono esters or to those with

---

[23] For subsequent reports detailing catalytic enantioselective transformations involving allylstannanes, see: (a) "Catalytic Approach for the Formation of Optically Active Allyl α-Amino Acids by Addition of Allylic Metal Compounds to α-Imino Esters," Fang, X.; Johannsen, M.; Yao, S.; Gathergood, N.; Hazell, R. G.; Jørgensen, K. A. *J. Org. Chem.* **1999**, *64*, 4844–4849. (b) "Highly Enantioselective Allylation of Imines with a Chiral Zirconium Catalyst," Gastner, T.; Ishitani, H.; Akiyama, R.; Kobayashi, S. *Angew. Chem., Int. Ed.* **2001**, *40*, 1896–1898. (c) "Synthesis and Catalytic Application of Chiral 1,1'-Bi-2-naphthol- and Biphenanathrol-Based Pincer Complexes: Selective Allylation of Sulfonimines with Allyl Stannane and Allyl Trifluoroborate," Aydin, J.; Kumar, K. S.; Sayah, M. J.; Wallner, O. A.; Szabó, K. J. *J. Org. Chem.* **2007**, *72*, 4689–4697.

[24] For catalytic enantioselective methods that utilize allylsilanes, see: (a) "Catalytic, Enantioselective Alkylation of α-Imino Esters: The Synthesis of Nonnatural α-Amino Acid Derivatives," Ferraris, D.; Young, B.; Cox, C.; Dudding, T.; Drury, W. J., III; Ryzhkov, L.; Taggi, A. E.; Lectka, T. *J. Am. Chem. Soc.* **2002**, *124*, 67–77. (b) "Catalytic Asymmetric Allylation of Hydrazono Esters in Aqueous Media by

electron-withdrawing aryl substituents. For example, only the more reactive 2-substituted allyltrimethylsilanes[25] proceed in Cu-catalyzed additions to *N*-acyl α-imino ester **2.3** to provide allylglycine derivatives such as **2.5a** in 76% yield and 96.5:3.5 e.r. (Scheme

Scheme 2.3 Cu-Catalyzed Additions of 2-Substituted Allylsilanes to *N*-Acyl α-Imino Esters **2.3**.

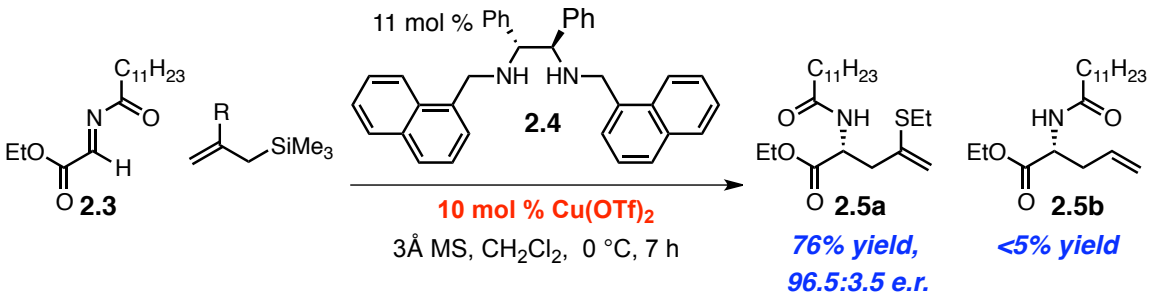

2.3);[23c] there is only trace conversion to α-amino ester **2.5b** when unsubstituted trimethylallylsilane is employed with the Cu–diamine **2.4** complex as catalyst. The catalytic enantioselective three-component coupling reported by List and coworkers further highlights the inadequate reactivity of trimethylallylsilane. The synthesis of fluorenyl carbamates **2.7a** and **2.7b** requires *ten days* in the presence of 10 mol % of

---

Using ZnF_2–Chiral Diamine," Hamada, T.; Manabe, K.; Kobayashi, S. *Angew. Chem., Int. Ed.* **2003**, *42*, 3927–3930. (c) "Enantiomerically Enriched Allylglycine Derivatives through the Catalytic Asymmetric Allylation of Iminoesters and Iminophosphonates with Allylsilanes," Kiyohara, H.; Nakamura, Y.; Matsubara, R.; Kobayashi, S. *Angew. Chem., Int. Ed.* **2006**, *45*, 1615–1617. (d) "First Enantioselective Organocatalytic Allylation of Simple Aldimines with Allyltrichlorosilane," Jagtap, S. B.; Tsogoeva, S. B. *Chem. Commun.* **2006**, 4747–4749. (f) "Enantioselective Ag-Catalyzed Allylation of Aldimines," Naodovic, M.; Wadamoto, M.; Yamamoto, H. *Eur. J. Org. Chem.* **2009**, 5129–5131. (g) "Chiral Brønsted Acid Catalysis for Enantioselective Hosomi–Sakurai Reaction of Imines with Allyltrimethylsilane," Momiyama, N.; Nishimoto, H.; Terada, M. *Org. Lett.* **2011**, *13*, 2126–2129. (h) "Catalytic Asymmetric Three-Component Synthesis of Homoallylic Amines," Gandhi, S.; List, B. *Angew. Chem., Int. Ed.* **2013**, *52*, 2573–2576.

[25] Studies indicate that replacement of the internal olefinic proton of allyltrimethylsilane with a methyl group (2-methylallyltrimethylsilane) results in 1700-fold increase in rate of reaction. Moreover, in comparison with the corresponding allyltributyltin reagents, the allylsilanes are less reactive by four orders of magnitude. For a description of the data cited, see: "Scales of Nucleophilicity and Electrophilicity: A System for Ordering Polar Organic and Organometallic Reactions," Mayr, H.; Patz, M. *Angew. Chem., Int. Ed. Engl.* **1994**, *33*, 938–957.

Scheme 2.4 Catalytic Enantioselective Three Component Synthesis of Homoallylic Carbamates

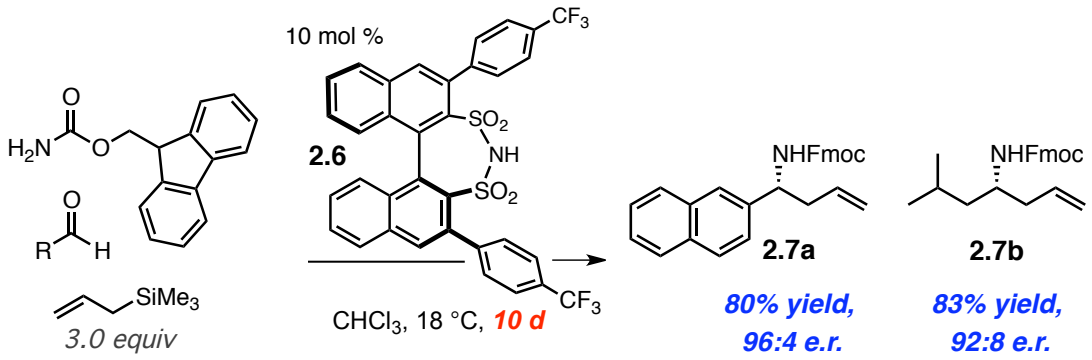

Brønsted acid catalyst disulfonimide **2.6** to obtain 80–83% yield and 92:8–96:4 e.r. Silyl-based allyl reagents, although versatile and effective partners for allyl additions to carbonyls, do not demonstrate the requisite nucleophilicities to efficiently participate in reactions with less electrophilic imines.

Allylindiums represent an attractive class of allyl metals due to their low toxicity, high functional group tolerance, and selectivity profile. A number of diclosures report high efficiency in allyl transfer reactions to *N*-acyl hydrazones under Barbier-type conditions in which the allylindium species are produced *in situ* from allylic halides and super stoichiometric quantities of In^0 (1.75–3.0 equivalents).[26] Sulfinamide urea catalyst **2.8** pairs a Lewis basic sulfoxide terminus, to activate the allylindium species, with a Lewis acidic urea to engage the benzoyl hydrazone in hydrogen–bonding.[25b] Aryl and

[26] For catalytic enantioselective approaches which *in situ* generate allylindium species from allyl halides and super stoichiometric amounts of In (0), see: (a) "Catalytic Enantioselective Indium-Mediated Allylation of Hydrazones," Cook, G. R.; Kargbo, R.; Maity, B. *Org. Lett.* **2005**, *7*, 2767–2770. (b) "Indium-Mediated Asymmetric Allylation of Acylhydrazones Using a Chiral Urea Catalyst," Tan, K. L.; Jacobsen, E. N. *Angew. Chem., Int. Ed.* **2007**, *46*, 1315–1317. (c) "Readily Accessible, Modular, and Tuneable BINOL 3,3'-Perfluoroalkylsulfones: Highly Efficient Catalysts for Enantioselective In-Mediated Imine Allylation," Kargbo, R.; Takahashi, Y.; Bhor, S.; Cook, G. R.; Lloyd-Jones, G. C.; Shepperson, I. R. *J. Am. Chem. Soc.* **2007**, *129*, 3846–3847. (d) "Indium-Mediated Catalytic Enantioselective Allylation of *N*-Benzoylhydrazones Using a Protonated Chiral Amine," Kim. S. J.; Jang, D. O. *J. Am. Chem. Soc.* **2010**, *132*, 12168–12169.

Scheme 2.5 Indium-Mediated Enantioselective Allyl Addition to Hydrazones Using a Chiral Urea Catalyst

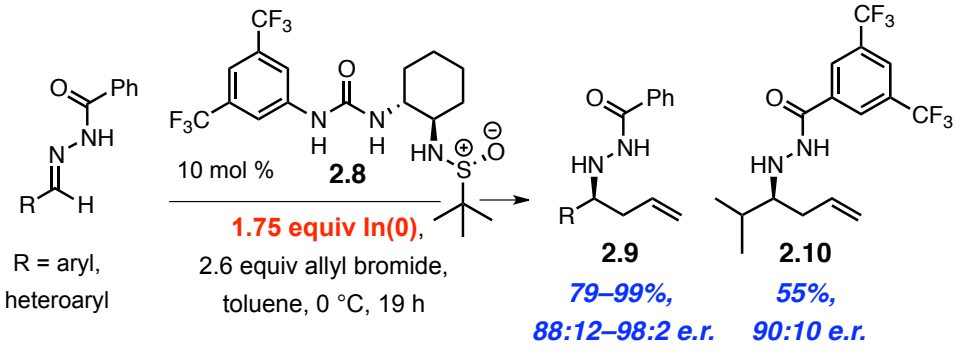

heteroaryl-substituted hydrazines **2.9** are afforded in 79–99% yield and 88:12–98:2 e.r., while reactions of aliphatic hydrazones prove less selective (<75:25 e.r.). Use of a more electron deficient *N*-acyl group and performing the reaction at –40 °C allows access to *iso*-propyl substituted **2.10** in 55% yield and 90:10 e.r. (Scheme 2.5).

Rather than use superstoichiometric equivalents of indium(0), Kobayashi and coworkers discovered that an allylindium species could be generated *in situ* with a *catalytic quantity* of indium iodide and allyl boronic acid pinacol ester **2.11**.[27] The generated chiral In(I)–semicorrin **2.12** complex promotes reaction with aryl- and heteroaryl-substituted *N*-benzoyl hydrazones to afford allyl adducts **2.13** in >88% yield and in 92:8–98:2 e.r. (Scheme 2.6). However, cyclohexyl-bearing **2.14** is obtained with diminished selectivity of 65:35 e.r.. A similar strategy to generate a chiral allylindium(I) species from allylboron **2.11** is used for reactions with *N,O*-aminals; generated iminium

[27] For catalytic enantioselective methods which *in situ* generate allylindium species from allylboronic acid pinacol ester and *catalytic* amounts of InI, see: (a) "Indium(I)-Catalyzed Asymmetric Allylation, Crotylation, and α-Chloroallylation of Hydrazones with Rare Constitutional and High Configurational Selectivities," Chakrabarti, A.; Konishi, H.; Yamaguchi, M.; Schneider, U.; Kobayashi, S. *Angew. Chem., Int. Ed.* **2010**, *49*, 1838–1841. (b) "A Catalytic Asymmetric Borono Variant of Hosomi–Sakurai Reactions with N,O-Aminals," Huang, Y-Y.; Chakrabarti, A.; Morita, N.; Schneider, U.; Kobayashi, S. *Angew. Chem., Int. Ed.* **2011**, *50*, 11121–11124.

Scheme 2.6 Indium-Catalyzed Enantioselective Reactions of Allylborons and Hydrazones

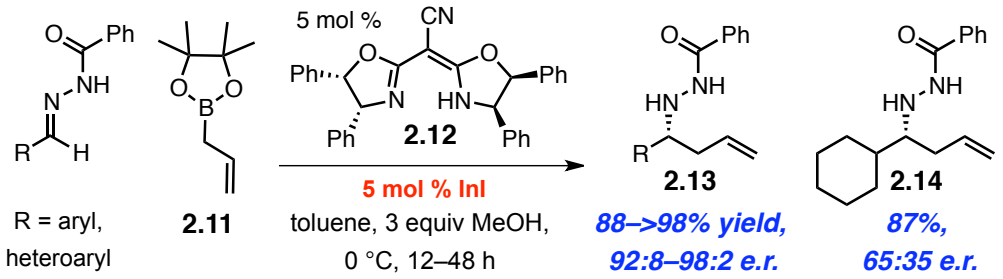

ions are paired with a chiral counterion catalyst to afford the homoallylic amides in excellent yields and selectivities.[26b] Although allylindiums display unique levels of reactivity and selectivity, the long-term sustainability of indium-promoted transformations is contentious, particularly due to the rising application of indium tin oxide in emerging technologies such as touch panels, and plasma and liquid crystal displays.[28]

Boron-based allyl reagents,[29] like **2.11** used for transmetalation to indium, are readily accessible or commercially available, stable, and environmentally benign. Although allylboronic acid derivatives are not intrinsically highly nucleophilic (HOMO is not high in energy), the partially empty p orbital on boron provides a handle for their activation towards allyl transfer. There are two strategies often employed with allylboron reagents to increase the rate of their transmetalation or allylboration; either, treatment with a mild Lewis base, to complex with the p-orbital of the boron center, or, the action of a Lewis acid, to coordinate the oxygen of B–O bond. Both methods engender higher

[28] Prices of indium will continue to soar as its demand for use in technologies rises, see: "Managing the Scarcity of Chemical Elements," Nakamura, E.; Sato, K. *Nature Mater*. **2011**, *10*, 158–161.
[29] (a) "Organoboron Compounds as Mild Nucleophiles in Lewis Acid- and Transition Metal-catalyzed C–C Bond-forming Reactions," Batey, R. A.; Quach, T. D.; Shen, M.; Thadani, A. N.; Smil, D. V.; Li, S-W.; MacKay, D. B. *Pure Appl. Chem*. **2002**, *74*, 43–55. For a comprehensive analysis of boronic acids and their derivatives, see: (b) Hall, D. G. *Boronic Acids:Preparation and Applications in Organic Synthesis, Medicine and Materials, 2nd Edition*; Wiley-VCH: Weinheim, Germany, **2011**.

reactivity as a result of a more electron deficient boron center. For example, allylborations proceed rapidly with aldehydes as the Lewis basic carbonyl can coordinate boron, raising the electron density at the allyl group, leading to a Zimmerman-Traxler-type cyclic transition state.[28] Allylborations, however, do not occur as readily with aldimines; the C=N bond is less polarized and, as such, imines are much weaker Lewis bases and therefore do not engender enough activation.[30] Catalysts that take advantage of the unique properties of the Lewis acidity of boron to realize enantioselective allyl transfers to imines have recently been disclosed.

The lability of acyclic dialkoxyallylboron **2.16** is exploited in allylborations catalyzed by a chiral biphenol **2.17** described by Schaus and coworkers.[31] When the diol catalyst exchanges with the *iso*-propoxy units of the boron reagent,[32] the Lewis acidity at boron increases, a result of the inferior electron donation and overlap between the phenolic oxygen lone pairs and the empty boron p orbital. Catalyst-bound allylboron is activated for coordination of the *N*-acyl imine for an ensuing chair-like transition state for transfer of the allyl group. A broad range of substitution on the imine is tolerated producing **2.18a**–**2.18f** in 80–87% yield and >95:5 e.r. (Scheme 2.7). The benzoyl group on the imine serves to withdraw electron density, aiding *N*-coordination, and, is

---

[30] Discovery of a unique catalyst structure to promote allylborations of imines to overcome the low reactivity will be discussed in Chapter 4.

[31] (a) "Asymmetric Allylboration of Acyl Imines Catalyzed by Chiral Diols," Lou, S.; Moquist, P. N.; Schaus, S. E. *J. Am. Chem. Soc.* **2007**, *129*, 15398–15404. For the catalysis of allyl additions to ketones, see: (b) "Asymmetric Allylboration of Ketones Catalyzed by Chiral Diols," Lou, S.; Moquist, P. N.; Schaus, S. E. *J. Am. Chem. Soc.* **2006**, *128*, 12660–12661. (c) "The Mechanism and an Improved Asymmetric Allylboration of Ketones Catalyzed by Chiral Biphenols," Barnett, D. S.; Moquist, P. N.; Schaus, S. E. *Angew. Chem., Int. Ed.* **2009**, *48*, 8679–8682. For catalyzed additions of other organoborons (besides allyl) to imines, see: (d) "Enantioselective Addition of Boronates to Acyl Imines Catalyzed by Chiral Biphenols," Bishop, J. A.; Lou, S.; Schaus, S. E. *Angew. Chem., Int. Ed.* **2009**, *48*, 4337–4340.

[32] Schaus postulates that there is only mono-displacement, leaving one phenol free for H-bonding (see inset of Scheme 2.7), however, computational studies on the allylboration of ketones suggest that a small quantity of a more active cyclic bisphenolic allylboron is formed. See, "Mechanistic Insights into the Catalytic Asymmetric Allylboration of Ketones: Brønsted of Lewis Acid Activation?" Paton, R. S.; Goodman, J. M.; Pellegrinet, S. C. *Org. Lett.* **2009**, *11*, 37–40.

Scheme 2.7 Enantioselective Allylboration of Benzoyl Imines Catalyzed by Chiral BINOL Derivatives

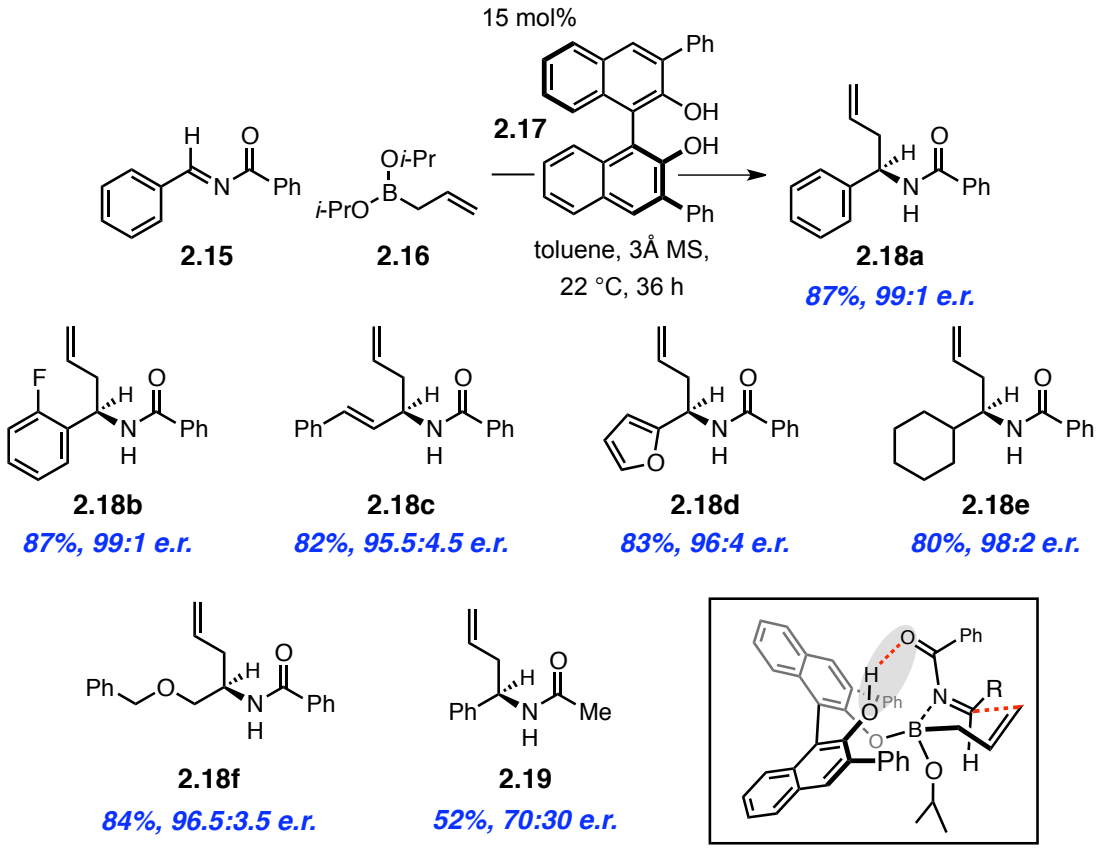

postulated to engage the phenolic proton in H–bonding in the transition state for C–C bond formation (see inset); imines bearing weaker H-bond acceptors, such as carbamates or an acetyl group, are less efficient and selective (**2.19** in 52% yield and 70:30 e.r.). Despite the significant advance represented by this method for the stereoselective generation of homoallylic amides, the inefficiency of imine allylboration is pronounced through the elongated reaction times, high catalyst loadings, and the required use of highly activated and protolytically unstable reacting partners.

Mild activation of allylboron reagents can also result in facile transmetalation to metals, a strategy that has been invoked for enantioselective metal-catalyzed allyl group

additions to imines.[33] In this regard, Shibasaki has developed Cu–phosphine complexes that engage allylboron **2.11** to *in situ* prepare phosphine–Cu-allyl complexes capable of generating *O*- or *N*-substituted quaternary carbon stereogenic centers.[34] Aryl-substituted *N*-benzyl ketoimines are transformed to the derived homoallylic amines **2.22** in 82–97% yield and 91:9–96.5:3.5 e.r. (Scheme 2.8). Kinetic studies indicate the transmetalation event leading to the bisphosphine–Cu-allyl complex to be rate-limiting. Rate acceleration is noted with the incorporation of 30 mol % lithium *iso*-propoxide suggesting that either the fluoride or *iso*-propoxide anions can expedite alkylation of the copper through the

Scheme 2.8 Enantioselective Cu-Catalyzed Allyl Additions to Ketoimines

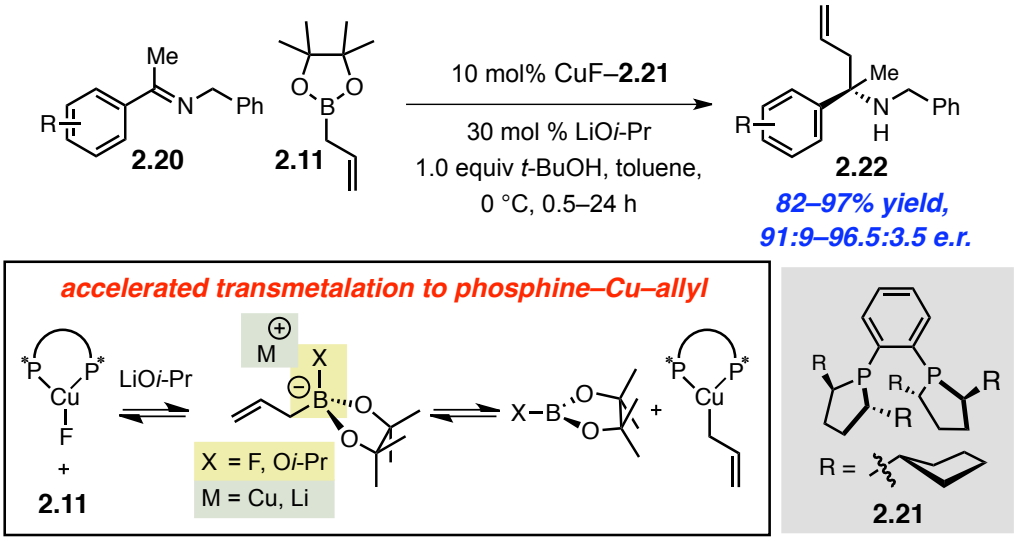

[33] For examples describing catalytic enantioselective transformations that make use of transmetalation events with allylborons, see: (a) "Zinc-Catalyzed Asymmetric Allylation for the Synthesis of Optically Active Allylglycine Derivatives. Regio- and Stereoselective Formal α-Addition of Allylboronates to Hydrazono Esters," Fujita, M.; Nagano, T.; Schneider, U.; Hamada, T.; Ogawa, C.; Kobayashi, S. *J. Am. Chem. Soc.* **2008**, *130*, 2914–2915. (b) "Enantioselective Rhodium-Catalyzed Nucleophilic Allylation of Cyclic Imines with Allylboron Reagents," Luo, Y.; Hepburn, H. B.; Chotsaeng, N.; Lam, H. W. *Angew. Chem., Int. Ed.* **2012**, *51*, 8309–8313.

[34] (a) "Catalytic Enantioselective Allylboration of Ketones," Wada, R.; Oisaki, K.; Kanai, M.; Shibasaki, M. *J. Am. Chem. Soc.* **2004**, *126*, 8910–8911. (b) "Catalytic Enantioselective Allylation of Ketoimines," Wada, R.; Shibuguchi, T.; Makino, S.; Oisaki, K.; Kanai, M.; Shibasaki, M. *J. Am. Chem. Soc.* **2006**, *128*, 7687–7691. (c) "Cu(I)-catalyzed Asymmetric Allylation of Ketones and Ketimines," Kanai, M.; Wada, R.; Shibuguchi, T.; Shibasaki, M. *Pure Appl. Chem.* **2008**, *80*, 1055–1062.

intermediacy of an sp^3-hybridized allylic borate (see boxed inset, Scheme 2.8). Despite the efficiency with which the Cu–DuPhos derivatives provide enantioenriched tertiary carbamines, the reactions to afford the corresponding secondary carbamines are not reported.

The strategies outlined for the *diastereoselective* or *enantioselective* additions of allyl units to imines are all flawed with one or more of the following limitations: inadequate substrate scope (many methods are solely effective for α-hydrazono esters while highly selective alkylations of alkyl-substituted aldimines remain a challenge), demanding chemoselective *N*-protecting group removals (several equivalents of SmI_2 are required to cleave a hydrazine[32a] and an *N*-benzoyl group[30a] can be excised with a two-step sequence involving di*iso*butylaluminum hydride and hydrochloric acid), high loadings of costly or difficult-to-access catalysts, and long reaction times. Moreover, issues pertaining to sustainability (departure from strategies reliant on palladium and indium) and practicality (use of easy to handle, non-toxic commercially available reagents) must be considered in evaluating synthetic avenues for prolonged and widespread application. Powerful new catalysts that lower the activation barrier for allyl transfer to imines are required to address the aforementioned shortcomings.

2.3 Ag-Catalysis in Allyl Addition Reactions

Analysis of the reported catalytic methods for the installation of an allyl group into a C=N bond led us to identify allylboron reagents as promising nucleophiles for new reaction development. Moreover, allyl boronic acid pinacol ester **2.11** is a commercially available and stable reagent which can be readily activated under either Lewis acid or Lewis base catalysis regimes. The bifunctional Ag-based catalysts, described in Chapter

1, are fitted with a Lewis basic *C*-terminus amide particularly efficacious for the activation of silyl-based nucleophiles[35] for Mannich-type additions, and, as such, we

Scheme 2.9 Ag-Catalyzed Allyl Additions to Imines Using Amino Acid-Based Phosphine Ligands

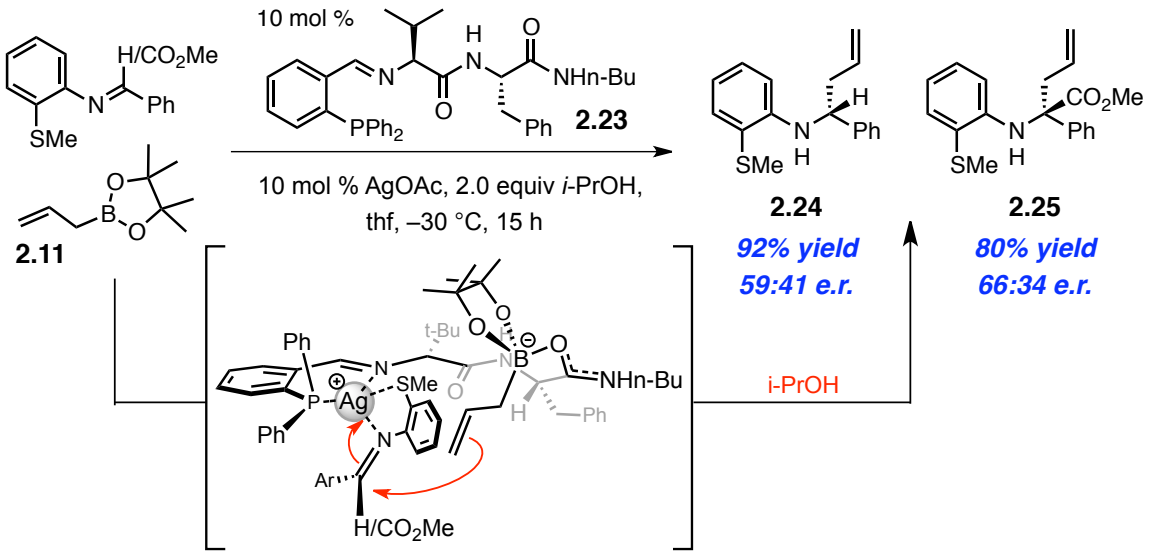

conjectured that the same activation strategy might be applicable for allylborons. The Mannich-type reactions are proposed to occur through a nucleophilic hypervalent silicon species resulting from Lewis basic complexation with the amino acid-derived catalyst. We thus postulated that, analogously, the catalyst's amide could form a Lewis acid-base adduct with the boronic ester inducing activation of the pendant allyl group (Scheme 2.9).

We found that Ag–phosphine **2.23** complex is competent in promoting reaction between allylboron **2.11** and an *N*-aryl aldimine or an α-ketoiminoester in excellent yields but with <66:34 e.r.. Reactions were believed to proceed through Lewis acidic activation of the imine through bidentate coordination with the silver center, in addition to concomitant boronate formation. This dual action of the catalyst results in induced

[35] The mechanistic investigations into this class of Ag-based catalysts are detailed in Section 1.4 of Chapter 1.

Figure 2.2 Catalyst and Additive Screening for Reactions of Allylboron with Benzaldehyde-derived *N*-Aryl Aldimine **2.26**

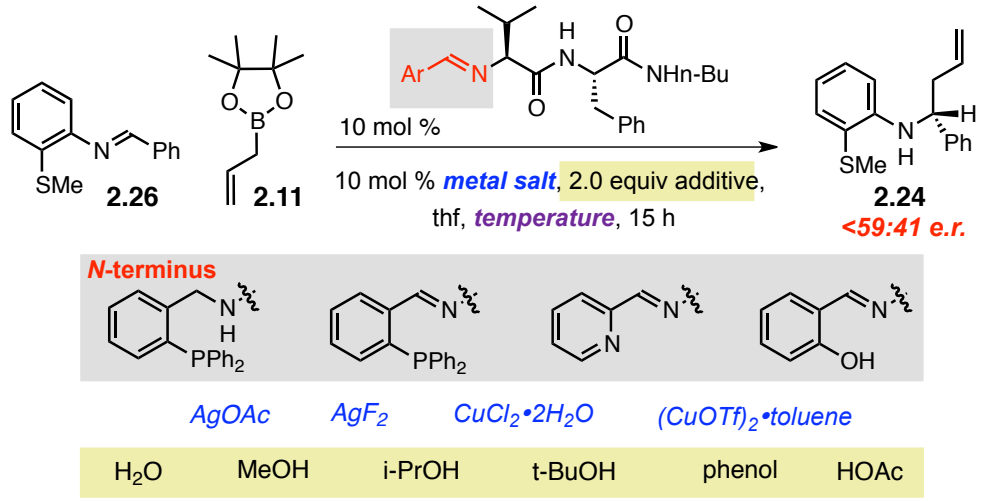

intramolecularity of the allyl transfer. The excellent efficiencies for the formation of both tertiary and quaternary stereogenic centers with measurable optical purities seemed to support the outlined mechanism for catalysis. Efforts to alter the reaction conditions, modify the catalyst structure, and/or the identity of the metal cation employed all failed to promote enhanced facial discrimination, such that catalyzed additions to *N*-aryl aldimine **2.26** were consistently obtained with poor stereoselectivity (<59:41 e.r., Figure 2.2). Investigations aimed at interpretation of the unsatisfactory stereoselectivity revealed an effective adventitious allyl addition when the reaction is performed with catalytic silver

Figure 2.3 Postulated Decomposition Pathway of Ag–allyl Species Resulting in Uncatalyzed Allyl Additions

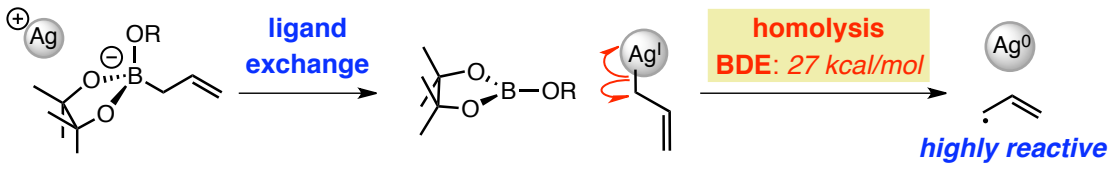

the absence acetate in of a chiral ligand;[36] this competitive uncatalyzed process can rationalize the low stereoinduction. It is likely that unligated silver acetate can react with an activated tetrahedral allyl boronate[37] in a ligand exchange process generating allylsilver (Figure 2.3). This unstable organometallic species, prone to Ag–C bond

Figure 2.4 Bond Homolysis Energies for Allylic Compounds

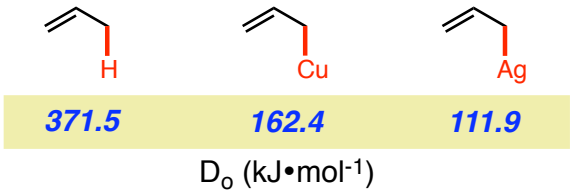

calculated BDEs at the M06/SDD:6-31+G(d) level

homolysis (D_o = 111.9 kJ/mol,[37c] Figure 2.4), collapses leading to reduction of the metal salt to Ag^0 and formation of a highly reactive allyl radical, capable of reacting with the imine unsaturation without catalysis.[38]

Mechanistic understanding accrued on a similar class of Ag–phosphine complexes described in Chapter 1, revealed the dynamic nature and lability of phosphine complexation.[39] An uncatalyzed pathway, which can be initiated by a minute

---

[36] Notably, visible inspection of the reaction appears to have resulted in reduction of the Ag(I) salt to metallic silver (silver mirror formation on the reaction vessel).

[37] Mild activation of the allyl boron can occur with the alcohol additive, *iso*propanol, or with coordinating solvent molecules, tetrahydrofuran.

[38] Organosilver compounds are known to be more susceptible to bond homolysis, calculated and experimental bond dissociation energies are lower in comparison to other corresponding organometallics. For theoretical approaches to understanding the stability of various organometallic reagents, see: (a) "Theoretical Studies of the First– and Second–row Transition-metal Methyl and Their Positive Ions," Bauschlicher, C. W., Jr.; Langhoff, S. R.; Partridge, H.; Barnes, L. A. *J. Chem. Phys.* **1989**, *91*, 2399–2411. (b) "Alkyl Coupling on Copper, Silver, and Gold: Correlation Between the Coupling Rate and the Metal–Alkyl Bond Strength," Paul, A.; Bent. B. E. *J. Catal.* **1994**, *147*, 264–271. (c) "Theoretical Approaches to Estimating Homolytic Bond Dissociation Energies of Organocopper and Organosilver Compounds," Rijs N. J.; Brookes, N. J.; O'Hair, R. A. J.; Yates, B. F. *J. Phys. Chem. A* **2012**, *116*, 8910–8917.

[39] Multinuclear spectroscopy of tetrahydrofuran solutions of amino acid-based triarylphosphines and silver acetate provided evidence of rapidly equilibrating mixtures of mono-phosphine and bis-phosphine ligated complexes at temperatures above –50° C.

concentration of free silver(I) available by facile triarylphosphine dissociation,[40] may be too robust for catalyzed additions to outcompete. Due to facile transmetalation of allylborons and the facility of decomposition of organosilver compounds, we concluded that the mechanistic picture in Scheme 2.9 would not likely constitute an effective solution for the enantioselective synthesis of homoallylic amines.

We postulated that more effective stabilization of the generated allylic metal, alongside stronger coordination to discourage ligand dissociation, may lead to the discovery of a reliable allyl transfer catalyst. *N*-Heterocyclic carbenes[41] (NHCs), a class of ligands recognized for a higher degree of σ-donation than phosphines, were subsequently considered. NHCs can be generated through deprotonation of an imidazolium or

Figure 2.5 *N*–Heterocyclic Carbenes as Strong σ-Donors

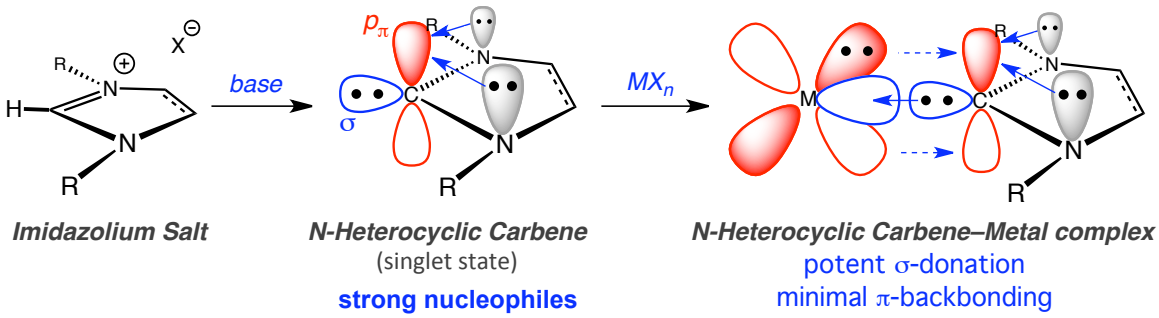

[40] Allyl radical formation can also originate from Ag–C bond homolysis from the chiral phosphine-ligated Ag^{I}–allyl complex. However, the Ag–C should be electronically stabilized through σ–donation from the phosphine.

[41] For reviews outlining the utility of *N*-Heterocyclic carbenes (NHCs) in organometallic chemistry and catalysis, see: (a) "Stable Carbenes," Bourissou, D.; Guerret O.; Gabbaï, F. P.; Bertrand, G. *Chem. Rev.* **2000**, *100*, 39–91. (b) "*N*-Heterocyclic Carbenes: A New Concept in Organometallic Catalysis," Herrmann, W. A. *Angew. Chem., Int. Ed.* **2002**, *41*, 1290–1309. (c) "Coinage Metal–*N*-Heterocyclic Carbene Complexes," Lin, J. C. Y.; Huang, R. T. W.; Lee, C. S.; Bhattacharyya, A.; Hwang, W. S.; Lin, I. J. B. *Chem. Rev.* **2009**, *109*, 3561–3598. (d) "Ag(I) *N*-Heterocyclic Carbene Complexes: Synthesis, Structure, and Application," Garrison, J. C.; Youngs, W. J. *Chem. Rev.* **2005**, *105*, 3978–4008. (e) "Heterocyclic Carbenes: Synthesis and Coordination Chemistry," Hahn, F. E.; Jahnke, M. C. *Angew. Chem., Int. Ed.* **2008**, *47*, 3122–3172. (f) "*N*-Heterocyclic Carbenes in Late Transition Metal Catalysis," Díez-González, S.; Marion, N.; Nolan, S. P. *Chem. Rev.* **2009**, *109*, 3612–3676. (g) "Understanding the M–(NHC) (NHC = *N*-Heterocyclic Carbene) Bond," Jacobsen, H,; Correa, A.; Poater, A.; Costabile, C.; Cavallo, L. *Coord. Chem. Rev.* **2009**, *253*, 687–703. (h) "The Measure of All Rings–*N*-Heterocyclic Carbenes," Dröge, T.; Glorius, F. *Angew. Chem., Int. Ed.* **2010**, *49*, 6940–6952.

imidazolinium salt, the resultant divalent carbon is sp^2-hybridized and the singlet state, in which two electrons reside in the σ orbital, is normally the lowest energy configuration. Triplet state configurations, with electrons occupying the p_π orbital, are significantly raised in energy due to filled-filled interactions arising from the flanking *N*–lone pairs. Diaminocarbenes that reside in five-membered rings, such that *N* nonbonding electron pairs are aligned for optimal delocalization, exist as singlet state carbenes of increased stability, a feature that accounts for the potency of their electronic donation (Figure 2.5). NHCs can serve as nucleophiles or ligands for metal complexes and often exhibit strong σ-donation and minimal π-backbonding (flow of electron denisity from metal into the NHC ligand: $d^{metal} \rightarrow p_\pi$). In our efforts to study the activation of allylboron reagents for additions to carbonyl derivatives, we surmised that we could utilize the unique properties of NHCs as *both* nucleophilic organocatalysts[42] and as stabilizing features in metal complexes.[40]

Firstly, chiral *N*-heterocyclic carbene–Ag complexes were investigated in allyl addition reactions with the expectation that preisolated carbene–Ag complexes would not undergo dissociation to the free silver salt.[43] The electronic stabilization imparted by the NHC ligand (vs. triarylphosphine **2.23**) could potentially eradicate the issues with uncatalyzed allyl additions, presumably a result of decomposition of the allylmetal to allyl radical species. Unfortunately, reactions promoted by **NHC–Ag I–III** afford homoallylic amine **2.24** in up to >98% conversion but in <55:45 e.r. (Scheme 2.10). It is

[42] For reviews outlining organic transformations promoted by NHCs, see: (a) "Organocatalysis by *N*-Heterocyclic Carbenes," Enders, D.; Niemeier, O.; Henseler, A. *Chem. Rev.* **2007**, *107*, 5606–5655. (b) "*N*-Heterocyclic Carbenes as Organocatalysts," Marion, N.; Díez-González, S.; Nolan, S. P. *Angew. Chem., Int. Ed.* **2007**, *46*, 2988–3000. (c) "Synthesis and Reactions of *N*-Heterocyclic Carbene Boranes," Curran, D. P.; Solovyev, A.; Brahmi, M. M.; Fensterbank, L.; Malacria, M.; Lacôte, E. *Angew. Chem., Int. Ed.* **2011**, *50*, 10294–10317.

[43] NHC dissociation values for NHC–Ag-Cl complexes are calculated to be ~53 kcal/mol, see: "The Significance of p Interactions in Group 11 Complexes with N-Heterocyclic Carbenes," Nemcsok, D.; Wichmann, K.; Frenking, G. *Organometallics* **2004**, *23*, 3640–3646.

possible that the electronic donation of the carbene ligands cannot overcome the low energetic barriers to Ag–C bond dissociation. As such, silver-based catalysts, due to the

Scheme 2.10 NHC–Ag-Catalyzed Allyl Additions to Imines

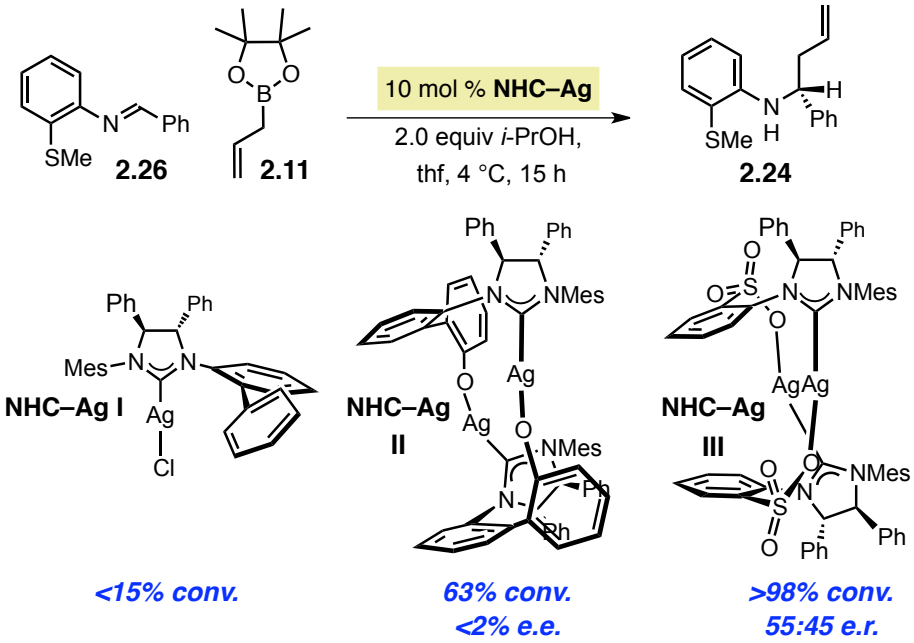

instability of the nucleophilic intermediates involved, are unlikely to provide a solution for enantioselective C–C bond formation in this context. Hence, new catalysts, that activate allylboron reagents to provide stable, yet nucleophilic, species were sought.

2.4 Lewis Bases as Potent Catalysts for C–B Bond Activation

The ensuing studies concentrated on utilizing the nucleophilic character of *N*-heterocyclic carbenes to function as Lewis basic activators of boron-based allyl reagents. We hypothesized that the ensuing electronic reorganization of the derived Lewis base-Lewis acid complex would sufficiently raise the energy of the HOMO of the allyl group for additions to imines; the C–C bond-formation could then be rendered enantioselective through action of a chiral NHC. We had previously demonstrated the capacity of an NHC

Scheme 2.11 Activation of a B–B Bond for Conjugate Additions to Enones through Catalysis with an NHC.

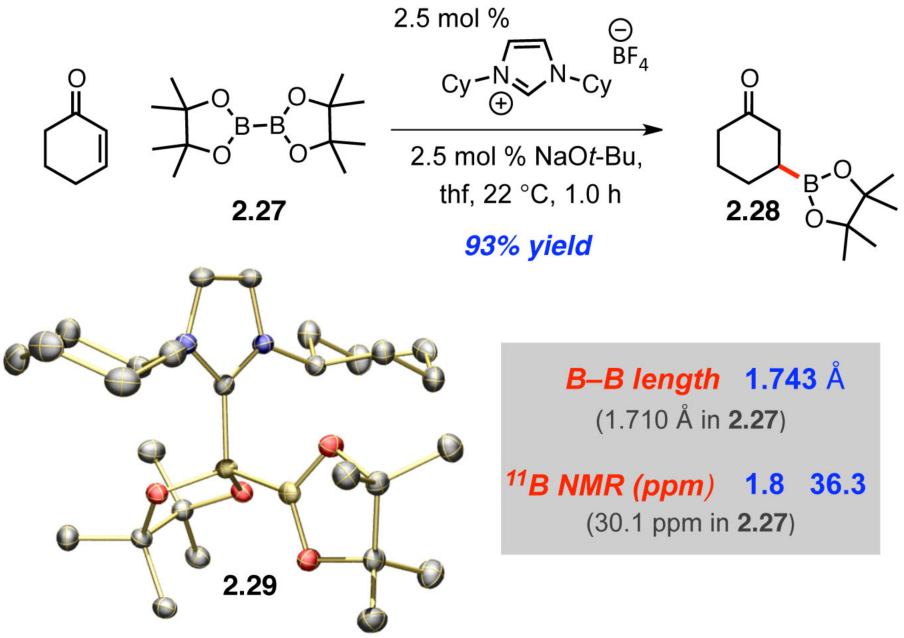

to complex with an empty p-orbital of a diboron reagent. Complexation led to adequate activation of the B–B bond to catalyze nucleophilic boron conjugate additions to enones (Scheme 2.11).[44] A Lewis base-acid adduct of the biscyclohexyl-substituted carbene with diboron reagent **2.27** was postulated to be the catalytically active nucleophilic intermediate and its existence was investigated spectroscopically. The observed singlet at δ 30.1 ppm for **2.27** in the ^{11}B NMR spectra disappears when the diboron reagent is treated with a carbene, resulting in two new distinct peaks. The new chemical shifts of 36.3 and 1.8 ppm, suggestive of one sp^2 and an sp^3-hybridized boronate respectively, correlate well with expected shifts for complex **2.29**. The electronic reorganization resulting from Lewis basic activation of the bound boron causes electron density to

[44] "Efficient C–B Bond Formation Promoted by *N*-Heterocyclic Carbenes: Synthesis of Tertiary and Quaternary B-Substituted Carbons through Metal-Free Catalytic Boron Conjugate Additions to Cyclic and Acyclic α,β-Unsaturated Carbonyls," Lee, K-s.; Zhugralin, A. R.; Hoveyda, A. H. *J. Am. Chem. Soc.* **2009**, *131*, 7253–7255. And a correction published in: *J. Am. Chem. Soc.* **2010**, *132*, 12766.

cumulate on the unchelated sp^2-hybridized boron center. Furthermore, the B–B bond is weakened by the σ-donation of the NHC, ultimately leading to reaction with the low-lying LUMO of the enone, generating β-boryl cyclic ketones, such as **2.28**, in excellent yields. The hypothesized Lewis base-acid adduct **2.29** was later corroborated with an X-ray crystal structure; from this structure we observe an elongation of the B–B bond from 1.710 Å in native diboron **2.27** to 1.743 Å when complexed.[45] This lengthening is indicative of a weakened B–B bond and is clearly induced through electronic activation by the carbene catalyst. Furthermore, this catalytic process was successfully rendered enantioselective; a chiral NHC was shown to effectively control the facial selectivity of boron conjugate addition.[46]

Analogous to activation of the B–B bond of a diboron reagent to enhance its nucleophilicity, we envisioned *N*-heterocyclic carbenes functioning as Lewis basic catalysts to promote activation of the C–B bond of an allylboron reagent. Preliminary calculations[47] supported the feasibility of complexation between the Lewis acidic boron center of **2.11** with an NHC, as well as the desired resultant electronic reorganization. The calculated partial atomic charges on the allyl unit in adduct **2.30** are increased from the inherent charges on parent **2.11** (Figure 2.6), this electronic disparity is consistent with the expected electronic distribution characteristic of Lewis base-bound Lewis acids

---

[45] For characterization of adduct **2.28** with spectroscopic evidence which correlate well with our own observed results, see: "Spectroscopic and Structural Characterization of the CyNHC Adduct of B_2pin_2 in Solution and in the Solid State," Kleeberg, C.; Crawford, A. G.; Batsanov, A. S.; Hodgkinson, P.; Apperley, D. C.; Cheung, M. S.; Lin, Z.; Marder, T. B. *J. Org. Chem.* **2012**, *77*, 785–789.

[46] For an application of NHC catalysis for the enantioselective construction of β-boryl ketones, see: "Metal-Free Catalytic Enantioselective C–B Bond Formation: (Pinacolato)boron Conjugate Additions to α,β-Unsaturated Ketones, Esters, Weinreb Amides, and Aldehydes Promoted by Chiral N-Heterocyclic Carbenes," Wu, H.; Radomkit, S.; O'Brien, J. M.; Hoveyda, A. H. *J. Am. Chem. Soc.* **2012**, *134*, 8277–8285.

[47] I am grateful to my colleague Dr. A. R. Zhugralin for performing these revealing computational studies in the earlier phases of my study.

Figure 2.6 *N*-Heterocylic Carbenes as Lewis Basic Activators of Allylboron **2.11**

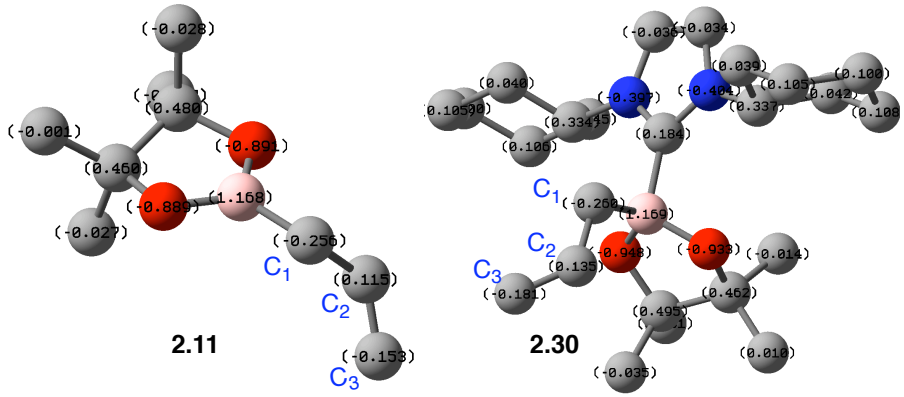

comparison of partial atomic charges			
C_1	–0.256	C_1	–0.260
C_2	0.115	C_2	0.135
C_3	–0.153	C_3	–0.181

B98/6–311G(d,p) + on N and O, Cioslowski GAPT charges

(electron density is diverged from the Lewis acid to its more electronegative ligands).[48]

Moreover, spectroscopic evidence of the formation of adduct **2.30** was observed. The ^{11}B NMR spectrum of a solution of allylboron **2.11** treated with biscyclohexyl-bearing NHC reveals almost complete consumption of the allylboron reagent (δ = 31.2 ppm) with the appearance of three new upfield shifts[49] between 3.98 and –2.28 ppm, chemical shifts indicative of the formation of sp^3-hybridized boronate-containing adducts. Additionally, the ^{1}H NMR spectrum of the reaction between an NHC and allylboron **2.11** is characterized by a change in the multiplicity, coupling constants, and chemical shifts representing the internal and terminal olefinic protons (Figure 2.8). The broad nature and divergence of the two terminal olefin protons may be indicative of either, the presence of

[48] "Lewis Base Catalysis in Organic Synthesis," Denmark, S. E.; Beutner, G. L. *Angew. Chem., Int. Ed.* **2008**, *47*, 1560–1638.

[49] The exact chemical shift corresponding to **2.30** is unclear as organoborons can be contaminated with minor impurities and peaks due to borosilicate glass in the NMR tube. For analysis of the composition of a boron-containing sample using ^{11}B NMR spectroscopy, see the correction in reference 42 and reference 43 for clarification.

Figure 2.7 160 MHz ^{11}B NMR of Allylboron **2.11** Treated with an *N*-Heterocylic Carbene in d_8-Tetrahydrofuran

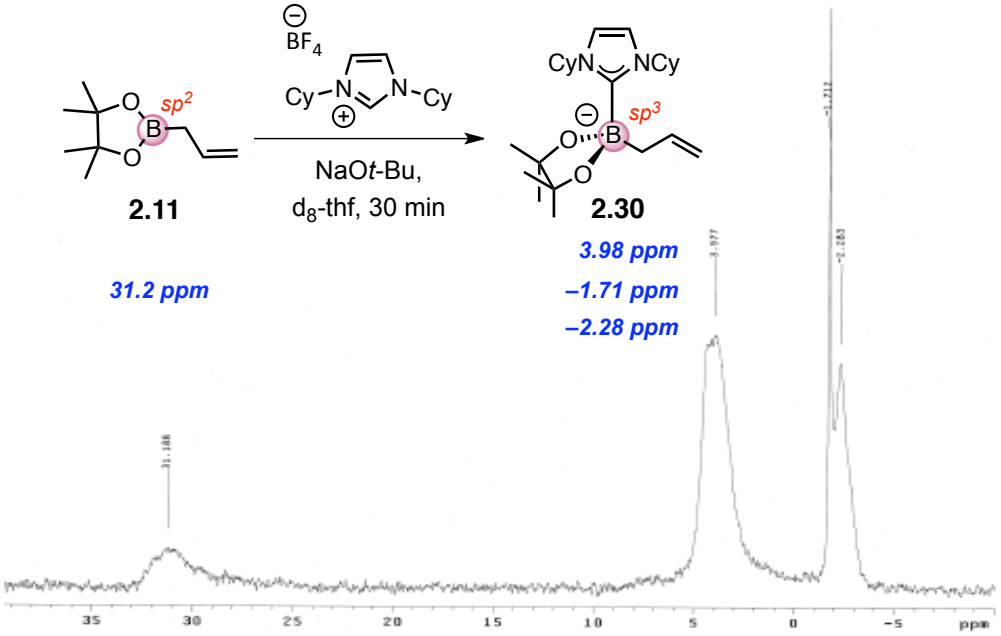

Figure 2.8 400 MHz ^{1}H NMR Spectra of Allylboron **2.11** and Its Reaction with an *N*-Heterocylic Carbene in d_8-Tetrahydrofuran

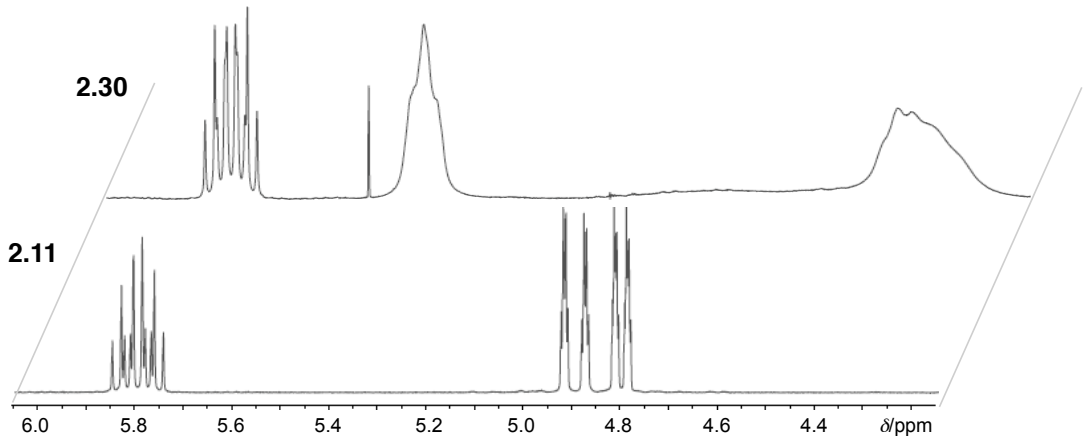

rapidly interconverting complexed species, or, an established equilibrium between ligated and unbound allylboron **2.11**. Initial investigations on the capacity for an NHC to *stoichiometrically* engage an allylboron through Lewis basic activation encouraged us to

examine whether this complexation would result in *catalytic activity* towards the promotion of allyl transfer reactions.

Promotion of reactions between allylboron **2.11** and, either diphenylphosphinoyl aldimine **2.31a**,[50] or various ketones with catalytic quantities of carbenes derived from dialkyl-substituted imidazolium salt (**ICy**), and aryl-substituted imidazolium (**IMes**) and imidazolinium (**SIMes**) salts were studied (Scheme 2.12). Although the catalyst obtained from **ICy** (the optimal NHC for boryl conjugate additions, Scheme 2.11) provides homoallylic amide **2.32a** with the highest efficiency, transformations of ketones occur at

Scheme 2.12 Efficiencies of NHC-catalyzed Reactions of Allylboron **2.11** with Aldimines and Ketones

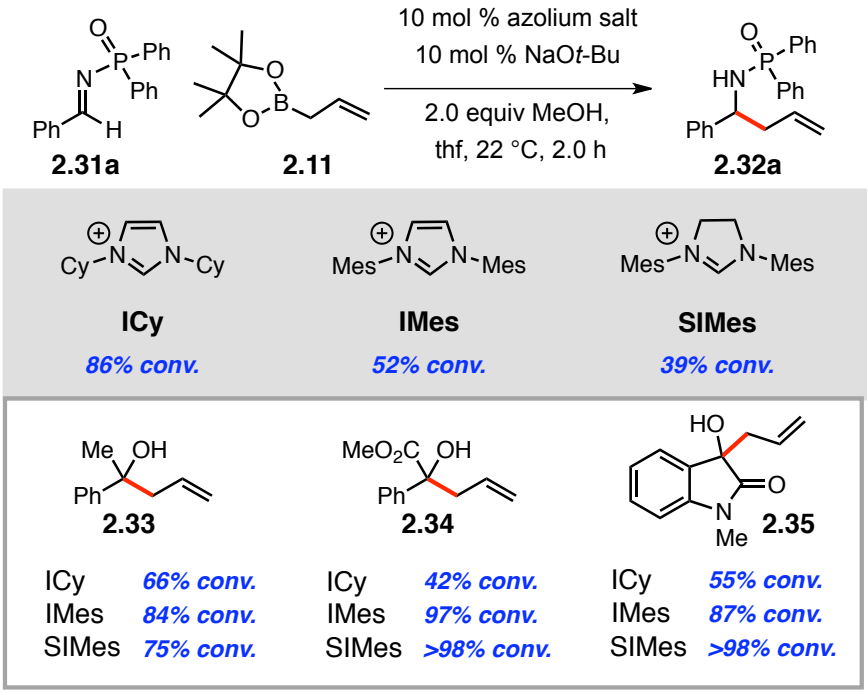

[50] Consequently, diphenylphosphinoyl aldimines were selected as substrates for their ability to react as Michael acceptors (in a 1,4-fashion), emulating the successful NHC-catalyzed boron conjugate additions (1,4) to cyclic and acyclic enones. Their increased electrophilicity, accessibility, crystallinity, and ease of deprotection led us to focus our investigations on this class of aldimines. For a review on their synthetic utility, see: "*N*–Phosphinoylimines: An Emerging Class of Reactive Intermediates for Stereoselective Organic Synthesis," Weinreb, S. M.; Orr, R. K. *Synthesis*, **2005**, *8*, 1205–1227.

accelerated rates in the presence of the carbene derived from saturated imidazolinium salt **SIMes**[51] (Scheme 2.12). Tertiary homoallylic alcohols **2.33**–**2.25** are obtained with 75 to >98% conversion within two hours.

In correspondence with our hypothesis, the described catalytic allyl addition processes promoted by NHCs are proposed to proceed through the intermediacy of NHC–allylboron complex **2.30** (Figure 2.9). The nucleophilic activation raises the electron density of the allyl unit to engage the imine or ketone in allyl transfer.[52] A product-bound boronate, generated after allyl addition, requires the action of an alcohol for protolytic release of the product and the boric acid derivative. The carbene catalyst dissociates in favor of complexation with a molecule of the more Lewis acidic allylboron **2.11**. Based

Figure 2.9 Mechanistic Proposal for NHC-catalyzed Allyl Transfer Reactions

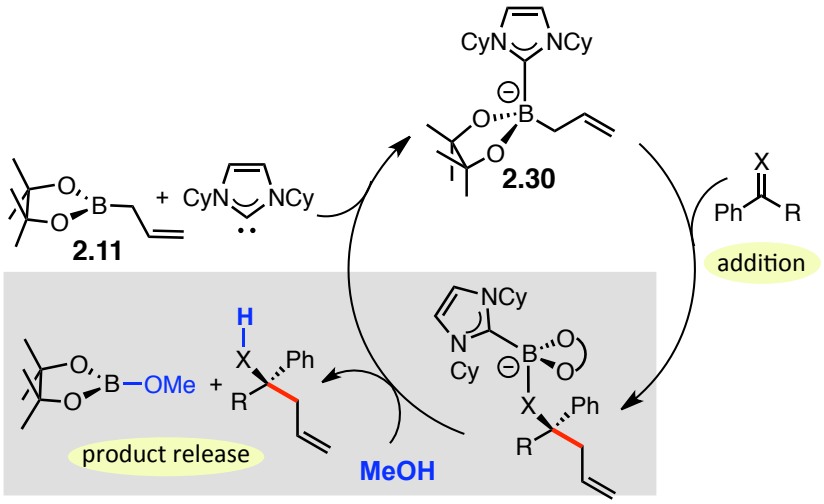

[51] The effectiveness of reactions promoted by saturated carbenes is significant since the chiral NHCs employed for the enantioselective variants are derivatives bearing a 5-membered saturated N-heterocycle.
[52] Allylborons typically react as Type I reagents with allyl group transfer occurring through closed cyclic Zimmerman-Traxler-type transition states induced by initial substrate coordination to the boron center. The active proposed boronate complex in NHC catalyzed transformations is coordinatively saturated and incapable of precomplexation. Either the mechanism has changed to a Type II addition characterized by acyclic open transition states, or, a ligand on the boronate (one of the alcohols of pinacol) can be released to allow for the Type I mechanism. For a discussion regarding mechanism and stereoselection in the context of allyl transfer reactions to carbonyl derivatives, see: "Catalytic Enantioselective Addition of Allylic Organometallic Reagents to Aldehydes and Ketones," Denmark, S. E.; Fu, J. *Chem. Rev.* **2003**, *103*, 2763–2794.

on the available transition states for the C–C bond forming step,[49] we reasoned that the chiral NHC may be too distant to influence facial discrimination of the substrate approach.

The ability for NHC catalysts to impart enantiocontrol was investigated for allyl group additions to phosphinoyl aldimine **2.31a** (Scheme 2.13). Carbenes derived from bidentate sulfonate-containing **2.36** or biphenol **2.37** provide 30 and 13% conversion respectively in two hours, while a monodentate carbene, based on bulkier C_2-symmetric imidazolinium salt **2.38**, proves ineffective. The low efficiencies observed for transformations promoted by chiral carbenes derived from sterically hindered saturated imidazolinium salts were unsurprising, considering the achiral carbene derived from **SIMes** provided the slowest reaction rate for this class of aldimine (39% conversion, Scheme 2.12). Moreover, in accordance with our concerns regarding the challenge of chirality transfer from the distally positioned stereogenicity on the catalyst, chiral NHCs afford homoallylic amide **2.32a** with poor stereoselectivity, up to 54.5:46.5 e.r. While

Scheme 2.13 Enantioselective Allyl Additions to a Phosphinoyl Aldimine with Chiral *N*-Heterocyclic Carbene Catalysts

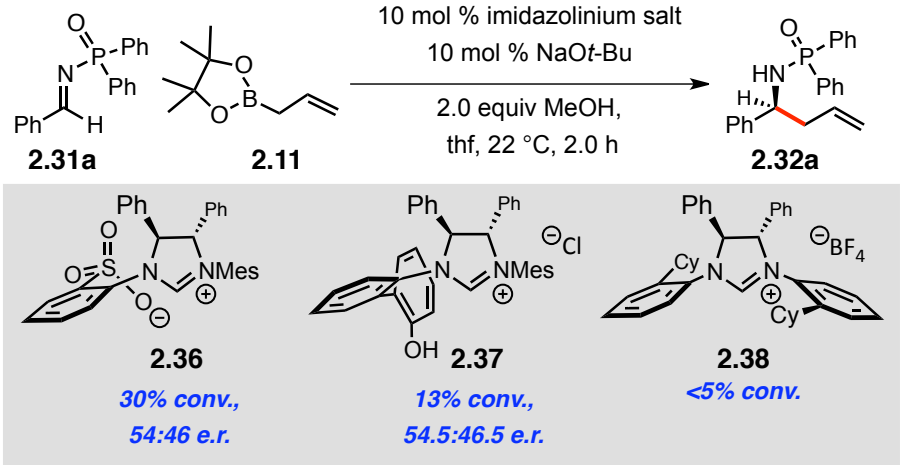

catalysis by carbenes may pose a viable strategy for reactions of ketones, the combination of low efficiency and selectivity in the synthesis of chiral amines prompted the pursuit for more reactive catalysts.

As a result of the studies towards application of *N*-heterocyclic carbenes as Lewis basic catalysts for the allyl additions to imines, we encountered that sodium *tert*-butoxide, the base utilized to *in situ* deprotonate the azolium salts, was a more competent promoter of allyl transfer from allylboron **2.11**. In the presence of 10 mol % sodium *tert*-butoxide, homoallylic amide **2.32a** is afforded in 72% conversion in two hours. The efficiency with which sodium alkoxides promote reactions of aldimines was the subject of further investigations. These studies ultimately resulted in the discovery of an amino acid-derived phenol that can promote highly efficient and selective reactions with unsaturated organoborons. The identification of the phenolic catalyst and the unique mechanism by which it operates will be described in detail in Chapter 4.

2.5 Allyl Additions Promoted by NHC–Cu Complexes

We next postulated that an organometallic allylic reagent would provide the requisite nucleophilicity, as well as afford the desired organized Zimmerman Traxler-type mechanism for allyl transfer (Type I).[51] Furthermore, an organometallic species can be suited with a chiral modifier such that it is proximal to the C–C bond formation in the six-membered transition state. Copper, an abundant, sustainable, and inexpensive Lewis acidic metal, has proven to be uniquely reactive in reactions with allylboron **2.11**[34] (in reactions of ketoimines, see Scheme 2.8). Additionally, allylcoppers, unlike the aforementioned allylsilver species, are more stable to bond dissociation (D_o = 39 vs. 27

kcal/mol[37c] for allylcopper vs. allylsilver, see Figure 2.4). We thus theorized that an NHC-based copper complex could result in a stabilized yet reactive allyl nucleophile; the NHC ligand could both impart stability to the Cu–C bond, as well as increase the electron density of the allyl unit.

In 2010, Ball and coworkers disclosed an approach for the synthesis of NHC–Cu-allyl complexes.[53] The strategy involved facile transmetalation of allylsilanes with an NHC–Cu-F complex, a thermodynamically favorable event due to the formation of a new Si–F bond (a driving force of 135 kcal/mol, see Scheme 2.14). Allyl transfers to the NHC–Cu-F complex are rapid, complete within minutes, and likely occur through a cyclic transition state after Si–F precoordination. The NHC–Cu-allyl complexes afforded are stable enough to be isolated and characterized (X-ray structure of **2.39**), yet are

Scheme 2.14 Formation of an NHC–Cu(I)-allyl Complex from Transmetalation Between Trimethoxyallylsilane and an NHC–Cu-F

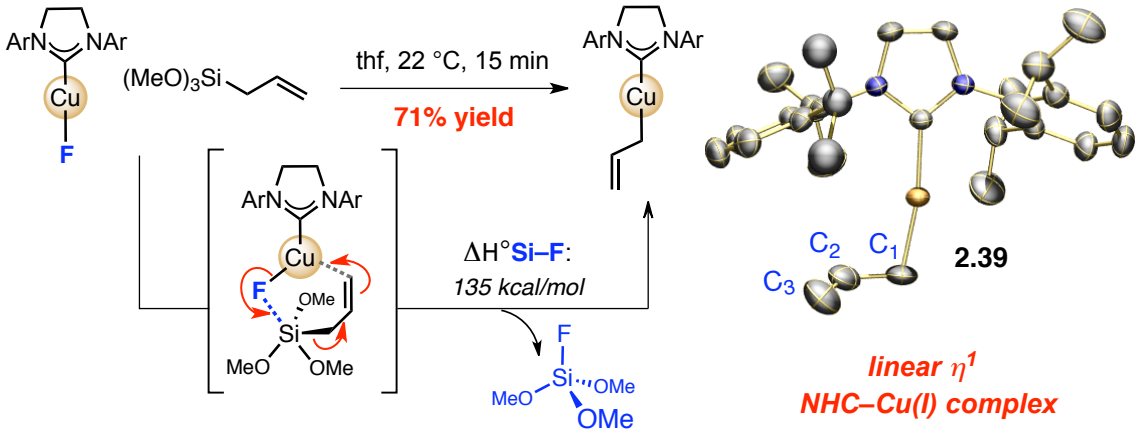

[53] For generation of NHC–Cu-allyl complexes from transmetalation of allylsilanes, see: (a) "Synthesis and Reactivity of Functionalized Arylcopper Compounds by Transmetalation of Organosilanes," Herron, J. R.; Ball, Z. T. *J. Am. Chem. Soc.* **2008**, *130*, 16486–16487. (b) "Allylcopper Intermediates with *N*-Heterocyclic Carbene Ligands: Synthesis, Structure, and Catalysis," Russo, V.; Herron, J. R.; Ball, Z. T. *Org. Lett.* **2010**, *12*, 220–223.

competent as catalytic nucleophiles for allyl additions to aldehydes.[52] The structure of the NHC-bound allylcopper **2.39** is revealed to be a nearly perfect linear η^1-allylCu(I) complex. Moreover, there is no evidence of interactions involving coordination of the π–system to the Cu center: 1) The C_2=C_3 bond length is 1.306 Å, an expected distance for a free C=C double bond, suggestive that there is no elongation from η^3 binding. 2) The dihedral angle for Cu–C_1–C_2–C_3 is 108°, an anticlinal alignment suggestive of hyperconjugation between the filled metal d orbitals and the π* molecular orbital (an electronic interaction maximized with a τ of 100°).[54] Although generation of a Si–F bond is an exceptionally favorable process, the requisite Cu–F complex requires preparation from the corresponding Cu–O*t*-Bu and buffered hydrogen fluoride, as well as glove-box techniques for their isolation and use.

In a similar vein, Sadighi and coworkers demonstrated the synthesis of NHC–Cu(I)-boryl complex **2.40** through a thermodynamically driven σ–bond metathesis event

Scheme 2.15 Formation of an NHC–Cu(I)-boryl Complex from Transmetalation Between Diboron **2.27** and an NHC–Cu-O*t*-Bu Complex

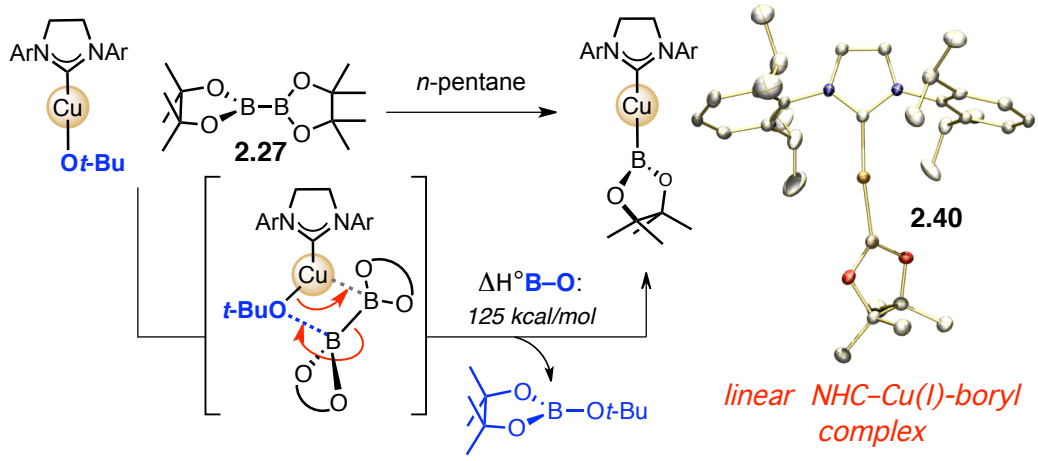

[54] For a discussion regarding the conformational aspects for (η^1-allyl)palladium complexes, see: "Umpolung of the Allylpalladium Reactivity: Mechanism and Regioselectivity of the Electrophilic Attack on Bis-Allylpalladium Complexes Formed in Palladium-Catalyzed Transformations," Szabó, K. J. *Chem. Eur. J.* **2000**, *6*, 4413–4421.

between an NHC–Cu-O*t*-Bu and the B–B bond of diboron reagent **2.27** (ΔH° B–O = 125 kcal/mol, see Scheme 2.15).[55] The *N*-heterocylic carbene ligand bestows adequate stabilization of the Cu–B bond such that complex **2.40** can be isolated and characterized, however, is sufficiently reactive to engage in insertion reactions in the presence of carbon dioxide or styrene. Based on the advances made in the reports from Ball and Sadighi, we surmised that, in an analogous fashion, a catalytic, *in situ* prepared NHC–Cu-alkoxide complex would react with the C–B bond of allylboron **2.11**, energetically driven by the formation of a B–O bond, for the generation of reactive NHC–Cu(I)-allyl species.

Copper(I) complexes, derived *in situ* from copper(I) chloride, saturated imidazolinium salt **SIMes**, and base, were discovered to catalytically promote allyl transfer reactions. In concurrence with our hypothesis, an intermediate NHC–Cu-alkoxide (generated from displacement of the Cu–Cl bond with the alkoxide base) can

Scheme 2.16 NHC–Cu(I)-Catalyzed Allyl Additions to Aldimine **2.31a** and Ketones with Allylboron **2.11**

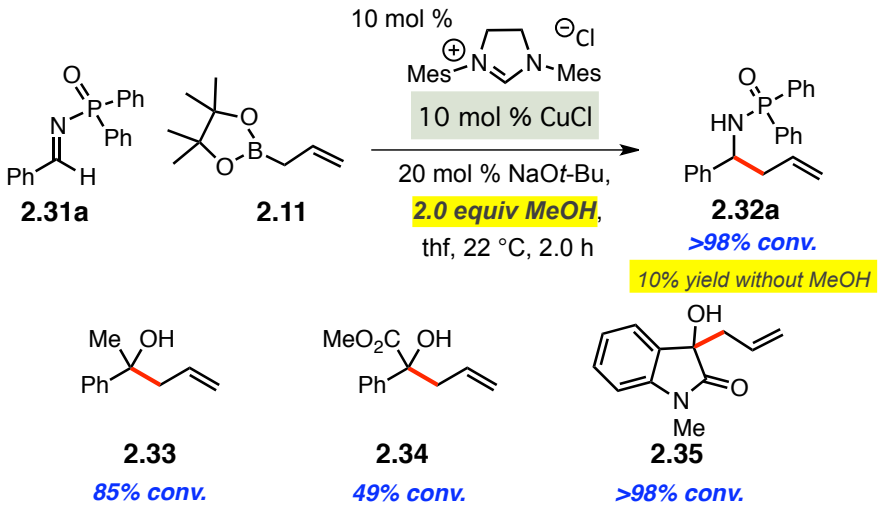

[55] (a) "Efficient Homogeneous Catalysis in the Reduction of CO_2 to CO," Laitar, D. S. Muller, P.; Sadighi, J. P. *J. Am. Chem. Soc.* **2005**, *127*, 17196–17197. (b) "Copper(I) β-Boroalkyls from Alkene Insertion: Isolation and Rearrangement," Laitar, D. S.; Tsui, E. Y.; Sadighi, J. P. *Organometallics* **2006**, *25*, 2405–2408.

react with the C–B bond to produce an NHC–Cu-allyl species nucleophilic enough to alkylate imines or ketones (Scheme 2.16). Excellent efficiencies, however, required the introduction of an alcohol additive; in the absence of methanol, NHC–Cu-catalyzed allyl addition to phosphinoylbenzaldimine affords homoallylic amide **2.32a** in 10% yield, while complete conversion is obtained after two hours with two equivalents of methanol. Methanol is postulated to be vital in the rapid regeneration of catalytically engaged NHC–Cu-OMe ***i*** (Figure 2.10). A ligand exchange event (***TS I***) between NHC–Cu-OMe ***i*** and allylboron **2.11** generates linear η^1-allylcopper intermediate ***ii***, which upon substrate coordination, transfers the allyl group through cylic ***TS II***. Reaction of the resultant NHC–Cu-amide ***iii*** with a molecule of allylboron, to directly regenerate NHC–Cu-allyl ***ii***,

Figure 2.10 Proposed Catalytic Cycle for NHC–Cu-catalyzed Allyl Transfer Reactions to Phosphinoyl Aldimine **2.31a**

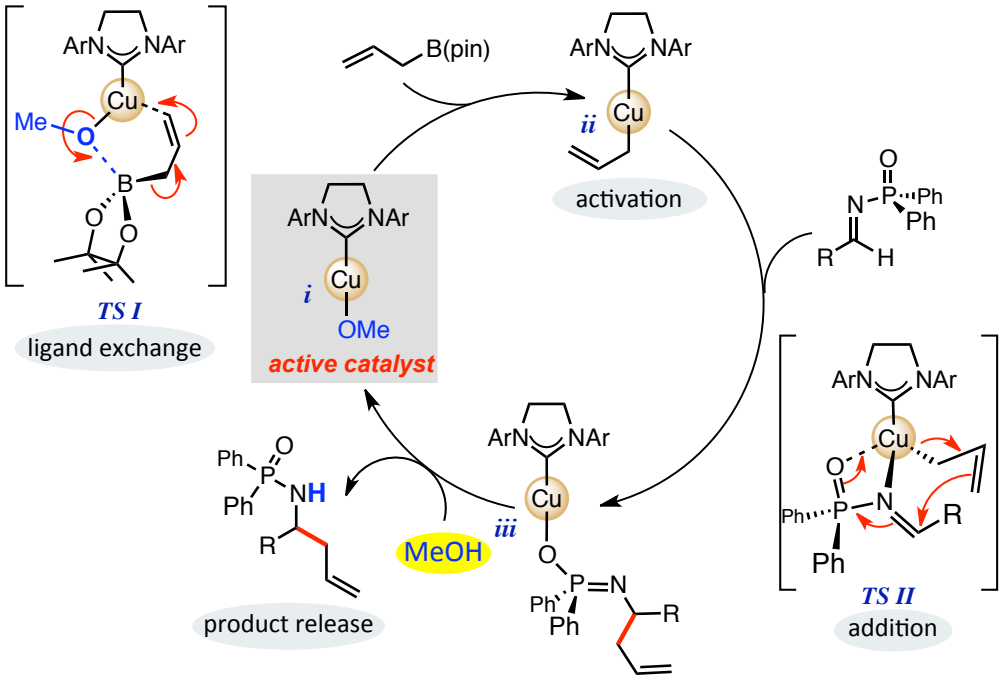

is likely unproductive. In comparison with active NHC–Cu-OMe ***i***, NHC–Cu-amide ***iii*** is presumably too hindered and electronically deactivated to coordinate allylboron **2.11** for

ligand exchange (akin to ***TS I***); instead, methanol can protolytically release the product with concomitant reestablishment of the Cu–O bond for allylboron activation. Remarkably, methanol must *chemoselectively* react with the more sterically encumbered Cu complex ***iii*** while avoiding unproductive protonation of NHC–Cu-allyl ***ii***. To justify this extraordinary selectivity, we presume the existence of a modified active Cu complex ***i***, in which the phosphinoyl imine behaves as a perpetual bidentate ligand for copper.[56] In this case, the active species would be tetrahedral substrate-bound NHC–Cu(I)-OMe

Figure 2.11 Alternative Intermediates in the Catalytic Cycle for Allyl Addition

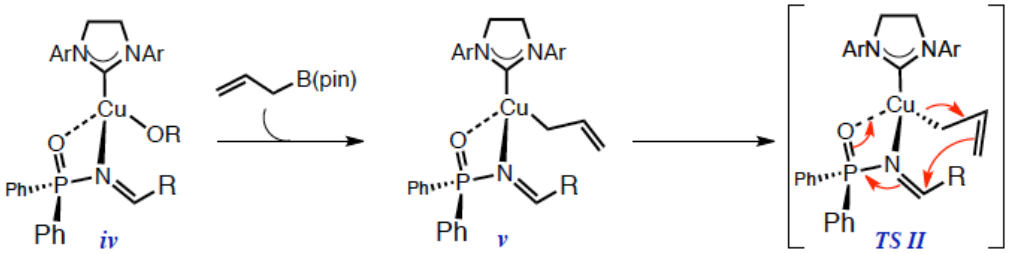

complex ***iv***, which, upon ligand exchange (OMe → allyl), would result in intermediate ***v*** poised for the C–C bond formation in ***TS II*** (Figure 2.11). In this mechanistic sequence, methanol would be less likely to react with the more hindered allylcopper ***v***, particularly if there is a low energetic barrier to ***TS II*** such that it is rapidly converted to the amide–Cu complex ***iii***. Further studies have implicated the role of methanol in facilitation of catalyst turnover; in the presence of stoichiometric NHC–Cu catalyst, in the absence of the additive, complete conversion to the homoallylic amide is observed.

NHC–Cu catalysts derived from saturated imidazolinium salts activate allylboron **2.11** to generate stable yet highly nucleophilic allyl donors. With the appropriate

[56] For evidence of the feasibility of N, O–bidentate coordination of an *N*-phosphinyl group to a Cu metal center, see: "Reactions of 3Z-Hydroxyiminoflavanone with Chlorodiphenylphosphine and 0,0-Diethylphosphorochloridite and Investigations of Cu(II) Complexing Properties," Zyner, E.; Ochocki, J.; Kostka, K. *Pol. J. Chem.* **1991**, *65*, 1829–1834.

substitution on a chiral NHC, we intended to control the facial selectivity of the allyl addition. We thus set out to investigate the ability for the chiral five-membered cyclic diaminocarbenes, derived from enantiomerically pure diphenylethylene diamine, developed in these laboratories,[57] to control the absolute configuration of the resulting homoallylic alcohols and amides (Schemes 2.17 and 2.18). Catalytic enantioselective allyl additions to *N*-methylated isatin generally proceed with excellent efficiencies (>84% conversion in two hours) to obtain 3-hydroxy-2-oxindole **2.35** with enantioselectivity levels ranging from 52:48 to 74:26 e.r. (Scheme 2.17). The catalyst proceeding from C_1-symmetric imidazolinium salt **2.43** provides the highest stereoselectivity; *meta*-methyl substitution on the biaryl ring[58] enhances facial selectivity (57:43→74:26 e.r. from **2.42** to **2.43**), however, further steric modifications at this site prove deleterious.

Transformations with acetophenone in the presence of monodentate NHC–Cu complexes produce the tertiary alcohols with >93% conversion in two hours, however, with poor levels of enantioinduction (<58:42 e.r., Scheme 2.17). Copper complexes derived from *bidentate* NHCs **2.36** and **2.37**, which likely possess a tetrahedral geometry rather than the linear orientation of monodentate NHC–Cu complexes, afford lower efficiencies and racemic homoallylic alcohol **2.33**. The chiral catalysts investigated do

---

[57] For bidentate sulfonate or phenoxy-containing chiral imidazolinium salts, see: (a) "A Readily Available Chiral Ag-Based *N*-Heterocyclic Carbene Complex for Use in Efficient and Highly Enantioselective Ru-Catalyzed Olefin Metathesis and Cu-Catalyzed Allylic Alkylation Reactions," Van Veldhuizen, J. J.; Campbell, J. E.; Giudici, R. E.; Hoveyda, A. H. *J. Am. Chem. Soc.* **2005**, *127*, 6877–6882. (b) "All-Carbon Quaternary Stereogenic Centers by Enantioselective Cu-Catalyzed Conjugate Additions Promoted by a Chiral *N*-Heterocyclic Carbene," Brown, M. K.; May, T. L.; Baxter, C. A.; Hoveyda, A. H. *Angew. Chem., Int. Ed.* **2007**, *46*, 1097–1100. For the development and application of monodentate chiral analogs, see: (c) "Monodentate Non-C_2-symmetric Chiral *N*-Heterocyclic Carbene Complexes for Enantioselective Synthesis. Cu-Catalyzed Conjugate Additions of Aryl-and Alkenylsilylfluorides to Cyclic Enones," Lee, K-s.; Hoveyda, A. H. *J. Org. Chem.* **2009**, *74*, 4455–4462.

[58] Conformational effects caused by differing substitution patterns on the *N*-aryl substituents will be discussed in greater detail in the forthcoming sections in the context of catalyst development for the catalytic enantioselective additions to phosphinoyl aldimines.

Scheme ***2.17*** Catalytic Enantioselective NHC–Cu-catalyzed Allyl Additions to Acetophenone and *N*-Me Isatin

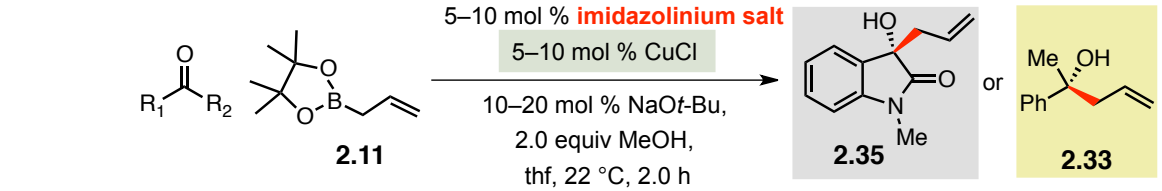

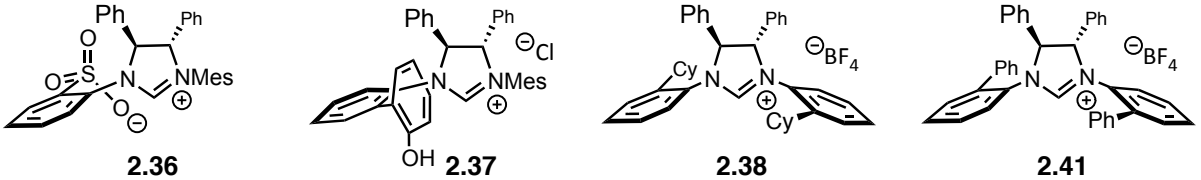

2.36	2.37	2.38	2.41
>98% conv., 60:40 e.r.	*>98% conv., 57:43 e.r.*	*84% conv., 69:31 e.r.*	*>98% conv., 69:31 e.r.*
52% conv., <2% e.e.	*29% conv., <2% e.e.*	***>98% conv., 55:45 e.r.***	*93% conv., 54:46 e.r.*

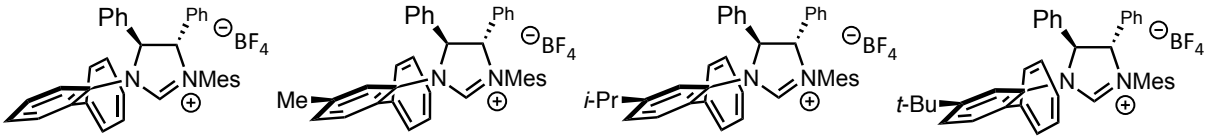

2.42	2.43	2.44	2.45
>98% conv., 57:43 e.r.	***>98% conv., 74:26 e.r.***	*>98% conv., 68:32 e.r.*	*>98% conv., 65:35 e.r.*
>98% conv., 54:46 e.r.	*83% conv., 54:46 e.r.*	*>98% conv., <2% e.e.*	*>98% conv., <2% e.e.*

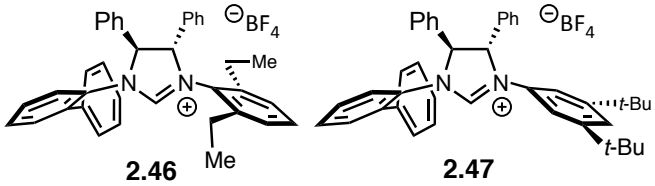

2.46	2.47
>98% conv., 52:48 e.r.	*>98% conv., 59:41 e.r.*
>98% conv., 58:42 e.r.	--

not provide sufficient energetic differentiation of the possible coordination modes of the carbonyl, therefore, allyl transfer can occur through various six-membered transition states of relatively equal energy (Figure 2.12).[59] Possible approaches of the prochiral

[59] The transition states depicted in Figure 2.12 are representative examples. There is also the possibility for boat-like (vs. chair) transition states to be operative. Elucidation of energetic profiles of the various pathways would require computational assistance.

ketones are represented by **I–III**, all of which are depicted with the smaller ketone substituent (R_s) residing in the pseudo-axial position of the chair-like transition states.

Figure 2.12 Possible Transition States for the Allyl Transfer to Ketones

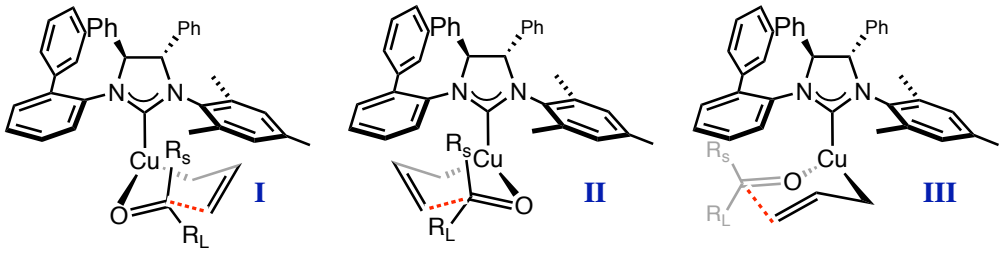

Development of a carbene that affects allyl additions with excellent facial selectivity requires adjustments to the *N*-substituents such that the imposed steric constraints limit substrate approach to a single lowest energy pathway.

In contrast, an assessment of the enantiocontrol afforded by various NHC–Cu complexes in allyl additions to diphenylphosphinoyl aldimine **2.31a** led to the discovery of a highly stereoselective catalyst (Scheme 2.18). Catalysts derived from bidentate, as well as C_1 and C_2-symmetric monodentate imidazolinium salts, are efficacious at promoting allyl transfer to the imine (>72% conversion in two hours at ambient temperature). Integration of facial selectivity alongside catalyst activity was addressed with a rationally designed template (see Figure 2.13). Since the transition state for C–C bond formation is postulated to invoke a tetrahedral Cu(I) complex with two coordination sites occupied by the bidentate phosphinoyl aldimine, a model for the least hindered approach of the substrate can be derived. If the NHC ligand is constrained to the apical position of the tetrahedron, we note that the steric presence of the substituents carried on the carbene's *N*-aryl groups carves out a specific open volume around the copper center. The allyl unit, being the smallest of the ligands on copper, will occupy the most sterically-demanding quadrant, limiting the accessible approaches of the bidentate

Scheme 2.18 Catalytic Enantioselective NHC–Cu-catalyzed Allyl Additions to Diphenylphosphinoyl Aldimine **2.31a**

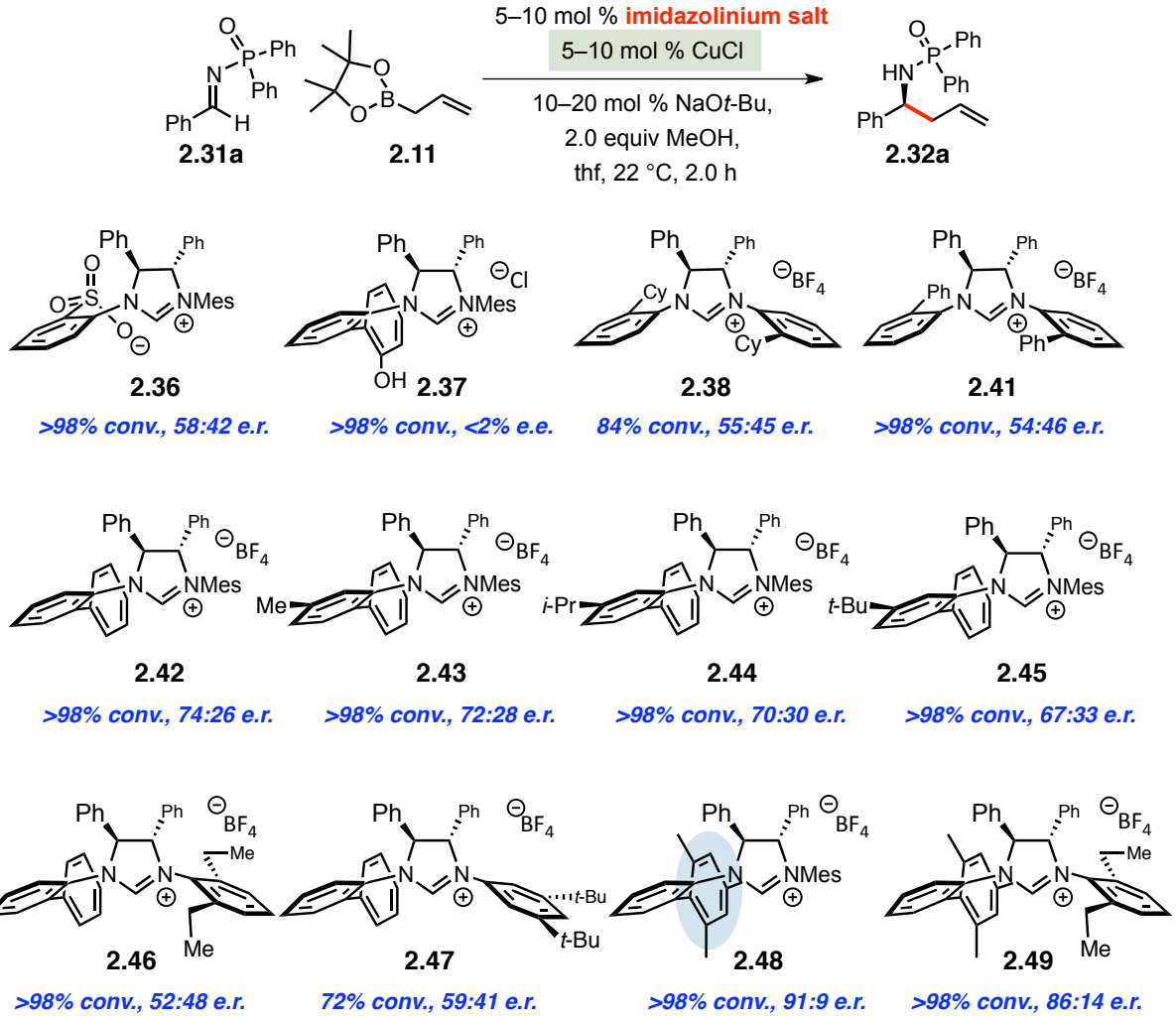

substrate. With this reasoning, the structural design of chiral carbenes typically involves decoration of the *N*-aryl groups with *ortho*-substituents ***a–c*** to block three of the four ligation sites around copper, freeing one quadrant for substrate binding.

A 3:1 selectivity for the intended mode of addition is observed with the catalyst derived from biphenyl-containing **2.42**. We postulated that selectivity between the competing transition states could be improved with logical structural modifications: The energy of the *desired* transition state (pictured in the box in Figure 2.13) can be lowered

Figure 2.13 A Blueprint for Catalyst Design and Its Successful Implementation for the Enantioselective Synthesis of Homoallylamines

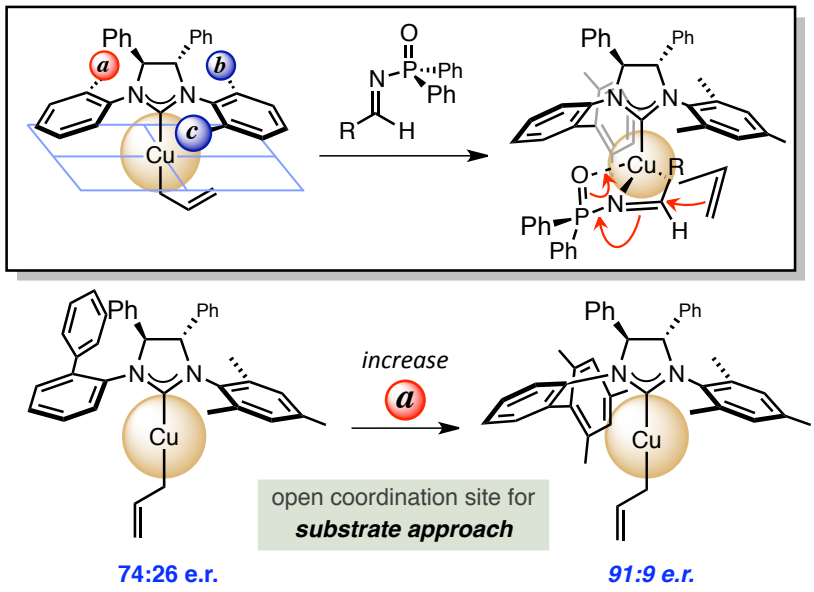

if the area encompassing the copper center is fashioned in a way to diminish steric interactions with the bulky imine protecting group; the lowest energy coordination mode of the substrate is primarily spatially governed, such that modifications to the NHC target an optimized "fit" for the imine.[60] Augmentation of the volume available for substrate approach was accomplished with replacement of the biphenyl substituent in **2.42** with an *N*-aryl group bearing a larger *ortho*-mesityl substituent in **2.48**; the larger *ortho*-substituent induces a large shift in the torsion angle, a rotation around the C–N bond that minimizes steric interactions between the mesityl ring and the backbone phenyl group.[61] As represented in Figure 2.13, this structural modification improved selectivity

[60] The energy of the transition state must be lowered *in comparison* to any competing approaches, particularly allyl transfer to the opposite enantiotopic face of the coordinated imine resulting in the other enantiomer.

[61] In a forthcoming section, the effect of various substituents on the structure of the carbene ligand, including shifts in torsion angles and the interplay of the five aryl groups, will be discussed in detail.

towards the desired mode of addition that leads to (*S*)-**2.32a** from 3:1 to 10:1 (91:9 e.r. with catalyst from **2.48**)[62].

In the presence of the Cu-based catalyst derived from **2.48**, the selectivity with which **2.32a** is obtained can be further improved from 91:9 e.r. to 97:3 e.r. when the reaction temperature is lowered to –50 °C. The activity of the catalyst is not diminished: transformations are complete within six hours with 5 mol % catalyst loading. With optimal conditions identified, the scope of phosphinoyl aldimines that participate in enantioselective additions of allyl groups was investigated (Table 2.1). A wide range of aryl- and heteroaryl-substituted imines are transformed to the corresponding α-chiral amines in >72% yield and with stereoselectivities ranging from 84:16 to 98.5:1.5 e.r.. There are several noteworthy points regarding the findings detailed in Table 2.1: 1) Imines that are significantly electron deficient react at slower rates than those bearing groups that can donate electron density (80% conversion of **2.31k**, entry 11). This observation is consistent with a mechanism in which coordination of the imine to the Lewis acidic copper center is rate-limiting (whereas if allyl addition was rate-limiting, electron-rich imines would be expected to react with slower rates).[63] 2) Reactions of sterically-encumbered substrates, naphthyl-bearing **2.31b** and those with bulky *ortho*-substituted aryl groups (entries 5 and 6), proceed efficiently but provide diminished enantioselectivities (products obtained in 84:16–88:12 e.r.). 3) Substrates carrying Lewis basic heteroatoms are well tolerated; the efficiencies and selectivities obtained in entries

[62] Reaction with the catalyst derived from **2.48** proceeds through competing transition states whose difference in energy ($\Delta\Delta G^{\ddagger}$) is 1.37 kcal/mol. The catalyst modification thus differentiated the two competitive addition modes (by either lowering the energy of one or raising the energy of the other) by an extra 0.72 kcal/mol.

[63] Further experimentation to support this claim (studies to elucidate the kinetics, or Hammett plot correlations) were not performed to verify these mechanistic nuances.

Table 2.1 NHC–Cu-catalyzed Allyl Additions to Aryl- and Heteroaryl-substituted Phosphinoyl Aldimines **2.31**

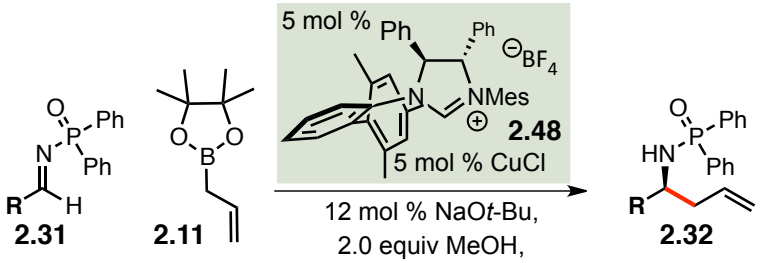

entry	**R**		conv. (%)[a]	yield (%)[b]	er[c]
1	C_6H_5	**2.32a**	>98	95	97:3
2	2-naphthyl	**2.32b**	>98	89	88:12
3	*o*-FC_6H_4	**2.32c**	>98	95	98:2
4	*o*-BrC_6H_4	**2.32d**	>98	92	98:2
5	*o*-MeC_6H_4	**2.32e**	>98	79	84:16
6	*o*-$OMeC_6H_4$	**2.32f**	>98	82	87.5:12.5
7	*m*-BrC_6H_4	**2.32g**	>98	88	96:4
8	*p*-ClC_6H_4	**2.32h**	>98	90	98:2
9	*p*-BrC_6H_4	**2.32i**	>98	92	98.5:1.5
10	*p*-FC_6H_4	**2.32j**	>98	90	97.5:2.5
11	*p*-$CF_3C_6H_4$	**2.32k**	80	72	98.5:1.5
12	*p*-$OMeC_6H_4$	**2.32l**	98	78	91.5:8.5
13	2-furyl	**2.32m**	>98	91	95:5
14	3-furyl	**2.32n**	>98	78	93:7
15	3-thienyl	**2.32o**	>98	86	98:2

[a]Determined by analysis of 400 MHz ^{1}H NMR spectra of unpurified reaction mixtures; [b]Isolated yields of purified products; [c]Enantiomer ratio values were determined by HPLC analysis.

13–15 suggest that competitive chelation of the heteroatoms to the copper center does not lead to significant disruption of the desired pathway. 4) Allyl additions described in Table 2.1 are scalable and practical to perform large-scale synthesis; a gram-scale transformation of phenyl-substituted **2.31a** can be promoted with 1 mol % catalyst

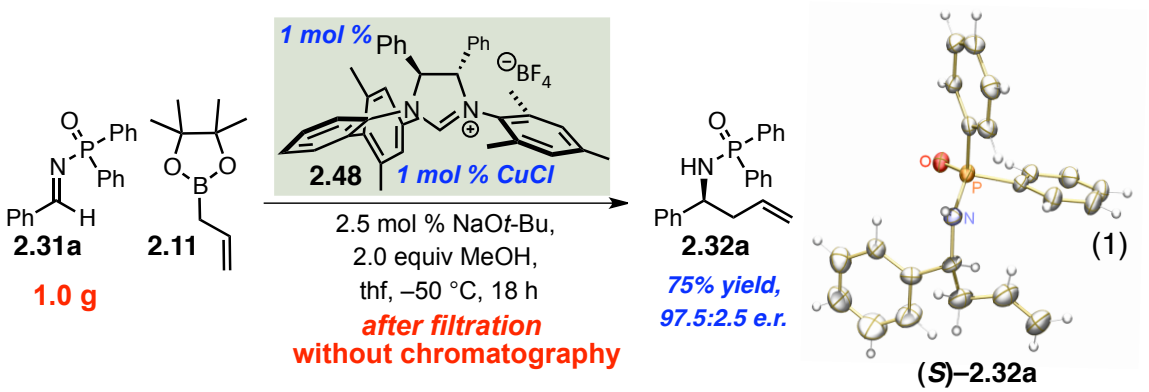

loading to afford analytically pure homoallylamide **2.32a**, after filtration, in 75% yield and 97.5:2.5 e.r. (equation 1). The diphenylphosphinamide imparts crystallinity allowing for both, isolation of the products without chromatography, and determination of the absolute stereochemistry (single X-ray diffraction analysis reveal that the (*S*)-enantiomer is formed preferentially).

Bisalkyl-substituted α-chiral amines represent a class of amines that are notoriously difficult to access, of which, those bearing an allyl group on the stereogenic carbon center are amongst the most challenging.[64] The difficulties arise from the minimized steric differentiation of the two imine substituents (H vs. methine, instead of H vs. aryl), as well as the instability of aliphatic imine precursors; those carrying an α-proton can tautomerize to eneamides leading to undesired byproducts and side reactions. Phosphinoyl aldimines derived from aliphatic aldehydes can be transformed to the corresponding homoallylic amides in the presence of 2.5–5.0 mol % NHC–Cu catalyst derived from carbene precursor **2.48** (Figure 2.14). While *β*-branched **2.32p** and linear alkyl-substituted **2.32q** are afforded in >96:4 e.r., α-branched **2.32s**–**u** are obtained in

[64] Examples of the low selectivities and efficiencies obtained in allyl nucleophile additions to aliphatic aldimines were presented in the Section 2.2. For discussion of the available methods and limitations for chiral amine synthesis, see: (a) "Chiral Amine Synthesis–Recent Developments and Trends for Enamide Reduction, Reductive Amination, and Imine Reduction," Nugent, T. C.; El-Shazly, M. *Adv. Synth. Catal.* **2010**, *352*, 753–819. (b) Chiral Amine Synthesis (Ed.: T. C. Nugent),Wiley-VCH, Weinheim, **2010**.

Figure 2.14 NHC–Cu-catalyzed Allyl Additions to Alkenyl- and Aliphatic-substituted Phosphinoyl Aldimines **2.31**

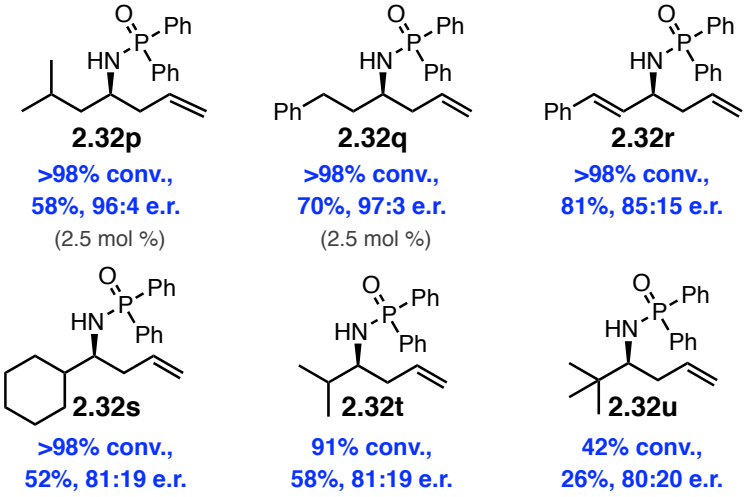

Reactions performed with the conditions shown for Table 2.1.

approximately 80:20 e.r. (4:1 selectivity). Efficiency of the C–C bond formation is only diminished for allyl addition to provide *tert*-butyl substituted **2.32u** (42% conversion). The reduced isolated yields for the synthesis of aliphatic homoallylic amides (52–70%) is a product of their instability and the inability to isolate or purify the aldimines.[65]

Limitations discovered in investigations of the scope, particularly the low selectivities obtained with sterically-hindered, electron-rich, and α-branched aldimines, prompted the development of new chiral carbenes that create more accommodating substrate binding pockets at copper. As previously illustrated, minor modifications to the substituents on the carbene ligands can have remarkable effects on the preferred conformation and reactivity of the Cu-based catalysts. Targeted structural alteration led to the synthesis of carbene precursor **2.50** bearing a dissymmetric *ortho*-methyl-*ortho-iso*-

[65] Alkyl-substituted aldimines are freshly prepared and used immediately from the elimination reaction of the corresponding sulfinyl adducts, see: (a) Côté, A.; Boezio, A. A.; Charette, A. B. *Proc. Natl. Acad. Sci.* **2004**, *101*, 5405. (b) Yamaguchi, A.; Matsunaga, S.; Shibasaki, M. *Tetrahedron Lett.* **2006**, *47*, 3985.

propyl *N*-aryl unit, in place of symmetric mesityl group in **2.48**.[66] Reactions promoted by the Cu catalyst derived from imidazolinium salt **2.50** induced excellent enantioinduction (>94.5:5.5 e.r.) in allyl transfers for a range of previously challenging aldimines (compare Table 2.1 and Figure 2.13 with the results described in Scheme 2.19). For example, reactions to provide sterically conjested **2.32b**, **2.32e**, and **2.32f**, attained in <88:12 e.r. with mesityl-substituted **2.48** (Table 2.1), are produced in >96:4 e.r. with the catalyst modified to bear a 2-methyl-6-*iso*propyl aryl group.

Scheme 2.19 A New NHC–Cu Catalyst Affording Improved Enantioselectivities

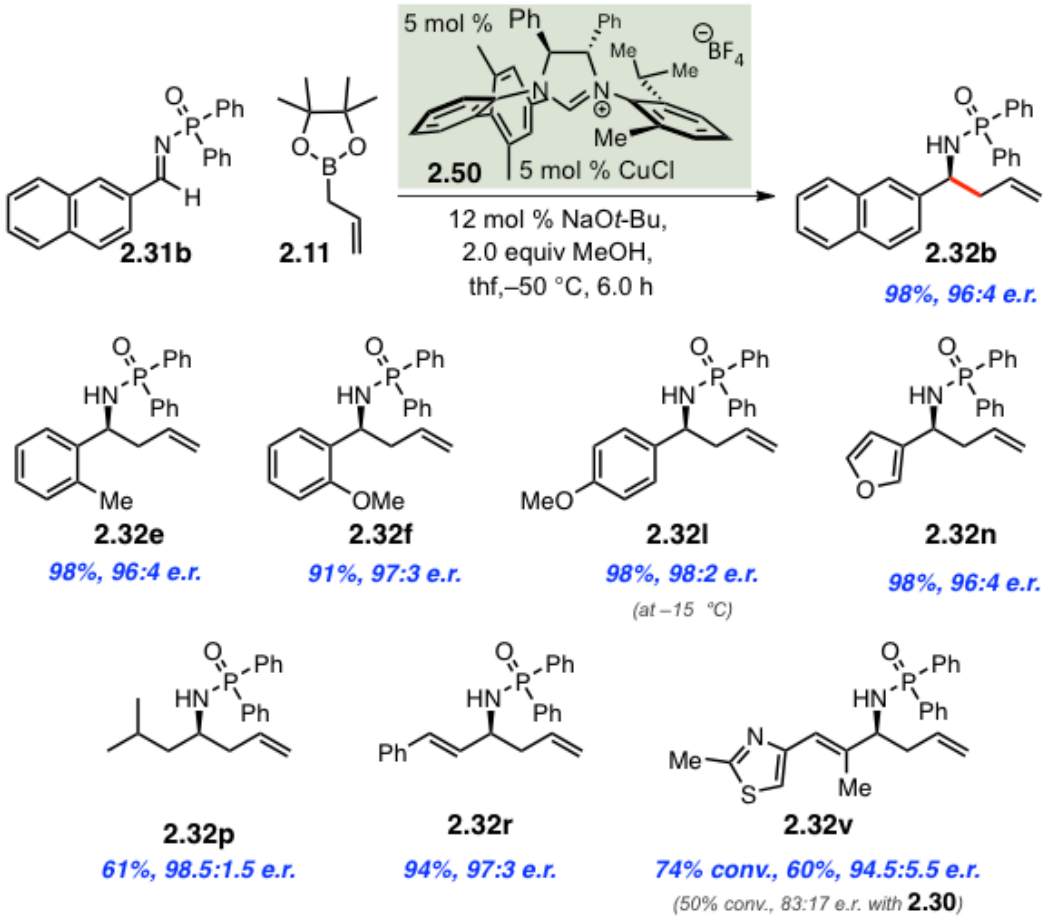

[66] This structural modification marked the synthesis of the first carbene precursor, in our laboratories, that did not bear at least one symmetric *N*-aryl substituent. Since then, we have found that added dissymmetry in the catalyst can result in improved enantiodifferentiation in a number of transformations.

Reactions of electron-rich aldimines are also more stereoselective with disymmetrically substituted NHC–Cu complex derived from **2.50**; *para*-methoxyaryl amide **2.32b** and 3-furyl amide **2.32n** are obtained in 98:2 and 96:4 er, respectively (Scheme 2.19). In these cases, lower stereoelectivities with **2.48** (91.5:8.5 and 93:7 e.r., respectively) may have been due to an altered energy profile, in which coordination to the copper complex is no longer rate-limiting. With electron deficient imines, coordination is a potentially stereo-defining and rate-limiting event, however, reactions with substrates bearing electron-donating substitutents (where coordination may be fast) could behave differently, in that allyl group transfer (or product release/catalyst regeneration) may be turnover-limiting instead.[61] As such, we postulate that the improved enantioselectivities afforded with the Cu-complex derived from **2.50** are an artifact of a change in the kinetics of the catalytic cycle; as a more efficient and competent allyl transfer catalyst, it may reinstate coordination to copper as the rate-limiting and stereo-defining step.

Finally, the stereogenic center in allylic amides **2.32r** and **2.32v** can be set in 97:3 and 94.5:5.5 e.r., respectively, in the presence of the Cu-catalyst derived from **2.50**. Notably, enantiomerically enriched complex tri-substituted allylic amide **2.32v** can be employed towards the synthesis of the aza-epothilones (such as ixabepilone in Scheme 2.2),[8] a class of potent anti-cancer drug targets, through a ring closing metathesis strategy to yield the macrocyclic lactam.

To understand how the chiral Cu-based catalyst derived from **2.50** (or **2.48**) influences the energetic differentiation of the competing modes for substrate coordination, we undertook investigations to elucidate the preferred conformations of the imidazolinium salt and its derived copper complex. Synthesis of the carbene precursors studied begins with two consecutive palladium-catalyzed Buchwald-Hartwig cross

coupling reactions between diphenylethylene diamine and the corresponding *ortho*-substituted aryl halides, yielding the bisarylated diamines. En route to preparation of **2.50**, cyclization of the resultant diamine provides the imidazolinium tetrafluoroborate

Scheme 2.20 Synthetic Route to Chiral Imidazolinium Tetrafluoroborate **2.50**

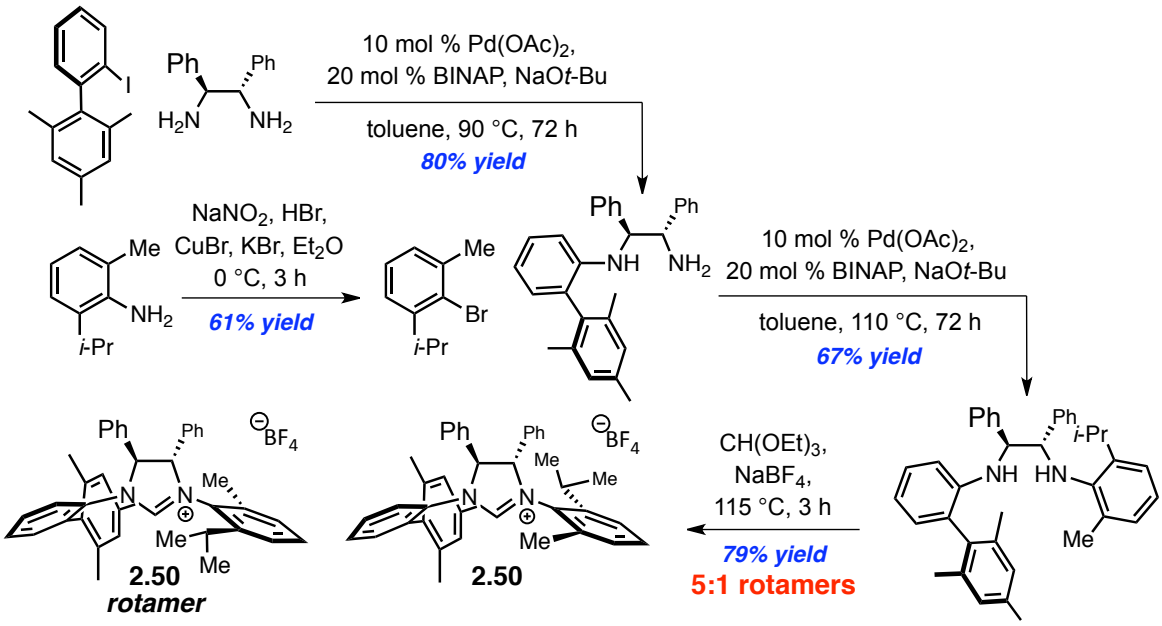

salt as a 5:1 mixture of rotamers (Scheme 2.20). The presence of rotational isomers is a consequence of the two dissymmetric groups appended to the heterocycle. The identity of the predominant stereoisomer in solution, as established by nOe experiments, is confirmed through analysis of the X-ray structure (pictured in Figure 2.15). The preferential conformation, surprisingly, rotates the dissymmetric bis*ortho*-substituted *N*-aryl group such that the bulkier *iso*propyl group is positioned *syn* to the phenyl group on the adjacent backbone stereogenic center (opposed to **2.50 rotamer** in which the smaller methyl group is oriented *syn*, see Scheme 2.20). Notably, the two stereoisomers freely interconvert in solution at ambient temperature; the ^{1}H NMR spectra (22° C, $CDCl_3$) of a sample of the crystal, isomerically pure **2.50** proven by solid state structure analysis, indicates a rapid reestablishment of the original 5:1 mixture of rotamers, likely

Figure 2.15 X-Ray Crystal Structure of Both Imidazolinium Salt **2.50** and the Derived Complex with CuCl **2.51**

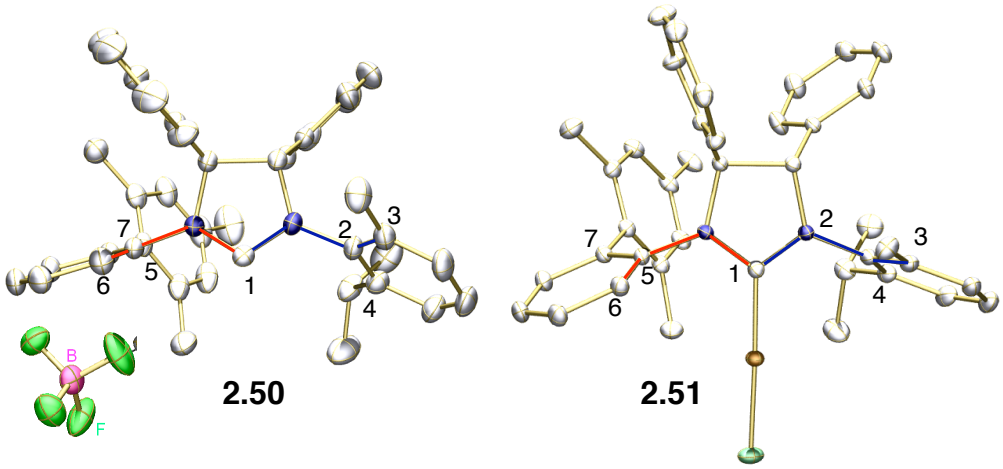

θ N–C_1–N = 114.6°
C_1–N = 1.315, 1.304 Å

C_1–N–C_5–C_6 = ***77.7°***
C_1–N–C_5–C_7 = ***105.4°***
C_1–N–C_2–C_3 = ***74.2°***
C_1–N–C_2–C_4 = ***103.4°***

θ N–C_1–N = 108.8°
C_1–N = 1.334, 1.343 Å
C_1–Cu = 1.89 Å

C_1–N–C_5–C_6 = ***80.9°***
C_1–N–C_5–C_7 = ***96.2°***
C_1–N–C_2–C_3 = ***89.7°***
C_1–N–C_2–C_4 = ***90.3°***

representing the thermodynamic equilibrium. Steric repulsion between the protruding phenyl group of the imidazolinium backbone and the *ortho-iso*propyl substituent leads to significant tilting of the *N*-aryl group in the major rotamer (*syn* orientation). The altered dihedral angles of ϕ = 74.2° and 103.4° position the other *ortho* unit of the *N*-aryl group (methyl) in close proximity with the backbone of the carbene.[67] It thus appears that the alternative rotation, where the methyl is *syn* to the backbone phenyl, is a higher energy conformer, mainly due to the engendered negative interaction between the *iso*propyl group and the backbone.[68] The same conformational preference is retained in the derived

[67] There is an nOe enhancement noted between the methyl group and the backbone proton indicating the propinquity of the nuclei (see Experimentals Section 2.8 for further details). The distance is measured to be 2.169 and 2.220 Å in the X-ray structures of **2.50** and **2.51**, respectively.
[68] For a similar argument to explain the favorable positioning of an *ortho*-substituted sulfonate *syn* to the phenyl ring on the backbone, see: "Stereogenic-at-Metal Zn- and Al-Based N-Heterocyclic Carbene (NHC)

Cu complex; deprotonation of **2.50** and complexation with copper(I) chloride results in the NHC–Cu-Cl complex **2.51,** the X-ray structure[69] of which reveals the same *syn* positioning of the *iso*propyl group in respect to the backbone phenyl ring. While most of the structural elements remain similar, there are several important features that can be noted in comparison of the two molecular structures (Figure 2.15).[70] 1) In comparison to the imidazolinium salt **2.50**, the N–C_1 bond lengths of the derived Cu complex **2.51** are elongated to 1.334 and 1.343 Å, from 1.304 and 1.315 Å, while the N–C_1–N angle is contracted (θ = 114.6° → 108.8°); these observations are consistent with increased π character of the carbene (greater electron donation into the out-of-plane p_π orbital of the carbene carbon) and a marked decrease in π-delocalization in the *N*-heterocycle. Therefore, the degree of donation from the flanking nitrogen atoms is increased upon metal complexation, a result that can be noted by the lengthening of the N–C_1 bond lengths. The higher degree of σ-bond character is characteristic of minimized electronic contribution from the iminium resonance structure (C=N double bond). 2) The dihedral angles ϕ, values representative of the degree of "twisting" or out of plane positioning of the *N*-aryl substituents, are similar yet unique for the Cu-complex in relation to the precursor salt. The effects on the structural attributes of the imidazole ring (C–N bond elongation and N–C–N angle contraction) have a significant influence on the conformation of the five aryl rings. For example, while the downward tilt characterized

---

Complexes as Bifunctional Catalysts in Cu-Free Enantioselective Allylic Alkylations," Lee, Y.; Li, B.; Hoveyda, A. H. *J. Am. Chem. Soc.* **2009**, *131*, 11625–11633.

[69] I am indebted to the work of my colleague Nicholas Mszar for his resolve in obtaining crystals to enrich our understanding of the structural influence of our carbene ligands. This molecular structure determined by single crystal X-ray diffraction represents the first example of an elucidated structure of a chiral monodentate NHC complexed with copper from our laboratory. The comparison of the structural information derived from the imidazolinium salt and its Cu complex have been invaluable.

[70] The coordination chemistry of carbenes with late transition metals is the subject of several reviews, see references 40d, g, and 40h and the references cited therein as well as in the early work from Arduengo in, "A Stable Crystalline Carbene," Arduengo, A. J., III.; Harlow, R. L.; Kline, M. *J. Am. Chem. Soc.* **1991**, *113*, 361–363.

by the *ortho*-mesityl substitution on the *N*-biaryl unit persists in the Cu-complex (ϕ = 80.9° and 96.2° in contrast to 77.7° and 105.4° for **2.50**), the dramatic angling effect produced by substitution with dissymmetric 2-methyl-6-*iso*propylphenyl observed for the carbene precursor, however, is less pronounced in NHC–Cu complex **2.51** (blue dihedral angles highlighted in Figure 2.15)[71]

With a better understanding of the conformational attributes of C_1-symmetric **2.50**, we focused on deducing the impact of its conformation on the stereoselectivity and efficacy of the derived Cu catalyst. Cu catalysts bearing diaminocarbene ligands derived from **2.42** and **2.50** both promote efficient allyl transfer to phosphinoyl aldimines, however, the former results in significantly lower enantioselectivity (76:24 e.r., see Scheme 2.19, vs. 94:6 e.r. at 22 °C for **2.50**). The basis for this discrepancy in activity of the two catalysts can be gathered from comparative analysis of the solid state molecular structures of the two corresponding imidazolinium salts (Figure 2.16). They carry distinct structural features, all of which influence the available volume encompassing the copper centers in the corresponding metal complexes. Beginning on the heterocycle, substitution with a sizable 2-methyl-6-*iso*propylphenyl group in **2.50** results in a longer N–C_1 bond length of 1.315 Å. Moreover, the dissymmetry of the bis*ortho*-substitution (versus 2,4,6-trimethylphenyl in **2.42**) produces a substantial shift in the positioning of the *N*-aryl unit on the right-hand side of the molecule. The observed dihedral angle ϕ, conferring the spatial relationship of C_4 with respect to the heterocycle, is 74.2° with *iso*propyl group substitution in **2.50** while the methyl group in **2.42** results in a torsional angle of 58.8°.

[71] The evidence obtained from the solid state structure may not be completely reflective of in solution behavior (as was noted for the single conformer obtained in solid state for imidazolinium salt **2.50** versus its in solution formation of rotamers); crystal-packing forces may have a significant influence on the conformation. Moreover, in the context of the transition state for allyl transfer to aldimines, it is the ability for the two *N*-aryl rings to tilt out of the way to allow for substrate approach/C–C bond formation that is significant.

Figure 2.16 Comparison of the Structural Features Using the X-Ray Crystal Structures of Imidazolinium Salts **2.42** and **2.50**

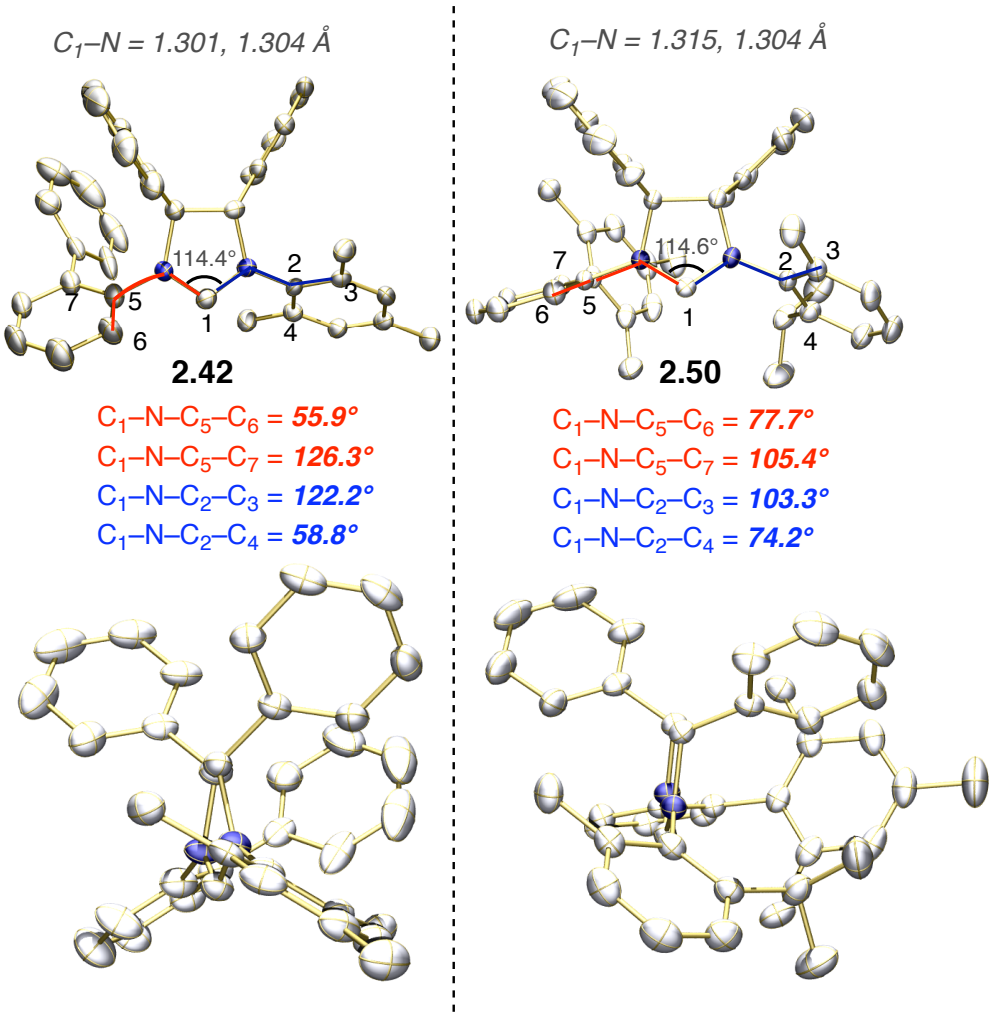

Effectively, modification of one of the *ortho*-methyl groups of the mesityl unit to an *iso*propyl group tilts the aryl ring by approximately 20°; this angling has a significant effect on the space occupied in both the front and back right quadrants surrounding copper.

The left-hand sides of the molecules, bearing a biaryl substituent, display a similar shift. Exchange of the biphenyl group of **2.42** for an *ortho*-mesitylphenyl group in **2.50** affords a 22° displacement of the C_6 carbon in relation to C_1 (C_1–N–C_5–C_6 ϕ = 55.9° with

biphenyl substitution and 77.7° with replacement with a mesityl group in **2.50**). The cumulative effects outlined above are highlighted in the contrasted side profiles of the imidazolinium salts in Figure 2.16; the sterically accessible volume beneath the ligands is substantially differentiated in two examples shown. The stereocontrol imposed by the catalyst is a direct result of its ability to limit the approach of the bidentate imine, and as such, the excellent facial selectivity observed with the Cu catalyst derived from **2.50** suggests that it possesses a coordination site at the copper center with the appropriate volume suited for substrate approach.

The identity of the enantiomer obtained after C–C bond formation is dependent on the orientation of the bound prochiral imine. Bidentate coordination to the tetrahedral copper(I) center is postulated to occur exclusively from the front face in the competing transition states; the carbene substituents (a mesityl and *iso*propyl group) are tactfully positioned to occupy and block the back-side approach to the copper center. In the *favored* transition state, the imine substituent sits underneath the space carved out by the right-hand side *N*-aryl substituent (either a mesityl or 2-methyl-6-*iso*propylphenyl group), while the bulky protecting group can occupy the more open area beneath the biaryl group

Figure 2.17 Competing Transition States in NHC–Cu-catalyzed Allyl Transfer to Phosphinoyl Aldimines

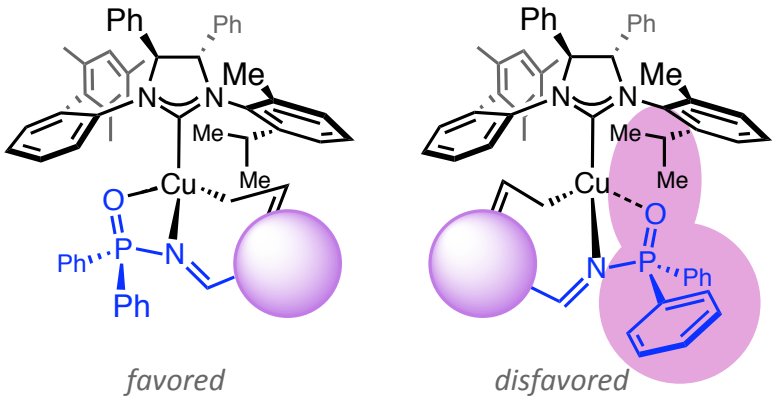

of the NHC (*favored* in Figure 2.17). Addition of the allyl group from this lower energy transition state affords the observed (*S*)-enantiomer of **2.32**. The opposing *disfavored* pathway, furnishing allyl additions to the reverse face of the prochiral imine, positions the imine substituent beneath the biaryl forcing the bulky diphenylphosphinoyl group beneath the mesityl ring of **2.48** (or 2-methyl-6-*iso*propylphenyl group in **2.50**). The *disfavored*, higher energy transition state generates adverse steric interactions between the protecting group and substitutents of the right-hand side *N*-aryl group. However, when aldimines with greater steric congestion approach the Cu-catalyst derived from mesityl-bearing **2.48,** the two modes of coordination are of comparable energies (selectivities are approximately 85:15 e.r.); large imine substituents energetically penalize the *favored* pathway, due to steric clash with the methyl of the mesityl group, such that its energy is more similar to that of the *disfavored* transition state. However, with the catalyst composed from **2.50**, the 20° tilt associated with 2-methyl-6-*iso*propylphenyl substitution leads to better accommodation of the larger imine substituents, reinstating the lower energy of the *favored* binding mode. The *disfavored* approach, in contrast, remains less attainable; the volume allotted by the 2-methyl-6-*iso*propylaryl unit is insufficient for positioning of the phosphinoyl group.

The outlined mechanistic scenario establishes the importance of the large diphenylphosphinoyl group for discrimination in binding the enantiotopic faces. Congruently, catalytic enantioselective allyl additions to *N*-aryl protected aldimine **2.26** proceed efficiently, but provide racemic homoallylamine **2.24**. Although *ortho*-thiomethyl aniline-derived aldimine also provides bidentate chelation to the copper center, allyl addition is nondiscriminatory since the two aryl substituents of the C=N

unsaturation are of similar size (i.e., the favored and unfavored binding modes in Figure 2.16 are energetically equivalent).

The catalyst afforded from **2.50** addresses many of the discovered limitations in scope, however, aldimines bearing α-branched aliphatic substituents remained a challenging substitution pattern for the catalysts described (i.e., 80:20 e.r. with *iso*propyl, cyclohexyl, or *tert*-butyl-bearing aldimines, Figure 2.14). Unlike the reactions described in Scheme 2.19, there is only a nominal improvement with sterically modified **2.50** (82:18 e.r., entry 7, Table 2.2); coordination of imines containing substituted sp^3-

Table 2.2 Catalyst Screening for the Enantioselective Allyl Group Addition to Aldimines with α-Branched Substituents

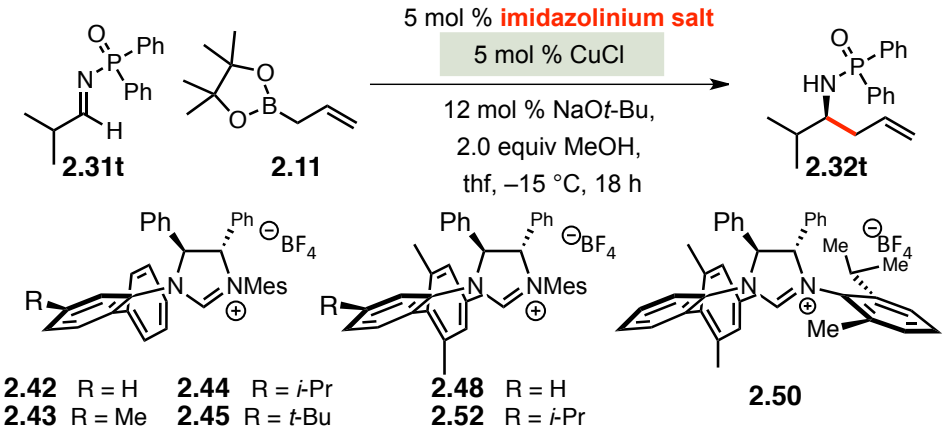

entry	**NHC–Cu complex**	conv. (%)[a]	e.r.[b]
1	**2.42**	64	76:24
2	**2.43**	62	84:16
3	**2.44**	80	88:12
4	**2.45**	82	87:13
5	**2.48**	>98	81:19
6	**2.52**	55	62:38
7	**2.50**	75	82:18

[a]Determined by analysis of 400 MHz ^{1}H NMR spectra of unpurified reaction mixtures; [b]Enantiomer ratio values were determined by HPLC analysis.

hybridized centers is not accommodated in the binding pockets designed for planar aryl-substituted aldimines. A different approach to affect the volume accessible to the substrate involves steric modifications to the left-hand biaryl *N*-substituent; the *meta*-position of the biaryl juts out into the space above the left front quadrant, and as such, addition of steric bulk at this position could potentially increase the energy of the *disfavored* transition state, a binding mode that would force the imine substituent to point into the added bulk. Accordingly, the optimal enantiodifferentiation is observed with the catalyst derived from *meta-iso*propyl containing **2.44**, affording aliphatic homoallylic amide **2.32t** in 80% conversion and 88:12 e.r. (entry 3). Although the improvements are incremental, they confirm the validity of our model, supporting its use as a predictive tool to successfully and rationally design catalysts for specific substrates.

The next phase of our study probed the scope of allylic boron reagents that participate in the enantioselective NHC–Cu-catalyzed protocol. We investigated the capacity for β-substituted allylborons[72] to react with an NHC–Cu complex to provide active nucleophiles for additions to phosphinoyl aldimine **2.31a**. In the presence of the optimal Cu-based catalysts discovered for transformations with unsubstituted allylboron, β-methyl substituted allylboron **2.53** is engaged in reaction with the aldimine derived from benzaldehyde to provide the derived amide **2.54**, bearing a 1,1-disubstituted olefin, in 18 hours in 84–96% yield and up to 95:5 e.r. (Scheme 2.21). With respect to transfers

[72] Transformations that provide the corresponding homoallylic amines bearing 1,1-disubtituted terminal olefins are rare. For catalytic enantioselective examples that provide access to various substitution at the 2-position, see: references 21c, 22a-b, 23a and 23c. For selected methods that invoke the use of a chiral amine, see: (a) "Diastereoselective Barbier-Type and Palladium-Mediated Allylation of Optically Active Aldimine with Allylindium Reagents," Yanada, R.; Kaieda, A.; Takemoto, Y. *J. Org. Chem.* **2001**, *66*, 7516–7518. (b) "3-Component Palladium–Indium Mediated Diastereoselective Cascade Allylation of Imines with Allenes and Aryl Iodides," Cooper, I. R.; Grigg, R.; MacLachlan, W. S.; Thornton-Pett, M.; Sridharan, V. *Chem. Comm.* **2002**, 1372–1373. (c) "Stereoselective Synthesis of Pyrrolidin-3-ols from Homoallylamines," Medjahdi, M.; González-Gómez, J. C.; Foubelo, F.; Yus, M. *Heterocycles* **2008**, *76*, 569–581.

Scheme 2.21 Catalytic Enantioselective Additions of a Methallyl Group to Phosphinoyl Aldimines

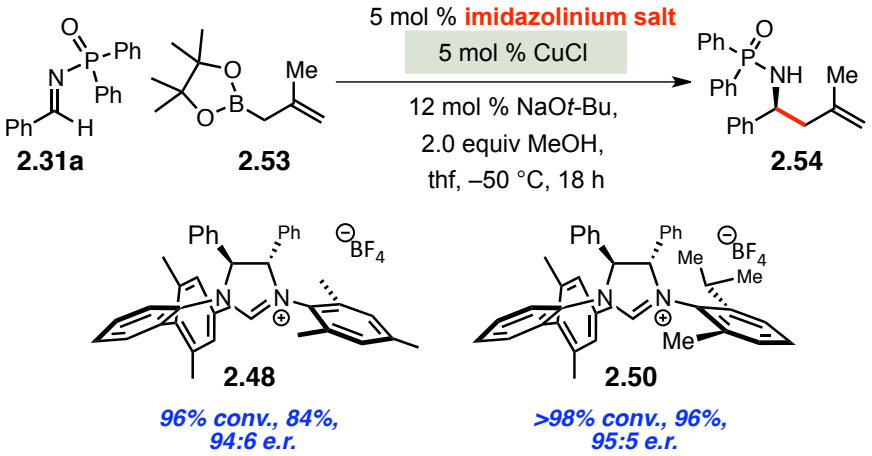

of methylallyl groups from the copper center, the relative energies of the competing transition states (analogous to those in Figure 2.17) are not significantly affected by the added methyl substitution. In contrast, there is a significant influence on the energies of the transition states for C–C bond formation in the Cu-catalyzed reactions with *β*-phenyl substituted allylboron **2.55** (Scheme 2.22).

The efficiencies, with which additions that afford homoallylic amide **2.56** occur, are significantly diminished; reactions proceed sluggishly at –50 °C, and must be performed at –15 °C to ensure adequate reactivity of the NHC–Cu-complex. The selected screening of carbene ligands in Scheme 2.22 demonstrates the consequence of substitution pattern on the biaryl group of the catalyst (modifications to the left-hand side); for example, placement of an *iso*propyl group in the *meta* position of the biphenyl substituent was found to improve the selectivity from 65:35 to 70:30 e.r. (reactions with **2.42** versus **2.44**). Moreover, installation of an *ortho*-mesityl group (versus phenyl) on the biaryl *N*-substituent, an advantageous modification in related processes involving unsubstituted allylboron **2.11**, also provides a substantial boost in the enantiotopic

Scheme 2.22 Catalytic Enantioselective Additions of β-Phenyl Substituted Allyl Groups to Phosphinoyl Aldimines

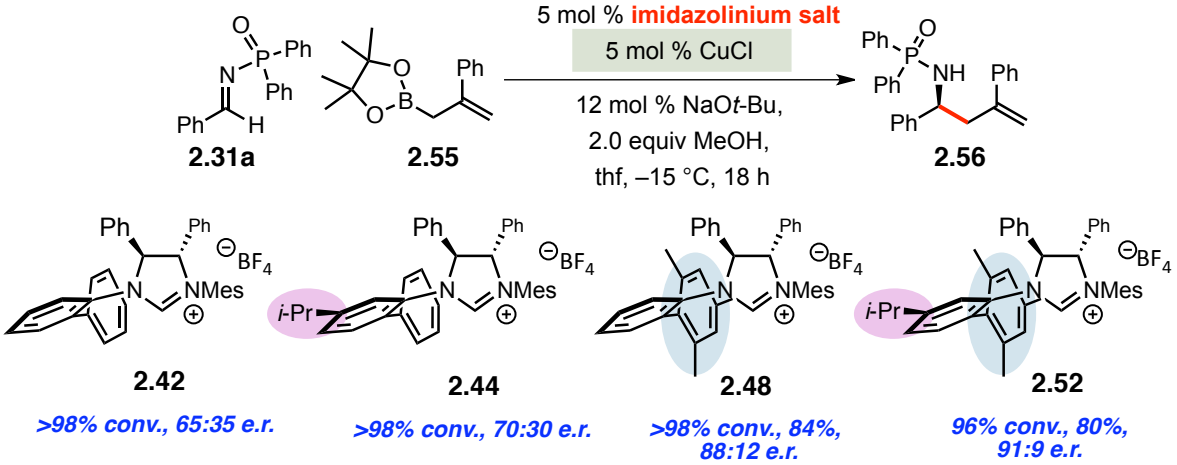

differentiation provided by the catalyst (88:12 e.r. with **2.48** vs. 65:35 e.r. with **2.44**). Finally, the optimal angle for the placement of the biaryl *N*-substituent is achieved with 2-mesityl-5-*iso*propylphenyl bearing imidazolinium salt **2.52**,[73] the derived catalyst of which provides substituted homoallylamide **2.56** in 80% yield and 91:9 e.r. (Scheme 2.22). The incremental improvements in stereoselectivity provide a direct reflection of the influence each catalyst imposes on the relative energies of the competing addition pathways. The described enantioselective reactions with 2-substituted allylborons, a class of stable and readily accessible reagents,[74] provide an additional site in the chiral amine

[73] Analysis of the X-ray structure of imidazolinium salt **2.52**, procured by my colleague Hao Wu and solved by crystallographer Dr. Bo Li, reveals the effect on conformation imposed by the substitution with the *meta-iso*propyl unit; the dihedral angles that describe the positioning of the biaryl unit are measured to be ϕ = 62.4° and 119.1° (in contrast to 77.7° and 105.4° for H-substituted **2.50**). The result is a moderation in the angling of the biaryl unit, such that preferential stationing is between that of unsubstituted biphenyl **2.42** and *ortho*-mesitylphenyl containing **2.50**.

[74] For recent examples for the synthesis of 2-substituted allylborons, see: (a) "A Synthesis of Allylboronates *via* the Palladium(0)-Catalyzed Cross-Coupling Reaction of Bis(pinacolato)diboron with Allylic Acetates," Ishiyama, T.; Ahiko, T.; Miyaura, N. *Tetrahedron Lett*. **1996**, *37*, 6889–6892. (b) "NHC–Cu-Catalyzed Enantioselective Hydroboration of Acyclic and Exocyclic 1,1-Disubstituted Aryl Alkenes," Corberan, R.; Mszar, N. W.; Hoveyda, A. H. *Angew. Chem., Int. Ed*. **2011**, *50*, 7079–7082. (c) "Ni- and Pd-Catalyzed Synthesis of Substituted and Functionalized Allylic Boronates" Zhang, P.; Roundtree, I. A.; Morken, J. P. *Org. Lett*. **2012**, *14*, 1416–1419, and references cited therein.

products to which molecular complexity can be installed. Moreover, these transformations allow direct synthetic access to biologically active natural products, such as eponemycin (pictured in Scheme 2.2).

The processes described thus far present catalytic and enantioselective additions of *symmetric* allyl units, altogether forgoing the potential issues of diastereo- and site-selectivity in the additions of substituted allylic metals (i.e., addition from either C_1 or the C_3 carbons of the allylcopper provide identical amide products with reactions of allylborons **2.11**, **2.53**, and **2.55**). Issues regarding selectivity of reactions with *dissymmetric* allyl nucleophiles, suited with substituents on either C_1 or C_3, are evidenced by the formation of regioisomeric and diastereomeric product mixtures. The stereospecificty of the NHC–Cu catalysts reported herein was first examined in deuterium labeling experiments. Catalyzed reactions of **d_2–2.11** and phosphinoyl aldimine **2.31a** yield an equimolar mixture of the two possible bis-deuteride substituted positional isomers **d_2–2.32a** (Scheme 2.23). The observed scrambling of the deuterium-label is suggestive of a rapid η^1 to η^1 interconversion pathway[75] for the allylcopper intermediate; isomerization provides both α-d_2 and γ-d_2-allylcoppers, species that react with the imine at equal rates through cyclic transition states. In a parallel fashion, crotyl additions, initiated from stereoisomerically pure *cis* or *trans*-crotylborons, afford C–C bond formations with minimal diastereocontrol. In the presence of the NHC–Cu catalyst derived from carbene precursor **2.48**, transformations with *cis*-crotylboronic acid pinacol

[75] For spectroscopic evidence of σ-bonding in allylcoppers and cuprates, see: (a) "New Methodology for Conjugate Additions of Allylic Ligands to α,β-Unsaturated Ketones: Synthetic and Spectroscopic Studies," Lipshutz, B. H.; Ellsworth, E. L.; Dimock, S. H.; Smith, R. A. J. *J. Am. Chem. Soc.* **1990**, *112*, 4404–4410. For a discussion regarding the accessible mechanisms for isomerization of the isoelectronic allylzinc(II) d^{10} complexes, see: (b) "Bis(allyl)zinc Revisted: Sigma Versus Pi Bonding of Allyl Coordination," Licthenberg, C.; Engel, J.; Spaniol, T. P.; Englert, U.; Raabe, G.; Okuda, J. *J. Am. Chem. Soc.* **2012**, *134*, 9805–9811.

ester **2.57** and aldimine **2.31a**, proceed with complete γ-selectivity, exclusively affording homoallylamides bearing an adjacent all-carbon tertiary stereogenic center. The generated methyl-substituted stereogenic centers, however, are afforded as a 58:42 diastereomeric ratio of **syn–2.58** and **anti–2.58**.[76] The high enantioselectivities of the two isomers (88:12 and 92:8 e.r.) suggest that the crotyl transfer occurs through a

Scheme 2.23 Extension of Catalytic Enantioselective NHC–Cu-Catalyzed Additions to Transformations with Dissymmetric Allylborons

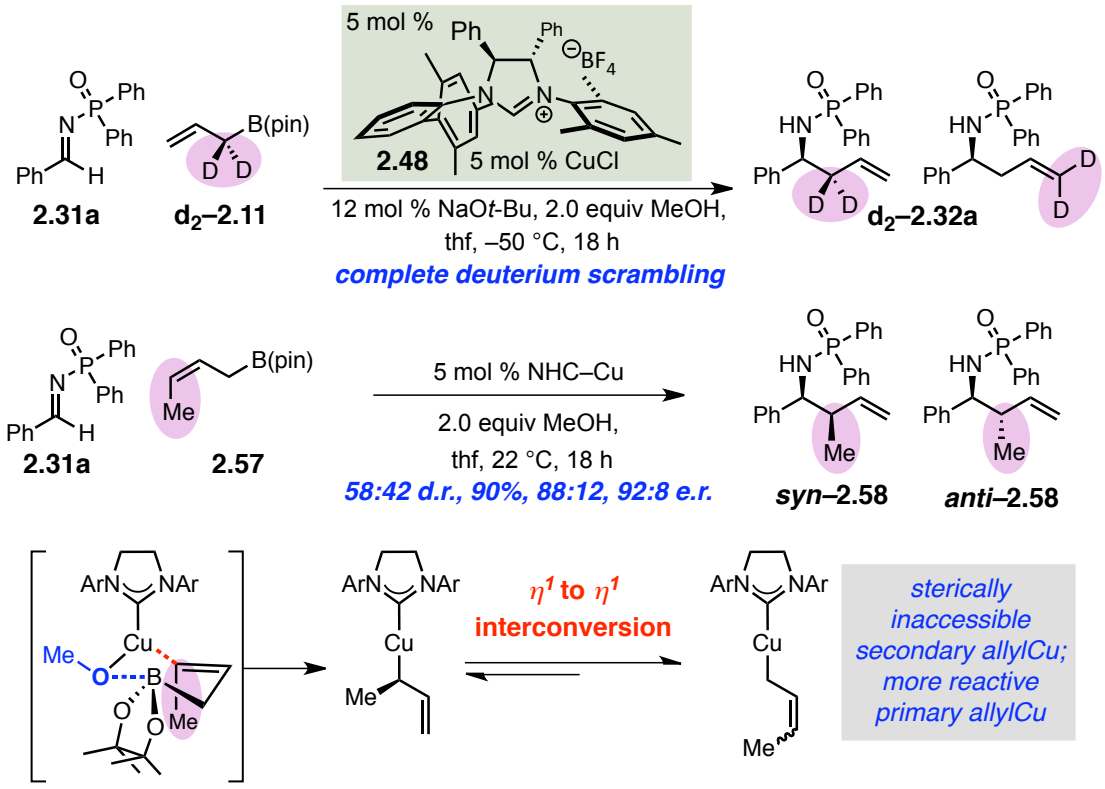

parallel transition state to the *favored* pathway in Figure 2.17, however, through a crotylcopper intermediate in which the stereochemical identity of the olefin has been lost.

[76] The identity of the major diastereomer (the relationship of the all-carbon stereogenic center to the *N*-substituted center) was not confirmed.

The poor diastereocontrol is indicative of an isomerization event of the olefin geometry prior to C–C bond formation.

As depicted in Scheme 2.23, although *in situ* generation of the substituted NHC–Cu-allyl species may occur stereospecifically through a 6-membered alkylation of the NHC–Cu-methoxide complex with isomerically pure *cis*-allylboron, the stereochemistry may be destroyed in the transition state involved in η^1 to η^1 interconversion of the allylmetal.[77] Furthermore, there is perfect site-selectivity (exclusive reaction with the primary γ-substituted allylcopper) despite the facility of interconversion between the α and γ-substituted isomeric allylcoppers. We postulate that the bulky NHC-ligated Cu preferentially resides as the less sterically encumbered primary allylcopper; additionally, the secondary alkylcopper center may be sterically inaccessible for coordination of the phosphinoyl aldimine, such that allyl transfers from the *E*/*Z* isomerized primary allycopper are energetically favored.[78]

The mechanism by which a σ-coordinated allylcopper can rapidly interconvert from the α to γ-bound isomers can occur either intra- or intermolecularly (Figure 2.18). Collapse to a π-bound η^3–allylcopper complex can result in intramolecular allyl

---

[77] Reactions with *trans*-γ-phenyl-substituted allylboron were investigated in an attempt to raise the energy required to reach the transition state for allyl interconversion. If the allyl exchange could be halted, the stereochemistry might be retained for transfer to the amine products. Unfortunately, reactions proceed with similarly poor diastereoselectivity (55:45 d.r.).

[78] Excellent site-selectivities of reactions with *in situ* prepared NHC–Cu-allyl species (2-boryl-substituted allylcoppers catalytically accessed from Cu–B additions to allenes), in either protonations or allyl transfers to aldehydes and ketones, have been observed in investigations in these laboratories. Moreover, the site-selectivity, at least in protonations of the NHC–Cu-allyl intermediates, is found to be highly dependent on the size of the carbene ligand associated with the Cu catalyst, e.g., small NHCs display a reversal in site-selectivity from complexes with encumbered ligands. For a detailed account, see: (a) "NHC–Cu-Catalyzed Protoboration of Monosubstituted Allenes. Ligand-Controlled Site Selectivity, Application to Synthesis and Mechanism," Meng, F.; Jung, B.; Haeffner, F.; Hoveyda, A. H. *Org. Lett.* **2013**, *15*, 1414–1417. (b) "Cu-Catalyzed Chemoselective Preparation of 2-(Pinacolato)boron-Substituted Allylcopper Complexes and their In Situ Site-, Diastereo-, and Enantioselective Additions to Aldehydes and Ketones," Meng, F.; Jang, H.; Jung, B.; Hoveyda, A. H. *Angew. Chem., Int. Ed.* **2013**, *52*, 5046–5051.

isomerization, notably, the stereochemical identity of an α–stereocenter or of a geometrically-pure olefin isomer can be eroded through the intermediacy of a π-allyl complex. An intermolecular mechanism, that does not invoke π-interactions, proceeds through a bimolecular interchange of allyl groups. The intermolecular allyl exchange

Figure 2.18 Potential Mechanisms for Intra- and Intermolecular η^1 to η^1 Allyl Exchanges for AllylCopper(I) Species

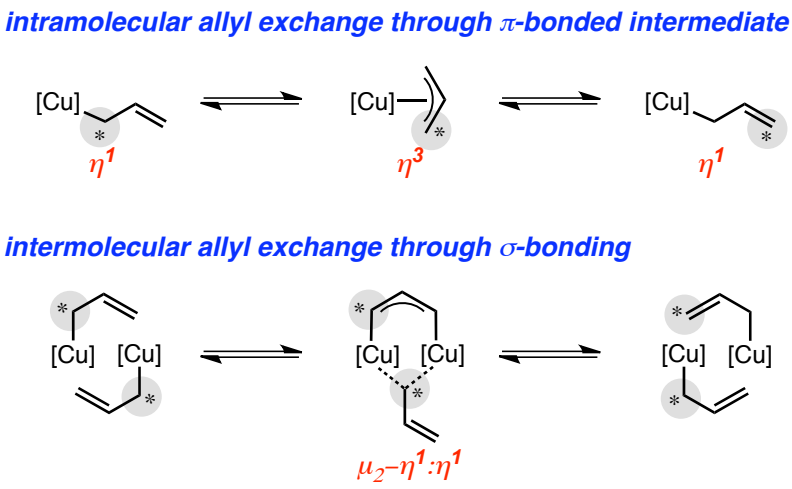

involves a σ-coordinated bimetallic μ_2–η^1: η^1 transition state and is found to be the predominate pathway for exchange of bis(allyl)zinc,[73a] a d^{10} metal center isoelectronic to allylcopper(I). Additionally, as discussed earlier in regards to the first disclosed X-ray structure of an NHC–Cu(I)-allyl complex **2.39** (Scheme 2.14), the low energy isolated conformer is suggestive of a filled $d^{Cu} \rightarrow \pi^*$ interaction with no evidence of $\pi \rightarrow d^{Cu}$; the preference for σ-binding with Cu(I) is consistent with higher energy filled-filled interactions. Preservation of stereochemistry in reactions involving allylmetals, despite the rapid kinetics of isomerization associated with either of the considered pathways, is a challenging yet attainable goal; thus far, high levels of diastereocontrol have been

attained with rare examples of configurationally stable allylmetals[79] or in protocols that provide only one of the possible isomers.[80]

Nevertheless, rather than contending with the configurational instability of allylcoppers, our focus shifted to the identification of *metal-free* catalysts that would promote highly diastereo- and enantioselective additions of γ-substituted allylborons. The potency of Lewis bases, such as *N*-heterocyclic carbenes and metal alkoxides, as *metal-free* catalysts for the activation of C–B bonds, described in section 2.4, motivated our interest. The development of chiral phenoxides as *metal-free* catalysts, their unique mechanism and complementarity to the Cu–catalyzed transformations discussed herein, are among the topics discussed in Chapter 4.

2.6 Limitations and Future Studies

Subsequent studies concentrated on the discovery of new classes of transformations amenable to copper catalysis. The high level of reactivity observed for allyl aditions to imines derived from aldehydes encouraged studies aimed at the formation of the related *N*-substituted quaternary stereogenic centers. **SIMes–**NHC–Cu-catalyzed *allyl additions to ketoimines* proceed with varied efficiencies; unexpectedly, *ortho*-thiomethylaniline **2.25** was provided in 95% conversion while the corresponding

[79] For a configurationally stable allylrhodium complex, see reference 33b. For references regarding allylzinc complexes that do not readily isomerize or preferentially react as the *trans*-allylzinc, see references 19e and 20c for their use in diastereoselective additions, and 33a for a chiral Zn catalyst.

[80] For unique α-selective additions of allylindium that provide one of the two possible isomers, see reference 27a. For allyliridium or allylrhodium catalysts that provide high *anti*-diastereoselectivity (however not with additions to imines), see: (b) "*anti*-Diastereo- and Enantioselective Carbonyl Crotylation from the Alcohol or Aldehyde Oxidation Level Employing a Cyclometallated Iridium Catalyst: α-Methyl Allyl Acetate as a Surrogate to Preformed Crotylmetal Reagents," Kim, I. S.; Han, S. B.; Krische, M. J. *J. Am. Chem. Soc.* **2009**, *131*, 2514–2520. (c) "Enantioselective C-H Crotylation of Primary Alcohols via Hydrohydroxyalkylation of Butadiene," Zbieg, J. R.; Yamaguchi, E.; McInturff, E. L.; Krische, M. J. *Science* **2012**, *336*, 324–327. And references cited therein.

diphenyl phosphinoyl-protected ketoimine participates in allyl transfers at a much slower rate (25% conversion, Scheme 2.24).[81] The phosphinoyl ketoimine synthesized from

Scheme 2.24 Extension of NHC–Cu-Catalyzed Allyl Additions to Ketoimines

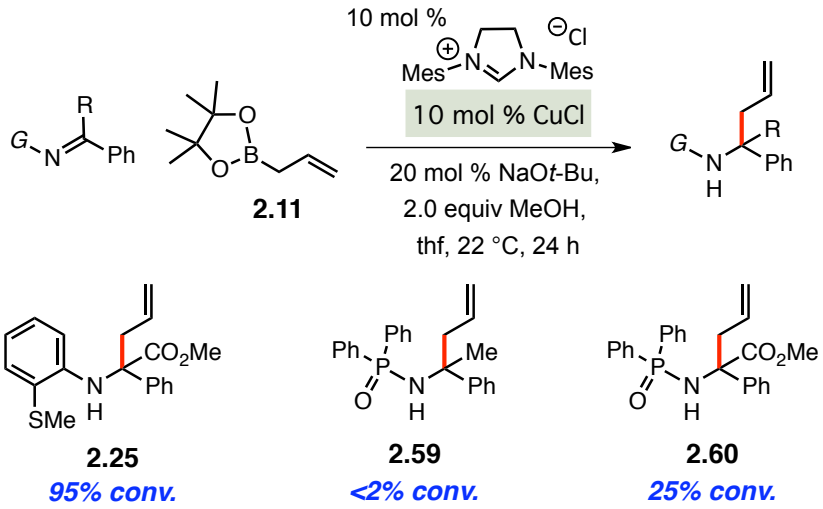

acetophenone is inactive towards allyl transfer; the electrophilicity of the prochiral carbon in the C=N unsaturation is significantly enhanced with the addition of an electron-withdrawing α-ester group. Notably, the reactivity of the NHC–Cu-based catalyst pales in comparison to the excellent efficiencies with which additions are afforded by the phosphine–Cu-allyl complex described by Shibasaki and coworkers; in this case, additions to *unactivated* benzyl-protected ketoimines promoted by an achiral phosphine–Cu-F complex and La(O*i*-Pr)$_3$ generate the allyl-substituted tertiary carbamines in 85–98% yield within four hours (see Scheme 2.8 for the chiral catalytic system, the achiral catalyst system described here is not pictured).[34b] Nevertheless, we examined the enantiocontrol with which the NHC–Cu-catalyst derived from **2.48** could afford α-

[81] Calculated natural atomic charges of various acetaldehyde-derived imines reveal that those bearing *N*-aryl substitutents had charges of +0.19 and 0.20 while phosphinoyl aldimines showed a positive charge of +0.26 (in comparison to the much higher electropositivity on the acetaldehyde carbon of +0.51). For details, see: "Copper-Catalyzed Asymmetric Alkylation of Imines with Dialkylzinc and Related Reactions," Yamada, K.; Tomioka, K. *Chem. Rev.* **2008**, *108*, 2874–2886.

disubstituted amino acid derivative **2.60**; unfortunately, the homoallylic amide is provided with only 32% conversion and as a 62:38 mixture of enantiomers (equation 2).

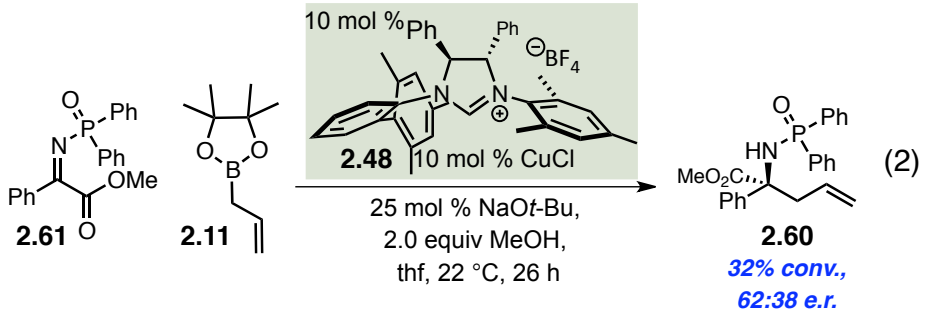

(2)

Another strategy for the preparation of enantioenriched homoallylic amides was explored to exploit the reactivity of the discovered NHC–Cu-allyl complexes. The NHC–Cu-O*t*-Bu complex, prepared *in situ* from commericially available achiral imidazolinium salt **SIMes**, promotes diastereoselective additions to imines derived from *N-tert*-butanesulfinamide, a chiral auxillary developed by Ellman.[20] (*R*)-*tert*-Butanesulfinyl imine **2.62** is transformed to the corresponding homoallylic sulfinamide **2.63** within three hours, in the presence of 5 mol % **SIMes**–Cu-O*t*-Bu, with 95:5 d.r. (Scheme 2.25). Transfer of the stereogenicity is imposed by the Zimmerman Traxler-type cyclic transition state; bidentate chelation of the N and O of the sulfinyl imine to the copper center favors allyl transfer from the *si*-face of the imine. Transformations in the absence of the carbene ligand are promoted by Cu-O*t*-Bu to 70% conversion in four hours, however, with diminished stereoselection (only 74:26 d.r., data not shown). Moreover, a range of diastereoselectivities for the allyl addition are observed with varying carbene ligands, suggestive that the donation from the NHC is likely responsible for enhancing the Lewis acidity of copper, thereby reinforcing a tight cyclic geometry for the transition state.

Scheme 2.25 NHC–Cu-Catalyzed Diastereoselective Allyl Additions to Enantiopure *N-tert*-Butanesulfinyl Imines

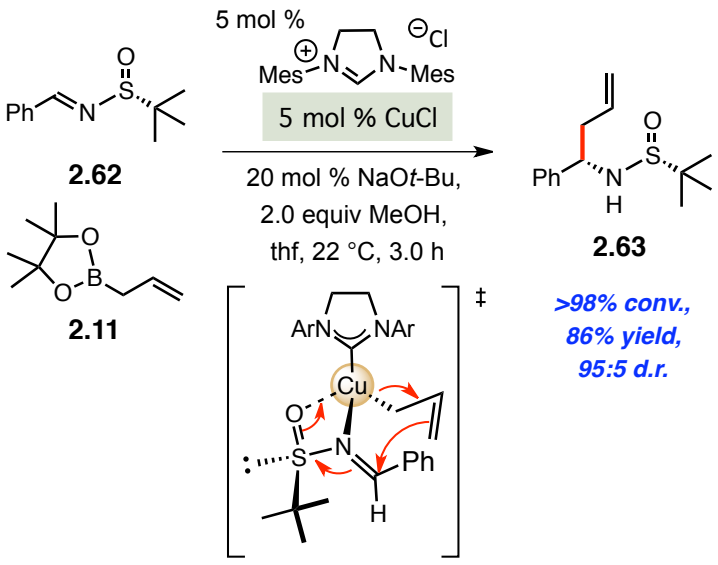

2.7 Conclusions

Detailed in this chapter are our efforts to provide new, sustainable, and reactive catalysts for the preparation of enantioenriched homoallylic amines, entities that display unique synthetic versatility, particularly towards the synthesis of biologically active molecules. Studies initiated by Ag-catalyzed reactions of allyl boronic acid pinacol ester have led to the identification of both Lewis base and Lewis acid catalysts for the activation of this class of allyl nucleophiles. *N*-Heterocylic carbenes (NHCs), potent two electron donors, were central to these studies, both in serving as nucleophilic catalysts and as stabilizing ligands in complexes with metals. We have demonstrated Cu-complexes of chiral NHCs to be effective and general catalysts for the activation of C–B bonds, allowing for rapid entry to a broad class of enantioenriched homoallylic amines. A model for stereoinduction, amenable to describing a wide class of chiral monodentate

carbene ligands and their metal complexes, was derived; targeted modification of the three-dimensional structure of the catalysts revealed the vital blueprint that led to the optimal facial selectivities in additions to phosphinoyl aldimines.

Limitations employing allylmetals, particularly NHC–Cu-allyl complexes, were discovered, of utmost significance, being the inability to control the configuration of copper complexes bearing dissymmetric allyl units. Studies to be described in the following chapters will address the shortcomings of the present Cu-catalyzed process: modification of the allylcopper to a configurationally stable allenylcopper for highly selective propargyl additions (Chapter 3) and the development of a *metal-free* catalyst for allyl and allenyl additions that offer unique and complementary reactivity to the Cu-catalyzed transformations detailed herein (Chapter 4).

2.8 Experimentals

General. Infrared (IR) spectra were recorded on a Bruker alpha spectrophotometer, n_{max} in cm^{-1}. Bands are characterized as broad (br), strong (s), medium (m), and weak (w). ^{1}H NMR spectra were recorded on a Varian Unity INOVA 400 (400 MHz) spectrometer. Chemical shifts are reported in ppm from tetramethylsilane with the solvent resonance as the internal standard ($CDCl_3$: δ 7.26 ppm). Data are reported as follows: chemical shift, integration, multiplicity (s = singlet, d = doublet, t = triplet, q = quartet, sept = septet, br = broad, m = multiplet), and coupling constants (Hz). ^{13}C NMR spectra were recorded on a Varian Unity INOVA 400 (100 MHz) or a Varian Unity INOVA 500 (125 MHz) spectrometer with complete proton decoupling. Chemical shifts are reported in ppm from tetramethylsilane with the solvent resonance as the internal standard ($CDCl_3$: δ 77.16 ppm). ^{11}B NMR spectra were recorded on a Varian Unity INOVA 550 (160 MHz)

spectrometer. High-resolution mass spectrometry was performed on a JEOL AccuTOF-DART (positive mode) at the Mass Spectrometry Facility, Boston College. Enantiomer ratio (e.r.) values were determined by HPLC analysis (Chiral Technologies Chiralcel OD (4.6 x 250 mm), Chiral Technologies Chiralcel OD-H (4.6 x 250 mm), Chiral Technologies Chiralcel OJ-H (4.6 x 250 mm), Chiral Technologies Chiralpak AD-H (4.6 x 250 mm)). Specific rotations were measured on a Rudolph Research Analytical Autopol IV Polarimeter.

Unless otherwise noted, all reactions were carried out with distilled and degassed solvents under an atmosphere of dry N_2 in oven- (135 °C) or flame-dried glassware with standard dry box or vacuum-line techniques. Tetrahydrofuran (Aldrich) was purified by distillation from sodium benzophenone ketyl immediately prior to use unless otherwise specified. Methanol (Acros) was purified by distillation from Mg (Strem) prior to use. All work-up and purification procedures were carried out with reagent grade solvents (purchased from Fisher) in air. Allylboronic acid pinacol ester **2.11** and *cis*-crotylboronic acid pinacol ester **2.57** were purchased from Aldrich or received from Frontier Scientific, Inc and distilled prior to use. Allylboronates substituted at the 2-position (**2.53** and **2.55**) were synthesized through a Pd-catalyzed cross-coupling of bis(pinacolato)diboron and the corresponding allyl acetates.[82] Achiral azolium salts (**SiMes**, **IMes**, and **ICy**) were purchased from Aldrich and recrystallized prior to use. Sodium *tert*-butoxide and copper(I) chloride were purchased from Strem and used as received. Aryl-, heteroaryl-, and alkene- *N*-diphenylphosphinoyl imines were synthesized through the use of a condensation promoted by $TiCl_4$ between *P*,*P*-diphenylphosphinic

[82] "A Synthesis of Allylboronates *via* the Palladium(0)-Catalyzed Cross-Coupling Reaction of Bis(pinacolato)diboron with Allylic Acetates," Ishiyama, T.; Ahiko, T-a.; Miyaura, N. *Tetrahedron Lett.* **1996**, *37*, 6889–6892.

amide and the corresponding aldehyde.[83] Alkyl-substituted aldimines were synthesized through the intermediacy of the corresponding sulfinyl adducts according to previously disclosed methods.[84] Chiral bidentate and monodentate imidazolinium salts and their respective silver complexes were prepared as previously disclosed.[85]

▪ **Representative experimental procedure for Ag-catalyzed addition of allylboronic acid pinacolic ester 2.11 to *ortho*-thiomethylaniline derived imines***:* An oven-dried 13x100 mm test tube equipped with a stir bar is charged with AgOAc (1.7 mg, 10.0 μmol), **2.23** (6.5 mg, 10.0 μmol), and amino acid-derived phosphine **2.26** (22.7 mg, 0.100 mmol). The test tube is sealed with a septum and electrical tape, after which it is evacuated and filled with an atmosphere of N_2. Freshly distilled tetrahyrdofuran (1.00 mL) and *iso*-propanol (10.0 μL, 0.200 mmol) is added. Allyl boronic pincaol ester **2.11** (26.2 μL, 0.140 mmol) is added to the solution with a synringe. The resulting homogenous solution is allowed to cool to –30 °C for three hours before addition of 500 μL of saturated aqueous solution of $NaHCO_3$. The water layer is washed with Et_2O (3 x 2

[82] (a) "The Titanium Tetrachloride Induced Synthesis of *N*-Phosphinoylimines and *N*-Sulphoylimines Directly from Aromatic Aldehydes," Jennings, W. B.; Lovely, C. J. *Tetrahedron.* **1991**, *47*, 5561–5568. (b) "The First Catalytic Asymmetric Nitro-Mannich-type Reaction Promoted by a New Heterobimetallic Complex," Yamada, K-i.; Harwood, S. J.; Gröger, H.; Shibasaki, M. *Angew. Chem., Int. Ed.* **1999**, *38*, 3504–3506.

[84] (a) "Catalytic Asymmetric Addition of Diorganozinc Reagents to *N*-Phosphinoylalkylimines," Côté, A.; Boezio, A. A.; Charette, A. B. *Proc. Natl. Acad. Sci.* **2004**, *101*, 5405–5410. (b) "Direct Catalytic Asymmetric Mannich-type Reactions of Isomerizable Aliphatic Imines: Chemoselective Enolate Formations from a Hydroxyketones by a Zn-Catalyst," Yamaguchi, A.; Matsunaga, S.; Shibasaki, M. *Tetrahedron Lett.* **2006**, *47*, 3985–3989.

[85] (a) "A Readily Available Chiral Ag-Based *N*-Heterocyclic Carbene Complex for Use in Efficient and Highly Enantioselective Ru-Catalyzed Olefin Metathesis and Cu-Catalyzed Allylic Alkylation Reactions," Van Veldhuizen, J. J.; Campbell, J. E.; Giudici, R. E.; Hoveyda, A. H. *J. Am. Chem. Soc.* **2005**, *127*, 6877–6882. (b) "All-Carbon Quaternary Stereogenic Centers by Enantioselective Cu-Catalyzed Conjugate Additions Promoted by a Chiral *N*-Heterocyclic Carbene," Brown, M. K.; May, T. L.; Baxter, C. A.; Hoveyda, A. H. *Angew. Chem., Int. Ed.* **2007**, *46*, 1097–1100. (c) "Monodentate Non-C_2-symmetric Chiral *N*-Heterocyclic Carbene Complexes for Enantioselective Synthesis. Cu-Catalyzed Conjugate Additions of Aryl- and Alkenylsilylfluorides to Cyclic Enones," Lee, K.-s.; Hoveyda, A. H. *J. Org. Chem.* **2009**, *74*, 4455–4462.

mL), the organic layers are combined, dried over $MgSO_4$, and the volatiles are removed *in vacuo*. The unpurified residue obtained as an off-white oil is purified by silica gel chromatography (200:1 hexanes:EtOAc) to yield pure **2.24** as a colorless oil in 92% yield.

(*R*)-2-(methylthio)-*N*-(1-phenylbut-3-en-1-yl)aniline (**2.24**): IR (neat): 3363 (w, br), 3063 (w), 2854 (w), 1585 (s), 1497 (s), 1449 (s), 1317 (m), 1283 (m), 1037 (m), 992 (m), 919 (m), 743 (s), 699 (s), 465 (s) cm^{-1}. ^1H NMR (400 MHz, $CDCl_3$): δ 7.41–7.39 (1H, dd, J = 7.6, 1.6 Hz), 7.37–7.31 (4H, m), 7.26–7.22 (1H, m), 7.02–6.98 (1H, m), 6.60 (1H, ddd, J = 7.6, 7.6, 1.2 Hz), 6.31 (1H, dd, J = 8.4, 1.2 Hz), 5.82 (1H, dddd, J = 17.2, 10.4, 7.2, 7.2 Hz), 5.55 (1H, br d, J = 4.4 Hz), 5.29–5.18 (2H, m), 4.46 (1H, dddd, J = 8.0, 8.0, 5.0 Hz), 2.72–2.55 (2H, m), 2.39 (3H, s). ^{13}C NMR (100 MHz, $CDCl_3$): δ 147.4, 143.4, 134.6, 134.2, 129.4, 128.7, 127.1, 126.4, 119.9, 118.5, 117.1, 111.5, 57.3, 43.6, 18.3. HRMS Calcd for $C_{17}H_{20}NS$ $[M + H]^+$: 270.13164; Found: 270.13280. The enantiomeric purity of this compound was determined by HPLC analysis in comparison with authentic racemic material (Chiralcel OD, 98:2 hexanes:*i*-PrOH, 0.5 mL/min, 220 nm): t_R : 9 min (minor) and 12 min (major).

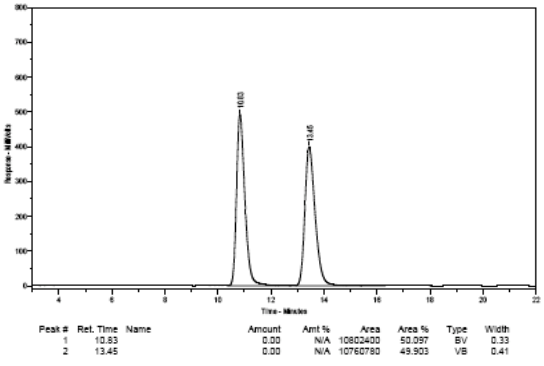

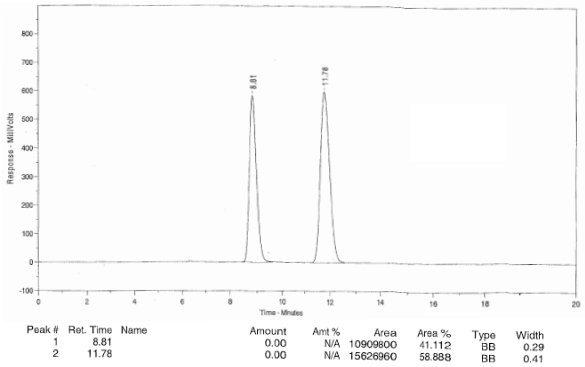

Peak #	Ret. Time	Area %	Peak #	Ret. Time	Area %
1	10.8 min	50.097	1	8.8 min	41.112
2	13.4 min	49.903	2	11.8 min	58.888

(*R*)-Methyl 2-((2-(methylthio)phenyl)amino)-2-phenylpent-4-enoate (**2.25**): ^{1}H NMR (400 MHz, $CDCl_3$): δ 7.59–7.58 (1H, m), 7.43 (1H, dd, *J* = 1.6, 7.6 Hz), 7.38–7.28 (3H, m), 6.87–6.83 (1H, m), 6.60 (1H, s), 6.58 (1H, ddd, *J* = 7.6, 7.6, 1.2 Hz), 6.02 (1H, dd, *J* = 8.0, 0.8 Hz), 5.61 (1H, dddd, *J* = 17.2, 10.0, 7.2, 7.2 Hz), 5.10–5.02 (2H, m), 3.69 (3H, s), 3.27 (2H, app d, *J* = 7.2 Hz), 2.42 (3H, s); The enantiomeric purity of this compound was determined by HPLC analysis in comparison with authentic racemic material (Chiralcel OD, 100% hexanes, 0.4 mL/min, 220 nm): t_R : 77 min (major) and 92 min (minor).

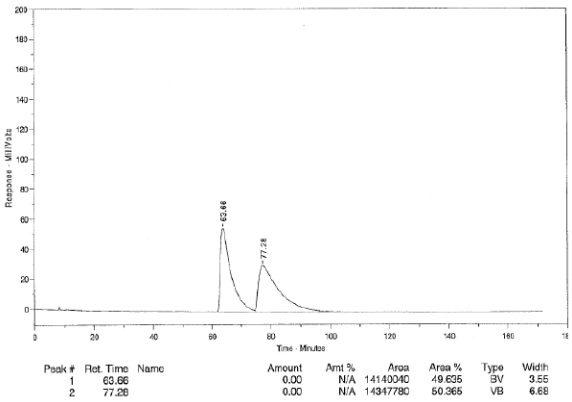

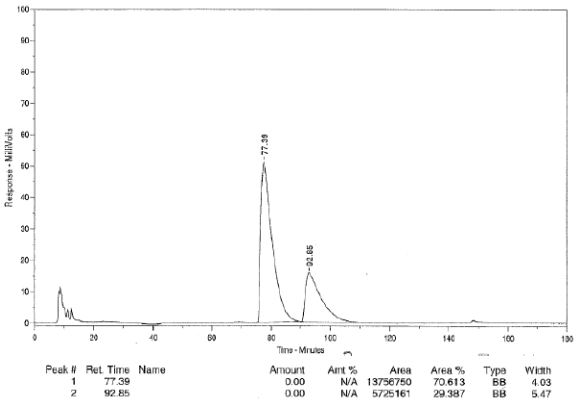

Peak #	Ret. Time	Area %	Peak #	Ret. Time	Area %
1	63.7 min	49.635	1	77.3 min	70.613
2	77.3 min	50.365	2	92.8 min	29.387

▪ **Representative experimental procedure for *NHC-catalyzed* additions of allylboronic acid pinacolic ester 2.11 to *ketones:*** In a N_2-filled glovebox, an oven-dried vial equipped with a stir bar is charged with NaO*t*-Bu (1.0 mg, 10.0 μmol), **SIMes** (3.5 mg, 10.0 μmol). Freshly distilled tetrahyrdofuran (1.00 mL) is added and the vial is sealed with a septum and electrical tape, and allowed to premix for one hour. A separate oven-dried vial is charged with the ketone (0.100 mmol), tetrahyrofuran, and methanol

(8.0 μL, 0.200 mmol). The milky catalyst solution is removed from the glovebox and allylboron **2.11** (26.2 μL, 0.140 mmol) is added with a syringe. The catalyst solution is then added to the vial containing the substrate and the resulting homogenous solution is allowed to stir at 22 ºC for two hours, after which the volatiles are removed *in vacuo*. The unpurified residue, obtained as an off-white oil, is purified by silica gel chromatography.

2-Phenylpent-4-en-2-ol (**2.33**): ^{1}H NMR (400 MHz, $CDCl_3$): δ 7.46–7.43 (2H, m), 7.37–7.33 (2H, m), 7.27–7.22 (1H, m), 5.68–5.57 (1H, m), 2.72–2.67 (1H, m), 2.53–2.48 (1H, m), 2.06 (1H, s), 1.56 (3H, s); The enantiomeric purity of this compound was determined by HPLC analysis in comparison with authentic racemic material (Chiralcel OJ–H 97:3 hexanes:*i*-propanol, 1.0 mL/min, 220 nm): t_R : 9 min (major) and 11 min (minor).

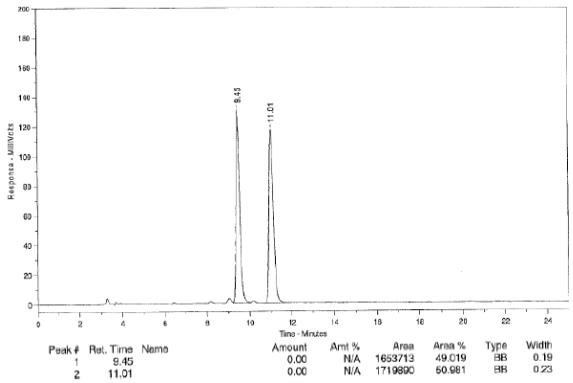

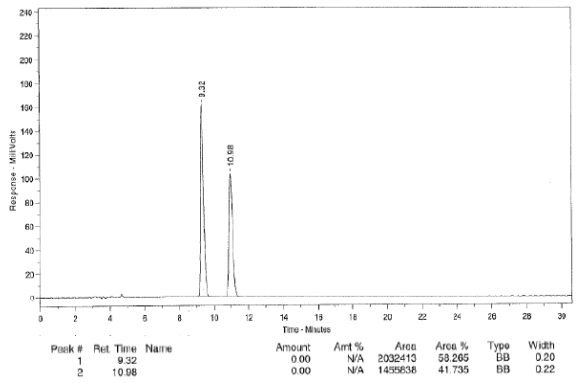

Peak #	Ret. Time	Area %
1	9.4 min	49.019
2	11.0 min	50.981

Peak #	Ret. Time	Area %
1	9.3 min	58.265
2	11.0 min	41.735

Methyl 2-hydroxy-2-phenylpent-4-enoate (**2.34**): clear oil; ^{1}H NMR (400 MHz, $CDCl_3$): δ 7.62–7.59 (2H, m), 7.39–7.30 (4H, m), 5.85–5.75 (1H, m), 5.21–5.13 (2H, m), 3.78 (3H, s), 3.01–2.95 (1H, m), 2.80–2.74 (1H, m).

3-Allyl-3-hydroxy-1-methylindolin-2-one (**2.35**): IR (neat): 3292 (s, br), 1692 (s), 1615 (m), 1469 (m), 1437 (m), 1383 (s), 1304 (m), 1211 (m), 1094 (s), 1014 (m), 941 (m), 756 (m), 636 (s), 494 (m) cm^{-1}. ^{1}H NMR (400 MHz, $CDCl_3$): δ 7.40-7.38 (1H, m), 7.32 (1H, ddd, *J*= 7.6, 1.2, 1.2 Hz), 7.09 (1H, ddd, *J*= 7.6, 0.8, 0.8 Hz), 6.82 (1H, d, *J*= 7.6 Hz), 5.68–5.58 (1H, m), 5.12–5.06 (2H, m), 3.41 (1H, s), 3.17 (3H, s), 2.78–2.72 (1H, m), 2.64–2.58 (1H, m); ^{13}C NMR (100 MHz, $CDCl_3$): δ 177.9, 143.4, 130.6, 129.83, 129.76, 124.2, 123.2, 120.5, 76.6, 42.9, 26.3. The optical purity of the compound is determined by HPLC analysis in comparison with authentic racemic material (OD, 92:8 hexanes:*i*-PrOH, 1.0 mL/min, 220 nm) t_R of **2.50**: 8 min (minor) and 10 min (major).

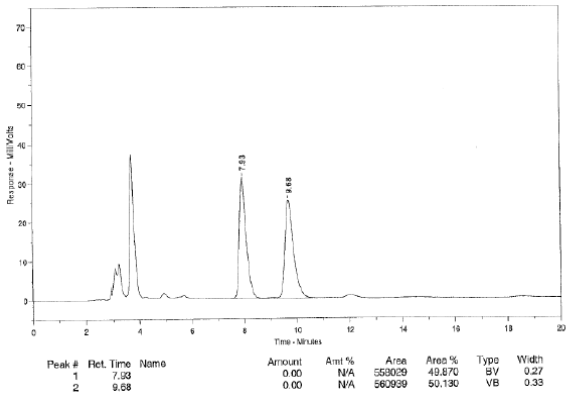

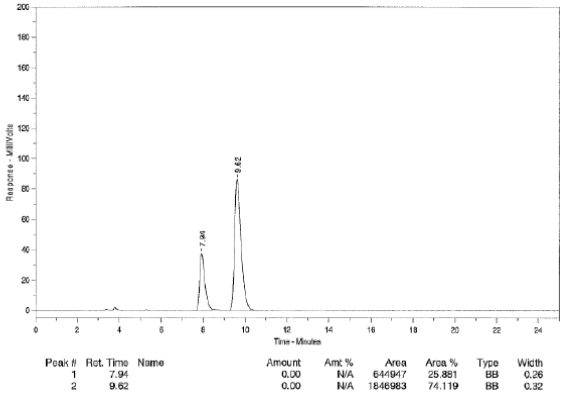

Peak #	Ret. Time	Area %	Peak #	Ret. Time	Area %
1	7.9 min	49.870	1	7.9 min	25.881
2	9.7 min	50.130	2	9.6 min	74.119

▪ ***NHC–Cu catalyzed allyl additions to phosphinoyl aldimines:*** Chiral C_1- and C_2-symmetric imidazolinium salts were prepared through the synthetic route outlined in Scheme 2.20 developed by Dr. Kang Sang Lee and as described in the literature.[84c] Through our studies for the enantioselective allyl additions to aldimines, two new carbene precursors were discovered:

Imidazolinium Tetrafluoroborate Salt (**2.50**): Imidazolinium salt **2.50** was prepared according to a previously disclosed procedure.[84c] The requisite 2-iodo or 2-bromo-1-isopropyl-3-methylbenzene for the synthesis of **2.50** can be prepared through a reported Sandmeyer reaction[86] of commercially available 2-isopropyl-6-methylaniline. **2.50**: IR (neat): 3064 (w, br), 2966 (w, br), 1617 (s), 1586 (m), 1455 (m), 1268 (m), 1220 (m), 1055 (s), 912 (m), 761 (m), 728 (s), 701 (m) cm^{-1}; ^1H NMR (400 MHz, $CDCl_3$) 5:1 mixture of rotamers: δ 9.09 (0.2H, s), 8.81 (1H, s), 8.16 (1H, dd, *J* = 8.0, 1.2 Hz), 7.99 (1H, dd, *J* = 8.0, 1.2 Hz), 7.54–7.50 (1.2H, m), 7.47–7.42 (4H, m), 7.40–7.28 (5H, m), 7.26–7.18 (4H, m), 7.16–7.11 (5H, m), 6.92 (1H, dd, *J* = 8.0, 1.2 Hz), 6.84–6.81 (0.2H, m), 6.41–6.39 (2.4H, m), 5.43 (0.2H, d, *J* = 6.8 Hz), 5.39 (1H, d, *J* = 7.6 Hz), 5.20 (1H, d, *J* = 7.6 Hz), 5.04 (0.2H, d, *J* = 6.8 Hz), 3.09 (0.2H, sept, *J* = 6.8 Hz), 2.56 (6H, s), 2.53 (0.6H, s), 2.26 (1H, sept, *J* = 6.8 Hz), 2.07 (0.6H, s), 2.04 (3H, s), 1.91 (3H, s), 1.89 (0.6H, s), 1.47 (0.6H, d, *J* = 6.8 Hz), 1.22 (0.6H, d, *J* = 6.8 Hz), 1.09 (1H, d, *J* = 6.8 Hz), 0.31 (1H, d, *J* = 6.4 Hz); ^{13}C NMR (100 MHz, $CDCl_3$) 5:1 mixture of rotamers: δ 158.2 (minor), 157.7, 146.3, 146.2 (minor), 139.0, 137.0, 136.6, 136.55, 136.52, 136.4, 136.0, 135.9, 135.6, 134.5, 132.6, 132.4, 131.6, 131.4, 130.9, 130.8, 130.7, 130.6, 130.4, 130.3, 130.2, 130.12, 130.08, 130.00, 129.8, 129.7, 129.4, 129.3, 129.13, 129.07, 129.0, 128.9, 128.8, 128.7, 127.1, 126.6, 125.4, 124.6, 77.9 (minor), 75.8, 72.4, 71.9 (minor), 53.6, 28.9, 28.5, 26.0, 24.6, 24.1, 22.8, 21.55, 21.50, 21.4, 20.71, 20.67, 18.9, 17.9; HRMS Calcd for $C_{40}H_{41}N_2$ $[M - BF_4]^+$: 549.3270; Found: 549.3273. $[\alpha]^{24}_D = -171.4$ (*c* = 0.275, $CHCl_3$).

[86] "Efficient One-pot Transformation of Aminoarenes to Haloarenes Using Halodimethylsulfonium Halides Generated *in situ*," Baik, W.; Luan, W.; Lee, H. J.; Yoon, C. H.; Koo, S.; Kim, B. H. *Can. J. Chem.* **2005**, *83*, 213–219.

Imidazolinium Tetrafluoroborate Salt (2.52): Imidazolinium salt **2.52** was prepared according to a previously disclosed procedure.[84c] The requisite biaryl iodide for the synthesis of **2.52** can be prepared through an *ortho*-iodination of commercially available 4-isopropylaniline[87] followed by a modifed Sandmeyer reaction[88]. **2.52**: IR (neat): 3062 (w, br), 2963 (w, br), 1621 (s), 1602 (m), 1455 (m), 1268 (m), 1220 (m), 1059 (s), 1034 (s), 911 (m), 758 (m), 782 (m) cm^{-1}; ^1H NMR (400 MHz, $CDCl_3$): δ 8.76 (1H, s), 7.90 (1H, d, *J* = 1.6 Hz), 7.46–7.37 (5H, m), 7.31–7.28 (2H, m), 7.20 (1H, br s), 7.16–7.10 (3H, m), 7.01 (1H, d, *J* = 7.6 Hz), 6.92 (1H, br s), 6.60 (1H, br s), 6.44–6.41 (2H, m), 5.35 (1H, d, *J* = 7.2 Hz), 5.21 (1H, d, *J* = 7.2 Hz), 3.04 (1H, sept, *J* = 6.8 Hz), 2.52 (3H, s), 2.50 (3H, s), 2.18 (3H, s), 2.06 (3H, s), 1.93 (3H, s), 1.59 (3H, s), 1.25 (6H, d, *J* = 7.2 Hz); ^{13}C NMR (100 MHz, $CDCl_3$): δ 157.8, 151.4, 140.2, 138.6, 137.1, 136.7, 136.1, 135.6, 134.9, 134.7, 133.6, 133.1, 132.2, 131.2, 130.8, 130.3, 130.0, 129.9, 129.6, 129.5, 129.3, 129.1, 129.0, 128.8, 128.6, 128.3, 127.4, 75.5, 72.5, 33.6, 24.1, 23.1, 21.52, 21.50, 21.1, 21.0, 18.7, 17.7. HRMS Calcd for $C_{42}H_{45}N_2$ $[M - BF_4]^+$: 577.3583; Found: 577.3607. $[\alpha]^{25}_D = -167.2$ (*c* = 0.275, $CHCl_3$).

▪ **Representative Procedure for NHC–Cu-Catalyzed Enantioselective Allyl Additions to *N*-diphenylphosphinoyl imines:** *Preparation of the chiral NHC–Cu catalyst:* An oven-dried vial equipped with a stir bar was charged with imidazolinium salt **2.48** (12.5 mg, 20.0 μmol), NaO*t*-Bu (4.6 mg, 48 μmol), and CuCl (1.9 mg, 20 μmol) in a N_2 filled glovebox. The vial was sealed with a cap (phenolic open top cap with a red

[87] "Carbon Networks Based on Dehydrobenzoannulenes. 4. Synthesis of "Star" and "Trefoil" Graphdiyne Substructures via Sixfold Cross-Coupling of Hexaiodobenzene," Wan, W. B.; Haley, M. M. *J. Org. Chem.* **2001**, *66*, 3893–3901.

[88] (a) "Reactive Annulenones: A Comparative Study," Gaviña, F.; Costero, A. M.; González, A. M. *J. Org. Chem.* **1990**, *55*, 2060–2063. (b) "Avoiding the Classical Resolution During the Synthesis of MeO-BIPHEP and 3,3'-Disubstituted Derivatives," Gorobets, E.; Wheatley, B. M. M.; Hopkins, J. M.; McDonald, R.; Keay, B. A. *Tetrahedron Lett.* **2005**, *46*, 3843–3846.

PFTE/white silicone septa) and electrical tape, and removed from the glovebox. Freshly distilled thf (1.00 mL) was added and the mixture was allowed to stir for one hour under N_2 at 22 °C.

Another oven-dried vial equipped with a stir bar was charged with aldimine **2.31a** (30.5 mg, 0.100 mmol). The vial was sealed with a septum and electrical tape and purged with N_2. Freshly distilled thf (250 μL) and MeOH (8.1 μL, 0.20 mmol) were added and the solution was allowed to cool to –50 °C (dry ice/acetone bath). An appropriate portion of the stock solution of the NHC–Cu complex (250 μL) was transferred to the vial containing substrate **2.31a** at –50 °C. To the solution, allyl boronate **2.11** (26.2 μL, 0.140 mmol) was added and the mixture was allowed to stir for six hours at –50 °C before addition of 1.0 mL of 1 M aqueous solution of HCl (to quench any unreaction aldimine). The solution was allowed to warm to 22 °C and the reaction mixture was diluted with AcOEt. The layers were separated and the water layer was washed with AcOEt (3 x 2 mL). The organic layers were combined and dried with $MgSO_4$ and the volatiles were removed *in vacuo*. The unpurified residue obtained as an off-white solid is purified by silica gel chromatography (a gradient from 1:1 hexanes:Et_2O to 100% Et_2O is used to remove pinacol from the mixture followed by 4:1 AcOEt:hexanes with 5% Et_3N to 100% AcOEt with 5% Et_3N) to yield 32.5 mg (0.094 mmol, 94% yield) of pure **2.32a** as a white crystalline solid in 97:3 er (94% ee).

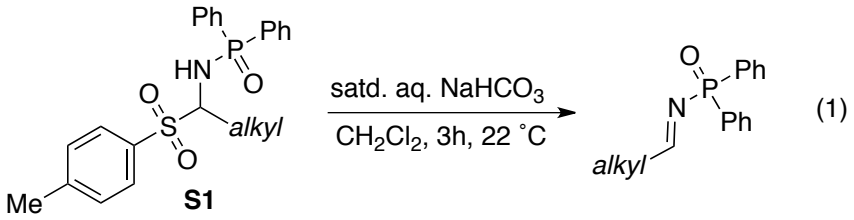

(1)

▪ **Representative Procedure for NHC–Cu-Catalyzed Enantioselective Allyl Additions to Alkyl-Substituted *N*-diphenylphosphinoyl imines**: *Preparation of the alkyl-substituted aldimine:* A vial equipped with a stir bar was charged with sulfinyl adduct **S1** (0.06 mmol) to which was added CH_2Cl_2 (12.0 mL) and a saturated aqueous solution of $NaHCO_3$ (12.0 mL) consecutively. The biphasic mixture was allowed to stir for three hours at 22 °C. The organic layer was separated and the aqueous phase was washed with CH_2Cl_2 (2 x 6 mL). The combined organic layers were dried over $MgSO_4$. The volatiles were removed under reduced pressure and the unpurified imine was used without further purification in the Cu-catalyzed allyl addition.

In an oven-dried vial equipped with a stir bar was charged the abovementioned freshly prepared alkyl-substituted aldimine as a solution in freshly distilled thf (0.2 M) and MeOH (2.0 equiv). The vial was sealed with a septum and electrical tape and purged with N_2. The solution was allowed to cool to –50 ˚C (dry ice/acetone bath) and an appropriate portion of the stock solution of the NHC–Cu complex (see above) was transferred to the vial containing the substrate at –50 °C. To the solution, allyl boronate **2.11** was added and the mixture was allowed to stir for 6 h at –50 °C before addition of 1.0 mL of a 1 M aqueous solution of HCl. The solution was allowed to warm to 22 °C and the reaction mixture was diluted with AcOEt. The organic layer was separated and the aqueous layer was washed with AcOEt (3 x 2 mL). The organic layers were combined and dried with $MgSO_4$. The volatiles were removed *in vacuo*. The unpurified residue obtained as an off-white solid was purified by silica gel chromatography (the same

conditions in the general procedure for allyl addition to aldimine **2.31a**).

▪ ***Analytical Data for Homoallylamides*** **2.32a–2.32v**

(*S*)–*P*,*P*-Diphenyl-*N*-(1-phenylbut-3-en-1-yl)phosphinic amide (**2.32a**): mp = 143–144 °C. IR (neat): 3176 (w, br), 1437 (m), 1184 (s), 1123 (m), 915 (m), 724 (m), 696 (s), 535 (m) cm^{-1}; ^1H NMR (400 MHz, $CDCl_3$): δ 7.89–7.84 (2H, m), 7.79–7.74 (2H, m), 7.51–7.47 (1H, m), 7.45–7.41 (3H, m), 7.34–7.18 (7H, m), 5.61 (1H, dddd, *J* = 17.2, 10.0, 7.2, 7.2 Hz), 5.11–5.03 (2H, m), 4.47 (1H, dddd, *J* = 10.4, 10.4, 6.4, 6.4 Hz), 3.35 (1H, br dd, *J* = 9.6, 6.0 Hz), 2.74–2.60 (2H, m); ^{13}C NMR (100 MHz, $CDCl_3$): δ 143.1 (d, *J* = 5.2 Hz), 133.8, 133.3 (d, *J* = 130 Hz, only peak at 133.9 visible, the other is overlapping), 132.6 (d, *J* = 9.6 Hz), 132.2 (d, *J* = 130 Hz), 131.95 (d, *J* = 3.0 Hz), 131.93 (d, *J* = 9.7 Hz), 131.8 (d, *J* = 3.0 Hz), 128.6 (d, *J* = 12.6 Hz), 128.5, 128.4 (d, *J* = 12.6 Hz), 127.2, 126.6, 118.9, 54.6, 43.8 (d, *J* = 3.7 Hz); HRMS Calcd for $C_{22}H_{23}NOP$ $[M + H]^+$: 348.15173; Found: 348.15315. $[\alpha]^{25}_D$ = –46.0 (*c* = 1.00, $CHCl_3$) for a 99:1 e.r. sample. The enantiomeric purity of this compound was determined by HPLC analysis in comparison with authentic racemic material (Chiracel OD, 92:8 hexanes:*i*-PrOH, 1.0 mL/min, 220 nm): t_R of **2.32a**: 8 min (minor) and 10 min (major).

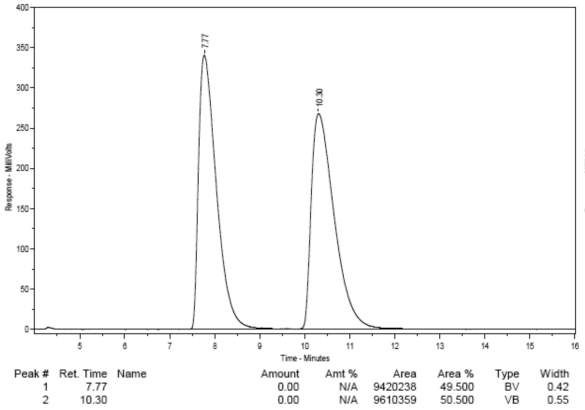

Peak #	Ret. Time	Name	Amount	Amt %	Area	Area %	Type	Width
1	7.77		0.00	N/A	9420238	49.500	BV	0.42
2	10.30		0.00	N/A	9610359	50.500	VB	0.55

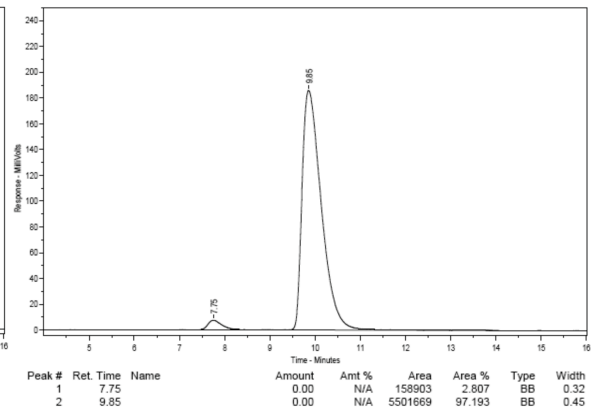

Peak #	Ret. Time	Name	Amount	Amt %	Area	Area %	Type	Width
1	7.75		0.00	N/A	158903	2.807	BB	0.32
2	9.85		0.00	N/A	5501669	97.193	BB	0.45

Peak #	Ret. Time	Area %
1	7.8 min	49.500
2	10.3 min	50.500

Peak #	Ret. Time	Area %
1	7.8 min	2.807
2	9.9 min	97.193

(*S*)–*N*-(1-(Naphthalen-2-yl)but-3-en-1-yl)-*P*,*P*-diphenylphosphinic amide (**2.32b**): mp = 134–136 °C. IR (neat): 3132 (w, br), 1436 (m), 1181 (s), 1123 (m), 1107 (m), 1070 (m), 915 (m), 817 (m), 745 (m), 721 (m), 694 (s), 553 (s), 516 (m) cm^{-1}; ^1H NMR (400 MHz, $CDCl_3$) δ 7.91–7.86 (2H, m), 7.82–7.75 (5H, m), 7.58 (1H, br s), 7.52–7.40 (5H, m), 7.38–7.35 (2H, m), 7.29–7.25 (2H, m), 5.60 (1H, dddd, *J* = 17.2, 10.0, 7.2, 7.2 Hz), 5.14–5.03 (2H, m), 4.52 (1H, dddd, *J* = 10.0, 10.0, 6.4, 6.4 Hz), 3.47 (1H, br dd, *J* = 9.6, 6.0 Hz), 2.84–2.69 (2H, m); ^{13}C NMR (100 MHz, $CDCl_3$): δ 140.4 (d, *J* = 5.2 Hz), 133.7, 133.33, 133.27 (d, *J* = 127 Hz), 132.8, 132.6 (d, *J* = 9.6 Hz), 132.1 (d, *J* = 130 Hz), 132.0 (d, *J* = 3.0 Hz), 131.9 (d, *J* = 9.7 Hz), 131.8 (d, *J* = 3.0 Hz), 128.6 (d, *J* = 12.6 Hz), 128.42, 128.41 (d, *J* = 12.6 Hz), 128.0, 127.7, 126.2, 125.9, 125.4, 124.7, 119.1, 54.8, 43.7 (d, *J* = 3.7 Hz); HRMS Calcd for $C_{26}H_{25}NOP$ $[M + H]^+$: 398.16738; Found: 398.16725. $[\alpha]^{25}_D$ = –42.7 (*c* = 1.00, $CHCl_3$) for a 97:3 e.r. sample. The enantiomeric purity of this compound was determined by HPLC analysis in comparison with authentic racemic material (Chiracel OD, 92:8 hexanes:*i*-PrOH, 1.0 mL/min, 220 nm): t_R of **2.32b**: 13 min (minor) and 16 min (major).

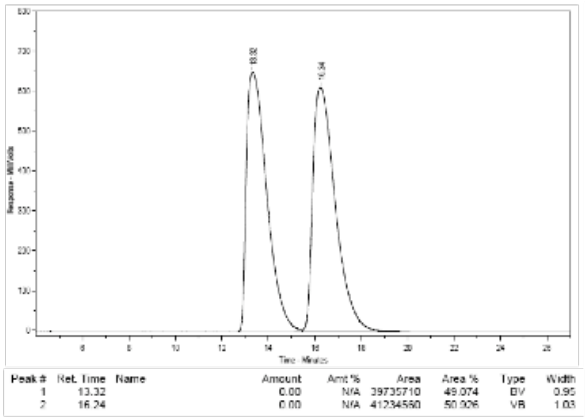

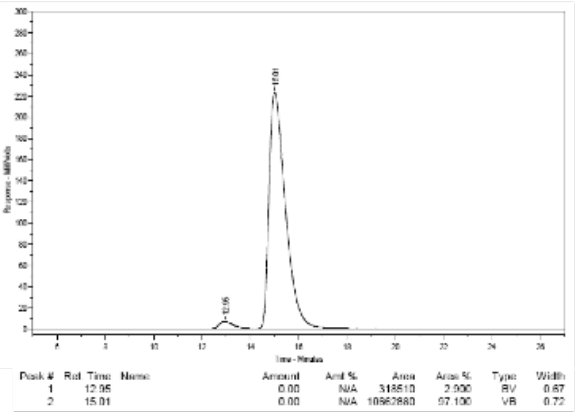

Peak #	Ret. Time	Area %	Peak #	Ret. Time	Area %
1	13.3 min	49.074	1	13.0 min	2.900
2	16.2 min	50.926	2	15.0 min	97.100

(*S*)–*N*-(1-(2-Fluorophenyl)but-3-en-1-yl)-*P*,*P*-diphenylphosphinic amide (**2.32c**): mp = 141–142 °C. IR (neat): 3157 (w, br), 2898 (w, br), 1487 (m), 1461 (m), 1436 (m), 1176 (m), 1123 (m), 1108 (m), 1075 (m), 913 (m), 718 (m), 693 (m), 651 (m), 528 (m), 514 (s) cm^{-1}; ^{1}H NMR (400 MHz, $CDCl_3$): δ 7.87–7.82 (2H, m), 7.78–7.72 (2H, m), 7.51–7.47 (1H, m), 7.44–7.39 (3H, m), 7.34–7.29 (2H, m), 7.23–7.18 (1H, m), 7.15 (1H, ddd, *J* = 7.6, 7.6, 1.6 Hz), 7.05 (1H, ddd, *J* = 7.6, 7.6, 1.2 Hz), 6.97 (1H, ddd, *J* = 10.8, 8.0, 0.8 Hz), 5.61 (1H, dddd, *J* = 17.2, 10.0, 7.2, 7.2 Hz), 5.09–5.01 (2H, m), 4.47 (1H, dddd, *J* = 10.4, 10.4, 6.4, 6.4 Hz), 3.56 (1H, br dd, *J* =10.4, 6.8 Hz), 2.78–2.60 (2H, m); ^{13}C NMR (100 MHz, $CDCl_3$): δ 160.4 (d, *J* = 244 Hz), 133.8, 133.0 (d, *J* = 127 Hz), 132.6 (d, *J* = 9.6 Hz), 132.1 (d, *J* = 130 Hz), 132.0 (d, *J* = 3.0 Hz), 131.95 (d, *J* = 9.7 Hz), 131.89 (d, *J* = 3.0 Hz), 130.1 (dd, *J* = 12.7, 5.2 Hz), 128.9 (d, *J* = 5.3 Hz), 128.8 (d, *J* = 2.3 Hz), 128.6 (d, *J* = 12.7 Hz), 128.4 (d, *J* = 12.6 Hz), 124.1 (d, *J* = 3.7 Hz), 118.8, 115.7 (d, *J* = 21.6 Hz), 125.4, 51.0, 42.7 (dd, *J* = 4.4, 3.7 Hz); HRMS Calcd for $C_{22}H_{22}FNOP$ $[M + H]^+$: 366.14230; Found: 366.14205. $[\alpha]^{26}_{D}$ = –33.0 (*c* = 1.00, $CHCl_3$) for a 98.5:1.5 e.r.

sample. The enantiomeric purity of this compound was determined by HPLC analysis in comparison with authentic racemic material (Chiracel OD, 92:8 hexanes:*i*-PrOH, 0.6 mL/min, 220 nm): t_R of **2.32c**: 15 min (minor) and 17 min (major).

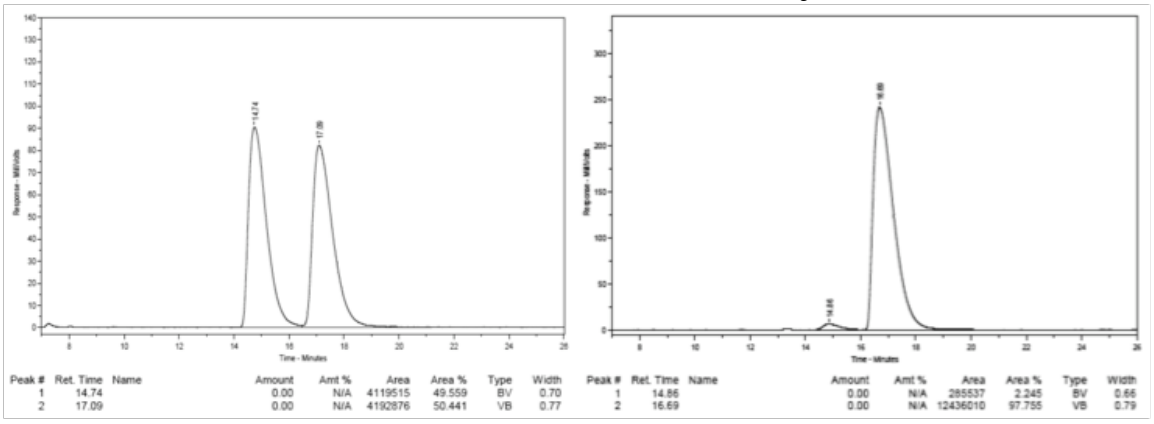

Peak #	Ret. Time	Area %	Peak #	Ret. Time	Area %
1	14.7 min	49.559	1	14.9 min	2.245
2	17.1 min	50.441	2	16.7 min	97.755

(*S*)–*N*-(1-(2-Bromophenyl)but-3-en-1-yl)-*P*,*P*-diphenylphosphinic amide (**2.32d**): mp = 130–131 °C. IR (neat): 3167 (w, br), 1438 (m), 1185 (s), 1109 (m), 1021 (m), 912 (m), 751 (m), 724 (s), 696 (m), 528 (m) cm^{-1}. ^1H NMR (400 MHz, $CDCl_3$): δ 7.87–7.82 (2H, m), 7.75–7.70 (2H, m), 7.51–7.47 (1H, m), 7.44–7.39 (4H, m), 7.35–7.27 (4H, m), 7.07 (1H, ddd, *J* = 8.8, 8.0, 2.0 Hz), 5.64 (1H, dddd, *J* = 17.4, 10.4, 7.2, 7.2 Hz), 5.14–5.10 (2H, m), 4.71 (1H, dddd, *J* = 10.4, 10.4, 6.0, 6.0 Hz), 3.56 (1H, br dd, *J* = 9.6, 6.0 Hz), 2.64 (2H, app t, *J* = 6.4 Hz). ^{13}C NMR (100 MHz, $CDCl_3$): δ 142.0 (d, *J* = 4.5 Hz), 133.4, 133.0, 132.7 (d, *J* = 127 Hz), 132.5 (d, *J* = 9.6 Hz), 132.01 (d, *J* = 2.2 Hz), 131.97 (d, *J* = 8.9 Hz), 131.8 (d, *J* = 127 Hz, only the peak at 131.15 ppm is visible, the other is overlapping), 131.87 (d, *J* = 3.0 Hz), 128.61 (d, *J* = 11.9 Hz), 128.58, 128.4 (d, *J* = 12.7 Hz), 127.5, 122.5, 119.4, 53.9, 42.1 (d, *J* = 4.5 Hz); HRMS Calcd for $C_{22}H_{22}BrNOP$ [M +

H]$^+$: 426.06224; Found: 426.06290. $[\alpha]^{24}_D$ = –2.71 (*c* = 1.00, $CHCl_3$) for a 98:2 e.r. sample. The enantiomeric purity of this compound was determined by HPLC analysis in comparison with authentic racemic material (Chiracel OJ-H, 92:8 hexanes:*i*-PrOH, 0.8 mL/min, 220 nm): t_R of **2.32d**: 7 min (major) and 16 min (minor).

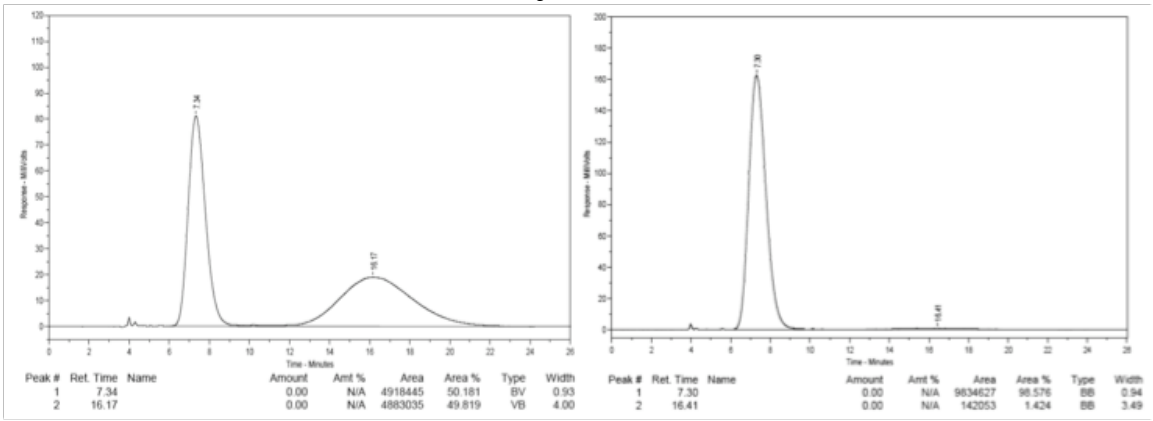

Peak #	Ret. Time	Area %	Peak #	Ret. Time	Area %
1	7.3 min	50.181	1	7.3 min	98.576
2	16.2 min	49.819	2	16.4 min	1.424

(*S*)–*P*,*P*-Diphenyl-*N*-(1-(*o*-tolyl)but-3-en-1-yl)phosphinic amide (**2.32e**): mp = 157–159 °C. IR (neat): 3163 (w, br), 3058 (w, br), 2953 (w, br), 1465 (m), 1438 (m), 1183 (s), 1121 (m), 1108 (m), 1069 (m), 918 (w), 742 (m), 722 (s), 695 (s), 549 (m), 530 (m) cm^{-1}; ^1H NMR (400 MHz, $CDCl_3$): δ 7.88–7.83 (2H, m), 7.72–7.67 (2H, m), 7.50–7.46 (1H, m), 7.44–7.38 (3H, m), 7.35–7.33 (1H, m), 7.29–7.21 (3H, m), 7.12 (1H, ddd, *J* = 8.4, 7.6, 1.6 Hz), 7.00 (1H, m), 5.61 (1H, dddd, *J* = 17.2, 10.0, 7.2, 7.2 Hz), 5.11–5.03 (2H, m), 4.54 (1H, dddd, *J* = 10.0, 10.0, 6.4, 6.4 Hz), 3.43 (1H, br dd, *J* = 9.6, 6.4 Hz), 2.65–2.52 (2H, m), 1.91 (3H, s); ^{13}C NMR (100 MHz, $CDCl_3$): δ 141.7 (d, *J* = 4.5 Hz), 134.6, 133.7, 133.3 (d, *J* = 126 Hz, only the peak at 133.9 is visible, the other is overlapping), 132.7 (d, *J* = 9.6 Hz), 132.0 (d, *J* = 126 Hz, only the peak at 131.33 is visible, the other is overlapping), 131.96 (d, *J* = 2.2 Hz), 131.9 (d, *J* = 8.9 Hz), 131.7 (d, *J* = 3.0 Hz), 130.4,

128.6 (d, J = 12.6 Hz), 128.3 (d, J = 12.6 Hz), 126.9, 126.3, 125.8, 118.9, 50.4, 43.3 (d, J = 2.9 Hz), 19.1; HRMS Calcd for $C_{23}H_{25}NOP$ $[M + H]^+$: 362.16738; Found: 362.16809. $[\alpha]^{25}_D$ = –3.51 (c = 1.00, $CHCl_3$) for a 98:2 e.r. sample. The enantiomeric purity is determined by HPLC analysis in comparison with authentic racemic material (Chiracel OJ-H, 93:7 hexanes:*i*-PrOH, 0.6 mL/min, 220 nm): t_R of **2.32e**: 9 min (major) and 19 min (minor).

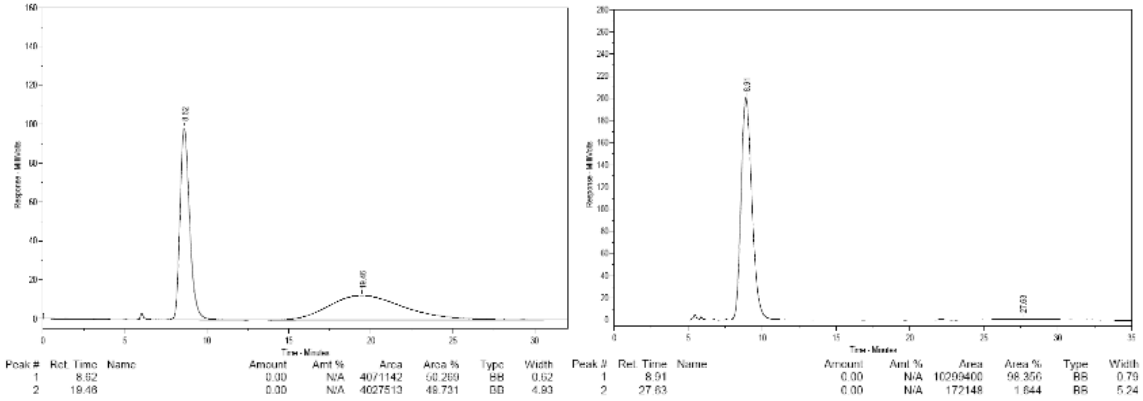

Peak #	Ret. Time	Area %	Peak #	Ret. Time	Area %
1	8.6 min	50.269	1	8.9 min	98.356
2	19.5 min	49.731	2	27.6 min	1.644

(*S*)–*N*-(1-(2-Methoxyphenyl)but-3-en-1-yl)-*P*,*P*-diphenylphosphinic amide (**2.32f**): mp = 119–121 °C. IR (neat): 3187 (w, br), 3058 (w, br), 2930 (w, br), 1600 (w), 1588 (w), 1437 (m), 1240 (m), 1186 (s), 1109 (m), 1070 (m), 1027 (m), 910 (m, br), 750 (m), 722 (s), 694 (s), 553 (m), 523 (m) cm^{-1}; ^1H NMR (400 MHz, $CDCl_3$): δ 7.86–7.81 (2H, m), 7.78–7.72 (2H, m), 7.49–7.38 (4H, m), 7.33–7.29 (2H, m), 7.21 (1H, ddd, J = 9.2, 7.6, 2.0 Hz), 7.12 (1H, ddd, J= 7.2, 7.2, 1.2 Hz), 7.01 (1H, dd, J= 7.6, 2.0 Hz), 6.88 (1H, ddd, J= 7.2, 7.2, 0.8 Hz), 6.83 (1H, dd, J = 8.4, 0.8 Hz), 5.58 (1H, dddd, J = 17.2, 10.0, 7.6, 7.6 Hz), 5.02-4.94 (2H, m), 4.41 (1H, dddd, J = 17.4, 7.2, 6.0, 6.0 Hz), 3.94 (1H, br dd, J= 11.2, 8.4 Hz), 3.73 (3H, s), 2.78-2.63 (2H, m); ^{13}C NMR (100 MHz, $CDCl_3$): δ

156.8, 135.0, 133.6 (d, J = 127 Hz), 132.7 (d, J = 9.6 Hz), 132.5 (d, J = 130 Hz), 131.9 (d, J = 9.7 Hz), 131.8 (d, J = 3.0 Hz), 131.6 (d, J = 3.0 Hz), 130.9 (d, J = 5.2 Hz), 128.51 (d, J = 11.9 Hz), 128.49, 128.30 (d, J = 12.7 Hz), 128.25, 120.6, 117.7, 111.0, 55.3, 52.8, 42.3 (d, J = 3.8 Hz); HRMS Calcd for $C_{23}H_{25}NO_2P$ $[M + H]^+$: 378.16229; Found: 378.16227. $[\alpha]^{26}_D$ = –11.8 (c = 1.00, $CHCl_3$) for a 97:3 e.r. sample. The enantiomeric purity is determined by HPLC analysis in comparison with authentic racemic material (Chiracel OD, 92:8 hexanes:*i*-PrOH, 0.8 mL/min, 220 nm): t_R of **2.32f**: 12 min (minor) and 14 min (major).

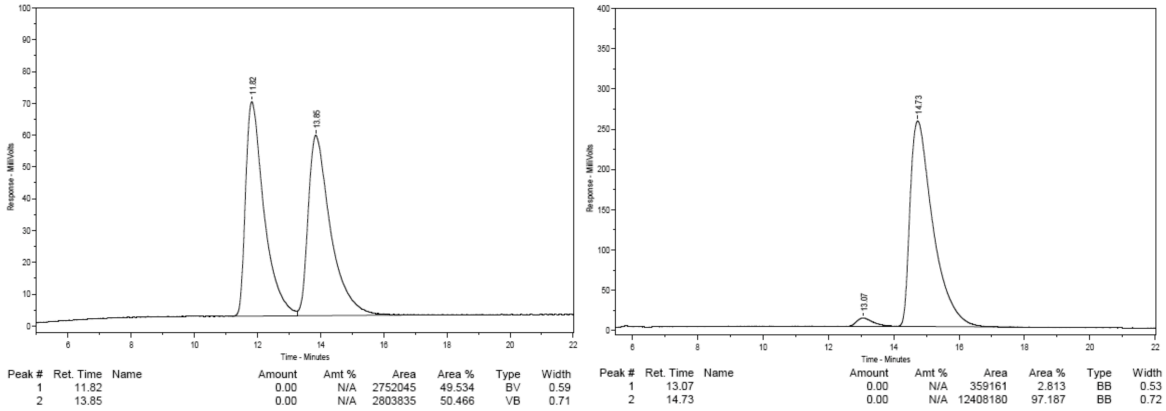

Peak #	Ret. Time	Name	Amount	Amt %	Area	Area %	Type	Width
1	11.82		0.00	N/A	2752045	49.534	BV	0.59
2	13.85		0.00	N/A	2803835	50.466	VB	0.71

Peak #	Ret. Time	Name	Amount	Amt %	Area	Area %	Type	Width
1	13.07		0.00	N/A	359161	2.813	BB	0.53
2	14.73		0.00	N/A	12408160	97.187	BB	0.72

Peak #	Ret. Time	Area %
1	11.8 min	49.534
2	13.9 min	50.466

Peak #	Ret. Time	Area %
1	13.1 min	2.813
2	14.7 min	97.187

(*S*)–*N*-(1-(3-Bromophenyl)but-3-en-1-yl)-*P*,*P*-diphenylphosphinic amide (**2.32g**): mp = 139–140 °C. IR (neat): 3216 (w, br), 1466 (m), 1407 (w), 1229 (s), 1123 (m), 1079 (m), 989 (m), 870 (m), 783 (m), 726 (m), 694 (s), 552 (s), 527 (s), 441 (m) cm^{-1}; ^1H NMR (400 MHz, $CDCl_3$): δ 7.87–7.82 (2H, m), 7.77–7.71 (2H, m), 7.53–7.47 (1H, m), 7.45–7.40 (3H, m), 7.35–7.30 (4H, m), 7.13–7.11 (2H, m), 5.58 (1H, dddd, J = 17.2, 10.0, 7.2, 7.2 Hz), 5.13–5.07 (2H, m), 4.31 (1H, dddd, J = 10.0, 10.0, 6.4, 6.4 Hz), 3.42 (1H, br dd, J = 9.4, 6.0 Hz), 2.67–2.58 (2H, m); ^{13}C NMR (100 MHz, $CDCl_3$): δ 145.5 (d, J = 4.4

Hz), 133.3, 132.9 (d, J = 127 Hz), 132.5 (d, J = 9.7 Hz), 132.1 (d, J = 3.0 Hz), 132.0 (d, J = 3.0 Hz), 131.91 (d, J = 127 Hz, only the peak at 133.3 is visible, the other is overlapping), 131.90 (d, J = 9.7 Hz), 130.3, 130.1, 129.7, 128.7 (d, J = 12.6 Hz), 128.4 (d, J = 12.6 Hz), 125.4, 122.6, 119.4, 54.1, 43.6 (d, J = 4.5 Hz); HRMS Calcd for $C_{22}H_{22}BrNOP$ $[M + H]^+$: 426.06224; Found: 426.06208. $[\alpha]^{26}_D$ = –49.7 (c = 1.00, $CHCl_3$) for a 96:4 e.r. sample. The enantiomeric purity of this compound was determined by HPLC analysis in comparison with authentic racemic material (Chiracel OD, 92:8 hexanes:*i*-PrOH, 0.6 mL/min, 220 nm): t_R of **2.32g**: 14 min (minor) and 17 min (major).

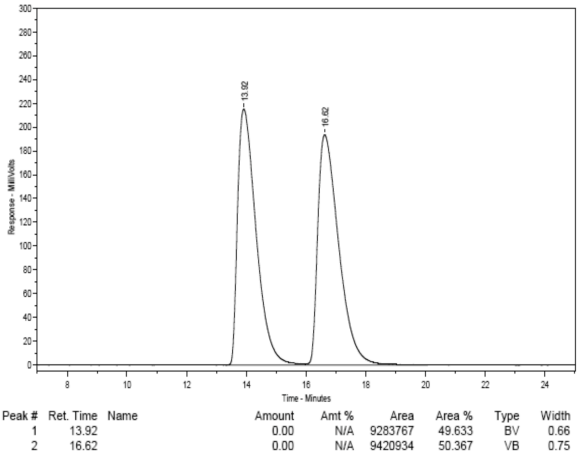

Peak #	Ret. Time	Name	Amount	Amt %	Area	Area %	Type	Width
1	13.92		0.00	N/A	9283767	49.633	BV	0.66
2	16.62		0.00	N/A	9420934	50.367	VB	0.75

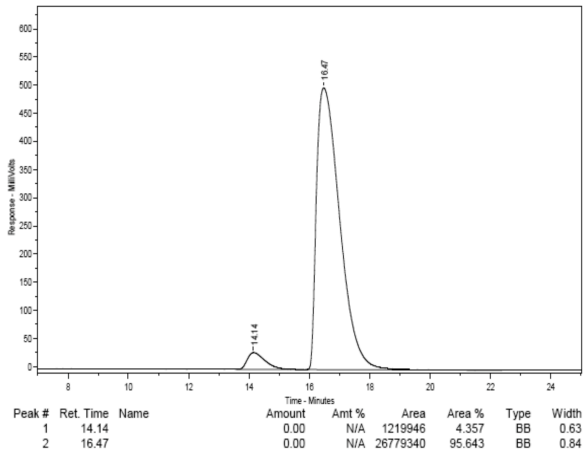

Peak #	Ret. Time	Name	Amount	Amt %	Area	Area %	Type	Width
1	14.14		0.00	N/A	1219946	4.357	BB	0.63
2	16.47		0.00	N/A	26779340	95.643	BB	0.84

Peak #	Ret. Time	Area %
1	13.9 min	49.633
2	16.6 min	50.367

Peak #	Ret. Time	Area %
1	14.1 min	4.357
2	16.5 min	95.643

(*S*)–*N*-(1-(4-Chlorophenyl)but-3-en-1-yl)-*P*,*P*-diphenylphosphinic amide (**2.32h**): mp: 152–154 °C. IR (neat): 3172 (w, br), 2901 (w, br), 1492 (m), 1438 (m), 1184 (s), 1124 (m), 1110 (m), 1072 (m), 724 (m), 696 (m), 540 (s) cm^{-1}; ^1H NMR (400 MHz, $CDCl_3$): δ 7.88–7.82 (2H, m) 7.78–7.72 (2H, m), 7.52–7.47 (1H, m), 7.46–7.40 (3H, m), 7.35–7.30 (2H, m), 7.25–7.22 (2H, m), 7.14–7.11 (2H, m), 5.57 (1H, dddd, J = 16.8, 10.0, 7.2, 7.2 Hz), 5.12–5.05 (2H, m), 4.32 (1H, dddd, J = 9.6, 9.6, 6.4, 6.4 Hz), 3.30

(1H, br dd, J = 9.6, 6.0 Hz), 2.69–2.55 (2H, m); ^{13}C NMR (100 MHz, $CDCl_3$): δ 141.7 (d, J = 5.3 Hz), 133.4, 133.0 (d, J = 126 Hz), 132.9, 132.5 (d, J = 9.7 Hz), 132.11 (d, J = 130 Hz), 132.09 (d, J = 3.0 Hz), 131.96 (d, J = 9.7 Hz), 131.95 (d, J = 3.0 Hz), 128.7 (d, J = 12.6 Hz), 128.6, 128.5 (d, J = 12.6 Hz), 128.1, 119.4, 54.0, 43.6 (d, J = 4.5 Hz); HRMS Calcd for $C_{22}H_{22}ClNOP$ [M + H]$^+$: 382.11275; Found: 382.11274. $[\alpha]^{26}_D$ = –64.4 (c = 1.00, $CHCl_3$) for a 98:2 e.r. sample. The enantiomeric purity of this compound was determined by HPLC analysis in comparison with authentic racemic material (Chiracel OD, 92:8 hexanes:*i*-PrOH, 0.6 mL/min, 220 nm): t_R of **2.32h**: 15 min (minor) and 16 min (major).

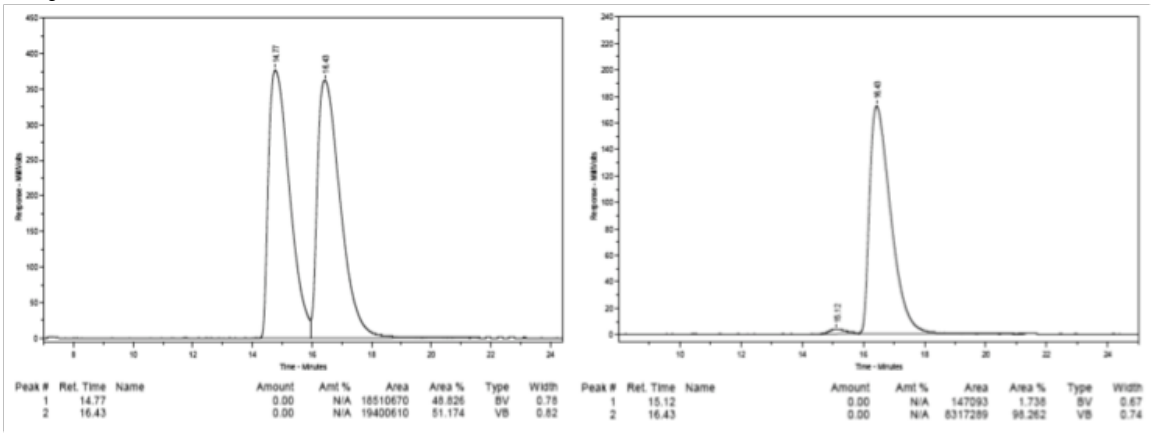

Peak #	Ret. Time	Area %	Peak #	Ret. Time	Area %
1	14.8 min	48.826	1	15.1 min	1.738
2	16.4 min	51.174	2	16.4 min	98.262

(*S*)–*N*-(1-(4-Bromophenyl)but-3-en-1-yl)-*P*,*P*-diphenylphosphinic amide (**2.32i**): mp: 174–176 °C. IR (neat): 3164 (w, br), 1437 (m), 1183 (s), 1123 (m), 1072 (m), 1010 (m), 914 (w), 821 (w), 725 (m), 696 (m), 535 (m) cm^{-1}; ^{1}H NMR (400 MHz, $CDCl_3$): δ 7.88–7.82 (2H, m) 7.78–7.72 (2H, m), 7.53–7.31 (8H, m), 7.08–7.06 (2H, m), 5.57 (1H, dddd, J = 16.8, 10.0, 7.2, 7.2 Hz), 5.13–5.06 (2H, m), 4.31 (1H, dddd, J = 10.0, 10.0, 6.4, 6.4 Hz), 3.30 (1H, br dd, J = 9.6, 5.6 Hz), 2.69–2.55 (2H, m); ^{13}C NMR (100 MHz, $CDCl_3$): δ

142.2 (d, J = 5.2 Hz), 133.3, 132.9 (d, J = 127 Hz), 132.5 (d, J = 9.7 Hz), 132.10 (d, J = 3.0 Hz), 132.09 (d, J = 129 Hz), 131.97 (d, J = 3.0 Hz), 131.96 (d, J = 9.7 Hz), 128.7 (d, J = 12.6 Hz), 128.5 (d, J = 12.6 Hz, overlaps with the peak at 128.4), 128.4, 121.0, 119.4, 54.1, 43.6 (d, J = 4.4 Hz); HRMS Calcd for $C_{22}H_{22}BrNOP$ $[M + H]^+$: 426.06224; Found: 426.06129. $[\alpha]^{25}_D$ = –72.3 (c = 1.00, $CHCl_3$) for a 98:2 e.r. sample. The enantiomeric purity of this compound was determined by HPLC analysis in comparison with authentic racemic material (Chiracel OD, 92:8 hexanes:*i*-PrOH, 0.8 mL/min, 220 nm): t_R of **2.32i**: 12 min (minor) and 13 min (major).

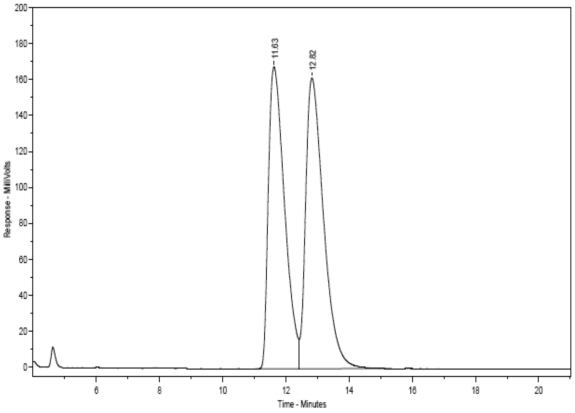

Peak #	Ret. Time	Name	Amount	Amt %	Area	Area %	Type	Width
1	11.63		0.00	N/A	5975165	48.443	BV	0.56
2	12.82		0.00	N/A	6359250	51.557	VB	0.60

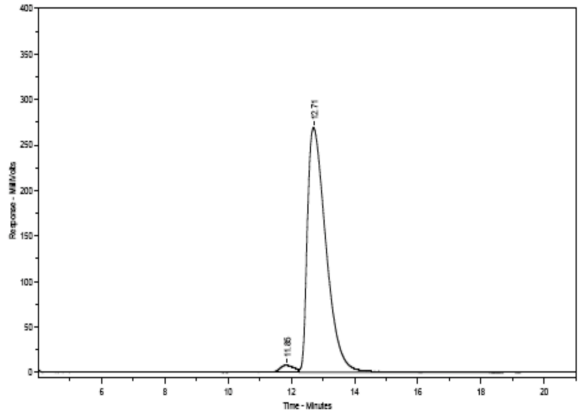

Peak #	Ret. Time	Name	Amount	Amt %	Area	Area %	Type	Width
1	11.85		0.00	N/A	242928	2.168	BB	0.54
2	12.71		0.00	N/A	10964700	97.832	BB	0.62

Peak #	Ret. Time	Area %
1	11.6 min	48.443
2	12.8 min	51.557

Peak #	Ret. Time	Area %
1	11.8 min	2.168
2	12.7 min	97.832

(*S*)–*P*,*P*-Diphenyl-*N*-(1-(4-fluorophenyl)but-3-en-1-yl)phosphinic amide (**2.32j**): mp: 133–134 °C. IR (neat): 3171 (w, br), 1604 (w), 1509 (m), 1438 (m), 1221 (s), 1183 (m), 1122 (m), 996 (w), 918 (m), 832 (m), 725 (s), 694 (s), 561 (m), 527 (s) cm^{-1}; ^1H NMR (400 MHz, $CDCl_3$): δ 7.87–7.82 (2H, m) 7.78–7.72 (2H, m), 7.51–7.40 (4H, m), 7.34–7.30 (2H, m), 7.18–7.13 (2H, m), 6.98–6.92 (2H, m), 5.59 (1H, dddd, J = 17.2, 12.0, 7.2, 7.2 Hz), 5.11–5.04 (2H, m), 4.34 (1H, dddd, J = 10.0, 10.0, 6.4, 6.4 Hz), 3.35 (1H, br dd,

J = 9.6, 5.6 Hz), 2.70–2.55 (2H, m); ^{13}C NMR (100 MHz, $CDCl_3$): δ 161.9 (d, J = 244 Hz), 139.9 (d, J = 5.2 Hz), 133.6, 133.0 (d, J = 126 Hz), 132.5 (d, J = 9.7 Hz), 132.2 (d, J = 129 Hz), 132.0 (d, J = 3.0 Hz), 131.9 (d, J = 8.9 Hz), 128.60 (d, J = 20.8 Hz), 128.58, 128.29 (d, J = 17.1 Hz), 128.28, 119.2, 115.4, 115.2, 53.9, 43.8 (d, J = 4.4 Hz); HRMS Calcd for $C_{22}H_{22}FNOP$ $[M + H]^+$: 366.14230; Found: 366.14199. $[\alpha]^{25}_D$ = –20.1 (c = 1.00, $CHCl_3$) for a 98:2 e.r. sample. The enantiomeric purity of this compound was determined by HPLC analysis in comparison with authentic racemic material (Chiracel OD, 92:8 hexanes:*i*-PrOH, 0.6 mL/min, 220 nm): t_R of **2.32j**: 14 min (minor) and 16 min (major).

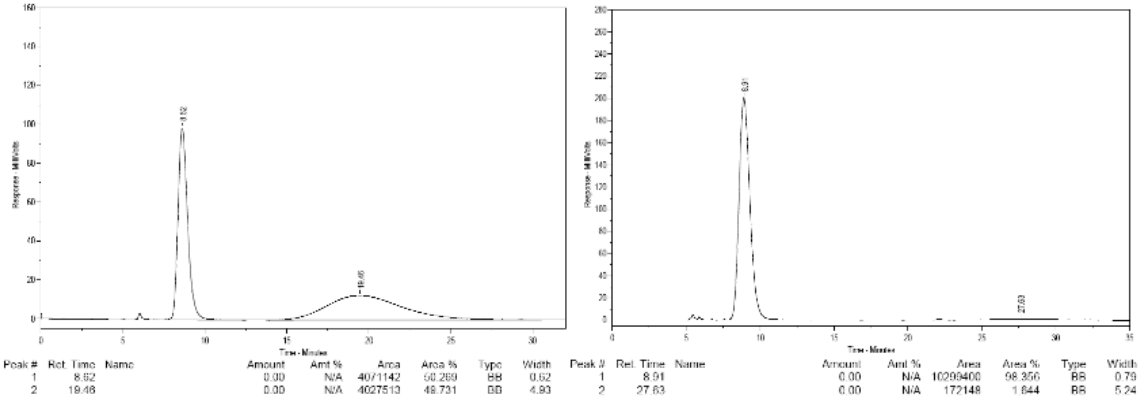

Peak #	Ret. Time	Area %	Peak #	Ret. Time	Area %
1	14.2 min	49.824	1	14.5 min	2.018
2	16.3 min	50.176	2	16.3 min	97.962

(*S*)–*P*,*P*-Diphenyl-*N*-(1-(4-(trifluoromethyl)phenyl)but-3-en-1-yl)phosphinic amide (**2.32k**): mp = 158–159 °C. IR (neat): 3158 (w, br), 2963 (w), 1438 (m), 1326 (s), 1261 (m), 1182 (m), 1121 (s), 1069 (s), 1019 (m), 799 (m), 725 (m), 696 (m), 533 (m) cm^{-1}; ^{1}H NMR (400 MHz, $CDCl_3$): δ 7.88–7.83 (2H, m) 7.75–7.70 (2H, m), 7.52–7.48 (3H, m), 7.45–7.40 (3H, m), 7.32–7.28 (4H, m), 5.58 (1H, dddd, J = 17.2, 10.0, 7.2, 7.2 Hz), 5.14–5.08 (2H, m), 4.41 (1H, dddd, J = 9.6, 9.6, 6.4, 6.4 Hz), 3.49 (1H, br dd, J = 8.8, 6.2

Hz), 2.71–2.58 (2H, m); ^{13}C NMR (100 MHz, $CDCl_3$): δ 147.2 (d, J = 3.8 Hz), 133.1, 132.7 (d, J = 127 Hz), 132.4 (d, J = 9.7 Hz), 132.1 (d, J = 3.0 Hz), 131.98 (d, J = 3.0 Hz, overlaps with doublet at 131.95), 131.97 (d, J = 129 Hz), 131.95 (d, J = 9.7 Hz), 129.4 (q, J = 32.0 Hz), 128.7 (d, J = 12.6 Hz), 128.5 (d, J = 12.7 Hz), 127.1, 125.4 (q, J = 3.7 Hz), 124.2 (q, J = 135 Hz), 119.6, 54.2, 43.5 (d, J = 4.4 Hz); HRMS Calcd for $C_{23}H_{22}F_3NOP$ $[M + H]^+$: 416.13911; Found: 416.13900. $[\alpha]^{25}_D$ = +47.2 (c = 1.00, $CHCl_3$) for a 98:2 e.r. sample. The enantiomeric purity of this compound was determined by HPLC analysis in comparison with authentic racemic material (Chiracel OD, 92:8 hexanes:*i*-PrOH, 0.6 mL/min, 220 nm): t_R of **2.32k**: 14 min (minor) and 16 min (major).

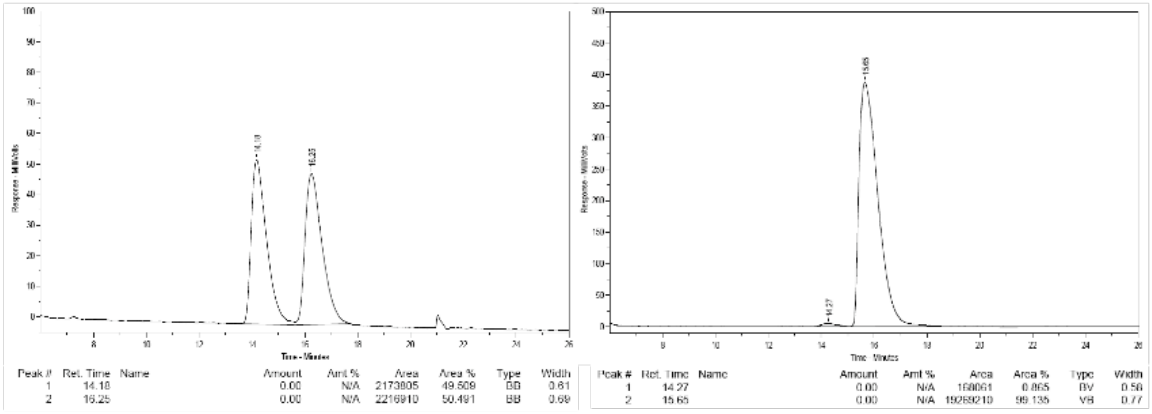

Peak #	Ret. Time	Area %	Peak #	Ret. Time	Area %
1	14.2 min	49.509	1	14.3 min	0.865
2	16.3 min	50.491	2	15.6 min	99.135

(*S*)–*N*-(1-(4-Methoxyphenyl)but-3-en-1-yl)-*P*,*P*-diphenylphosphinic amide (2.32l): mp = 115–116 °C. IR (neat): 3176 (w, br), 1612 (w), 1513 (m), 1438 (m), 1246 (m), 1181 (s), 1122 (m), 1110 (m), 1070 (m), 697 (m), 670 (m), 545 (m), 527 (m) cm^{-1}; ^{1}H NMR (400 MHz, $CDCl_3$): δ 7.88–7.83 (2H, m), 7.80–7.75 (2H, m), 7.51–7.47 (1H, m), 7.45–7.40 (3H, m), 7.36–7.31 (2H, m), 7.13–7.10 (2H, m), 6.83–6.80 (2H, m), 5.56 (1H, dddd, J = 17.2, 10.4, 6.8, 6.8 Hz), 5.10–5.02 (2H, m), 4.30 (1H, dddd, J = 9.6, 9.6, 6.4, 6.4 Hz),

3.79 (3H, s), 3.28 (1H, br dd, J = 9.6, 6.0 Hz), 2.72–2.57 (2H, m); ^{13}C NMR (100 MHz, $CDCl_3$): δ 158.7 135.3 (d, J = 5.9 Hz), 134.6 (d, J = 127 Hz, only the peak at 133.9 is visible, the other is overlapping), 134.0, 132.6 (d, J = 9.6 Hz), 132.3 (d, J = 129 Hz), 132.0 (d, J = 9.7 Hz), 131.9 (d, J = 2.9 Hz, peak overlaps with doublet at 132.0 ppm), 131.8 (d, J = 2.9 Hz), 128.6 (d, J = 12.7 Hz), 128.4 (d, J = 12.6 Hz), 127.8, 113.9, 55.4, 54.2, 43.8; HRMS Calcd for $C_{23}H_{25}NO_2P$ [M + H]$^+$: 378.16229; Found: 378.16177. $[\alpha]^{24}_D$ = –29.9 (c = 1.00, $CHCl_3$) for a 98:2 e.r. sample. The enantiomeric purity of this compound was determined by HPLC analysis in comparison with authentic racemic material (Chiracel OJ-H, 92:8 hexanes:*i*-PrOH, 0.8 mL/min, 220 nm): t_R of **2.32l**: 11 min (major) and 18 min (minor).

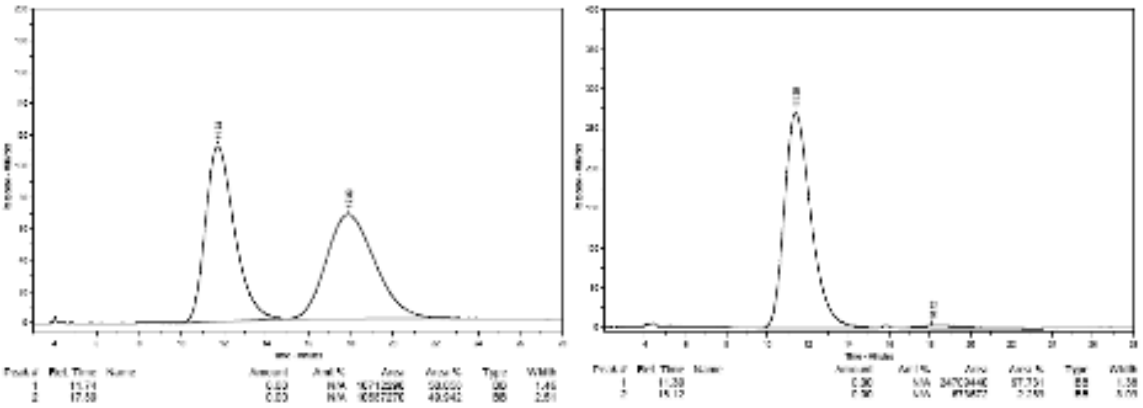

Peak #	Ret. Time	Area %	Peak #	Ret. Time	Area %
1	11.7 min	50.058	1	11.4 min	97.731
2	17.9 min	49.942	2	18.1 min	2.269

(*S*)–*N*-(1-(Furan-2-yl)but-3-en-1-yl)-*P*,*P*-diphenylphosphinic amide (**2.32m**): mp = 91–92 °C. IR (neat): 3171 (w, br), 2913 (w, br), 1436 (m), 1184 (s), 1149 (m), 1122 (m), 1109 (m), 914 (m), 722 (s), 695 (s), 535 (s) cm^{-1}; ^{1}H NMR (400 MHz, $CDCl_3$): δ 7.89–7.82 (4H, m), 7.50–7.37 (6H, m), 7.32–7.31 (1H, m), 6.25–6.24 (1H, m), 6.12–6.11 (1H, m), 5.63 (1H, dddd, J = 17.6, 10.0, 7.6, 7.6 Hz), 5.14–5.05 (2H, m), 4.37 (1H, dddd, J =

10.0, 10.0, 6.4, 6.4 Hz), 3.34 (1H, br dd, J = 10.4, 7.2 Hz), 2.79–2.61 (2H, m); ^{13}C NMR (100 MHz, $CDCl_3$): δ 155.3 (d, J = 6.7 Hz), 141.8, 133.5, 133.2 (d, J = 127 Hz), 132.6 (d, J = 9.6 Hz), 132.1 (d, J = 130 Hz), 132.0 (d, J = 2.3 Hz), 131.93 (d, J = 3.0 Hz), 131.92 (d, J = 9.7 Hz), 128.6 (d, J = 12.7 Hz), 128.5 (d, J = 12.6 Hz), 119.0, 110.2, 106.7, 48.9, 41.0 (d, J = 3.7 Hz); HRMS Calcd for $C_{20}H_{21}NO_2P$ $[M + H]^+$: 338.13099; Found: 338.13123. $[\alpha]^{25}_D$ = –7.17 (c = 0.500, $CHCl_3$) for a 95:5 e.r. sample. The enantiomeric purity of this compound was determined by HPLC analysis in comparison with authentic racemic material (Chiracel OD, 92:8 hexanes:*i*-PrOH, 1.0 mL/min, 220 nm): t_R of **2.32m**: 10 min (minor) and 11 min (major).

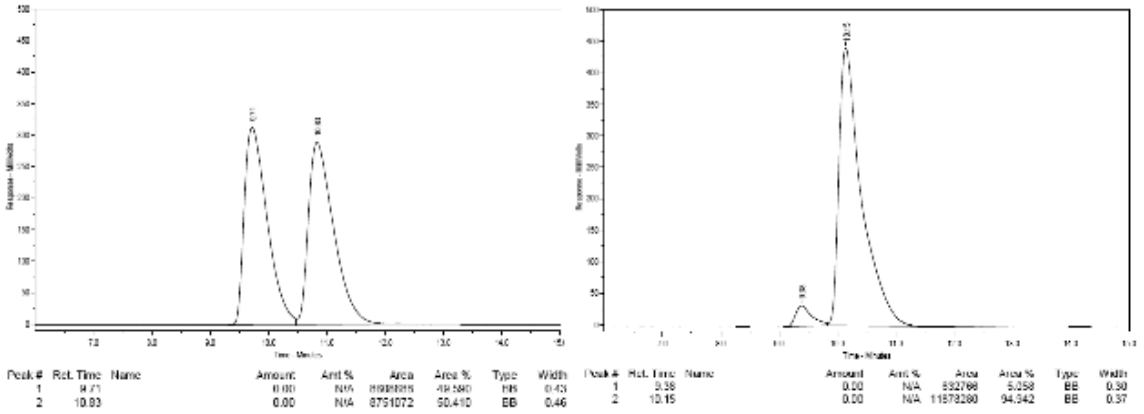

Peak #	Ret. Time	Area %	Peak #	Ret. Time	Area %
1	9.7 min	49.590	1	9.4 min	5.058
2	10.8 min	50.410	2	10.2 min	94.942

(*S*)–*N*-(1-(furan-3-yl)but-3-en-1-yl)-*P*,*P*-diphenylphosphinic amide (**2.32n**): mp = 97–100 °C. IR (neat): 3076 (w, br), 1438 (m), 1187 (s), 1161 (m), 1123 (m), 1110 (m), 915 (w), 725 (m), 697 (m), 553 (m), 529 (m) cm^{-1}; ^{1}H NMR (400 MHz, $CDCl_3$): δ 7.90–7.86 (4H, m), 7.51–7.39 (6H, m), 7.35–7.34 (1H, m), 7.32 (1H, s), 6.38 (1H, s), 5.69 (1H, dddd, J = 11.6. 6.4, 5.2, 5.2 Hz), 5.18–5.10 (2H, m), 4.30 (1H, dddd, J = 8.4, 8.4, 4.8, 4.8 Hz), 3.18 (1H, br dd, J = 7.6, 4.8 Hz), 2.67–2.56 (2H, m); ^{13}C NMR (125 MHz, $CDCl_3$):

δ 143.4, 139.6, 133.7, 132.9 (d, J = 129 Hz), 132.48 (d, J = 130 Hz), 132.47 (d, J = 9.6 Hz), 132.1 (d, J = 9.3 Hz), 132.02 (d, J = 2.8 Hz), 132.01 (d, J = 2.8 Hz), 128.64 (d, J = 12.5 Hz), 128.59 (d, J = 12.8 Hz), 128.1 (d, J = 4.8 Hz), 119.2, 109.4, 47.1, 42.3 (d, J = 3.3 Hz); HRMS Calcd for $C_{20}H_{21}NO_2P$ $[M + H]^+$: 338.13099; Found: 338.13037. $[\alpha]^{25}_D$ = –14.2 (c = 1.00, $CHCl_3$) for a 92:8 e.r. sample. The enantiomeric purity of this compound was determined by HPLC analysis in comparison with authentic racemic material (Chiracel OD, 92:8 hexanes:*i*-PrOH, 0.8 mL/min, 220 nm): t_R of **2.32n**: 10 min (minor) and 13 min (major).

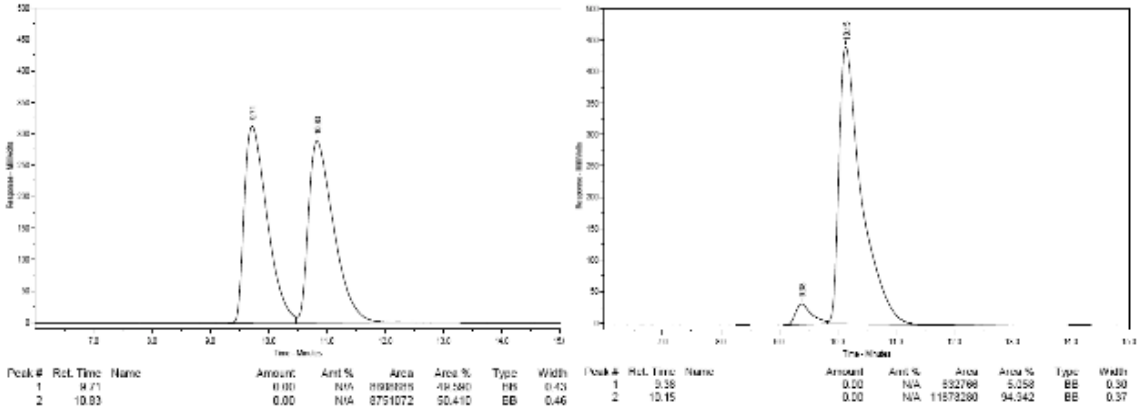

Peak #	Ret. Time	Area %	Peak #	Ret. Time	Area %
1	10.2 min	49.970	1	11.4 min	2.831
2	12.5 min	50.030	2	13.4 min	97.169

(*S*)–*P*,*P*-Diphenyl-*N*-(1-(thiophen-3-yl)but-3-en-1-yl)phosphinic amide (**2.32o**): mp = 128-129 °C. IR (neat): 3171 (w, br), 1437 (m), 1184 (s), 1123 (m), 1109 (m), 1071 (m), 912 (w), 725 (m), 696 (s), 552 (m), 526 (m) cm^{-1}; ^1H NMR (400 MHz, $CDCl_3$): δ 7.90–7.81 (4H, m), 7.51–7.35 (6H, m), 7.24 (1H, dd, J = 5.2, 3.2 Hz), 7.09–7.08 (1H, m), 7.02 (1H, dd, J = 4.8, 1.6 Hz), 5.63 (1H, dddd, J = 14.4, 7.6, 6.4, 6.4 Hz), 5.16–5.06 (2H, m), 4.43 (1H, dddd, J = 10.0, 10.0, 6.0, 6.0 Hz), 3.03 (1H, br dd, J = 10.4, 6.4 Hz), 2.75–2.61 (2H, m); ^{13}C NMR (125 MHz, $CDCl_3$): δ 144.5 (d, J = 5.9 Hz), 133.7, 133.1 (d, J = 127

Hz), 132.5 (d, J = 9.7 Hz), 132.3 (d, J = 130 Hz), 132.02 (d, J = 8.9 Hz), 132.01 (d, J = 2.8 Hz), 132.01 (d, J = 3.0 Hz, peak overlaps with doublet at 132.02), 128.7 (d, J = 12.7 Hz), 128.6 (d, J = 12.6 Hz), 126.3, 126.2, 121.4, 119.1, 50.7, 43.0 (d, J = 3.7 Hz); HRMS Calcd for $C_{20}H_{21}NOPS$ $[M + H]^+$: 354.10815; Found: 354.10785. $[\alpha]^{24}_D$ = –27.4 (c = 1.00, $CHCl_3$) for a 98:2 e.r. sample. The enantiomeric purity of this compound was determined by HPLC analysis in comparison with authentic racemic material (Chiracel OD, 92:8 hexanes:*i*-PrOH, 0.8 mL/min, 220 nm): t_R of **2.32o**: 11 min (minor) and 15 min (major).

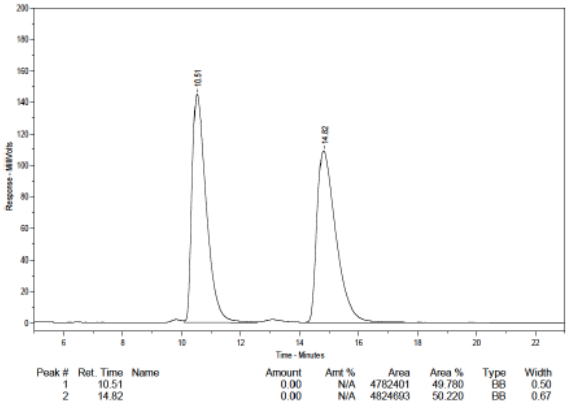

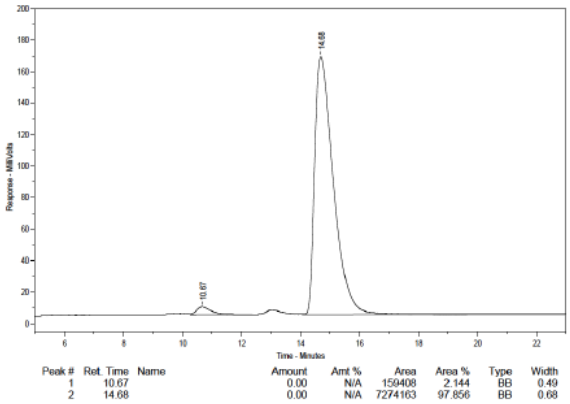

Peak #	Ret. Time	Area %	Peak #	Ret. Time	Area %
1	10.5 min	49.780	1	10.7 min	2.144
2	14.8 min	50.220	2	14.7 min	97.856

(*R*)–*N*-(6-Methylhept-1-en-4-yl)-*P*,*P*-diphenylphosphinic amide (**2.32p**): mp = 92–94 °C. IR (neat): 3170 (w, br), 2925 (w, br), 1437 (m), 1121 (m), 1109 (m), 910 (m), 749 (m), 722 (m), 693 (s), 565 (m), 528 (s) cm^{-1}; ^1H NMR (400 MHz, $CDCl_3$): δ 7.94–7.87 (4H, m), 7.51–7.40 (6H, m), 5.79 (1H, dddd, J = 17.6, 10.4, 7.6, 7.6 Hz), 5.14–5.10 (2H, m), 3.24–3.13 (1H, m), 2.75 (1H, br dd, J = 10.8, 6.0 Hz), 2.39–2.28 (2H, m), 1.82–1.72 (1H, m), 1.42–1.28 (2H, m), 0.80–0.75 (6H, m); ^{13}C NMR (100 MHz, $CDCl_3$): δ 134.1, 133.2 (d, J = 129 Hz), 133.0 (d, J = 129 Hz), 132.4 (d, J = 8.9 Hz), 132.2 (d, J = 9.0 Hz), 131.8 (d, J = 2.3 Hz), 128.52 (d, J = 12.7 Hz), 128.49 (d, J = 12.7 Hz), 118.6, 49.2

(d, J = 1.5 Hz), 46.1 (d, J = 6.0 Hz), 41.4 (d, J = 3.7 Hz), 24.7 (d, J = 3.8 Hz), 22.7, 22.6; HRMS Calcd for $C_{20}H_{18}N_2O_7$ $[M + H]^+$: 399.11923; Found: 399.11946. $[\alpha]^{25}_D$ = +20.4 (*c* = 1.00, $CHCl_3$) for a 97.5:2.5 e.r. sample. The enantiomeric purity of this compound was determined by HPLC analysis in comparison with authentic racemic material (Chiracel OD-H, 95:5 hexanes:*i*-PrOH, 0.6 mL/min, 220 nm): t_R of **2.32p**: 13 min (major) and 14 min (minor).

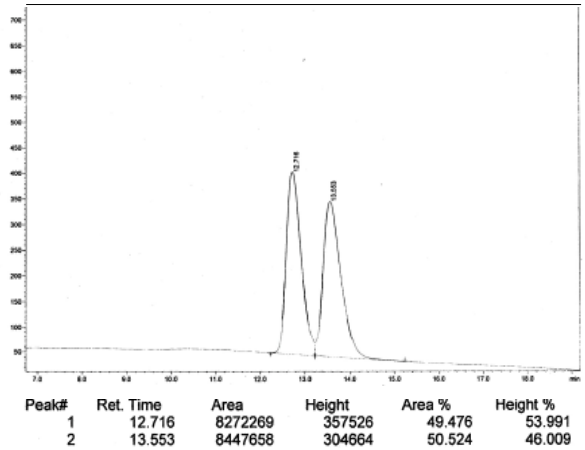

Peak#	Ret. Time	Area	Height	Area %	Height %
1	12.716	8272269	357526	49.476	53.991
2	13.553	8447658	304664	50.524	46.009

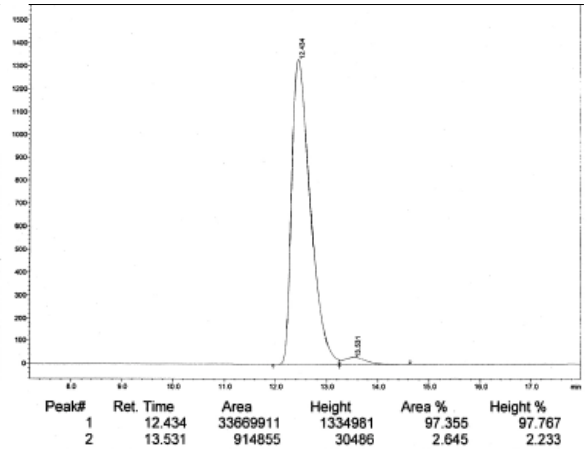

Peak#	Ret. Time	Area	Height	Area %	Height %
1	12.434	33669911	1334981	97.355	97.767
2	13.531	914855	30486	2.645	2.233

Peak #	Ret. Time	Area %	Peak #	Ret. Time	Area %
1	12.7 min	49.476	1	12.4 min	97.355
2	13.5 min	50.524	2	13.5 min	2.645

(*R*)–*P*,*P*-Diphenyl-*N*-(1-phenylhex-5-en-3-yl)phosphinic amide (**2.32q**): mp = 96–98 °C. IR (neat): 3175 (w, br), 2923 (w, br), 1437 (m), 1184 (s), 1122 (m), 1109 (m), 996 (w), 911 (w), 723 (m), 696 (s), 556 (m), 532 (m) cm^{-1}; ^1H NMR (400 MHz, $CDCl_3$): δ 7.91–7.84 (4H, m), 7.49–7.39 (6H, m), 7.24–7.19 (2H, m), 7.15–7.10 (3H, m), 5.78 (1H, dddd, J = 17.2, 10.4, 7.6, 7.6 Hz), 5.14–5.10 (2H, m), 3.26–3.18 (1H, m), 2.84 (1H, br dd, J = 10.8, 6.4 Hz), 2.76–2.60 (2H, m), 2.39–2.36 (2H, m), 1.86–1.80 (2H, m); ^{13}C NMR (100 MHz, $CDCl_3$): δ 141.9, 134.1, 133.1 (d, J = 128 Hz), 133.0 (d, J = 128 Hz, only the peak at 133.6 is visible, the other is overlapping), 132.3 (d, J = 9.7 Hz), 132.2

(d, J = 8.9 Hz), 131.88 (d, J = 3.0 Hz), 131.86 (d, J = 3.0 Hz, only the peak at 131.9 is visible, the other may be overlapping), 128.63 (d, J = 12.6 Hz), 128.56 (d, J = 12.6 Hz), 128.5, 128.4, 125.9, 118.7, 50.8 (d, J = 1.5 Hz), 41.1 (d, J = 4.4 Hz), 38.1 (d, J = 5.2 Hz), 32.2; HRMS Calcd for $C_{24}H_{27}NOP$ $[M + H]^+$: 376.18303; Found: 376.18236. $[\alpha]^{26}_D$ = –1.85 (c = 1.00, $CHCl_3$) for a 97:3 e.r. sample. The enantiomeric purity of this compound was determined by HPLC analysis in comparison with authentic racemic material (Chiracel OD-H, 95:5 hexanes:*i*-PrOH, 0.6 mL/min, 220 nm): t_R of **2.32q**: 23 min (minor) and 27 min (major).

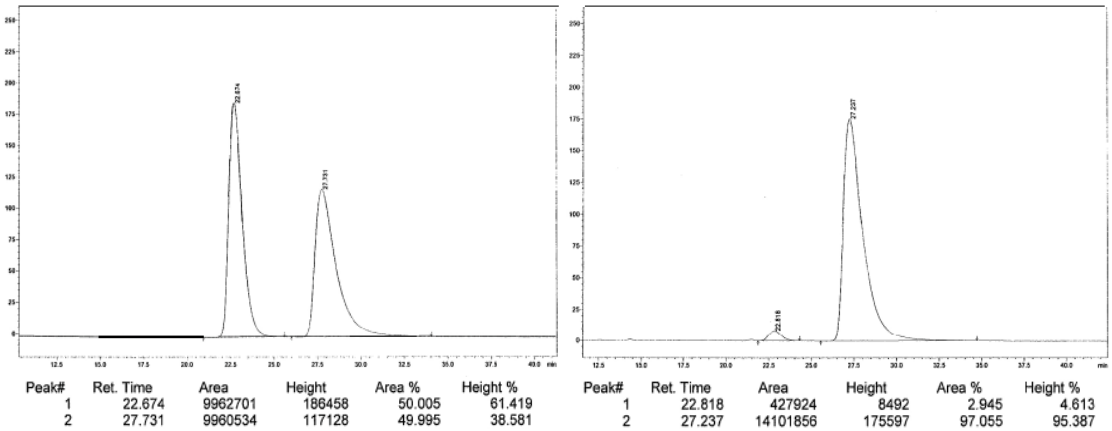

Peak#	Ret. Time	Area	Height	Area %	Height %
1	22.674	9962701	186458	50.005	61.419
2	27.731	9960534	117128	49.995	38.581

Peak#	Ret. Time	Area	Height	Area %	Height %
1	22.818	427924	8492	2.945	4.613
2	27.237	14101856	175597	97.055	95.387

Peak #	Ret. Time	Area %
1	22.7 min	50.005
2	27.7 min	49.995

Peak #	Ret. Time	Area %
1	22.8 min	2.945
2	27.2 min	97.055

(*S*,*E*)–*P*,*P*-Diphenyl-*N*-(1-phenylhexa-1,5-dien-3-yl)phosphinic amide (**2.32r**): mp = 106–109 °C. IR (neat): 3165 (w, br), 2923 (w, br), 1437 (m), 1260 (m), 1183 (m), 1108 (m), 1067 (m), 913 (m), 800 (m), 746 (m), 723 (m), 692 (s), 557 (m), 539 (s) cm^{-1}; ^1H NMR (400 MHz, $CDCl_3$): δ 7.96–7.88 (4H, m), 7.51–7.39 (6H, m), 7.31–7.27 (4H, m), 7.25–7.20 (1H, m), 6.44 (1H, dd, J = 15.6, 1.6 Hz), 6.15 (1H, dd, J = 16.0, 6.4 Hz), 5.78 (1H, dddd, J = 14.4, 7.6, 6.8, 6.8 Hz), 5.21–5.12 (2H, m), 4.02–3.92 (1H, m), 3.09 (1H, br dd, J = 9.6, 6.0 Hz), 2.59–2.45 (2H, m); ^{13}C NMR (100 MHz, $CDCl_3$): δ 136.8, 133.7,

133.2 (d, J = 127 Hz), 132.64 (d, J = 127 Hz, only the peak at 133.3 ppm is visible, the other is overlapping), 132.59 (d, J = 9.7 Hz), 132.00 (d, J = 9.0 Hz), 131.96 (d, J = 2.3 Hz, peak overlaps with doublet at 132.00 ppm), 131.94 (d, J = 2.9 Hz, peak overlaps with doublet at 132.00 ppm), 131.5 (d, J = 5.9 Hz), 130.5, 128.64 (d, J = 12.7 Hz), 128.60, 128.58 (d, J = 12.6 Hz), 127.7, 126.6, 119.2, 52.8, 42.1 (d, J = 4.5 Hz); HRMS Calcd for $C_{24}H_{25}NOP$ $[M + H]^+$: 374.16738; Found: 374.16773. $[\alpha]^{25}_D$ = +54.6 (c = 1.00, $CHCl_3$) for a 96:4 e.r. sample. The enantiomeric purity of this compound was determined by HPLC analysis in comparison with authentic racemic material (Chiracel OD-H, 95:5 hexanes:*i*-PrOH, 0.6 mL/min, 220 nm): t_R of **2.32r**: 11 min (minor) and 13 min (major).

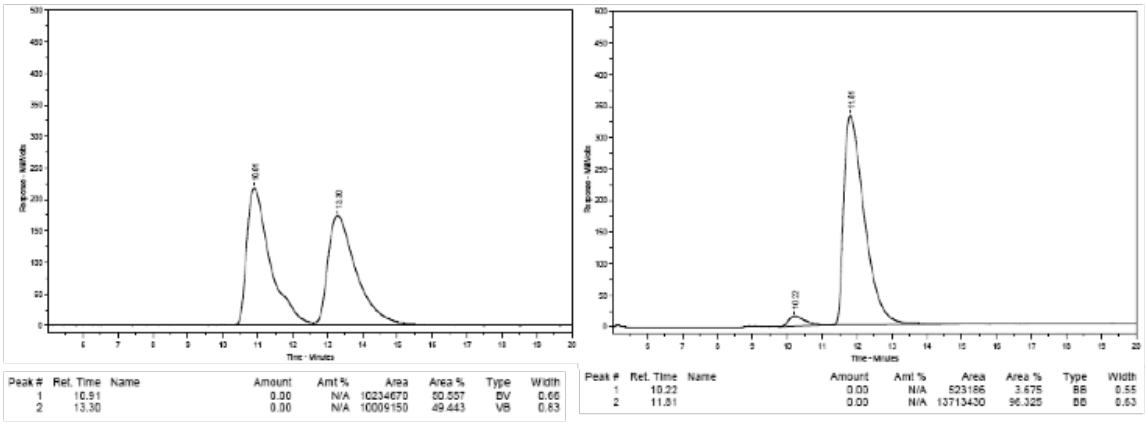

Peak #	Ret. Time	Area %	Peak #	Ret. Time	Area %
1	10.9 min	50.557	1	10.2 min	3.675
2	13.3 min	49.443	2	11.8 min	96.325

(*S*)–*N*-(1-cyclohexylbut-3-en-1-yl)-*P*,*P*-diphenylphosphinic amide (**2.32s**): mp = 120–122 °C. IR (neat): 3207 (w, br), 3075 (w), 3057 (w), 2921 (m), 2850 (m), 1639 (w), 1436 (s), 1187 (s), 1123 (s), 1108 (s), 1067 (m), 994 (w), 909 (m), 722 (s), 694 (s), 533 (s) cm^{-1}; ^1H NMR (400 MHz, CDCl3): δ 7.93–7.87 (4H, m), 7.50–7.42 (6H, m), 5.77 (1H, dddd, J = 17.3, 10.1, 7.3, 7.3 Hz), 5.12–5.06 (2H, m), 3.02–2.87 (1H, m), 2.77 (1H, br dd, J = 10.7, 6.1 Hz), 2.09 (2H, app t, J = 6.5 Hz), 1.82–1.61 (5H, m), 1.46–1.41 (1H, m), 1.24–

1.15 (4H, m), 0.98-0.92 (1H, m); 13C NMR (100 MHz, CDCl3): δ 135.1, 133.3 (d, *J* = 128.7 Hz), 133.2(d, *J* = 129.8 Hz, only peak at 132.8 is visible, the other is overlapping), 132.5 (d, *J* = 9.3Hz), 132.3 (d, *J* = 9.3 Hz), 131.80 (d, *J* = 1.4 Hz), 131.78 (d, *J* = 1.4 Hz), 127.50 (d, *J* = 2.5 Hz), 127.48 (d, *J* = 12.5 Hz), 117.8, 55.9 (d, *J* = 2.2 Hz), 42.1 (d, *J* = 5.1 Hz), 38.5 (d, *J* = 4.2 Hz), 29.5, 28.8, 26.6, 26.5, 26.4; HRMS Calcd for $C_{22}H_{29}NOP$ $[M + H]^+$: 354.19868; Found: 354.19835. $[\alpha]^{25}_D$ = +13.53 (*c* = 1.00, $CHCl_3$) for a 82:18 e.r. sample. The enantiomeric purity of this compound was determined by HPLC analysis in comparison with authentic racemic material (Chiracel OD-H, 95:5 hexanes:*i*-PrOH, 0.6 mL/min, 220 nm): t_R of **2.32s**: 12 min (major) and 16 min (minor).

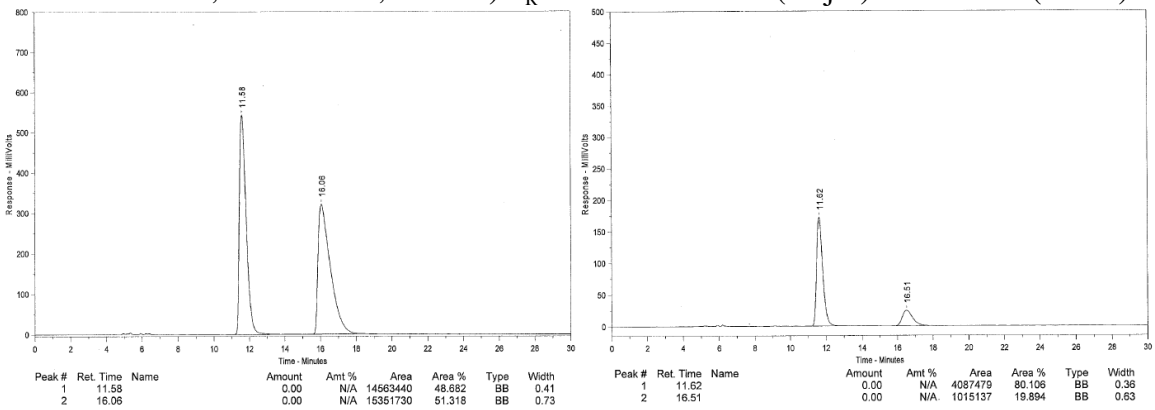

Peak #	Ret. Time	Area %	Peak #	Ret. Time	Area %
1	11.6 min	48.682	1	11.6 min	80.106
2	16.1 min	51.318	2	16.5 min	19.894

(*S*)–*N*-(2-methylhex-5-en-3-yl)-*P*,*P*-diphenylphosphinic amide (**2.32t**): mp = 117–120 °C. IR (neat): 3205 (w, br), 2959 (w, br), 1435 (m), 1183 (m), 1122 (m), 1107 (m), 990 (m), 960 (m), 748 (m), 722 (m), 692 (s), 531 (s) cm^{-1}; ^1H NMR (400 MHz, $CDCl_3$): δ 7.93–7.87 (4H, m), 7.51–7.39 (6H, m), 5.78 (1H, dddd, *J* = 17.2, 10.0, 7.2, 7.2 Hz), 5.12–5.06 (2H, m), 3.02–2.93 (1H, m), 2.75 (1H, br dd, *J* = 10.4, 6.0 Hz), 2.32–2.27 (2H, m), 1.90–1.82 (1H, m), 0.93–0.88 (6H, m); ^{13}C NMR (100 MHz, $CDCl_3$): δ 135.3, 133.2

(d, J = 127 Hz), 132.5, 132.4 (d, J = 8.9 Hz), 132.3 (d, J = 9.0 Hz), 131.8 (d, J = 3.0 Hz), 128.48 (d, J = 12.7 Hz), 128.47 (d, J = 12.7 Hz), 117.7, 56.4 (d, J = 6.0 Hz), 38.3 (d, J = 4.5 Hz), 32.1 (d, J = 5.2 Hz), 18.8, 18.1; HRMS Calcd for $C_{19}H_{25}NOP$ [M + H]$^+$: 314.16738; Found: 314.16816. $[\alpha]^{25}_D$ = +13.53 (c = 1.00, $CHCl_3$) for a 82:18 e.r. sample. The enantiomeric purity of this compound was determined by HPLC analysis in comparison with authentic racemic material (Chiracel OD-H, 95:5 hexanes:*i*-PrOH, 0.6 mL/min, 220 nm): t_R of **2.32t**: 13 min (major) and 18 min (minor).

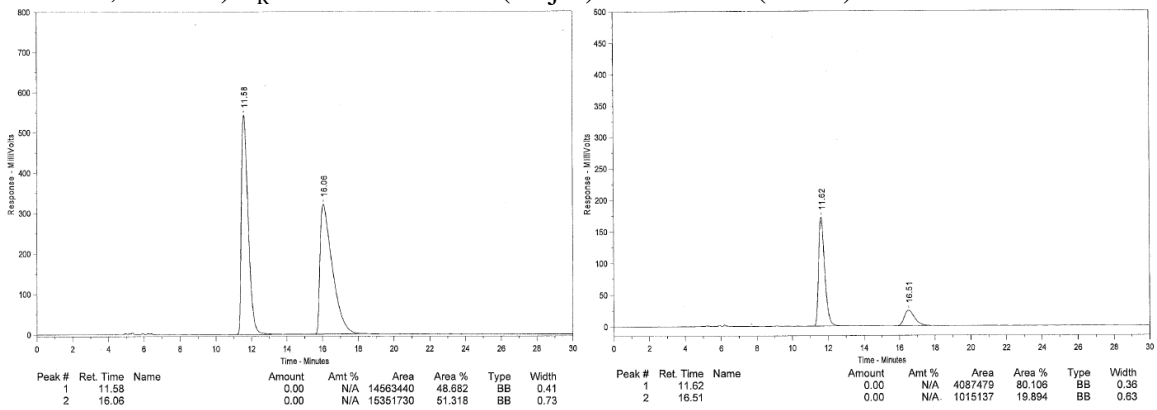

Peak #	Ret. Time	Area %	Peak #	Ret. Time	Area %
1	13.5 min	49.835	1	12.7 min	87.998
2	17.8 min	50.165	2	17.3 min	12.002

(*S*)–*N*-(2,2-Dimethylhex-5-en-3-yl)-*P*,*P*-diphenylphosphinic amide (**2.32u**): mp = 112–115 °C. ^{1}H NMR (400 MHz, $CDCl_3$): δ 7.94–7.85 (4H, m), 7.51–7.43 (6H, m), 5.88 (1H, dddd, J = 16.8, 10.0, 6.8, 6.8 Hz), 5.09–5.01 (2H, m), 2.92–2.84 (1H, m), 2.66 (1H, br dd, J = 11.2, 7.2 Hz), 2.49–2.43 (2H, m), 2.23–2.15 (1H, m), 0.92 (9H, s); HRMS Calcd for $C_{20}H_{27}NOP$ [M + H]$^+$: 328.18303; Found: 328.18324. The enantiomeric purity of this compound was determined by HPLC analysis in comparison with authentic racemic material (Chiracel OD-H, 95:5 hexanes:*i*-PrOH, 0.6 mL/min, 220 nm): t_R of **2.32u**: 12 min (major) and 16 min (minor).

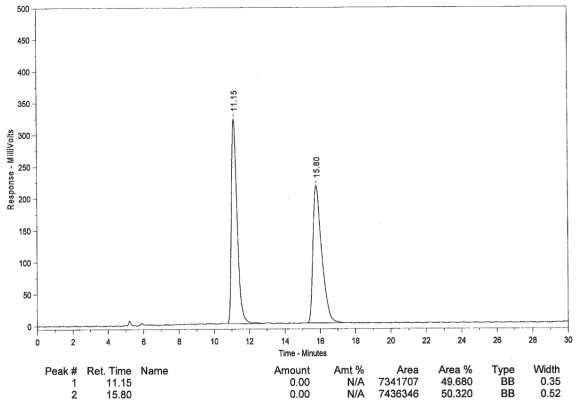

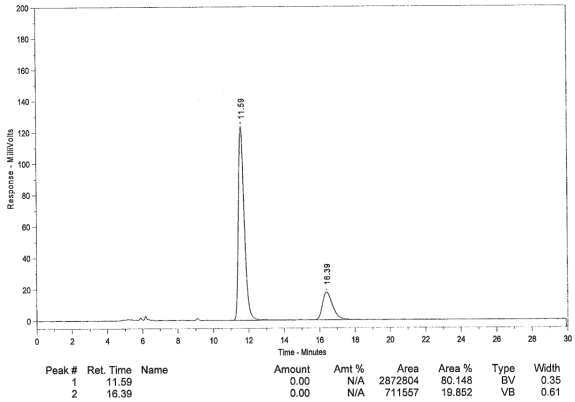

Peak #	Ret. Time	Area %
1	11.2 min	49.680
2	15.8 min	50.320

Peak #	Ret. Time	Area %
1	11.6 min	80.148
2	16.4 min	19.852

(*S*,*E*)–*N*-(2-methyl-1-(2-methylthiazol-4-yl)hexa-1,5-dien-3-yl)-*P*,*P*-diphenylphosphinic amide (**2.32v**): IR (neat): 3357 (w, br), 3193 (w, br), 3076 (w), 3058 (w), 2966 (w), 2926 (w), 2871 (w), 1574 (w), 1437 (m), 1184 (s), 1121(m), 1108 (m), 952 (m), 910 (m), 723 (s), 694 (s), 525 (s) cm^{-1}; ^1H NMR (400 MHz, $CDCl_3$): δ 7.92–7.84 (4H, m), 7.40–7.37 (6H, m), 6.83 (1H, s), 6.30 (1H, s), 5.70 (1H, dddd, *J* = 17.1, 9.9, 7.2, 7.2 Hz), 5.14–5.06 (2H, m), 3.81 (1H, dddd, *J* = 9.4, 9.4, 6.6, 6.6 Hz), 3.16 (1H, dd, *J* = 9.5, 5.6 Hz), 2.69 (3H, s), 2.60–2.53 (1H, m), 2.50–2.43 (1H, m), 2.00 (3H, s); ^{13}C NMR (100 MHz, $CDCl_3$): δ 164.5, 152.9, 139.9 (d, *J* = 5.0 Hz), 133.9, 133.1 (d, *J* = 127.6 Hz), 132.6 (d, *J* = 9.5 Hz), 132.4 (d, *J* = 131.1 Hz), 131.9 (d, *J* = 9.5 Hz), 131.9 (d, *J* = 2.8 Hz), 131.8 (d, *J* = 2.8 Hz), 128.6 (d, *J* = 12.6 Hz), 128.5 (d, *J* = 12.7 Hz), 120.2, 118.6, 115.7, 58.0, 40.4 (d, *J* = 4.3 Hz), 19.3, 15.5; HRMS Calcd for $C_{24}H_{26}N_2OPS$ $[M + H]^+$: 409.15034; Found: 409.15018. The enantiomeric purity of this compound was determined by HPLC analysis in comparison with authentic racemic material (Chiracel AD-H, 91:9 hexanes:*i*-PrOH, 0.8 mL/min, 220 nm): t_R of **2.32v**: 41 min (major) and 63 min (minor).

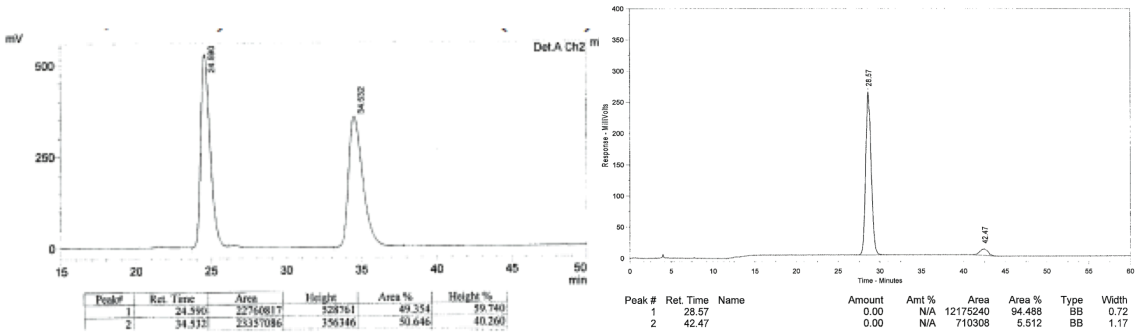

Peak #	Ret. Time	Area %	Peak #	Ret. Time	Area %
1	24.6 min	49.354	1	28.6 min	94.488
2	34.5 min	50.646	2	42.5 min	5.512

▪ **Representative Procedure for NHC–Cu-Catalyzed Enantioselective Allyl Additions of Substituted Allylboron Reagents to Aldimine 2.31a:** Preparation of the chiral NHC–Cu catalyst as a 0.2 M solution in thf is performed as described above. Another oven-dried vial equipped with a stir bar was charged with 2-substituted allylboron **2.53** (25.5 mg, 0.140 mmol). The vial was sealed with a septum and electrical tape and purged with N_2. An appropriate portion of the stock solution of the NHC–Cu complex (250 μL) was transferred to the vial containing substrate **2.31a** at 22 °C. After the mixture is allowed to stir for five minutes, the solution was allowed to cool to –78 °C (dry ice/acetone bath). A stock solution of aldimine **2.31a** (30.5 mg, 0.100 mmol in 500 μL freshly distilled thf) and MeOH (8.1 μL, 0.20 mmol) were added and the reaction was transferred to a –50 °C cryocool and allowed to stir for 18 hours before addition of 1.0 mL of a 1 M aqueous solution of HCl. The solution was allowed to warm to 22 °C and the reaction mixture was diluted with AcOEt. The layers were separated and the water layer was washed with AcOEt (3 x 2 mL). The organic layers were combined and dried with $MgSO_4$ and the volatiles were removed *in vacuo*. The unpurified residue obtained as an off-white solid is purified by silica gel chromatography (a gradient from 1:1

hexanes:Et_2O to 100% Et_2O is used to remove pinacol from the mixture followed by 4:1 AcOEt:hexanes with 5% Et_3N to 100% AcOEt with 5% Et_3N) to yield 34.6 mg (0.096 mmol, 96% yield) of pure **2.54** as a white crystalline solid in 95:5 e.r. (90% ee).

(*S*)–*N*-(3-methyl-1-phenylbut-3-en-1-yl)-*P*,*P*-diphenylphosphinic amide (**2.54**): mp = 166–168 °C. IR (neat): 3173 (w, br), 1436 (m), 1181 (s), 1122 (m), 1108 (m), 1069 (m), 889 (m), 748 (m), 723 (m), 692 (s), 527 (s) cm^{-1}; ^1H NMR (400 MHz, $CDCl_3$): δ 7.86–7.80 (2H, m), 7.76–7.70 (2H, m), 7.50–7.46 (1H, m), 7.44–7.38 (3H, m), 7.31–7.27 (2H, m), 7.26–7.16 (5H, m), 4.79–4.77 (1H, m), 4.69–4.68 (1H, m), 4.43–4.34 (1H, m), 3.32 (1H, br dd, *J* = 8.0, 6.0 Hz), 2.62 (1H, dd, *J* = 13.6 Hz, 7.2 Hz), 2.53 (1H, dd, *J* = 14.0 Hz, 7.2 Hz), 1.58 (3H, s); ^{13}C NMR (100 MHz, $CDCl_3$): δ 143.1 (d, *J* = 5.2 Hz), 142.1, 133.2 (d, *J* = 127 Hz), 132.6 (d, *J* = 8.9 Hz), 132.2 (d, *J* = 129 Hz), 131.93 (d, *J* = 3.0 Hz), 131.92 (d, *J* = 9.7 Hz), 131.7 (d, *J* = 3.0 Hz), 128.6 (d, *J* = 12.7 Hz), 128.4, 128.3 (d, *J* = 12.6 Hz), 127.2, 126.7, 114.5, 53.6, 48.3 (d, *J* = 5.2 Hz), 22.4; HRMS Calcd for $C_{23}H_{25}NOP$ $[M + H]^+$: 362.16738; Found: 362.16615. $[\alpha]^{25}_D = -17.6$ (*c* = 1.00, $CHCl_3$) for a 95:5 e.r. sample. The enantiomeric purity of this compound was determined by HPLC analysis in comparison with authentic racemic material (Chiracel OD, 92:8 hexanes:*i*-PrOH, 0.8 mL/min, 220 nm): t_R of **2.54**: 10 min (minor) and 13 min (major).

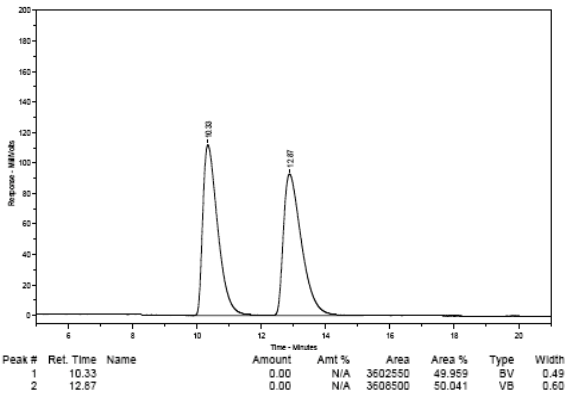

Peak #	Ret. Time	Name	Amount	Amt %	Area	Area %	Type	Width
1	10.33		0.00	N/A	3602550	49.959	BV	0.49
2	12.87		0.00	N/A	3608500	50.041	VB	0.60

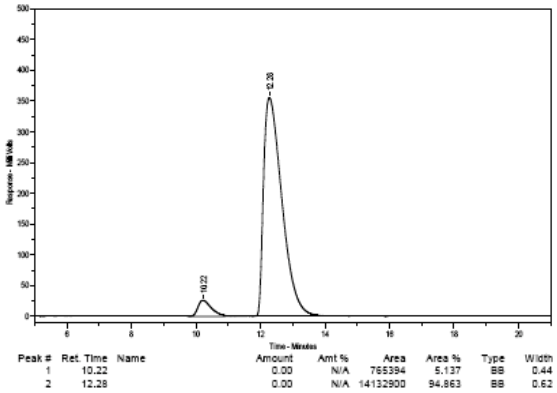

Peak #	Ret. Time	Name	Amount	Amt %	Area	Area %	Type	Width
1	10.22		0.00	N/A	765394	5.137	BB	0.44
2	12.28		0.00	N/A	14132900	94.863	BB	0.62

Peak #	Ret. Time	Area %	Peak #	Ret. Time	Area %
1	10.3 min	49.959	1	10.2 min	5.137
2	12.9 min	50.041	2	12.3 min	94.863

(*S*)–*N*-(1,3-diphenylbut-3-en-1-yl)-*P*,*P*-diphenylphosphinic amide (**2.56**): mp = 150–151 °C. IR (neat): 3173 (w, br), 1436 (m), 1181 (s), 1122 (m), 1108 (m), 1069 (m), 889 (m), 748 (m), 723 (m), 692 (s), 527 (s) cm^{-1}; ^{1}H NMR (400 MHz, $CDCl_3$): δ 7.76–7.70 (4H, m), 7.47–7.40 (2H, m), 7.37–7.30 (4H, m), 7.27–7.16 (8H, m), 7.07–7.00 (2H, m), 5.21 (1H, d, *J* = 1.2 Hz), 4.87 (1H, d, *J* = 1.2 Hz), 4.27 (1H, dddd, *J* = 8.4, 8.4, 6.4, 6.4 Hz), 3.29 (1H, br dd, *J* = 8.8, 5.6 Hz), 3.25 (1H, dd, *J* = 14.0, 6.0 Hz), 2.99 (1H, dd, *J* = 14.0, 8.0 Hz); ^{13}C NMR (100 MHz, $CDCl_3$): δ 144.5, 143.0 (d, *J* = 5.3 Hz), 140.1, 132.8 (d, *J* = 127 Hz), 132.44 (d, *J* = 9.7 Hz), 132.37 (d, *J* = 129 Hz), 132.0 (d, *J* = 9.7 Hz), 131.81 (d, *J* = 3.0 Hz), 131.78 (d, *J* = 3.0 Hz), 128.52, 128.50 (d, *J* = 12.6 Hz), 128.42 (d, *J* = 12.6 Hz), 128.40, 127.6, 127.3, 126.7, 126.4, 116.0, 54.8, 45.7 (d, *J* = 5.2 Hz); HRMS Calcd for $C_{28}H_{27}NOP$ $[M + H]^+$: 424.18303; Found: 424.18230. $[\alpha]^{25}_D$ = –17.6 (*c* = 1.00, $CHCl_3$) for a 95:5 e.r. sample. The enantiomeric purity of this compound was determined by HPLC analysis in comparison with authentic racemic material (Chiracel OD, 92:8 hexanes:*i*-PrOH, 0.8 mL/min, 220 nm): t_R of **2.56**: 14 min (major) and 16 min (minor).

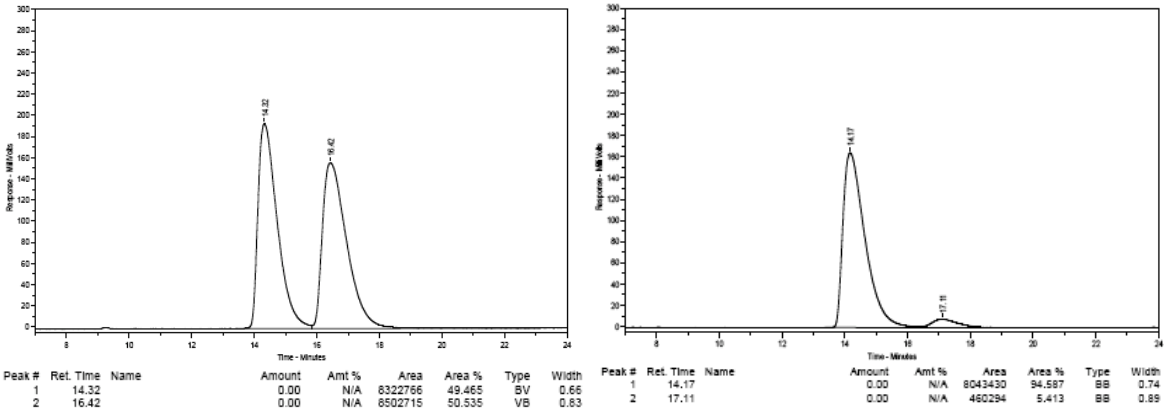

Peak #	Ret. Time	Area %	Peak #	Ret. Time	Area %
1	14.3 min	49.465	1	14.2 min	5.413
2	16.4 min	50.535	2	17.1 min	94.587

▪ **NHC–Cu Catalyzed Addition of *cis*-Crotylboronic Acid Pinacol Ester:** *See representative procedure for additions of susbstituted allylboronates*. An inseparable mixture of a 60:40 ratio of *syn* and *anti* diastereomers was obtained: ***N*–((1*S*)-2-methyl-1-phenylbut-3-en-1-yl)-*P*,*P*-diphenylphosphinic amide** (**2.58**): mp = 136–138 °C. IR (neat): 3158 (w, br), 3056 (w, br), 1454 (m), 1436 (m), 1181 (m), 1122 (m), 1106 (m), 1063 (m), 912 (m), 746 (m), 724 (m), 694 (s), 535 (s) cm^{-1}; ^1H NMR (400 MHz, $CDCl_3$) for a 4:3 mixture of diastereomers: δ 7.85–7.78 (3H, m), 7.70–7.61 (3H, m), 7.51–7.33 (6H, m), 7.28–7.15 (8H, m), 7.11–7.08 (2H, m), 7.05–7.02 (2H, m), 5.81 (1H, ddd, *J* = 18.0, 10.6, 7.6 Hz), 5.58–5.49 (1H, m), 5.18–5.07 (3.3H, m), 4.16–4.04 (1.75H, m), 3.60 (1H, br dd, *J* = 10.4, 6.4 Hz), 3.39 (0.75H, br dd, *J* = 8.0, 6.4 Hz), 3.29 (1H, br dd, *J* = 8.8, 5.6 Hz), 2.73 (1H, ddd, *J* = 13.2, 13.2, 6.4 Hz), 2.56 (0.75H, ddd, *J* = 13.2, 13.2, 6.4 Hz), 0.99 (2.2H, d, *J* = 6.8 Hz), 0.93 (3H, d, *J* = 6.8 Hz); ^{13}C NMR (100 MHz, $CDCl_3$) for a 4:3 mixture of diastereomers: δ 142.72, 142.69, 141.0, 140.2, 139.3, 132.8, 132.75, 132.72, 132.6, 131.95, 131.93, 131.87, 131.83, 131.78, 131.76, 131.60, 131.59, 131.3, 128.7, 128.63, 128.55, 128.5, 128.4, 128.23, 128.21, 128.18, 128.1, 128.0, 127.7, 127.3, 127.1, 127.09, 127.06, 117.4, 116.8, 59.5, 59.0, 45.9, 45.8, 45.71, 45.66, 17.5, 17.2. HRMS Calcd for $C_{23}H_{25}NOP$ $[M + H]^+$: 362.16738; Found: 362.16645. The enantiomeric purity of this compound was determined by HPLC analysis in comparison with authentic racemic material (Chiralpak AD-H, 98:2 hexanes:*i*-PrOH, 0.7 mL/min, 220 nm): t_R of major diastereomer: 121 min (major) and 128 min (minor); t_R of minor diastereomer: 138 min (major) and 296 min (minor).

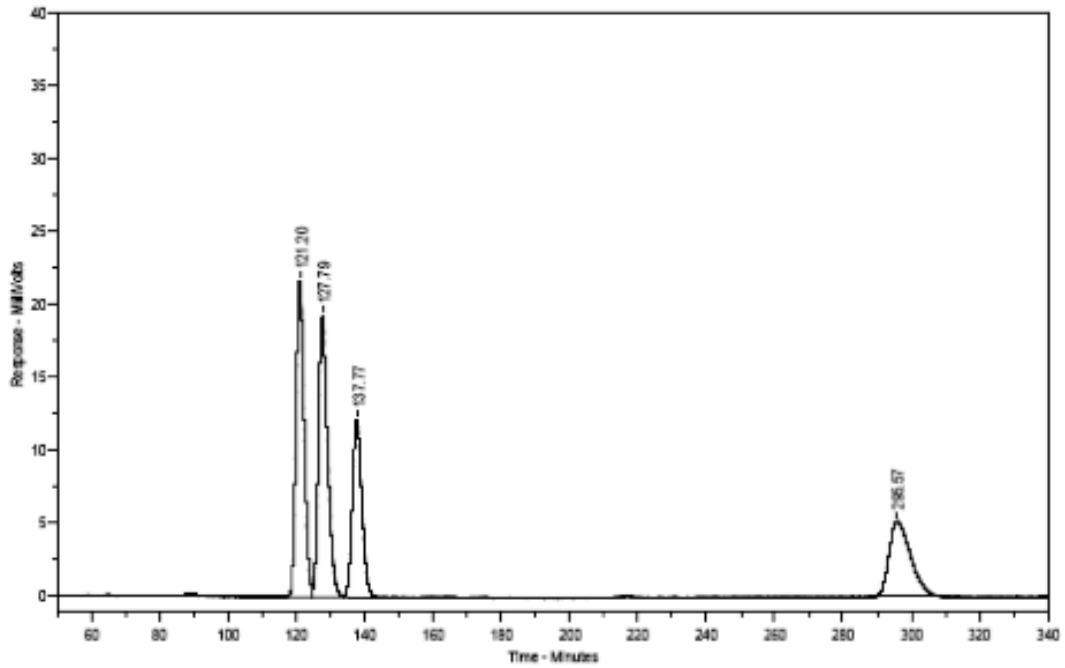

Peak #	Ret. Time	Name	Amount	Amt %	Area	Area %	Type	Width
1	121.20		0.00	N/A	3580950	30.423	BV	2.56
2	127.79		0.00	N/A	3604940	30.627	VV	2.68
3	137.77		0.00	N/A	2327149	19.771	VB	2.95
4	295.57		0.00	N/A	2257546	19.180	BB	6.90

Peak #	Ret. Time	Area %
1	121.2 min	30.423
2	127.8 min	30.627
3	137.8 min	19.711
4	295.6 min	19.180

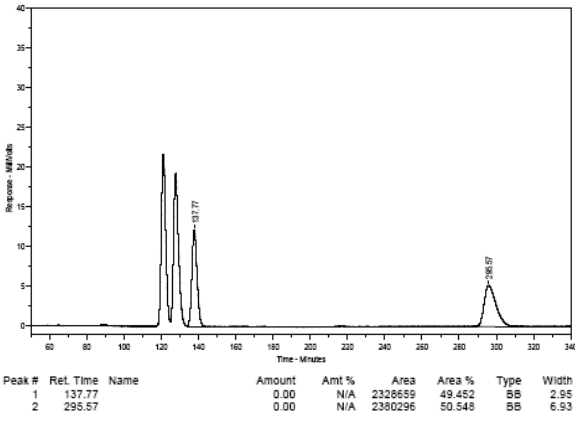

Peak #	Ret. Time	Name	Amount	Amt %	Area	Area %	Type	Width
1	137.77		0.00	N/A	2328659	49.452	BB	2.95
2	295.57		0.00	N/A	2380296	50.548	BB	6.93

Peak #	Ret. Time	Area %
1	137.8 min	49.452
2	295.6 min	50.548

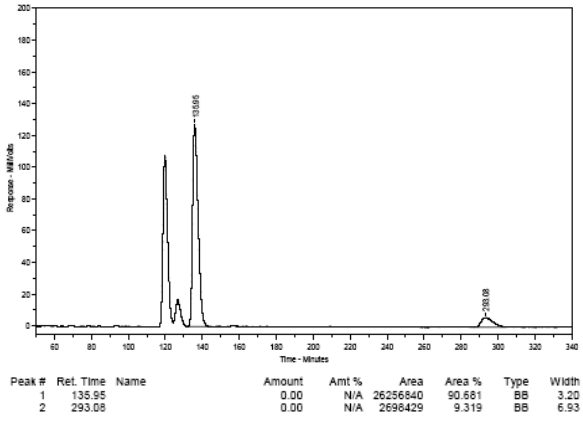

Peak #	Ret. Time	Name	Amount	Amt %	Area	Area %	Type	Width
1	135.95		0.00	N/A	26256840	90.681	BB	3.20
2	293.08		0.00	N/A	2698429	9.319	BB	6.93

Peak #	Ret. Time	Area %
1	136.0 min	90.681
2	293.1 min	9.319

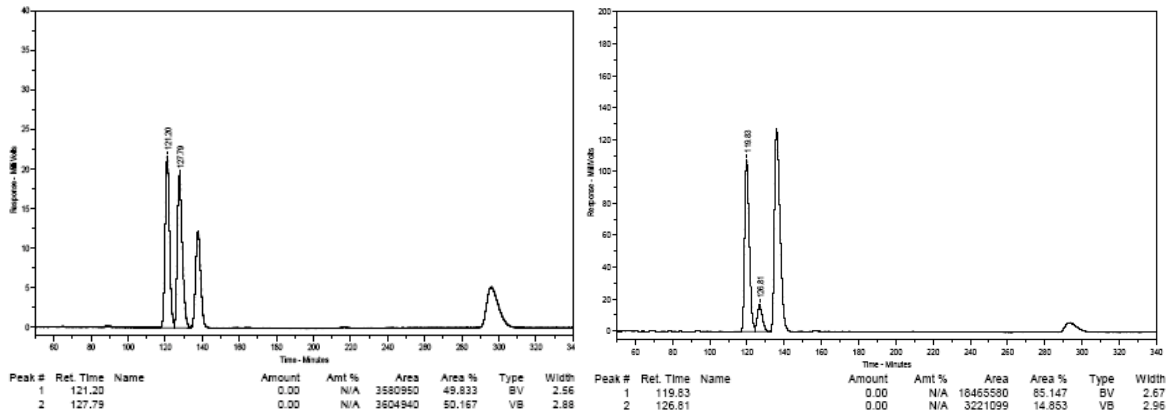

Peak #	Ret. Time	Area %	Peak #	Ret. Time	Area %
1	121.2 min	49.833	1	119.8 min	85.147
2	127.8 min	50.167	2	126.8 min	14.853

▪ **NHC–Cu-Catalyzed Enantioselective Allyl Additions to *o*-Thiomethylaniline-derived Aldimines:** *See representative procedure for additions of allylboron* **2.11** *catalyzed by the NHC–Cu complex derived from* **2.48** *to N-diphenylphosphinoyl imines*. The unpurified product is obtained as a pale yellow oil and was purified by silica gel chromatography (100% Hexanes to 20:1 Hexanes:Et_2O) to yield 26.2 mg (0.097 mmol, 97% yield) of pure 2-(methylthio)-*N*-(1-phenylbut-3-en-1-yl)aniline as a colorless oil in 53:47 e.r. (6% ee). **2-(methylthio)-*N*-(1-phenylbut-3-en-1-yl)aniline** (**2.24**): IR (neat): 3363 (w, br), 3063 (w), 2854 (w), 1585 (s), 1497 (s), 1449 (s), 1317 (m), 1283 (m), 1037 (m), 992 (m), 919 (m), 743 (s), 699 (s), 465 (s) cm^{-1}. ^1H NMR (400 MHz, $CDCl_3$): δ 7.41–7.39 (1H, dd, *J* = 7.6, 1.6 Hz), 7.37–7.31 (4H, m), 7.26–7.22 (1H, m), 7.02–6.98 (1H, m), 6.60 (1H, ddd, *J* = 7.6, 7.6, 1.2 Hz), 6.31 (1H, dd, *J* = 8.4, 1.2 Hz), 5.82 (1H, dddd, *J* = 17.2, 10.4, 7.2, 7.2 Hz), 5.55 (1H, br d, *J* = 4.4 Hz), 5.29–5.18 (2H, m), 4.46

(1H, dddd, J = 8.0, 8.0, 5.0, 5.0 Hz), 2.72–2.55 (2H, m), 2.39 (3H, s). ^{13}C NMR (100 MHz, $CDCl_3$): δ 147.4, 143.4, 134.6, 134.2, 129.4, 128.7, 127.1, 126.4, 119.9, 118.5, 117.1, 111.5, 57.3, 43.6, 18.3. HRMS Calcd for $C_{17}H_{20}NS$ $[M + H]^+$: 270.13164; Found: 270.13280. The enantiomeric purity of this compound was determined by HPLC analysis in comparison with authentic racemic material (Chiracel OD, 98:2 hexanes:*i*-PrOH, 0.5 mL/min, 220 nm):): t_R of **2.24**: 11 min (minor) and 13 min (major).

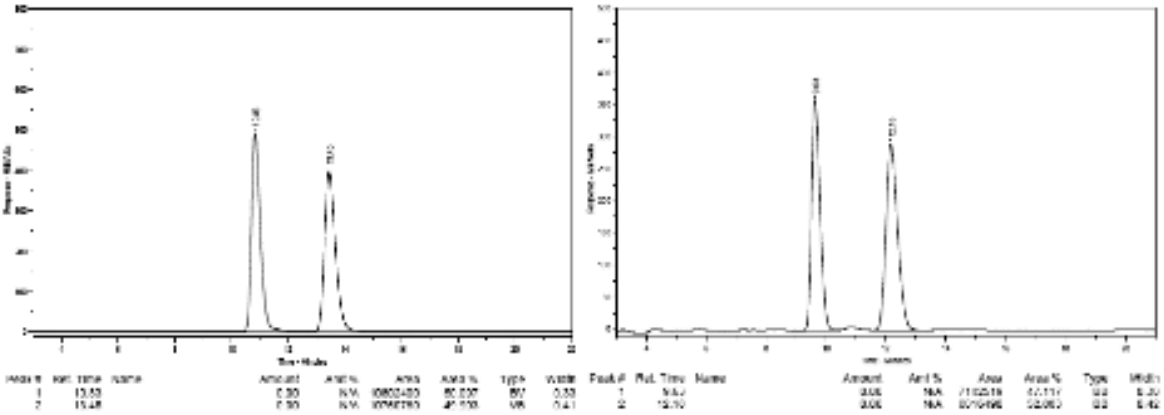

Peak #	Ret. Time	Area %	Peak #	Ret. Time	Area %
1	10.8 min	50.097	1	9.6 min	47.117
2	13.4 min	49.903	2	12.2 min	52.883

▪ **Absolute Configuration of the EVM products:** ***X-ray Crystal Structure of Homoallylamide (S)-*** **2.32a*****: Proof of Absolute Stereochemistry:*** Please note that the absolute stereochemistry of the major product enantiomers are inferred from that obtained through the X-ray crystal structure of homoallylamide **2.32a**

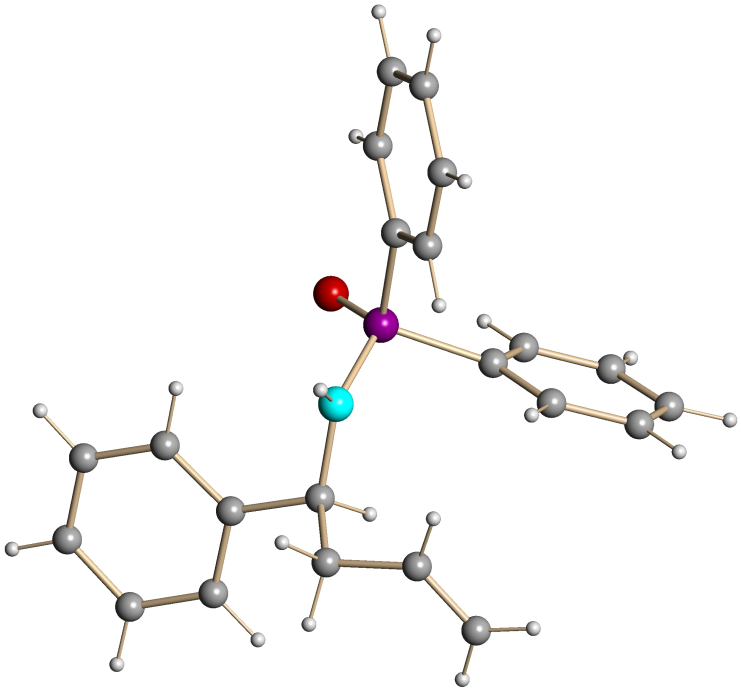

Table 1. *Crystal data and structure refinement for $C_{22}H_{22}NOP$*

Identification code	$C_{22}H_{22}NOP$	
Empirical formula	$C_{22}H_{22}NOP$	
Formula weight	347.38	
Temperature	173(2) K	
Wavelength	0.71073 ≈	
Crystal system	Triclinic	
Space group	P 1	
Unit cell dimensions	a = 8.6853(5) ≈	a= 74.297(3)∞.
	b = 11.3946(6) ≈	b= 79.005(3)∞.
	c = 20.2971(11) ≈	g = 89.123(3)∞.
Volume	1896.85(18) $≈^3$	
Z	4	
Density (calculated)	1.216 mg/m^3	

Absorption coefficient	0.154 mm^{-1}
F(000)	736
Crystal size	0.18 x 0.04 x 0.03 mm^3
Theta range for data collection	1.86 to 27.00∞.
Index ranges	-11<=h<=11, -14<=k<=14, -25<=l<=25
Reflections collected	57723
Independent reflections	16102 [R(int) = 0.0737]
Completeness to theta = 27.00∞	100.0 %
Absorption correction	Semi-empirical from equivalents
Max. and min. transmission	0.9954 and 0.9729
Refinement method	Full-matrix least-squares on F^2
Data / restraints / parameters	16102 / 6 / 910
Goodness-of-fit on F^2	1.000
Final R indices [I>2sigma(I)]	R1 = 0.0590, wR2 = 0.1352
R indices (all data)	R1 = 0.0966, wR2 = 0.1560
Absolute structure parameter	0.11(8)
Extinction coefficient	na
Largest diff. peak and hole	0.761 and -0.290 e.≈$^{-3}$

Table 2. *Atomic coordinates (x 10^4) and equivalent isotropic displacement parameters ($\approx^2$x 10^3) for $C_{22}H_{22}NOP$. U(eq) is defined as one third of the trace of the orthogonalized U^{ij} tensor*

	x	y	z	U(eq)
P(1)	9105(1)	2240(1)	4866(1)	30(1)
O(1)	9735(3)	3024(2)	5236(1)	36(1)
N(1)	7871(4)	2812(3)	4351(2)	33(1)
C(1)	7970(5)	949(3)	5481(2)	33(1)
C(2)	7041(5)	173(3)	5282(2)	38(1)
C(3)	6261(5)	-843(4)	5771(2)	42(1)
C(4)	6392(5)	-1073(4)	6461(2)	42(1)
C(5)	7287(5)	-311(4)	6669(2)	43(1)
C(6)	8094(5)	711(3)	6174(2)	34(1)
C(7)	10694(5)	1629(3)	4359(2)	33(1)
C(8)	10413(6)	939(4)	3914(2)	46(1)
C(9)	11677(6)	418(4)	3580(2)	53(1)
C(10)	13175(6)	559(4)	3684(2)	56(1)
C(11)	13447(6)	1258(4)	4111(2)	52(1)
C(12)	12211(5)	1781(4)	4444(2)	38(1)
C(13)	8315(5)	3822(4)	3704(2)	38(1)
C(14)	7295(6)	3680(4)	3181(2)	52(1)
C(15)	7578(6)	2568(5)	2942(2)	58(1)
C(16)	8442(7)	2532(6)	2348(3)	68(2)
C(17)	8165(5)	5078(4)	3818(2)	42(1)
C(18)	8741(7)	6096(5)	3265(3)	69(2)
C(19)	8562(9)	7261(5)	3360(3)	88(2)
C(20)	7933(8)	7433(5)	3994(3)	72(2)
C(21)	7390(6)	6449(4)	4543(3)	58(1)

C(22)	7520(5)	5296(4)	4445(2)	44(1)
P(2)	3744(1)	3254(1)	5740(1)	27(1)
O(2)	4874(3)	2766(2)	5242(1)	33(1)
N(2)	2435(4)	4199(2)	5446(2)	30(1)
C(23)	4784(5)	4029(3)	6207(2)	29(1)
C(24)	4028(5)	4854(3)	6548(2)	35(1)
C(25)	4842(5)	5354(4)	6937(2)	41(1)
C(26)	6353(6)	5076(4)	6982(2)	49(1)
C(27)	7112(5)	4277(4)	6631(2)	45(1)
C(28)	6319(5)	3754(4)	6248(2)	35(1)
C(29)	2550(4)	2042(3)	6385(2)	28(1)
C(30)	1349(5)	2256(3)	6892(2)	33(1)
C(31)	528(5)	1289(4)	7401(2)	35(1)
C(32)	881(5)	102(4)	7402(2)	40(1)
C(33)	2056(5)	-119(4)	6891(2)	44(1)
C(34)	2905(5)	851(3)	6387(2)	36(1)
C(35)	2934(5)	5396(3)	4955(2)	32(1)
C(36)	2711(6)	5421(4)	4218(2)	46(1)
C(37)	3601(12)	6504(7)	3678(3)	38(2)
C(38)	2904(13)	7356(8)	3283(5)	69(4)
C(37X)	2907(17)	6654(11)	3705(7)	47(4)
C(38X)	4180(20)	6897(18)	3228(10)	105(7)
C(39)	2074(5)	6396(3)	5220(2)	32(1)
C(40)	2873(6)	7472(4)	5172(2)	45(1)
C(41)	2088(7)	8394(4)	5414(2)	52(1)
C(42)	538(7)	8260(4)	5683(2)	53(1)
C(43)	-297(6)	7201(4)	5729(3)	58(1)
C(44)	497(5)	6279(4)	5484(2)	47(1)
P(3)	6719(1)	4460(1)	134(1)	27(1)
O(3)	7686(3)	3642(2)	-217(1)	32(1)
N(3)	5020(4)	3945(3)	656(2)	31(1)

C(45)	6138(4)	5751(3)	-498(2)	27(1)
C(46)	6877(5)	5954(3)	-1192(2)	31(1)
C(47)	6521(5)	6964(3)	-1691(2)	40(1)
C(48)	5447(5)	7769(4)	-1508(2)	38(1)
C(49)	4713(5)	7572(3)	-823(2)	38(1)
C(50)	5040(4)	6563(3)	-316(2)	34(1)
C(51)	7839(5)	5082(3)	631(2)	30(1)
C(52)	9441(5)	4949(4)	530(2)	37(1)
C(53)	10383(6)	5491(4)	854(2)	46(1)
C(54)	9724(6)	6170(4)	1284(2)	48(1)
C(55)	8115(6)	6322(4)	1396(2)	49(1)
C(56)	7177(5)	5790(4)	1074(2)	41(1)
C(57)	4930(5)	2982(4)	1305(2)	36(1)
C(58)	3324(6)	3055(4)	1781(2)	48(1)
C(59)	3134(6)	4188(5)	2018(2)	58(1)
C(60)	2790(8)	4228(6)	2640(3)	82(2)
C(61)	5121(5)	1705(4)	1220(2)	39(1)
C(62)	5575(6)	785(4)	1747(2)	55(1)
C(63)	5765(7)	-377(5)	1691(3)	69(2)
C(64)	5419(7)	-681(4)	1122(4)	74(2)
C(65)	4964(7)	209(4)	591(3)	63(1)
C(66)	4827(5)	1399(4)	634(2)	46(1)
P(4)	2159(1)	3388(1)	9274(1)	26(1)
O(4)	2817(3)	3858(2)	9782(1)	32(1)
N(4)	615(4)	2445(3)	9563(2)	30(1)
C(67)	1526(4)	4608(3)	8629(2)	28(1)
C(68)	757(5)	4408(3)	8122(2)	32(1)
C(69)	389(5)	5381(4)	7604(2)	37(1)
C(70)	780(5)	6560(4)	7592(2)	39(1)
C(71)	1521(6)	6770(4)	8095(2)	45(1)
C(72)	1919(5)	5801(3)	8608(2)	34(1)

C(73)	3634(4)	2613(3)	8809(2)	26(1)
C(74)	3216(5)	1816(3)	8450(2)	33(1)
C(75)	4370(5)	1315(4)	8055(2)	39(1)
C(76)	5926(6)	1591(4)	8012(2)	48(1)
C(77)	6345(5)	2357(4)	8379(2)	47(1)
C(78)	5183(5)	2877(3)	8773(2)	36(1)
C(79)	722(5)	1231(3)	10035(2)	29(1)
C(80)	-81(6)	1178(4)	10785(2)	40(1)
C(81)	60(6)	-31(4)	11279(2)	46(1)
C(82)	1025(7)	-262(5)	11727(2)	68(2)
C(83)	66(4)	256(3)	9766(2)	29(1)
C(84)	851(5)	-812(3)	9774(2)	40(1)
C(85)	249(6)	-1710(4)	9535(2)	48(1)
C(86)	-1128(6)	-1552(4)	9299(2)	48(1)
C(87)	-1918(6)	-497(4)	9285(3)	54(1)
C(88)	-1324(5)	399(4)	9530(2)	44(1)

▪ **Crystal Structure of Imidazolinium Tetrafluoroborate Salt 2.50:**

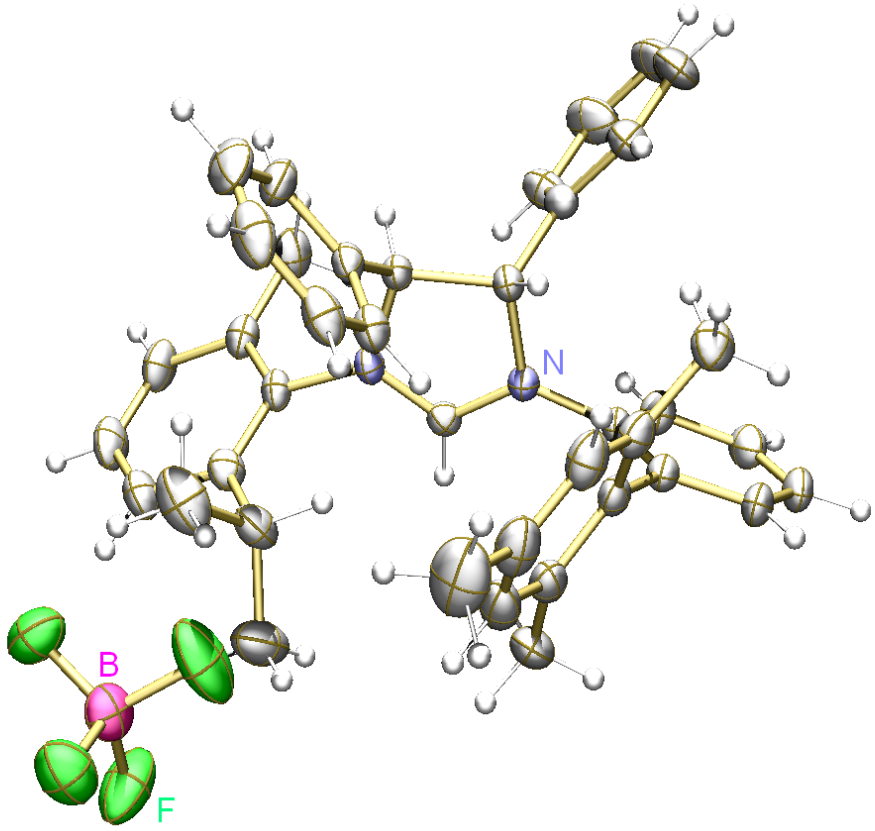

Table 1. *Crystal data and structure refinement for* $C_{41}H_{43}BCl_2F_4N_2$

Identification code	$C_{41}H_{43}BCl_2F_4N_2$	
Empirical formula	C_{41} H_{43} B Cl_2 F_4 N_2	
Formula weight	721.48	
Temperature	173(2) K	
Wavelength	0.71073 ≈	
Crystal system	Monoclinic	
Space group	P 2(1)	
Unit cell dimensions	a = 9.4246(11) ≈	a= 90∞.

	b = 17.954(2) ≈	b= 110.801(2)∞.
	c = 11.7320(14) ≈	g = 90∞.
Volume	1855.8(4) ≈^{3}	
Z	2	
Density (calculated)	1.291 mg/m^3	
Absorption coefficient	0.227 mm^{-1}	
F(000)	756	
Crystal size	0.13 x 0.11 x 0.09 mm^3	
Theta range for data collection	2.18 to 28.00∞.	
Index ranges	-12<=h<=12, -23<=k<=23, -15<=l<=15	
Reflections collected	28922	
Independent reflections	8925 [R(int) = 0.0267]	
Completeness to theta = 28.00∞	99.9 %	
Absorption correction	Semi-empirical from equivalents	
Max. and min. transmission	0.9799 and 0.9711	
Refinement method	Full-matrix least-squares on F^2	
Data / restraints / parameters	8925 / 83 / 470	
Goodness-of-fit on F^2	1.044	
Final R indices [I>2sigma(I)]	R1 = 0.0554, wR2 = 0.1518	
R indices (all data)	R1 = 0.0614, wR2 = 0.1581	
Absolute structure parameter	0.01(8)	
Extinction coefficient	na	
Largest diff. peak and hole	0.824 and -0.432 e.≈$^{-3}$	

Table 2. *Atomic coordinates (x 10^4) and equivalent isotropic displacement parameters ($\approx^2$x 10^3) for $C_{41}H_{43}BCl_2F_4N_2$. U(eq) is defined as one third of the trace of the orthogonalized U^{ij} tensor*

	x	y	z	U(eq)
N(1)	2888(2)	968(1)	7715(2)	25(1)
N(2)	1876(2)	2016(1)	6814(1)	25(1)
C(1)	3094(2)	1669(1)	7533(2)	24(1)
C(2)	1263(2)	760(1)	7102(2)	25(1)
C(3)	557(2)	1495(1)	6424(2)	25(1)
C(4)	3995(2)	439(1)	8440(2)	26(1)
C(5)	4401(3)	462(1)	9696(2)	34(1)
C(6)	5399(3)	-82(1)	10391(2)	37(1)
C(7)	5920(3)	-633(1)	9828(2)	37(1)
C(8)	5517(2)	-643(1)	8570(2)	33(1)
C(9)	4556(2)	-95(1)	7851(2)	27(1)
C(10)	4210(2)	-90(1)	6505(2)	29(1)
C(11)	3177(3)	-601(1)	5745(2)	33(1)
C(12)	2905(3)	-581(2)	4493(2)	42(1)
C(13)	3635(3)	-83(2)	3991(2)	46(1)
C(14)	4660(3)	406(2)	4755(2)	46(1)
C(15)	4993(3)	413(1)	6015(2)	36(1)
C(16)	2391(3)	-1177(1)	6234(2)	41(1)
C(17)	3335(5)	-73(2)	2636(3)	70(1)
C(18)	6200(3)	921(2)	6826(3)	46(1)
C(19)	582(2)	496(1)	8024(2)	30(1)
C(20)	-73(3)	-201(1)	7919(3)	43(1)
C(21)	-663(3)	-440(2)	8796(3)	58(1)
C(22)	-598(3)	17(2)	9745(3)	60(1)
C(23)	52(4)	712(2)	9858(2)	55(1)

C(24)	643(3)	952(2)	8995(2)	40(1)
C(25)	-148(2)	1405(1)	5056(2)	27(1)
C(26)	-1603(3)	1683(1)	4444(2)	40(1)
C(27)	-2293(3)	1577(2)	3191(3)	55(1)
C(28)	-1509(4)	1209(2)	2556(2)	51(1)
C(29)	-93(3)	945(1)	3148(2)	42(1)
C(30)	601(3)	1033(1)	4406(2)	32(1)
C(31)	1842(2)	2804(1)	6514(2)	27(1)
C(32)	1164(2)	3295(1)	7100(2)	32(1)
C(33)	1243(3)	4053(1)	6876(2)	40(1)
C(34)	1954(3)	4307(1)	6107(2)	45(1)
C(35)	2570(3)	3816(1)	5520(2)	42(1)
C(36)	2526(2)	3046(1)	5701(2)	32(1)
C(37)	392(3)	3042(2)	7951(2)	42(1)
C(38)	3111(3)	2530(1)	4945(2)	39(1)
C(39)	2068(4)	2587(2)	3596(3)	59(1)
C(40)	4759(4)	2702(2)	5088(4)	62(1)
B(1)	3568(4)	2355(2)	1002(3)	42(1)
F(1)	4898(2)	2651(1)	1803(2)	68(1)
F(2)	3307(3)	1671(1)	1419(2)	76(1)
F(3)	3715(2)	2269(1)	-132(2)	59(1)
F(4)	2400(2)	2849(1)	887(2)	55(1)
C(1S)	6992(5)	3130(4)	10057(4)	76(1)
Cl(1)	6056(2)	3089(1)	8488(1)	94(1)
Cl(2)	8809(2)	2742(1)	10548(2)	100(1)
C(1SA)	7400(30)	3331(15)	9830(20)	76(1)
Cl(1A)	6614(13)	2702(8)	8540(12)	100(1)
Cl(2A)	8665(16)	2855(7)	11110(10)	94(1)

Table 3. *Selected bond lengths [≈] and angles [∞] for $C_{41}H_{43}BCl_2F_4N_2$*

N(1)-C(1)	1.304(3)
N(2)-C(1)	1.315(2)
C(1)-N(1)-C(4)	127.84(17)
C(1)-N(1)-C(2)	110.47(16)
C(4)-N(1)-C(2)	121.63(16)
C(1)-N(2)-C(31)	123.69(17)
C(1)-N(2)-C(3)	109.98(15)
N(1)-C(1)-N(2)	114.59(17)
C(19)-C(2)-C(3)	114.62(16)
N(2)-C(3)-C(25)	113.39(15)
N(2)-C(3)-C(2)	102.49(14)
C(5)-C(4)-N(1)	118.47(18)
C(9)-C(4)-N(1)	118.90(17)

Table 4. *Selected torsion angles [∞] for $C_{41}H_{43}BCl_2F_4N_2$*

C(4)-N(1)-C(1)-N(2)	179.25(17)
C(2)-N(1)-C(1)-N(2)	-3.6(2)
C(31)-N(2)-C(1)-N(1)	178.44(17)
C(3)-N(2)-C(1)-N(1)	1.4(2)
C(1)-N(1)-C(2)-C(19)	-118.64(19)
C(4)-N(1)-C(2)-C(19)	58.7(2)
C(1)-N(1)-C(2)-C(3)	4.0(2)
C(4)-N(1)-C(2)-C(3)	-178.61(16)
C(1)-N(2)-C(3)-C(25)	-121.42(17)
C(31)-N(2)-C(3)-C(25)	61.6(2)
C(1)-N(2)-C(3)-C(2)	1.27(19)
C(31)-N(2)-C(3)-C(2)	-175.68(17)
N(1)-C(2)-C(3)-N(2)	-3.01(17)

C(19)-C(2)-C(3)-N(2)	117.14(18)
N(1)-C(2)-C(3)-C(25)	119.62(17)
C(19)-C(2)-C(3)-C(25)	-120.23(19)
C(1)-N(1)-C(4)-C(5)	77.7(3)
C(2)-N(1)-C(4)-C(5)	-99.1(2)
C(1)-N(1)-C(4)-C(9)	-105.4(2)
C(2)-N(1)-C(4)-C(9)	77.7(2)
C(9)-C(4)-C(5)-C(6)	-0.9(3)
N(1)-C(4)-C(5)-C(6)	175.84(19)
N(1)-C(4)-C(9)-C(8)	-174.09(18)
C(5)-C(4)-C(9)-C(10)	-175.5(2)
N(1)-C(4)-C(9)-C(10)	7.8(3)
N(1)-C(2)-C(19)-C(20)	-123.0(2)
C(3)-C(2)-C(19)-C(20)	121.8(2)
N(1)-C(2)-C(19)-C(24)	55.7(3)
C(2)-C(19)-C(24)-C(23)	-178.8(2)
N(2)-C(3)-C(25)-C(30)	70.1(2)
C(2)-C(3)-C(25)-C(30)	-46.3(2)
N(2)-C(3)-C(25)-C(26)	-111.9(2)
C(1)-N(2)-C(31)-C(32)	-103.4(2)
C(3)-N(2)-C(31)-C(32)	73.2(2)
C(36)-C(31)-C(32)-C(33)	-2.3(3)
N(2)-C(31)-C(32)-C(33)	175.19(19)
N(2)-C(31)-C(32)-C(37)	-4.1(3)
N(2)-C(31)-C(36)-C(35)	-174.9(2)
N(2)-C(31)-C(36)-C(38)	9.7(3)

▪ **Crystal Structure of NHC–Cu-complex 2.51:**

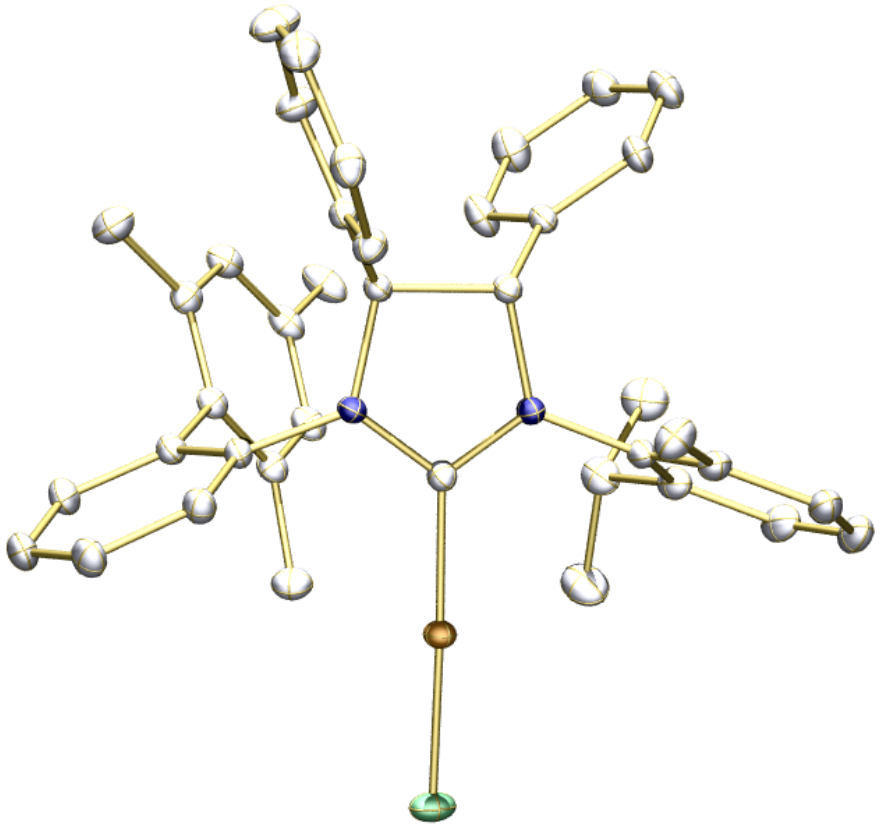

Table 1. *Crystal data and structure refinement for $C_{41}H_{42}Cl_3CuN_2$.*

Identification code	$C_{41}H_{42}Cl_3CuN_2$	
Empirical formula	$C_{41}H_{42}Cl_3CuN_2$	
Formula weight	732.66	
Temperature	100(2) K	
Wavelength	0.71073 ≈	
Crystal system	Orthorhombic	
Space group	P2(1)2(1)2(1)	
Unit cell dimensions	a = 9.6086(7) ≈	a= 90∞.
	b = 19.3742(15) ≈	b= 90∞.
	c = 19.6842(15) ≈	g = 90∞.

Volume	3664.4(5) ≈^{3}
Z	4
Density (calculated)	1.328 Mg/m^3
Absorption coefficient	0.846 mm^{-1}
F(000)	1528
Crystal size	0.20 x 0.10 x 0.08 mm^3
Theta range for data collection	1.47 to 37.42∞.
Index ranges	-16<=h<=15, -33<=k<=30, -33<=l<=31
Reflections collected	93048
Independent reflections	18479 [R(int) = 0.0451]
Completeness to theta = 37.42∞	99.7 %
Absorption correction	Semi-empirical from equivalents
Max. and min. transmission	0.9354 and 0.8490
Refinement method	Full-matrix least-squares on F^2
Data / restraints / parameters	18479 / 15 / 449
Goodness-of-fit on F^2	1.019
Final R indices [I>2sigma(I)]	R1 = 0.0350, wR2 = 0.0801
R indices (all data)	R1 = 0.0496, wR2 = 0.0850
Absolute structure parameter	0.004(5)
Extinction coefficient	na
Largest diff. peak and hole	0.453 and -0.922 e.≈$^{-3}$

Table 2. *Atomic coordinates (x 10^4) and equivalent isotropic displacement parameters ($\approx^2$x 10^3) for $C_{41}H_{42}Cl_3CuN_2$. U(eq) is defined as one third of the trace of the orthogonalized U^{ij} tensor.*

	x	y	z	U(eq)
Cu(1)	9606(1)	1498(1)	5511(1)	16(1)
Cl(1)	10801(1)	1160(1)	4675(1)	25(1)
N(1)	9027(1)	2252(1)	6744(1)	14(1)
N(2)	7561(1)	1413(1)	6574(1)	14(1)
C(1)	8659(1)	1744(1)	6316(1)	14(1)
C(2)	8159(1)	2280(1)	7365(1)	13(1)
C(3)	7037(1)	1722(1)	7216(1)	13(1)
C(4)	10294(1)	2635(1)	6668(1)	14(1)
C(5)	10315(1)	3173(1)	6197(1)	17(1)
C(6)	11552(1)	3528(1)	6075(1)	21(1)
C(7)	12742(1)	3358(1)	6434(1)	21(1)
C(8)	12704(1)	2834(1)	6916(1)	19(1)
C(9)	11490(1)	2453(1)	7035(1)	15(1)
C(10)	11510(1)	1853(1)	7514(1)	15(1)
C(11)	11750(1)	1183(1)	7265(1)	17(1)
C(12)	11730(1)	627(1)	7715(1)	19(1)
C(13)	11534(1)	716(1)	8411(1)	20(1)
C(14)	11364(1)	1386(1)	8653(1)	20(1)
C(15)	11346(1)	1956(1)	8219(1)	18(1)
C(16)	12097(2)	1050(1)	6532(1)	22(1)
C(17)	11532(2)	102(1)	8880(1)	28(1)
C(18)	11188(2)	2675(1)	8507(1)	24(1)
C(19)	7502(1)	2973(1)	7512(1)	15(1)
C(20)	6841(1)	3350(1)	7003(1)	17(1)
C(21)	6122(1)	3952(1)	7164(1)	20(1)

C(22)	6046(2)	4178(1)	7834(1)	24(1)
C(23)	6708(2)	3805(1)	8341(1)	28(1)
C(24)	7441(2)	3202(1)	8182(1)	22(1)
C(25)	6801(1)	1221(1)	7794(1)	14(1)
C(26)	7902(1)	971(1)	8189(1)	22(1)
C(27)	7648(2)	551(1)	8746(1)	26(1)
C(28)	6300(2)	357(1)	8909(1)	24(1)
C(29)	5205(1)	591(1)	8514(1)	24(1)
C(30)	5450(1)	1024(1)	7961(1)	19(1)
C(31)	6797(1)	900(1)	6204(1)	16(1)
C(32)	7196(1)	205(1)	6254(1)	19(1)
C(33)	6418(2)	-279(1)	5888(1)	25(1)
C(34)	5295(2)	-79(1)	5497(1)	26(1)
C(35)	4922(1)	613(1)	5447(1)	22(1)
C(36)	5679(1)	1114(1)	5797(1)	17(1)
C(37)	8438(2)	-37(1)	6666(1)	24(1)
C(38)	7986(2)	-528(1)	7237(1)	30(1)
C(39)	9518(2)	-384(1)	6206(1)	33(1)
C(40)	5317(2)	1868(1)	5713(1)	23(1)
C(41)	5545(3)	7114(1)	5506(2)	65(1)
Cl(2)	6162(2)	6468(1)	4955(1)	40(1)
Cl(3)	6110(2)	7931(1)	5114(1)	65(1)
C(41X)	5545(3)	7114(1)	5506(2)	65(1)
Cl(2X)	6155(4)	6496(2)	4954(2)	65(1)
Cl(3X)	5523(3)	7958(1)	5321(1)	60(1)
C(41Y)	5545(3)	7114(1)	5506(2)	65(1)
Cl(2Y)	6373(11)	7750(5)	4998(5)	78(2)
Cl(3Y)	3733(5)	7105(5)	5411(5)	78(2)

Table 3. *Selected bond lengths [≈] and angles [∞] for $C_{41}H_{42}Cl_3CuN_2$.*

Cu(1)-C(1)	1.8896(12)
Cu(1)-Cl(1)	2.1108(4)
N(1)-C(1)	1.3428(16)
N(1)-C(4)	1.4337(15)
N(1)-C(2)	1.4811(15)
N(2)-C(1)	1.3345(15)
N(2)-C(31)	1.4349(16)
N(2)-C(3)	1.4868(15)
C(1)-Cu(1)-Cl(1)	173.98(4)
C(1)-N(1)-C(4)	122.52(10)
C(1)-N(1)-C(2)	113.35(9)
C(4)-N(1)-C(2)	123.07(10)
C(1)-N(2)-C(31)	122.99(10)
C(1)-N(2)-C(3)	113.44(10)
C(31)-N(2)-C(3)	122.51(9)
N(2)-C(1)-N(1)	108.79(10)
N(2)-C(1)-Cu(1)	125.36(9)
N(1)-C(1)-Cu(1)	125.74(9)
N(1)-C(2)-C(19)	115.20(10)
N(1)-C(2)-C(3)	102.08(9)
N(2)-C(3)-C(25)	115.67(10)
N(2)-C(3)-C(2)	101.85(9)

Table 6. *Selected torsion angles [∞] for $C_{41}H_{42}Cl_3CuN_2$.*

C(31)-N(2)-C(1)-N(1)	171.79(11)
C(3)-N(2)-C(1)-N(1)	3.28(14)
C(31)-N(2)-C(1)-Cu(1)	-11.78(17)

C(3)-N(2)-C(1)-Cu(1)	179.72(8)
C(4)-N(1)-C(1)-N(2)	170.24(10)
C(2)-N(1)-C(1)-N(2)	1.73(14)
C(4)-N(1)-C(1)-Cu(1)	-6.18(16)
C(2)-N(1)-C(1)-Cu(1)	-174.69(8)
Cl(1)-Cu(1)-C(1)-N(2)	-90.9(4)
Cl(1)-Cu(1)-C(1)-N(1)	85.0(4)
C(1)-N(1)-C(2)-C(3)	-5.52(13)
C(4)-N(1)-C(2)-C(3)	-173.95(10)
C(1)-N(2)-C(3)-C(25)	-130.73(11)
C(31)-N(2)-C(3)-C(25)	60.70(14)
C(1)-N(2)-C(3)-C(2)	-6.43(13)
C(31)-N(2)-C(3)-C(2)	-175.01(10)
N(1)-C(2)-C(3)-N(2)	6.58(11)
C(19)-C(2)-C(3)-N(2)	130.03(10)
N(1)-C(2)-C(3)-C(25)	131.93(10)
C(19)-C(2)-C(3)-C(25)	-104.63(11)
C(1)-N(1)-C(4)-C(5)	80.92(15)
C(2)-N(1)-C(4)-C(5)	-111.69(13)
C(1)-N(1)-C(4)-C(9)	-96.27(14)
C(2)-N(1)-C(4)-C(9)	71.13(15)
C(9)-C(4)-C(5)-C(6)	1.41(19)
N(1)-C(4)-C(5)-C(6)	-175.75(11)
N(1)-C(4)-C(9)-C(8)	177.64(11)
C(3)-C(2)-C(19)-C(20)	-69.74(14)
N(2)-C(3)-C(25)-C(26)	78.63(15)
C(1)-N(2)-C(31)-C(32)	90.35(15)
C(3)-N(2)-C(31)-C(32)	-102.16(14)
C(1)-N(2)-C(31)-C(36)	-89.07(14)
C(3)-N(2)-C(31)-C(36)	78.41(15)

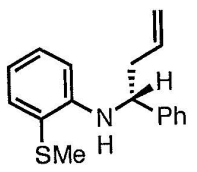
H
N
Ph
H
SMe

2.24

ppm
0
1
2
3
4
5
6
7
8
9
2.18
2.91
1.05
2.66
1.00
1.00
0.98
1.01
0.95
1.00

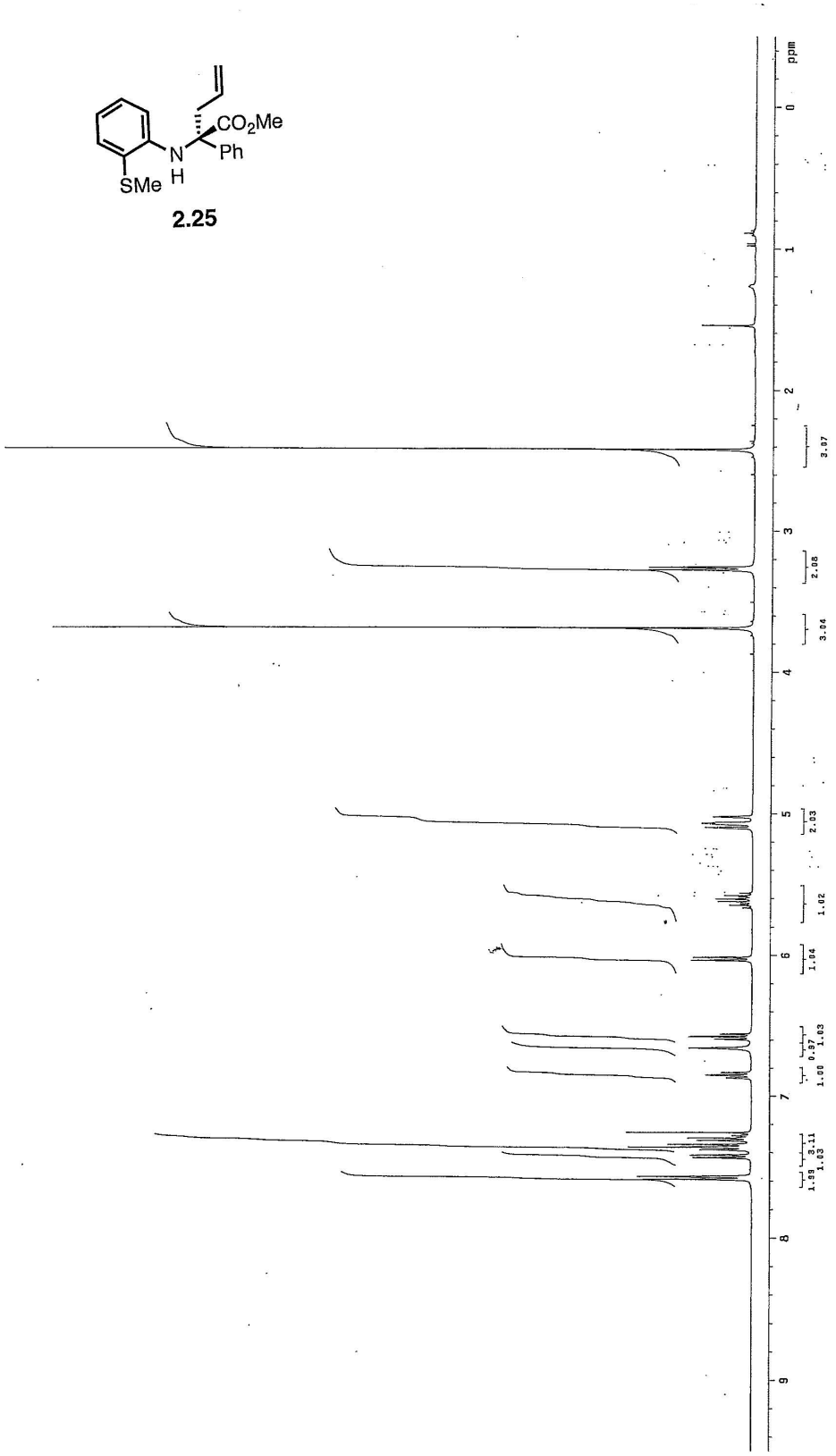
CO2Me
Ph
N
H
SMe
2.25
ppm
0
1
2
3
4
5
6
7
8
9
3.07
2.08
3.04
2.03
1.02
1.04
0.97
1.63
1.00
3.11
1.93
1.03

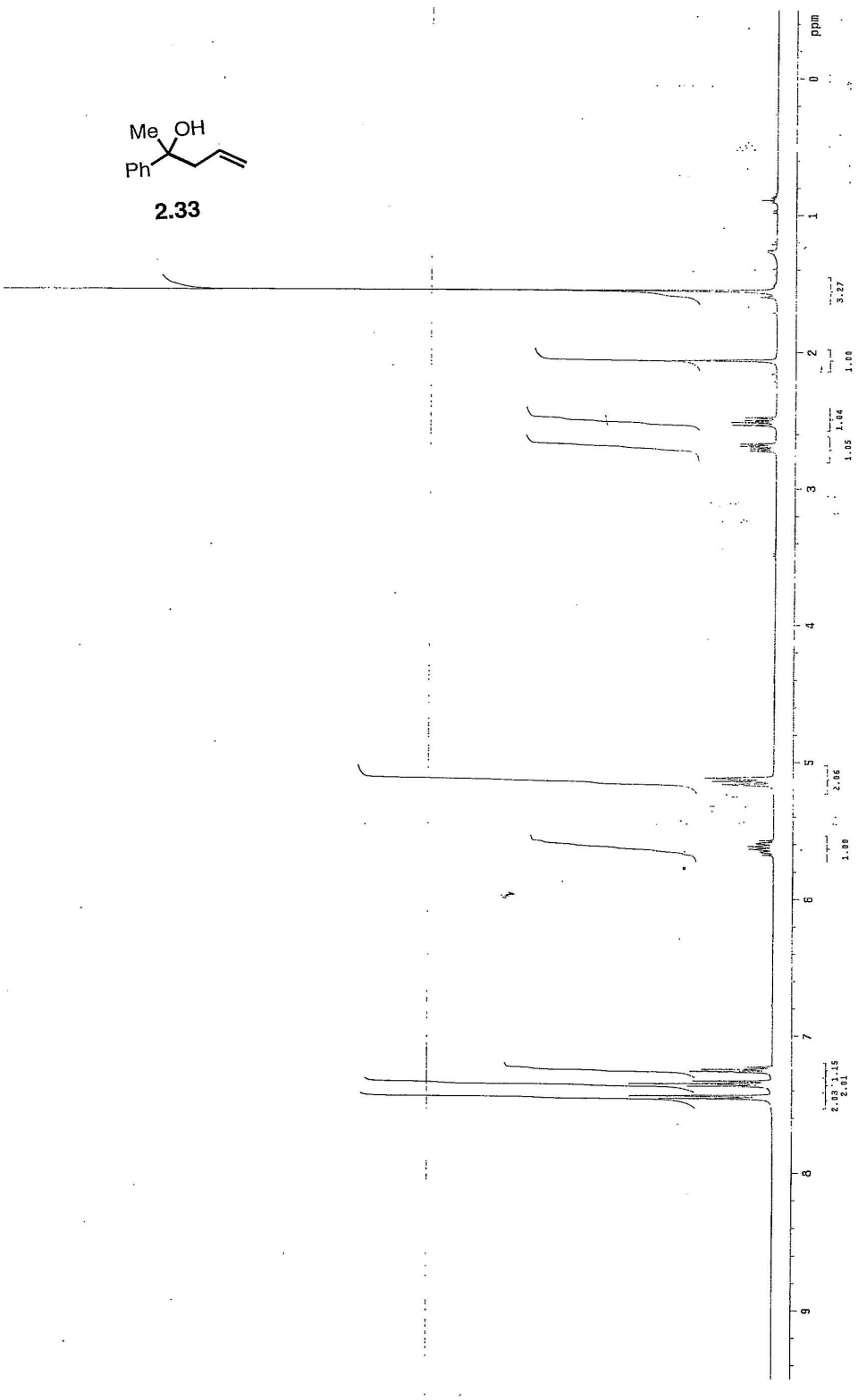
Me
OH
Ph
2.33
ppm
0
1
2
3
4
5
6
7
8
9
3.27
1.00
1.64
1.05
2.06
1.00
2.03
1.15
2.01

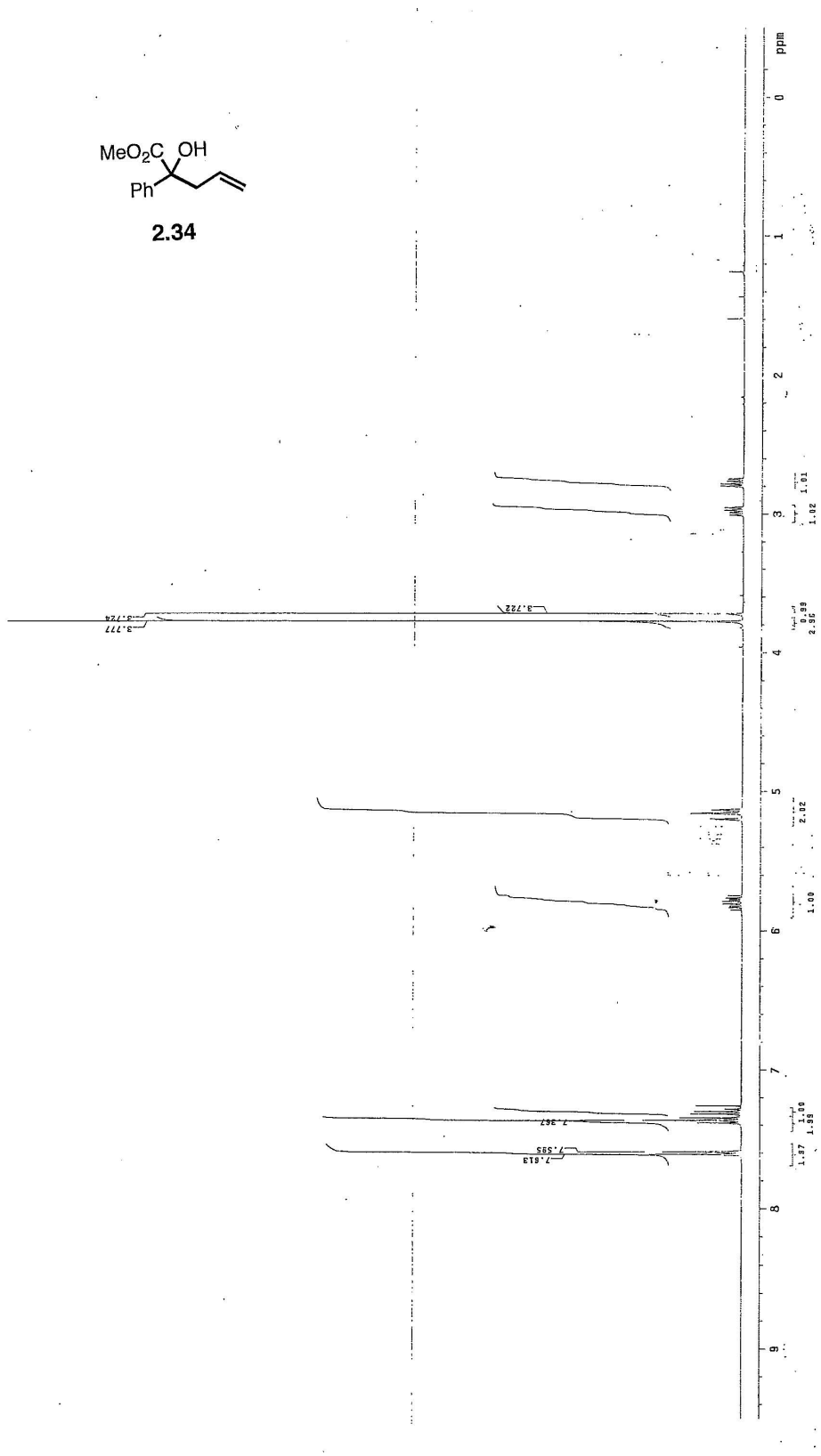
MeO2C
OH
Ph
2.34
ppm
3.722
3.777
3.724
7.367
7.595
7.613

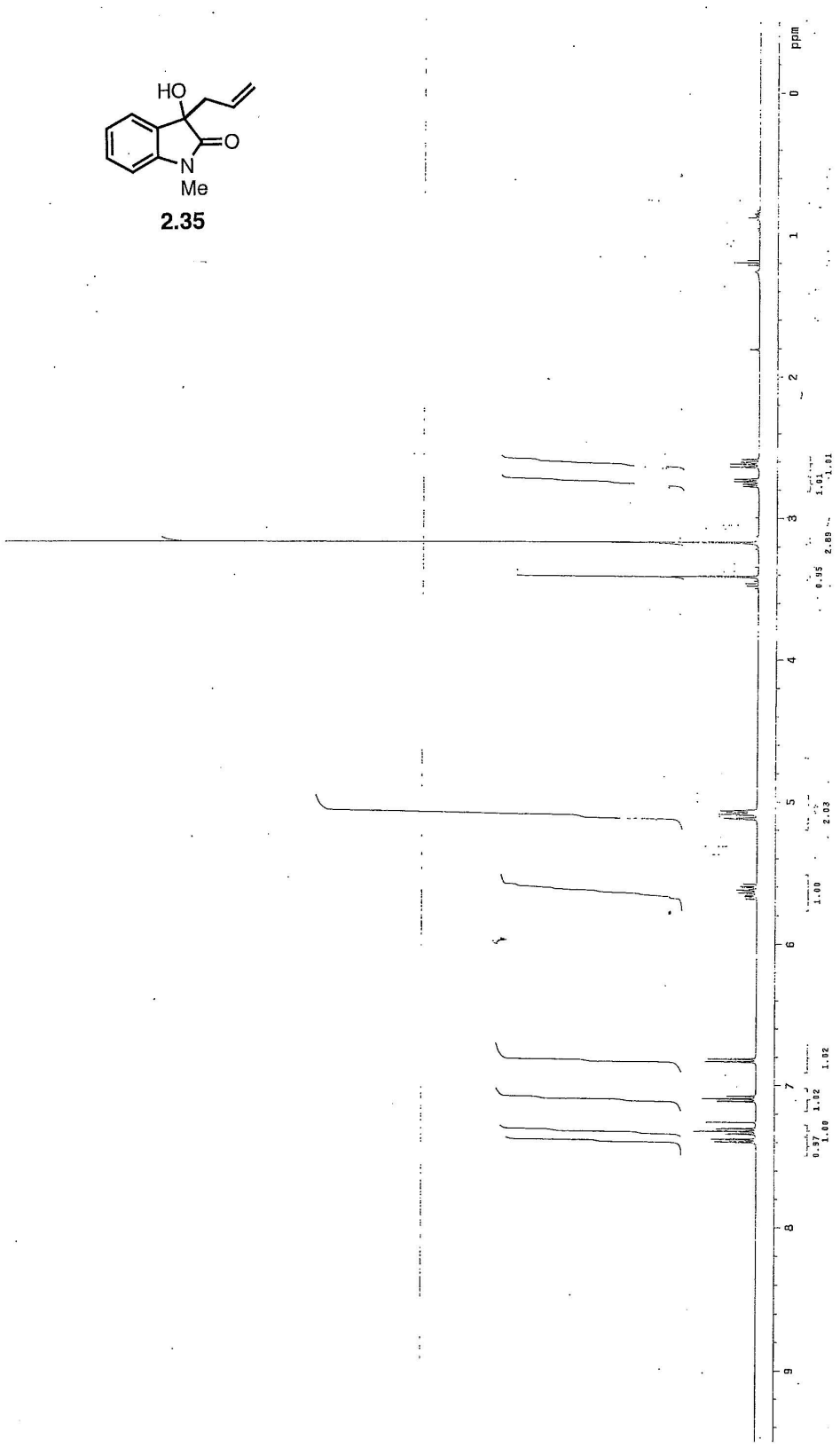
HO
O
N
Me
2.35
ppm
0
1
2
3
4
5
6
7
8
9
1.61
1.01
2.89
0.95
2.03
1.00
1.02
1.02
0.97
1.00

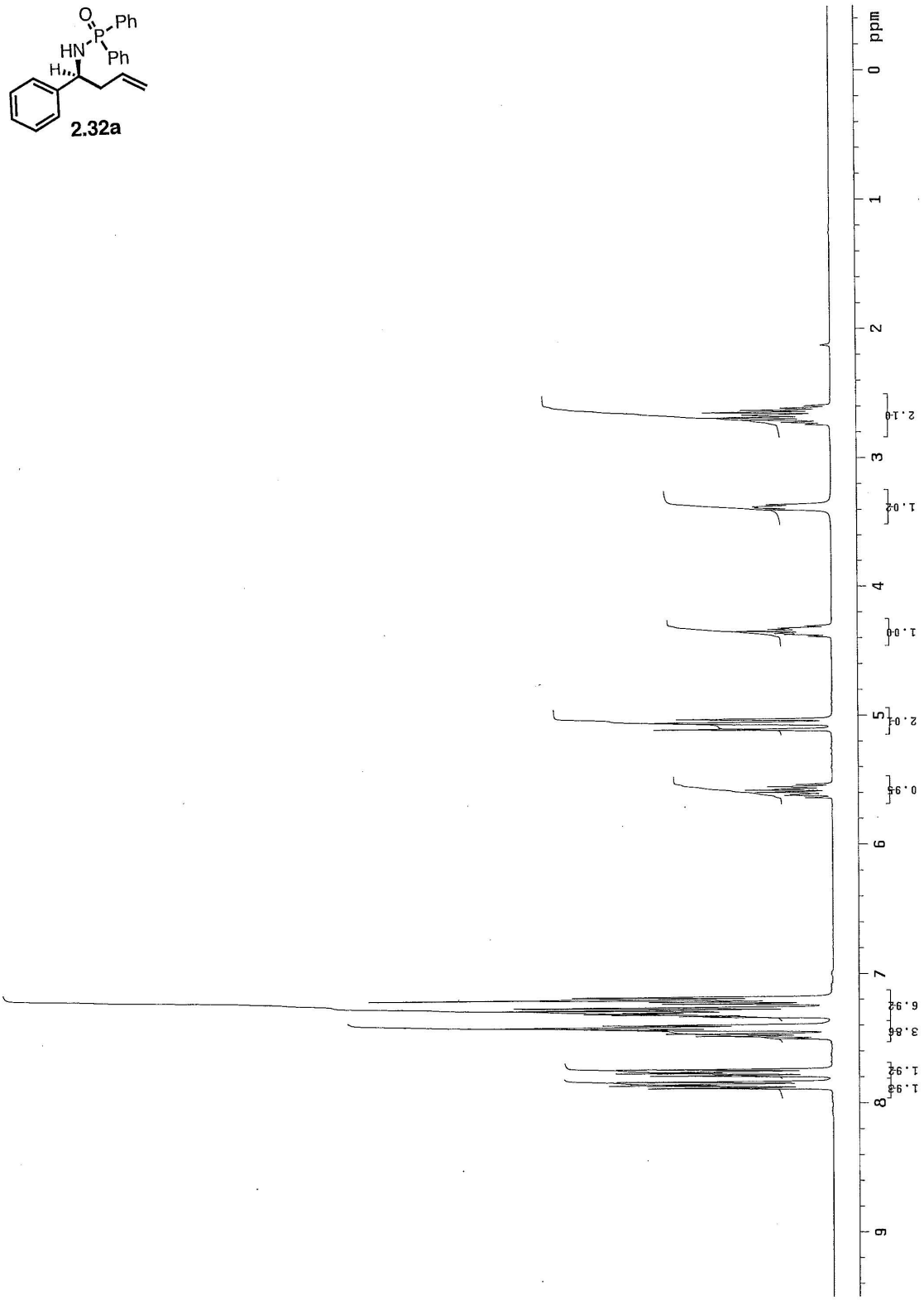
O
P
Ph
HN
Ph
H
2.32a
ppm
0
1
2
3
4
5
6
7
8
9
2.10
1.02
1.00
2.01
0.95
6.92
3.86
1.92
1.93

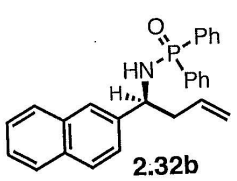
O
Ph
HN
P
Ph
H

2.32b

ppm
0
1
2
3
4
5
6
7
8
9
2.02
1.02
1.04
1.99
0.96
2.24
5.76
1.01
4.86
1.85

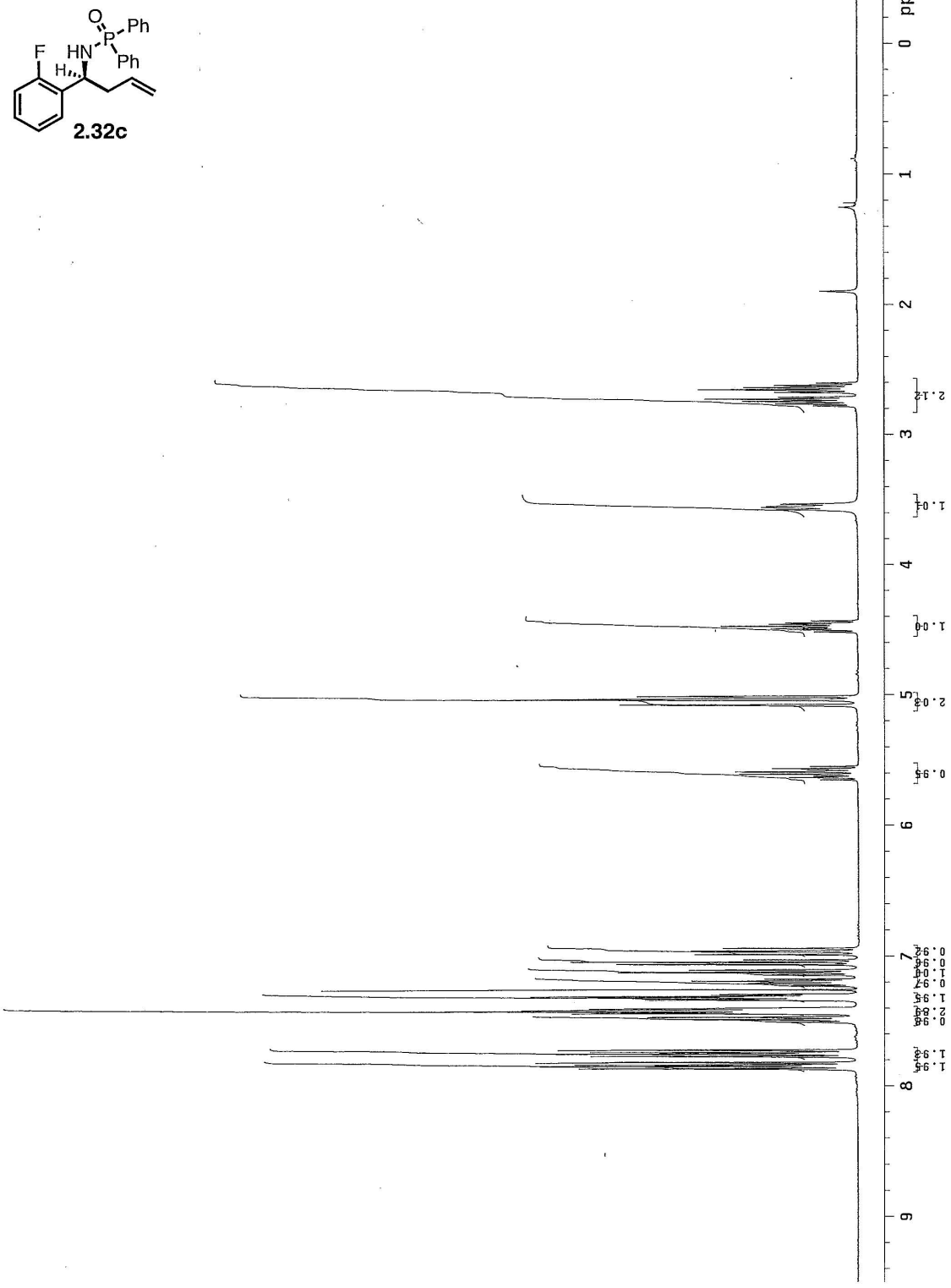
O
Ph
P
F
HN
Ph
H
2.32c
ppm
0
1
2
3
4
5
6
7
8
9
2.12
1.01
1.00
2.03
0.95
0.97
0.97
1.01
0.97
1.94
2.03
0.95
1.94

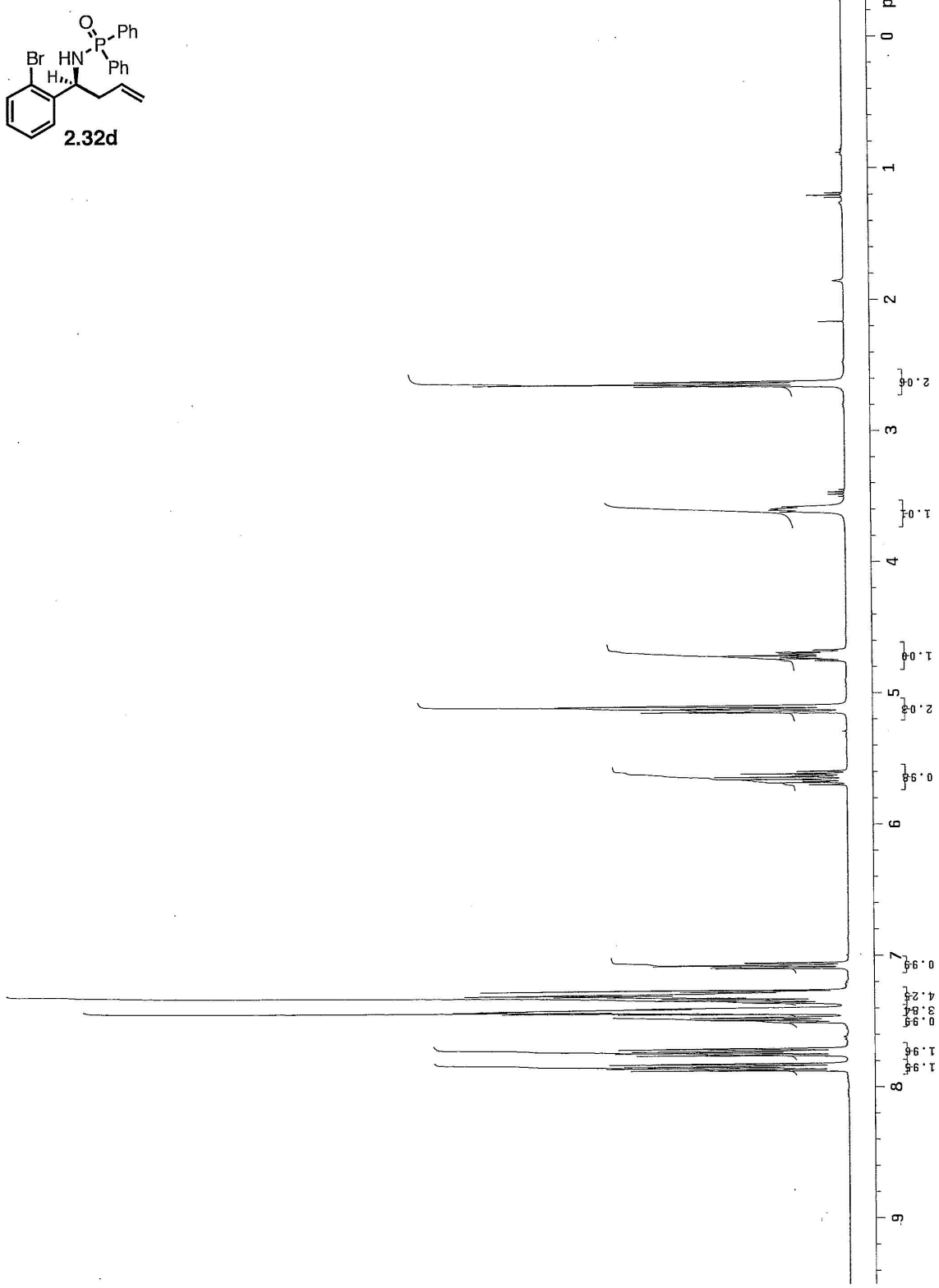
O
Ph
P
Br
HN
H
Ph
2.32d
ppm
0
1
2
3
4
5
6
7
8
9
2.06
1.01
1.00
2.05
0.98
0.99
3.84
4.25
1.96
1.95

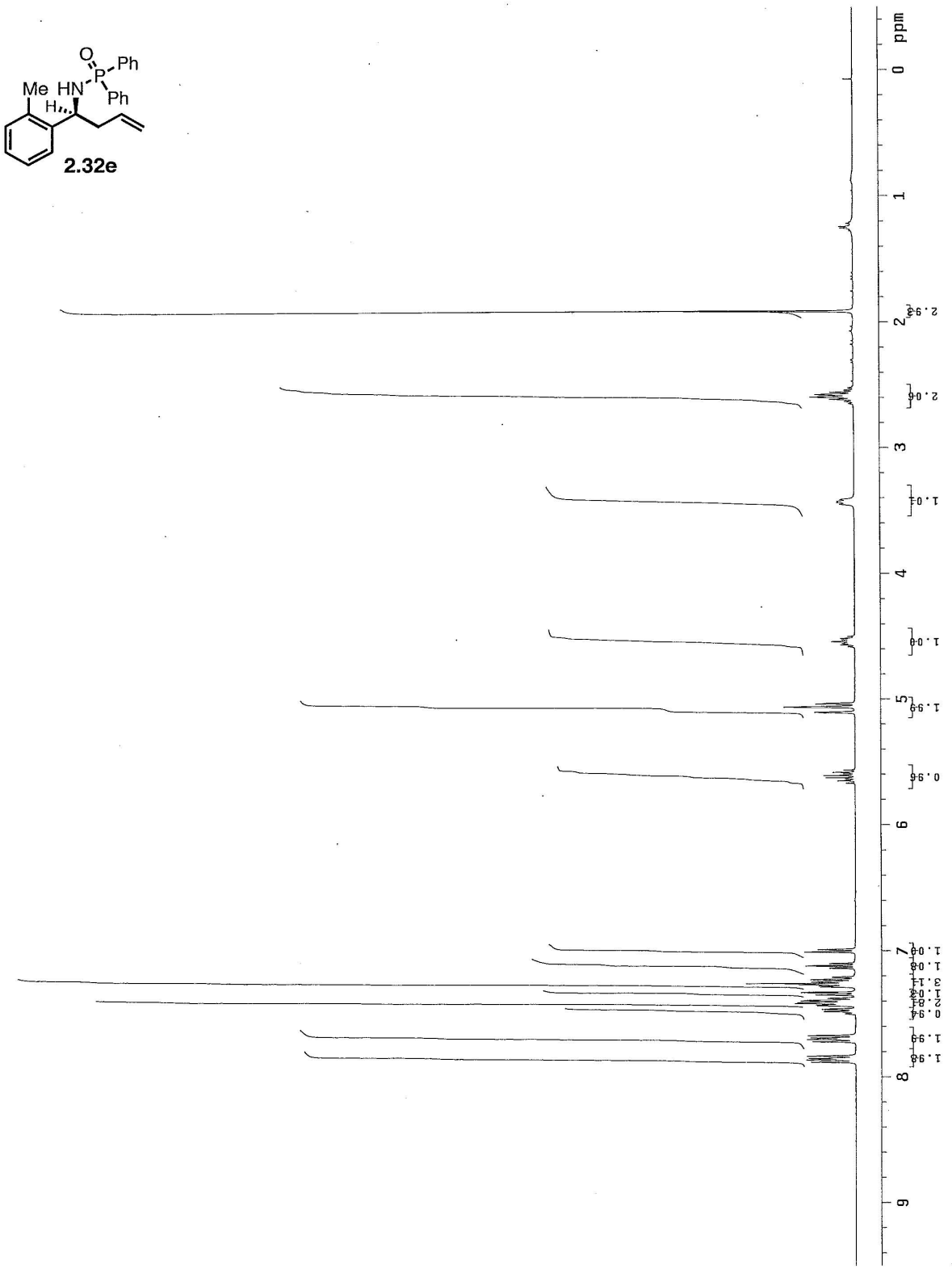
O
Ph
P
Me HN
H
Ph
2.32e
ppm
0
1
2
3
4
5
6
7
8
9

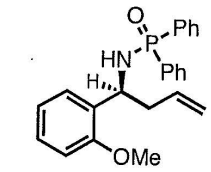
O
Ph
HN
P
Ph
H
OMe

2.32f

ppm
0
1
2
3
4
5
6
7
8
9
2.08
3.04
1.04
1.04
2.04
0.94
1.96
1.04
1.02
1.94
3.84
3.78

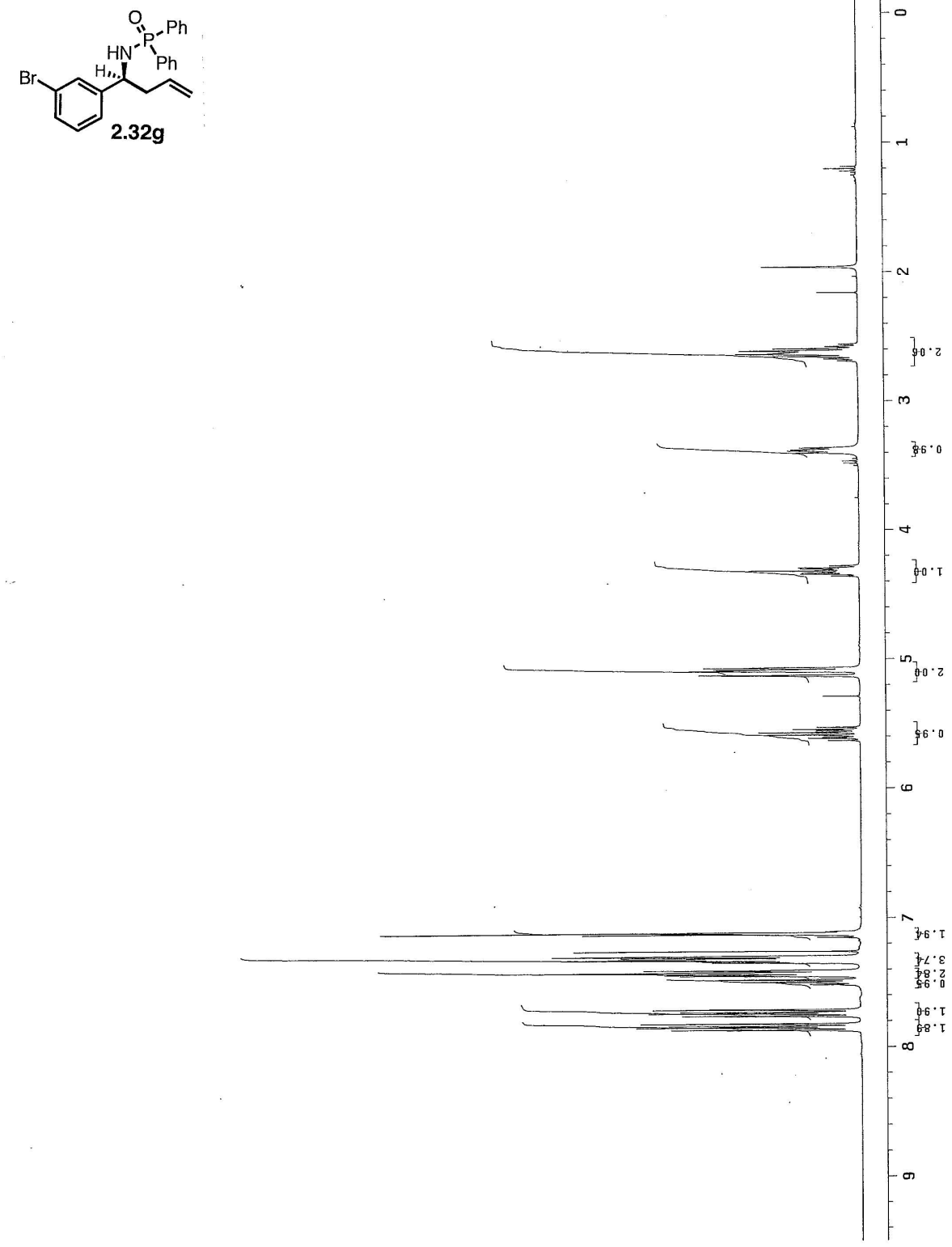
O
Ph
HN
P
Ph
H
Br
2.32g
ppm
0
1
2
3
4
5
6
7
8
9
2.00
0.98
1.00
2.00
0.95
1.94
3.74
2.84
0.95
1.90
1.89

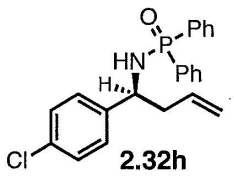
O
Ph
HN
P
Ph
H
Cl

2.32h

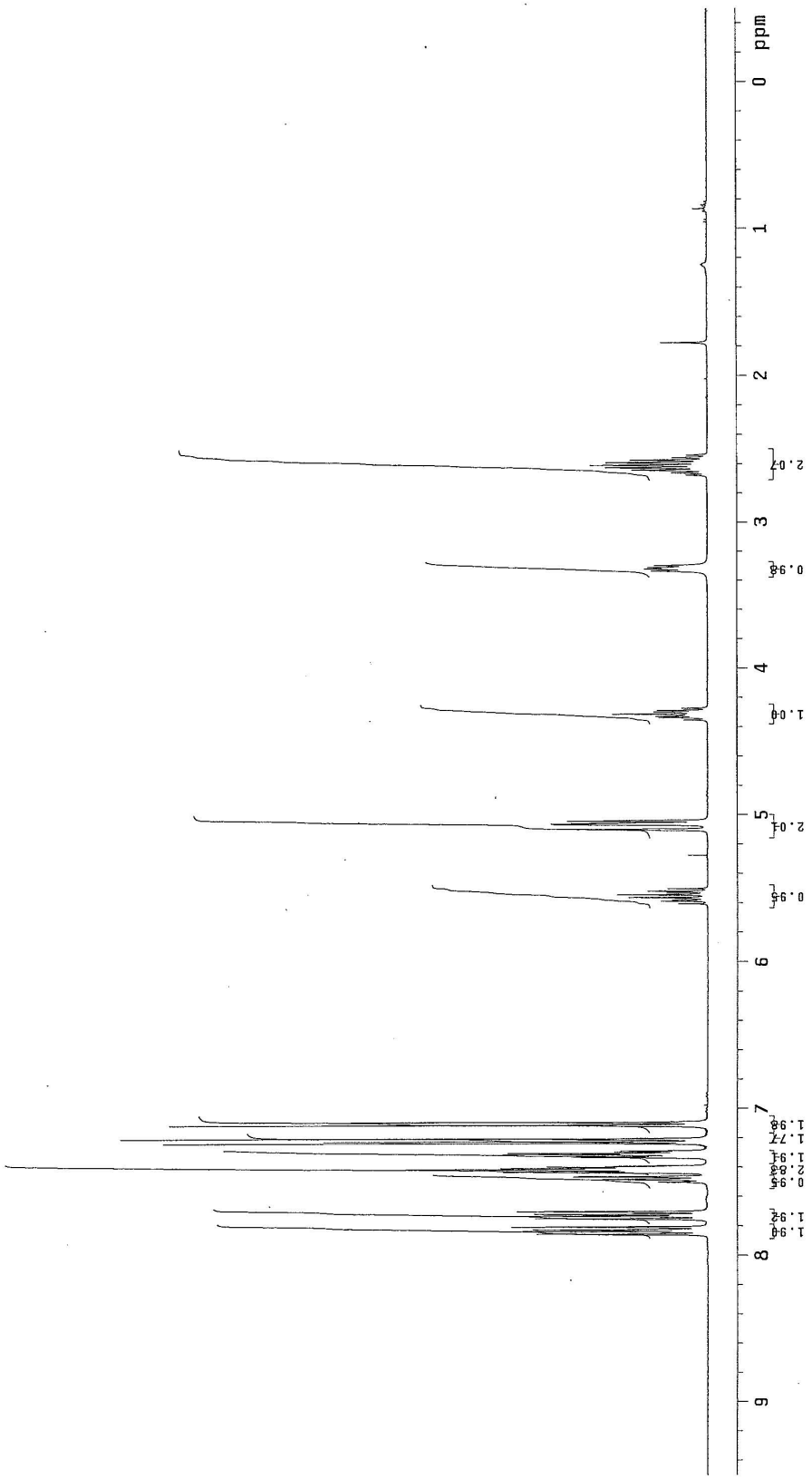
ppm
0
1
2
3
4
5
6
7
8
9
2.07
0.98
1.04
2.01
0.95
1.98
1.77
1.91
2.83
0.95
1.92
1.96

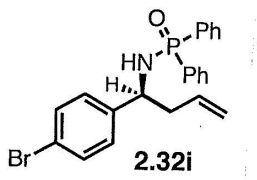
O
Ph
HN
P
Ph
H
Br

2.32i

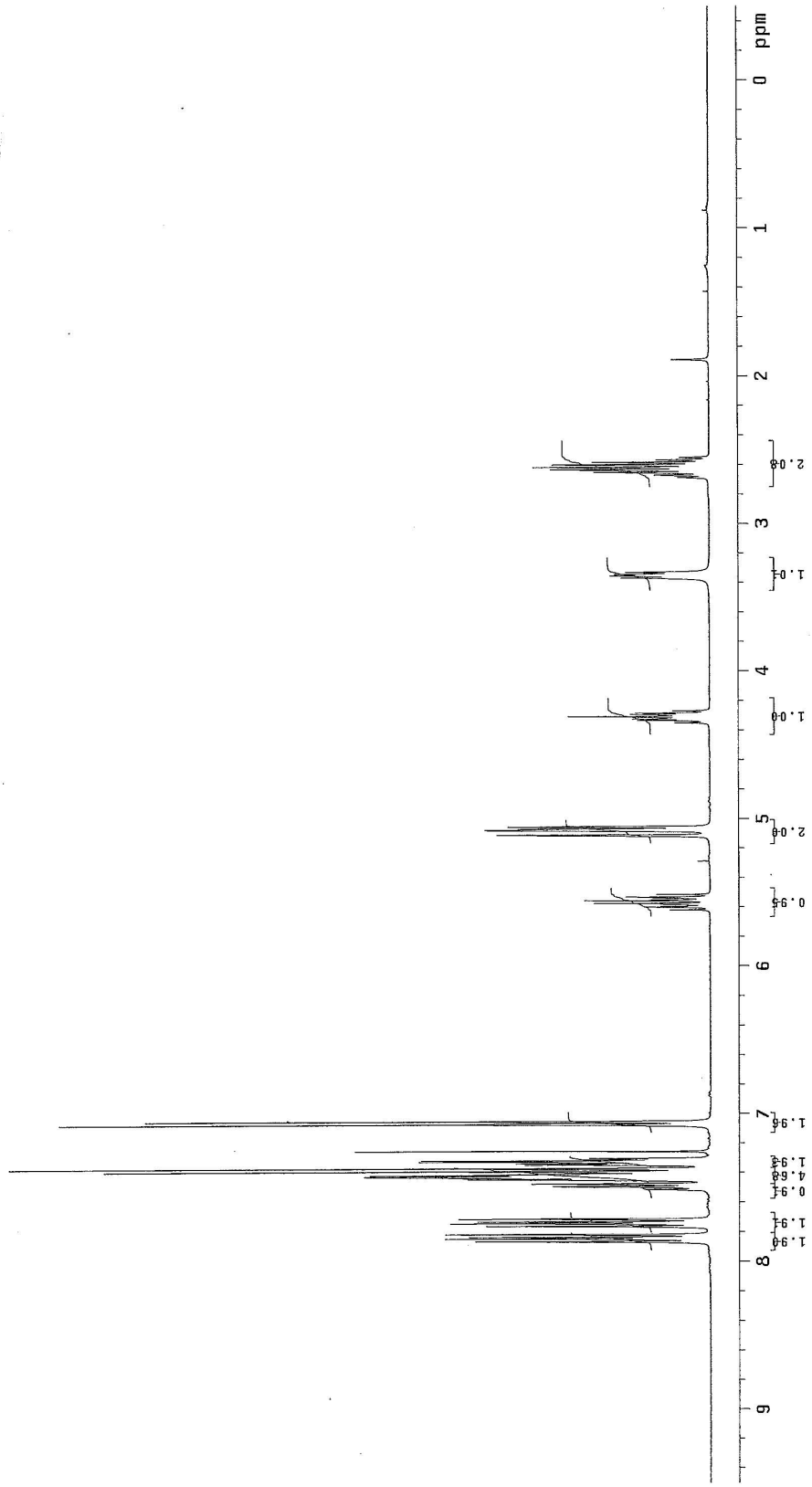
ppm
0
1
2
3
4
5
6
7
8
9
2.00
1.01
1.00
2.00
0.95
1.96
1.94
4.68
0.91
1.91
1.90

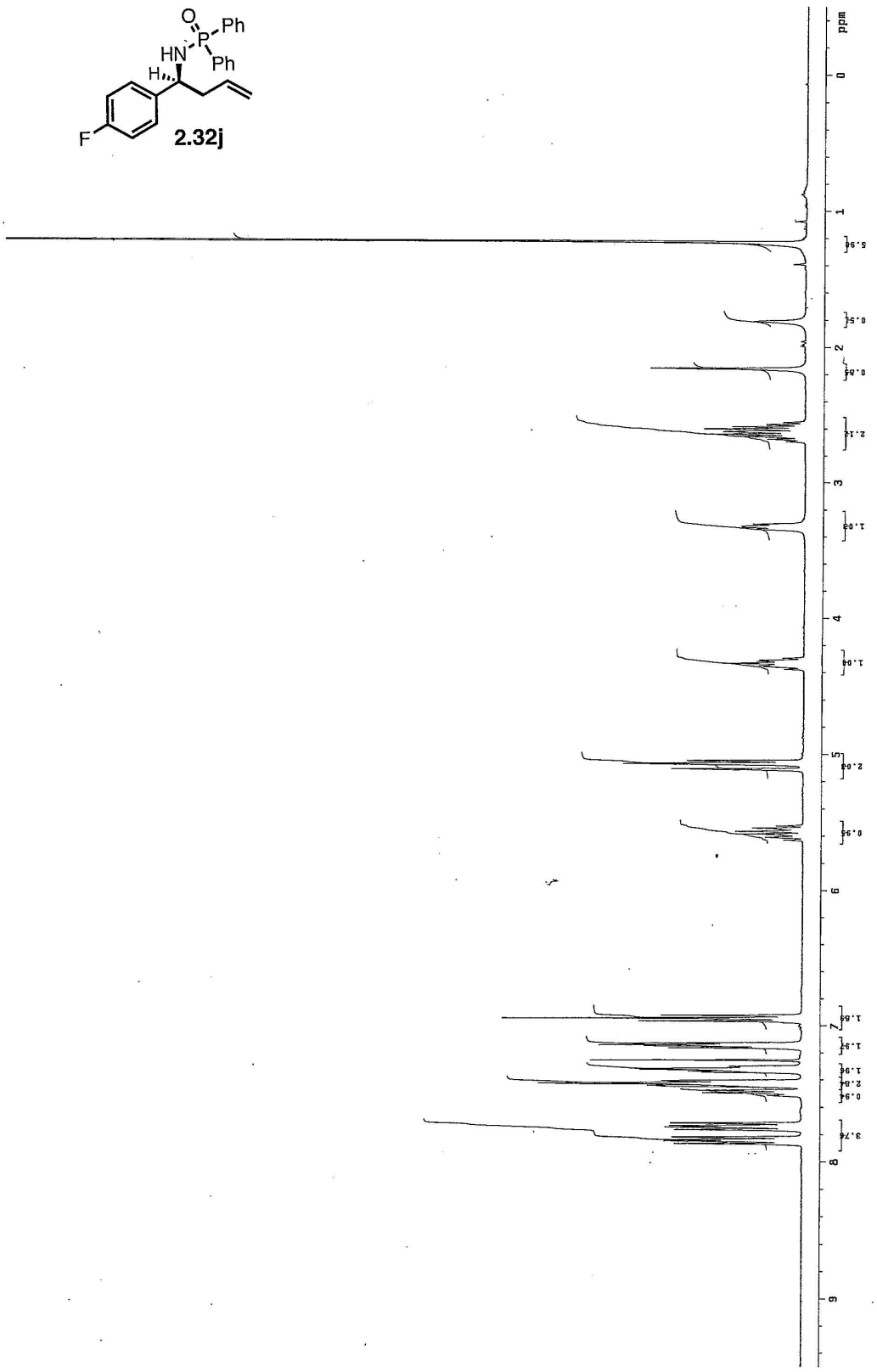
O
Ph
HN
P
Ph
H
F
2.32j
ppm
0
1
2
3
4
5
6
7
8
9
5.94
0.54
0.84
2.12
1.08
1.00
2.03
0.95
1.69
1.37
1.96
2.04
0.94
3.76

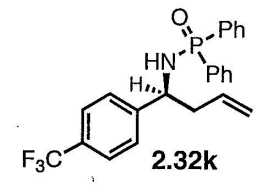
O
Ph
HN
P
Ph
H
F3C

2.32k

ppm
0
1
2
3
4
5
6
7
8
9
2.06
1.00
1.00
2.01
0.95
3.84
2.88
2.79
1.94
1.89

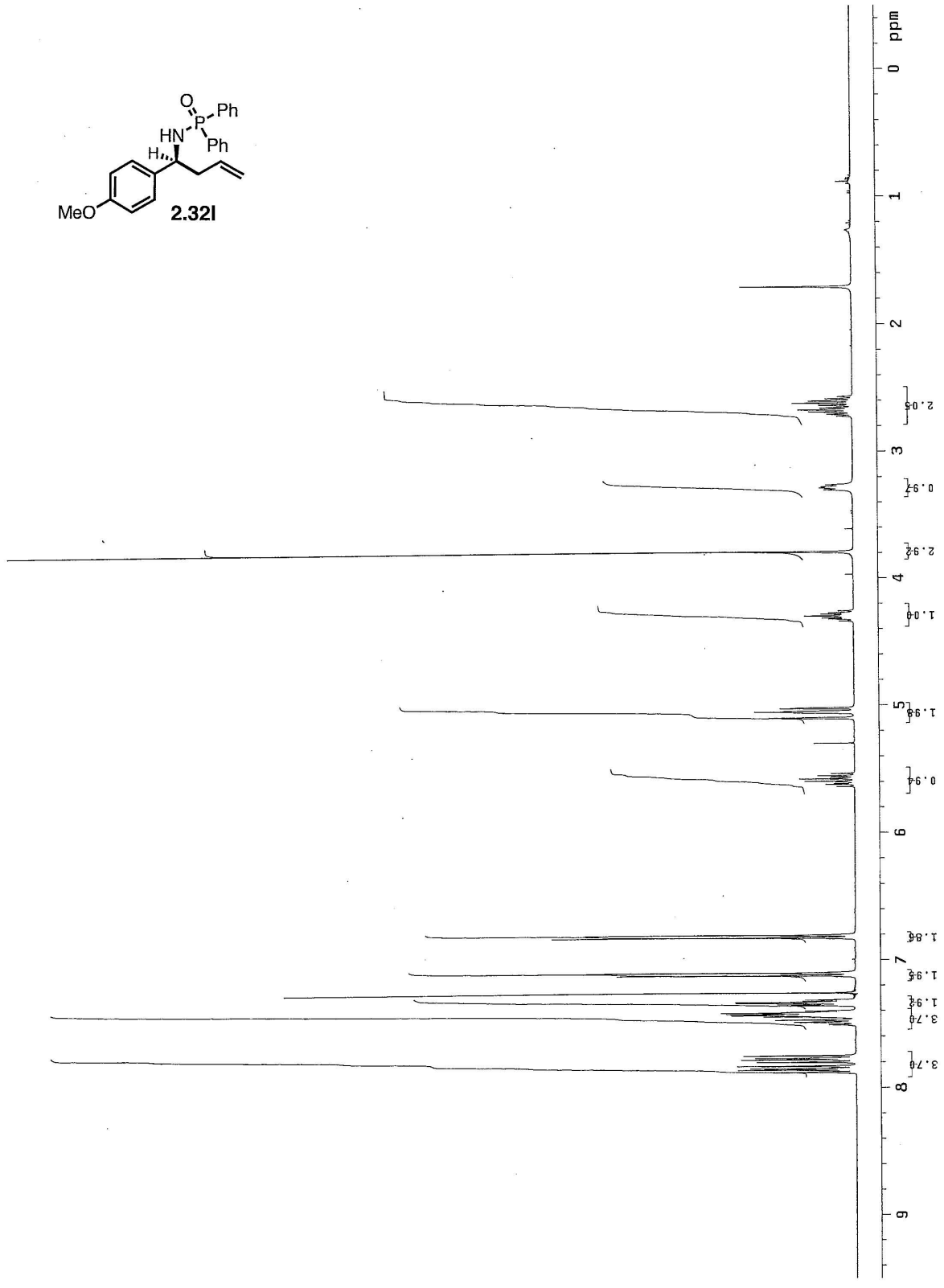
O
Ph
HN
P
Ph
H
MeO
2.32l
ppm
0
1
2
3
4
5
6
7
8
9
2.05
0.97
2.92
1.00
1.98
0.94
1.86
1.95
1.92
3.70
3.70

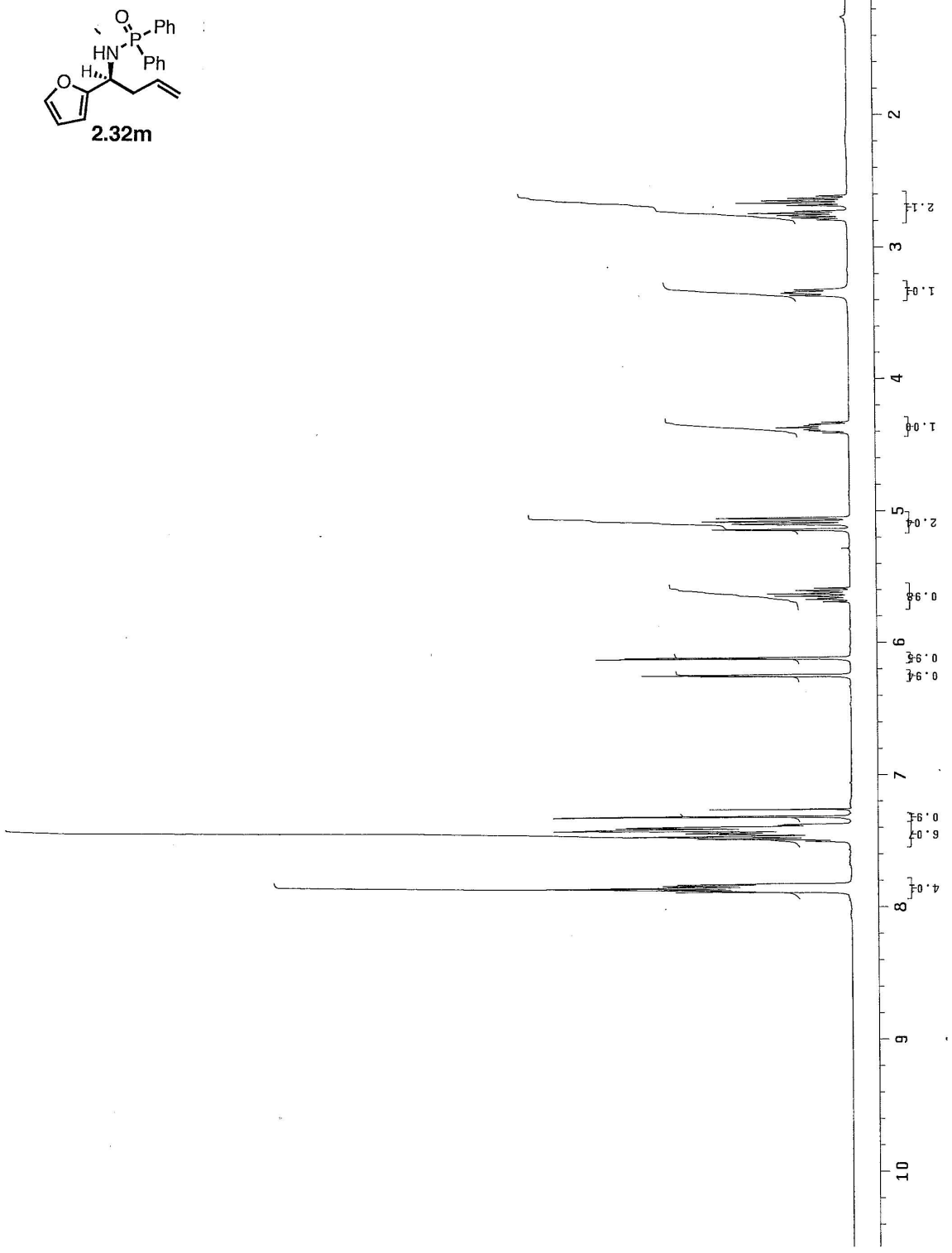
O
Ph
HN
P
Ph
H
O
2.32m
1 ppm
2
3
4
5
6
7
8
9
10
2.14
1.04
1.00
2.04
0.98
0.94
0.94
6.04
4.04

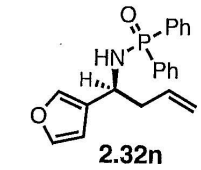
O
Ph
HN
P
Ph
H
O

2.32n

ppm
0
1
2
3
4
5
6
7
8
9
2.17
1.02
1.00
2.10
0.98
0.94
0.91
0.90
6.02
3.97

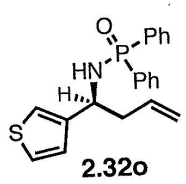
O
Ph
P
HN
Ph
H
S

2.32o

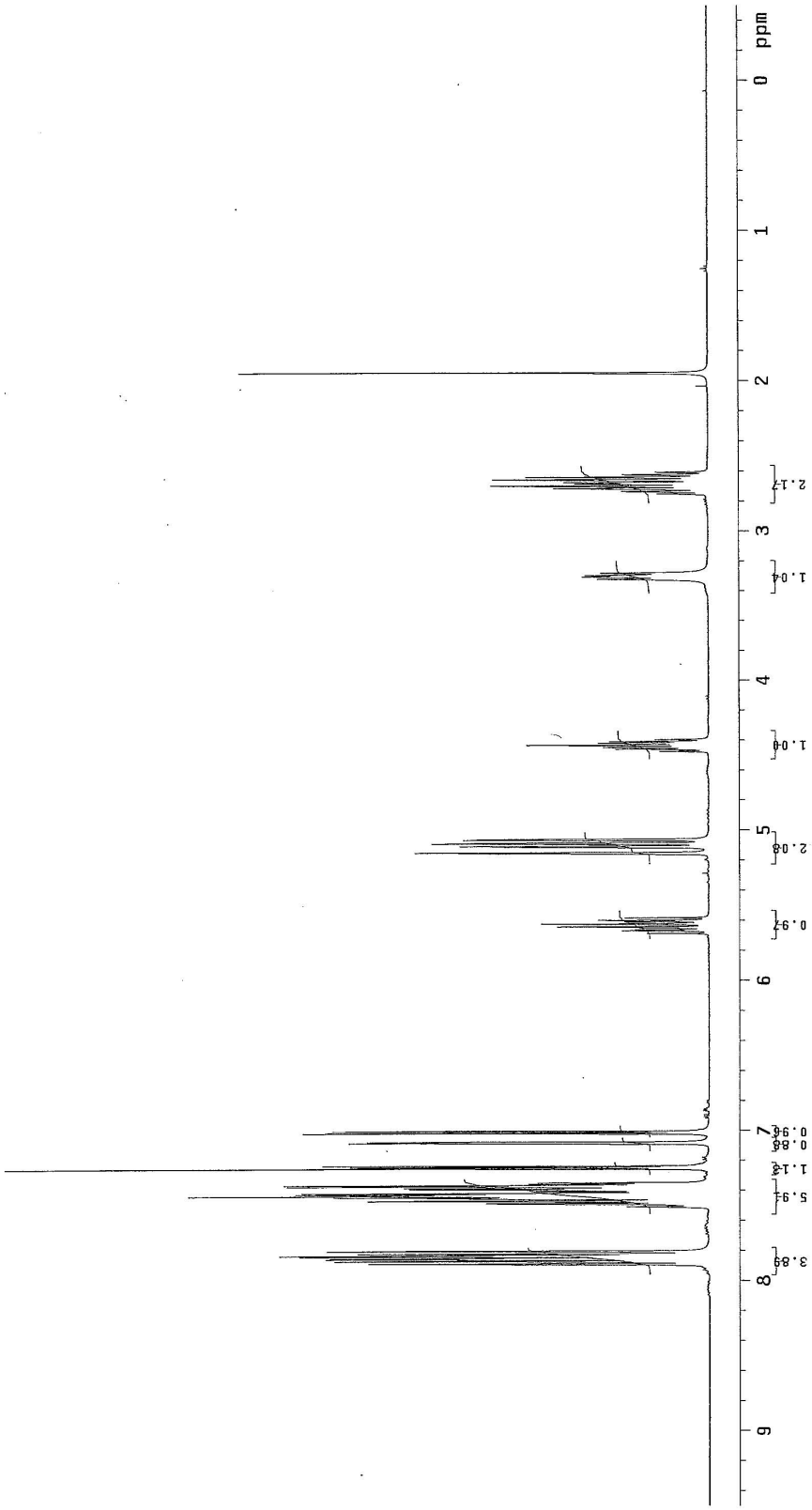
ppm
0
1
2
3
4
5
6
7
8
9
2.17
1.04
1.00
2.08
0.97
0.96
0.88
1.12
5.91
3.89

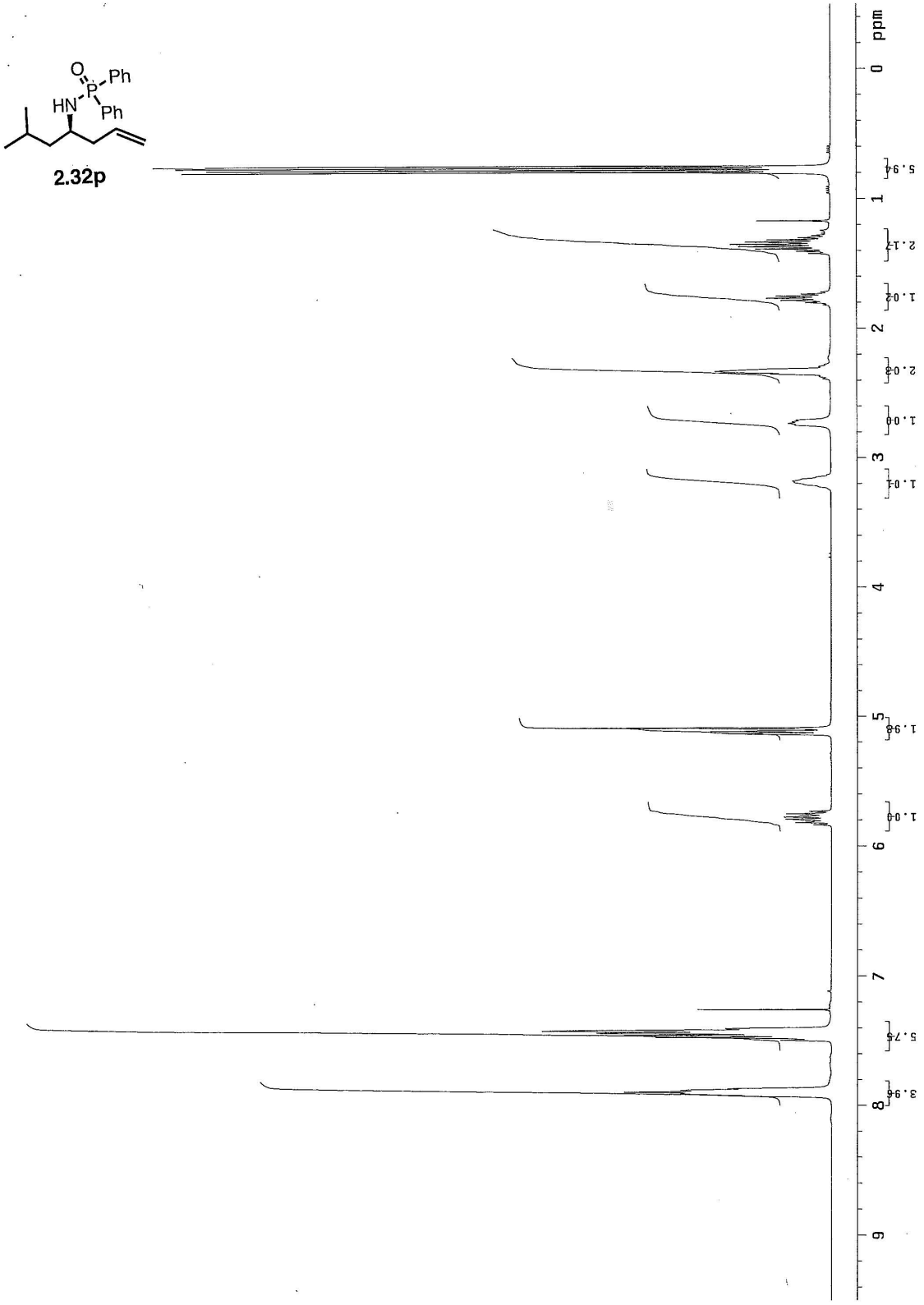
O
Ph
P
HN
Ph
2.32p
ppm
0
1
2
3
4
5
6
7
8
9
5.94
2.17
1.02
2.03
1.00
1.01
1.96
1.00
5.75
3.96

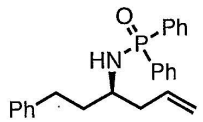
O
Ph
HN
P
Ph
Ph

2.32q

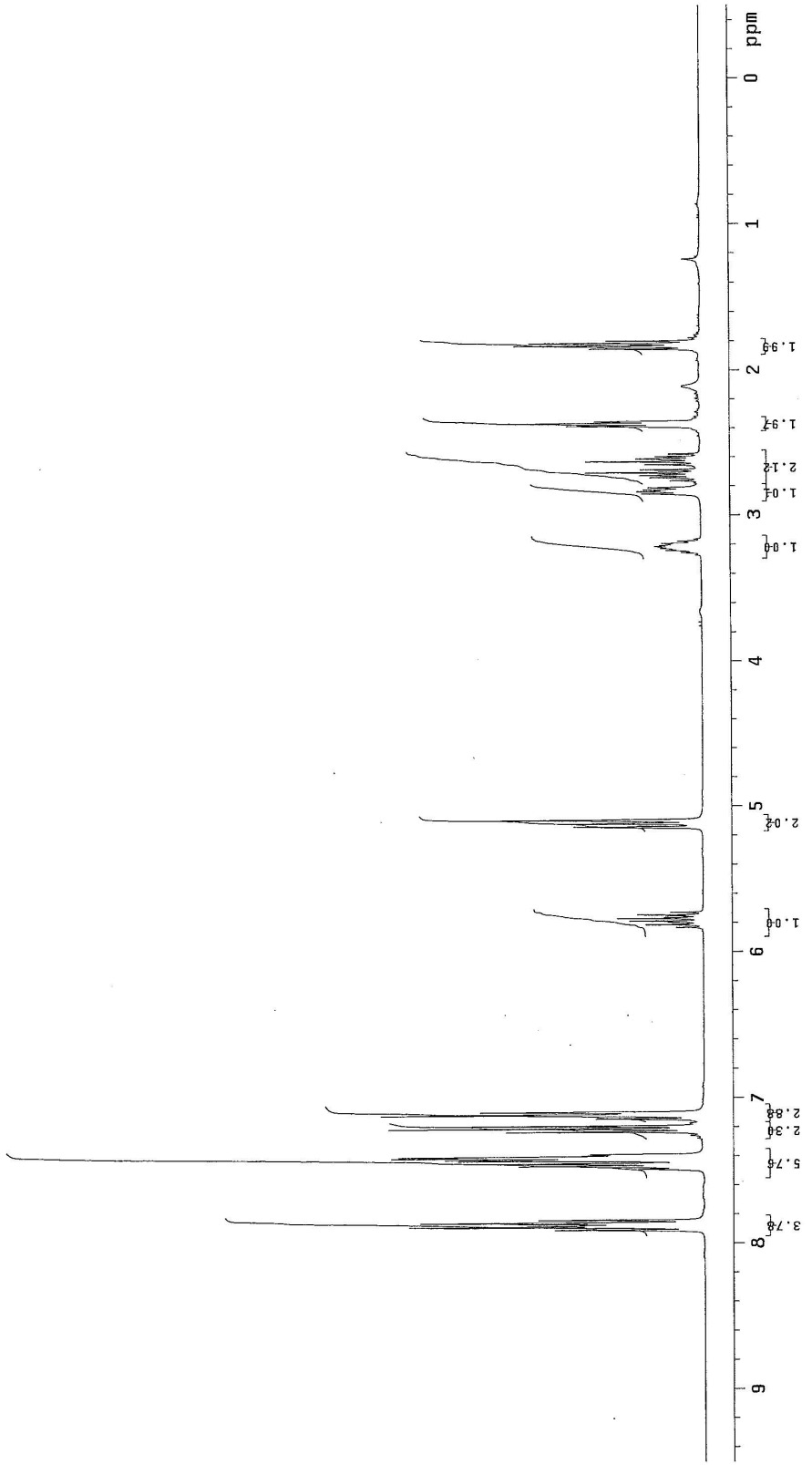
ppm
0
1
2
3
4
5
6
7
8
9
1.99
1.97
2.12
1.04
1.00
2.04
1.00
2.88
2.34
5.76
3.74

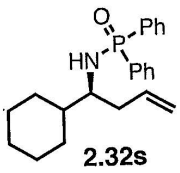
O
Ph
HN
P
Ph

2.32s

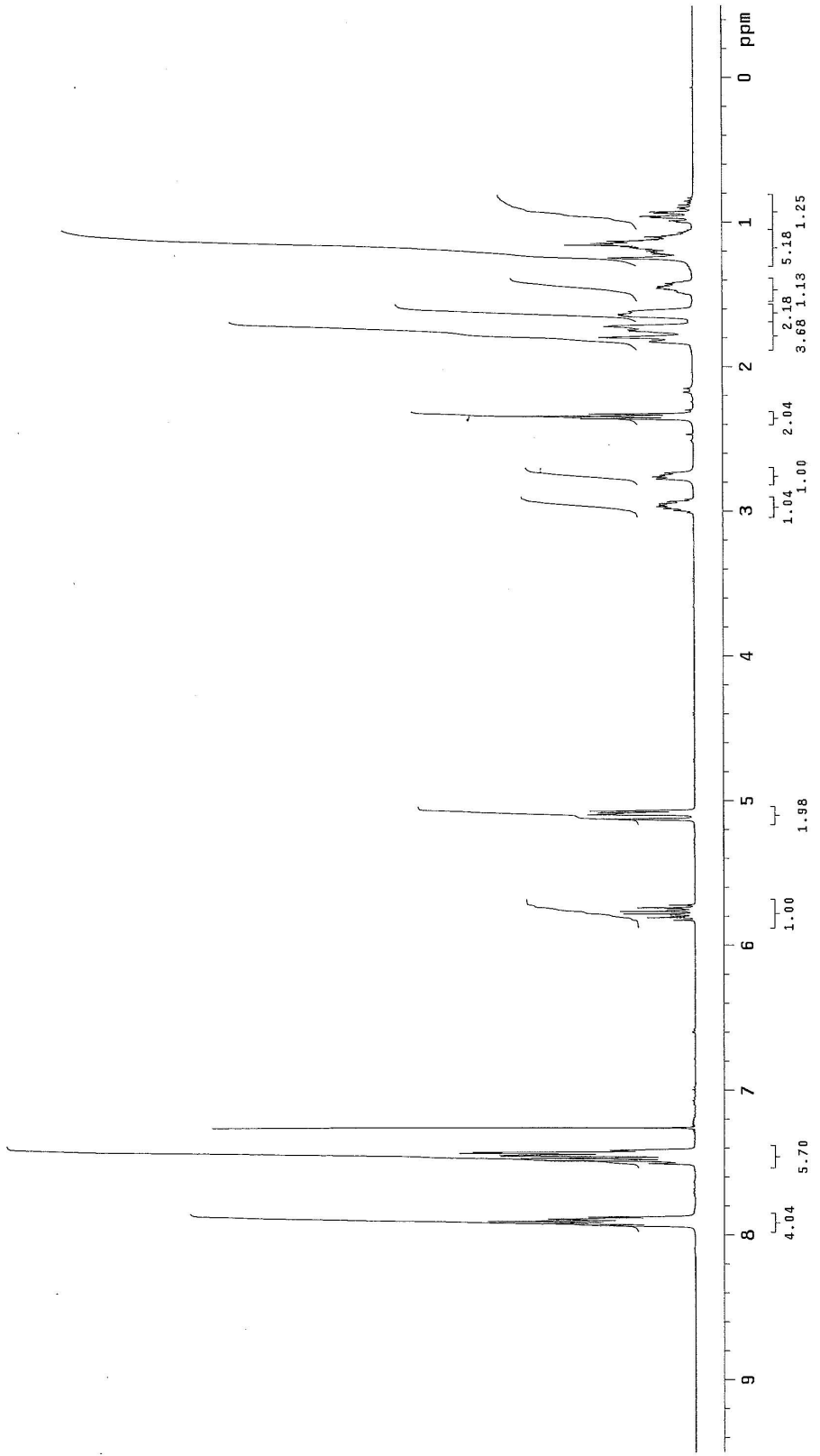
ppm
0
1
2
3
4
5
6
7
8
9
5.18
1.25
2.18
1.13
3.68
2.04
1.04
1.00
1.98
1.00
4.04
5.70

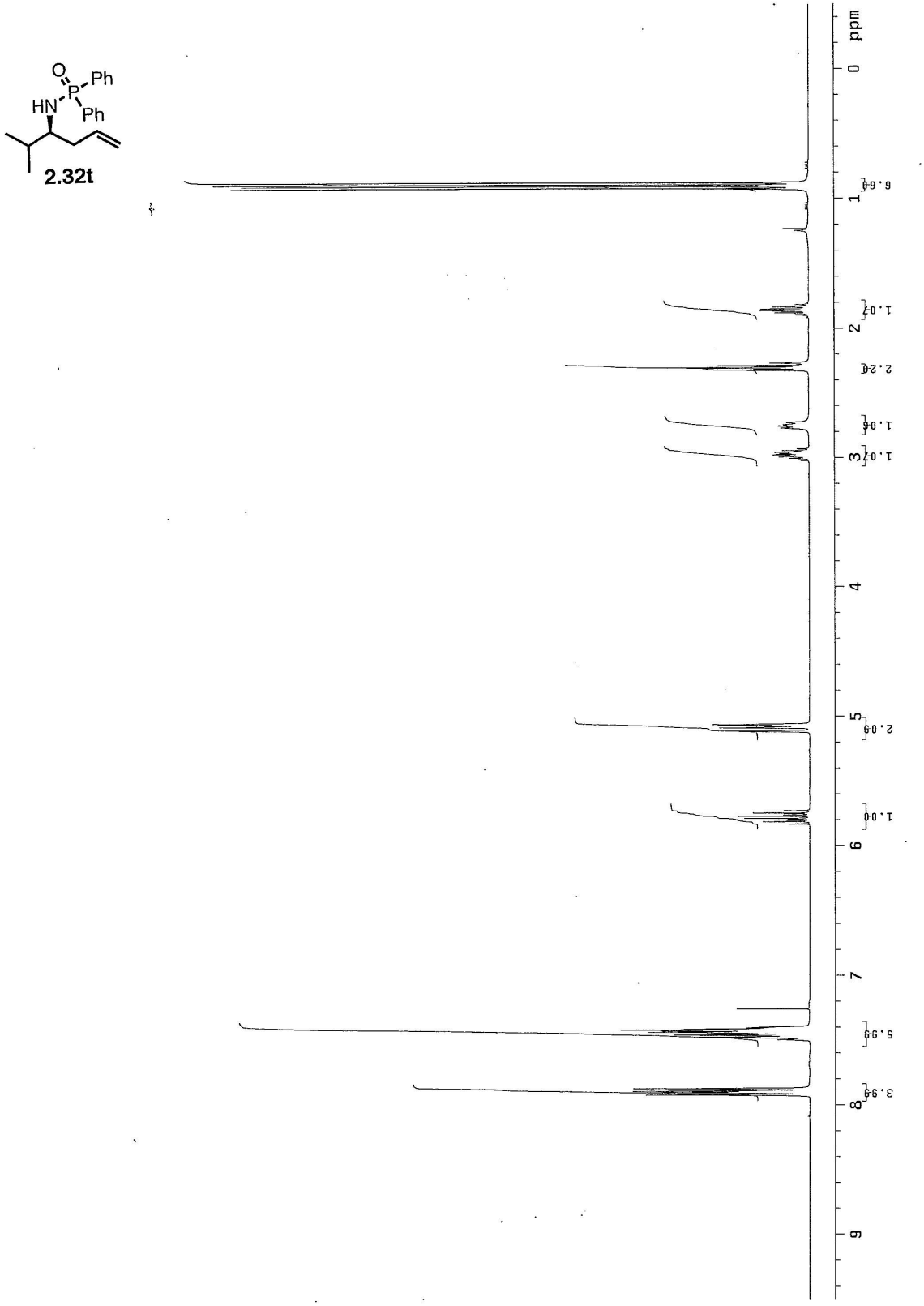
O
Ph
HN
P
Ph
2.32t
ppm
0
1
2
3
4
5
6
7
8
9
6.66
1.07
2.24
1.04
1.02
2.04
1.00
5.99
3.94

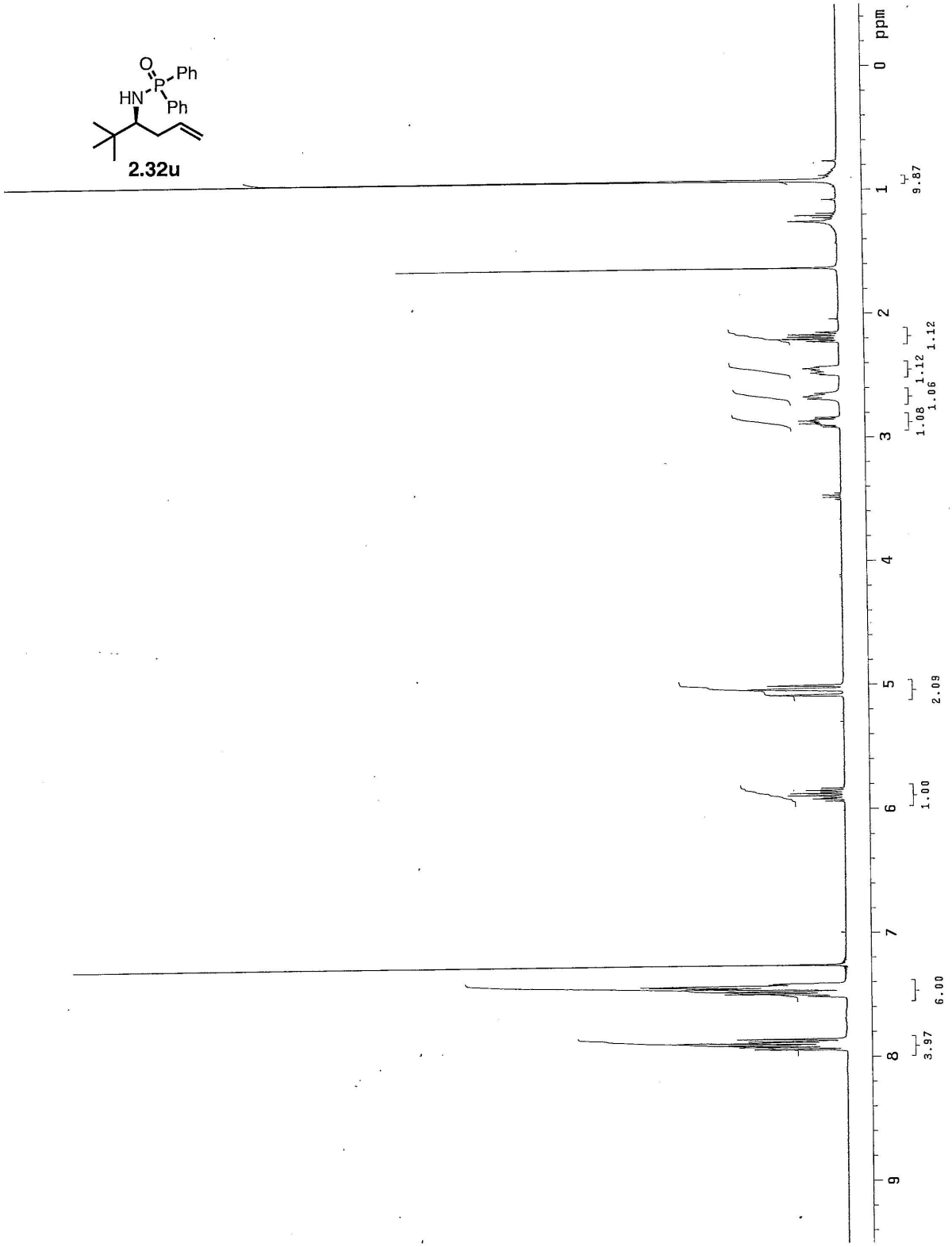
O
Ph
HN
P
Ph
2.32u
ppm
0
1
2
3
4
5
6
7
8
9
9.87
1.08
1.12
1.06
1.12
2.09
1.00
6.00
3.97

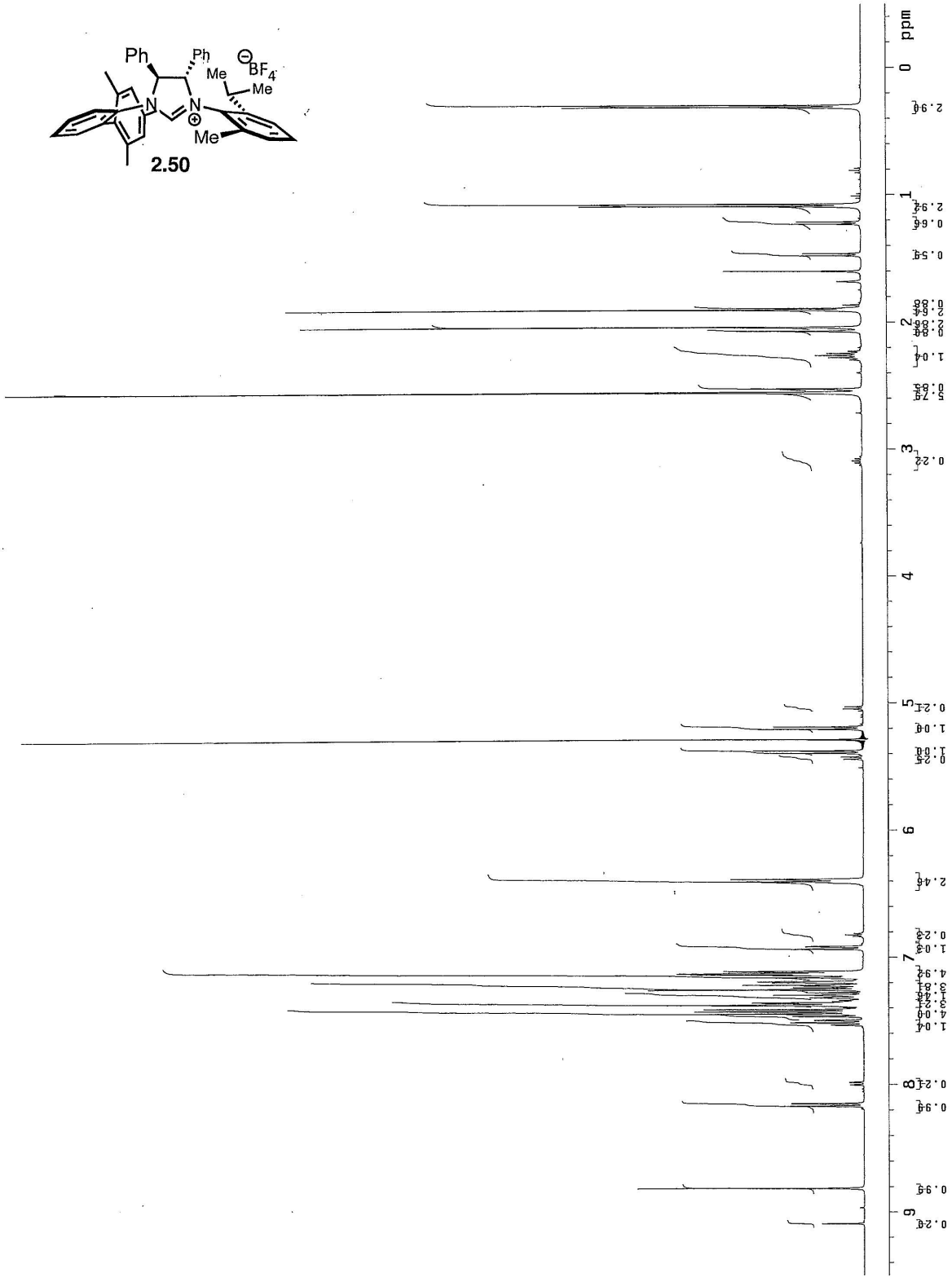
Ph
Ph
Me
$\ominus BF_4$
Me
N
N
Me
2.50
ppm
0
1
2
3
4
5
6
7
8
9
2.94
2.94
0.64
0.54
0.80
2.64
2.86
0.88
1.04
5.29
0.63
0.22
0.21
1.04
1.00
0.25
2.46
0.24
1.03
4.92
3.13
4.04
1.04
0.21
0.94
0.94
0.24

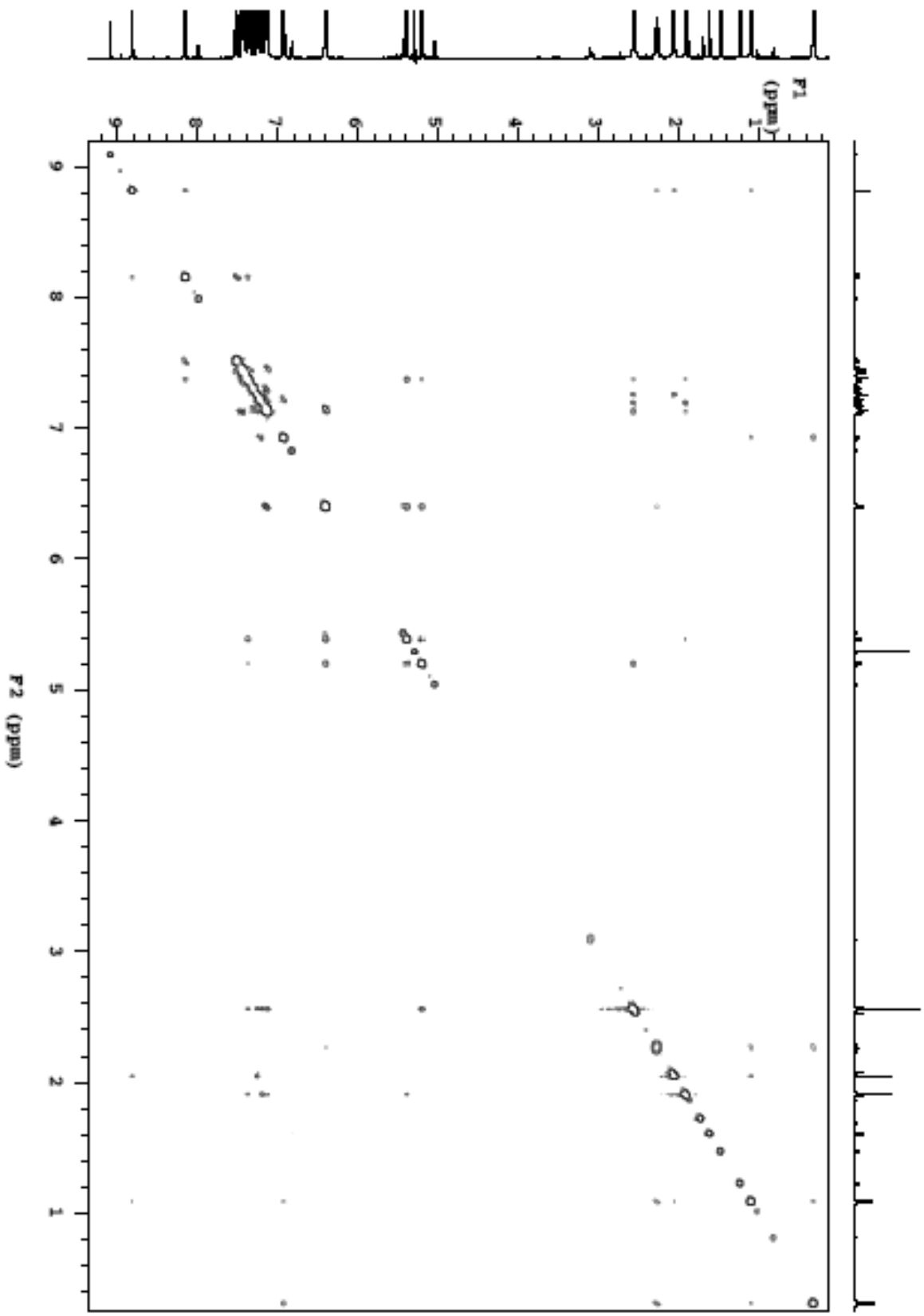
F1 (ppm)
F2 (ppm)

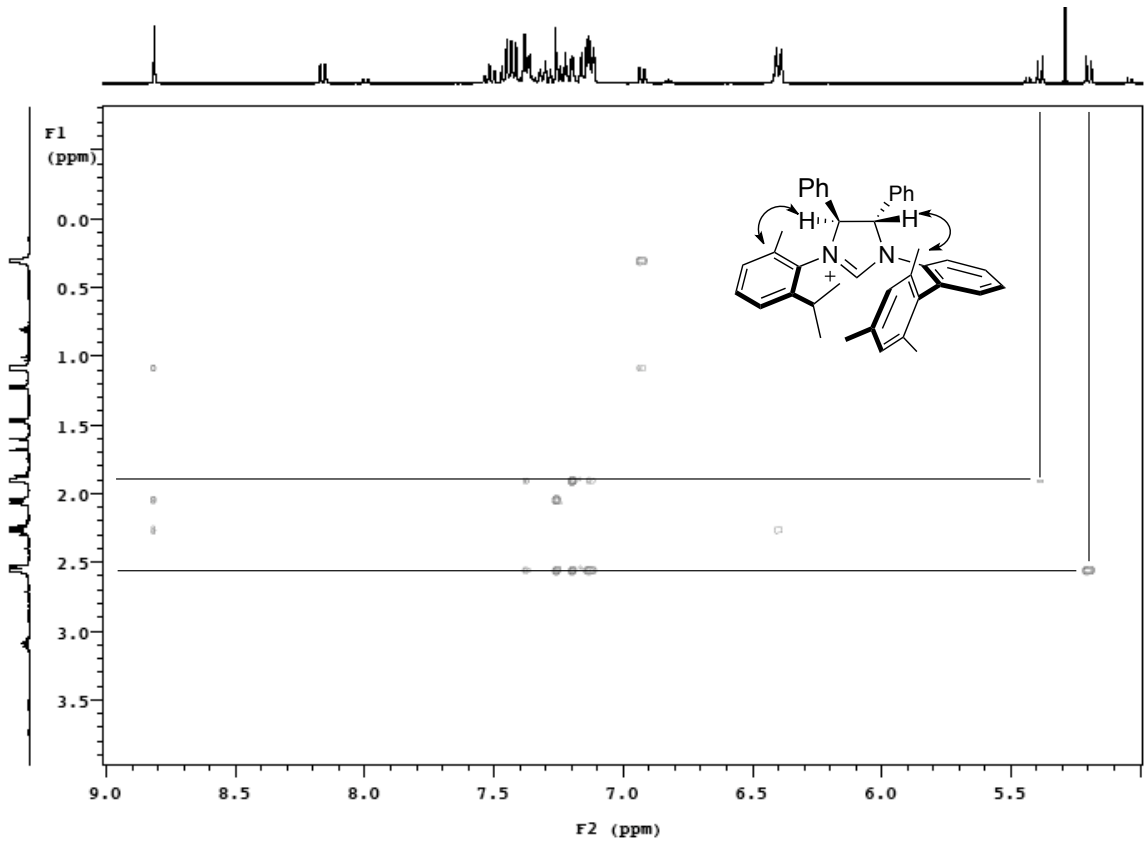
F1
(ppm)
0.0
0.5
1.0
1.5
2.0
2.5
3.0
3.5
9.0
8.5
8.0
7.5
7.0
6.5
6.0
5.5
F2 (ppm)
Ph
H
Ph
H
N
N
+

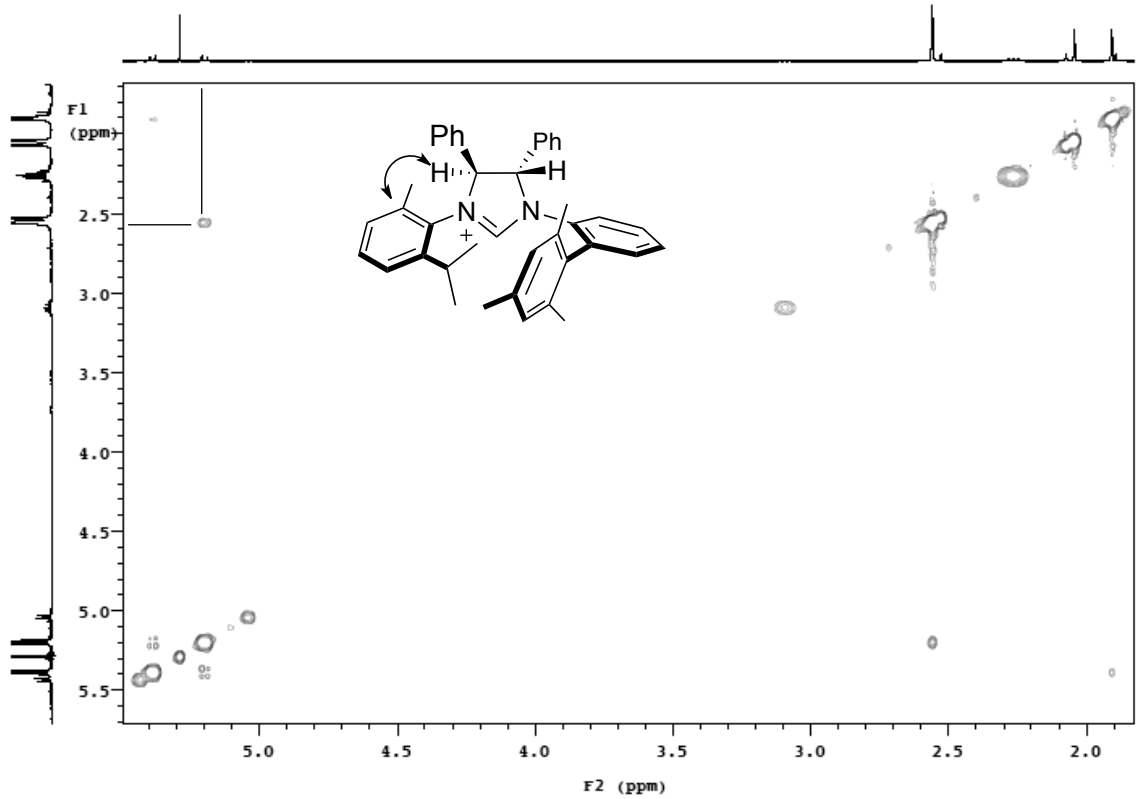
F1
(ppm)
2.5
3.0
3.5
4.0
4.5
5.0
5.5
5.0
4.5
4.0
3.5
3.0
2.5
2.0
F2 (ppm)
Ph
H
Ph
H
N
N
+

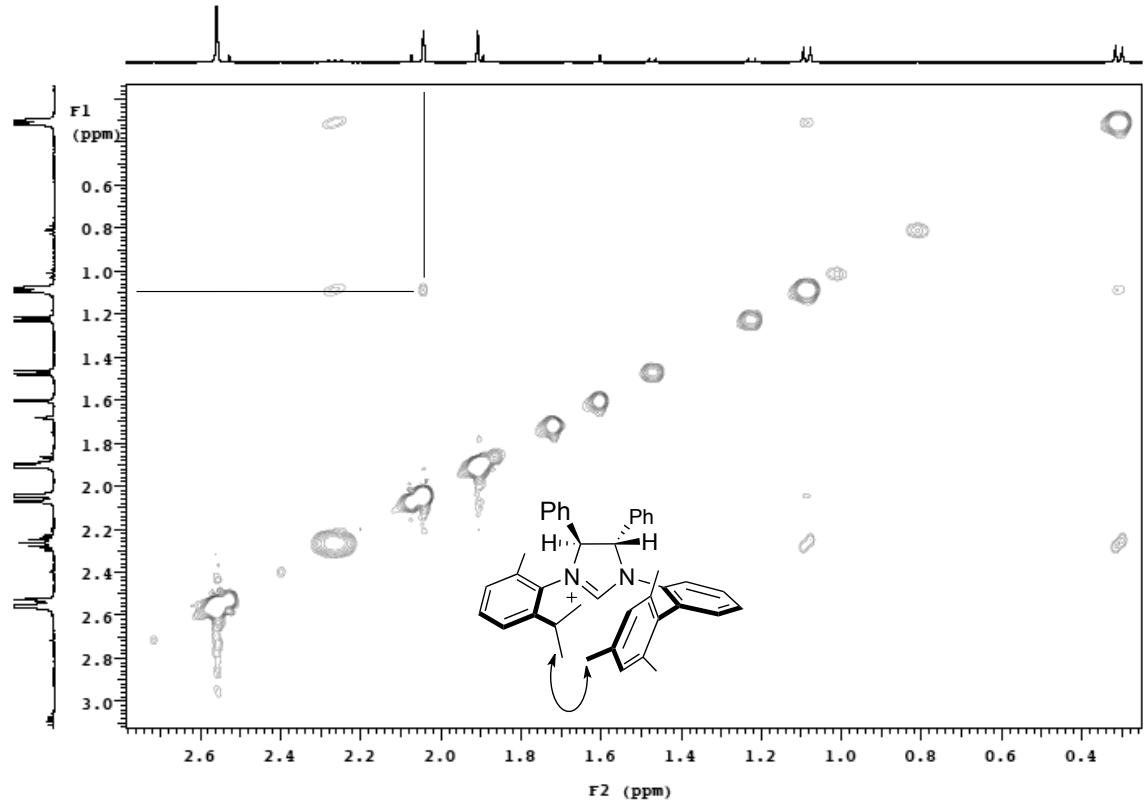
F1 (ppm)
F2 (ppm)
Ph
Ph
H
H
N
N
+

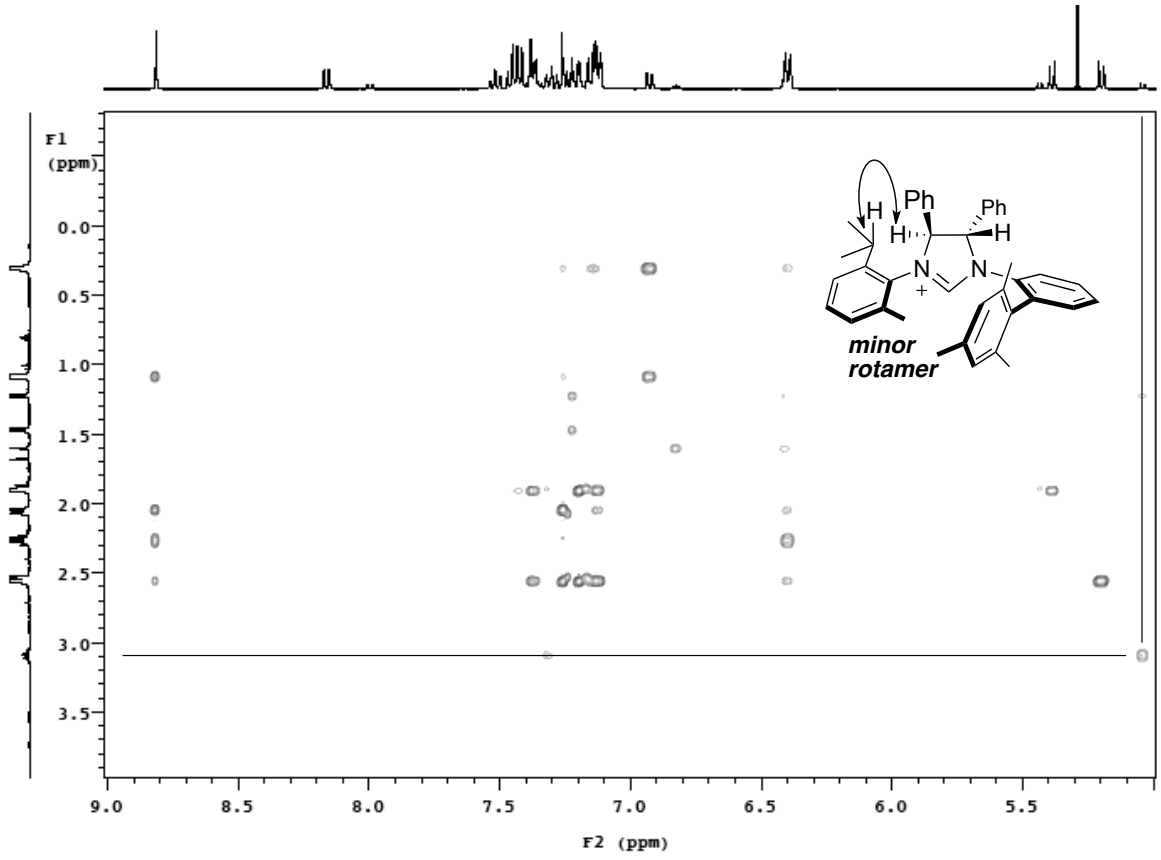
F1 (ppm)
F2 (ppm)
H
Ph
Ph
H
H
N
N
+
minor
rotamer

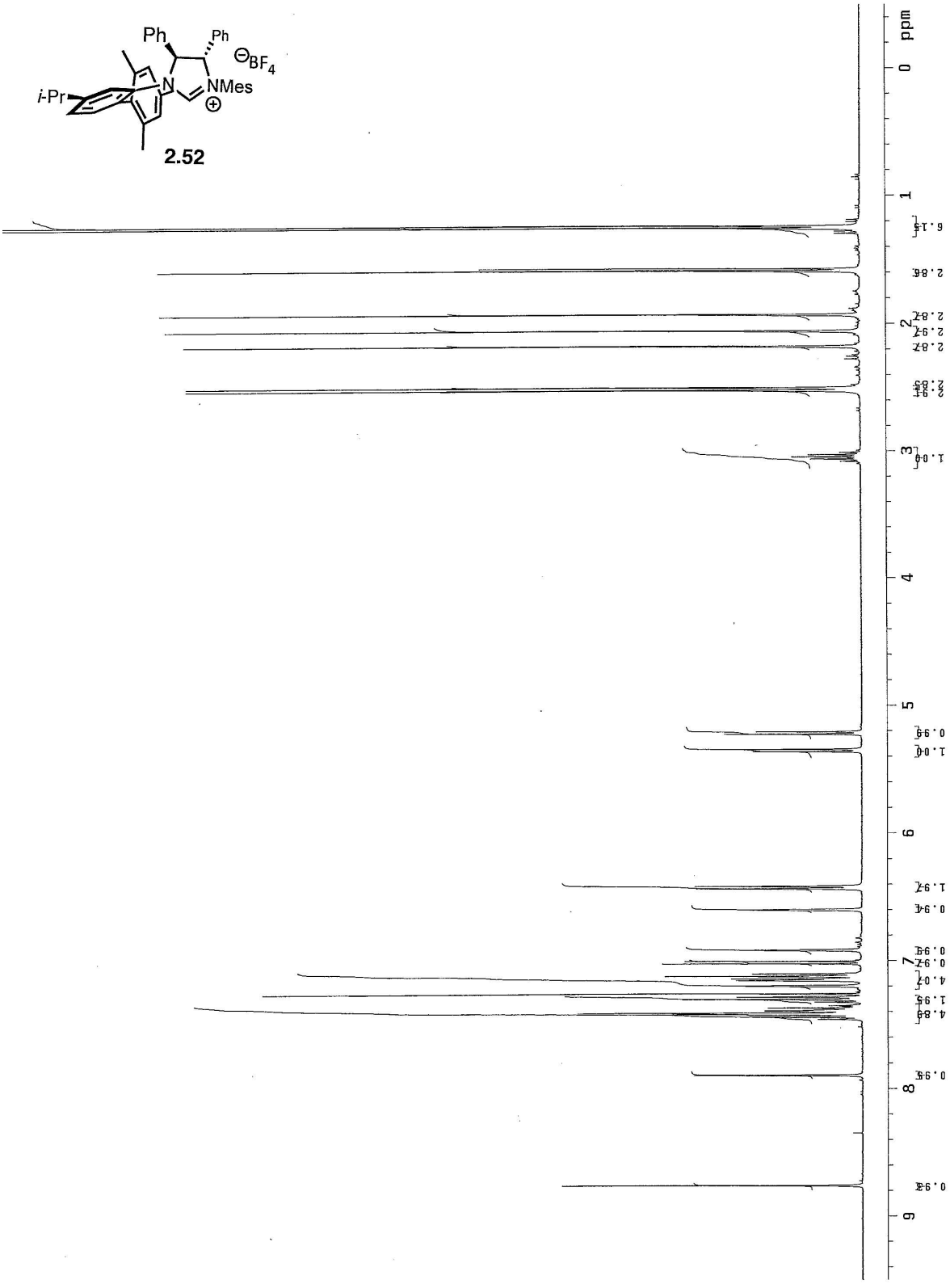
Ph
Ph
⊖BF4
i-Pr
N
NMes
⊕
2.52
ppm
0
1
2
3
4
5
6
7
8
9
6.15
2.86
2.87
2.97
2.87
2.93
1.00
0.99
1.00
1.97
0.94
0.97
0.93
4.07
1.95
4.89
0.95
0.93

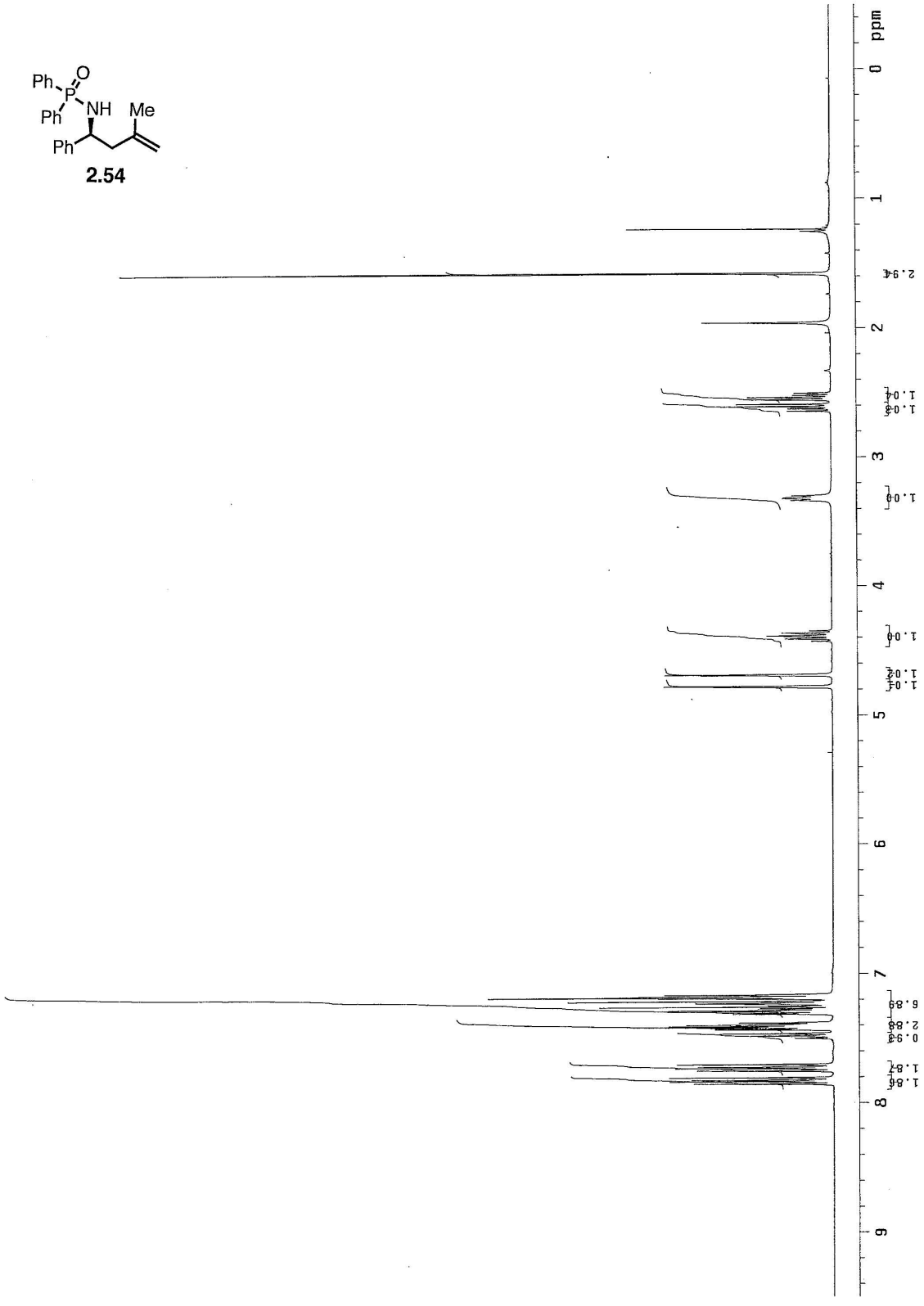
Ph
O
P
Ph
NH
Me
Ph
2.54
ppm
0
1
2
3
4
5
6
7
8
9
2.94
1.04
1.05
1.00
1.00
1.01
1.01
6.89
2.88
0.93
1.87
1.86

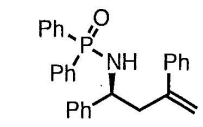
Ph
O
P
Ph
NH
Ph
Ph

2.56

ppm
0
1
2
3
4
5
6
7
8
9
1.01
1.07
0.98
1.00
1.01
1.00
1.98
1.87
5.77
3.92
1.95
3.69

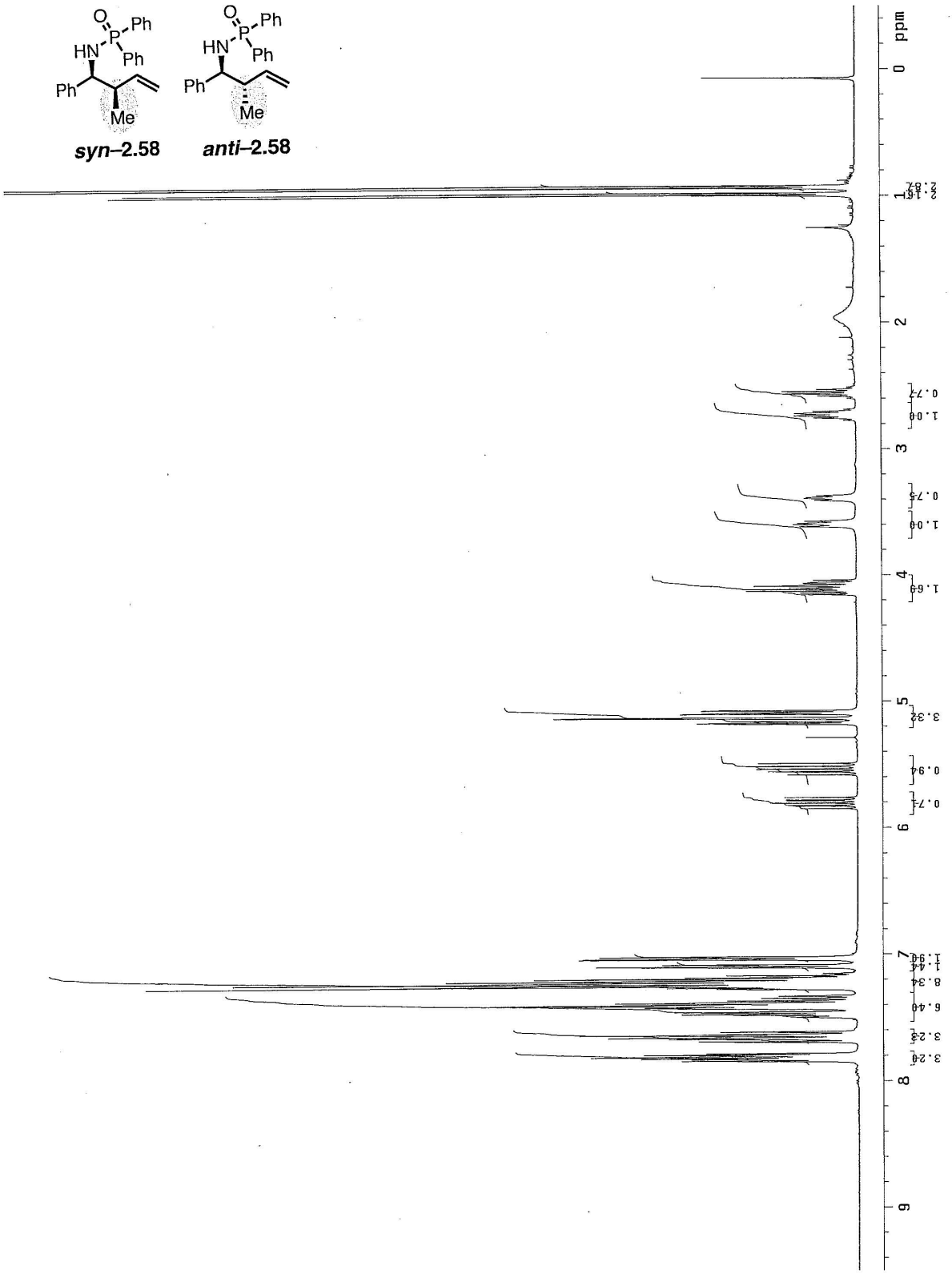

***syn*–2.58** ***anti*–2.58**

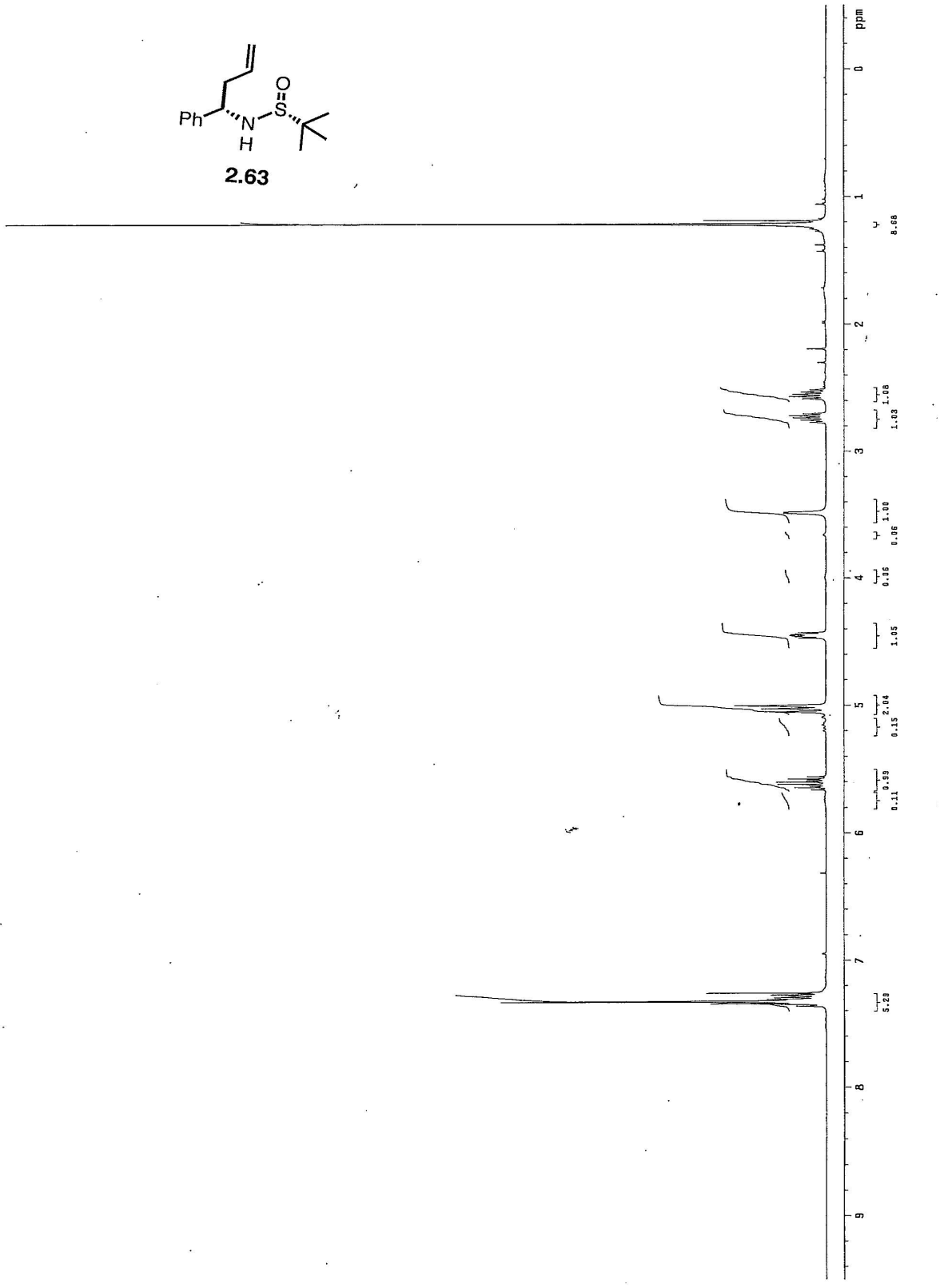
Ph
N
H
S
O
2.63
ppm
0
1
2
3
4
5
6
7
8
9
8.68
1.08
1.03
1.00
0.06
0.06
1.05
2.04
0.15
0.89
0.11
5.28

Chapter Three

NHC–Cu-Catalyzed Enantioselective Propargyl Group Additions to Phosphinoylaldimines

3.1 Introduction

As discussed in the previous two chapters, enantiomerically enriched α-branched amines are ubiquitous structural motifs in biologically relevant molecules, and, as such, synthetic methods for their efficient preparation are in constant development.[1] Moreover, classes of α-chiral amines, which can be synthesized with additional molecular complexity and are readily converted to a myriad of *N*-containing building blocks, are of significant utility. The Mannich bases described in Chapter 1 and the homoallylamines discussed in Chapter 2 fit this grouping; catalyzed transformations with the appropriately substituted silyl ketene acetals or allylborons result in amines bearing an additional *β*-stereogenic center alongside a handle for further manipulation, a butenolide or olefin, respectively. In an analogous fashion, protocols for the enantioselective addition of a propargyl group to an imine are equally desirable; the three carbon homologation can set two stereocenters to provide enantiopure homopropargylic amines of exceptional synthetic versatility. The resultant amines, substituted with a *β*-alkyne moiety, can be engaged in metal-promoted intramolecular cyclization strategies for the preparation of

[1] (a) "Chiral Amine Synthesis–Recent Developments and Trends for Enamide Reduction, Reductive Amination, and Imine Reduction," Nugent, T. C.; El-Shazly, M. *Adv. Synth. Catal.* **2010**, *352*, 753–819. (b) Nugent, T. C. In *Process Chemistry in the Pharmaceutical Industry* Braish, T. F.; Gadamasetii, K. Eds.; CRC Press-Taylor and Francis Group: New York, **2008**, 137–156.

various *N*-heterocycles,[2] including stereodefined pyrroles[3] and piperidines.[4] The capacity to convert homopropargylic amines to saturated *N*-heterocycles has prompted their implementation towards the synthesis of a broad range of natural products and pharmaceutical agents.[5] The functional diversity of the amines in Figure 3.1, each of which has been prepared through the intermediacy of a β-alkynyl amine, serves as a testament to the synthetic flexibility allowed by the alkyne precursors. Synthesis of aryl-quinolizidine alkaloid subcosine II is achieved through a gold-catalyzed cyclization of the aryl-substituted homoproparylic amine, followed by subsequent one-pot reduction/Ferrier rearrangement to afford the piperidin-4-ol core.[4a] Alternatively, the alkyne can be engaged to participate in a ruthenium-catalyzed cylcoisomerization event yielding an

---

[2] For methods to convert homopropargylic amines to a variety of *N*-heterocycles, see: Via a Pauson-Khand cyclization, see: (a) "Solid Phase Synthesis of Fused Bicyclic Amino Acid Derivatives via Intramolecular Pauson-Khand Cyclization: Versatile Scaffolds for Combinatorial Chemistry," Bolton, G. L.; Hodes, J. C.; Rubin, J. R. *Tetrahedron*, **1997**, *53*, 6611–6634. (b) "One-pot Synthesis of Chiral Dehydroproline Esters: [3+2]-type Cycloaddition Reaction of Allenylstannane and α-Imino Ester," Fuchibe, K.; Hatemata, R.; Akiyama, T. *Tetrahedron,* **2006**, *62*, 11304–11310. (c) "Stereochemical and Skeletal Diversity Arising from Amino Propargylic Alcohols," Pizzirani, D.; Kaya, T.; Clemons, P. A.; Schreiber, S. L. *Org. Lett.* **2010**, *12*, 2822–2825. (d) "Gold-Catalyzed Synthesis of 3-Pyrrolidinones and Nitrones from *N*-Sulfonyl Hydroxylamines via Oxygen-Transfer Redox and 1,3-Sulfonyl Migration," Yeom, H-S.; So, E.; Shin, S. *Chem. Eur. J.* **2011**, *17*, 1764–1767. (e) "Gold-Catalyzed Tandem 1,3-Migration/[2+2] Cycloaddition of 1,7-Enyne Benzoates to Azabicyclo[4.2.0]oct-5-enes," Rao, W.; Susanti, D.; Chan, P. W. H. *J. Am. Chem. Soc.* **2011**, *133*, 15248–15251. For the synthesis of enantioenriched γ-lactams, see: (f) "Gold-Catalyzed Oxidative Cyclization of Chiral Homopropargyl Amides: Synthesis of Enantioenriched γ-Lactams," Shu, C.; Liu, M-Q.; Wang, S-S.; Li, L.; Ye, L-W. *J. Org. Chem.* **2013***, 78*, 3292–3299.

[3] For methods to convert homopropargylic amines to pyrroles, see: (a) "A Novel Pyrrole Synthesis," Agarwal, S.; Knölker, H-J. *Org. Biomol. Chem.* **2004**, *2*, 3060–3062. (b) "Gold-Catalzed Synthesis of 2-Aryl-3-fluoropyrroles," Surmont, R.; Verniest, G.; De Kimpe, N. *Org. Lett.* **2009**, *11*, 2920–2923.

[4] For methods to convert homopropargylic amines to piperidines, see: (a) (a) "A Modular, Efficient, and Stereoselective Synthesis of Substituted Piperidin-4-ols," Cui, L.; Li, C.; Zhang, L. *Angew. Chem., Int. Ed.* **2010**, *49*, 9178–9181. (b) "Stereodefinied *N,O*-Acetals: Pd-Catalyzed Synthesis from Homopropargylic Amines and Utility in the Flexible Synthesis of 2,6-Substituted Piperidines," Kim, H.; Rhee, Y. H. *J. Am. Chem. Soc.* **2012**, *134*, 4011–4014.

[5] For examples of the utility of homopropargylic amine building blocks in drug discovery, see: (a) "Design and Synthesis of Potent, Selective Inhibitors of Endothelin-Converting Enzyme," Wallace, E. M.; Moliterni, J. A.; Moskal, M. A.; Neubert, A. D.; Marcopulos, N.; Stamford, L. B.; Trapani, A. J.; Savage, P.; Chou, M.; Jeng, A. Y. *J. Med. Chem.* **1998**, *41*, 1513–1523. (b) "A New Strategy for the Development of Highly Potent and Selective Plasmin Inhibitors," Saupe, S. M.; Steinmetzer, T. *J. Med. Chem.* **2012**, *55*, 1171–1180.

Figure 3.1 Natural Products Synthesized Through the Intermediacy of a Homompropargylic Amine

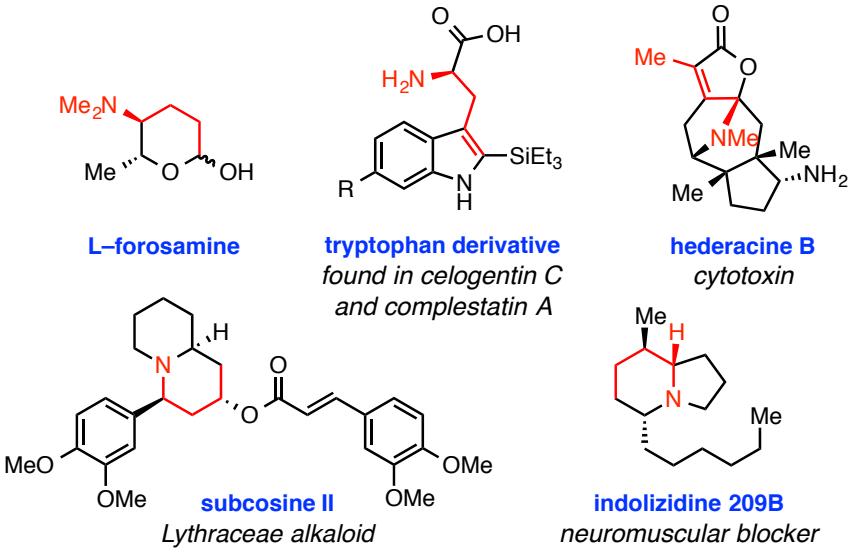

amine-substituted dihydropyran, an intermediate en route to L-forosamine, a biologically significant glycoside that appears in the spiramycins and related macrolactones.[6] The pyrrolidines embedded in the structures of tropane alkaloid hederacine B[7] and indolizidine alkaloid 209B[8] can also be accessed through intramolecular cyclization of the amine. Finally, palladium-catalyzed heteroannulation of the alkyne unit results in the efficient synthesis of β-indole substituted amines, an essential strategy to access uniquely substituted tryptophan derivatives for the preparation of natural products such as antitumor agent celogentin C[9] and antiviral complestatin A.[10]

---

[6] (a) "Chemoselectivity of the Ru-Catalyzed Cycloisomerization Reaction for the Synthesis of Dihydropyrans; Application to the Synthesis of L-Forosamine," Zacuto, M. J.; Tomita, D.; Pirzada, Z.; Xu, F. *Org. Lett.* **2010**, *12*, 684–687. For a multi-step synthesis of forosamine in the preparation of spinosyn G, see: (b) "Spinosyn G: Proof of Structure by Semisynthesis," Graupner, P. R.; Martynow, J.; Anzeveno, P. B. *J. Org. Chem.* **2005**, *70*, 2154–2160.

[7] "Toward the Racemic Total Synthesis of Hederacines A and B: Construction of an Advances Tricyclic Intermediate," Yamashita, M.; Yamashita, T.; Aoyagi, S. *Org. Lett.* **2011**, *13*, 2204–2207.

[8] "A Concise Asymmetric Synthesis of 5,8-Disubstituted Indolizidine Alkaloids. Total Synthesis of (–)-indolizidine 209B," Song, Y.; Okamoto, S.; Sato, F. *Tetrahedron Lett.* **2002**, *43*, 8635–8637.

[9] For a catalytic enantioselective method for the preparation of homopropargylic amino esters and the synthesis of the central tryptophan of celogentin C, see: "Catalytic Asymmetric Synthesis of the Central Tryptophan Residue of Celogentin C," Castle, S. L. Srikanth, G. S. C. *Org. Lett.* **2003**, *5*, 3611–3614.

The most efficient and practical route to access enantiomerically enriched homopropargylic amines involves the nucleophilic addition of a propargyl or allenylmetal reagent[11] to an imine, an approach that can be rendered diastereo- or enantioselective. Although significant progress has been made regarding both diastereoselective and catalytic transformations for the synthesis of the corresponding enantiopure secondary[12] or tertiary homopropargylic alcohols,[13] few reports have surfaced describing reactions with amine precursors. The difficulties associated with additions to imines[14] can be exacerbated by the complications incurred with transformations involving allenic or propargylic organometallic reagents (Figure 3.2). Control of the configuration of the

---

[10] "Synthesis and Stereochemical Determination of Complestatin A and B (Neuroprotectin A and B)," Breazzano, S. P.; Boger, D. L. *J. Am. Chem. Soc.* **2011**, *133*, 18495–18502.

[11] For a comprehensive review regarding this approach for the synthesis of homopropargylic amines and alcohols, see: "Catalytic Asymmetric Propargylation," Ding, C-H.; Hou, X-L. *Chem. Rev.* **2011**, *111*, 1914–1937.

[12] For a diastereoselective reaction of aldehydes with enantiopure allenylboron reagents, see: (a) "A Practical and General Enantioselective Synthesis of Chiral Propa-1,2-dienyl and Propargyl Carbinols," Corey, E. J.; Yu, C-M.; Lee, D-H. *J. Am. Chem. Soc.* **1990**, *112*, 879–881. For selected examples of catalytic enantioselective methods, see: (b) "Asymmetric Nozaki–Hiyama Propargylation of Aldehydes: Enhancement of Enantioselectivity by Cobalt Co-Catalysis," Usanov, D. L.; Yamamoto, H. *Angew. Chem., Int. Ed.* **2010**, *49*, 8169–8172. (c) "Copper Catalyzed Asymmetric Propargylation of Aldehydes," Fandrick, D. R.; Fandrick, K. R.; Reeves, J. T.; Tan, Z.; Tang, W.; Cappaci, A. G.; Rodriguez, S.; Song, J. J.; Lee, H.; Yee, N. K.; Senanayake, C. H. *J. Am. Chem. Soc.* **2010**, *132*, 7600–7601. (d) "Diastereo- and Enantioselective Iridium-Catalyzed Carbonyl Propargylation from the Alcohol or Aldehyde Oxidation Level: 1,2-Enynes as Allenylmetal Equivalents," Geary, L. M.; Woo, S. K.; Leung, J. C.; Krische, M. J. *Angew. Chem., Int. Ed.* **2012**, *51*, 2972–2976. (f) "Enantioselective Synthesis of *anti*- and *syn*-Homopropargyl Alcohols via Chiral Brønsted Acid Catalyzed Asymmetric Allenylboration Reactions," Chen, M.; Roush, W. R. *J. Am. Chem. Soc.* **2012**, *134*, 10947–10952. And references cited therein.

[13] For the synthesis of tertiary homopropargylic alcohols from enantiopure allenylboron reagents, see: (a) "*B*-Allenyl- and *B*-(γ-Trimethylsilylpropargyl)-10-phenyl-9-borabicyclo[3.3.2]decanes: Asymmetric Synthesis of Propargyl and α-Allenyl 3°-Carbinols from Ketones," Hernandez, E.; Burgos, C. H.; Alicea, E.; Soderquist, J. A. *Org. Lett.* **2006**, *8*, 4089–4091. For catalytic enantioselective additions of propargyl groups, see: (b) "Identification of Modular Chiral Bisphosphines Effective for Cu(I)-Catalyzed Asymmetric Allylation and Propargylation of Ketones," Shi, S-L.; Xu, L-W.; Oisaki, K.; Kanai, M.; Shibasaki, M. *J. Am. Chem. Soc.* **2010**, *132*, 6638–6639. (c) "A General Copper–BINAP-Catalyzed Asymmetric Propargylation of Ketones with Propargyl Boronates," Fandrick, K. R.; Fandrick, D. R.; Reeves, J. T.; Gao, J.; Ma, S.; Li, W.; Lee, H.; Grinberg, N.; Lu, B.; Senanayake, C. H. *J. Am. Chem. Soc.* **2011**, *133*, 10332–10335. (d) "Asymmetric Propargylation of Ketones Using Allenylboronates Catalyzed by Chiral Biphenols," Barnett, D. S.; Schaus, S. E. *Org. Lett.* **2011**, *13*, 4020–4023. (e) "Silver-Catalyzed Allenylation and Enantioselective Propargylation Reactions of Ketones," Kohn, B. L.; Ichiishi, N.; Jarvo, E. R. *Angew. Chem., Int. Ed.* **2013**, *52*, 4414–4417.

[14] For a discussion regarding the challenges accompanying transformations of aldimines and ketoimines as electrophiles, see Section 1.1 of Chapter 1.

reagents can be problematic: typically a thermodynamic equilibrium, k_{eq}, between the isomeric allenyl and propargylmetals is established due to the low barrier for their interconversion. Moreover, preference towards either the propargylic metal or the allenic analogue is subject to the influence of a number of factors, including: the nature of the metal center, substitution at the α or γ-carbons, and the reactivity of the electrophilic reaction partner. Additionally, their preparation, typically from reaction of a propargylic metal or halide with another metal (M, in Figure 3.2), can occur through two distinct mechanisms; reaction through the α–carbon provides the propargylmetal through an S_E2

Figure 3.2 Preparation of Allenyl and Propargylmetals, Their Interconversion, and Their Reactions with Electrophiles

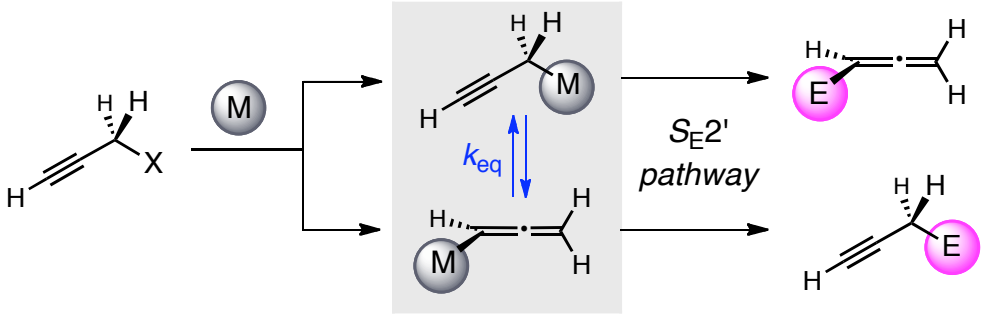

pathway, while the allenic metal can be directly generated if the C–M bond is formed at the γ-carbon through an S_E2' mechanism. Analogously, the allenic and propargylic organometallic species can react with electrophiles (E, in Figure 3.2) through either an S_E2 (reaction occurs at the α-carbon) or S_E2' pathway (C–C bond formation occurs at the γ-carbon, the pathway depicted in Figure 3.2). As such, a significant impediment faced in reactions with this class of nucleophiles is group transfer selectivity,[15] an issue that is worsened by the low reactivity of imine partners.

[15] Typically, the issue of selectivity arises due to the equilibrating nature of the allenic and propargylic metal species. This issue is of particular consequence when the two isomeric nucleophilic species react

3.2 Background

Thus far, a majority of the methods disclosed for the stereoselective synthesis of homopropargylic amines are diastereoselective, such that a chiral modifier is covalently bound to one of the reacting partners. One such strategy involves the use of enantiopure allenylborons or allenylsilanes, taking advantage of their configurational stability and preference to undergo reaction through an S_E2' mechanism. The first disclosure detailed allenylboration reactions between enantiopure allenylborane **3.2** and a silylated imine

Scheme 3.1 Preparation of Enantioenriched β-Silyl Amines Through the Use of Chiral Allenylboron **3.2**

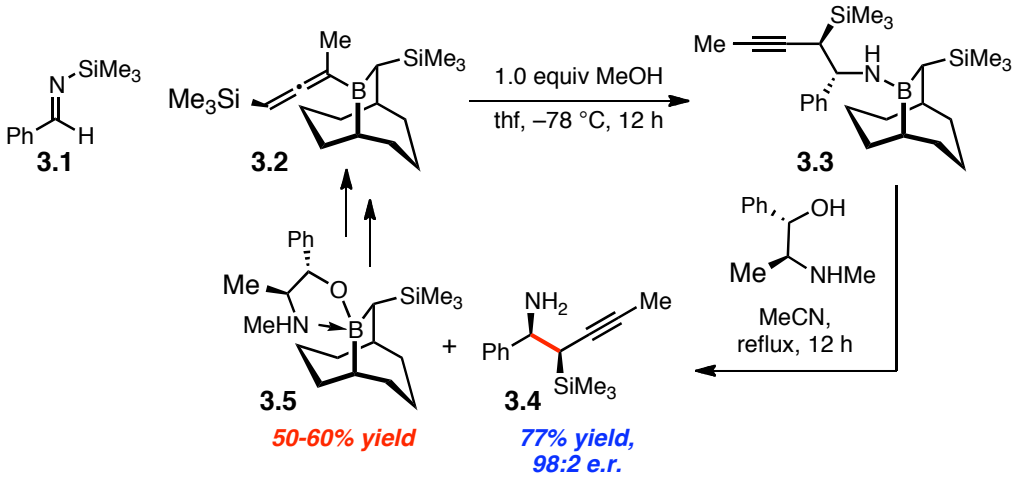

leading to the formation of boron-bound β-silyl homopropargylic amine **3.3** (Scheme 3.1).[16] Ligand exchange of borane **3.3** with pseudoephedrine affords the free amine **3.4** in 77% yield and 98:2 e.r. alongside 50–60% yield of the enantiomerically pure borane **3.5**, which can be recycled for the preparation of chiral allenylborane **3.2**.

---

with an electrophile with equal rates, resulting in likely inseparable mixtures of both allenyl and propargyl adducts.

[16] "β-Silylated Homopropargylic Amines via the Asymmetric Allenylboration of Aldimines," Gonzalez, A. Z.; Soderquist, J. A. *Org. Lett.* **2007**, *9*, 1081–1084.

Similarly, a disclosure from Panek and coworkers outlined the ability for enantiomerically pure allenyl silane **3.6** to transfer its axial chirality to point stereogenicity in homopropargyl sulfonamides **3.7** (Scheme 3.2).[17] S_E2' alkylation of the *in situ* generated iminium ions occurs through acyclic transition states with either antiperiplanar or synclinal approach of the nucleophile. The three component transformations result in the selective formation of the *syn* diastereomers with 5:1–>20:1 preference. While incorporation of an aliphatic substituent leads to products that can be

Scheme 3.2 Transfer of Axial Chirality of Enantiopure Allenylsilane **3.6** to Point Stereogenicity in Homopropargylic Sulfonamides **3.7**

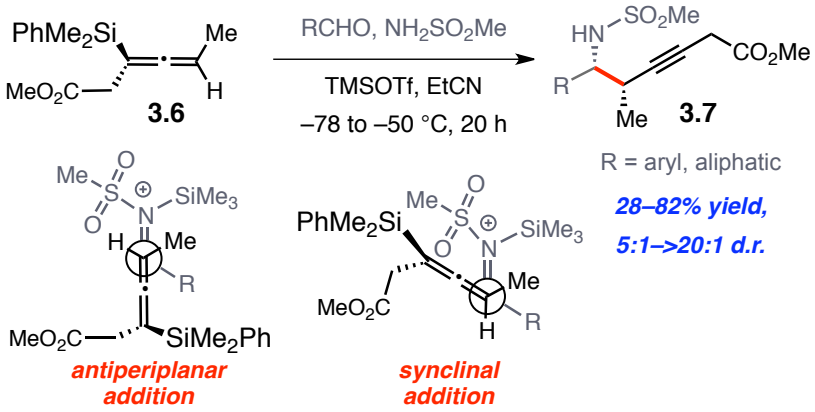

obtained in 69–82% yield, reactions with aryl aldehydes are less efficient producing the benzylic amines in 28–59% yields, presumably due to competitive decomposition pathways of the aryl-substituted iminium species. The strategies described herein provide methods for highly diastereoselective and exclusive formation of propargyl adducts, however, their reliance on stoichiometric chiral allenyl reagents for facial discrimination is restrictive due to the multi-step and costly procedures required for their preparation.

---

[17] "Synthesis of Enantioenriched Homopropargylic Sulfonamides by a Three Component Reaction of Aldehydes, Sulfonamides, and Chiral Allenylsilanes," Brawn, R. A.; Panek, J. S. *Org. Lett.* **2009**, *11*, 4362–4365.

Another strategy involves the preparation of imines from readily available chiral amines, positioning the chiral modifier in close proximity to the site of C–C bond formation; moreover, the chiral auxiliary can be readily removed after the reaction to access the enantiomerically enriched amines. The *tert*-butanesulfinyl imines, developed by Ellman and coworkers, undergo highly diastereoselective alkylations with a wide

Scheme 3.3 Highly Diastereoselective Reactions of *tert*-Butanesulfinyl Imines with Racemic Allenylzinc Reagent **3.9**

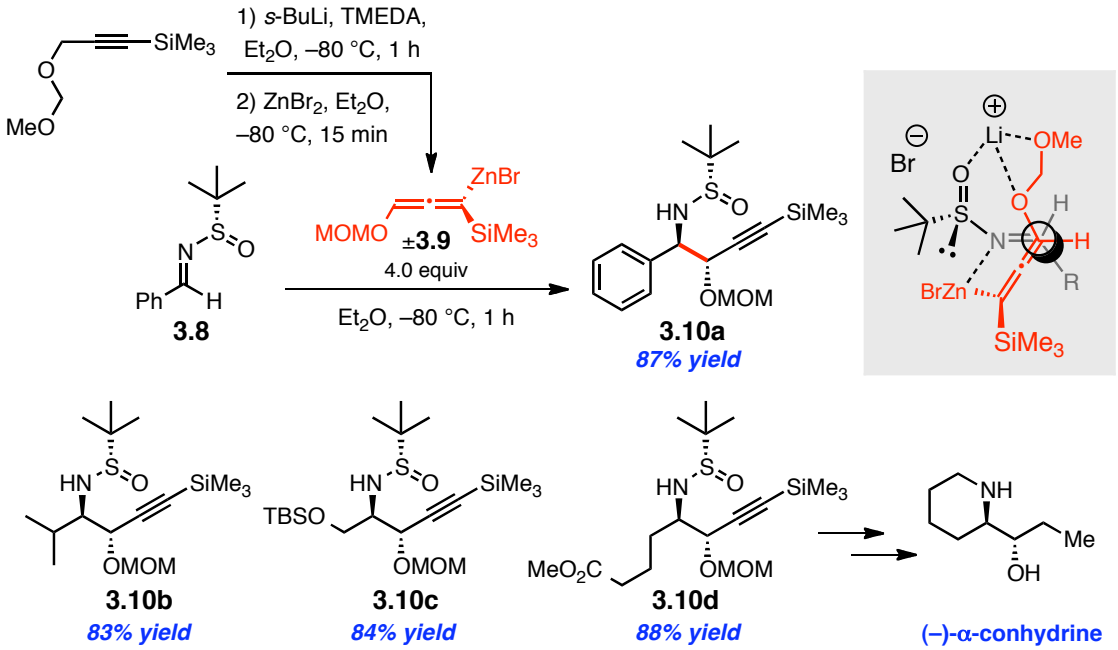

range of nucleophiles providing access to α-chiral amines of variable substitution patterns, and, as such, have likewise been exploited for the stereoselective synthesis of homopropargylic amines.[18] In particular, additions of allenylzinc reagents have been well

[18] For selected examples of methods that describe propargyl group additions to imines suited with Ellman's chiral auxiliary, see: (a) "Highly Diastereoselective Zinc-Catalyzed Propargylation of *tert*-Butanesulfinyl Imines," Fandrick, D. R.; Johnson, C. S.; Fandrick, K. R.; Reeves, J. T.; Tan, Z.; Lee, H.; Song, J. J.; Yee, N. K.; Senanayake, C. H. *Org. Lett.* **2010**, *12*, 748–751. (b) "Diastereoselective Synthesis of Enantiopure Homopropargylic *N-tert*-Butylsulfinylamines," Cyklinsky, M.; Botuha, C.; Chemla, F.; Ferreira, F.; Pérez-Luna, A. *Synlett*, **2011**, 2681–2684. (c) "Indium-Promoted Diastereo- and Regioselective Propargylation of Chiral Sulfinylimines," García-Muñoz, M. J.; Zacconi, F.; Foubelo, F.; Yus, M. *Eur. J. Org. Chem.* **2013**, 1287–1295.

studied, in part due to the high degree of covalency of the C–Zn bond, a feature that results in configurational stability and preference for reactions via a S_E2' mechanism. One enantiomer of racemic allenylzinc bromide **3.9** can efficiently engage a sulfinylimine in a chelate-controlled cyclic transition state to selectively access the *anti* α-amino propargylic ethers **3.10a–d** in 83–88% yield (Scheme 3.3).[19] The kinetic resolution described allows access to *anti* 1,2-amino alcohols, structural motifs found in the framework of alkaloids, such as α-conhydrine,[19e] and the sphingolipids.[19c]

In a related method, propargyl borolane **3.11** was found to react with catalytic diethylzinc, through an S_E2' mechanism, to *in situ* prepare an analogous silicon-substituted allenylzinc.[18a] The generated allenylzincs react with *N-tert*butansesulfinyl

Scheme 3.4 Highly Diastereoselective Reactions of *tert*-Butanesulfinyl Imines with *in situ* Generated Allenylzinc Reagents

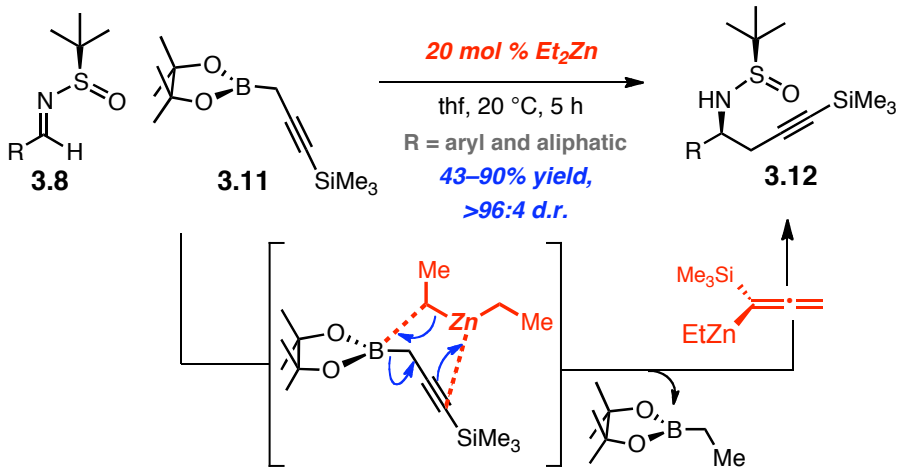

[19] (a) "Synthesis of Diastereoenriched Acetylenic α-*N*-*tert*-Butanesulfinamidoalkyl Methoxymethyl Ethers," Chemla, F.; Ferreira, F. *Synlett*, **2006**, 2613–2616. (b) "Stereo- and Enantioselective Synthesis of Acetylenic 2-Amino-1,3-diol Stereotriads," Voituriez, A.; Pérez-Luna, A.; Ferreira, F.; Botuha, C.; Chemla, F. *Org. Lett.* **2009**, *11*, 931–934. (c) "High-Yielding Synthesis of Sphingoid-Type Bases," Séguin, C.; Ferreira, F.; Botuha, C.; Chemla, F.; Pérez-Luna, A. *J. Org. Chem.* **2009**, *74*, 6986–6992. (d) "Expeditious Synthesis of a Common Intermediate of $_L$-1-Deoxyallonojirimycin and $_L$-1-Deoxymannojirimycin," Ferreira, F.; Botuha, C.; Chemla, F.; Pérez-Luna, A. *J. Org. Chem.* **2009**, *74*, 2238–2241. (e) "Stereoselective Synthesis of *syn*-β-Amino Propargylic Ethers: Application to the Asymmetric Syntheses of (+)-β-Conhydrine and (–)-Balanol," Louvel, J.; Chemla, F.; Demont, E.; Ferreira, F.; Pérez-Luna, A.; Voituriez, A. *Adv. Synth. Catal.* **2011**, *353*, 2137–2151.

imines **3.8** to provide a range of aromatic and aliphatic-substituted homopropargylic sulfinamides in >96:4 d.r. and in 43–90% yield (Scheme 3.4). Despite the synthetic advance represented by the diastereoselective strategies described, practical and efficient transformations that can be performed with a substoichiometric chiral source would be of significant value.

Disclosures that describe the catalytic and enantioselective addition of a propargyl group to an imine, however, are strikingly scarce.[20] The first report employs a Lewis acidic copper(I) salt in combination with BINAP derivative **3.13** to promote reaction between allenyltributylstannane and a tosyl-protected α-imino ester (equation 1).[21] The resultant alkyne-substituted sulfonamide **3.14** is afforded with 97% group selectivity (3% allene addition), 93:7 e.r., and 96% yield, however, as the sole example reported. A more recent disclosure from Jarvo and coworkers expands the scope of accessible tosylamines, beyond those bearing α-ester substitution, through an enantioselective Ag–phosphine catalyzed transformation of tosylimines with allenyl boronic acid pinacol ester **3.15**

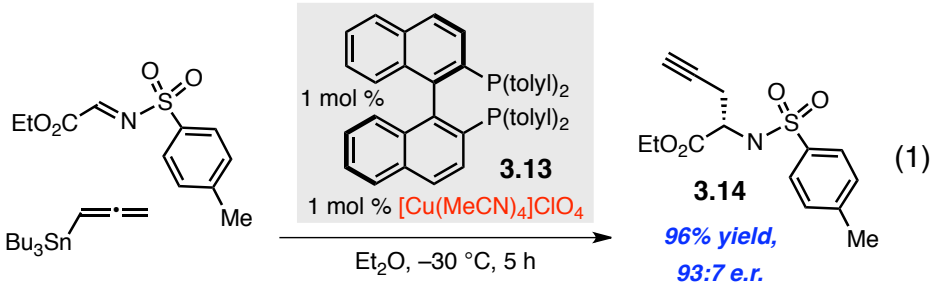

(1)

[20] For a single example of a catalyzed addition of an allenyltrichlorsilane to an *N*-acylhydrazone, providing the phenyl-substituted homopropargylamine in 53% yield and 89:11 e.r., see: (a) "Helical Chiral 2,2'-Bipyrdine *N*-Monoxides as Catalysts in the Enantioselective Propargylation of Aldehydes with Allenyltrichlorosilane," Chen, J.; Captain, B.; Takenaka, N. *Org. Lett.* **2011**, *13*, 1654–1657. Furthermore, in a recent study, homopropargyl amines were obtained as minor byproducts; see: (b) "A Catalytic Asymmetric Borono Variant of Hosomi–Sakurai Reactions with N,O-Aminals," Huang, Y-Y.; Chakrabarti, A.; Morita, N.; Schneider, U.; Kobayashi, S. *Angew. Chem., Int. Ed.* **2011**, *50*, 11121–11124..

[21] (a) "Catalytic, Enantioselective Propargyl- and Allenylation Reactions of α-Imino Ester," Kagoshima, H.; Uzawa,T.; Akiyama, T. *Chem. Lett.* **2002**, 298–299. (b) "One-pot Synthesis of Chiral Dehydroproline Esters: [3 + 2]-type Cycloaddition Reactions of Allenylstannane and α-Imino Ester," Fuchibe, K.; Hatemata, R.; Akiyama, T. *Tetrahedron*, **2006**, *62*, 11304–11310.

(Scheme 3.5).[22] The chiral phosphine–silver(I) complex is postulated to transmetalate with the allenylboron reagent such that the resultant allenylsilver transfers the propargyl group to the tosyl-protected imines with high facial and S_E2' selectivity. Notably, unligated allenylsilver is not configurationally stable; the rapid isomerization to the propargylic metal that ensues is evidenced by the one to one ratio of allene and propargyl

Scheme 3.5 Enantioselective Ag-Catalyzed Propargyl Additions to Sulfonyl-Protected Aldimines

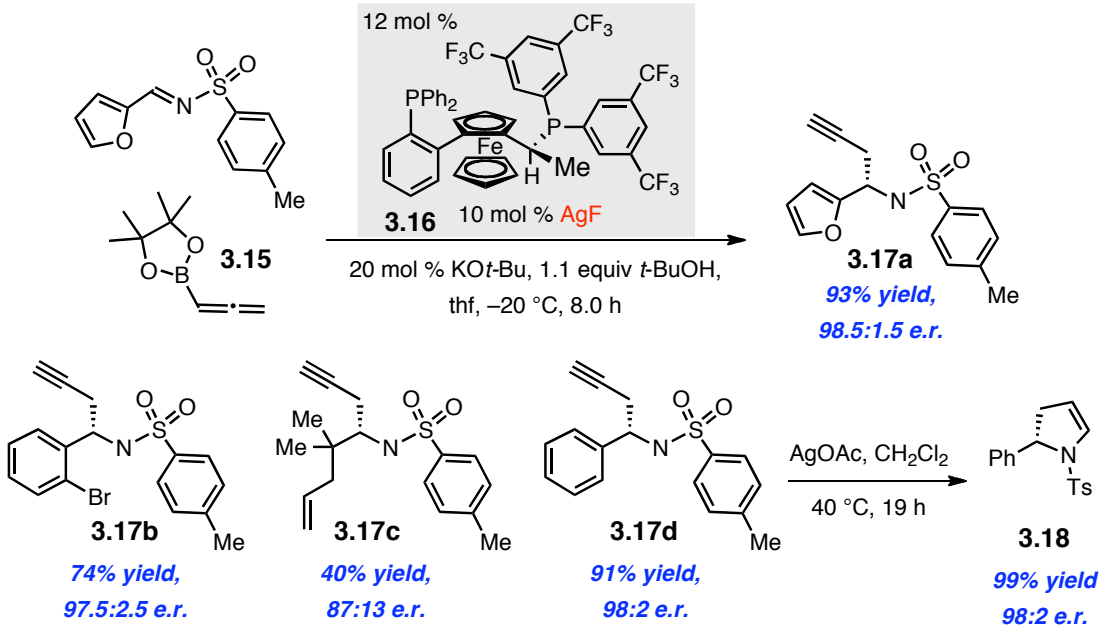

transfer products obtained in the absence of a phosphine ligand.[23] Bisphosphines, particularly Walphos W001-1 **3.16**, however, are found to impart sufficient stabilization of the allenylsilver complex such that only trace quantities of the allenic carbamines are observed. Homopropargylic aryl-, heteroaryl-, and alkyl-substituted sulfonamides,

[22] "Enantioselective Silver-Catalyzed Propargylation of Imines," Wisniewska, H. M.; Jarvo, E. R. *Chem. Sci.* **2011**, *2*, 807–810.

[23] Note that when the reaction is performed with 10 mol % AgF and 20 mol % KO*t*-Bu with 1.1 equivalents of *tert*butanol, but in the absence of any ligand, there is a 1:1 ratio of allenyl and propargyl transfer. However, under these conditions, it is not clear what the active catalyst is, for example, in our laboratories we have discovered metal alkoxides to be potent activators of C–B bonds (see Section 2.4 in Chapter 2).

represented by **3.17a**–**d**, are obtained in >87:13 e.r. and in 40–99% yield. A facile silver-mediated intramolecular hydroamination of the alkyne in **3.17d** provides access to the derived 2-pyrroline **3.18** in 99% yield and with no erosion of the stereochemistry. Despite the significant advance exemplified by the exceptional group and stereoselectivities of the silver-catalyzed process, the demonstrated substrate scope is limited; decreased reactivity and yield of sterically hindered and electron-rich aldimines is observed, while the only alkyl-substituted example, bishomoallylic amide **3.17c**, is devoid of α-protons (a feature that is typically challenging in reactions of aldimines). Moreover, the transformations suffer from competitive and unselective reactions promoted by unligated silver fluoride, particularly at temperatures above –20 °C; precomplexation and isolation of the bisphosphine–AgF complex is thus required to obtain high levels of selectivity. Practical and efficient enantioselective propargyl additions promoted by a sustainable and inexpensive catalyst to a broad range of aldimines remained a challenging objective.

3.3 NHC–Cu-catalyzed Enantioselective Propargyl Additions

We envisioned that, within the context of our studies on the copper-catalyzed enantioselective allyl additions to phosphinoyl aldimines with allylboronic acid pinacol ester,[24] reactions with the corresponding allenylboron **3.15** may proceed with similar levels of efficiency. In our previous studies, we have demonstrated the capacity for an *in situ* prepared Cu-complex of an *N*-heterocyclic carbene (NHC) to serve as a competent

[24] For a detailed account of this research see Chapter 2, and "Enantioselective Synthesis of Homoallylic Amines through Reactions of (Pinacolato)allylborons with Aryl-, Heteroaryl-, Alkyl-, or Alkene-Substituted Aldimines Catalyzed by Chiral C_1-Symmetric NHC–Cu Complexes," Vieira, E. M.; Snapper, M. L.; Hoveyda, A. H. *J. Am. Chem. Soc.* **2011**, *133*, 3332–3335.

Figure 3.3 Comparison of the Stability and Activity of an NHC–Cu-allyl and the Corresponding NHC–Cu-allene

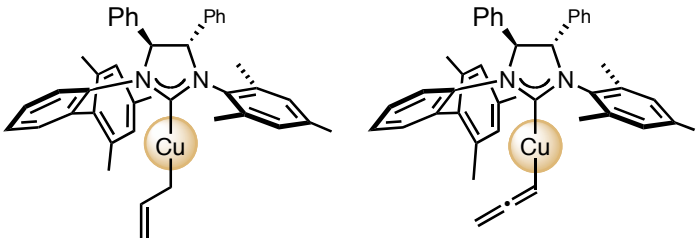

configurationally unstable
sensitive to H_2O and O_2

configurational stability?
activity of vinylCu?

catalyst for the activation of an allylboron towards ligand exchange; the resulting NHC–Cu-allyl intermediate can react with a diphenylphosphinoyl aldimine with high levels of efficiency and stereospecificity. However, the generated allylcopper(I) species were discovered to be highly reactive, configurationally unstable, and exceedingly sensitive to oxidative processes (formation of copper(I) oxide) and protonolysis. These ascribed weaknesses of the copper-catalyzed protocols could conceivably be resolved in reactions with the corresponding allenylcopper complex (Figure 3.3).

With the copper center bound to an sp^2-hybridized carbon, rather than the C_{sp^3}–Cu bond of an allylcopper, the homologous allenylcopper complexes are expected to be lower in energy with the imparted stabilization of the C–Cu bond. However, the additional stability of the organometallic reagent can result in a lack of the required reactivity for reactions with imines. Moreover, although the allenylcopper complex is lower in energy, the corresponding higher energy propargylic isomer would be more reactive by comparison. The success of the design of the catalytic cycle in Figure 3.4 hinged on the relative kinetics of the individual steps: of primary concern, the rate of propargyl transfer to the electrophile, from the NHC–bound allenylcopper ***ii***, should be

greater than the rate of its isomerization k_{eq}, i.e., if the activation barrier for addition were too high, then competitive, or possibly exclusive, allenyl group addition from propargylic complex ***i*** could occur. Additionally, we presumed that additions from either copper-based complex to phosphinoylaldimines would occur stereospecifically and through an S_E2' mechanism, by way of the favored addition transition state in Figure 3.4, a proposal that emerged from the investigations on allyl additions outlined in Chapter 2. Furthermore, methanol would continue to serve as a critical additive for concomitant

Figure 3.4 Proposed Catalytic Cycle for NHC–Cu-Catalyzed Propargyl Additions to Phosphinoyl Aldimines

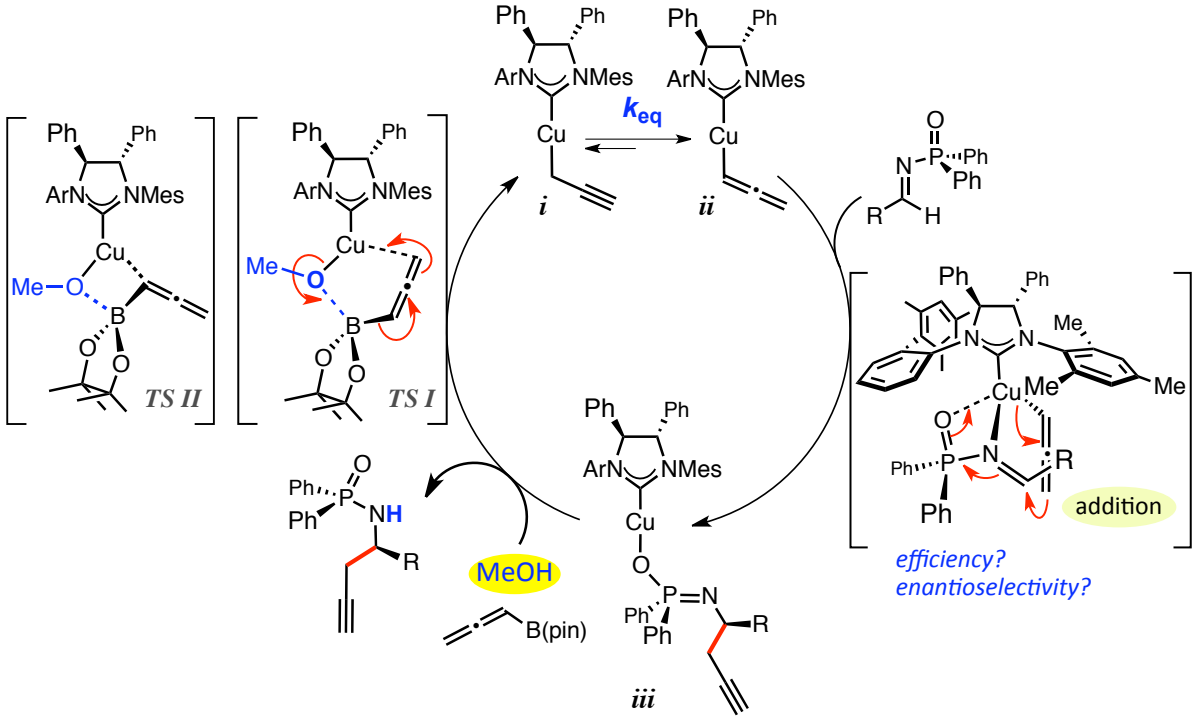

product release and catalyst regeneration from NHC–Cu-amide ***iii***. Finally, allenylboron **3.15** could react with the produced NHC–Cu-OMe through either ***TS I*** or ***TS II***. The four-atom centered sigma-bond metathesis event in ***TS II*** affords allenylcopper ***ii***, while an S_E2' alkylation, depicted in ***TS I***, would generate the propargylic species ***i***.

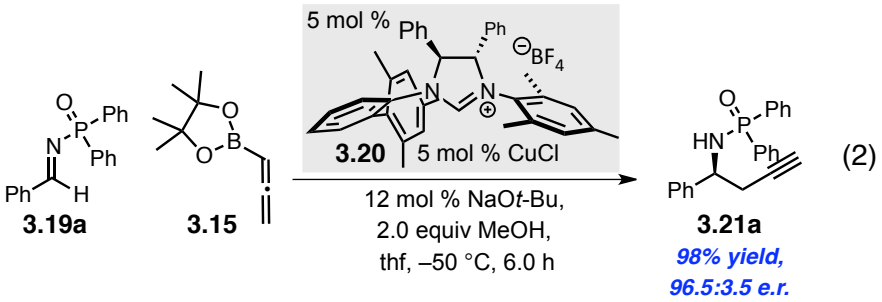

(2)

Employing the optimized conditions for allyl transfer reactions, with the NHC–Cu catalyst derived *in situ* from chiral C_1-symmetric imidazolinium salt **3.20**,[24] reaction of phosphinoylaldimine **3.19a** and allenylboron **3.15** provides exclusive formation of homopropargylic amide **3.21a** (<2% allene addition product observed). Furthermore, transformations are complete within six hours and the alkyne-substituted amine is obtained in 96.5:3.5 e.r. (equation 2). The stabilization imparted by the allene ligand to the copper-based nucleophile, does not appear to significantly diminish its reactivity, as had been anticipated. In fact, judging by the amount of catalyst required to completely

Table 3.1 Examination of Catalyst Loading in Enantioselective NHC–Cu-catalyzed Propargyl Group Additions to Aldimine **3.19c**

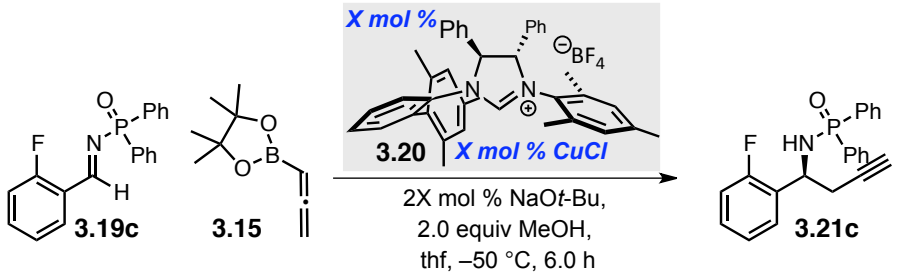

entry	**mol %**	conv. (%)[a]	yield (%)[b]	e.r.[c]
1	**5**	>98	>98	97.5:2.5
2	**2**	>98	94	97.5:2.5
3	**1**	>98	91	98:2
4	**0.5**	91	82	97:3
5	**0.25**	86	80	97.5:2.5

[a]Determined by analysis of 400 MHz ^{1}H NMR spectra of unpurified reaction mixtures; [b]Isolated yields of purified products; [c]Enantiomer ratio values were determined by HPLC analysis.

convert aldimine **3.19c** to homopropargyl amide **3.21c**, the generated NHC–Cu-allene complex displays increased reactivity (Table 3.1). With only 0.25 mol % catalyst loading, there is 86% conversion towards the exclusive formation of propargyl adduct **3.21c** (within six hours at –50 ºC, entry 5). There is no erosion of activity or enantioselectivity with reduced concentration of the active catalyst, such that *ortho*-fluorophenyl substituted amide **3.21c** is consistently obtained in >80% yield with approximately 97.5:2.5 e.r. (Table 3.1).

Table 3.2 Examination of the Scope of the Enantioselective NHC–Cu-catalyzed Propargyl Group Additions

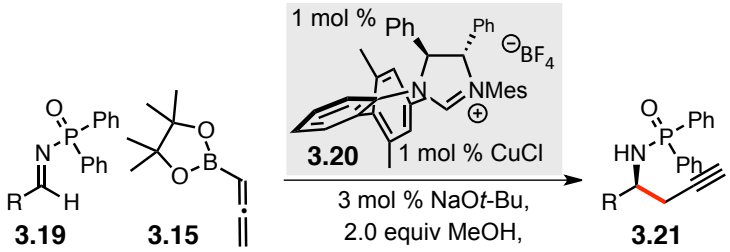

entry	**R**		yield (%)[a]	e.r.[b]
1	C_6H_5	**3.21a**	98	98:2
2	2-naphthyl	**3.21b**	96	95:5
3	*o*-FC_6H_4	**3.21c**	96	97.5:2.5
4	*o*-MeC_6H_4	**3.21d**	93	97.5:2.5
5	*o*-$OMeC_6H_4$	**3.21e**	97	97:3
6	*m*-BrC_6H_4	**3.21f**	97	96:4
7	*p*-ClC_6H_4	**3.21g**	92	97:3
8	*p*-$OMeC_6H_4$	**3.21h**	98	97:3
9	2-furyl	**3.21i**	>98	96.5:3.5
10	3-thienyl	**3.21j**	91	99:1
11	3-pyridyl	**3.21k**	95	97:3

Reactions are performed in an N_2 atmosphere with 1.4 equiv. of **3.15**; >98% conversion and <2% allene addition is observed in all cases. [a]Isolated yields of purified products; [b]Enantiomer ratio values were determined by HPLC analysis.

The scope of the enantioselective propargyl additions promoted by 1 mol % of the Cu catalyst derived from **3.20** was subsequently investigated (Table 3.2). Unlike the analogous transformations with allylboronic acid pinacol ester, which required an alternate modified catalyst for high stereoselectivity in reactions of electron-rich and sterically encumbered aldimines, propargyl additions deliver products with >95:5 e.r. derived from a wide range of aryl- and heteroaryl-susbstituted phosphinoylaldimines **3.19**. For example, the allyl-substituted analog of **3.21d** is obtained in 79% yield and 84:16 e.r., while propargyl group transfer occurs with improved facial discrimination affording the propargyl adduct in 97.5:2.5 e.r. under the same conditions (entry 4).[25] Notably, for all cases, there is <2% allene addition and the homopropargyl amides can be isolated in >90% yield. Additionally, the Cu-catalyzed process is not inhibited by substrates bearing coordinating heteroatoms, such that pyridyl-substituted **3.21k** is obtained with equal efficiency and in 95% yield and 97:3 e.r. (entry 11).

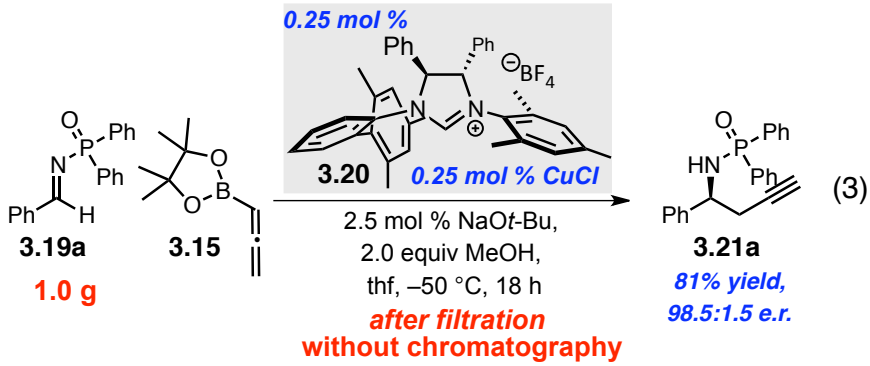

Reactions depicted in Table 3.2 are amenable to gram-scale operations. Propargyl addition to **3.19a** proceeds with facility in the presence of reduced quantities of the NHC–Cu-catalyst (0.25 mol %). Trituration of the reaction solution precipitates

[25] To compare the selectivities obtained from the Cu-catalyzed allyl and propargyl addition reactions, see Table 3.2 and Table 2.1 in Chapter 2, the only distinction being reactions of allenylboron are performed with 1 (vs. 5) mol % catalyst.

homopropargyl amide **3.21a** such that it can be obtained in 81% yield after filtration in 98.5:1.5 e.r. (equation 3). However, due to the postulated stability and robustness of the allenyl-substituted NHC–Cu(I) intermediate, we speculated that the propargyl additions could constitute a more practical and tolerant set of reactions. The air and moisture-sensitivity of the copper(I) intermediates in the allyl group additions necessitated stringent exclusion of these impurities and the implementation of dry-box techniques. A more practical set of conditions would allow reaction set up on benchtop and would preclude use of the air and moisture sensitive Cu(I) salts. Based on earlier investigations that generated a catalytically active Cu(I) species *in situ* from a diboron reagent and a Cu(II) salt,[26] we envisioned generation of the active NHC–Cu(I)-allene complex from inexpensive, and air-stable copper(II) chloride dihydrate. Accordingly, in the presence of 0.25 mol % imidazolinium salt **3.20**, 0.25 mol % copper(II) chloride dihydrate, and 2.5 mol% NaO*t*-Bu, gram-scale propargyl addition proceeds to >98% conversion at –50 ºC

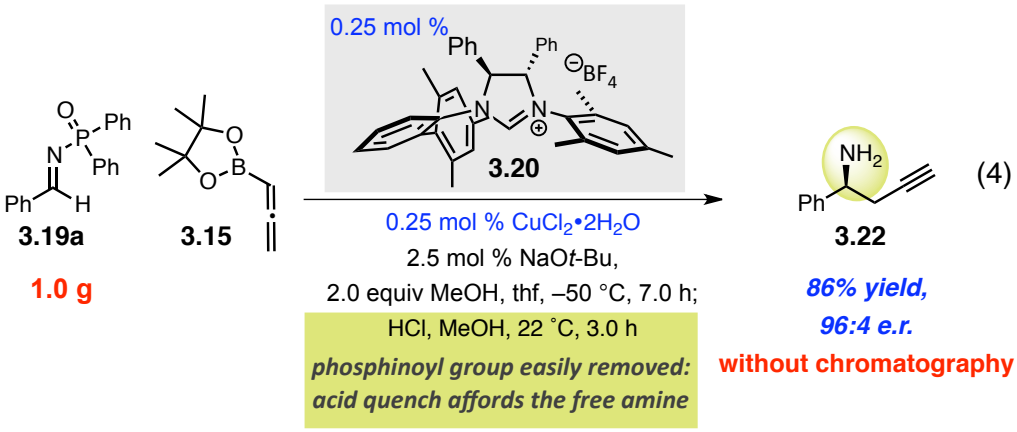

[26] For selected examples, see: (a) "Enantioselective Synthesis of Allylboronates Bearing a Tertiary or Quaternary B-Substituted Stereogenic Carbon by NHC–Cu-Catalyzed Substitution Reactions," Guzman-Martinez, A.; Hoveyda, A. H. *J. Am. Chem. Soc.* **2010**, *132*, 10634–10637. (b) "One-Pot Three Component Catalytic Enantioselective Synthesis of Homoallylboronates," Ibrahem, I.; Breistein, P.; Córdova, A. *Angew. Chem., Int. Ed.* **2011**, *50*, 12036–12041.

within seven hours.[27] Subsequent treatment of the reaction solution with concentrated aqueous hydrogen chloride and methanol for three hours results in cleavage of the phosphinoyl group, such that the free homopropargylic amine can be obtained in 86% yield and 96:4 e.r. after aqueous extraction (equation 4). The practical one-pot operation allows for the conversion of readily available starting materials to high-value enantioenriched amine building blocks with the action of a small quantity of chiral catalyst. There are two qualities of the phosphinamide products that are highlighted by the gram-scale processes in equations 3 and 4: 1) their crystallinity for ease of purification and 2) the facile and inexpensive conditions for removal of the protecting group. These attributes constitute the principal advantages for this class of protected imines, which compensate for their perceived lack of atom economy.

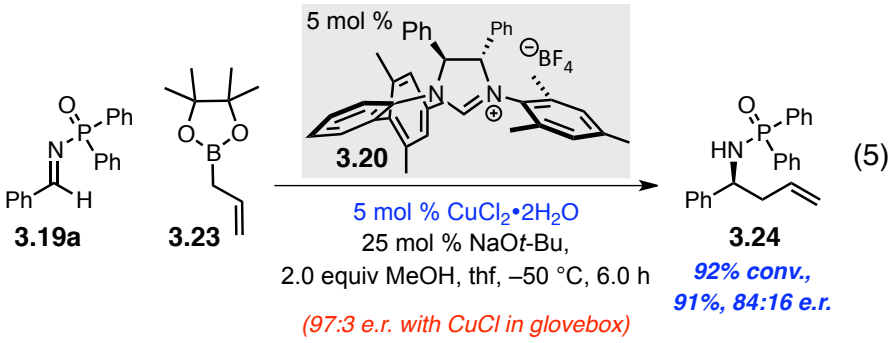

(5)

In concurrence with the postulated robust nature of allenylcopper to undesired side processes, such as oxidation, homolysis, and protonation, in relation to the more susceptible allylcopper counterparts, reactions initiated by a Cu(II) salt are less efficacious in transformations with allylboron **3.23** (equation 5). In the presence of 5 mol % of a Cu-based catalyst derived from copper(II) chloride dihydrate, there is 92%

[27] Reduction of copper(II) chloride may be due to the excess sodium *tert*-butoxide. An alternate route for reduction involves reaction of NHC–Cu(II)Cl(O*t*-Bu) with **3.15** to generate (pin)B-OtBu and NHC–Cu(II)Cl(allene). Subsequent homolytic Cu–C bond cleavage affords NHC–Cu(I)Cl and the product from allene dimerization.

conversion to homoallylic amide **3.24** in 84:16 e.r., this in comparison to 97:3 e.r. when the catalyst is generated from copper(I) chloride in the glovebox. In the case of reactions that proceed through the intermediacy of an NHC–Cu-allyl complex, adventitious moisture and oxygen can react with the active complex generating alternative active species (potentially a copper oxide complex) that promote allyl additions with poor discrimination. Reactions that result in propargyl transfer proceed through an allenylcopper intermediate that, either does not react with these impurities, or, can outcompete reactions from other generated copper complexes.

Due to the added simplicity of the reaction set up for transformations promoted by the air stable Cu(II) salt,[28] the scope and utility of the propargyl addition reactions were further investigated. Optimization of the required reaction time for complete conversion of benzaldehyde-derived **3.19a** to propargyl adduct **3.21a**, revealed that reactions are typically complete within thirty minutes. Moreover, moderation of the reaction temperature indicated that performing the propargyl transfer at –15 ºC provided similar selectivity levels so long as the reaction components were combined at –78 ºC.[29] The scope of the transformation was reinvestigated with the conditions discovered for additions initiated from copper(II) chloride dihydrate (Table 3.3). Propargyl additions are driven to completion with 1 mol % catalyst loading derived from imidazolinium salt **3.20** and the Cu(II) salt within an hour. A range of aryl- and heteroaromatic-substituted imines react to provide the derived propargyl adducts (<2% allene addition in all cases) in >88%

[28] Reactions can be set up and performed on bench-top. A nitrogen atmosphere, however, is still required for optimal reactivity and selectivity.

[29] With these conditions, **3.21a** is obtained in 95% yield and 96:4 e.r. (entry 1, Table 3.3), if, however, the components are not mixed first at –78 ºC and the reaction is performed at –15 ºC, the selectivity is diminished to 93:7 e.r.. There is no reaction observed at –78 ºC, therefore, a majority of the reaction occurs upon warming the reaction solution to –15 ºC.

Table 3.3 Examination of the Scope of Enantioselective Propargyl Group Additions Promoted by an NHC–Cu Catalyst Derived from a Cu(II) Salt

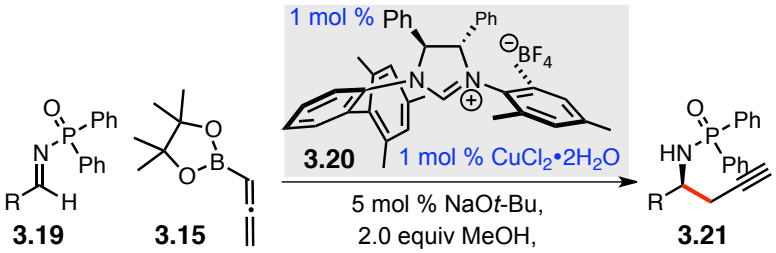

entry	**R**		yield (%)[a]	e.r.[b]
1	C_6H_5	**3.21a**	95	96:4
2	2-naphthyl	**3.21b**	95	94:6
3	*o*-FC_6H_4	**3.21c**	96	95:5
4	*o*-MeC_6H_4	**3.21d**	92	94:6
5	*o*-$OMeC_6H_4$	**3.21e**	98	94:6
6	*m*-BrC_6H_4	**3.21f**	93	93:7
7	*p*-ClC_6H_4	**3.21g**	88	96:4
8	*p*-$OMeC_6H_4$	**3.21h**	92	96:4
9	2-furyl	**3.21i**	94	96.5:3.5
10	3-thienyl	**3.21j**	97	97:3
11	3-pyridyl	**3.21k**	>98	94:6

Reactions are performed in an N_2 atmosphere with 1.4 equiv. of **3.15**; >98% conversion and <2% allene addition is observed in all cases. [a]Isolated yields of purified products; [b]Enantiomer ratio values were determined by HPLC analysis.

yield and in 93:7–97:3 e.r. (Table 3.3). There is little diminution of facial selectivity in comparison of the transformations performed with the Cu(II) salt (Table 3.3) versus those that are directly promoted by the Cu(I) salt (Table 3.2).[30]

Furthermore, substrates bearing di- or trisubstituted alkenes, and linear, α- or β-branched alkyl substituents participate in enantioselective propargyl additions to afford homopropargylic amides **3.21l–q** in 65–98% yield and 92:8–97:3 e.r. employing the

[30] The selectivities are within 3% difference. The similar trends in selectivity indicate that, in fact, the same catalytic species is operative, whether initated by copper(I) chloride or copper(II) chloride dihydrate.

conditions identified in Table 3.3 (Figure 3.5). The diminished yields observed for alkyl-substituted amines **3.21o–q** is a result of the instability of the precursor imines, which are prone to hemiaminal or enamine formation, precluding their isolation and/or purification. Notably, α-branched alkyl-substitution on the substrate does not pose a significant hurdle to facial discrimination as it did for the related transition states for allyl

Figure 3.5 NHC–Cu-Catalyzed Propargyl Additions to Alkenyl- and Alkyl-Substituted Phosphinoyl Aldimines

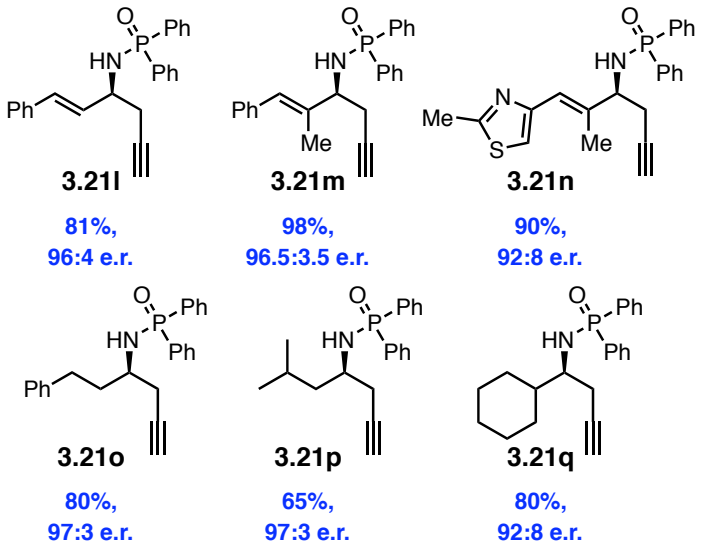

Reactions are performed in an N_2 atmosphere with 1.4 equiv. of **3.15** with conditions in Table 3.3; >98% conversion and <2% allene addition is observed in all cases. [a]Isolated yields of purified products; [b]Enantiomer ratio values were determined by HPLC analysis.

transfer, such that cyclohexyl-bearing homopropargyl amide **3.21q** can be obtained in 92:8 e.r. with the catalyst derived from **3.20** (this catalyst provides 80:20 e.r. for the analogous allyl addition).

3.4 Mechanistic Attributes of NHC–Cu-allene

Despite the similarities between the NHC–Cu-catalyzed allyl and propargyl additions to phosphinoyl aldimines, there are several distinctions: 1) As already noted, reactions with allenylboron are more efficient, require lower catalyst loadings, and do not require low temperatures. This is likely a result of adventitious reactions of the Cu(I)-allyl catalyst that reduce the effective concentration of the active species; propargyl additions do not suffer as significantly, due to the stability of the allenylcopper intermediate. 2) Allylcopper species are not configurationally stable, such that a mixture of isomeric products is obtained with complexes bearing dissymmetric allyl units. In contrast, the allenylcopper appears to be stable, despite the propensity for isomerization observed in related systems.[31] 3) Allyl addition processes are significantly affected by the substitution pattern on the electrophilic reaction partner, with diminished stereoselectivity for *ortho*-aryl-substituted or α-branched alkyl-containing aldimines.[32] A similar trend is not observed in the synthesis of sterically encumbered homopropargylic amides despite the closely related proposed transition states (Figure 3.6). Both NHC–Cu-allyl and NHC–Cu-allene intermediates preferentially coordinate the phosphinoyl aldimine through the mode depicted as the *favored* transition state, as confirmed by the (*S*)-configuration of the derived homoallylic and homopropargylic amides (X-ray crystal structure of **3.21f** corroborates the absolute sense of addition observed, Figure 3.6). The differences in the selectivity profiles (between allylcopper and allenylcopper) are likely spatial in nature;

---

[31] For Cu(II)-catalyzed additions of allenylboron **3.15** that provide hydrazines with up to 26% allene additions, see: "Copper(II) and Bismuth(III) Hydroxide Catalyzed Addition Reactions of Hydrazonoester with Allenylboronate in Aqueous Media," Kobayashi, S.; Kitanosono, T.; Ueno, M. *Synlett* **2010**, *13*, 2033–2036.

[32] For a detailed discussion regarding the competing pathways for allyl transfers and the modified catalyst structures, which led to improved facial selectivities in these cases, see Section 2.5 in Chapter 2.

Figure 3.6 Competing Transition States for Propargyl Additions with the Favored Approach Confirmed by the X-ray Structure of **3.21f**

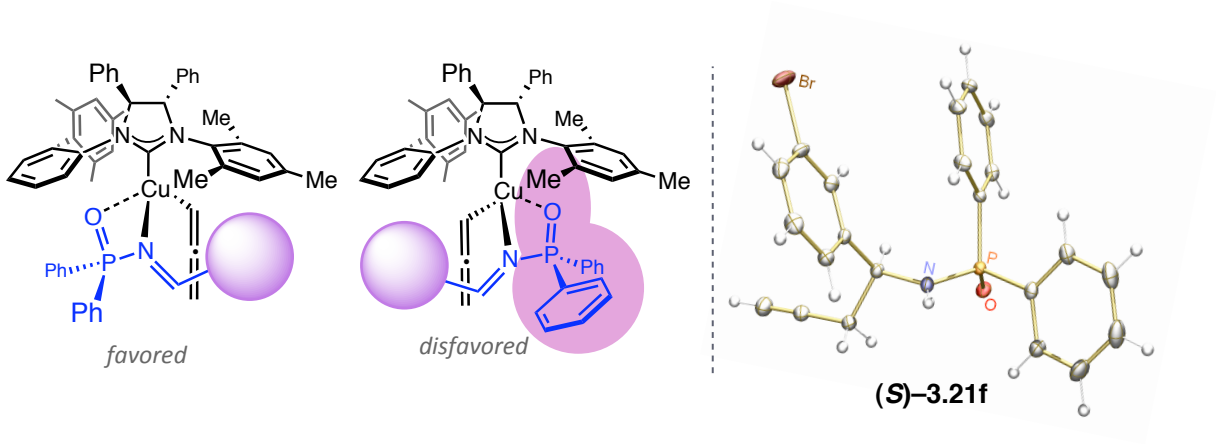

the sp-hybridized central carbon of the allene dictates a 180° conformation, such that alignment of the prochiral carbon of the imine for C–C bond formation may require a tilted substrate coordination (versus the chair-like 109° angles for the cyclic transition states in allyl additions). This alignment may position the imine substituent further from the right-hand side aryl-substituent of the carbene ligand in the *favored* pathway, while the *disfavored* transition state is not ameliorated.

Computational studies[33] are congruent with the hypothesized competing pathways (Figure 3.7). The calculated transition state structures in Figure 3.7 provide a viewpoint of the incipient C–C bond (a 180° rotation from the depicted competing transition states in Figure 3.6). The required alignment of the π* of the C=N bond with the filled π-system of the allene unit is energetically preferable in the *favored* pathway. When the opposite face of the imine is coordinated, the *disfavored* approach, the calculated structure predicts

[33] I am grateful to the mechanistic elucidation provided by the computational investigations set forth by my colleague Dr. Fredrik Haeffner.

Figure 3.7 Calculated Conformations and Energies of the Competing Pathways for Propargyl Addition from the NHC–Cu-allene Complex

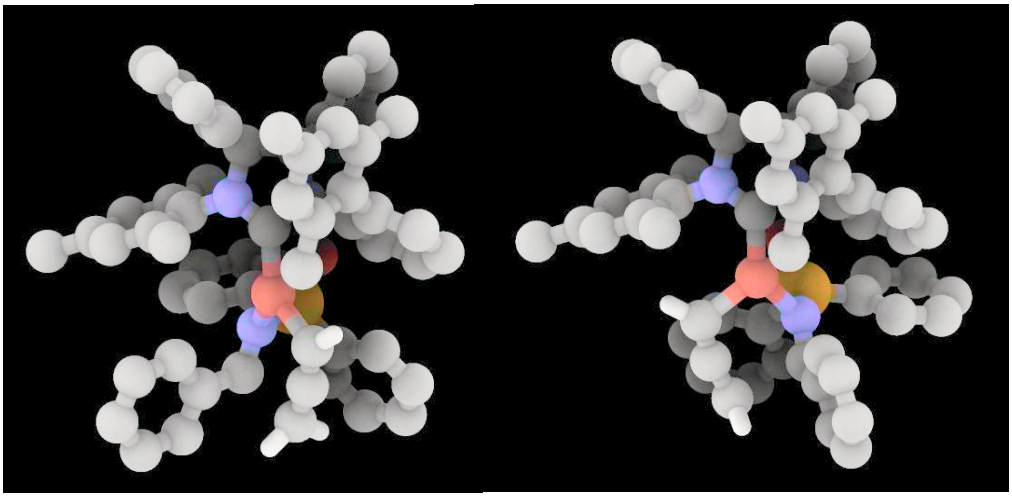

favored *disfavored*

a severe steric interaction between the phenyl unit of the phosphinoyl group and the biaryl *N*-substituent. Moreover, the energetic differentiation between the two possible transition states is calculated to be 2.5 kcal/mol.[34]

Computational experiments were also undertaken to elucidate the energetic profile of the potential isomerization event of the NHC–Cu-allene complex to the corresponding propargyl complex (Figure 3.8). The calculated free energies of the isomeric complexes reveal the allene-substituted copper to be 9.9 kcal/mol lower in energy than its constitutional isomer. The transition state for the intramolecular isomerization pathway[35] is calculated to be 16.8 kcal/mol. Moreover, attempts to estimate

---

[34] Such an energetic distinction should result in nearly perfect selectivity for the *S* enantiomer (>99:1 e.r.). Higher level calculations are required to produce more precise values for the Gibbs free energy activation barriers.

[35] Other possible methods for isomerization, such as the *intermolecular* pathway discussed for isomerization of the allylcopper species in Section 2.5, were not examined. For an account on the isomerization pathways available to isoelectronic allylzincs, see: "Bis(allyl)zinc Revisited: Sigma versus Pi Bonding of Allyl Coordination," Lictenberg, C.; Engel, J.; Spaniol, T. P.; Englert, U.; Raabe, G.; Okuda, J. *J. Am. Chem. Soc.* **2012**, *134*, 9805–9811.

Figure 3.8 Calculated Conformations and Energies of the Competing Pathways for Propargyl Addition from the NHC–Cu-allene Complex

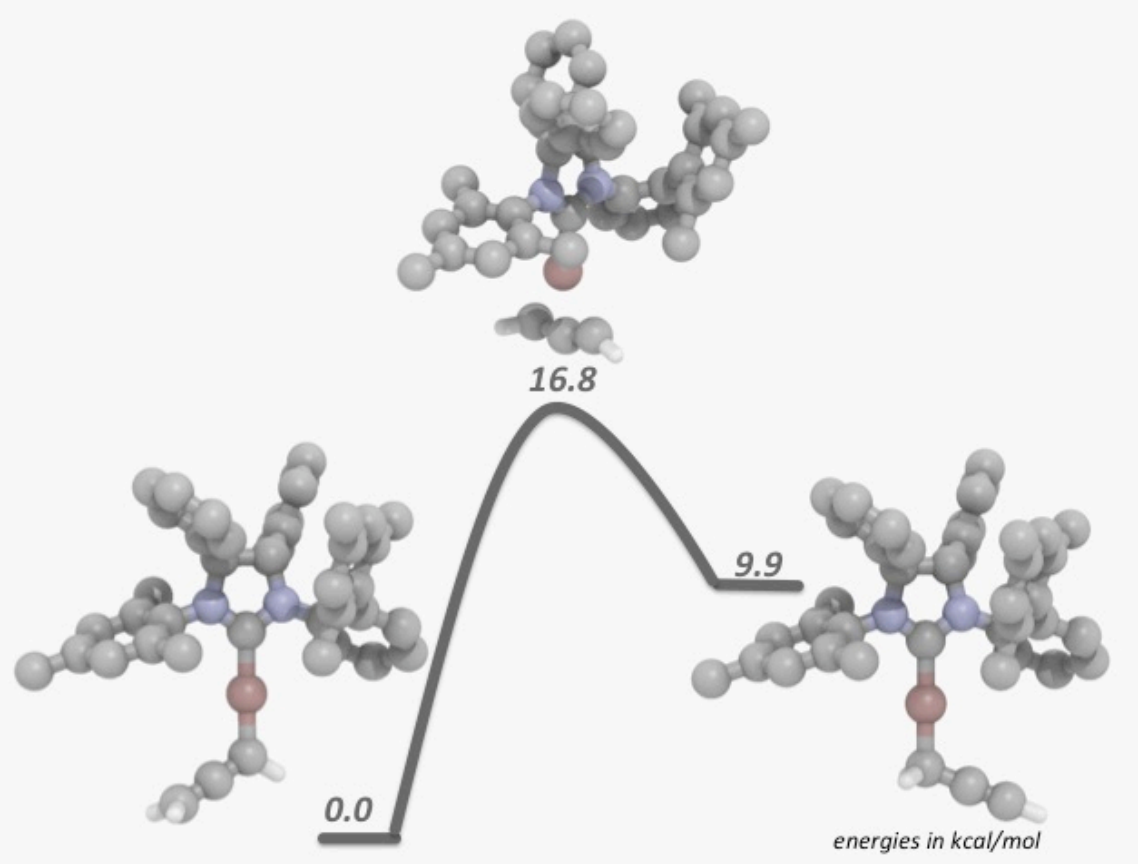

the requisite energy for propargyl transfer from the allenylcopper revealed a barrierless transition state, suggesting rapid C–C bond formation once the imine is bound or ligand transfer (O*t*-Bu→allene) occurs. This energetic profile has implications regarding the mechanism of ligand transfer between the NHC–Cu-OMe intermediate and allenylboron **3.15** for regeneration of the active NHC–Cu-allene intermediate (see ***TS I*** and ***TS II*** in Figure 3.4). There are two possibilities: either, sigma bond metathesis in ***TS II*** is operable such that NHC–Cu-allene ***ii*** is directly generated and its barrier to coordinate and react with a molecule of aldimine is lower than intramolecular isomerization; or, the ligand exchange occurs through an S_E2' mechanism, affording NHC–Cu-propargyl

complex ***i***, whose barrier to convert to the lower energy allene complex must be lower than the energy required for productive reaction with the substrate. Regardless of the mechanism of ligand transfer, reaction of an 85:15 isomeric mixture of propargyl borolane **3.25** (15% allenylboron **3.15**) provides evidence that isomerization prior to addition may be a viable pathway (equation 6).[36] Complete conversion to propargyl adduct **3.21a** suggests that the allenylcopper complex is the dominant active catalyst and all of the reaction must funnel through this intermediate.

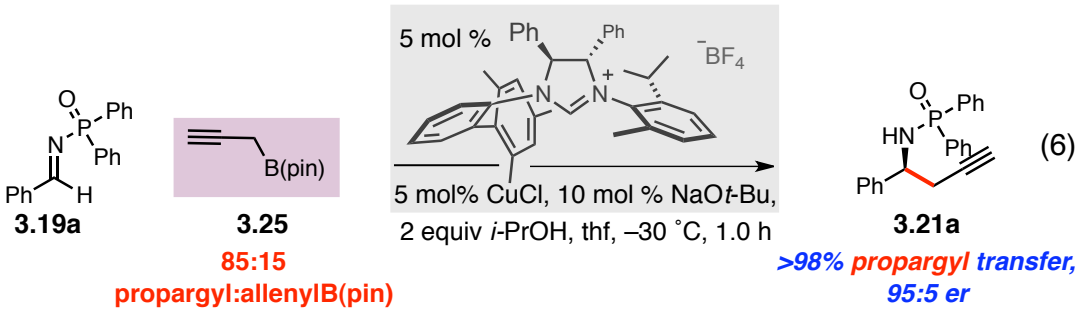

(6)

Due to the large discrepancy in energy between the corresponding NHC–Cu-allenyl and propargyl complexes (9.9 kcal/mol), there appeared to be minimal opportunity to affect the reaction so as to provide the unattainable allenic carbamines. The system would have to be altered in such a way to generate an effective concentration of the propargyl-substituted copper complex, such that S_E2' reaction with a phosphinoylaldimine would provide access to the α-allenyl amides. We postulated that steric modification of the allenyl/propargyl moiety could destabilize one of the isomerizing complexes, thereby affecting the k_{eq}. Transformations with γ-substituted propargylboron **3.26** would result in the isomeric copper complexes depicted in Scheme

[36] Reaction in equation 6 was performed by my colleague Nicholas Mszar towards our joint efforts for the discovery of conditions that provide allenic carbamines, the isomeric products unattainable from reactions with allenylboron **3.15**. The conditions employed: 2 equivalents of *iso*propanol, at –30 ºC with the Cu-catalyst derived from imidazolinium salt **3.27**, were identified, by Mr. Mszar, as optimal in the related transformations with propargyl borolane **3.26** in Scheme 3.6.

3.6; the trimethylsilyl substituent proximal to the copper center in the Cu-allene complex should raise the energy of this complex, in comparison to its proteo-analog, such that the ground state energies of the equilibrating species in Scheme 3.6 are less disparate (calculated to be 1.1 kcal/mol versus the 9.9 kcal/mol in the energy diagram in Figure 3.8). Correspondingly, transformations with trimethylsilylalkyne **3.26**, in the presence of the NHC–Cu complex derived from imidazolinium salt **3.27**, afford the silylated allene-bearing amide **3.28** in 95% yield and 95:5 e.r. within one hour.[36] The allene addition occurs with >95% selectivity, suggesting that, although there may be rapid equilibration, reaction occurs predominantly through the propargylcopper complex. It is also likely that the

Scheme 3.6 The Effect of Silicon-Substitution on the Product Distribution in the Reactions of Propargylboron **3.26**

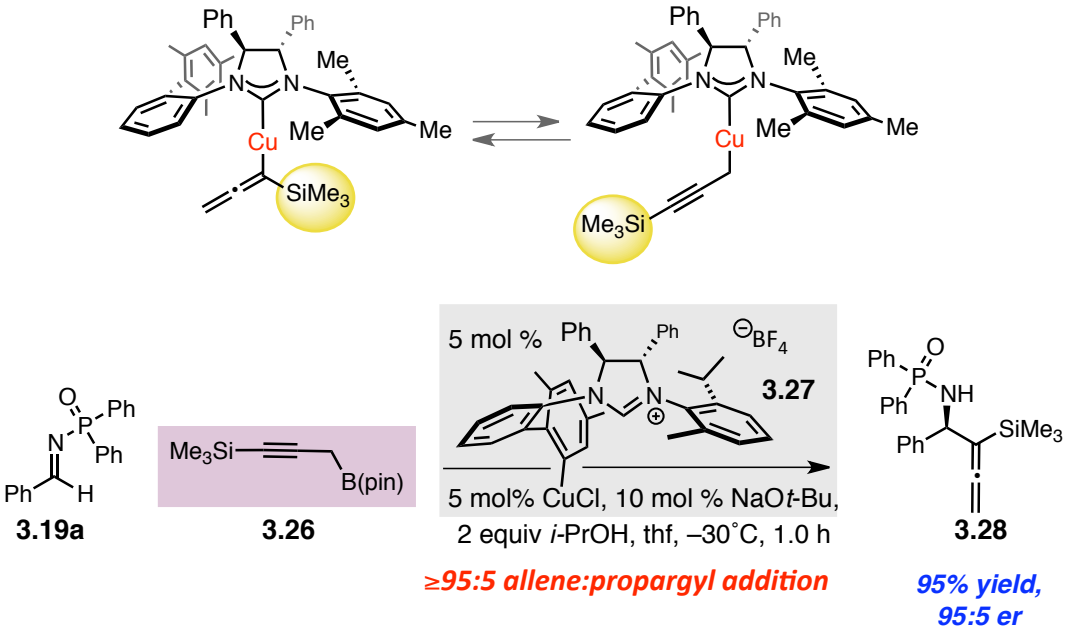

silyl-substitution may raise the barrier for substrate coordination/propargyl transfer from the allenylcopper due to the increased steric encumbrance at the copper center. Similar to reactions of allylcopper (Cu–C_{sp^3} bond), the silylated propargylcopper complex is

extremely reactive and thus short-lived, requiring short reaction times (typically 15 minutes for completion) yet 5 mol % catalyst loading to provide an effective concentration of the active catalyst.

3.5 Alkyne as a Functional Handle

The utility of homopropargylamines in the context of synthetic chemistry has been amply demonstrated with their application for the formation of various *N*-heterocycles, as discussed in the Introduction of this Chapter. We perceived that the alkyne unit could further serve as a surrogate group for a number of difficult-to-access functionalities, one such group being stereo-defined olefins. Stereoselective hydrometalations or carbometalations, as well as hydrogenations are well known transformations of alkynes. Application of these methodologies to the homopropargylic amine products described herein, would provide access to homoallylic amines with isomerically pure di-, tri-, or even tetra-substituted olefins. We set out to the demonstrate the significance of such an

Figure 3.9 Access to the Macrocyclic Lactam of the Aza-epothilones through a Suzuki Cross-Coupling Disconnection

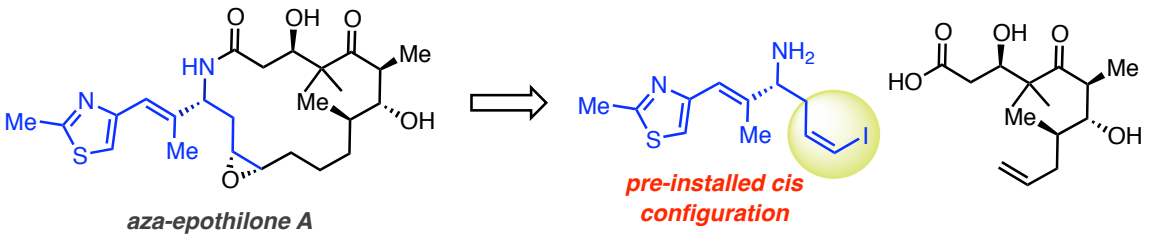

approach in the context of a synthetic strategy towards the biologically-relevant macrocyclic aza-epothilones.[37] The 16-membered macrolactam framework of the aza-

[37] (a) Preclinical Discovery of Ixabepilone, A Highly Active Antineoplastic Agent," Lee, F. Y. F.; Borzilleri, R.; Fairchild, C. R.; Kamath, A.; Smyklya, R.; Kramer, R.; Vite, G. *Cancer Chemother.*

epothilones can be disconnected in nearly equal parts, as shown in Figure 3.9. While amide-bond formations or macrolactamizations have been shown to proceed efficiently to bring together one part of the ring, C–C bond formation to unite the two halves of the molecule has proven much more challenging. Ring-closing metathesis strategies, uniting the two olefinic sites in ring closure, results in a thermodynamic mixture of *E*/Z-isomers of the new olefin, with the desired *cis*-olefin formed as half of the mixture at best.[38] A Wittig disconnection to afford the requisite *Z*-olefin also results in a equimolar mixture of the *cis* and *trans* olefin.[39] A more successful strategy entails cross-coupling technologies in which one of the cross partners has pre-defined stereochemistry.[40] In this vein, Danishefsky and coworkers employed a Suzuki cross-coupling, similar to the disconnection depicted in Figure 3.9, wherein the bishomoallylic alcohol undergoes

---

Pharamcol. **2008**, *63*, 157–166. (b) "Discovery of Ixabepilone," Hunt, J. T. *Mol*. *Cancer*. *Ther*. **2009**, *8*, 275–281.

[38] For a Ru-catalyzed RCM approach that resulted in a 5:1 ratio favoring the unnatural and poorly bioactive *E*-isomeric macrolactam, see: (a) "A Novel Application of a Pd(0)-Catalyzed Nucleophilic Substitution Reaction to the Regio- and Stereoselective Synthesis of Lactam Analogues of the Epothilone Natural Products," Borzilleri, R. M.; Zheng, X.; Schmidt, R. J.; Johnson, J. A.; Kim, S-H.; DiMarco, J. D.; Fairchild, C. R.; Gougoutas, J. Z.; Lee, F. Y. F.; Long, B. H.; Vite, G. D. *J. Am. Chem. Soc.* **2000**, *122*, 8890–8897. For a similar reactions that provides a 1:1 mixture of isomers, see: (b) "Synthesis and Biological Evaluation of Aza-Epothilones," Schinzer, D.; Altmann, K-H.; Stuhlmann, F.; Bauer, A.; Wartmann, M. *Chem. Bio. Chem.* **2000**, *1*, 67–70. For new molybdenum and tungsten-based RCM catalysts that have proven efficacious in providing *Z*-olefins in the synthesis of epothilones A–D, see: (c) "Synthesis of Macrocyclic Natural Products by Catalyst-Controlled Stereoselective Ring-Closing Metathesis," Yu, M.; Wang, C.; Kyle, A. F.; Jakubec, P.; Dixon, D. J.; Schrock, R. R.; Hoveyda, A. H. *Nature* **2011**, *479*, 88–93. (d) "Molybdenum-Based Complexes with Two Aryloxides and a Pentafluorimido Ligand: Catalysts for Efficient *Z*-Selective Synthesis of a Macrocyclic Trisubstituted Alkene by Ring-Closing Metathesis," Wang, C.; Haeffner, F.; Schrock, R. R. Hoveyda, A. H. *Angew. Chem., Int. Ed.* **2013**, *52*, 1939–1943.

[39] For a Witting strategy employed to access a similar framework for analogs of the epothilone series (lactone vs lactam rings), see: (a) "Total Syntheses of Epothilones A and B via a Macrolactonization-Based Strategy," Nicolaou, K. C.; Ninkovic, S.; Sarabia, F.; Vourloumis, D.; He, Y.; Vallberg, H.; Finlay, M. R> V.; Yang, Z. *J*. *Am*. *Chem*. *Soc*. **1997**, *119*, 7974–7991.(b) "Total Synthesis and Antitumor Activity of ZK-EPO: The First Fully Synthetic Epothilone in Clinical Development," Klar, U.; Buchmann, B.; Schwede, W.; Skuballa, W.; Hoffmann, J.; Lichtner, R. B. *Angew*. *Chem*., *Int*. *Ed*. **2006**, *45*, 7942–7948.

[40] (a) "On the Total Synthesis and Preliminary Biological Evaluations of 15(*R*) and 15(*S*) Aza-dEpoB: A Mitsunobu Inversion at C15 in Pre-Epothilone Fragments," Stachel, S. J.; Chappell, M. D.; Lee, C. B.; Danishefsky, S. J.; Chou, T-C.; He, L.; Horwitz, S. B. *Org. Lett.* **2000**, *2*, 1637–1639. (b) "On the Interactivity of Complex Synthesis and Tumor Pharmacology in the Drug Discovery Process: Total Synthesis and Comparative in Vivo Evaluations of the 15-Aza Epothilones," Stachel, S. J.; Lee, C. B.; Spassova, M.; Chappell, M. D.; Bornmann, W. G.; Danishefsky, S. J.; Chou, T-C.; Guam. Y. *J. Org. Chem.* **2001**, *66*, 4369–4378.

hydroboration followed by coupling of the resultant alkylborane with an amine-substituted *Z*-vinyl halide. We envisioned that straightforward installation of the requisite *Z*-olefin geometry for the Suzuki strategy set forth by Danishefsky for elaboration to the aza-epothilones, could be established through the intermediacy of the appropriately substituted homopropargylic amine.

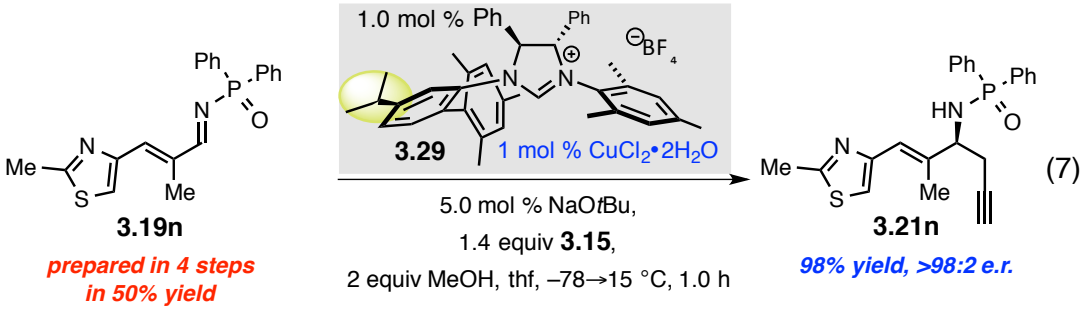

Over the course of examining the range of competent aldimine substrates that participate in highly selective propargyl group additions, we established that the thiazole-bearing tri-substituted olefin of **3.19n** was well tolerated, affording the derived propargyl adduct **3.21n** in 90% yield and 92:8 e.r. (with the catalyst derived from **3.20**, Figure 3.5). As demonstrated in equation 7, amide **3.21n**, required for elaboration to the aza-epothilones, can be obtained nearly quantitatively as a single enantiomer (>98:2 e.r.) in an hour. The catalyst prepared from copper(II) chloride dihydrate and imidazolinium salt **3.29**, a modified carbene precursor discovered for challenging additions of β-phenyl-substituted allyl units outlined in Chapter 2, is found to provide the superior facial selectivity.[41]

[41] Synthesis of sterically-demanding naphthyl-substituted **3.21b** can also be improved to 98:2 e.r. (from 95:5 e.r., see entry 2 in Table 3.2) with the Cu catalyst derived from *meta-iso*propyl substituted **3.29** vs. **3.20**. The change in the dihedral angle likely further destabilizes the *disfavored* approach (Figure 3.6) with steric interaction between the *iso*propyl group of the catalyst and the farther-extending imine substituent. See Section 2.5 in Chapter 2 for further details.

The strategies we conceived for conversion of the terminal alkyne in **3.21n** to the desired *cis*-vinyl halide entailed net-hydrogenation of the corresponding alkynyl iodide. The iodinated alkyne **3.30** can be readily prepared in quantitative yield with a Ag-catalyzed reaction with *N*-iodosuccinimide (Scheme 3.7). Many of the typical protocols for the *cis*-reduction of halo-alkynes, however, entail the use of highly Lewis acidic reagents, such as hydroboration/protonation or hydroalumination/protonation sequences, or Lindlar hydrogenations; unfortunately, such conditions are not compatible with the phosphinoyl-protected amines. The phosphine oxide moiety is a potent Lewis base donor, considerably more so than the π-system of the alkyne, leading to deactivation of boron and aluminum-based reagents, such that there is <2% conversion in the presence of dicyclochexylborane or di*iso*butylaluminum hydride. To avoid the added steps involved in protection of the amine with a less basic group, we searched for mild and compatible reagents for the *cis*-selective reduction. Reductions of iodoalkynes with *ortho*-nitrobenzenesulfonylhydrazide have proven to be a practical, functional group tolerant, and highly stereoselective method for the preparation of *cis*-vinyl iodides in a number of synthetic routes.[42] Reactions with *ortho*-nitrobenzenesulfonylhydrazide allow for mild conditions resulting in the slow-release of diimide, which reacts with the alkyne in a synchronous cyclic transtition state for the transfer of hydrogen.[43] Treatment of

[42] For selected examples of *cis*-reduction of iodoalkynes with *o*-NBSH, see: (a) "Studies toward Labeling Cytisine with [^{11}C]Phosgene: Rapid Synthesis of a δ-Lactam Involving a New Chemoselective Lithiation–Annulation Method," Rouden, J.; Seitz, T.; Lemoucheux, L.; Lasne, M-C. *J. Org. Chem.* **2004**, *69*, 3787–3793. (b) "Streamlined Syntheses of (–)-Dictyostatin, 16-Desmethyl-25, 26-dihydrodictyostatin, and 6-*epi*-16-Desmethyl-25,26-dihydrodictyostatin," Zhu, W.; Jimenez, M.; Jung W-H.; Camarco, D. P.; Balachandran, R.; Vogt, A.; Day, B. W.; Curran, D. P. *J. Am. Chem. Soc.* **2010**, *132*, 9175–9197.

[43] The higher energy *cis*-diimide has been implicated as the active hydrogen transfer reagent, as the process of hydrogen release has been calculated to be very exothermic from this species (~118 kcal/mol). For a detailed discussion of reductions with diimide, see: "Reduction with Diimide," Pasto, D. J.; Taylor, R. T. in *Organic Reactions Vol. 40* **1991**, John Wiley & Sons Inc. ed. Paquette, L. A.

Scheme 3.7 Elaboration of Alkyne **3.21n** to the Requisite *cis*-Vinyl Iodide for Elaboration to the Macrocyclic Lactam Core of the Aza-Epothilones

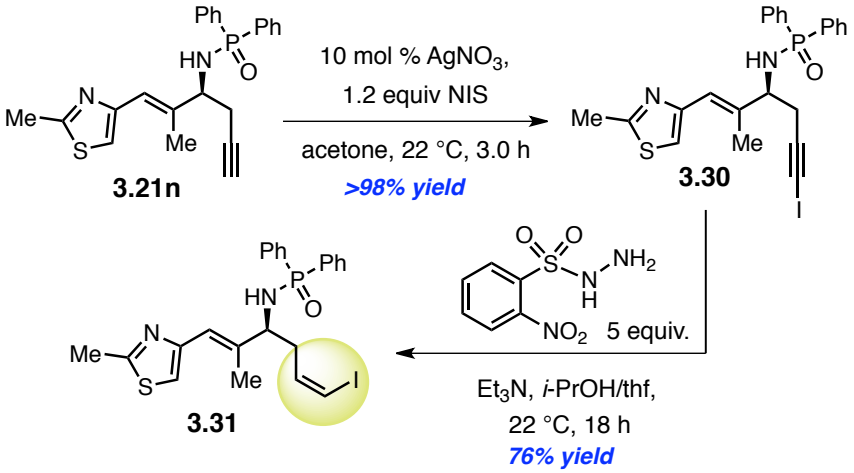

iodoalkyne **3.30** with five equivalents of *ortho*-nitrobenzenesulfonylhydrazide provides excellent site- and stereoselective reduction to afford *cis*-vinyl iodide **3.31** in 76% yield.[44] The practical and high-yielding synthesis of enantiopure amide **3.31** illustrates the potential for application of NHC–Cu-catalyzed propargyl additions towards the synthesis of the anti-cancer aza-epothilones, and derivatives thereof.

The versatility of the propargyl addition adducts can be further exemplified through an NHC–Cu catalyzed enantioselective diboration[45] of the alkyne unit (Scheme 3.8). In the presence of the NHC–Cu complex derived from copper(I) chloride and sulfonate-bearing imidazolinium salt **3.33**, homopropargylamide **3.21a** undergoes two consecutive Cu–B(pin) additions to install adjacent secondary and primary C–B bonds

[44] There is no reduction of the tri-substituted olefin, however, a small quantity of over-reduction to the alkyl iodide can be observed, but is readily separated from the vinyl iodide through treatment with an amine nucleophile (S_N2 displacement).

[45] For the mechanism and the rationalization for the site-selectivity of the two consecutive Cu-boryl additions to alkynes, see: "Vicinal Diboronates in High Enantiomeric Purity through Tandem Site-Selective NHC–Cu-Catalyzed Boron–Copper Additions to Terminal Alkynes," Lee, Y.; Jang, H.; Hoveyda, A. H. *J. Am. Chem. Soc.* **2009**, *131*, 18234–18235.

yielding highly functionalized amide **3.34** in 98% yield and 85:15 dr.[46] Moreover, the C–B bonds in 1,2-diboron **3.34** can be independently functionalized, through homologation, cross couplings, oxidation, and/or amination procedures to provide a vast array of enantioenriched small molecules. One such example is outlined in Scheme 3.8:

Scheme 3.8 NHC–Cu-Catalyzed Enantioselective Diboration of Alkyne **3.21a**, Synthesis of Versatile Diboron Intermediates **3.34**

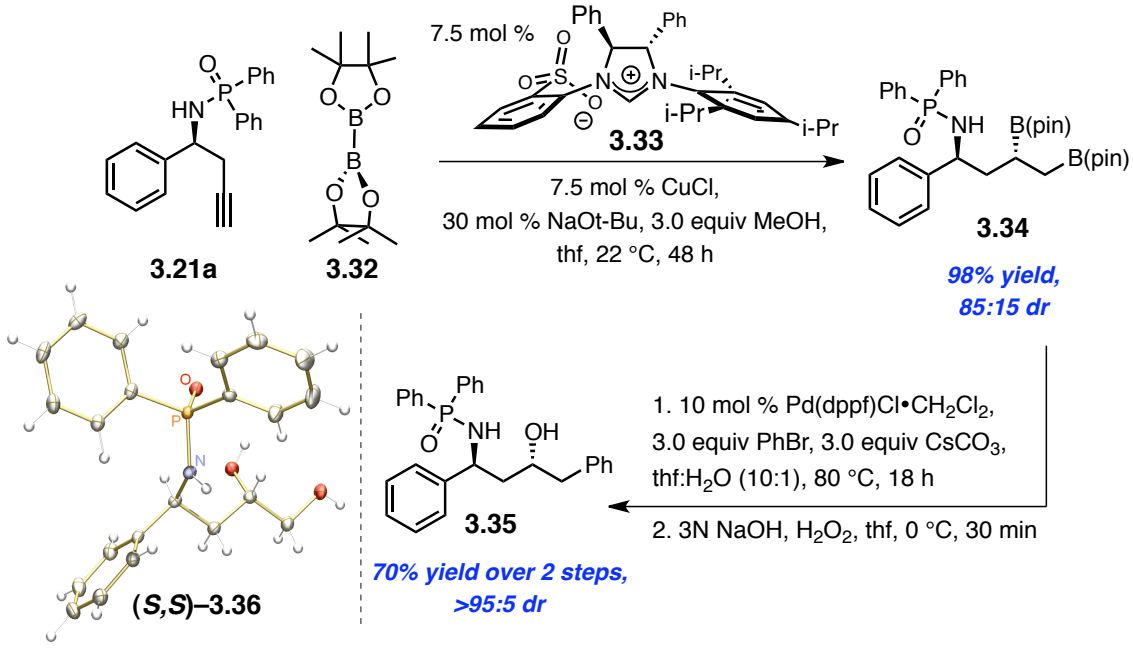

palladium-catalyzed Suzuki cross-coupling reaction of **3.34** selectively initiates the primary C–B bond to participate in C–C bond formation with bromobenzene, such that *anti*-1,3-aminoalcohol **3.35** can be isolated in >95:5 d.r. in 70% overall yield, after oxidation of the secondary C–B bond. Additionally, simple oxidation of the C–B bonds in **3.34** with aqueous hydrogen peroxide provides **(*S,S*)–3.36** in 80% yield after recrystallization (X-ray crystal structure in Scheme 3.8). The *anti* 1,3 relationship of the

[46] The major diastereomer of the bisboronate was identified as the *anti*-1,3 aminoboron through a crystal structure of the corresponding diol which can be accessed in >98% yield and shown in Scheme 3.8. The distereoselectivity of the transformation is catalyst and not substrate-controlled. Employing an achiral NHC–Cu catalyst provides the aminodiborons as a 1:1 mixture of diastereomers.

amine and alcohol moieties is a synthetically challenging structural motif encountered in the structures of biologically significant natural products.[47]

In addition to being a surrogate for the diol oxidation state that can be afforded by Cu-catalyzed diboration, the alkyne unit can be unmasked to provide the carboxylic acid oxidation state as well. A mild ruthenium-catalyzed oxidation[48] utilizing Oxone can be performed to transform alkyne **3.21p** to the homologous carboxylic acid **3.37** in 96% yield (Scheme 3.9). A deprotection can directly afford the β-amino acid, entities that have significant synthetic and biological applications.[49] There has been a great deal of

Scheme 3.9 Ru-Catalyzed Oxidation of Homopropargylic Amines to Access *β*-Amino Acid Derivatives

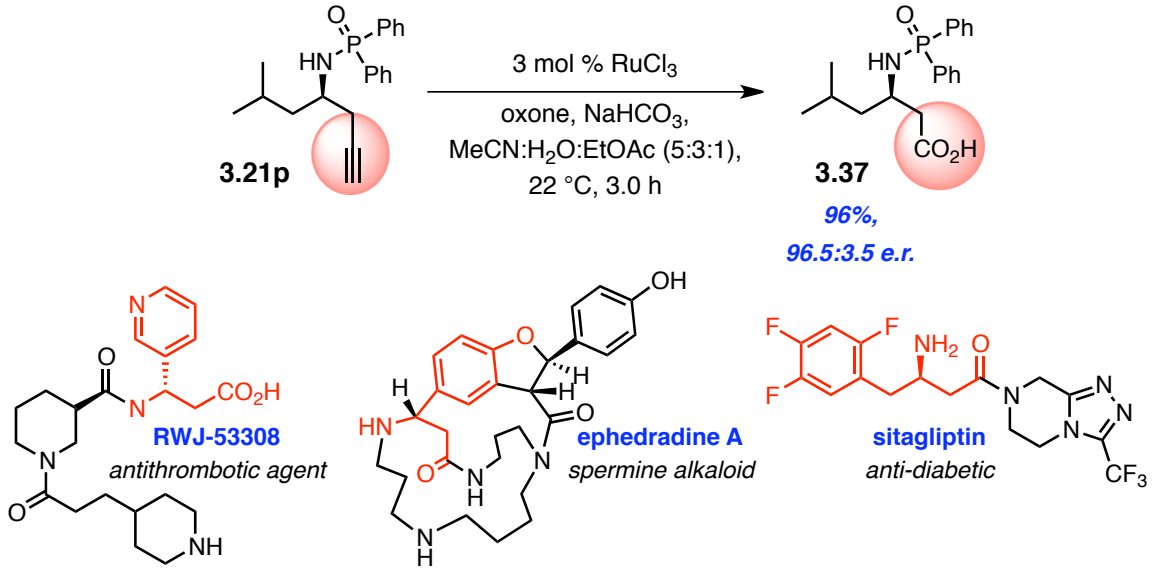

[47] For selected examples, see: (a) "First Synthesis of Polyoxin M," Shiro, Y.; Kato, K.; Fujii, M.; Ida, Y.; Akita, H. *Tetrahedron* **2006**, *62*, 8687–8695. (b) "Stereoselective Synthesis of Dendrobate Alkaloid (+)-241D and its C-4 epimer," Kumar, R. S. C.; Reddy, G. V.; Shankaraiah, G.; Babu, K. S.; Rao, J. M. *Tetrahedron Lett*. **2010**, *51*, 1114–1116.

[48] "Ruthenium-Catalyzed Oxidative Cleavage of Alkynes to Carboxylic Acids," Yang, D.; Chen, F.; Dong, Z-M.; Zhang, D-W. *J. Org. Chem*. **2004**, *69*, 2221–2223.

[49] For a review detailing the significance of β-amino acids, see: "The World of *β*- and *γ*-Peptides Comprised of Homologated Proteinogenic Amino Acids and Other Components," Seebach, D.; Beck, A. K.; Bierbaum, D. J. *Chem. Biodiversity* **2004**, *1*, 1111–1239.

synthetic effort to access the β-amino acid cores of biologically actives targets such as: RWJ-53308,[50] ephedradine A,[51] and sitagliptin,[52] the active pharmaceutical agent in Januvia®. The two-step protocol that imparts stereogenicity with concomitant three-carbon homologation, followed by oxidation represents a streamlined synthetic strategy to access these enantioenriched structural motifs.

3.6 Conclusions

The ability to promote facile ligand exchange between Cu-alkoxide complexes with boron-based reagents has enabled the discovery of the first practical, general, and efficient method for the catalytic enantioselective generation of homopropargylic amines. The protocol requires a catalyst that can be prepared *in situ* from an inexpensive and air-stable copper(II) salt, a chiral ligand that can be synthesized in four to five steps, and a commercially available and stable allenylboron. Transformations proceed with excellent group-transfer and facial selectivity with a broad range of aryl-, alkyl-, alkenyl-, and heterocycle-containing phosphinoyl aldimines to exclusively afford the alkyne-substituted products in >92:8 e.r. and >80% yield.

The utility of the alkyne-bearing products has been demonstrated through conversions to enantiomerically enriched amine-containing building blocks that are

---

[50] "Potent, Orally Active GPIIb/IIIa Antagonists Containing a Nipecotic Acid Subunit. Structure–Activity Studies Leading to the Discovery of RWJ-53308," Hoekstra, W. J.; Maryanoff, B. E.; Damiano, B. P.; Andrade-Gordon, P.; Cohen, J. H.; Constanzo, M. J.; Haertlein, B. J.; Hecker, L. R.; Hulshizer, B. L.; Kauffman, J. A.; Keane, P.; McComset, D. F.; Mitchell, J. A.; Scott, L.; Shah, R. D.; Yabut, S. C. *J. Med. Chem.* **1999**, *42*, 5254–5265.

[51] "Stereocontrolled Total Synthesis of (–)-Ephedradina A (Orantine)," Kurosawa, W.; Kan, T.; Fukuyama, T. *J. Am. Chem. Soc.* **2003**, *125*, 8112–8113.

[52] "Highly Efficient Asymmetric Synthesis of Sitagliptin," Hansen, K. B.; Hsiao, Y.; Xu, F.; Rivera, N.; Clausen, A.; Kubryk, M.; Krska, S.; Rosner, T.; Simmons, B.; Balsells, J.; Ikemoto, N.; Sun, Y.; Spindler, F.; Malan, C.; Grabowski, E. J. J.; Armstrong, J. D., III *J. Am. Chem. Soc.* **2009**, *131*, 8798–8804.

otherwise difficult to access. The appended alkyne unit can be transformed to an isomerically pure *cis*-vinyl iodide, a functionality that can allow for elaboration to the 15-aza-epothilones, a family of lactam macrocylces that exhibit superior pharmacokinetic profiles to their naturally-occurring lactone analogs. Enantioselective NHC–Cu-boryl additions to the unsaturations afford 1,2-diboron compounds that can be stereoselectively functionalized to access a myriad of α-chiral amines of various substitution patterns, such as *anti*-1,3-aminoalcohols. Finally, ruthenium-catalyzed oxidative cleavage of the alkyne was demonstrated as a strategy to rapidly access biologically significant β-amino acids.

Studies toward the extension of the NHC–Cu-catalyzed processes to a variety of electrophiles and to activation of other boron-based reagents, principally vinyl and propargyl-substituted borons, to afford reactive NHC–Cu species, are the subject of current investigations. Moreover, our research has begun to focus on transformations that can *in situ* generate the reactive Cu-based intermediates, described herein and in Chapter 2, through a tandem process, obviating the need for preformed allylboron or allenylboron reagents. Boron-substituted NHC–Cu-allyl complexes, for instance, can be accessed instead from site-selective Cu-boryl additions to allenes, producing competent nucleophiles for additions to carbonyls, imines, and allylic phosphates.

3.7 Experimentals

General. Infrared (IR) spectra were recorded on a Bruker FT–IR alpha (ATR mode) spectrophotometer, n_{max} in cm^{-1}. Bands are characterized as broad (br), strong (s), medium (m), and weak (w). ^{1}H NMR spectra were recorded on a Varian Unity INOVA 400 (400 MHz) spectrometer. Chemical shifts are reported in ppm from tetramethylsilane with the

solvent resonance as the internal standard ($CDCl_3$: δ 7.26 ppm). Data are reported as follows: chemical shift, integration, multiplicity (s = singlet, d = doublet, t = triplet, q = quartet, sept = septet, br = broad, m = multiplet), and coupling constants (Hz). ^{13}C NMR spectra were recorded on a Varian Unity INOVA 400 (100 MHz) spectrometer with complete proton decoupling. Chemical shifts are reported in ppm with the solvent resonance as the internal standard ($CDCl_3$: δ 77.16 ppm). High-resolution mass spectrometry was performed on a JEOL AccuTOF-DART (positive mode) at the Mass Spectrometry Facility, Boston College. Enantiomer ratio (e.r.) values were determined by analytical liquid chromatography (HPLC) analysis on a Shimadzu chromatograph (Chiral Technologies Chiralcel OD (4.6 x 250 mm), Chiral Technologies Chiralcel OD-H (4.6 x 250 mm), Chiral Technologies Chiralcel OJ-H (4.6 x 250 mm), Chiral Technologies Chiralpak AD-H (4.6 x 250 mm)). Specific rotations were measured on a Rudolph Research Analytical Autopol IV Polarimeter.

Unless otherwise noted, all reactions were carried out with distilled and degassed solvents under an atmosphere of dry N_2 in oven- (135 °C) or flame-dried glassware with standard dry box or vacuum-line techniques. All work-up and purification procedures were carried out with reagent grade solvents (purchased from Fisher) in air. Aryl-, heteroaryl-, and alkenyl- *N*-diphenylphosphinoyl imines were synthesized through the use of a condensation promoted by $TiCl_4$ between *P*,*P*-diphenylphosphinic amide and the corresponding aldehyde.[53] Alkyl-substituted aldimines as well as **2f** and **2g** were synthesized through the intermediacy of the corresponding sulfinyl adducts according to

[53] (a) "The Titanium Tetrachloride Induced Synthesis of *N*-Phosphinoylimines and *N*-Sulphoylimines Directly from Aromatic Aldehydes," Jennings, W. B.; Lovely, C. J. *Tetrahedron.* **1991**, *47*, 5561–5568. (b) "The First Catalytic Asymmetric Nitro-Mannich-type Reaction Promoted by a New Heterobimetallic Complex," Yamada, K-i.; Harwood, S. J.; Gröger, H.; Shibasaki, M. *Angew. Chem., Int. Ed.* **1999**, *38*, 3504–3506.

previously disclosed methods.[54]

▪ **Reagents:**

Acetone: Purchased from Aldrich (ACS reagent) and used as received.

Allenylboronic acid pinacol ester: Purchased from Frontier Scientific, Inc. and used as received.

Copper (I) Chloride: Purchased from Strem and used as received.

Copper (II) Chloride Dihydrate: Purchased from Aldrich and used as received.

Hydrochloric Acid: Purchased from Fisher and used as received.

Imidazolinium Tetrafluoroborate Salt 3.20: Prepared according to a previously reported procedure.[55]

Imidazolinium Tetrafluoroborate Salt 3.27 and 3.29: Prepared according to a previously reported procedure.[56]

Imidazolinium Tetrafluoroborate Salt 3.33: Prepared according to a previously reported procedure.[45]

Isopropanol: Purchased from Fisher and used as received.

Methanol: Purified by distillation from Mg (Strem) prior to use or anhydrous methanol (99.9%, Acroseal) purchased from Acros and used as received.

***N*-Iodosuccinimide**: Purchased from Aldrich and recrystallized prior to use.

Oxone: Purchased from Aldrich and used as received.

***ortho*-Nitrobenzenesulfonylhydrazide**: Prepared according to a previously reported

---

[54] (a) "Catalytic Asymmetric Addition of Diorganozinc Reagents to *N*-Phosphinoylalkylimines," Côté, A.; Boezio, A. A.; Charette, A. B. *Proc. Natl. Acad. Sci.* **2004**, *101*, 5405–5410. (b) "Direct Catalytic Asymmetric Mannich-type Reactions of Isomerizable Aliphatic Imines: Chemoselective Enolate Formations from a Hydroxyketones by a Zn-Catalyst," Yamaguchi, A.; Matsunaga, S.; Shibasaki, M. *Tetrahedron Lett.* **2006**, *47*, 3985–3989.

[55] "Monodentate Non-C_2-symmetric Chiral *N*-Heterocyclic Carbene Complexes for Enantioselective Synthesis. Cu-Catalyzed Conjugate Additions of Aryl- and Alkenylsilylfluorides to Cyclic Enones,"Lee, K-S.; Hoveyda, A. H. *J. Org. Chem.* **2009,** *74*, 4455–4462.

[56] "Enantioselective Synthesis of Homoallylic Amines through Reactions of (Pinacolato)allylborons with Aryl-, Heteroaryl-, Alkyl-, or Alkene-Substituted Aldimines Catalyzed by Chiral C_1-Symmetric NHC–Cu Complexes," Vieira, E. M.; Snapper, M. L.; Hoveyda, A. H. *J. Am. Chem. Soc.* **2011**, *133*, 3332–3335.

procedure.[57]

Ruthenium Trichloride: Purchased from Strem and used as received.

Silver Nitrate: Purchased from Aldrich and used as received.

Sodium Bicarbonate: Purchased from Fisher and used as received.

Sodium *tert*-butoxide: Purchased from Strem and used as received.

Tetrahydrofuran: Purchased from Aldrich and purified by distillation from sodium benzophenone ketyl immediately prior to use.

Triethylamine: Purchased from Aldrich and purified by distillation over CaH_2 prior to use.

▪ **Representative Procedure for NHC–Cu-Catalyzed Enantioselective Propargyl Group Additions to *N*-diphenylphosphinoylimines Using CuCl:** *Preparation of the chiral NHC–Cu catalyst:* An oven-dried vial equipped with a stir bar was charged with imidazolinium salt **3.20** (12.5 mg, 20.0 μmol), NaO*t*-Bu (4.6 mg, 48 μmol), and CuCl (1.9 mg, 20 μmol). The vial was sealed with a septum and Teflon tape and removed from the glovebox. Freshly distilled thf (1.00 mL) was added and the mixture was allowed to stir for 15 min under N_2 at 22 °C.

A separate oven-dried vial equipped with a stir bar was charged with allenylboron **3.15** (25.0 μL, 0.140 mmol). The vial was sealed with a septum and electrical tape and purged with N_2. An appropriate portion of the stock solution of the NHC–Cu complex (250. μL) was transferred to the vial and the solution was allowed to cool to –78 °C (dry ice/acetone bath). A solution of aldimine **3.19a** (35.0 mg, 0.100 mmol) in freshly distilled thf (250. μL) and MeOH (8.1 μL, 0.20 mmol) was then transferred to the vial

[57] "Preparation of the Reagent *o*-Nitrobenzenesulfonylhydrazide," Myers, A. G.; Zheng, B.; Movassaghi, M. *J. Org. Chem.* **1997**, *67*, 7507.

containing allenylboron **3.15** and the NHC–Cu complex at –78 °C. The mixture was allowed to stir for six hours at –50 °C before addition of an aqueous 1 M solution of HCl (1.0 mL). The solution was allowed to warm to 22 °C and the reaction mixture was diluted with AcOEt. The layers were separated and the water layer was washed with AcOEt (3 x 2 mL). The organic layers were combined and dried with $MgSO_4$ and the volatiles were removed *in vacuo*. The unpurified residue obtained as an off-white solid was purified by silica gel chromatography (a gradient from 1:1 hexanes:Et_2O to 100% Et_2O was used to remove pinacol from the mixture followed by 4:1 AcOEt:hexanes to 100% AcOEt) to yield 33.8 mg (0.094 mmol, 94% yield) of pure **3.21a** as a white crystalline solid in 96.5:3.5 e.r..

▪ **Representative Procedure for NHC–Cu-Catalyzed Enantioselective Propargyl Group Additions to *N*-diphenylphosphinoylimines Using $CuCl_2$•$2H_2O$:** *Preparation of the chiral NHC–Cu catalyst:* An oven-dried vial equipped with a stir bar was charged with imidazolinium salt **3.20** (6.2 mg, 10. μmol), NaO*t*-Bu (4.8 mg, 50. μmol), and $CuCl_2$•$2H_2O$ (1.7 mg, 10. μmol). The vial was sealed with a septa and electrical tape, and purged with a dry atmosphere of N_2. Freshly distilled thf (1.00 mL) was added and the mixture was allowed to stir for 15 min under N_2 at 22 °C.

Another oven-dried vial equipped with a stir bar was charged with allenylboron **3.15** (25.0 μL, 0.140 mmol). The vial was sealed with a septum and Teflon tape and purged with N_2. An appropriate portion of the stock solution of the NHC–Cu complex (100. μL) was transferred to the vial and the solution was allowed to cool to –78 °C (dry ice/acetone bath). A solution of aldimine **3.19a** (35.0 mg, 0.100 mmol) in freshly distilled thf (250. μL) and MeOH (8.1 μL, 0.20 mmol) was then transferred to the vial

containing allenylboron **3.15** and the NHC–Cu complex at –78 °C. The reaction mixture was then allowed to warm to –15 °C over the period of an hour before the addition of an aqueous 1 M solution of HCl (1.0 mL). The solution was allowed to warm to 22 °C and was diluted with AcOEt. The layers were separated and the water layer was washed with AcOEt (3 x 2 mL). The organic layers were combined and dried with $MgSO_4$ and the volatiles were removed *in vacuo* and the unpurified residue obtained was purified as described above to obtain 33.1 mg (0.096 mmol, 96% yield) of **3.21a** as a white crystalline solid in 96:4 e.r..

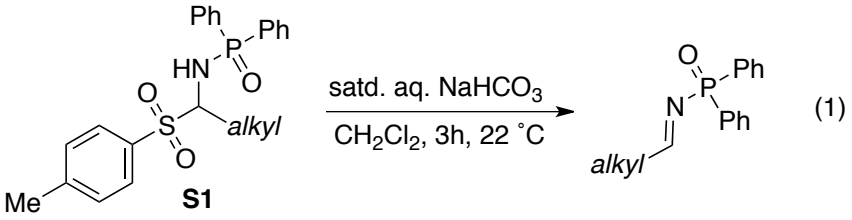

(1)

▪ **Representative Procedure for NHC–Cu-Catalyzed Enantioselective Propargyl Additions to Alkyl-Substituted *N*-diphenylphosphinoyl imines**: *Preparation of the alkyl-substituted aldimine (equation 1)*: A vial equipped with a stir bar was charged with sulfinyl adduct **S1** (0.06 mmol) to which was added CH_2Cl_2 (12.0 mL) and a saturated aqueous solution of $NaHCO_3$ (12.0 mL) consecutively. The biphasic mixture was allowed to stir vigorously for three hours at 22 °C. The organic layer was separated and the aqueous phase was washed with CH_2Cl_2 (2 x 6 mL). The combined organic layers were dried over $MgSO_4$. The volatiles were removed under reduced pressure and the unpurified imine was used without further purification in the Cu-catalyzed propargyl group additions.

An oven-dried vial equipped with a stir bar was charged with allenylboron **3.15** and the vial was sealed with a septum and electrical tape and purged with N_2. An appropriate portion of the stock solution of the NHC–Cu complex (see above) was transferred to the vial containing the boron reagent at 22 °C and allowed to stir for five minutes. The solution was then allowed to cool to –78 °C (dry ice/acetone bath) and an appropriate portion of the abovementioned freshly prepared alkyl-substituted aldimine as a solution in freshly distilled thf (0.2 M) and MeOH (2.0 equiv) was added. The reaction was then carried out as described above and quenched by the addition of an aqueous 1 M solution of HCl (1.0 mL). The solution was allowed to warm to 22 °C and the mixture diluted with AcOEt. The organic layer was separated and the aqueous layer was washed with AcOEt (3 x 2 mL). The organic layers were combined and dried with $MgSO_4$. The volatiles were removed *in vacuo*. The resulting residue obtained as an off-white solid was purified by silica gel chromatography (the same conditions in the general procedure for allyl addition to aldimine **3.19a**).

▪ ***Analytical Data for Hompropargylamides* 3.21a–3.32n**:

(*S*)–*P*,*P*-Diphenyl-*N*-(1-phenylbut-3-yn-1-yl)phosphinic amide (**3.21a**): mp = 135–137 °C. IR (neat): 3284 (w), 3133 (w, br), 1461 (m), 1438 (m), 1196 (s), 1181 (s), 1091 (m), 1068 (m), 950 (m), 721 (m), 693 (s), 570 (m), 519 (s) cm^{-1}; ^1H NMR (400 MHz, $CDCl_3$): δ 7.86–7.80 (2H, m), 7.78–7.72 (2H, m), 7.45–7.40 (1H, m), 7.39–7.34 (3H, m), 7.31–7.19 (7H, m), 4.46 (1H, dddd, *J* = 10.4, 6.4, 4.4, 4.4 Hz), 3.66 (1H, br dd, *J* = 10.4, 6.4 Hz), 2.86 (1H, ddd, *J* = 16.8, 6.4, 2.4 Hz), 2.71 (1H, ddd, *J* = 16.8, 4.0, 2.8 Hz), 1.91 (1H, t, *J* = 2.6 Hz); ^{13}C NMR (100 MHz, $CDCl_3$): δ 141.9 (d, *J* = 6.0 Hz), 132.9 (d, *J* = 127 Hz), 132.6 (d, *J* = 8.9 Hz), 132.11 (d, *J* = 2.9 Hz), 132.08 (d, *J* = 3.0 Hz, only the

peak at 132.1 is visible, the other is overlapping), 132.0 (d, J = 130 Hz), 131.97 (d, J = 9.7 Hz), 128.7 (d, J = 12.6 Hz), 128.6 (d, J = 12.6 Hz), 128.5, 127.6, 126.6, 80.1, 72.1, 52.8, 29.3 (d, J = 3.7 Hz); HRMS Calcd for $C_{22}H_{21}NOP$ $[M + H]^+$: 346.13608; Found: 346.13668. $[\alpha]^{25}_D$ = –21.3 (c = 1.00, $CHCl_3$) for a 97.5:2.5 e.r. sample. The enantiomeric purity of this compound was determined by HPLC analysis in comparison with authentic racemic material (Chiracel OJ-H, 91:9 hexanes:*i*-PrOH, 0.8 mL/min, 220 nm): t_R of **3.21a**: 13 min (major) and 22 min (minor).

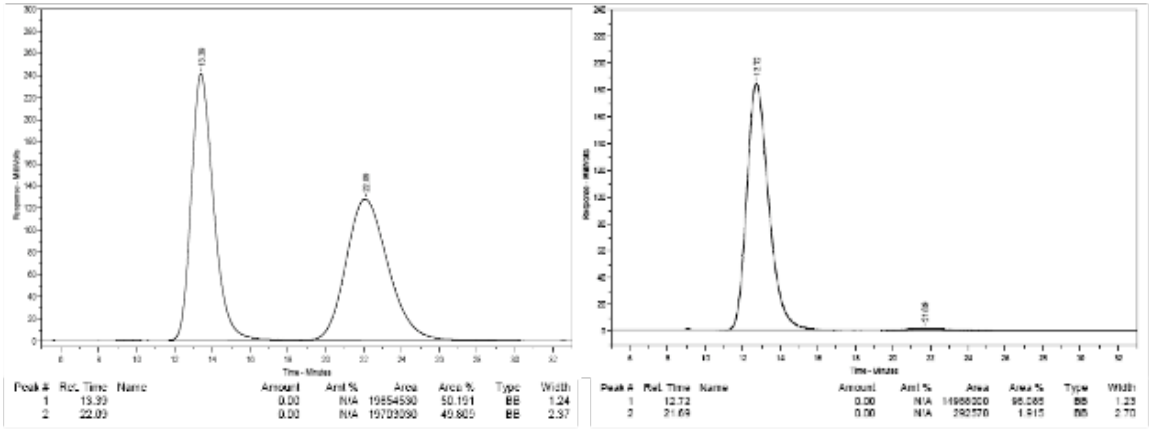

Peak #	Ret. Time	Area %	Peak #	Ret. Time	Area %
1	13.3 min	50.191	1	12.7 min	98.085
2	22.1 min	49.809	2	21.7 min	1.915

(*S*)–*N*-(1-(Naphthalen-2-yl)but-3-yn-1-yl)-*P*,*P*-diphenylphosphinic amide (3.21b): mp = 158–159 °C. IR (neat): 3167 (w, br), 1438 (m), 1185 (s), 1123 (m), 1109 (m), 1072 (m), 908 (m), 818 (m), 747 (m), 726 (s), 696 (s), 539 (m), 478 (m) cm^{-1}; ^1H NMR (400 MHz, $CDCl_3$) δ 7.96–7.90 (2H, m), 7.87–7.80 (5H, m), 7.75 (1H, br s), 7.55–7.42 (7H, m), 7.36–7.32 (2H, m), 4.64 (1H, dddd, J = 10.4, 6.4, 4.0, 4.0 Hz), 3.79 (1H, br dd, J = 10.4, 6.4 Hz), 3.03 (1H, ddd, J = 16.8, 6.4, 2.4 Hz), 2.88 (1H, ddd, J = 16.8, 4.0, 2.8 Hz), 1.97 (1H, t, J = 2.4 Hz); ^{13}C NMR (100 MHz, $CDCl_3$): δ 139.3 (d, J = 5.9 Hz), 133.2, 132.9, 132.88 (d, J = 127 Hz), 132.6 (d, J = 9.7 Hz), 132.1 (d, J = 2.2 Hz), 132.04 (d, J

= 3.0 Hz, only the peak at 132.1 is visible, the other is overlapping), 132.0 (d, J = 9.7 Hz), 131.9 (d, J = 130 Hz), 128.7 (d, J = 12.6 Hz), 128.6 (d, J = 12.7 Hz), 128.4, 128.2, 127.7, 126.3, 126.1, 125.4, 124.7, 80.1, 72.2, 53.0, 29.3 (d, J = 3.0 Hz); HRMS Calcd for $C_{26}H_{23}NOP$ $[M + H]^+$: 396.15173; Found: 396.15297. $[\alpha]^{25}_D$ = –47.2 (c = 1.00, $CHCl_3$) for a 98:2 e.r. sample. The enantiomeric purity of this compound was determined by HPLC analysis in comparison with authentic racemic material (Chiracel OJ-H, 90:10 hexanes:*i*-PrOH, 0.8 mL/min, 220 nm): t_R of **3.21b**: 15 min (major) and 34 min (minor).

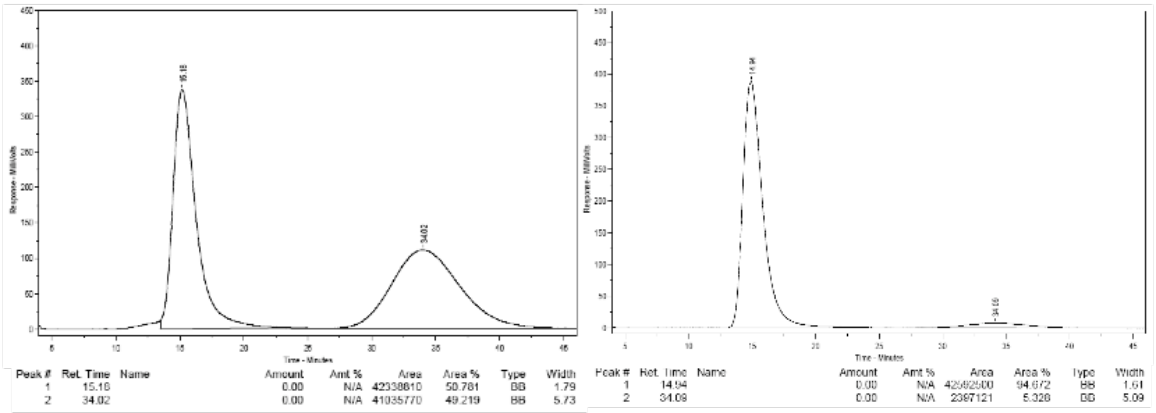

Peak #	Ret. Time	Area %	Peak #	Ret. Time	Area %
1	15.2 min	50.781	1	14.9 min	94.672
2	34.0 min	49.219	2	34.1 min	5.328

(*S*)–*N*-(1-(2-Fluorophenyl)but-3-yn-1-yl)-*P*,*P*-diphenylphosphinic amide (**3.21c**): mp = 138–139 °C. IR (neat): 3141 (w, br), 2893 (w, br), 1492 (m), 1456 (m), 1438 (m), 1194 (m), 1179 (m), 1108 (m), 1070 (m), 889 (m), 798 (m), 750 (m), 721 (s), 693 (s), 643 (m), 552 (m), 530 (s) cm^{-1}; ^1H NMR (400 MHz, $CDCl_3$): δ 7.91–7.85 (1H, m), 7.83–7.78 (2H, m), 7.53–7.41 (4H, m), 7.39–7.33 (3H, m), 7.13 (1H, ddd, J = 10.8, 8.0, 0.8 Hz), 6.98 (1H, ddd, J = 7.6, 7.6, 1.6 Hz), 4.65 (1H, dddd, J = 16.4, 6.8, 6.8, 4.8 Hz), 3.85 (1H, br dd, J = 11.6, 6.8 Hz), 2.93 (1H, ddd, J = 16.8, 6.8, 2.8 Hz), 2.82 (1H, ddd, J = 16.8, 4.8, 2.8 Hz), 1.95 (1H, t, J = 2.6 Hz); ^{13}C NMR (100 MHz, $CDCl_3$): δ 160.1 (d, J = 244 Hz),

132.6 (d, J = 127 Hz), 132.5 (d, J = 9.6 Hz), 132.2 (d, J = 3.0 Hz), 132.1 (d, J = 2.2 Hz), 132.0 (d, J = 9.7 Hz), 131.8 (d, J = 130 Hz), 129.3 (d, J = 8.1 Hz), 128.9 (dd, J = 12.7, 5.2 Hz), 128.71, 128.69 (d, J = 12.7 Hz), 128.6 (d, J = 12.7 Hz), 124.1 (d, J = 3.7 Hz), 115.6 (d, J = 21.6 Hz), 79.8, 71.9, 48.9, 28.5 (dd, J = 4.4, 3.7 Hz); HRMS Calcd for $C_{22}H_{20}FNOP$ $[M + H]^+$: 364.12665; Found: 364.12584. $[\alpha]^{25}_D$ = –19.6 (c = 1.00, $CHCl_3$) for a 97.5:2.5 e.r. sample. The enantiomeric purity of this compound was determined by HPLC analysis in comparison with authentic racemic material (Chiracel OJ-H, 92:8 hexanes:*i*-PrOH, 0.8 mL/min, 220 nm): t_R of **3.21c**: 13 min (major) and 19 min (minor).

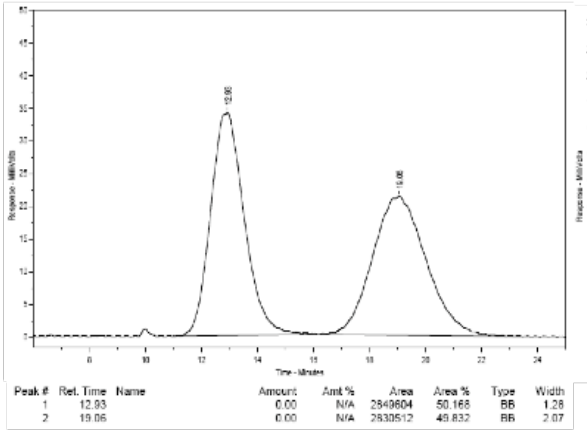

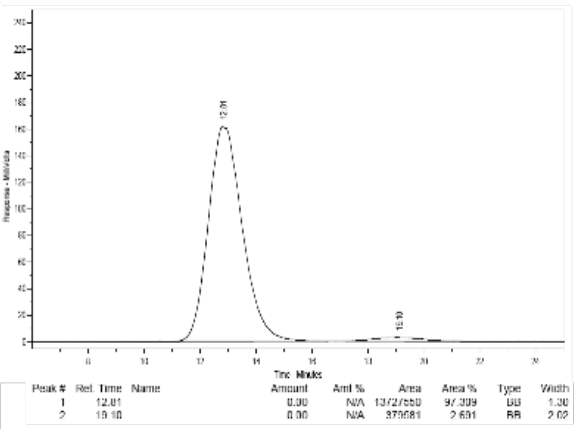

Peak #	Ret. Time	Area %	Peak #	Ret. Time	Area %
1	12.9 min	50.168	1	12.8 min	97.309
2	19.1 min	49.832	2	19.1 min	2.691

(*S*)–*P*,*P*-Diphenyl-*N*-(1-(*o*-Tolyl)but-3-yn-1-yl)phosphinic amide (**3.21d**): mp = 154–155 °C. IR (neat): 3165 (w, br), 3054 (w), 1438 (m), 1186 (s), 1123 (m), 1110 (m), 1071 (m), 744 (m), 724 (s), 697 (s), 638 (m), 551 (m), 531 (m) cm^{-1}; ^1H NMR (400 MHz, $CDCl_3$): δ 7.92–7.86 (2H, m), 7.77–7.72 (2H, m), 7.53–7.42 (5H, m), 7.35–7.24 (3H, m), 7.12 (1H, ddd, J = 7.6, 7.6, 1.2 Hz), 7.05 (1H, m), 4.67 (1H, dddd, J = 10.4, 6.8, 4.4, 4.4 Hz), 3.73 (1H, br dd, J = 9.6, 6.4 Hz), 2.89 (1H, ddd, J = 16.4, 6.8, 2.4 Hz), 2.68 (1H,

ddd, J = 16.4, 4.4, 2.8 Hz), 1.96–1.95 (4H, m); ^{13}C NMR (100 MHz, $CDCl_3$): δ 140.5 (d, J = 6.0 Hz), 134.5, 132.9 (d, J = 127 Hz), 132.6 (d, J = 9.7 Hz), 132.1 (d, J = 3.0 Hz), 132.0 (d, J = 3.0 Hz, only the peak at 131.9 is visible, the other is overlapping), 131.93 (d, J = 9.7 Hz), 131.87 (d, J = 130 Hz), 130.4, 128.7 (d, J = 11.9 Hz), 128.5 (d, J = 12.6 Hz), 127.4, 126.3, 125.8, 79.9, 71.9, 48.8, 28.9 (d, J = 3.7 Hz), 19.1; HRMS Calcd for $C_{23}H_{23}NOP$ $[M + H]^+$: 360.15173; Found: 360.15108. $[\alpha]^{27}_D$ = –33.0 (c = 1.00, $CHCl_3$) for a 98:2 e.r. sample. The enantiomeric purity is determined by HPLC analysis in comparison with authentic racemic material (Chiracel OJ-H, 91:9 hexanes:*i*-PrOH, 0.8 mL/min, 220 nm): t_R of **3.21d**: 8 min (major) and 19 min (minor).

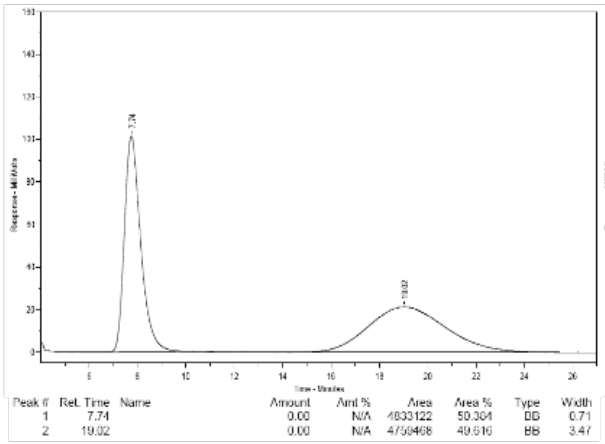

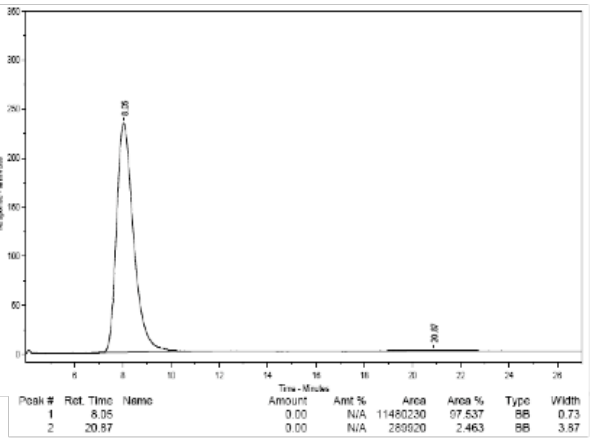

Peak #	Ret. Time	Area %	Peak #	Ret. Time	Area %
1	7.7 min	50.384	1	8.1 min	97.537
2	19.0 min	49.616	2	20.9 min	2.463

(*S*)–*N*-(1-(2-Methoxyphenyl)but-3-yn-1-yl)-*P*,*P*-diphenylphosphinic amide (3.21e): mp = 154–155 °C. IR (neat): 3185 (w, br), 3056 (w, br), 2915 (w, br), 1601 (w), 1589 (w), 1492 (m), 1462 (m), 1438 (m), 1241 (m), 1189 (s), 1121 (m), 1110 (m), 1027 (m), 953 (m), 751 (m), 722 (s), 695 (s), 552 (m), 519 (m) cm^{-1}; ^{1}H NMR (400 MHz, $CDCl_3$): δ 7.90–7.85 (2H, m), 7.83–7.77 (2H, m), 7.51–7.46 (1H, m), 7.45–7.40 (3H, m), 7.37–7.33

(2H, m), 7.28–7.21 (2H, m), 6.94 (1H, ddd, J = 7.6, 7.6, 0.8 Hz), 6.85–6.83 (1H, m), 4.57 (1H, dddd, J = 17.4, 7.2, 6.0, 6.0 Hz), 4.14 (1H, br dd, J = 11.6, 7.6 Hz), 3.73 (3H, s), 2.95 (1H, ddd, J = 16.4, 7.2, 2.8 Hz), 2.86 (1H, ddd, J = 16.4, 4.8, 2.8 Hz), 1.89 (1H, t, J = 2.4 Hz); ^{13}C NMR (100 MHz, $CDCl_3$): δ 156.4, 133.2 (d, J = 127 Hz), 132.6 (d, J = 9.7 Hz), 132.2 (d, J = 130 Hz), 131.94 (d, J = 8.9 Hz), 131.91 (d, J = 3.0 Hz), 131.8 (d, J = 3.0 Hz), 129.7, 129.6, 128.7, 128.6 (d, J = 11.9 Hz), 128.4 (d, J = 12.6 Hz), 120.5, 110.8, 81.0, 71.2, 55.3, 50.9, 27.8 (d, J = 2.9 Hz); HRMS Calcd for $C_{23}H_{23}NO_2P$ $[M + H]^+$: 376.14664; Found: 376.14594. $[\alpha]^{28}_D$ = –14.6 (c = 1.00, $CHCl_3$) for a 97.5:2.5 e.r. sample. The enantiomeric purity is determined by HPLC analysis in comparison with authentic racemic material (Chiracel OD-H, 96:4 hexanes:*i*-PrOH, 0.6 mL/min, 220 nm): t_R of **3.21e**: 16 min (major) and 22 min (minor).

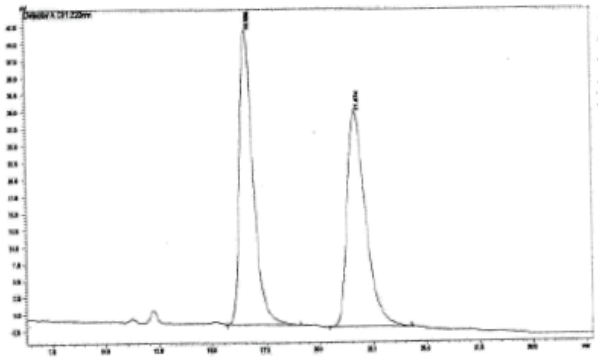

Peak#	Ret. Time	Area	Height	Area %	Height %
1	16.559	1935157	43514	50.223	57.604
2	21.674	1917978	32026	49.777	42.396
Total		3853135	75540	100.000	100.000

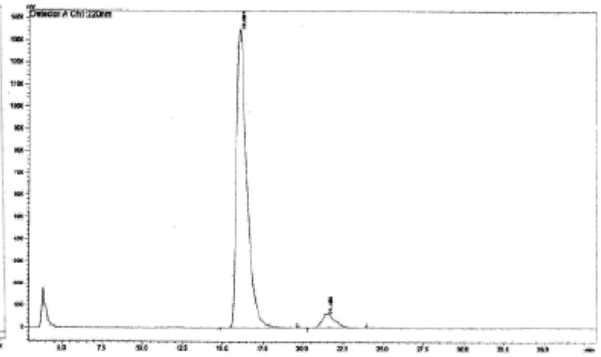

Peak#	Ret. Time	Area	Height	Area %	Height %
1	15.984	60258405	1348412	94.406	95.654
2	21.489	3570747	61271	5.594	4.346
Total		63829152	1409683	100.000	100.000

Peak #	Ret. Time	Area %	Peak #	Ret. Time	Area %
1	16.6 min	50.223	1	16.0 min	94.406
2	21.7 min	49.777	2	21.5 min	5.594

(*S*)–*N*-(1-(3-Bromophenyl)but-3-yn-1-yl)-*P*,*P*-diphenylphosphinic amide (**3.21f**): mp = 128–130 °C. IR (neat): 3157 (w, br), 1570 (w), 1437 (m), 1179 (m), 1122 (m), 1108 (m), 1070 (m), 724 (m), 692 (s), 636 (m), 520 (s), 436 (m) cm^{-1}; ^{1}H NMR (400 MHz,

$CDCl_3$): δ 7.91–7.85 (2H, m), 7.82–7.77 (2H, m), 7.53–7.48 (1H, m), 7.47–7.42 (4H, m), 7.39–7.35 (3H, m), 7.27–7.24 (1H, m), 7.19–7.15 (1H, m), 4.41 (1H, dddd, *J* = 10.8, 6.4, 4.4, 4.4 Hz), 3.79 (1H, br dd, *J* = 10.4, 6.4 Hz), 2.91 (1H, ddd, *J* = 16.4, 6.4, 2.8 Hz), 2.73 (1H, ddd, *J* = 16.8, 4.4, 2.8 Hz), 2.01 (1H, t, *J* = 2.8 Hz); ^{13}C NMR (100 MHz, $CDCl_3$): δ 144.3 (d, *J* = 5.2 Hz), 132.6 (d, *J* = 127 Hz, only the peak at 133.2 is visible, the other is overlapping), 132.5 (d, *J* = 9.7 Hz), 132.23 (d, *J* = 2.4 Hz), 132.17 (d, *J* = 2.2 Hz), 132.0 (d, *J* = 9.6 Hz), 131.8 (d, *J* = 128 Hz, only the peak at 131.2 is visible, the other is overlapping), 130.7, 130.1, 129.7, 128.7 (d, *J* = 11.9 Hz), 128.6 (d, *J* = 11.9 Hz), 125.4, 122.6, 79.6, 72.6, 52.4, 29.2 (d, *J* = 3.7 Hz); HRMS Calcd for $C_{22}H_{20}BrNOP$ [M + H]$^+$: 426.04454; Found: 426.04338. $[\alpha]^{27}_D$ = –25.0 (*c* = 1.00, $CHCl_3$) for a 96:4 e.r. sample. The enantiomeric purity of this compound was determined by HPLC analysis in comparison with authentic racemic material (Chiracel OJ-H, 95:5 hexanes:*i*-PrOH, 0.8 mL/min, 220 nm): t_R of **3.21f**: 11 min (major) and 15 min (minor).

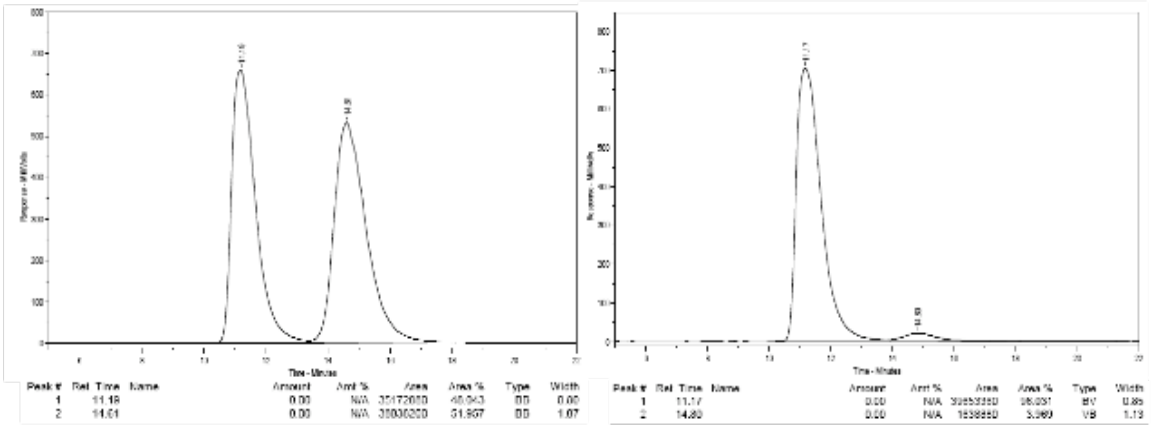

Peak #	Ret. Time	Area %	Peak #	Ret. Time	Area %
1	11.2 min	48.043	1	11.2 min	96.031
2	14.6 min	51.957	2	14.8 min	3.969

(*S*)–*N*-(1-(4-Chlorophenyl)but-3-yn-1-yl)-*P*,*P*-diphenylphosphinic amide (3.21g): mp: 134–135 °C. IR (neat): 3151 (w, br), 2887 (w, br), 1492 (m), 1437 (m), 1179 (s),

1122 (m), 1109 (m), 1089 (m), 724 (m), 695 (m), 638 (m), 530 (s) cm^{-1}; ^1H NMR (400 MHz, $CDCl_3$): δ 7.92–7.86 (2H, m) 7.83–7.78 (2H, m), 7.54–7.49 (1H, m), 7.48–7.43 (3H, m), 7.40–7.35 (2H, m), 7.30–7.25 (4H, m), 7.14–7.11 (2H, m), 4.44 (1H, dddd, *J* = 10.4, 6.4, 4.4, 4.4 Hz), 3.69 (1H, br dd, *J* = 10.4, 6.4 Hz), 2.91 (1H, ddd, *J* = 16.8, 6.4, 2.4 Hz), 2.73 (1H, ddd, *J* = 16.8, 4.0, 2.4 Hz), 2.00 (1H, t, *J* = 2.8 Hz); ^{13}C NMR (100 MHz, $CDCl_3$): δ 140.5 (d, *J* = 5.9 Hz), 133.4, 132.6 (d, *J* = 127 Hz), 132.4 (d, *J* = 9.7 Hz), 132.2 (d, *J* = 2.3 Hz), 132.1 (d, *J* = 3.0 Hz), 132.0 (d, *J* = 9.7 Hz), 131.9 (d, *J* = 130 Hz), 128.74 (d, *J* = 12.6 Hz, only the peak at 128.0 is visible, the other is overlapping), 128.67, 128.6 (d, *J* = 12.7 Hz), 128.0, 79.7, 72.4, 52.3, 29.2 (d, *J* = 4.5 Hz); HRMS Calcd for $C_{22}H_{20}ClNOP$ $[M + H]^+$: 380.09710; Found: 380.09728. $[\alpha]^{26}_D$ = –33.0 (*c* = 1.00, $CHCl_3$) for a 97:3 e.r. sample. The enantiomeric purity of this compound was determined by HPLC analysis in comparison with authentic racemic material (Chiracel OJ-H, 96:4 hexanes:*i*-PrOH, 0.8 mL/min, 220 nm): t_R of **3.21g**: 19 min (major) and 26 min (minor).

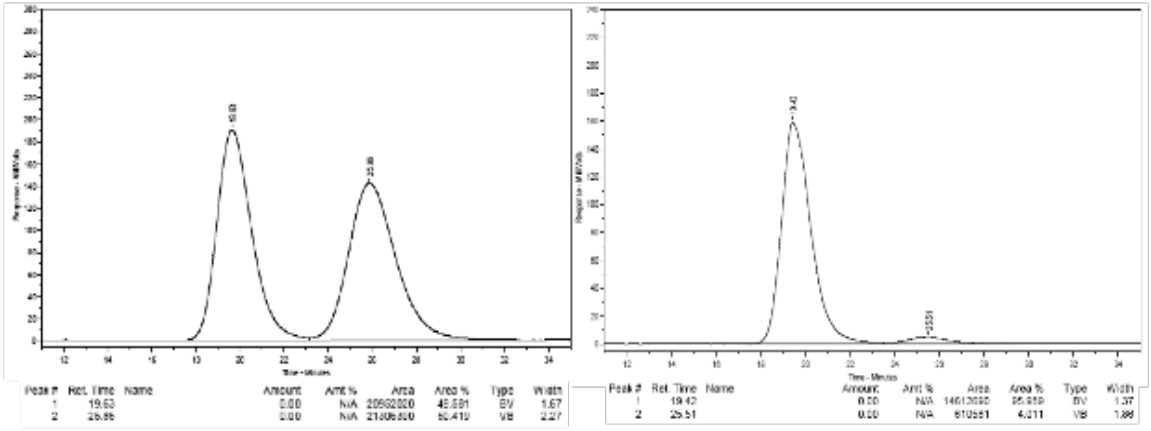

Peak #	Ret. Time	Area %	Peak #	Ret. Time	Area %
1	19.6 min	49.581	1	19.4 min	95.989
2	25.6 min	50.419	2	25.5 min	4.011

(*S*)–*N*-(1-(4-Methoxyphenyl)but-3-yn-1-yl)-*P*,*P*-diphenylphosphinic amide (3.21h): mp = 115–116 °C. IR (neat): 3175 (w, br), 1612 (w), 1513 (m), 1438 (m), 1246 (m), 1178

(s), 1122 (m), 1110 (m), 1070 (m), 1030 (m), 906 (m), 724 (s), 694 (s), 642 (m), 522 (s, br) cm^{-1}; ^1H NMR (400 MHz, $CDCl_3$): δ 7.92–7.80 (4H, m), 7.52–7.48 (1H, m), 7.47–7.41 (3H, m), 7.40–7.35 (2H, m), 7.27–7.23 (2H, m), 6.87–6.83 (2H, m), 4.41 (1H, dddd, *J* = 10.4, 6.4, 4.4, 4.4 Hz), 3.80 (3H, s), 3.65 (1H, br dd, *J* = 10.4, 6.4 Hz), 2.90 (1H, ddd, *J* = 16.8, 6.4, 2.8 Hz), 2.76 (1H, ddd, *J* = 16.8, 4.4, 2.8 Hz), 1.98 (1H, t, *J* = 2.8 Hz); ^{13}C NMR (100 MHz, $CDCl_3$): δ 159.0 134.2 (d, *J* = 5.9 Hz), 133.0 (d, *J* = 127 Hz), 132.5 (d, *J* = 9.7 Hz), 132.2 (d, *J* = 130 Hz), 132.04 (d, *J* = 3.0 Hz, only the peak at 132.1 is visible, the other is overlapping), 132.00 (d, *J* = 3.0 Hz), 131.99 (d, *J* = 9.7 Hz), 128.7 (d, *J* = 12.6 Hz), 128.6 (d, *J* = 12.6 Hz), 127.7, 113.9, 80.3, 72.0, 55.4, 52.4, 29.3 (d, *J* = 3.7 Hz); HRMS Calcd for $C_{23}H_{23}NO_2P$ $[M + H]^+$: 376.14664; Found: 376.14670. $[\alpha]^{27}_D$ = –28.4 (*c* = 1.00, $CHCl_3$) for a 97:3 e.r. sample. The enantiomeric purity of this compound was determined by HPLC analysis in comparison with authentic racemic material (Chiracel OJ-H, 92:8 hexanes:*i*-PrOH, 0.8 mL/min, 220 nm): t_R of **3.21h**: 18 min (major) and 29 min (minor).

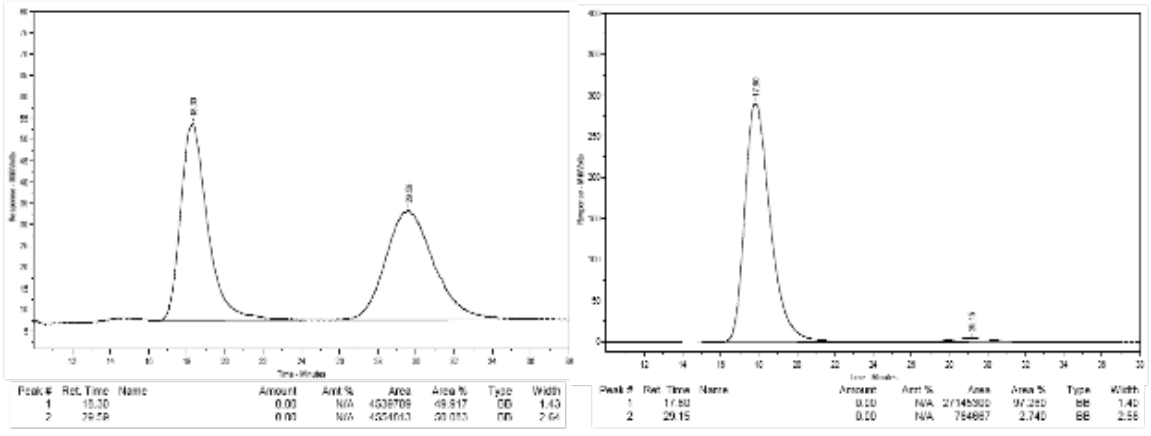

Peak #	Ret. Time	Area %	Peak #	Ret. Time	Area %
1	18.3 min	49.917	1	17.8 min	97.260
2	29.6 min	50.083	2	29.1 min	2.740

(*S*)–*N*-(1-(Furan-2-yl)but-3-yn-1-yl)-*P*,*P*-diphenylphosphinic amide (**3.21i**): mp = 109–110 °C. IR (neat): 3154 (w, br), 2881 (w, br), 1438 (m), 1188 (s), 1146 (m), 1123 (m), 1110 (m), 1071 (m), 726 (s), 696 (s), 569 (m, br), 530 (s) cm^{-1}; ^1H NMR (400 MHz, $CDCl_3$): δ 7.97–7.87 (4H, m), 7.52–7.49 (2H, m), 7.46–7.42 (4H, m), 7.35–7.35 (1H, m), 6.35–6.34 (1H, m), 6.32–6.30 (1H, m), 4.47 (1H, dddd, *J* = 14.4, 10.8, 5.6, 5.6 Hz), 3.63 (1H, br dd, *J* = 11.2, 7.2 Hz), 2.89 (2H, app dd, *J* = 5.2, 2.8 Hz), 1.99 (1H, t, *J* = 2.8 Hz); ^{13}C NMR (100 MHz, $CDCl_3$): δ 154.3 (d, *J* = 8.2 Hz), 142.1, 132.7 (d, *J* = 127 Hz), 132.6 (d, *J* = 9.6 Hz), 132.14 (d, *J* = 2.2 Hz), 132.12 (d, *J* = 3.0 Hz), 132.0 (d, *J* = 9.7 Hz), 131.9 (d, *J* = 130 Hz), 128.7 (d, *J* = 12.7 Hz), 110.4, 107.2, 79.9, 71.7, 47.9, 26.9 (d, *J* = 3.7 Hz); HRMS Calcd for $C_{20}H_{19}NO_2P$ $[M + H]^+$: 336.11534; Found: 336.11588. $[\alpha]^{24}_D$ = –22.0 (*c* = 1.00, $CHCl_3$) for a 96.5:3.5 e.r. sample. The enantiomeric purity of this compound was determined by HPLC analysis in comparison with authentic racemic material (Chiracel OD–H, 96:4 hexanes:*i*-PrOH, 0.6 mL/min, 220 nm): t_R of **3.21i**: 27 min (major) and 30 min (minor).

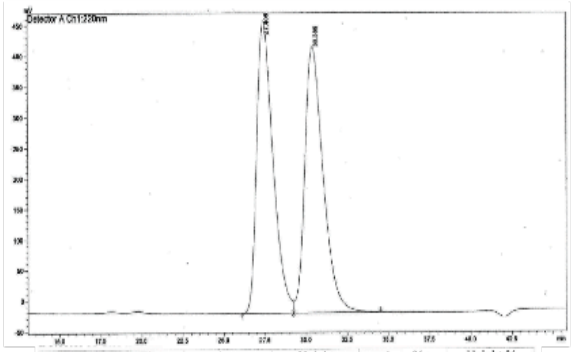

Peak#	Ret. Time	Area	Height	Area %	Height %
1	27.405	33280845	478860	49.430	52.371
2	30.389	34048101	435504	50.570	47.629
Total		67328947	914365	100.000	100.000

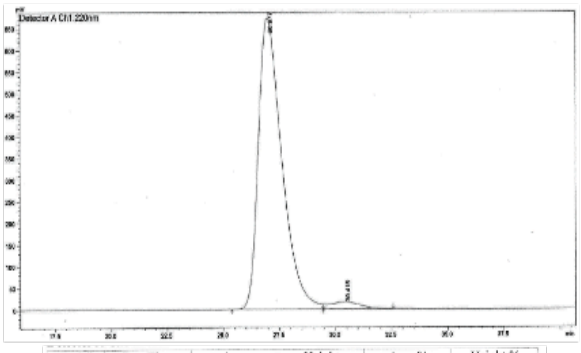

Peak#	Ret. Time	Area	Height	Area %	Height %
1	26.977	49397357	673386	97.152	97.693
2	30.415	1448312	15904	2.848	2.307
Total		50845668	689290	100.000	100.000

Peak #	Ret. Time	Area %	Peak #	Ret. Time	Area %
1	27.4 min	49.430	1	27.0 min	97.152
2	30.4 min	50.570	2	30.4 min	2.848

(*S*)–*P*,*P*-Diphenyl-*N*-(1-(thiophen-3-yl)but-3-yn-1-yl)phosphinic amide (**3.21j**): mp = 102–104 °C. IR (neat): 3171 (w, br), 1437 (m), 1182 (s), 1122 (m), 1109 (m), 1071 (m), 906 (m), 782 (m), 723 (s), 693 (s), 642 (m, br), 565 (m), 523 (s) cm^{-1}; ^{1}H NMR (400 MHz, $CDCl_3$): δ 7.92–7.84 (4H, m), 7.51–7.37 (6H, m), 7.26–7.25 (2H, m), 7.12–7.11 (1H, m), 4.49 (1H, dddd, *J* = 15.2, 6.4, 4.0, 4.0 Hz), 3.67 (1H, br dd, *J* = 10.8, 6.8 Hz), 2.91 (1H, ddd, *J* = 16.8, 6.0, 2.8 Hz), 2.78 (1H, ddd, *J* = 16.8, 4.0, 2.8 Hz), 2.01 (1H, t, *J* = 2.4 Hz); ^{13}C NMR (100 MHz, $CDCl_3$): δ 143.4 (d, *J* = 6.0 Hz), 132.7 (d, *J* = 128 Hz, only the peak at 133.3 is visible, the other is overlapping), 132.4 (d, *J* = 9.7 Hz), 132.2 (d, *J* = 130 Hz), 132.1 (d, *J* = 2.2 Hz), 132.0 (d, *J* = 9.7 Hz), 128.7 (d, *J* = 12.6 Hz), 128.6 (d, *J* = 12.6 Hz), 126.6, 126.1, 121.8, 80.3, 72.1, 49.2, 28.6 (d, *J* = 3.7 Hz); HRMS Calcd for $C_{20}H_{19}NOPS$ $[M + H]^+$: 352.09250; Found: 352.09141. $[\alpha]^{25}_D$ = –25.4 (*c* = 1.00, $CHCl_3$) for a 99:1 e.r. sample. The enantiomeric purity of this compound was determined by HPLC analysis in comparison with authentic racemic material (Chiracel OJ-H, 96:4 hexanes:*i*-PrOH, 0.8 mL/min, 220 nm): t_R of **3.21j**: 27 min (major) and 39 min (minor).

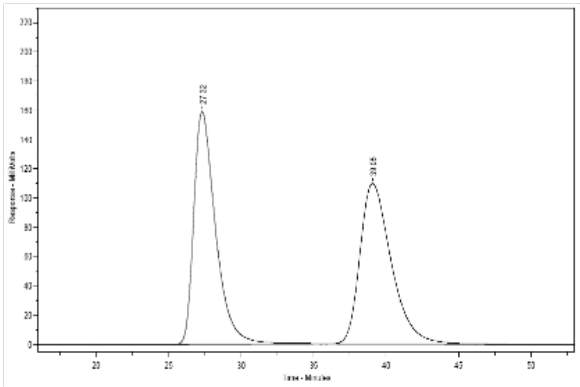

Peak #	Ret. Time	Name	Amount	Amt %	Area	Area %	Type	Width
1	27.32		0.00	N/A	16688010	50.170	BB	1.54
2	39.05		0.00	N/A	16572940	49.830	BB	2.27

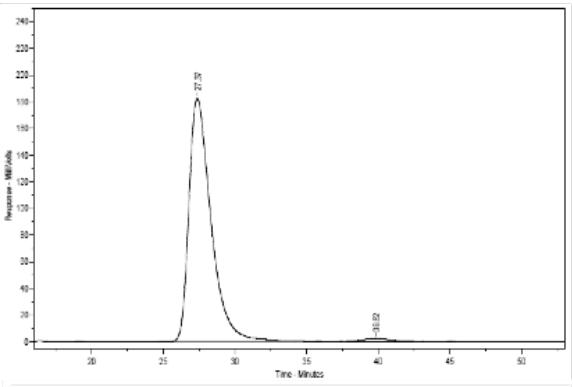

Peak #	Ret. Time	Name	Amount	Amt %	Area	Area %	Type	Width
1	27.37		0.00	N/A	19819890	98.351	BB	1.58
2	39.82		0.00	N/A	328907	1.649	BB	2.28

Peak #	Ret. Time	Area %	Peak #	Ret. Time	Area %
1	27.3 min	50.170	1	27.4 min	98.351
2	39.1 min	49.830	2	39.8 min	1.649

(*S*)–*P*,*P*-Diphenyl-*N*-(1-(pyridin-3-yl)but-3-yn-1-yl)phosphinic amide (**3.21k**): mp = 147–149 °C. IR (neat): 3171 (w, br), 1437 (m), 1184 (s), 1123 (m), 1109 (m), 1071 (m), 912 (w), 725 (m), 696 (s), 552 (m), 526 (m) cm^{-1}; ^1H NMR (400 MHz, $CDCl_3$): δ 8.56 (1H, d, *J* = 2.4 Hz), 8.52 (1H, dd, *J* = 4.4, 1.6 Hz), 7.92–7.87 (2H, m), 7.83–7.78 (2H, m), 7.72–7.69 (1H, m), 7.55–7.51 (1H, m), 7.49–7.44 (3H, m), 7.40–7.35 (2H, m), 7.27–7.24 (1H, m), 4.51 (1H, dddd, *J* = 10.4, 6.4, 4.4, 4.4 Hz), 3.77 (1H, m), 2.97 (1H, ddd, *J* = 16.8, 6.0, 2.8 Hz), 2.77 (1H, ddd, *J* = 16.8, 4.0, 2.4 Hz), 2.03 (1H, t, *J* = 2.8 Hz); ^{13}C NMR (125 MHz, $CDCl_3$): δ 148.9, 148.3, 137.4, 133.4, 132.4 (d, *J* = 9.7 Hz), 132.32 (d, *J* = 127 Hz), 132.27 (d, *J* = 3.0 Hz), 132.21 (d, *J* = 3.0 Hz), 132.0 (d, *J* = 9.7 Hz), 131.7 (d, *J* = 130 Hz, only the peak at 131.0 is visible, the other is overlapping), 128.8 (d, *J* = 12.7 Hz), 128.7 (d, *J* = 12.6 Hz), 123.4, 79.3, 72.7, 50.9, 29.0 (d, *J* = 3.7 Hz); HRMS Calcd for $C_{21}H_{20}N_2OP$ $[M + H]^+$: 347.13132; Found: 347.13078. $[\alpha]^{24}_D$ = –23.2 (*c* = 1.00, $CHCl_3$) for a 97:3 e.r. sample. The enantiomeric purity of this compound was determined by HPLC analysis in comparison with authentic racemic material (Chiracel OJ-H, 96:4 hexanes:*i*-PrOH, 0.6 mL/min, 220 nm): t_R of **3.21k**: 33 min (major) and 44 min (minor).

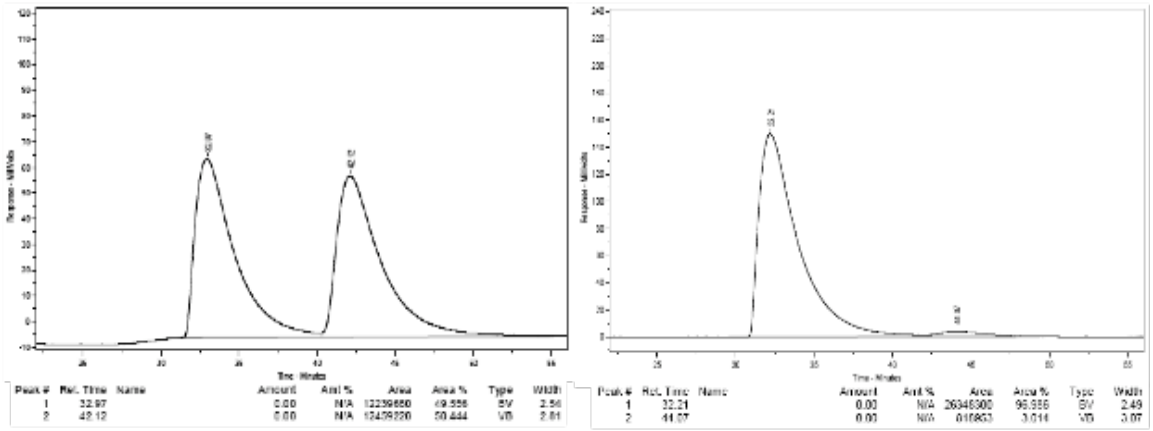

Peak #	Ret. Time	Area %	Peak #	Ret. Time	Area %
1	33.0 min	49.556	1	32.2 min	96.986
2	42.1 min	50.444	2	44.1 min	3.014

(*S*,*E*)–*P*,*P*-Diphenyl-*N*-(1-phenylhexa-1,5-dien-3-yl)phosphinic amide (**3.21l**): mp = 100–101 °C. IR (neat): 3162 (w, br), 2872 (w, br), 1437 (m), 1184 (m), 1122 (m), 1109 (m), 1069 (m), 964 (m), 908 (m), 747 (m), 723 (s), 691 (s), 641 (m), 529 (s) cm^{-1}; ^{1}H NMR (400 MHz, $CDCl_3$): δ 7.97–7.89 (4H, m), 7.53–7.41 (6H, m), 7.36–7.29 (4H, m), 7.26–7.22 (1H, m), 6.54 (1H, dd, *J* = 16.0, 0.8 Hz), 6.28 (1H, dd, *J* = 16.0, 6.4 Hz), 4.09–4.00 (1H, m), 3.43 (1H, br dd, *J* = 10.0, 6.4 Hz), 2.77 (1H, ddd, *J* = 16.8, 6.0, 2.8 Hz), 2.63 (1H, ddd, *J* = 16.8, 4.0, 2.8 Hz), 2.06 (1H, t, *J* = 2.8 Hz); ^{13}C NMR (100 MHz, $CDCl_3$): δ 136.6, 132.6 (d, *J* = 9.7 Hz), 132.1, 132.0 (d, *J* = 9.6 Hz), 131.1, 130.0 (d, *J* = 6.7 Hz), 130.5, 128.7 (d, *J* = 12.6 Hz), 128.65 (d, *J* = 12.7 Hz), 128.6, 127.8, 126.7, 80.2, 71.9, 51.3, 28.1 (d, *J* = 2.9 Hz); HRMS Calcd for $C_{24}H_{23}NOP$ $[M + H]^+$: 372.15173; Found: 372.15121. $[\alpha]^{25}_D$ = –49.3 (*c* = 1.00, $CHCl_3$) for a 98:2 e.r. sample. The enantiomeric purity of this compound was determined by HPLC analysis in comparison with authentic racemic material (Chiracel OJ-H, 95:5 hexanes:*i*-PrOH, 0.8 mL/min, 254 nm): t_R of **3.21l**: 27 min (minor) and 33 min (major).

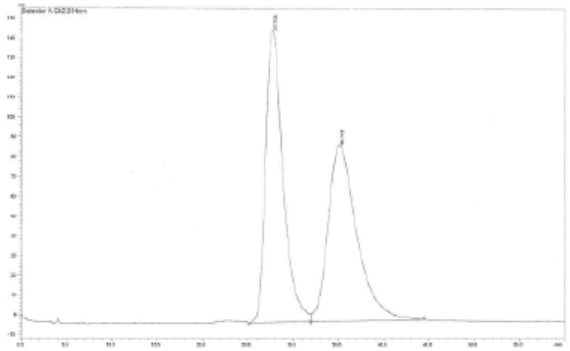

Peak#	Ret. Time	Area	Height	Area %	Height %
1	27.723	19614716	147743	49.968	62.385
2	35.112	19639493	89080	50.032	37.615
Total		39254209	236822	100.000	100.000

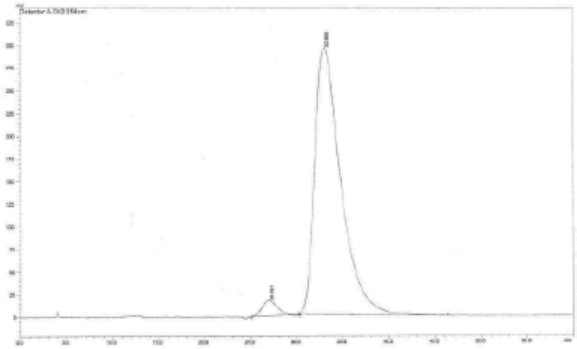

Peak#	Ret. Time	Area	Height	Area %	Height %
1	26.921	1934097	16882	3.213	5.394
2	32.955	58258687	295066	96.787	94.606
Total		60192784	312948	100.000	100.000

Peak #	Ret. Time	Area %	Peak #	Ret. Time	Area %
1	27.7 min	49.968	1	26.9 min	3.213
2	35.1 min	50.032	2	33.0 min	96.787

(*S*,*E*)–*N*-(2-Methyl-1-phenylhex-1-en-5-yn-3-yl)-*P*,*P*-diphenylphosphinic amide (**3.21m**): mp = 74–76 °C. IR (neat): 3300 (w, br), 3167 (w, br), 2915 (w, br), 1437 (m), 1184 (s), 1122 (m), 1109 (m), 1071 (m), 907 (w), 747 (m), 724 (s), 695 (s), 641 (m, br), 538 (m) cm^{-1}; ^1H NMR (400 MHz, $CDCl_3$): δ 7.99–7.89 (4H, m), 7.53–7.41 (6H, m), 7.34–7.31 (2H, m), 7.23–7.20 (3H, m), 6.45 (1H, s), 3.96–3.88 (1H, m), 3.49 (1H, br dd, *J* = 10.0, 6.4 Hz), 2.80–2.67 (2H, m), 2.05 (1H, t, *J* = 2.4 Hz), 1.84 (3H, d, *J* = 1.2 Hz); ^{13}C NMR (100 MHz, $CDCl_3$): δ 137.6, 137.3 (d, *J* = 5.2 Hz), 132.9 (d, *J* = 127 Hz), 132.6 (d, *J* = 9.6 Hz), 132.4 (d, *J* = 130 Hz), 132.1 (d, *J* = 2.2 Hz), 132.04 (d, *J* = 2.2 Hz, only the peak at 132.03 is visible, the other may be overlapping), 131.96 (d, *J* = 9.6 Hz), 129.1, 128.7 (d, *J* = 12.6 Hz), 128.6 (d, *J* = 12.6 Hz), 128.2, 127.3, 126.6, 80.2, 71.8, 56.1, 26.6 (d, *J* = 3.7 Hz), 14.9; HRMS Calcd for $C_{25}H_{25}NOP$ $[M + H]^+$: 386.16738; Found: 386.16661. $[\alpha]^{24}_D$ = –26.2 (*c* = 1.00, $CHCl_3$) for a 96.5:3.5 e.r. sample. The enantiomeric purity of this compound was determined by HPLC analysis in comparison with authentic racemic material (Chiracel AD-H, 88:12 hexanes:*i*-PrOH, 0.8 mL/min, 220 nm): t_R of **3.21m**: 15 min (major) and 17 min (minor).

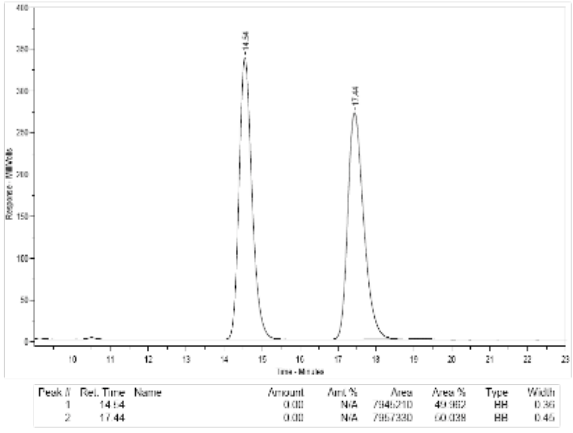

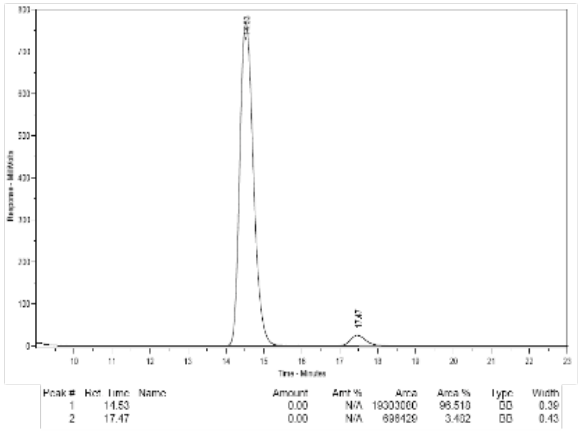

Peak #	Ret. Time	Area %
1	14.5 min	49.962
2	17.4 min	50.038

Peak #	Ret. Time	Area %
1	14.5 min	96.518
2	17.5 min	3.482

(*R*)–*P*,*P*-Diphenyl-*N*-(1-phenylhex-5-yn-3-yl)phosphinic amide (**3.21o**): mp = 117–119 °C. IR (neat): 3178 (w, br), 2924 (w, br), 1437 (m), 1183 (s), 1121 (m), 1109 (m), 978 (w), 746 (m), 722 (m), 694 (s), 635 (m, br), 523 (s) cm^{-1}; ^{1}H NMR (400 MHz, $CDCl_3$): δ 7.94–7.87 (4H, m), 7.53–7.42 (6H, m), 7.26–7.22 (2H, m), 7.17–7.13 (3H, m), 3.34–3.17 (2H, m), 2.77–2.61 (3H, m), 2.51–2.45 (1H, m), 2.08–1.94 (3H, m); ^{13}C NMR (100 MHz, $CDCl_3$): δ 141.5, 132.9 (d, J = 130 Hz, only the peak at 133.6 is visible, the other may be overlapping), 132.7 (d, J = 129 Hz), 132.3 (d, J = 8.9 Hz), 132.1 (d, J = 9.6 Hz), 132.0 (d, J = 3.0 Hz), 128.6 (d, J = 12.6 Hz), 128.5 (d, J = 8.2 Hz), 126.0, 80.3, 71.6, 49.1, 37.5 (d, J = 6.0 Hz), 32.4, 26.8 (d, J = 3.8 Hz); HRMS Calcd for $C_{24}H_{25}NOP$ $[M + H]^+$: 374.16738; Found: 374.16705. $[\alpha]^{26}_D$ = +14.4 (c = 1.00, $CHCl_3$) for a 97:3 e.r. sample. The enantiomeric purity of this compound was determined by HPLC analysis in comparison with authentic racemic material (Chiracel OD-H, 94:6 hexanes:*i*-PrOH, 0.8 mL/min, 220 nm): t_R of **3.21o**: 17 min (minor) and 19 min (major).

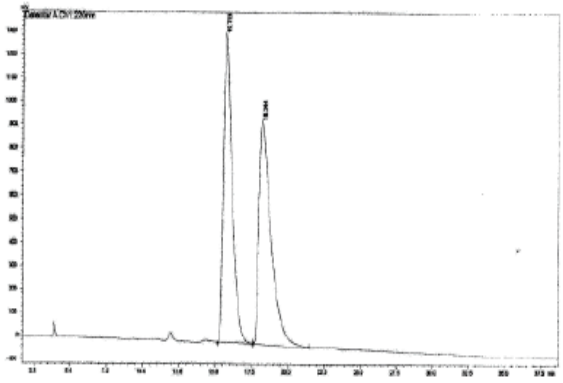

Peak#	Ret. Time	Area	Height	Area %	Height %
1	15.733	54657013	1320740	49.751	57.944
2	18.244	55203721	958584	50.249	42.056
Total		109860734	2279324	100.000	100.000

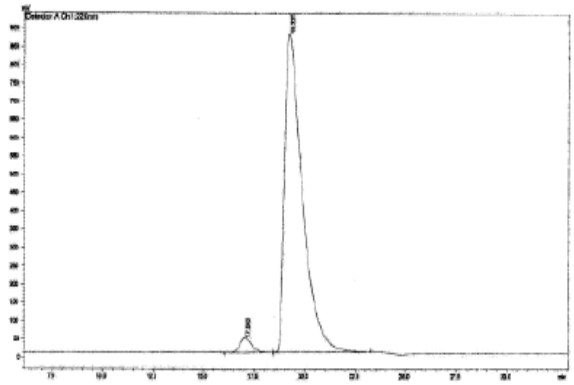

Peak#	Ret. Time	Area	Height	Area %	Height %
1	17.043	1660045	41100	3.004	4.493
2	19.227	53607097	873594	96.996	95.507
Total		55267142	914695	100.000	100.000

Peak #	Ret. Time	Area %	Peak #	Ret. Time	Area %
1	15.7 min	49.751	1	17.0 min	3.004
2	18.2 min	50.249	2	19.2 min	96.996

(*R*)–*N*-(6-Methylhept-1-yn-4-yl)-*P*,*P*-diphenylphosphinic amide (**3.21p**): mp = 108–110 °C. IR (neat): 3184 (w, br), 2868 (w, br), 1437 (m), 1184 (s), 1109 (m), 1122 (m), 1109 (m), 751 (w), 723 (s), 696 (s), 636 (m, br), 571 (m), 525 (s) cm^{-1}; ^{1}H NMR (400 MHz, $CDCl_3$): δ 7.94–7.88 (4H, m), 7.52–7.41 (6H, m), 3.32–3.21 (1H, m), 3.08 (1H, br dd, *J* = 11.2, 6.8 Hz), 2.63 (1H, ddd, *J* = 16.8, 5.2, 2.8 Hz), 2.40 (1H, ddd, *J* = 16.8, 2.8, 2.8 Hz), 2.01 (1H, t, *J* = 2.8 Hz), 1.78–1.68 (1H, m), 1.58–1.45 (2H, m), 0.80 (6H, app t, *J* = 6.4 Hz); ^{13}C NMR (100 MHz, $CDCl_3$): δ 133.1 (d, *J* = 129 Hz, only the peak at 133.7 is visible, the other may be overlapping), 132.8 (d, *J* = 130 Hz), 132.4 (d, *J* = 8.9 Hz), 132.1 (d, *J* = 9.6 Hz), 132.0 (d, *J* = 2.9 Hz), 131.9 (d, *J* = 3.0 Hz), 128.62 (d, *J* = 12.7 Hz), 128.58 (d, *J* = 12.6 Hz), 80.6, 71.4, 47.5 (d, *J* = 1.5 Hz), 45.5 (d, *J* = 5.9 Hz), 27.1 (d, *J* = 3.0 Hz), 24.8, 22.6 (d, *J* = 5.9 Hz); HRMS Calcd for $C_{20}H_{25}NOP$ $[M + H]^+$: 326.16738; Found: 326.16710. $[\alpha]^{25}_D$ = +39.2 (*c* = 1.00, $CHCl_3$) for a 98:2 e.r. sample. The enantiomeric purity of this compound was determined by HPLC analysis in comparison with authentic racemic material (Chiracel OD-H, 94:6 hexanes:*i*-PrOH, 0.8 mL/min, 220 nm): t_R of **3.21p**: 12 min (major) and 14 min (minor).

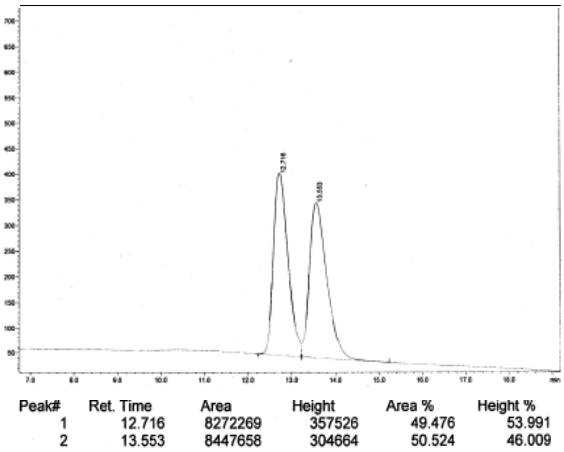

Peak#	Ret. Time	Area	Height	Area %	Height %
1	12.716	8272269	357526	49.476	53.991
2	13.553	8447658	304664	50.524	46.009

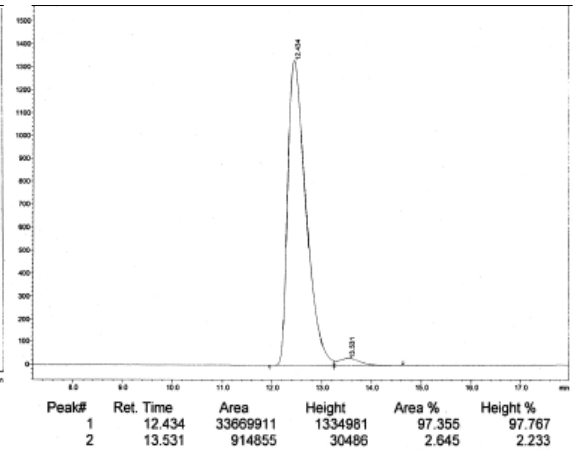

Peak#	Ret. Time	Area	Height	Area %	Height %
1	12.434	33669911	1334981	97.355	97.767
2	13.531	914855	30486	2.645	2.233

Peak #	Ret. Time	Area %	Peak #	Ret. Time	Area %
1	12.7 min	49.476	1	12.4 min	97.355
2	13.5 min	50.524	2	13.5 min	2.645

(*S*)–*N*-(1-Cyclohexylbut-3-yn-1-yl)-*P*,*P*-diphenylphosphinic amide (**3.21q**): mp = 96–98 °C. IR (neat): 3193 (w, br), 2923 (m), 2851 (w), 1437 (m), 1190 (m), 1121 (m), 1109 (m), 1070 (m), 723 (s), 694 (s), 641 (m), 568 (m), 525 (s) cm^{-1}; ^1H NMR (400 MHz, $CDCl_3$): δ 7.95–7.89 (4H, m), 7.52–7.41 (6H, m), 3.09 (1H, br dd, *J* = 11.2, 6.4 Hz), 3.00–2.91 (1H, m), 2.60 (1H, ddd, *J* = 16.8, 5.6, 2.8 Hz), 2.51 (1H, ddd, *J* = 16.8, 4.0, 2.8 Hz), 2.00 (1H, t, *J* = 2.8 Hz), 1.78–1.56 (5H, m), 1.28–0.87 (6H, m); ^{13}C NMR (100 MHz, $CDCl_3$): δ 133.1 (d, *J* = 129 Hz, only the peak at 133.8 is visible, the other may be overlapping), 132.7 (d, *J* = 129 Hz), 132.5 (d, *J* = 8.9 Hz), 132.2 (d, *J* = 9.7 Hz), 131.9 (d, *J* = 1.5 Hz), 128.6 (d, *J* = 12.7 Hz), 128.5 (d, *J* = 11.9 Hz), 81.0, 71.1, 54.2 (d, *J* = 2.2 Hz), 41.7 (d, *J* = 6.7 Hz), 29.6 (d, *J* = 53.6 Hz), 26.4, 26.3 (d, *J* = 4.5 Hz), 24.5 (d, *J* = 3.0 Hz); HRMS Calcd for $C_{22}H_{27}NOP$ $[M + H]^+$: 352.18303; Found: 352.18166; $[\alpha]^{25}_D$ = +25.7 (*c* = 1.00, $CHCl_3$) for a 91:9 e.r. sample. The enantiomeric purity of this compound was determined by HPLC analysis in comparison with authentic racemic material (Chiracel OD, 94:6 hexanes:*i*-PrOH, 0.8 mL/min, 220 nm): t_R of **3.21q**: 9 min (major) and 11 min (minor).

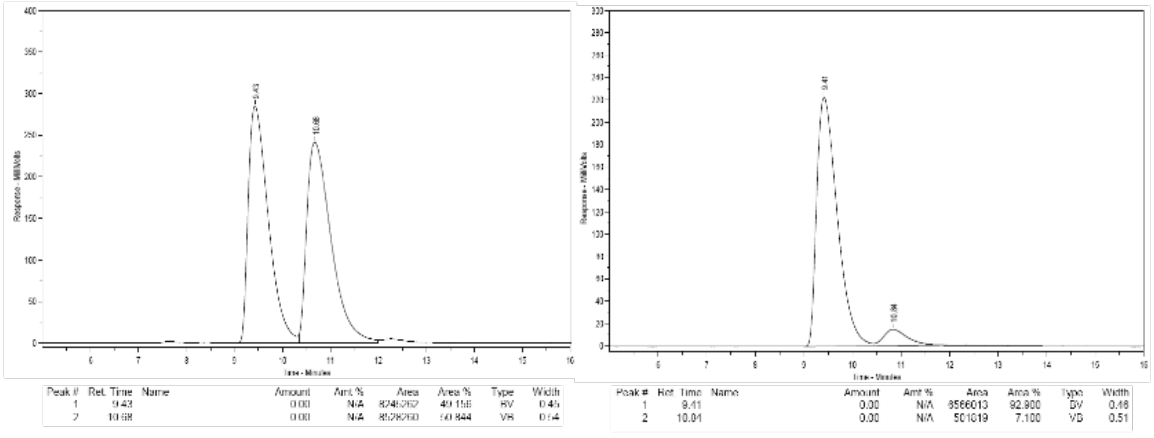

Peak #	Ret. Time	Area %	Peak #	Ret. Time	Area %
1	9.4 min	49.156	1	9.4 min	92.900
2	10.7 min	50.844	2	10.8 min	7.100

▪ **Procedure for Gram-Scale NHC–Cu-Catalyzed Enantioselective Propargyl Addition to Aldimine 3.19a to Afford Homopropargylamine 3.22**: On a benchtop, an oven-dried vial equipped with a stir bar was charged with imidazolinium salt **3.20** (5.5 mg, 8.8 μmol), NaO*t*-Bu (5.4 mg, 53 μmol), and $CuCl_2 \bullet 2H_2O$ (1.5 mg, 8.8 μmol). The vial was sealed with a septa and electrical tape, and purged with a dry atmosphere of N_2. Freshly distilled thf (2.00 mL) was added and the mixture was allowed to stir for 15 min under N_2 at 22 °C. To this solution, allenylboron **3.15** (750. μL, 4.17 mmol) is transferred and the resulting mixture is allowed to stir at 22 °C for 15 minutes. A flame-dried 50 mL round bottom flask equipped with a stir bar was charged with aldimine **3.19a** (1.07 g, 3.50 mmol), sealed with a septum and Teflon tape and purged with an atomosphere of N_2. Freshly distilled thf (6.0 mL) and MeOH (285 μL, 7.00 mmol) were added by synringe to the flask and the solution of aldimine was allowed to cool to –78 °C (dry ice/acetone bath). The pre-mixed solution of the NHC–Cu complex and allenylboron **3.15** were transferred to the flask at –78 °C rinsing the vial with thf (3 x 0.4 mL). The reaction mixture was then allowed to warm to –15 °C over the period of seven hours. The solution was allowed to warm to 22 °C and the reaction mixture is concentrated. The unpurified mixture is dissolved in 12 mL of MeOH and 4 mL of concentrated aqueous HCl is added dropwise. The mixture is allowed to stir for two hours at 22 °C after which the solution is concentrated to ~20% its volume. The resulting pale yellow oil is dissolved in an aqueous 1M solution of HCl, upon which the phosphinic acid precipitates from solution and can be removed through filtration. The aqueous filtrate is washed with AcOEt (5 x 40 mL) when the pH = 1 in order to remove pinacol from the solution. The aqueous layer is basified with a 3.0M solution of NaOH until pH is >12. The mixture is then washed with CH_2Cl_2 (5 x 40 mL). The CH_2Cl_2 washes were combined and dried with

Na_2SO_4 and the volatiles were removed *in vacuo* to obtain 439.5 mg (3.027 mmol, 87% yield) of free homopropargylamine **3.22** as a pale yellow oil.

(*S*)–1-Phenylbut-3-yn-1-amine (**3.22**): IR (neat): 3290 (m), 2911 (w, br), 1493 (w), 1423 (w), 837 (m), 759 (m), 699 (s), 636 (s), 536 (m) cm^{-1}; ^1H NMR (400 MHz, $CDCl_3$): δ 7.39–7.32 (4H, m), 7.29–7.25 (1H, m), 4.23–4,11 (1H, m), 2.59 (1H, ddd, J = 16.8, 4.8, 2.8 Hz), 2.49 (1H, ddd, J = 16.8, 8.2, 2.8 Hz), 2.05 (1H, t, J = 2.8 Hz), 1.78 (2H, br s); ^{13}C NMR (100 MHz, $CDCl_3$): δ 144.4, 128.6, 127.6, 126.3, 81.8, 70.6, 54.8, 29.8; HRMS Calcd for $C_{10}H_{12}N$ $[M + H]^+$: 146.09697; Found: 146.09686. $[\alpha]^{23}_D$ = –22.2 (c = 0.750, $CHCl_3$) for a 97:3 e.r. sample. Enantioselectivity is determined by protection of the free amine to afford the diphenylphosphinoyl amide **3.21a** and through HPLC analysis in comparison with authentic racemic material (Chiracel OJ-H, 91:9 hexanes:*i*-PrOH, 0.8 mL/min, 220 nm): t_R of **3.21a**: 13 min (major) and 22 min (minor).

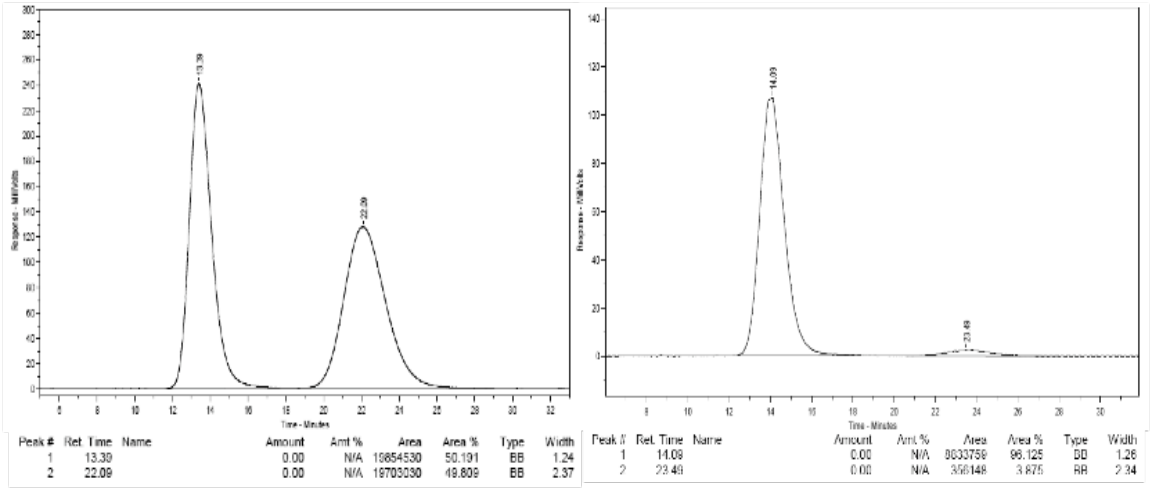

Peak #	Ret. Time	Area %	Peak #	Ret. Time	Area %
1	13.3 min	50.191	1	12.7 min	96.125
2	22.1 min	49.809	2	21.7 min	3.875

▪ **Synthesis of Key Fragment for Aza-epothilone Analogs**

***N*–((*E*)-2-Methyl-3-(2-methylthiazol-4-yl)allylidene)-*P*,*P*-diphenylphosphinic amide** (**3.19n**): The requisite phosphinoyl aldimine **3.19n** can be prepared from a Ti-mediated condensation[53] of diphenylphosphinamide with the corresponding aldehyde[58] to afford the diphenylphosphinoylimine as pale yellow to off white crystals. mp = 179–181 °C. IR (neat): 3453 (w, br), 3074 (w, br), 1588 (s), 1438 (w), 1202 (m), 1124 (m), 844 (m), 726 (m), 699 (m), 552 (m), 532 (m) cm^{-1}; ^1H NMR (400 MHz, $CDCl_3$): δ 8.94 (1H, d, *J* = 31.2 Hz), 7.94–7.89 (4H, m), 7.51–7.41 (6H, m), 7.38 (1H, s), 7.17 (1H, br s), 2.75 (3H, s), 2.43 (3H, d, *J* = 1.2 Hz); ^{13}C NMR (100 MHz, $CDCl_3$): δ 177.8 (d, *J* = 7.5 Hz), 165.8, 152.2 (d, *J* = 6.0 Hz), 139.4, 138.2, 138.0, 133.5 (d, *J* = 126 Hz), 131.8 (d, *J* = 3.0 Hz), 131.7 (d, *J* = 9.6 Hz), 128.6 (d, *J* = 12.6 Hz), 122.6, 19.5, 12.8; HRMS Calcd for $C_{20}H_{20}N_2OPS$ $[M + H]^+$: 367.10339; Found: 367.10415.

(*S*,*E*)–*N*-(2-Methyl-1-(2-methylthiazol-4-yl)hex-1-en-5-yn-3-yl)-*P*,*P*-diphenylphosphinic amide (**3.21n**): mp = 142–144 °C. IR (neat): 3173 (w, br), 2921 (w, br), 1438 (m), 1184 (s), 1122 (m), 1109 (m), 1071 (m), 907 (w), 724 (s), 697 (s), 642 (m), 540 (m) cm^{-1}; ^1H NMR (400 MHz, $CDCl_3$): δ 7.95–7.88 (4H, m), 7.52–7.38 (6H, m), 6.92 (1H, s), 6.51 (1H, br s), 3.89 (1H, dddd, *J* = 10.4, 10.4, 5.2, 5.2 Hz), 3.50 (1H, br dd, *J* = 10.4, 6.0 Hz), 2.79 (1H, ddd, *J* = 16.8, 6.4, 2.4 Hz), 2.73–2.67 (4H, m), 2.05 (3H, s), 2.01 (1H, t, *J* = 2.4 Hz); ^{13}C NMR (100 MHz, $CDCl_3$): δ 164.6, 152.8, 138.9 (d, *J* = 6.0 Hz), 133.2 (d, *J* = 126 Hz), 132.6 (d, *J* = 9.7 Hz), 132.2 (d, *J* = 130 Hz), 132.1 (d, *J* = 3.0 Hz), 132.0 (d, *J* = 2.2 Hz), 131.96 (d, *J* = 9.7 Hz), 128.7 (d, *J* = 12.7 Hz), 128.6 (d, *J* =

[58] "Total Syntheses of Epothilones A and B via a Macrolactonization-Based Strategy," Nicolaou, K. C.; Ninkovic, S.; Sarabia, D.; Vourloumis, D.; He, Y.; Vallberg, H.; Finlay, M. R. V.; Yang, Z. *J. Am. Chem. Soc.* **1997**, *119*, 7974–7991.

12.6 Hz), 120.3, 116.1, 80.0, 72.0, 56.1, 26.6 (d, J = 2.9 Hz), 19.3, 16.1; HRMS Calcd for $C_{23}H_{24}N_2OPS$ $[M + H]^+$: 407.13469; Found: 407.13332. $[\alpha]^{24}_D$ = –35.0 (c = 1.00, $CHCl_3$) for a 99:1 e.r. sample. The enantiomeric purity of this compound was determined by HPLC analysis in comparison with authentic racemic material (Chiracel OD-H, 92:8 hexanes:*i*-PrOH, 0.8 mL/min, 220 nm): t_R of **3.21n**: 15 min (major) and 19 min (minor).

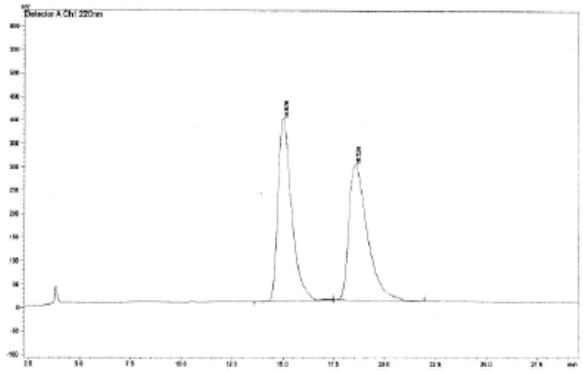

Peak#	Ret. Time	Area	Height	Area %	Height %
1	14.976	17968164	388753	49.813	57.339
2	18.524	18102821	289241	50.187	42.661
Total		36070985	677994	100.000	100.000

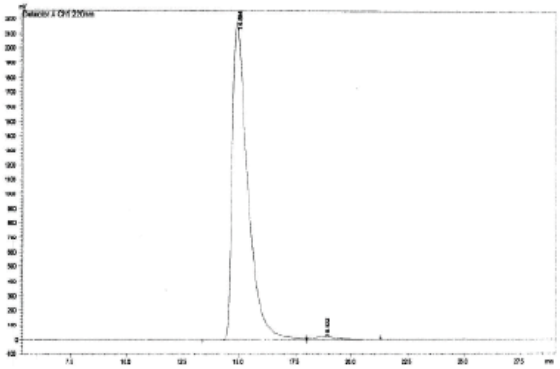

Peak#	Ret. Time	Area	Height	Area %	Height %
1	14.894	103679996	2178695	98.814	99.234
2	18.802	1243927	16809	1.186	0.766
Total		104923923	2195504	100.000	100.000

Peak #	Ret. Time	Area %
1	15.0 min	49.813
2	18.5 min	50.187

Peak #	Ret. Time	Area %
1	14.9 min	98.814
2	18.8 min	1.186

A vial equipped with a stir bar was charged with homopropargylamide **3.21n** (92.4 mg, 0.227 mmol), $AgNO_3$ (3.9 mg, 23 μmol), and *N*-iodosuccinimide (61.4 mg, 0.273 mmol). The vial was sealed with a septum and acetone (3.0 mL) is added by syringe. The mixture was allowed to stir in the dark for three hours. The volatiles were removed and the crude material is partitioned in equal parts H_2O and CH_2Cl_2 (15 mL each). The organic layer is separated and the aqueous layer is washed with CH_2Cl_2 (5 x 20 mL). The organic layers are combined and dried over $MgSO_4$ and the volatiles are removed *in vacuo* to afford the iodoalkyne **3.30** in 99% yield (120.1 mg, 0.226 mmol) as a pale yellow solid. The solid can be used without further purification or purified by silica gel chromatography if

required. **(*S*,*E*)–*N*-(6-Iodo-2-methyl-1-(2-methylthiazol-4-yl)hex-1-en-5-yn-3-yl)-*P*,*P*-diphenylphosphinic amide** (**3.30**): mp = 136–138 °C. IR (neat): 3165 (w, br), 2919 (w, br), 1438 (m), 1186 (s), 1122 (m), 1109 (m), 1072 (m), 1069 (m), 908 (w), 752 (s), 725 (s), 545 (m), 533 (m) cm^{-1}; ^1H NMR (400 MHz, $CDCl_3$): δ 7.95–7.87 (4H, m), 7.53–7.40 (6H, m), 6.92 (1H, s), 6.45 (1H, br s), 3.84 (1H, dddd, *J* = 10.4, 10.4, 5.2, 5.2 Hz), 3.43 (1H, br dd, *J* = 10.8, 6.4 Hz), 2.92 (1H, app dd, *J* = 16.8, 6.4 Hz), 2.84 (1H, app dd, *J* = 16.8, 5.2 Hz), 2.71 (3H, s), 2.04 (3H, s); ^{13}C NMR (100 MHz, $CDCl_3$): δ 164.7, 152.7, 139.0 (d, *J* = 5.2 Hz), 132.57 (d, *J* = 9.6 Hz), 132.56 (d, *J* = 127 Hz), 132.2 (d, *J* = 130 Hz), 132.1 (d, *J* = 3.0 Hz), 131.6 (d, *J* = 9.6 Hz), 128.73 (d, *J* = 12.6 Hz), 128.70 (d, *J* = 12.6 Hz), 120.4, 116.3, 90.5, 77.4, 56.8, 29.0 (d, *J* = 3.7 Hz), 19.4, 15.9; HRMS Calcd for $C_{23}H_{23}N_2OPSI$ $[M + H]^+$: 533.0314; Found: 533.0311. $[\alpha]^{25}_D$ = –25.6 (*c* = 1.00, $CHCl_3$) for a 99:1 e.r. sample.

A vial equipped with a stir bar was charged with iodoalkyne **3.30** (21.3 mg, 0.040 mmol) and *ortho*-nitrobenzensulfonylhydrazide (43.4 mg, 0.200 mmol). Equal parts tetrahyrdrofuran and *iso*-propanol were subsequently added. After allowing the solution to stir for five minutes, triethylamine (35.0 mL, 0.240 mmol) is added dropwise. The solution was allowed to stir in the dark for 18 hours after which the mixture was added to a 1:1 solution of AcOEt and a solution of saturated aqueous sodium bicarbonate (30 mL). The organic layer was separated and the aqueous layer was washed with AcOEt (3 x 15 mL). The organic layers were combined, dried over $MgSO_4$, and the volatiles removed. The unpurified residue obtained as an yellow oil was purified by silica gel chromatography a gradient from 100% Et_2O to 1:1 Et_2O:AcOEt to 100% AcOEt) to yield 15.6 mg (0.029 mmol, 73% yield) of pure **3.31** as a white crystalline solid.

***N*–((*S*,1*E*,5*Z*)-6-Iodo-2-methyl-1-(2-methylthiazol-4-yl)hexa-1,5-dien-3-yl)-*P*,*P*-diphenylphosphinic amide (3.31):** IR (neat): 3161 (w, br), 2923 (w, br), 1437 (m), 1184 (s), 1122 (m), 1109 (m), 1071 (m), 908 (w), 751 (m), 724 (s), 559 (m), 539 (m) cm^{-1}; ^1H NMR (400 MHz, $CDCl_3$): δ 7.93–7.87 (4H, m), 7.51–7.39 (6H, m), 6.87 (1H, s), 6.34–6.32 (1H, m), 6.27–6.23 (2H, m), 3.93–3.84 (1H, m), 3.12 (1H, br dd, *J* = 10.0, 6.0 Hz), 2.70 (3H, s), 2.65–2.55 (2H, m), 2.06 (3H, s),; ^{13}C NMR (100 MHz, $CDCl_3$): δ 164.7, 152.7, 139.0 (d, *J* = 5.2 Hz), 137.5, 132.9 (d, *J* = 127 Hz), 132.7 (d, *J* = 9.7 Hz), 132.4 (d, *J* = 130 Hz), 132.09 (d, *J* = 8.9 Hz), 132.08 (d *J* = 2.9 Hz), 132.0 (d, *J* = 2.2 Hz), 128.7 (d, *J* = 12.7 Hz), 128.5 (d, *J* = 12.6 Hz), 120.5, 116.1, 85.3, 77.4, 57.8, 41.4 (d, *J* = 4.5 Hz), 19.4, 15.2; HRMS Calcd for $C_{23}H_{25}N_2OPSI$ $[M + H]^+$: 535.04699; Found: 535.04792. $[\alpha]^{25}_D$ = –29.4 (*c* = 0.50, $CHCl_3$) for a 99:1 e.r. sample.

▪ **Representative Procedure for Conversion of Homopropargylamide 3.21a to 1,2-diboronate 3.34**: Under an inert atmosphere, an oven-dried vial equipped with a stir bar is charged with imidazolinium salt **3.33** (8.7 mg, 15 μmol), NaO*t*-Bu (5.8 mg, 60 μmol), and CuCl (1.5 mg, 15 μmol). The vial is sealed with a septum and Teflon tape and removed from the glovebox. Freshly distilled thf (300 μL) is added and the mixture is allowed to stir for 20 min under N_2 at 22 °C. A solution of bis(pinacolato)diboron **3.32** (111.7 mg, 0.440 mmol) in thf is transferred to the vial containing the NHC–Cu complex and allowed to stir for an additional 15 min. Subsequently, a solution of the homopropargylamide **3.21a** (69.1 mg, 0.20 mmol, 98.5:1.5 er) in 1.0 mL of thf is added to the solution of catalyst and the diboron reagent. The dark-colored reaction mixture is allowed to stir at 22 °C for 48 hours before filtration through a short column of silica gel topped with Celite with AcOEt. The volatiles are removed *in vacuo*. The unpurfied

mixture is purfied by silica gel chromatography (gradient from 1:2 AcOEt:hexanes to 100% AcOEt) to afford the 1,2-diboronate **3.34** (119.2 mg, 0.198 mmol) in 99% yield as a 85:15 mixture of diastereomers.

***P*,*P*–Diphenyl-*N*-((1*S*,3*S*)-1-phenyl-3,4-bis(4,4,5,5-tetramethyl-1,3,2-dioxaborolan-2-yl)butyl)phosphinic amide** (**3.34**): mp = 91–97 °C. IR (neat): 2977 (w, br), 2925 (w, br), 1371 (s), 1313 (m), 1196 (m), 1142 (s), 1110 (m), 967 (w), 846 (w), 754 (m), 724 (m), 698 (s), 528 (m) cm^{-1}; ^{1}H NMR (400 MHz, $CDCl_3$): δ 7.86–7.80 (2H, m), 7.78–7.72 (2H, m), 7.45–7.40 (1H, m), 7.39–7.34 (3H, m), 7.31–7.19 (7H, m), 4.31–4.23 (1H, m), 4.00 (1H, t, *J* = 8.0 Hz), 2.12–1.99 (1.15H, m), 1.82–1.71 (3H, m), 1.63 (12H, d, *J* = 6.8 Hz), 1.12 (12H, d, *J* = 0.8 Hz), 0.90–0.71 (2.5 H, m) ; ^{13}C NMR (100 MHz, $CDCl_3$): δ 144.6 (d, *J* = 3.7 Hz), 133.2 (d, *J* = 129 Hz, only the peak at 133.8 is visible, the other is overlapping), 132.8 (d, *J* = 129 Hz), 132.6 (d, *J* = 9.7 Hz), 132.4 (d, *J* = 9.7 Hz), 131.6 (d, *J* = 3.0 Hz), 131.5 (d, *J* = 2.9 Hz), 128.5 (d, *J* = 12.6 Hz), 128.3, 128.2 (d, *J* = 12.7 Hz), 126.7, 126.5, 83.2, 83.16, 18.09, 83.0, 55.2 (d, *J* = 1.5 Hz), 43.4 (d, *J* = 5.3 Hz), 25.0, 24.93, 24.87, 24.7, 24.6; HRMS Calcd for $C_{34}H_{46}NO_5PB_2Na$ $[M + Na]^+$: 624.3197; Found: 624.3203. $[\alpha]^{26}_D = -14.97$ (*c* = 1.00, $CHCl_3$).

▪ **Representative Procedure for Conversion of 1,2-diboronate 3.34 to 1,3-aminoalcohol 3.35**: A flame-dried 25 mL round-bottomed flask equipped with a stir bar is charged with 1,2-diboronate **3.34** (60.1 mg, 0.10 mmol), $Pd(dppf)Cl_2 \bullet CH_2Cl_2$ (7.3 mg, 10.0 μmol), and cesium carbonate (98.0 mg, 0.30 mmol). The flask is fitted with a reflux condenser and a septum and is sealed and placed under atomosphere of N_2. A degassed solution of 10:1 tetrahydrofuran:water is added by syringe. Lastly, distilled

bromobenzene (31.0 μL, 0.30 mmol) is added by syringe to the flask and the resulting brick red solution is allowed to stir at 80 °C for 20 hours. The reaction mixture is allowed to cool to 22 ºC and is subsequently filtered through a column of silica gel and Celite with ethyl acetate until the eluent is colorless. The mixture is concentrated and the unpurified foamy residue is taken up in 5 mL of a 1:1 solution of tetrahydofuran:water. The solution is treated with $NaBO_3 \bullet H_2O$ (99.1 mg, 10.0 mmol). The reaction mixture is allowed to stir at 22 °C for 1 hour before dilution with 10 mL each of water and ethyl acetate. The organic layer is removed and the aqueous layer is washed with ethyl acetate (3 x 10 mL). The combined organic layers are dried over $MgSO_4$ and the volatiles are removed *in vacuo*. The unpurified mixture is purified by silica gel chromatography (gradient from 1:2 AcOEt:hexanes to 100% AcOEt) to afford the 1,3-aminoalochol **3.35** (35.2 mg, 0.08 mmol) in 80% yield as a single diastereomer.

***N*–((1*S*,3*R*)-3-hydroxy-1,4-diphenylbutyl)-*P*,*P*-diphenylphosphinic amide** (**3.35**): mp = 170–173 °C. IR (neat): 3257 (m, br), 1438 (m), 1178 (m, br), 1124 (m), 1109 (m), 751 (w), 726 (m), 698 (s), 538 (m) cm^{-1}; ^1H NMR (400 MHz, $CDCl_3$): δ 7.85–7.80 (2H, m), 7.70–7.66 (2H, m), 7.53–7.50 (1H, m), 7.46–7.40 (3H, m), 7.31–7.15 (10H, m), 7.10–7.08 (1H, m), 4.51–4.43 (1H, m), 4.31–4.24 (1H, m), 3.26 (1H, t, *J* = 9.8 Hz), 2.99 (1H, dd, *J* = 13.6, 6.4 Hz), 2.70 (1H, dd, *J* = 13.6, 6.4 Hz), 1.86–1.66 (2H, *m*); ^{13}C NMR (100 MHz, $CDCl_3$): δ 144.5, 139.2, 132.34 (d, *J* = 2.9 Hz,), 132.32 (d, *J* = 148 Hz), 132.2 (d, *J* = 148 Hz), 132.1 (d, *J* = 2.9 Hz), 129.7, 128.8 (d, *J* = 12.6 Hz), 128.6, 128.44 (d, *J* = 12.6 Hz, only the peak at 128.5 is visible, the other is overlapping)), 128.37, 127.1, 126.1, 126.0, 67.9, 52.2, 46.7, 43.9.

▪ **Representative Procedure for the Oxidation of 1,2-diboronate 3.34 to diol 3.36**: A 10 mL vial equipped with a stir bar is charged with 1,2-diboronate **3.34** (60.1 mg, 0.10 mmol). The diboronate is dissolved in 1.0 mL of tetrahydofuran and the solution is allowed to cool to 0 ºC. A 2N aqueous solution of NaOH and hydrogen peroxide are subsequently added to the vial. The reaction mixture is allowed to stir at 22 °C for 30 minutes before dilution with 5 mL of dichlormethane. The organic layer is removed and the aqueous layer is washed with dichloromethane (3 x 10 mL). The combined organic layers are dried over Na_2SO_4 and the volatiles are removed *in vacuo*. The unpurified white residue is purified by silica gel chromatography (gradient from 1:1 AcOEt:Et_2O, to 100% AcOEt, to 4:1 AcOEt:MeOH) to afford the diol **3.36** (40.2 mg, 0.105 mmol) in >98% yield as a 83:17 mixture of diastereomers. The mixture of diastereomers can be recrystallized to afford the (*S*,*S*) diastereomer with >95% purity in 80% yield (30.5 mg, 0.080 mmol). The absolute configuration of the major diastereomeric product was established through single crystal X-ray crystallographic analysis (depicted below).

N–((1S,3S)-3,4-dihydroxy-1-phenylbutyl)-P,P-diphenylphosphinic amide (**3.36**): mp = 127–129 °C. ^{1}H NMR (400 MHz, $CDCl_3$): δ 7.85–7.80 (2H, m), 7.72–7.67 (2H, m), 7.54–7.50 (1H, m), 7.47–7.41 (3H, m), 7.34–7.24 (5H, m), 7.14–7.11 (2H, m), 5.85 (1H, s), 4.51–4.41 (1H, m), 4.27–4.19 (1H, m), 3.61–3.44 (3H, m), 2.74 (1H, br s), 1.83–1.63 (2H, *m*); ^{13}C NMR (125 MHz, $CDCl_3$): δ 144.3 (d, *J* = 6.5 Hz), 133.1 (d, *J* = 10.1 Hz,), 132.5 (d, *J* = 127 Hz), 132.4 (d, *J* = 3.0 Hz), 132.3 (d, *J* = 2.9 Hz), 131.6 (d, *J* = 9.7 Hz), 128.9 (d, *J* = 12.5 Hz), 128.7, 128.5 (d, *J* = 12.9 Hz), 127.2, 126.0, 67.9, 66.8, 52.1, 43.2. HRMS Calcd for $C_{22}H_{25}NO_3P$ $[M + H]^+$: 382.15720; Found: 382.15588.

▪ **Synthesis of Enantiomerically Enriched *β*–Amino Acid 3.37:** The procedure used is based on a previously reported protocol.[59] To a solution of homopropargylamide **3.21p** (48.0 mg, 0.147 mmol, 97:3 er) in MeCN:H_2O:AcOEt (1.5:1.0:0.3 mL) was added sodium bicarbonate (123 mg, 1.46 mmol) and Oxone (300. mg, 0.487 mmol). The solution was allowed to stir for three minutes before addition of $RuCl_3 \bullet 2H_2O$ (0.9 mg, 4. μmol). After three hours, the reaction was quenched by the addition of a solution of 10% aqueous sodium bisulfite. The solution was acidified to pH = 1 by addition of a 1.0 M solution of HCl. The aqueous layer was washed with AcOEt (2 x 10 mL) and with AcOEt:MeOH (4:1) (2 x 10 mL). The combined organic layers were then washed with brine and dried over Na_2SO_4 and the volatiles were removed *in vacuo*. The unpurified residue, obtained as a clear oil, was purified by silica gel chromatography (a gradient from 1:1 hexanes:AcOEt to 100% AcOEt ultimately flushing with 4:1 AcOEt:MeOH) to yield 48.7 mg (0.141 mmol, 96% yield) of pure **3.37** as a white crystalline solid in 96.5:3.5 e.r. (93% ee).

(*R*)–3-((Diphenylphosphoryl)amino)-5-methylhexanoic acid (**3.37**): mp = 191–194 °C. IR (neat): 3223 (w, br), 2956 (w, br), 2474 (w, br), 1698 (m), 1438 (m), 1299 (w), 1155 (s), 1121 (m), 1107 (m), 970 (w), 726 (m), 698 (m), 559 (m), 532 (m) cm^{-1}; ^1H NMR (400 MHz, CD_3OD): δ 7.93–7.86 (4H, m), 7.54–7.41 (6H, m), 3.86 (1H, br dd, *J* = 10.6, 4.6 Hz), 3.31–3.21 (1H, m), 2.93 (1H, dd, *J* = 16.0, 4.8 Hz), 2.47 (1H, ddd, *J* = 16.0, 3.2 Hz), 1.68 (1H, app sept, *J* = 6.8 Hz), 1.61–1.54 (1H, m), 1.46–1.39 (1H, m), 0.74 (6H, dd, *J* = 16.4, 6.4 Hz); ^{13}C NMR (100 MHz, CD_3OD): δ 175.1 (w, br), 133.7 (d, *J* = 131 Hz), 133.5 (d, *J* = 129 Hz), 133.45 (d, *J* = 9.3 Hz), 133.42 (d, *J* = 2.6 Hz, only

---

[59] "Ruthenium-Catalyzed Oxidative Cleavage of Alkynes to Carboxylic Acids," Yang, D.; Chen, F.; Dong, Z-M.; Zhang, D-W. *J. Org. Chem.* **2004**, *69*, 2221–2223.

the peak at 133.4 is visible, the other may be overlapping), 133.37 (d, J = 3.4 Hz, only the peak at 133.3 is visible, the other may be overlapping) 133.34 (d, J = 9.3 Hz), 129.83 (d, J = 12.6 Hz), 128.78 (d, J = 12.6 Hz), 48.6, 47.7 (d, J = 5.2 Hz), 25.9, 23.4, 22.7; HRMS Calcd for $C_{19}H_{25}NO_3P$ [M + H]$^+$: 346.15720 Found: 346.15721; $[\alpha]^{25}_D$ = +14.1 (c = 1.00, MeOH) for a 96:4 e.r. sample. The enantiomeric purity of this compound was determined by HPLC analysis in comparison with authentic racemic material (Chiracel AD–H, 92:8 hexanes:*i*-PrOH, 0.8 mL/min, 220 nm): t_R of **3.37**: 16 min (major) and 43 min (minor).

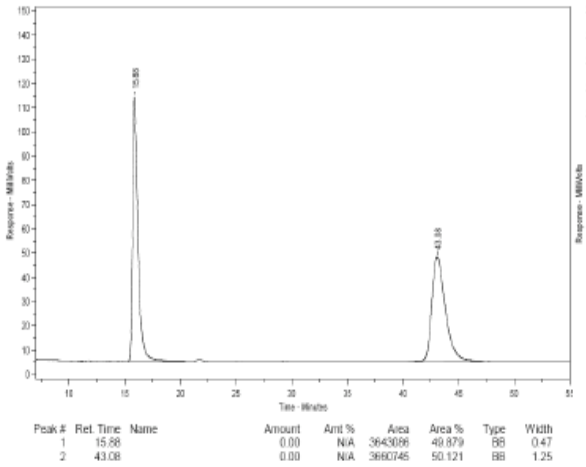

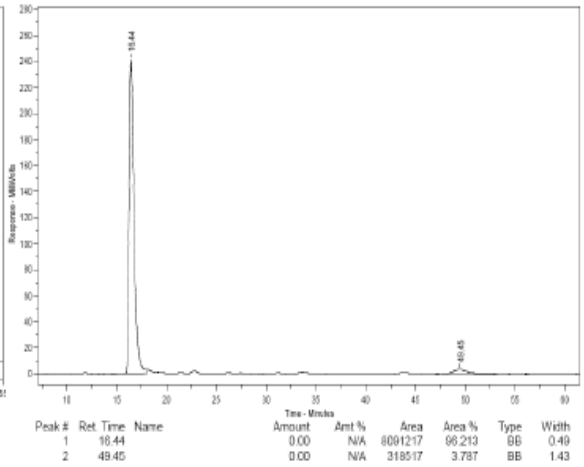

Peak #	Ret. Time	Area %	Peak #	Ret. Time	Area %
1	15.9 min	49.879	1	15.8 min	96.213
2	43.1 min	50.121	2	42.8 min	3.787

▪ **Absolute Configuration of 3.21f:** ***X-ray Crystal Structure of Homopropargylamide (S)-*** **3.21f*:***

Proof of Absolute Stereochemistry: Please note that the absolute stereochemistry of the major product enantiomers are inferred from that obtained through the X-ray crystal structure of homopropargylamine **3.21f.**

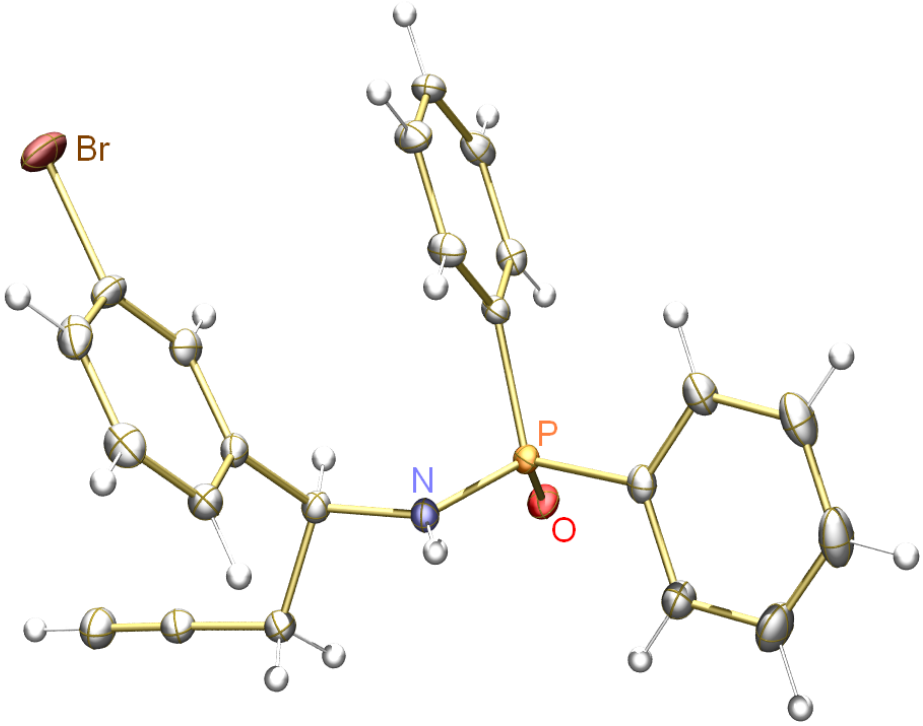

Table 1. *Crystal data and structure refinement for $C_{22}H_{19}BrNOP$.*

Identification code	$C_{22}H_{19}BrNOP$	
Empirical formula	$C_{22}H_{19}BrNOP$	
Formula weight	424.26	
Temperature	100(2) K	
Wavelength	0.71073 ≈	
Crystal system	Tetragonal	
Space group	P 4(1)	
Unit cell dimensions	a = 9.3962(2) ≈	a= 90∞.
	b = 9.3962(2) ≈	b= 90∞.

	c = 45.1252(9) ≈ g = 90∞.
Volume	3984.04(14) ≈^{3}
Z	8
Density (calculated)	1.415 Mg/m^3
Absorption coefficient	2.154 mm^{-1}
F(000)	1728
Crystal size	0.13 x 0.05 x 0.02 mm^3
Theta range for data collection	1.81 to 28.32∞.
Index ranges	-12<=h<=10, -12<=k<=12, -60<=l<=60
Reflections collected	75351
Independent reflections	9877 [R(int) = 0.0271]
Completeness to theta = 28.32∞	99.9 %
Absorption correction	Semi-empirical from equivalents
Max. and min. transmission	0.9582 and 0.7671
Refinement method	Full-matrix least-squares on F^2
Data / restraints / parameters	9877 / 3 / 475
Goodness-of-fit on F^2	1.046
Final R indices [I>2sigma(I)]	R1 = 0.0281, wR2 = 0.0669
R indices (all data)	R1 = 0.0305, wR2 = 0.0676
Absolute structure parameter	0.014(4)
Extinction coefficient	na
Largest diff. peak and hole	1.447 and -0.827 e.≈$^{-3}$

Table 2. *Atomic coordinates (x 10^4) and equivalent isotropic displacement parameters ($\approx^2$x 10^3) for $C_{22}H_{19}BrNOP$. U(eq) is defined as one third of the trace of the orthogonalized U^{ij} tensor.*

	x	y	z	U(eq)
Br(1)	-257(1)	1531(1)	8621(1)	32(1)
P(1)	3270(1)	-1188(1)	9863(1)	13(1)
O(1)	4590(2)	-2041(2)	9817(1)	19(1)
N(1)	1792(2)	-1866(2)	9736(1)	16(1)
C(1)	2891(2)	-890(2)	10247(1)	16(1)
C(2)	2764(3)	-2094(3)	10429(1)	22(1)
C(3)	2516(3)	-1930(3)	10729(1)	31(1)
C(4)	2400(3)	-582(3)	10852(1)	31(1)
C(5)	2521(3)	602(3)	10675(1)	28(1)
C(6)	2767(2)	463(3)	10372(1)	22(1)
C(7)	3427(2)	490(2)	9672(1)	14(1)
C(8)	4753(2)	890(2)	9561(1)	16(1)
C(9)	4871(2)	2097(2)	9383(1)	20(1)
C(10)	3679(3)	2903(2)	9319(1)	20(1)
C(11)	2364(2)	2530(2)	9436(1)	22(1)
C(12)	2240(2)	1321(2)	9611(1)	19(1)
C(13)	1659(2)	-2207(2)	9418(1)	15(1)
C(14)	383(2)	-1461(2)	9281(1)	16(1)
C(15)	591(3)	-486(2)	9055(1)	19(1)
C(16)	-567(3)	202(2)	8931(1)	21(1)
C(17)	-1946(3)	-68(2)	9026(1)	24(1)
C(18)	-2144(3)	-1050(3)	9251(1)	24(1)
C(19)	-993(2)	-1751(2)	9378(1)	19(1)
C(20)	1580(2)	-3835(2)	9381(1)	18(1)

C(21)	1489(2)	-4301(2)	9072(1)	21(1)
C(22)	1429(3)	-4705(3)	8824(1)	28(1)
Br(2)	5526(1)	6460(1)	8887(1)	35(1)
P(2)	8303(1)	6938(1)	10241(1)	12(1)
O(2)	9582(2)	6748(2)	10049(1)	17(1)
N(2)	6760(2)	6385(2)	10112(1)	14(1)
C(23)	8565(2)	5953(2)	10580(1)	15(1)
C(24)	9847(2)	5236(2)	10625(1)	22(1)
C(25)	10059(3)	4459(3)	10883(1)	29(1)
C(26)	9005(3)	4406(3)	11098(1)	28(1)
C(27)	7729(3)	5108(3)	11054(1)	26(1)
C(28)	7507(2)	5884(2)	10797(1)	20(1)
C(29)	7960(2)	8779(2)	10326(1)	14(1)
C(30)	9076(2)	9743(2)	10287(1)	21(1)
C(31)	8903(3)	11169(2)	10359(1)	24(1)
C(32)	7608(3)	11657(2)	10465(1)	20(1)
C(33)	6483(2)	10706(2)	10501(1)	19(1)
C(34)	6659(2)	9270(2)	10433(1)	18(1)
C(35)	6607(2)	4927(2)	10004(1)	15(1)
C(36)	7009(2)	4782(2)	9678(1)	16(1)
C(37)	6259(2)	5569(2)	9466(1)	18(1)
C(38)	6609(3)	5405(3)	9169(1)	24(1)
C(39)	7679(3)	4508(3)	9076(1)	30(1)
C(40)	8414(3)	3743(3)	9286(1)	30(1)
C(41)	8088(2)	3872(3)	9587(1)	24(1)
C(42)	5067(2)	4397(2)	10048(1)	19(1)
C(43)	4663(2)	4289(2)	10363(1)	20(1)
C(44)	4349(3)	4176(3)	10616(1)	29(1)

▪ **Absolute Configuration of 3.36:** ***X-ray Crystal Structure of Diol (S,S)-3.36:***

Proof of Absolute Stereochemistry: Please note that the NHC–Cu catalyst derived from imidazolinium salt **3.33** delivers enantioselective diboron addition to provide the new B-susbtituted stereocenter as the *R*-configuration regardless of the enantiomeric purity of the *N*-substituted stereocenter, i.e., the stereoselectivity is completely catalyst-controlled and not substrate-controlled.

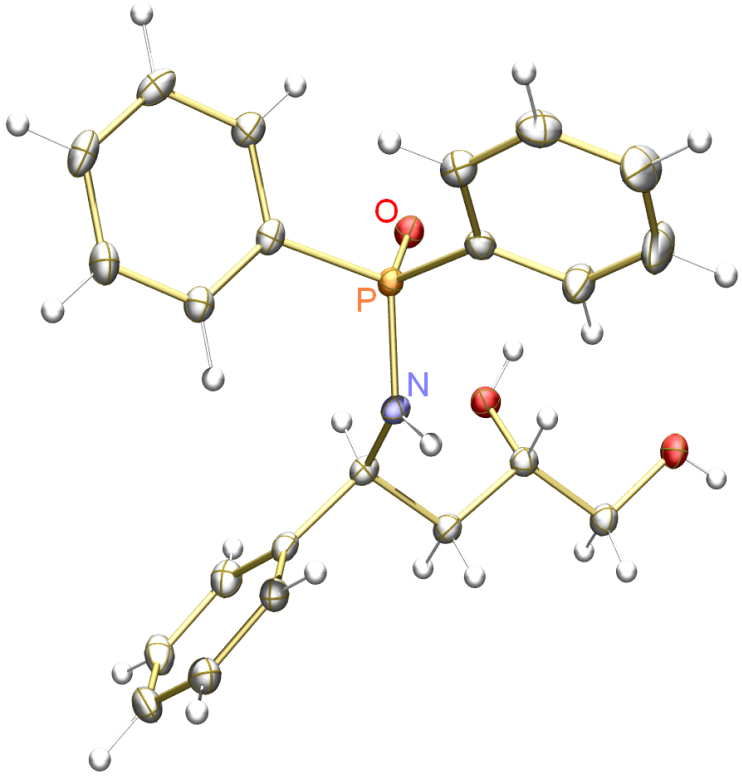

Table 1. *Crystal data and structure refinement for $C_{22}H_{24}NO_3P$.*

Identification code	$C_{22}H_{24}NO_3P$
Empirical formula	C_{22} H_{24} N O_3 P
Formula weight	381.39
Temperature	100(2) K
Wavelength	0.71073 ≈
Crystal system	Monoclinic
Space group	C 2

Unit cell dimensions	a = 20.2687(9) ≈	α= 90∞.
	b = 5.3404(3) ≈	β= 95.496(2)∞.
	c = 18.1190(8) ≈	γ = 90∞.
Volume	1952.24(16) ≈^{3}	
Z	4	
Density (calculated)	1.298 Mg/m^3	
Absorption coefficient	0.163 mm^{-1}	
F(000)	808	
Crystal size	0.24 x 0.05 x 0.04 mm^3	
Theta range for data collection	2.02 to 28.28∞.	
Index ranges	-27<=h<=27, -7<=k<=7, -24<=l<=24	
Reflections collected	24035	
Independent reflections	4793 [R(int) = 0.0277]	
Completeness to theta = 28.28∞	99.9 %	
Absorption correction	Semi-empirical from equivalents	
Max. and min. transmission	0.9935 and 0.9619	
Refinement method	Full-matrix least-squares on F^2	
Data / restraints / parameters	4793 / 6 / 259	
Goodness-of-fit on F^2	1.053	
Final R indices [I>2sigma(I)]	R1 = 0.0300, wR2 = 0.0742	
R indices (all data)	R1 = 0.0322, wR2 = 0.0759	
Absolute structure parameter	0.00(6)	
Extinction coefficient	na	
Largest diff. peak and hole	0.359 and -0.182 e.≈$^{-3}$	

Table 2. *Atomic coordinates (x 10^4) and equivalent isotropic displacement parameters (≈^{2}x 10^3) for $C_{22}H_{24}NO_3P$. U(eq) is defined as one third of the trace of the orthogonalized U^{ij} tensor*.

	x	y	z	U(eq)
P(1)	1887(1)	-1453(1)	2296(1)	14(1)
O(1)	2049(1)	-3789(2)	1893(1)	18(1)
O(2)	3285(1)	-2410(2)	902(1)	21(1)
O(3)	2914(1)	189(2)	-447(1)	22(1)
N(1)	2425(1)	823(2)	2264(1)	16(1)
C(1)	1792(1)	-2322(3)	3243(1)	17(1)
C(2)	2041(1)	-883(3)	3844(1)	19(1)
C(3)	1926(1)	-1596(4)	4563(1)	24(1)
C(4)	1564(1)	-3732(3)	4679(1)	24(1)
C(5)	1323(1)	-5203(3)	4081(1)	23(1)
C(6)	1438(1)	-4504(3)	3366(1)	20(1)
C(7)	1116(1)	-54(3)	1938(1)	17(1)
C(8)	539(1)	-274(3)	2298(1)	22(1)
C(9)	-61(1)	598(3)	1963(1)	27(1)
C(10)	-94(1)	1712(4)	1274(1)	36(1)
C(11)	481(1)	1980(4)	919(1)	41(1)
C(12)	1083(1)	1094(4)	1244(1)	28(1)
C(13)	3148(1)	479(3)	2267(1)	16(1)
C(14)	3536(1)	1785(3)	2919(1)	18(1)
C(15)	4170(1)	945(3)	3174(1)	23(1)
C(16)	4554(1)	2254(4)	3726(1)	28(1)
C(17)	4317(1)	4406(3)	4025(1)	28(1)
C(18)	3687(1)	5266(3)	3780(1)	25(1)
C(19)	3300(1)	3938(3)	3233(1)	20(1)

C(20)	3398(1)	1490(3)	1548(1)	18(1)
C(21)	3098(1)	161(3)	855(1)	17(1)
C(22)	3319(1)	1297(3)	151(1)	19(1)

Table 3. *Hydrogen bonds for $C_{22}H_{24}NO_3P$ [≈ and ∞].*

D-H...A	d(D-H)	d(H...A)	d(D...A)	<(DHA)
O(2)-H(2O)...O(3)#1	0.833(15)	1.976(15)	2.8014(15)	170(2)
O(3)-H(3O)...O(1)#2	0.822(15)	1.913(16)	2.6832(14)	156(2)
N(1)-H(1N)...O(1)#3	0.899(14)	2.143(15)	3.0359(16)	172.3(16)

Symmetry transformations used to generate equivalent atoms:

#1 -x+1/2,y-1/2,-z #2 -x+1/2,y+1/2,-z #3 x,y+1,z

▪**Gibbs Free Energy Surface of the Isomerization Event Between Model NHC–Cu–allene and Propargyl Complexes**: The geometries **A**-**C** were optimized with the B3LYP/6-31+G* method. Frequency calculations were carried out at the same level of theory. All computed frequencies are real except the transition state **B**, which has one imaginary frequency. Relative free energies are in kcal/mol and were computed at 298K.

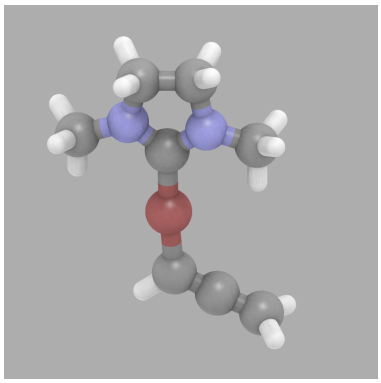

A

0.0

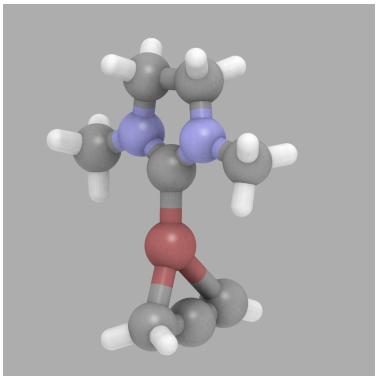

B

14.7

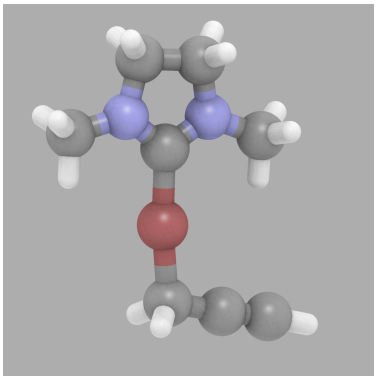

C

7.9

▪ **NHC–Cu-allene complex (A)**

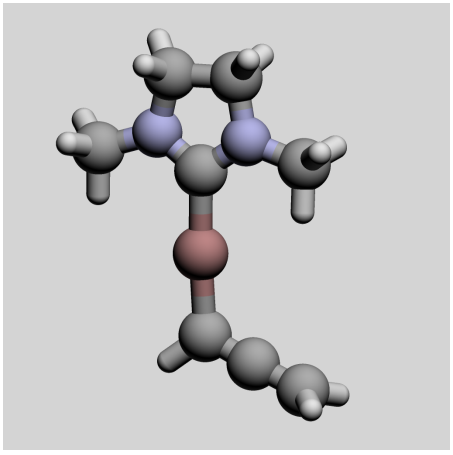

#b3lyp/6-31+G* freq geom=check guess=check

Cartesian coordinates (Angstroms):

H 3.121 -2.027 -0.072

H -2.412 -2.590 0.997

H	-3.742	-0.249	1.098
C	-2.045	-2.247	0.020
H	-0.786	3.151	0.774
N	-2.060	-0.799	-0.063
H	-3.255	2.073	0.704
C	-0.969	-0.008	-0.007
C	-3.319	-0.055	0.102
H	-2.678	-2.679	-0.764
N	-1.392	1.269	0.066
H	0.504	2.130	0.087
C	-2.852	1.401	-0.062
C	-0.537	2.439	-0.023
H	-4.056	-0.359	-0.649
H	-3.106	1.814	-1.049
H	-0.659	2.941	-0.993
H	-1.019	-2.596	-0.116
Cu	0.881	-0.564	-0.023
C	2.745	-0.999	-0.031
C	3.639	-0.045	0.014
C	4.498	0.960	0.063
H	4.871	1.346	1.011
H	4.885	1.425	-0.842

SCF Done: E(RB3LYP) = -2062.49255300 A.U. after 2 cycles

	1	2	3
	A	A	A
Frequencies --	16.9307	32.8673	67.1439
Red. masses --	3.6630	4.5481	2.7797

Zero-point correction= 0.197630 (Hartree/Particle)

Thermal correction to Energy= 0.211536

Thermal correction to Enthalpy=	0.212480
Thermal correction to Gibbs Free Energy=	0.154620
Sum of electronic and zero-point Energies=	–2062.294923
Sum of electronic and thermal Energies=	–2062.281017
Sum of electronic and thermal Enthalpies=	–2062.280073
Sum of electronic and thermal Free Energies=	–2062.337933

Item	Value	Threshold	Converged?
Maximum Force	0.000015	0.000450	YES
RMS Force	0.000003	0.000300	YES
Maximum Displacement	0.004173	0.001800	NO
RMS Displacement	0.000994	0.001200	YES

▪ **Model NHC–Cu-allene to propargyl isomerization transition state (B)**

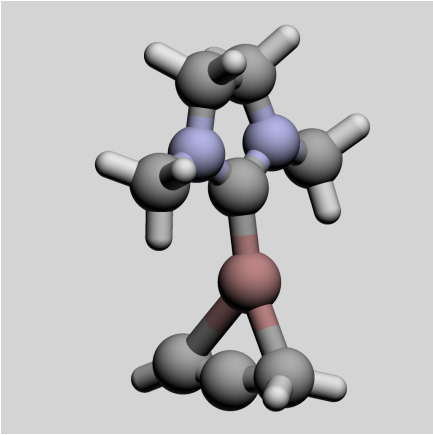

#b3lyp/6-31+G* freq guess=check geom=check

Cartesian coordinates (Angstroms):

H 1.451 -2.896 -0.964

H 3.425 -1.051 -0.922

C 1.138 -2.458 -0.005

H 1.686 3.089 -0.719

N	1.575	-1.081	0.109
H	3.662	1.301	-0.459
C	0.778	-0.003	-0.066
C	3.005	-0.748	0.050
H	1.563	-3.057	0.810
N	1.576	1.089	-0.102
H	0.052	2.478	-0.355
C	2.977	0.779	0.217
C	1.098	2.456	-0.043
H	3.564	-1.260	0.840
H	3.207	1.087	1.249
H	1.173	2.863	0.976
H	0.049	-2.491	0.060
Cu	-1.117	-0.010	-0.237
H	-3.142	0.058	2.620
C	-2.810	0.034	1.600
C	-3.116	0.004	0.389
C	-3.021	-0.030	-1.017
H	-3.321	-0.955	-1.512
H	-3.326	0.867	-1.557

SCF Done: E(RB3LYP) = -2062.46926506 A.U. after 7 cycles

	1	2	3
	A	A	A
Frequencies --	-129.2513	19.8979	54.6190
Red. masses --	10.4027	3.7280	3.6828

Zero-point correction=	0.196288 (Hartree/Particle)
Thermal correction to Energy=	0.209653
Thermal correction to Enthalpy=	0.210597
Thermal correction to Gibbs Free Energy=	0.154714

Sum of electronic and zero-point Energies=	–2062.272977
Sum of electronic and thermal Energies=	–2062.259612
Sum of electronic and thermal Enthalpies=	–2062.258668
Sum of electronic and thermal Free Energies=	–2062.314551

Item	Value	Threshold	Converged?
Maximum Force	0.000007	0.000450	YES
RMS Force	0.000001	0.000300	YES
Maximum Displacement	0.000384	0.001800	YES
RMS Displacement	0.000063	0.001200	YES

▪ **NHC–Cu-propargyl complex (C)**

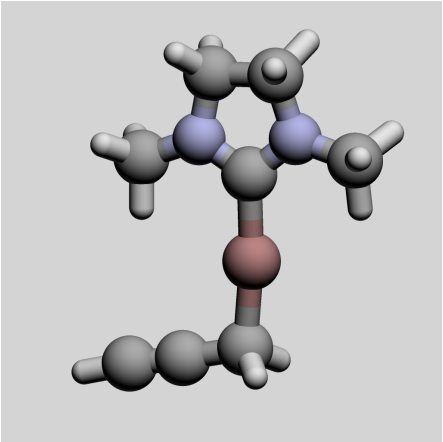

#b3lyp/6-31+G* freq geom=check guess=check

Cartesian coordinates (Angstroms):

H -4.632 2.182 0.108

H -3.079 -1.709 0.837

C -4.084 1.269 0.069

C -3.538 0.178 0.025

C -2.823 -1.080 -0.027

H -3.089 -1.642 -0.934

H 2.743 -2.612 -0.765

H	4.012	-0.227	-0.661
C	2.098	-2.209	0.025
H	0.475	2.918	-0.990
N	2.044	-0.763	-0.059
H	2.967	1.904	-1.047
C	0.917	-0.024	-0.008
C	3.267	0.042	0.096
H	2.491	-2.533	0.999
N	1.276	1.272	0.058
H	-0.661	2.044	0.069
C	2.729	1.474	-0.064
C	0.366	2.401	-0.027
H	3.708	-0.132	1.088
H	3.095	2.161	0.707
H	0.575	3.115	0.779
H	1.088	-2.606	-0.100
Cu	-0.915	-0.646	-0.021

SCF Done: E(RB3LYP) = -2062.47947801 A.U. after 2 cycles

	1	2	3
	A	A	A
Frequencies --	21.6616	32.3980	68.6886
Red. masses --	4.0503	5.2288	2.8496

Zero-point correction=	0.197036 (Hartree/Particle)
Thermal correction to Energy=	0.211112
Thermal correction to Enthalpy=	0.212056
Thermal correction to Gibbs Free Energy=	0.154202
Sum of electronic and zero-point Energies=	–2062.282442
Sum of electronic and thermal Energies=	–2062.268366
Sum of electronic and thermal Enthalpies=	–2062.267422

Sum of electronic and thermal Free Energies= –2062.325276

Item	Value	Threshold	Converged?
Maximum Force	0.000014	0.000450	YES
RMS Force	0.000003	0.000300	YES
Maximum Displacement	0.001120	0.001800	YES
RMS Displacement	0.000234	0.001200	YES

▪**Gibbs Free Energy Surface of the Isomerization Event Between NHC–Cu–allene and Propargyl Complexes**. The geometries **F–H** were optimized with the B3LYP/LANL2DZ method. Frequency calculations were carried out at the same level of theory as the geometry optimizations. All computed frequencies are real except for the transition state **G**, which has one imaginary frequency. Relative free energies are in kcal/mol and were computed at 298K (as shown under each figure).

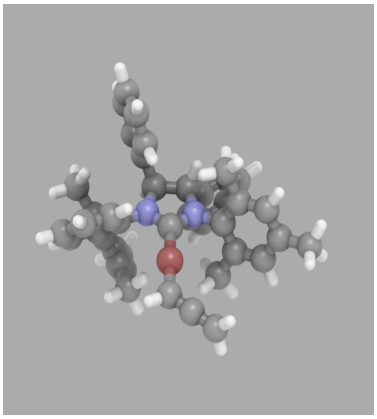

F

0.0

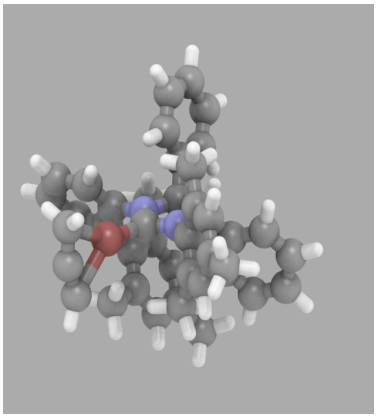

G

16.8

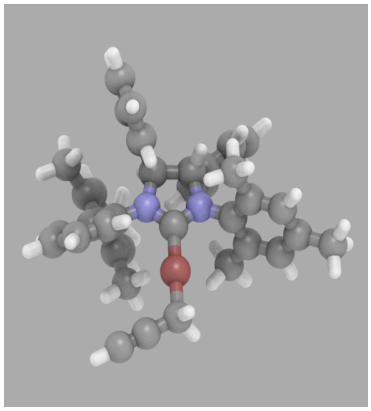

H

9.9

▪**NHC–Cu allene complex (F)**

#p b3lyp/lanl2dz freq geom=check guess=check

Cartesian coordinates (Angstroms):

C 0.246 1.414 1.000

N	1.249	0.398	0.500
C	-1.078	0.568	1.061
C	0.712	-0.828	0.265
N	-0.626	-0.772	0.545
C	-2.650	-1.904	-0.392
C	-3.459	-3.063	-0.418
C	-1.502	-1.916	0.442
C	-3.138	-4.209	0.327
C	-1.176	-3.068	1.187
C	-1.981	-4.215	1.127
C	2.846	0.608	2.947
C	3.433	0.846	1.567
C	4.798	1.175	1.446
C	2.660	0.710	0.386
C	5.411	1.353	0.191
C	6.890	1.671	0.079
C	3.251	0.866	-0.894
C	4.620	1.190	-0.963
C	2.471	0.650	-2.175
C	-4.967	-0.141	0.239
C	-4.449	1.123	-1.888
C	-4.115	0.080	-1.001
C	-4.117	2.471	-4.022
C	-3.731	1.344	-3.081
C	-3.006	-0.759	-1.300
C	-2.659	0.480	-3.377
C	-2.287	-0.573	-2.512
C	-1.165	-1.512	-2.922
C	0.715	5.057	-0.100
C	0.759	3.867	0.649
C	0.175	2.681	0.157

C	0.083	5.074	-1.357
C	-0.503	3.893	-1.856
C	-0.457	2.706	-1.106
C	-3.278	1.395	4.093
C	-2.763	1.354	2.784
C	-1.670	0.522	2.466
C	-2.708	0.594	5.100
C	-1.618	-0.243	4.789
C	-1.102	-0.275	3.483
H	0.536	1.704	2.014
H	-1.822	0.986	0.379
H	-4.337	-3.066	-1.061
H	-3.774	-5.089	0.274
H	-0.285	-3.059	1.808
H	-1.709	-5.098	1.700
H	3.644	0.410	3.671
H	2.167	-0.251	2.950
H	2.282	1.476	3.318
H	5.396	1.273	2.350
H	7.304	2.006	1.037
H	7.077	2.455	-0.665
H	7.457	0.783	-0.235
H	5.079	1.303	-1.943
H	2.338	-0.424	-2.367
H	3.008	1.077	-3.030
H	1.477	1.105	-2.130
H	-4.363	-0.357	1.126
H	-5.644	-0.996	0.104
H	-5.586	0.738	0.449
H	-5.292	1.769	-1.647
H	-3.443	2.524	-4.884

H -4.090 3.444 -3.512

H -5.138 2.336 -4.405

H -2.109 0.613 -4.307

H -1.517 -2.550 -2.976

H -0.331 -1.505 -2.210

H -0.767 -1.239 -3.906

H 1.171 5.963 0.293

H 1.250 3.860 1.620

H 0.046 5.992 -1.939

H -0.994 3.897 -2.826

H -0.917 1.808 -1.512

H -4.120 2.043 4.323

H -3.208 1.976 2.009

H -3.107 0.620 6.111

H -1.175 -0.868 5.561

H -0.261 -0.926 3.254

Cu 1.694 -2.382 -0.386

H 2.170 -4.896 -1.077

C 2.646 -3.905 -1.072

C 3.876 -3.833 -1.551

C 5.120 -3.718 -2.029

H 5.990 -3.837 -1.384

H 5.310 -3.510 -3.081

SCF Done: E(RB3LYP) = -1930.52741869 A.U. after 7 cycles

	1	2	3
	A	A	A
Frequencies --	9.6890	13.9326	19.1796
Red. masses --	4.1978	5.1121	5.3159

Zero-point correction= 0.715084 (Hartree/Particle)

Thermal correction to Energy=	0.759198
Thermal correction to Enthalpy=	0.760142
Thermal correction to Gibbs Free Energy=	0.631316
Sum of electronic and zero-point Energies=	–1929.812335
Sum of electronic and thermal Energies=	–1929.768221
Sum of electronic and thermal Enthalpies=	–1929.767277
Sum of electronic and thermal Free Energies=	–1929.896102

Item	Value	Threshold	Converged?
Maximum Force	0.000160	0.000450	YES
RMS Force	0.000014	0.000300	YES
Maximum Displacement	0.105403	0.001800	NO
RMS Displacement	0.009504	0.001200	NO

▪NHC–Cu-allene to propargyl isomerization transition state (G)

#p b3lyp/lanl2dz freq geom=check guess=check

Cartesian coordinates (Angstroms):

C	0.741	-0.920	0.005
N	1.382	0.221	0.384
C	2.803	0.448	0.223
H	-1.634	1.019	0.626
H	1.976	-3.004	-4.174
C	2.023	-3.098	-3.103
C	2.433	-3.824	-2.141
C	2.689	-4.289	-0.833
H	2.115	-5.139	-0.465
H	3.703	-4.208	-0.443
C	0.501	1.196	1.128
C	-0.876	0.439	1.157

N	-0.573	-0.816	0.387
C	-2.758	-1.611	-0.534
C	-3.665	-2.686	-0.687
C	-1.548	-1.857	0.166
C	-3.382	-3.971	-0.197
C	-1.260	-3.150	0.653
C	-2.164	-4.206	0.468
C	3.148	-0.280	2.660
C	3.663	0.252	1.334
C	5.039	0.509	1.178
C	5.579	0.939	-0.050
C	7.061	1.238	-0.189
C	3.321	0.844	-1.036
C	4.705	1.085	-1.145
C	2.441	0.964	-2.265
C	-4.854	0.172	0.610
C	-4.409	1.753	-1.312
C	-4.092	0.549	-0.651
C	-4.129	3.436	-3.202
C	-3.774	2.131	-2.513
C	-3.088	-0.300	-1.193
C	-2.811	1.258	-3.055
C	-2.458	0.046	-2.421
C	-1.458	-0.881	-3.088
C	1.182	4.937	0.635
C	1.187	3.631	1.158
C	0.467	2.596	0.527
C	0.449	5.224	-0.531
C	-0.275	4.196	-1.167
C	-0.266	2.892	-0.644
C	-2.729	0.890	4.486

C	-2.326	1.044	3.147
C	-1.359	0.187	2.583
C	-2.173	-0.133	5.276
C	-1.210	-0.997	4.718
C	-0.804	-0.836	3.382
H	0.884	1.284	2.151
H	-4.591	-2.507	-1.229
H	-4.094	-4.779	-0.343
H	-0.319	-3.321	1.166
H	-1.921	-5.197	0.842
H	3.983	-0.573	3.305
H	2.513	-1.161	2.509
H	2.555	0.463	3.212
H	5.702	0.352	2.027
H	7.657	0.646	0.515
H	7.270	2.299	0.016
H	7.419	1.024	-1.202
H	5.108	1.385	-2.111
H	2.128	-0.030	-2.612
H	2.984	1.452	-3.082
H	1.536	1.543	-2.061
H	-4.195	-0.220	1.392
H	-5.596	-0.611	0.403
H	-5.391	1.037	1.015
H	-5.172	2.403	-0.886
H	-3.642	3.518	-4.180
H	-3.820	4.301	-2.598
H	-5.213	3.524	-3.358
H	-2.332	1.513	-3.998
H	-1.883	-1.882	-3.240
H	-0.547	-1.023	-2.494

H -1.157 -0.491 -4.066

H 1.744 5.723 1.133

H 1.757 3.415 2.061

H 0.440 6.232 -0.938

H -0.844 4.408 -2.070

H -0.831 2.115 -1.152

H -3.474 1.560 4.908

H -2.761 1.837 2.540

H -2.486 -0.259 6.310

H -0.779 -1.794 5.320

H -0.061 -1.508 2.960

Cu 1.594 -2.416 -0.839

SCF Done: E(RB3LYP) = -1930.50041386 A.U. after 2 cycles

	1	2	3
	A	A	A
Frequencies --	-133.5321	14.0053	17.0093
Red. masses --	10.7502	2.3385	4.7785

Zero-point correction= 0.713558 (Hartree/Particle)

Thermal correction to Energy= 0.757276

Thermal correction to Enthalpy= 0.758221

Thermal correction to Gibbs Free Energy= 0.631040

Sum of electronic and zero-point Energies= –1929.786856

Sum of electronic and thermal Energies= –1929.743137

Sum of electronic and thermal Enthalpies= –1929.742193

Sum of electronic and thermal Free Energies= –1929.869374

Item	Value	Threshold	Converged?
Maximum Force	0.000000	0.000450	YES
RMS Force	0.000000	0.000300	YES
Maximum Displacement	0.000080	0.001800	YES

RMS Displacement 0.000010 0.001200 YES

▪NHC–Cu-allene to propargyl isomerization transition state (H)

#p b3lyp/lanl2dz freq geom=check guess=check

Cartesian coordinates (Angstroms):

C -0.698 -1.383 0.958

N -1.456 -0.213 0.370

C 0.742 -0.780 1.142

C -0.691 0.896 0.184

N 0.584 0.608 0.583

C 2.843 1.331 -0.202

C 3.860 2.313 -0.165

C 1.663 1.569 0.547

C 3.707 3.509 0.555

C 1.505 2.773 1.263

C 2.514 3.747 1.261

C -3.248 -0.002 2.675

C -3.760 -0.205 1.261

C -5.149 -0.299 1.036

C -2.886 -0.270 0.147

C -5.685 -0.440 -0.257

C -7.184 -0.523 -0.482

C -3.396 -0.390 -1.172

C -4.790 -0.477 -1.346

C -2.487 -0.382 -2.385

C 4.689 -0.883 0.561

C 4.103 -1.987 -1.638

C 3.917 -0.909 -0.749

C 3.700 -3.193 -3.844

C	3.456	-2.037	-2.889
C	3.029	0.143	-1.106
C	2.606	-0.971	-3.239
C	2.384	0.123	-2.374
C	1.504	1.272	-2.834
C	-1.707	-4.896	-0.203
C	-1.611	-3.707	0.543
C	-0.772	-2.654	0.121
C	-0.957	-5.047	-1.384
C	-0.115	-4.002	-1.812
C	-0.024	-2.814	-1.067
C	2.428	-1.967	4.374
C	2.054	-1.854	3.022
C	1.200	-0.816	2.596
C	1.957	-1.034	5.316
C	1.109	0.010	4.896
C	0.731	0.115	3.547
H	-1.127	-1.603	1.941
H	1.460	-1.334	0.533
H	4.766	2.142	-0.742
H	4.499	4.254	0.548
H	0.583	2.945	1.810
H	2.366	4.679	1.799
H	-4.052	0.361	3.324
H	-2.434	0.731	2.704
H	-2.869	-0.933	3.120
H	-5.823	-0.243	1.890
H	-7.727	-0.614	0.465
H	-7.446	-1.387	-1.107
H	-7.556	0.374	-0.996
H	-5.185	-0.568	-2.357

H -2.089 0.628 -2.562
H -3.037 -0.688 -3.282
H -1.633 -1.053 -2.258
H 4.061 -0.589 1.409
H 5.514 -0.159 0.518
H 5.123 -1.866 0.778
H 4.775 -2.795 -1.352
H 2.942 -3.227 -4.635
H 3.689 -4.156 -3.318
H 4.680 -3.101 -4.333
H 2.114 -0.977 -4.210
H 2.039 2.229 -2.794
H 0.613 1.392 -2.204
H 1.167 1.116 -3.865
H -2.359 -5.697 0.135
H -2.193 -3.597 1.456
H -1.026 -5.966 -1.962
H 0.471 -4.109 -2.722
H 0.630 -2.021 -1.419
H 3.085 -2.775 4.688
H 2.421 -2.580 2.298
H 2.250 -1.115 6.360
H 0.747 0.739 5.617
H 0.078 0.926 3.234
Cu -1.333 2.600 -0.521
H 0.784 6.735 -1.912
C -0.003 6.045 -1.718
C -0.919 5.250 -1.499
C -2.001 4.309 -1.227
H -2.698 4.729 -0.484
H -2.573 4.097 -2.145

SCF Done: E(RB3LYP) =	-1930.51606291	A.U. after	8 cycles
	1	2	3
	A	A	A
Frequencies --	-17.2975	-1.8200	16.5411
Red. masses --	4.7171	1.4203	4.2811

Zero-point correction=	0.714577 (Hartree/Particle)
Thermal correction to Energy=	0.756999
Thermal correction to Enthalpy=	0.757943
Thermal correction to Gibbs Free Energy=	0.635743
Sum of electronic and zero-point Energies=	–1929.801486
Sum of electronic and thermal Energies=	–1929.759064
Sum of electronic and thermal Enthalpies=	–1929.758119
Sum of electronic and thermal Free Energies=	–1929.880320

Item	Value	Threshold	Converged?
Maximum Force	0.000392	0.000450	YES
RMS Force	0.000092	0.000300	YES
Maximum Displacement	0.126994	0.001800	NO
RMS Displacement	0.018670	0.001200	NO

▪**Gibbs Free Activation Energy Barriers for Propargyl Addition to Phosphinoyl Aldimine 2a: J is the Calculated Diastereomeric Transition State which Leads to the Experimentally Observed Enantiomer**. The geometries **I–J** were optimized with the B3LYP/LANL2DZ method. Frequency calculations were carried out at the same level of theory as the geometry optimizations. All computed frequencies are real except for the transition states, which have one imaginary frequency. Relative free energies are in kcal/mol and were computed at 298K (as shown under each figure).

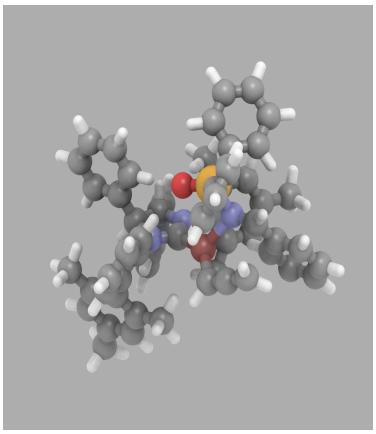

I

0.0

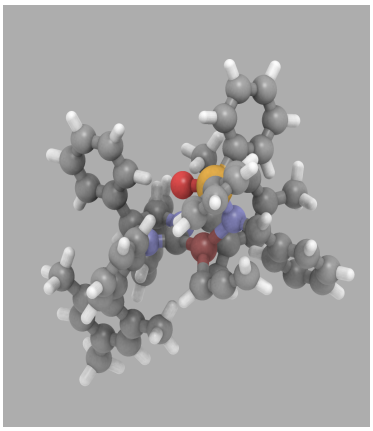

J

2.3

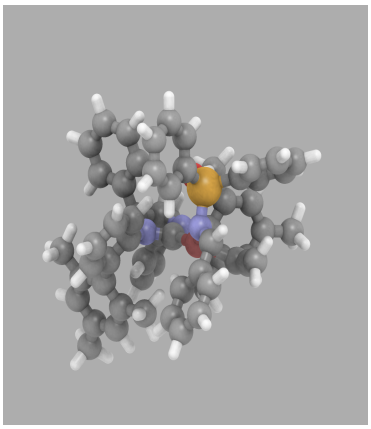

K

4.8

▪Ground State Complex (I)

#p b3lyp/lanl2dz freq geom=check guess=check

Cartesian coordinates (Angstroms):

H 7.337 -3.808 0.453

C 6.342 -3.652 0.045

H 6.481 -5.289 -1.367

H 5.911 -1.980 1.347

C 5.858 -4.486 -0.980

H 1.762 2.345 -1.486

C 5.534 -2.614 0.549

H 1.719 4.427 -2.857

C 2.615 2.616 -2.099

H 4.777 0.025 -1.309

C 2.603 3.794 -2.862

C 4.568 -4.278 -1.507

C 4.243 -2.411 0.023

H 4.195 -4.914 -2.306

C 3.819 0.558 -1.290

O	1.700	-1.714	1.224
C	3.758	1.780	-2.099
C	3.759	-3.242	-1.010
C	3.728	4.162	-3.625
H	3.713	5.076	-4.215
P	3.096	-1.102	0.702
N	2.807	0.145	-0.540
H	2.771	-3.072	-1.432
C	4.890	2.162	-2.863
C	4.878	3.343	-3.618
H	5.021	1.265	0.937
C	3.991	-0.253	2.104
H	5.770	1.520	-2.870
C	4.856	0.843	1.924
H	5.750	3.625	-4.203
H	3.063	-1.587	3.530
C	3.757	-0.761	3.399
C	5.497	1.422	3.037
H	6.160	2.272	2.894
C	4.401	-0.183	4.509
C	5.274	0.907	4.328
H	4.218	-0.577	5.505
H	5.770	1.356	5.186
C	-2.304	0.862	1.613
N	-1.157	1.134	0.663
C	-2.669	-0.623	1.262
C	-0.838	0.076	-0.137
N	-1.742	-0.920	0.116
C	-2.878	-2.603	-1.331
C	-2.843	-3.882	-1.933
C	-1.759	-2.202	-0.555

C -1.734 -4.733 -1.794
C -0.641 -3.050 -0.417
C -0.626 -4.308 -1.039
C 0.697 1.633 2.873
C 0.424 2.661 1.791
C 1.064 3.917 1.847
C -0.445 2.390 0.706
C 0.867 4.897 0.857
C 1.581 6.235 0.922
C -0.649 3.350 -0.320
C 0.009 4.591 -0.219
C -1.527 3.061 -1.522
C -5.474 -3.104 0.040
C -6.428 -1.173 -1.284
C -5.312 -1.974 -0.965
C -7.577 0.683 -2.597
C -6.353 -0.143 -2.243
C -4.067 -1.724 -1.605
C -5.117 0.076 -2.883
C -3.975 -0.699 -2.588
C -2.687 -0.455 -3.352
C -4.626 3.792 2.468
C -3.585 2.848 2.519
C -3.449 1.864 1.518
C -5.553 3.760 1.409
C -5.426 2.779 0.406
C -4.383 1.840 0.458
C -3.479 -2.761 4.343
C -3.618 -1.956 3.197
C -2.486 -1.563 2.451
C -2.201 -3.192 4.747

C	-1.070	-2.809	4.000
C	-1.205	-1.997	2.860
H	-1.910	0.902	2.633
H	-3.705	-0.684	0.920
H	-3.693	-4.194	-2.537
H	-1.733	-5.708	-2.275
H	0.205	-2.715	0.179
H	0.242	-4.953	-0.924
H	1.648	1.845	3.373
H	0.749	0.621	2.462
H	-0.084	1.639	3.649
H	1.738	4.124	2.677
H	2.023	6.407	1.910
H	0.896	7.066	0.708
H	2.393	6.283	0.182
H	-0.157	5.335	-0.996
H	-1.087	2.277	-2.152
H	-1.650	3.960	-2.135
H	-2.520	2.714	-1.221
H	-4.625	-3.173	0.728
H	-5.542	-4.076	-0.468
H	-6.389	-2.975	0.629
H	-7.374	-1.362	-0.778
H	-7.298	1.637	-3.060
H	-8.187	0.899	-1.710
H	-8.221	0.149	-3.311
H	-5.039	0.857	-3.637
H	-2.375	-1.357	-3.896
H	-1.856	-0.190	-2.688
H	-2.811	0.353	-4.081
H	-4.716	4.544	3.249

H	-2.873	2.876	3.342
H	-6.362	4.485	1.367
H	-6.138	2.743	-0.416
H	-4.306	1.094	-0.329
H	-4.360	-3.055	4.910
H	-4.608	-1.625	2.888
H	-2.090	-3.822	5.627
H	-0.080	-3.149	4.297
H	-0.316	-1.726	2.295
Cu	0.759	-0.177	-1.305
H	0.407	-1.365	-3.639
C	1.258	-0.979	-3.068
C	2.479	-1.063	-3.518
C	3.788	-1.078	-3.836
H	4.415	-1.942	-3.620
H	4.238	-0.269	-4.408

SCF Done: E(RB3LYP) = -2800.49540464 A.U. after 1 cycles

	1	2	3
	A	A	A
Frequencies --	12.8551	15.3229	17.1184
Red. masses --	5.6029	5.1457	5.2743

Zero-point correction=	1.017556 (Hartree/Particle)
Thermal correction to Energy=	1.081936
Thermal correction to Enthalpy=	1.082880
Thermal correction to Gibbs Free Energy=	0.909838
Sum of electronic and zero-point Energies=	–2799.477848
Sum of electronic and thermal Energies=	–2799.413469
Sum of electronic and thermal Enthalpies=	–2799.412524
Sum of electronic and thermal Free Energies=	–2799.585566

Item	Value	Threshold	Converged?
Maximum Force	0.000131	0.000450	YES
RMS Force	0.000012	0.000300	YES
Maximum Displacement	0.034773	0.001800	NO
RMS Displacement	0.005046	0.001200	NO

▪**Transition State for the Fast-forming Enantiomer (J)**

#p b3lyp/lanl2dz freq

Cartesian coordinates (Angstroms):

H 7.479 -3.488 -0.236
C 6.396 -3.517 -0.333
H 6.372 -5.428 -1.355
H 6.106 -1.622 0.671
C 5.772 -4.610 -0.963
H 1.750 2.193 -1.655
C 5.618 -2.459 0.176
H 1.748 4.323 -2.939
C 2.620 2.477 -2.238
H 4.780 -0.091 -1.391
C 2.630 3.687 -2.953
C 4.368 -4.645 -1.084
C 4.215 -2.494 0.053
H 3.884 -5.486 -1.574
C 3.790 0.362 -1.491
O 1.732 -1.679 1.268
C 3.755 1.633 -2.244
C 3.590 -3.589 -0.579
C 3.770 4.082 -3.677

H	3.773	5.018	-4.230
P	3.121	-1.109	0.671
N	2.797	0.032	-0.632
H	2.508	-3.608	-0.675
C	4.904	2.044	-2.968
C	4.914	3.255	-3.676
H	4.191	1.696	0.872
C	4.113	-0.181	1.952
H	5.786	1.405	-2.976
C	4.475	1.168	1.777
H	5.803	3.555	-4.226
H	4.148	-1.886	3.295
C	4.448	-0.851	3.149
C	5.188	1.840	2.789
H	5.467	2.881	2.649
C	5.158	-0.178	4.158
C	5.533	1.169	3.978
H	5.414	-0.697	5.078
H	6.083	1.690	4.758
C	-2.352	0.933	1.602
N	-1.191	1.169	0.659
C	-2.720	-0.560	1.291
C	-0.878	0.091	-0.114
N	-1.795	-0.889	0.150
C	-2.921	-2.606	-1.259
C	-2.891	-3.905	-1.817
C	-1.811	-2.192	-0.477
C	-1.797	-4.765	-1.623
C	-0.709	-3.049	-0.282
C	-0.700	-4.329	-0.858
C	0.725	1.575	2.836

C	0.463	2.628	1.775
C	1.148	3.860	1.829
C	-0.435	2.401	0.703
C	0.975	4.853	0.848
C	1.740	6.162	0.911
C	-0.615	3.373	-0.316
C	0.093	4.586	-0.219
C	-1.519	3.122	-1.507
C	-5.535	-3.058	0.087
C	-6.463	-1.158	-1.300
C	-5.355	-1.956	-0.945
C	-7.587	0.667	-2.675
C	-6.371	-0.154	-2.283
C	-4.100	-1.726	-1.574
C	-5.125	0.045	-2.910
C	-3.990	-0.725	-2.579
C	-2.689	-0.498	-3.325
C	-4.662	3.902	2.344
C	-3.626	2.954	2.433
C	-3.488	1.938	1.464
C	-5.580	3.842	1.279
C	-5.452	2.829	0.308
C	-4.414	1.886	0.398
C	-3.518	-2.651	4.407
C	-3.662	-1.871	3.245
C	-2.532	-1.472	2.501
C	-2.236	-3.049	4.831
C	-1.105	-2.659	4.086
C	-1.247	-1.873	2.929
H	-1.969	1.002	2.625
H	-3.757	-0.628	0.952

H -3.733 -4.229 -2.425
H -1.800 -5.757 -2.068
H 0.131 -2.703 0.316
H 0.153 -4.984 -0.699
H 1.630 1.818 3.402
H 0.862 0.583 2.392
H -0.100 1.502 3.559
H 1.840 4.036 2.651
H 2.215 6.303 1.889
H 1.080 7.021 0.729
H 2.531 6.191 0.149
H -0.051 5.339 -0.992
H -1.129 2.309 -2.134
H -1.599 4.020 -2.128
H -2.527 2.833 -1.193
H -4.690 -3.120 0.781
H -5.615 -4.042 -0.396
H -6.451 -2.901 0.669
H -7.416 -1.332 -0.802
H -7.299 1.592 -3.188
H -8.191 0.935 -1.799
H -8.239 0.104 -3.358
H -5.033 0.808 -3.682
H -2.354 -1.417 -3.824
H -1.878 -0.191 -2.655
H -2.807 0.276 -4.092
H -4.753 4.679 3.100
H -2.921 3.004 3.260
H -6.385 4.570 1.208
H -6.156 2.772 -0.518
H -4.334 1.117 -0.366

H -4.397 -2.951 4.973

H -4.656 -1.565 2.921

H -2.120 -3.658 5.725

H -0.111 -2.969 4.399

H -0.356 -1.598 2.368

Cu 0.815 -0.181 -1.118

H 0.157 -1.762 -3.215

C 1.063 -1.276 -2.872

C 2.271 -1.260 -3.296

C 3.622 -1.067 -3.428

H 4.307 -1.861 -3.130

H 4.003 -0.343 -4.145

SCF Done: E(RB3LYP) = -2800.49360174 A.U. after 26 cycles

	1	2	3
	A	A	A
Frequencies --	-179.0056	12.6832	13.5279
Red. masses --	7.4389	5.2185	5.0816

Zero-point correction= 1.017605 (Hartree/Particle)

Thermal correction to Energy= 1.080902

Thermal correction to Enthalpy= 1.081847

Thermal correction to Gibbs Free Energy= 0.911717

Sum of electronic and zero-point Energies= –2799.475997

Sum of electronic and thermal Energies= –2799.412699

Sum of electronic and thermal Enthalpies= –2799.411755

Sum of electronic and thermal Free Energies= –2799.581885

Item	Value	Threshold	Converged?
Maximum Force	0.000018	0.000450	YES
RMS Force	0.000003	0.000300	YES
Maximum Displacement	0.024744	0.001800	NO

RMS Displacement 0.004099 0.001200 NO

▪ **Transition State for the Slow-forming Enantiomer (K)**

#p b3lyp/lanl2dz freq

Cartesian coordinates (Angstroms):

H 5.615 -1.995 4.748
C 5.229 -2.159 3.745
H 5.810 -4.248 3.684
H 4.528 -0.125 3.519
C 5.337 -3.430 3.145
H 1.167 -1.751 -2.324
C 4.619 -1.102 3.048
H 0.639 -3.271 -4.226
C 1.958 -2.095 -2.983
H 4.705 -0.662 -1.431
C 1.667 -2.962 -4.049
C 4.826 -3.639 1.850
C 4.116 -1.308 1.745
H 4.902 -4.619 1.385
C 3.635 -0.772 -1.627
O 1.970 0.638 1.728
C 3.289 -1.676 -2.743
C 4.212 -2.582 1.152
C 2.694 -3.439 -4.886
H 2.465 -4.112 -5.709
P 3.256 0.120 0.898
N 2.725 -0.465 -0.676
H 3.806 -2.754 0.160
C 4.318 -2.167 -3.586

C	4.027	-3.040	-4.645
H	6.282	0.180	0.824
C	4.534	1.466	0.700
H	5.346	-1.853	-3.410
C	5.917	1.194	0.683
H	4.828	-3.409	-5.281
H	3.004	2.990	0.538
C	4.071	2.787	0.529
C	6.837	2.244	0.498
H	7.904	2.033	0.486
C	4.992	3.833	0.348
C	6.376	3.564	0.330
H	4.633	4.850	0.213
H	7.087	4.374	0.187
C	-2.647	1.308	1.283
N	-1.531	1.528	0.281
C	-2.546	-0.233	1.546
C	-0.880	0.386	-0.080
N	-1.499	-0.660	0.550
C	-1.962	-3.012	-0.124
C	-1.525	-4.356	-0.152
C	-1.096	-2.042	0.445
C	-0.270	-4.733	0.354
C	0.164	-2.417	0.951
C	0.581	-3.756	0.903
C	0.011	3.280	2.069
C	-0.499	3.735	0.714
C	-0.238	5.053	0.282
C	-1.193	2.863	-0.162
C	-0.628	5.514	-0.989
C	-0.325	6.931	-1.439

C	-1.586	3.292	-1.456
C	-1.295	4.613	-1.845
C	-2.259	2.354	-2.437
C	-4.487	-3.692	1.297
C	-5.737	-2.736	-0.681
C	-4.500	-3.014	-0.064
C	-7.157	-1.898	-2.624
C	-5.815	-2.153	-1.961
C	-3.294	-2.677	-0.737
C	-4.609	-1.843	-2.621
C	-3.351	-2.098	-2.035
C	-2.087	-1.783	-2.814
C	-5.738	3.551	0.945
C	-4.487	3.042	1.338
C	-4.008	1.818	0.825
C	-6.532	2.835	0.029
C	-6.063	1.611	-0.488
C	-4.811	1.108	-0.095
C	-2.840	-1.299	5.221
C	-3.145	-1.059	3.868
C	-2.165	-0.555	2.988
C	-1.544	-1.042	5.705
C	-0.560	-0.543	4.828
C	-0.864	-0.298	3.478
H	-2.383	1.845	2.199
H	-3.495	-0.721	1.310
H	-2.179	-5.106	-0.593
H	0.041	-5.774	0.316
H	0.799	-1.651	1.381
H	1.554	-4.031	1.301
H	0.624	4.064	2.528

H 0.627 2.376 1.981
H -0.804 3.059 2.772
H 0.293 5.726 0.953
H 0.093 7.531 -0.623
H -1.230 7.438 -1.800
H 0.401 6.938 -2.265
H -1.594 4.945 -2.838
H -1.563 1.570 -2.763
H -2.595 2.900 -3.326
H -3.127 1.856 -1.992
H -3.726 -3.274 1.964
H -4.262 -4.763 1.202
H -5.464 -3.603 1.787
H -6.656 -2.985 -0.153
H -7.098 -1.076 -3.348
H -7.929 -1.649 -1.886
H -7.503 -2.788 -3.169
H -4.644 -1.401 -3.615
H -1.442 -2.667 -2.894
H -1.493 -1.000 -2.327
H -2.326 -1.442 -3.828
H -6.090 4.497 1.350
H -3.878 3.600 2.047
H -7.501 3.223 -0.275
H -6.668 1.049 -1.195
H -4.469 0.164 -0.513
H -3.606 -1.686 5.889
H -4.151 -1.254 3.499
H -1.303 -1.230 6.749
H 0.446 -0.347 5.190
H -0.081 0.077 2.822

Cu	0.893	0.417	-1.000
H	0.819	2.681	-2.493
C	1.538	1.884	-2.337
C	2.722	1.678	-2.781
C	3.981	1.192	-3.014
H	4.198	0.647	-3.929
H	4.831	1.640	-2.500

SCF Done: E(RB3LYP) = -2800.49122937 A.U. after 26 cycles

	1	2	3
	A	A	A
Frequencies --	-170.0328	11.7437	13.2839
Red. masses --	7.1456	5.8141	5.5290

Zero-point correction= 1.018050 (Hartree/Particle)
Thermal correction to Energy= 1.081129
Thermal correction to Enthalpy= 1.082073
Thermal correction to Gibbs Free Energy= 0.913332
Sum of electronic and zero-point Energies= –2799.473180
Sum of electronic and thermal Energies= –2799.410100
Sum of electronic and thermal Enthalpies= –2799.409156
Sum of electronic and thermal Free Energies= –2799.577897

Item	Value	Threshold	Converged?
Maximum Force	0.000003	0.000450	YES
RMS Force	0.000001	0.000300	YES
Maximum Displacement	0.002451	0.001800	NO
RMS Displacement	0.000579	0.001200	YES

■ **^{1}H NMR Spectral Data for Homopropargylamides 3.21a–q and their Derivatives**

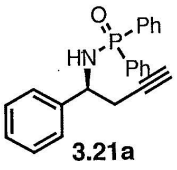

3.21a

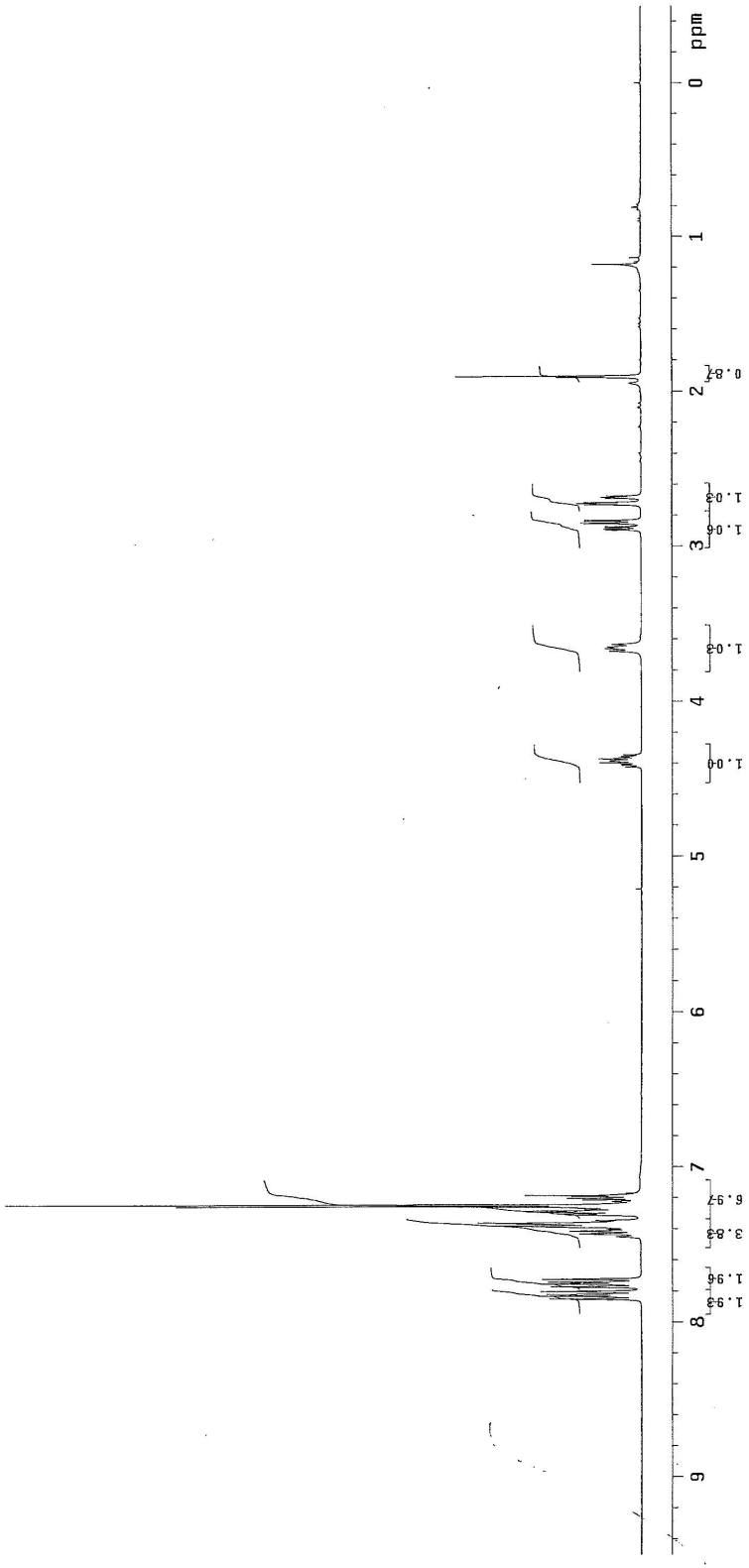

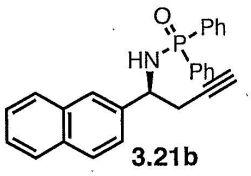
O
Ph
HN
P
Ph

3.21b

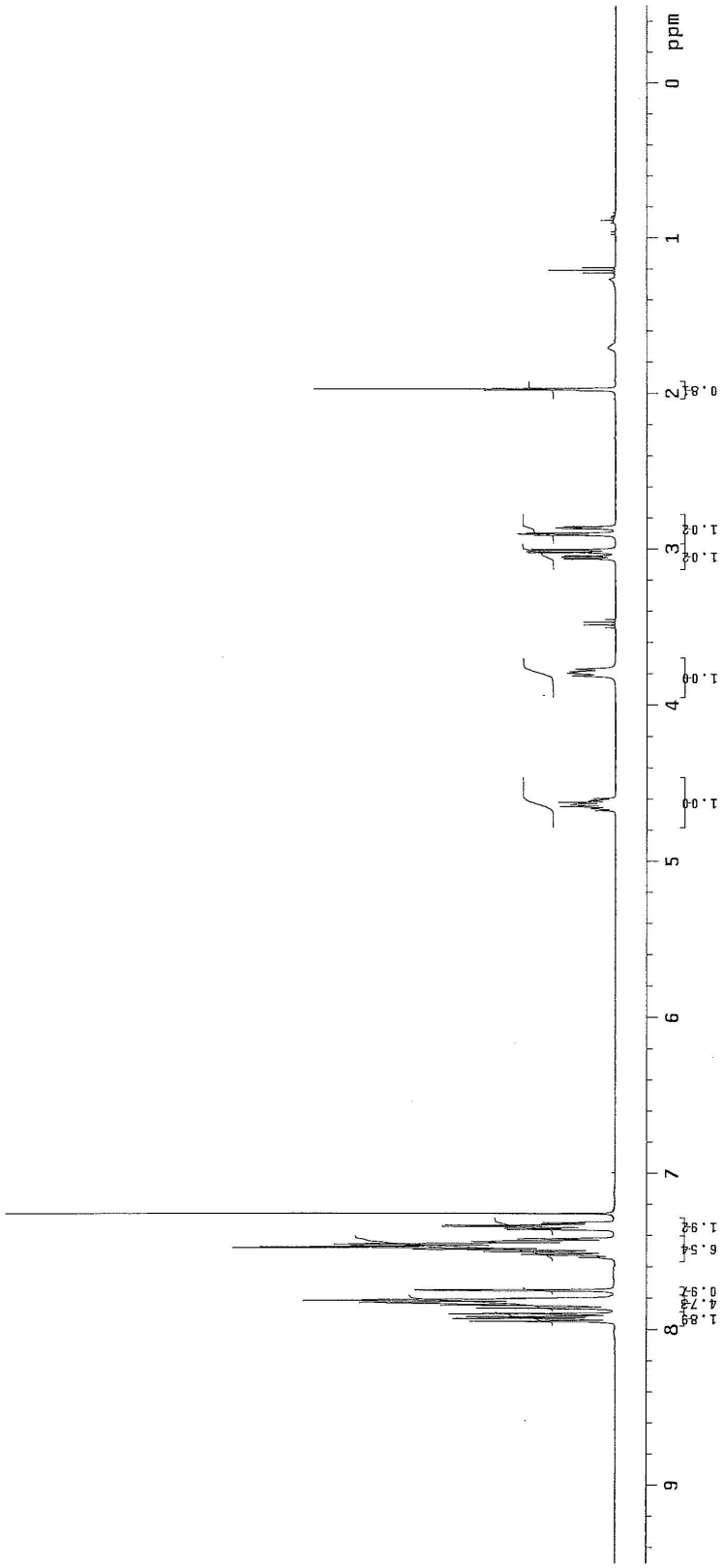
ppm
0
1
2
3
4
5
6
7
8
9
0.81
1.02
1.02
1.00
1.00
1.92
6.54
0.97
4.74
1.89

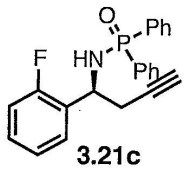
O
Ph
F
HN
P
Ph

3.21c

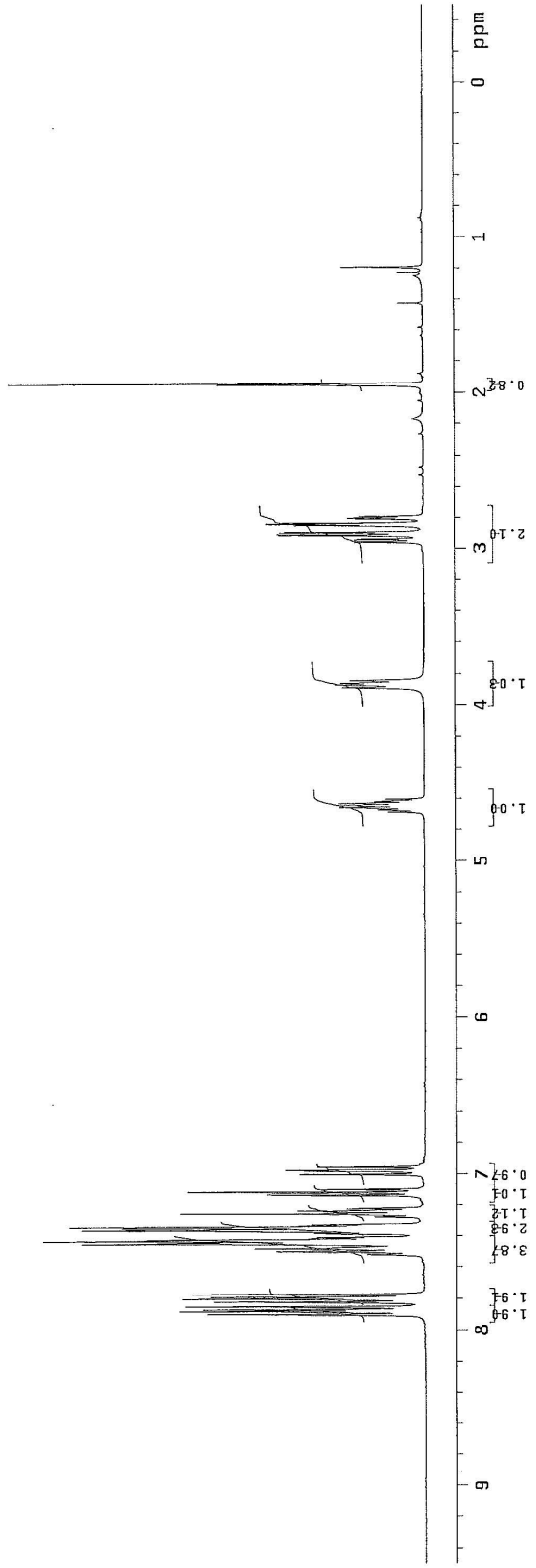
ppm
0
1
2
3
4
5
6
7
8
9
0.82
2.10
1.03
1.00
0.97
1.01
1.12
2.93
3.87
1.93
1.90

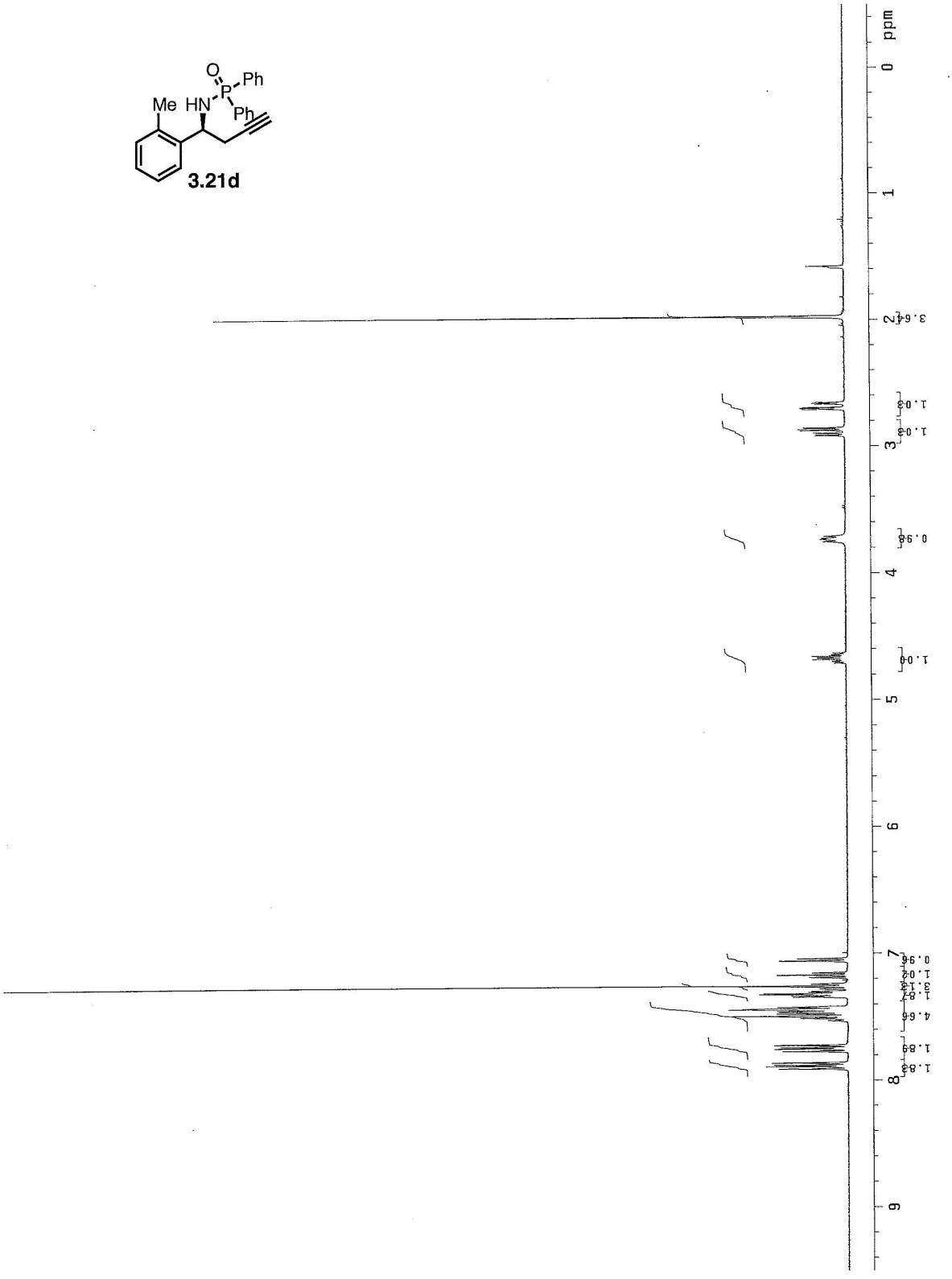
Me
HN
O
P
Ph
Ph
3.21d
ppm
0
1
2
3
4
5
6
7
8
9

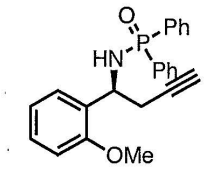
O
Ph
HN
P
Ph
OMe

3.21e

ppm
0
1
2
3
4
5
6
7
8
9
0.87
1.01
1.01
2.99
1.03
1.01
0.97
0.98
2.09
1.93
3.83
3.87

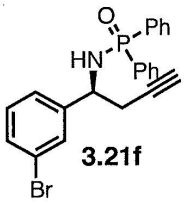

3.21f

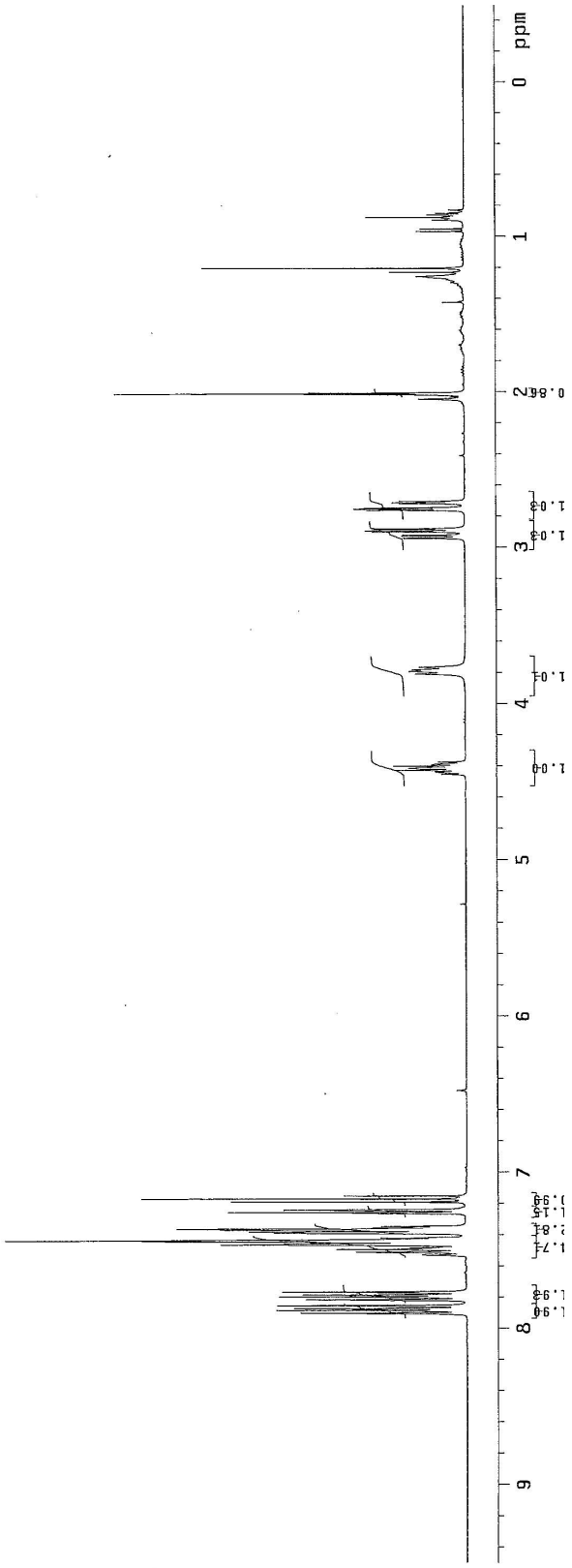

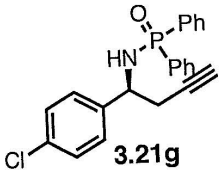
O
P
Ph
HN
Ph
Cl

3.21g

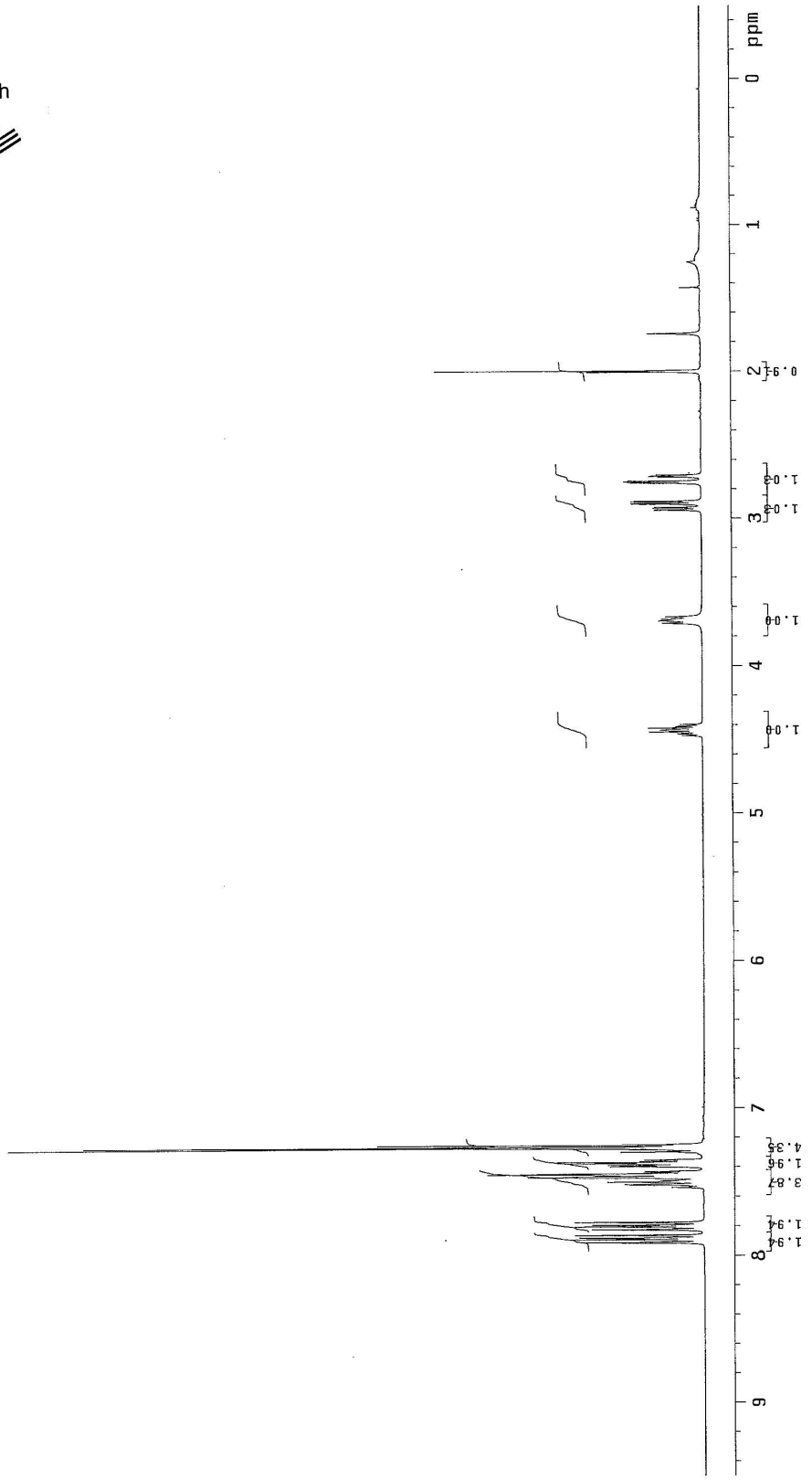
ppm
0
1
2
3
4
5
6
7
8
9
0.96
1.03
1.03
1.00
1.00
4.35
1.95
3.87
1.94
1.94

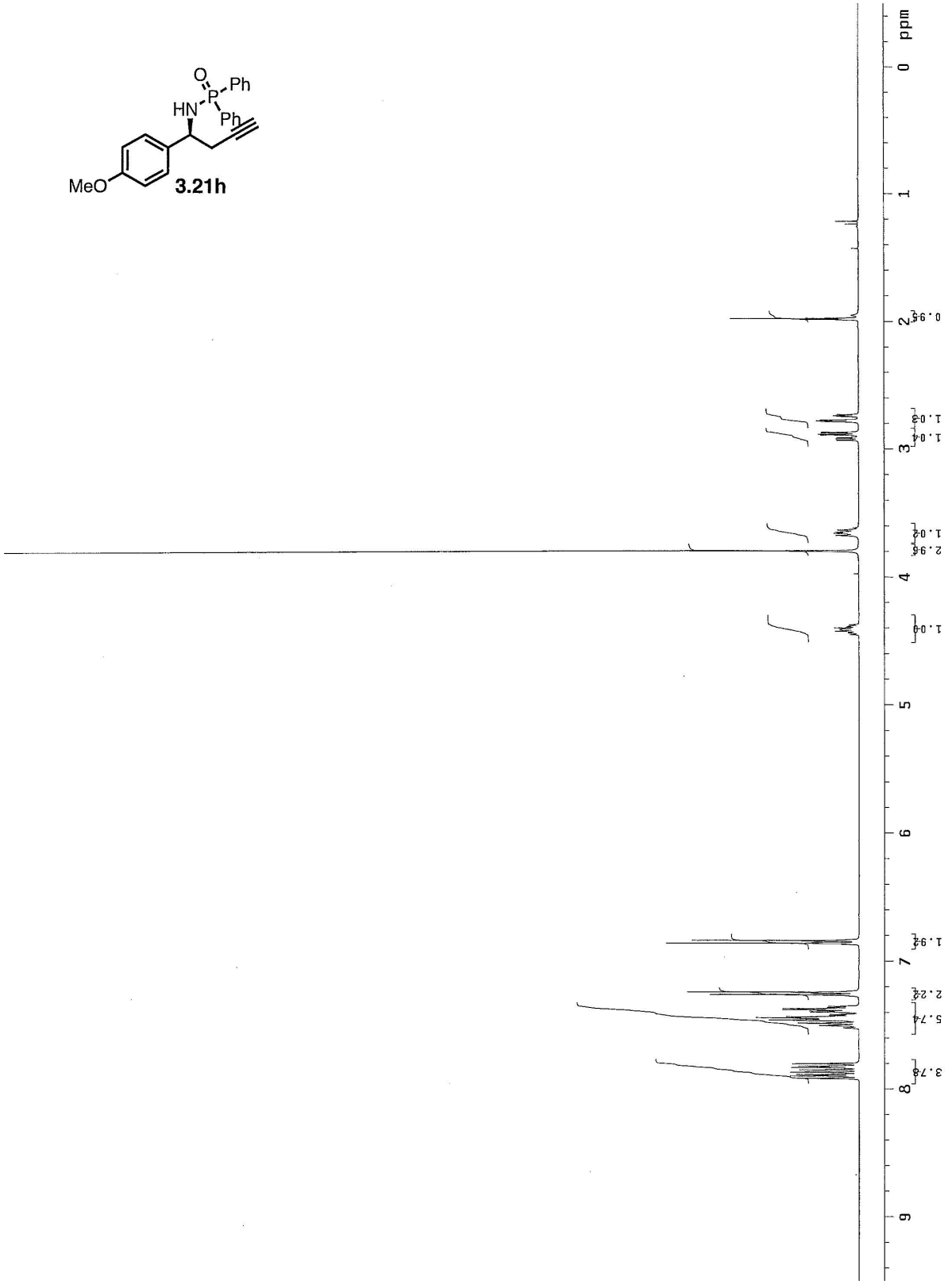
O
Ph
HN
P
Ph
MeO
3.21h
ppm
0
1
2
3
4
5
6
7
8
9
0.95
1.04
1.04
2.96
1.00
1.92
2.22
5.74
3.78

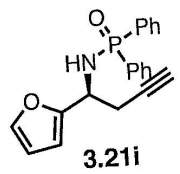

3.21i

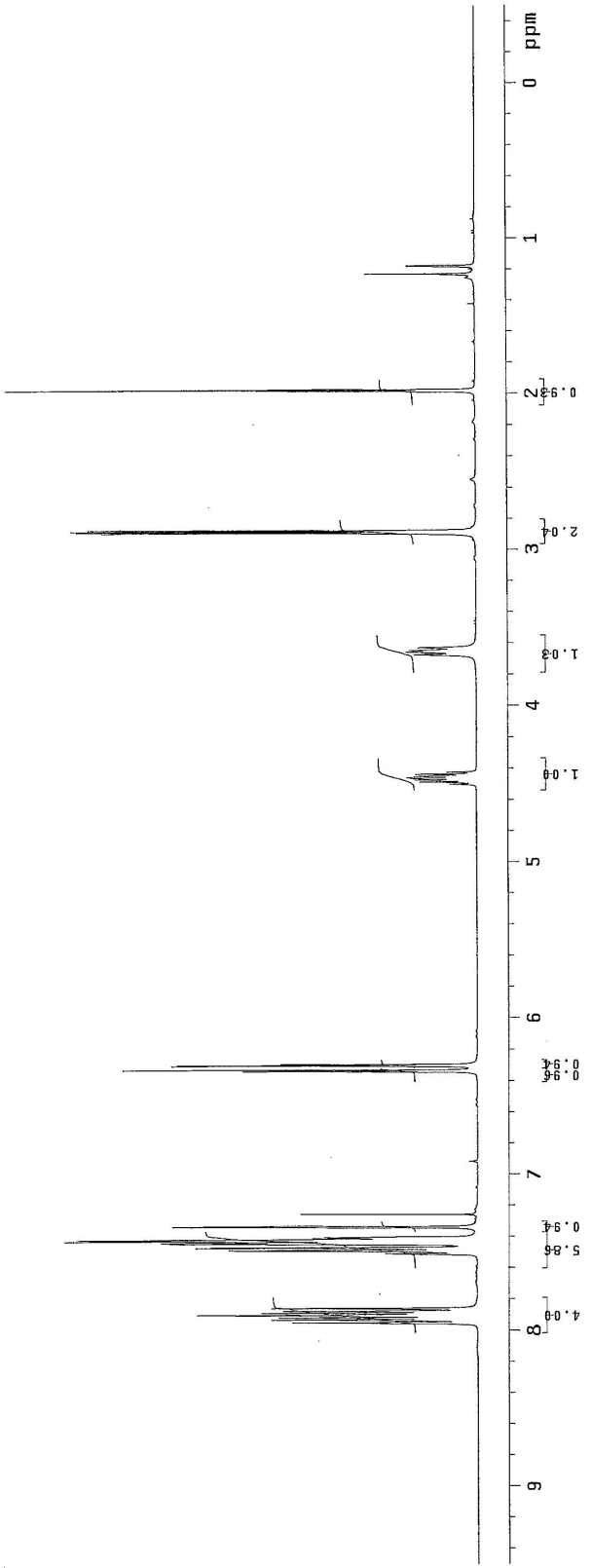

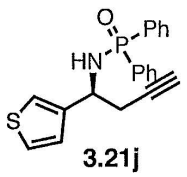

3.21j

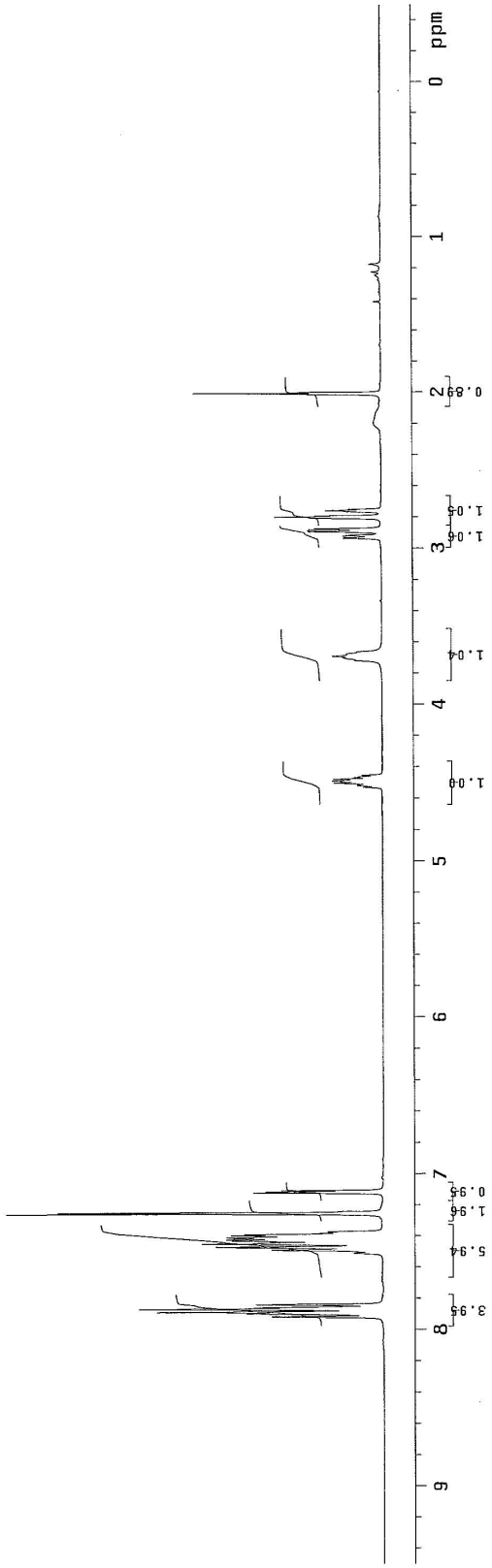

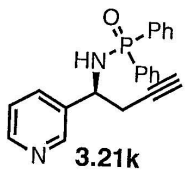

3.21k

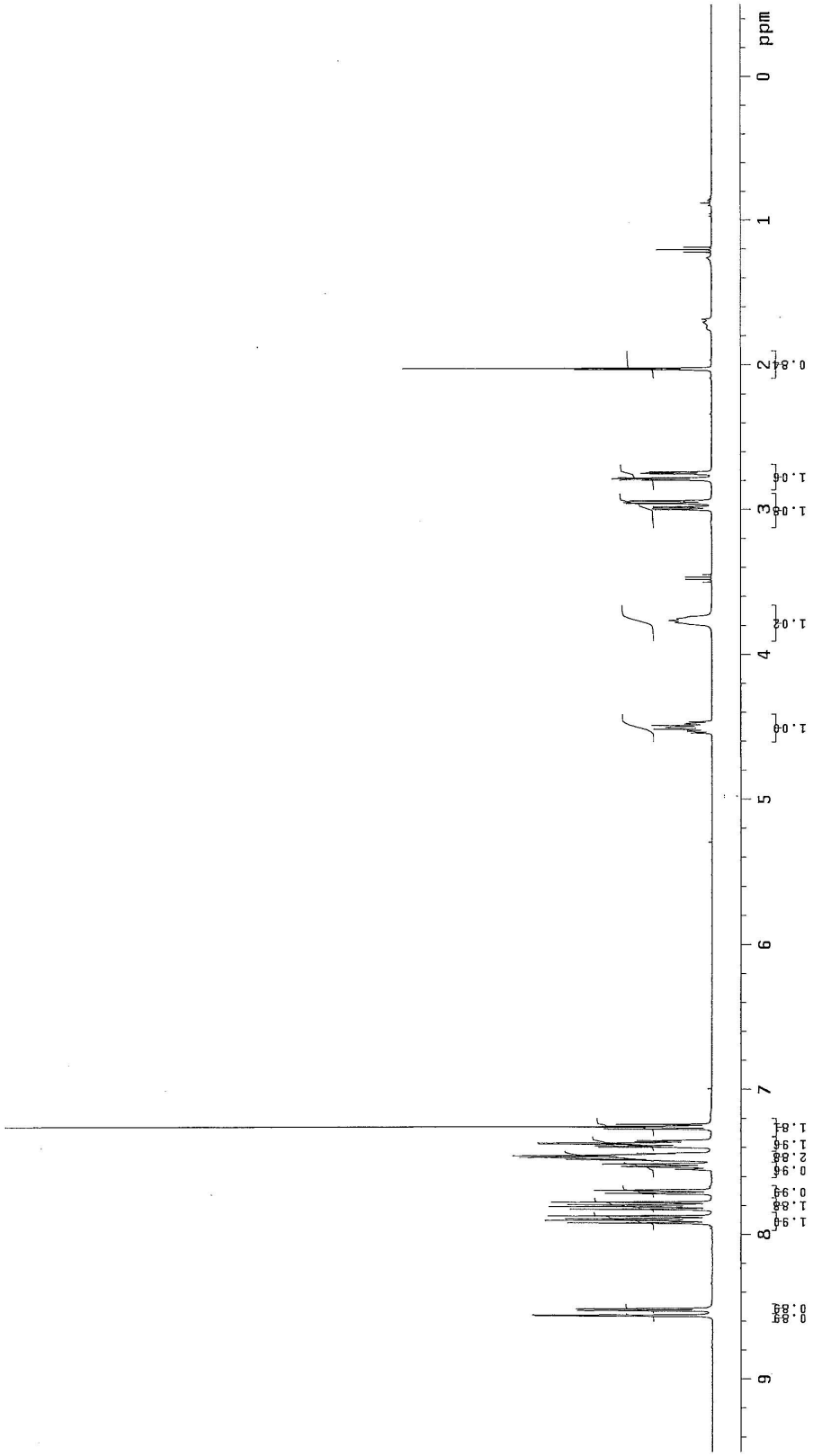

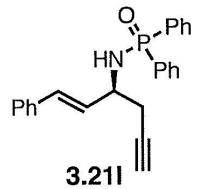
O
Ph
HN
P
Ph
Ph

3.21l

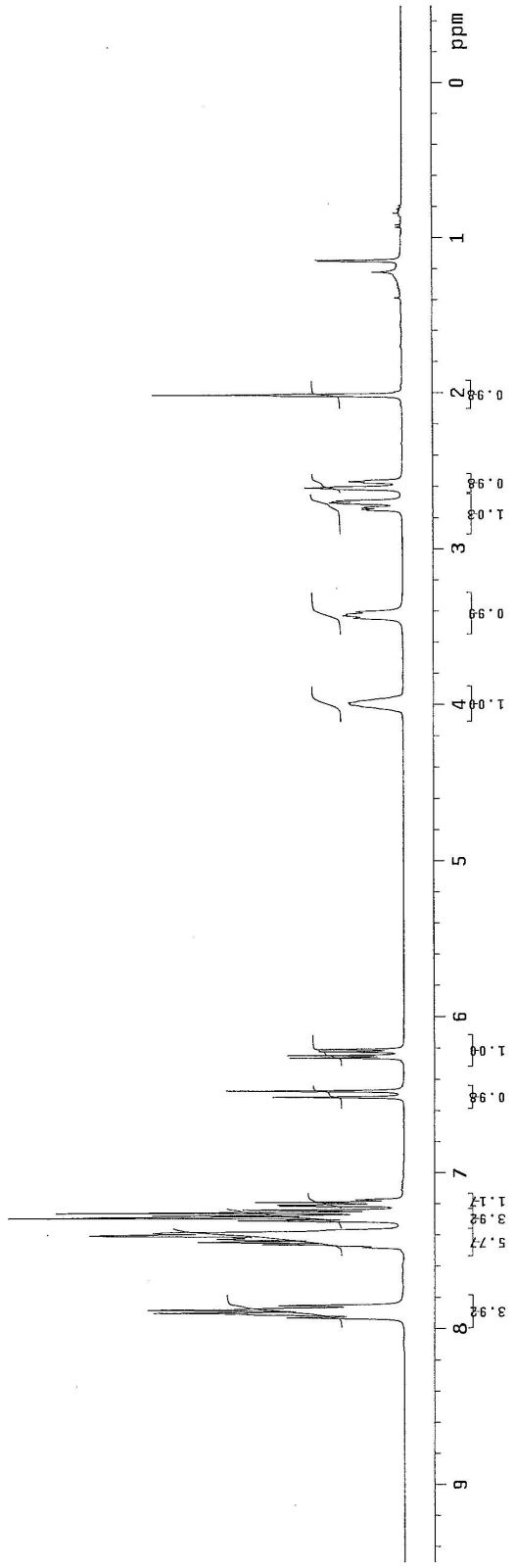
ppm
0
1
2
3
4
5
6
7
8
9
0.98
1.03
0.99
1.00
1.00
0.98
1.17
3.92
5.77
3.92

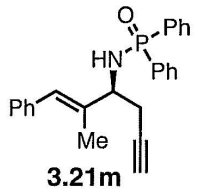
O
Ph
HN
P
Ph
Ph
Me

3.21m

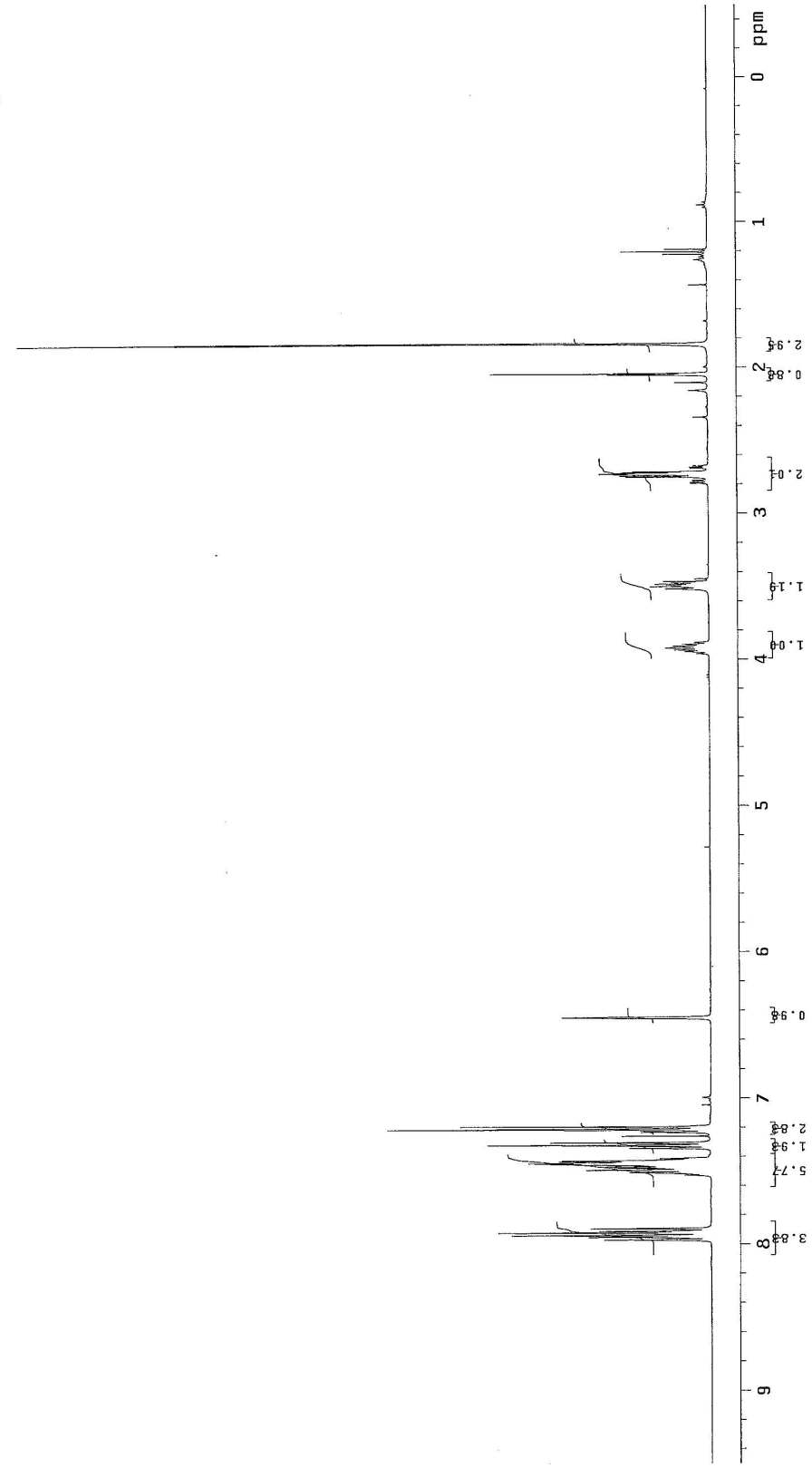
ppm
0
1
2
3
4
5
6
7
8
9
2.95
0.88
2.04
1.19
1.04
0.98
2.88
1.93
5.77
3.88

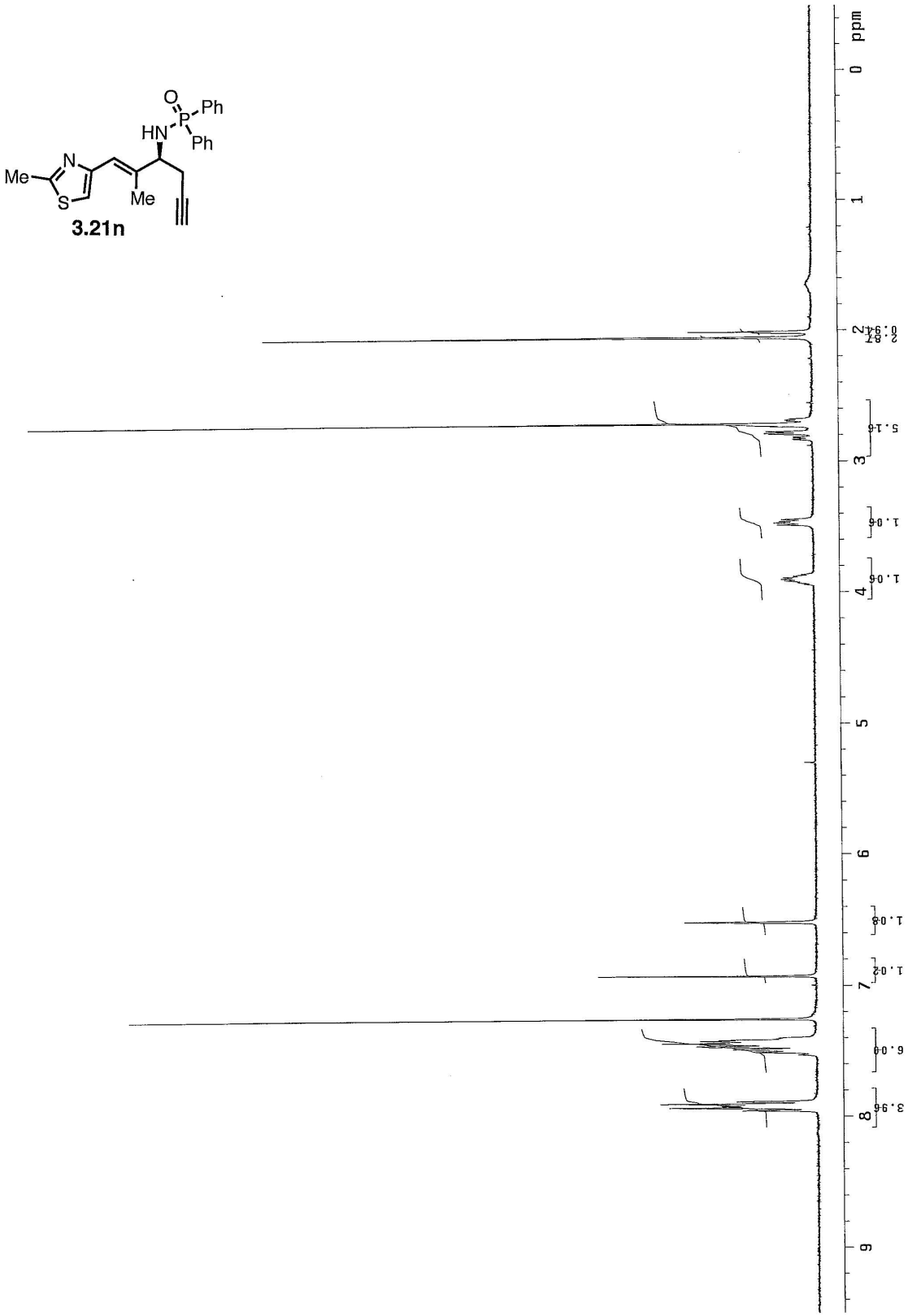
O
Ph
HN
P
Ph
N
Me
S
Me
3.21n
ppm
0
1
2
3
4
5
6
7
8
9
2.07
0.94
5.16
1.06
1.06
1.08
1.02
6.00
3.96

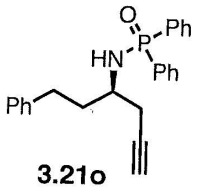
O
Ph
HN
P
Ph
Ph

3.21o

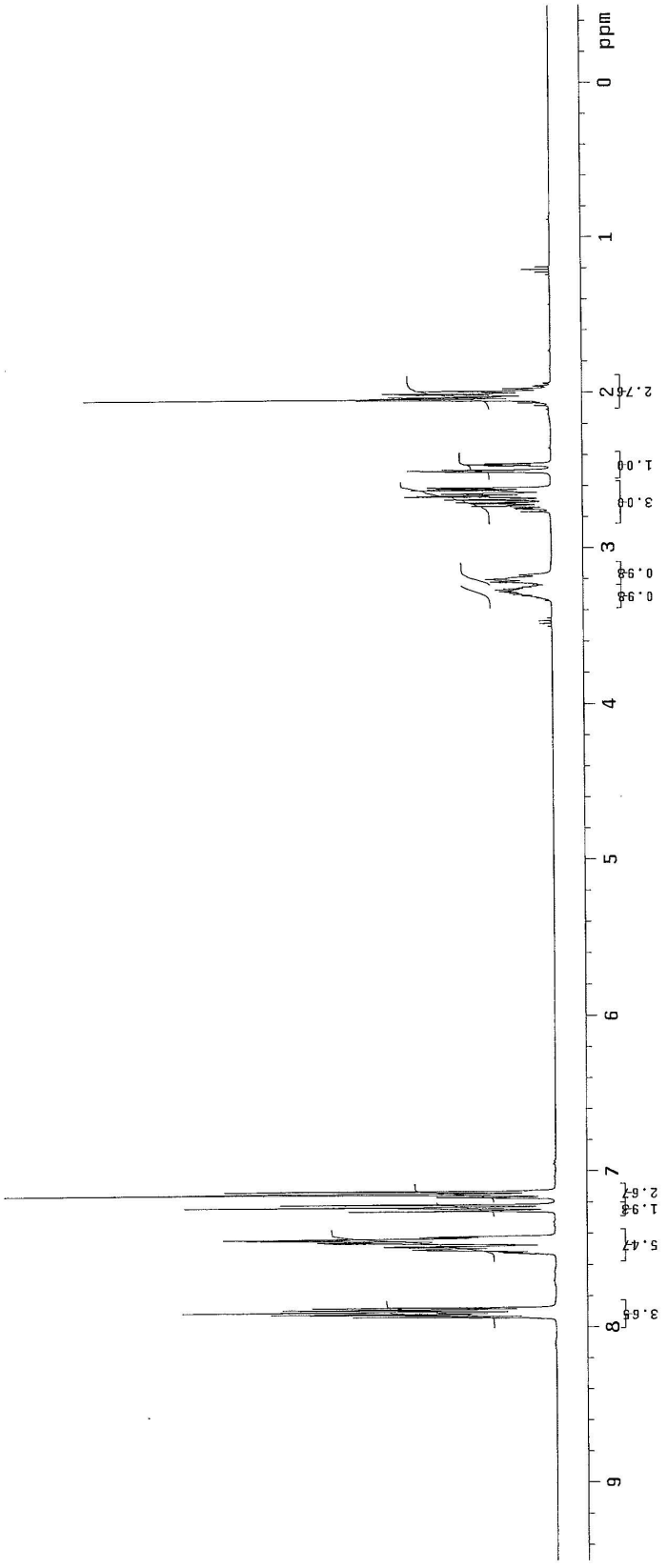
ppm
0
1
2
3
4
5
6
7
8
9
2.76
1.00
3.00
0.98
0.98
2.67
1.98
5.47
3.65

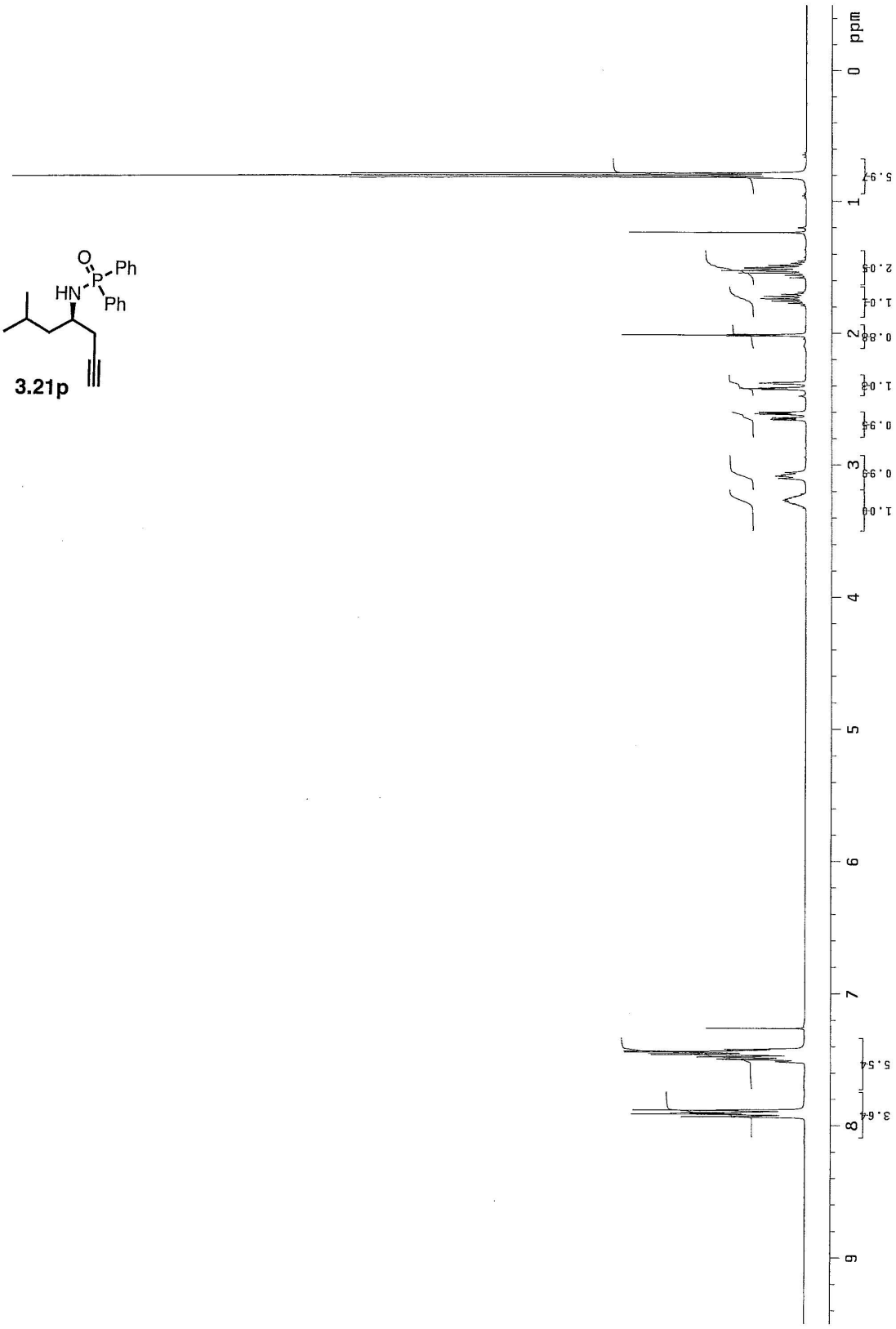
O
Ph
HN
P
Ph
3.21p
ppm
0
1
2
3
4
5
6
7
8
9
5.92
2.05
1.02
0.88
1.02
0.95
0.93
1.00
5.54
3.64

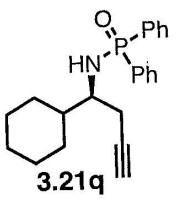

3.21q

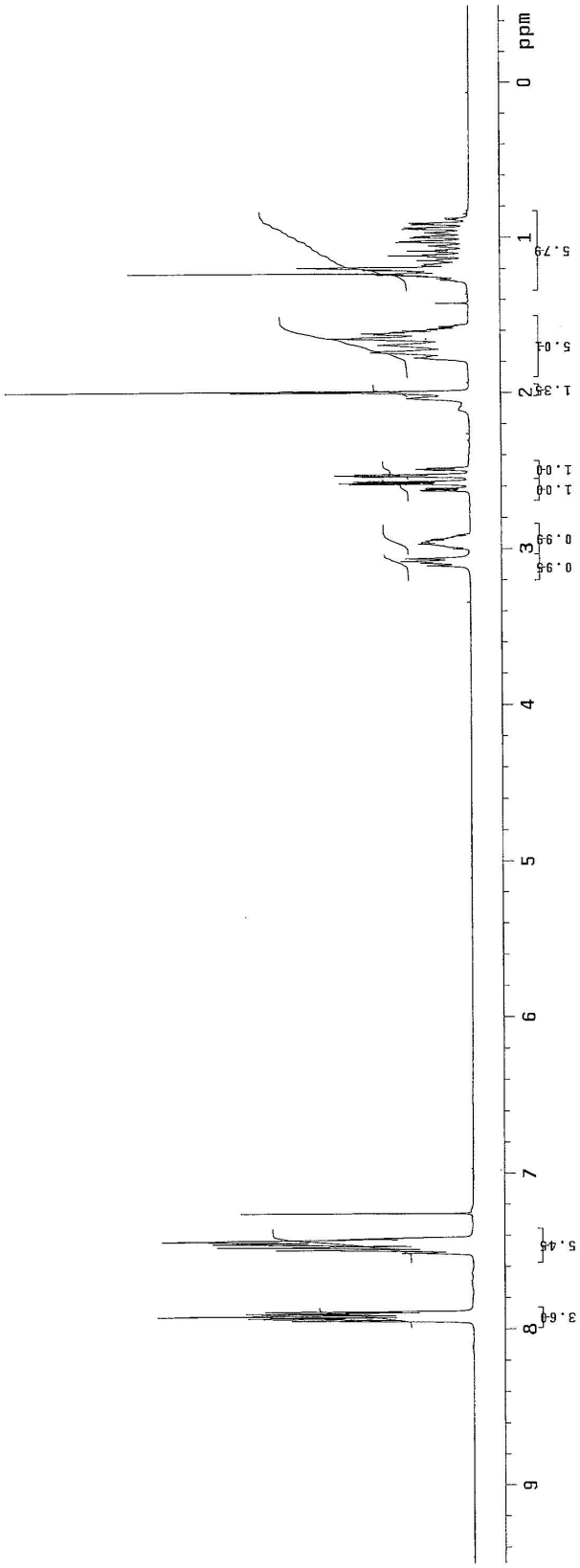

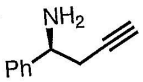

3.22

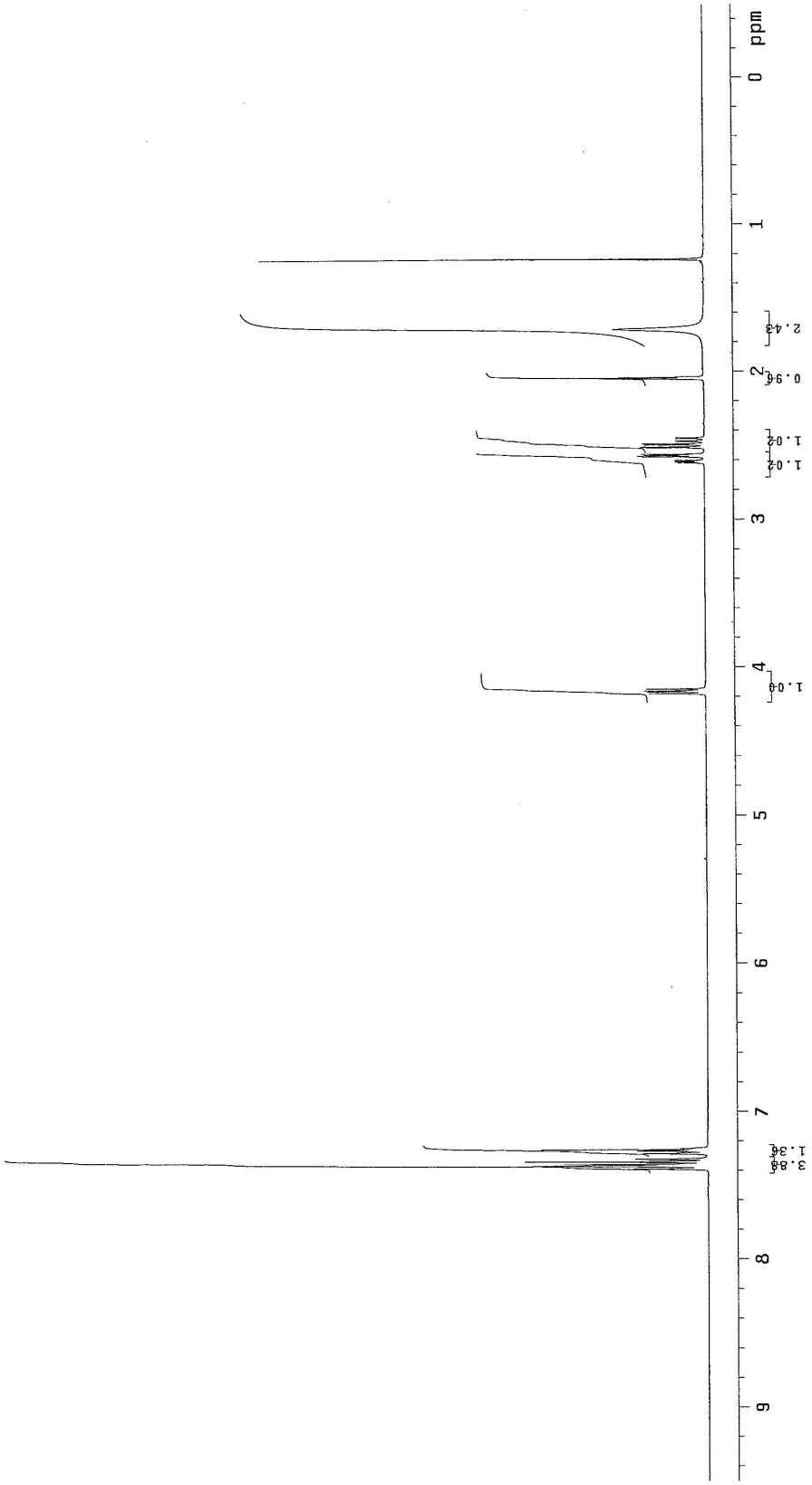

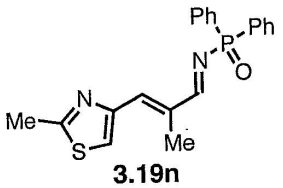

3.19n

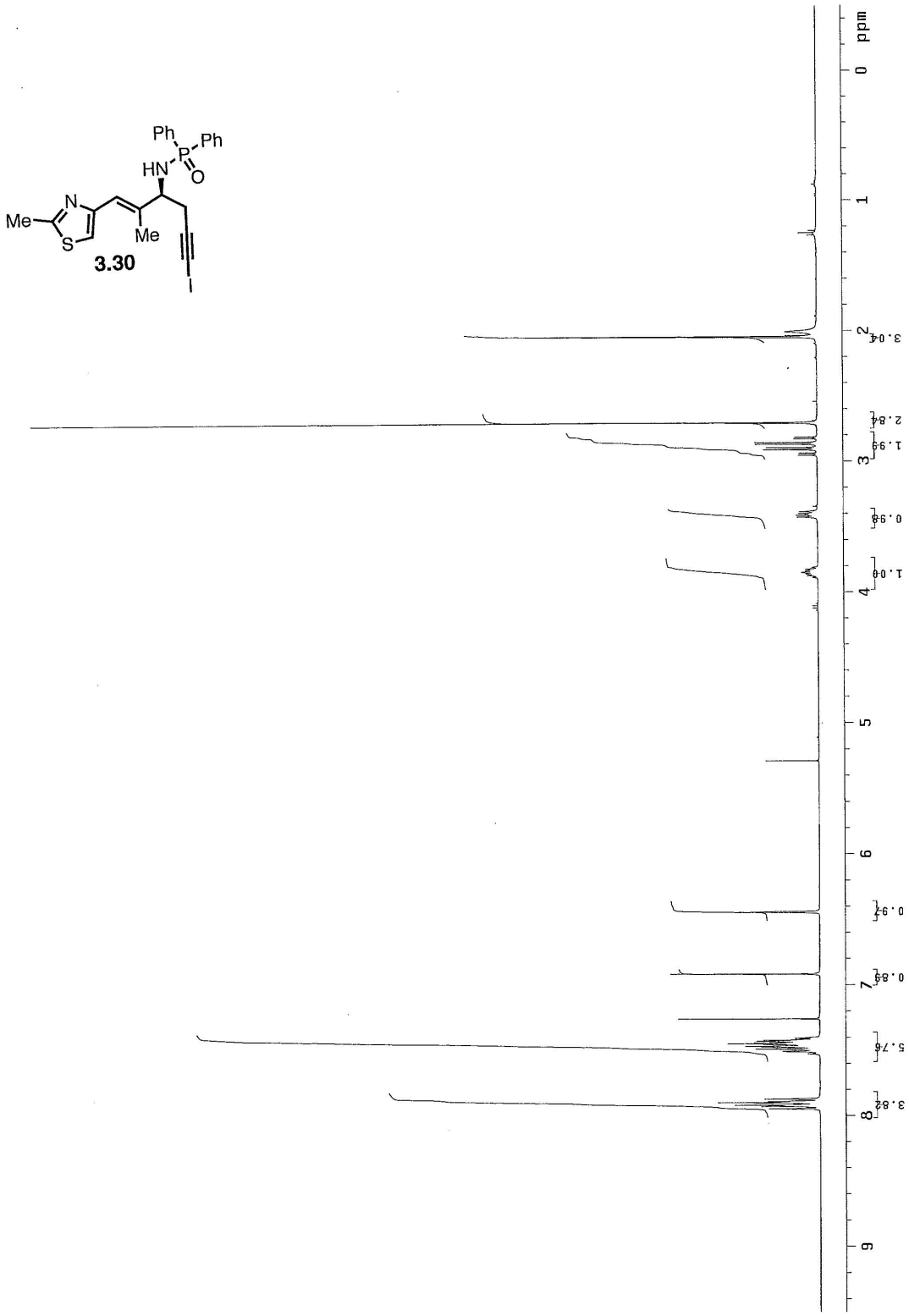
Ph
Ph
HN
P
O
N
Me
S
Me
3.30
ppm
0
1
2
3
4
5
6
7
8
9
3.04
2.84
1.99
0.98
1.00
0.97
0.89
5.76
3.82

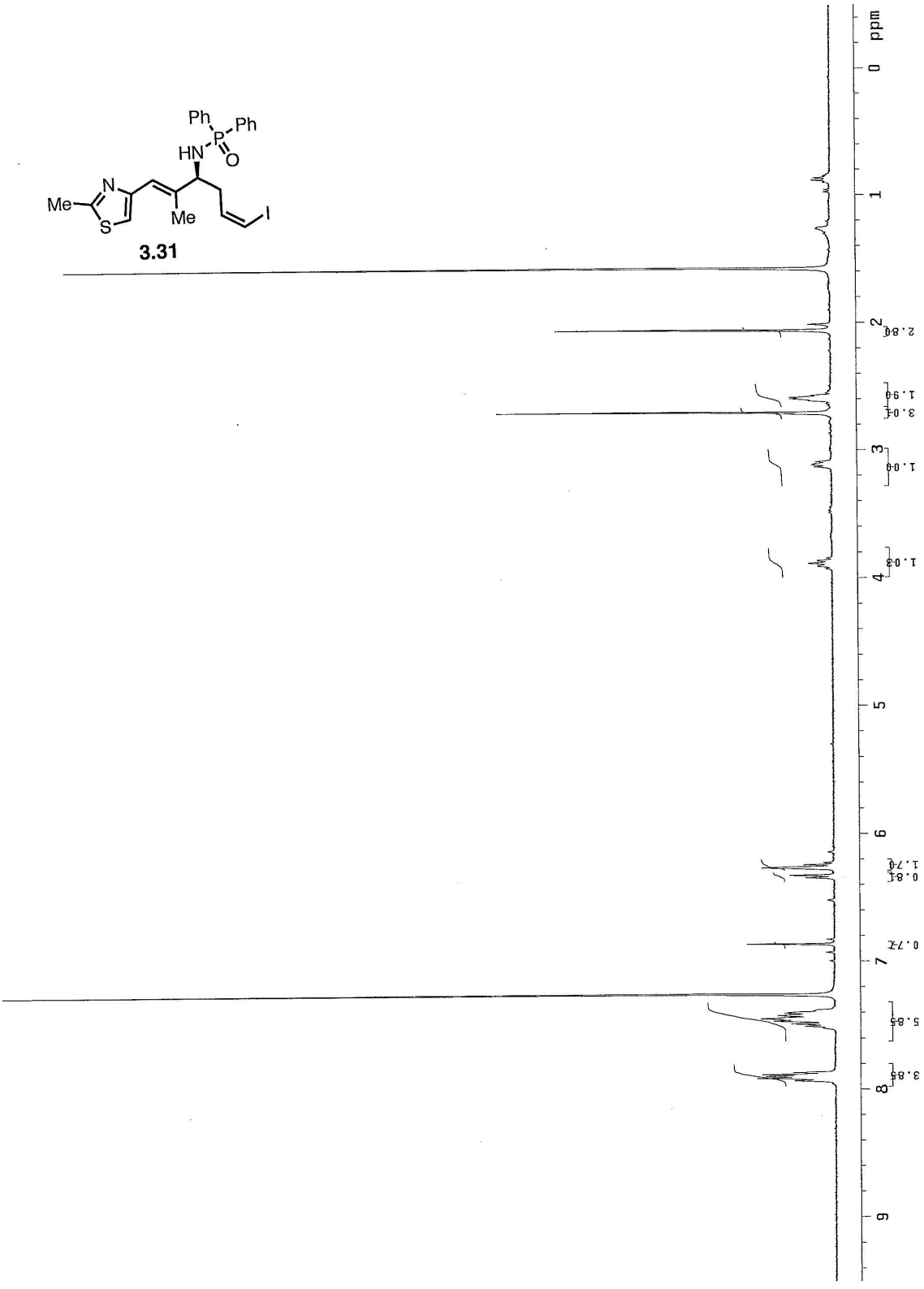
Ph
Ph
HN
P
O
N
Me
S
Me
I
3.31
ppm
0
1
2
3
4
5
6
7
8
9
2.80
1.90
3.04
1.00
1.03
1.70
0.81
0.72
5.85
3.85

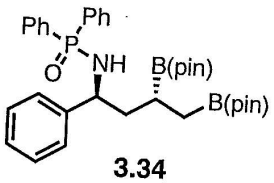

3.34

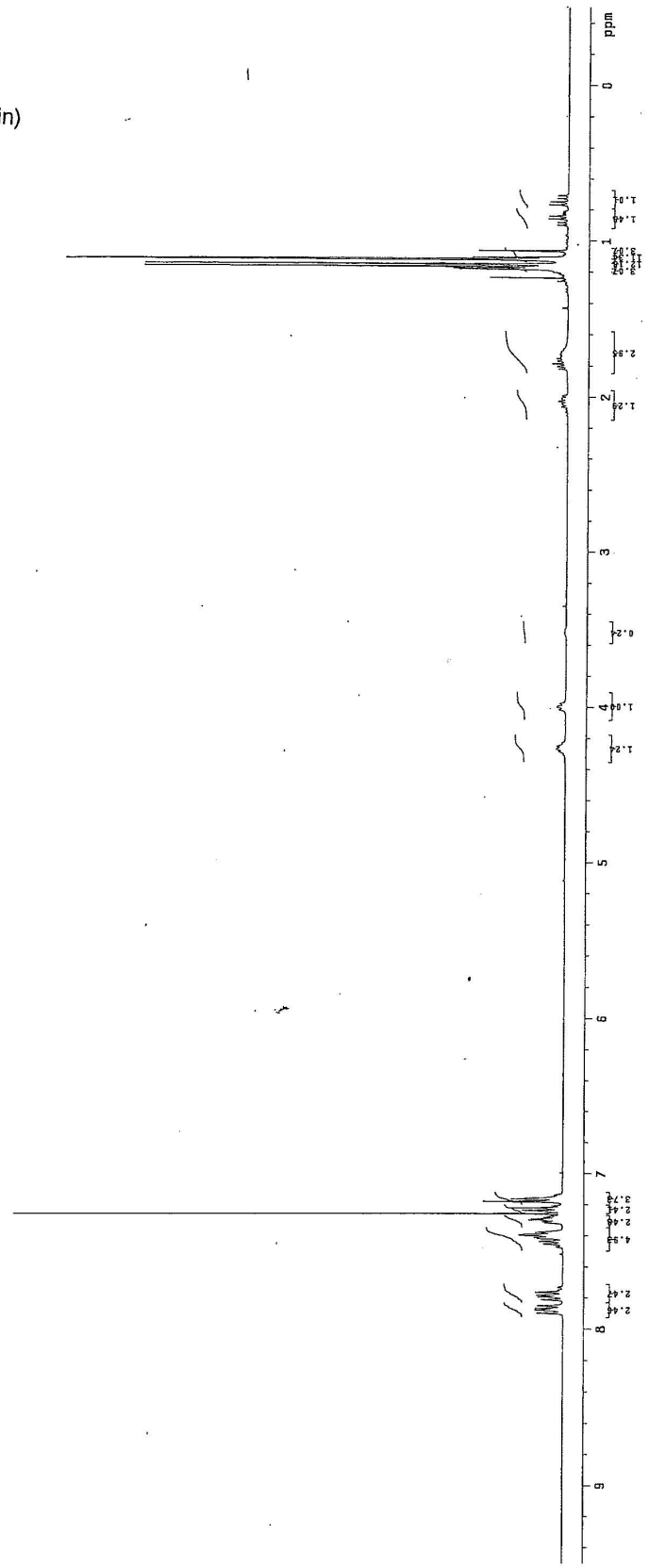

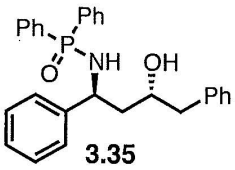

3.35

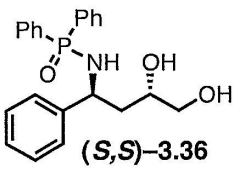

(*S,S*)–3.36

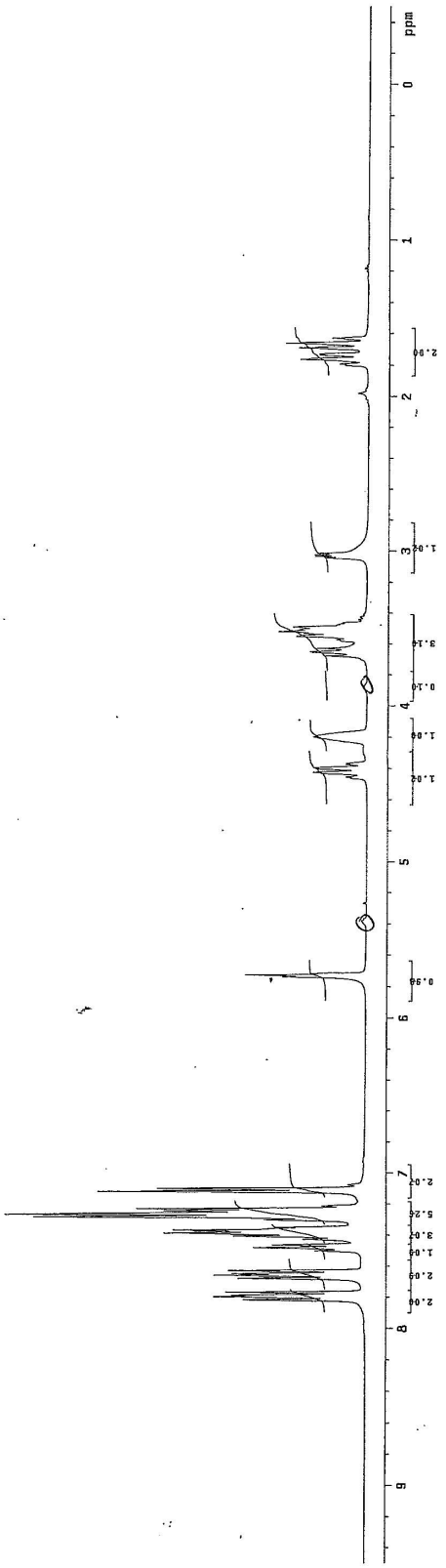

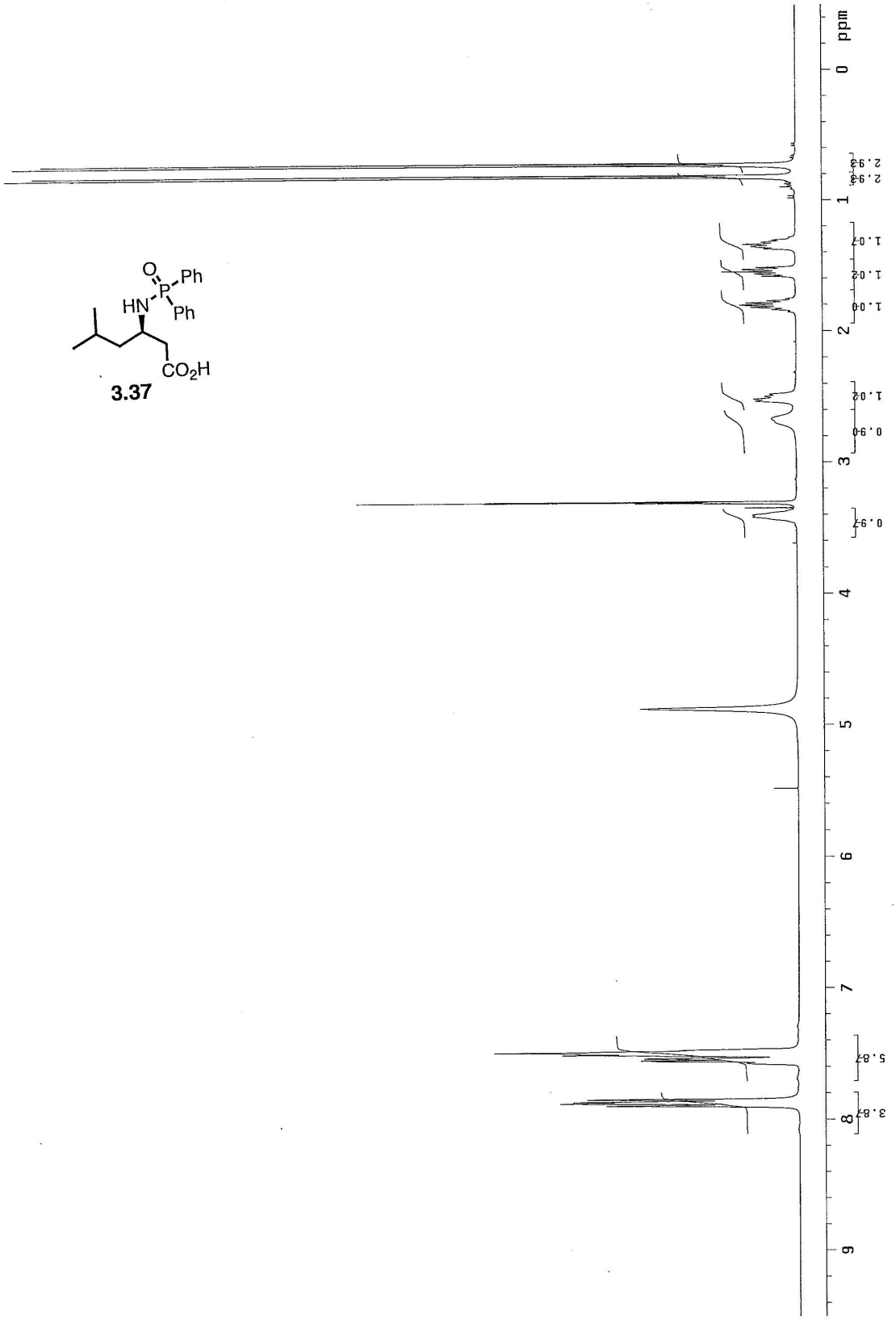
O
Ph
P
HN
Ph
CO2H
3.37
ppm
0
1
2
3
4
5
6
7
8
9
2.93
2.93
1.07
1.02
1.00
1.02
0.90
0.97
5.87
3.87

Chapter Four

Metal-Free Catalysts for Enantioselective Synthesis of Allenic Carbinols

4.1 Introduction

The development of new catalysts, and the processes that they govern, has the opportunity to significantly alter the manner in which molecules are prepared. Modern synthetic chemistry is a constantly evolving field, as what were once emerging technologies progress in sophistication. The field of enantioselective allyl addition to carbonyls and their derivatives is exemplary. As documented in Chapter 2, in the context of the formation of enantiomerically enriched homoallylic amines, pioneering methods relied on substrate control, employing prefunctionalized reaction partners that were suited with chiral auxiliaries to command the desired mode of addition. As the understanding of the factors that influence the transition states of these processes advanced, chiral *catalysts* were developed with the ability to alter and control the energetics of C–C bond formation. Currently, there are higher demands to be met to advance the field: Catalysts must work quickly, exhibiting high turnover rate to complete transformations rapidly with as little a quantity as possible. They must also be readily available and sustainable, as well as highly selective and general.

Moreover, the investigation of new catalysts can lead to the discovery of those that promote reactions with unique mechanisms, complementary to existing pathways. An analysis of the state-of-the-art catalysts that promote allyl additions revealed specific

Figure 4.1 Blueprint for the Development of a New Metal-Free Catalyst to Promote Reactions of Allylborons with Aldimines

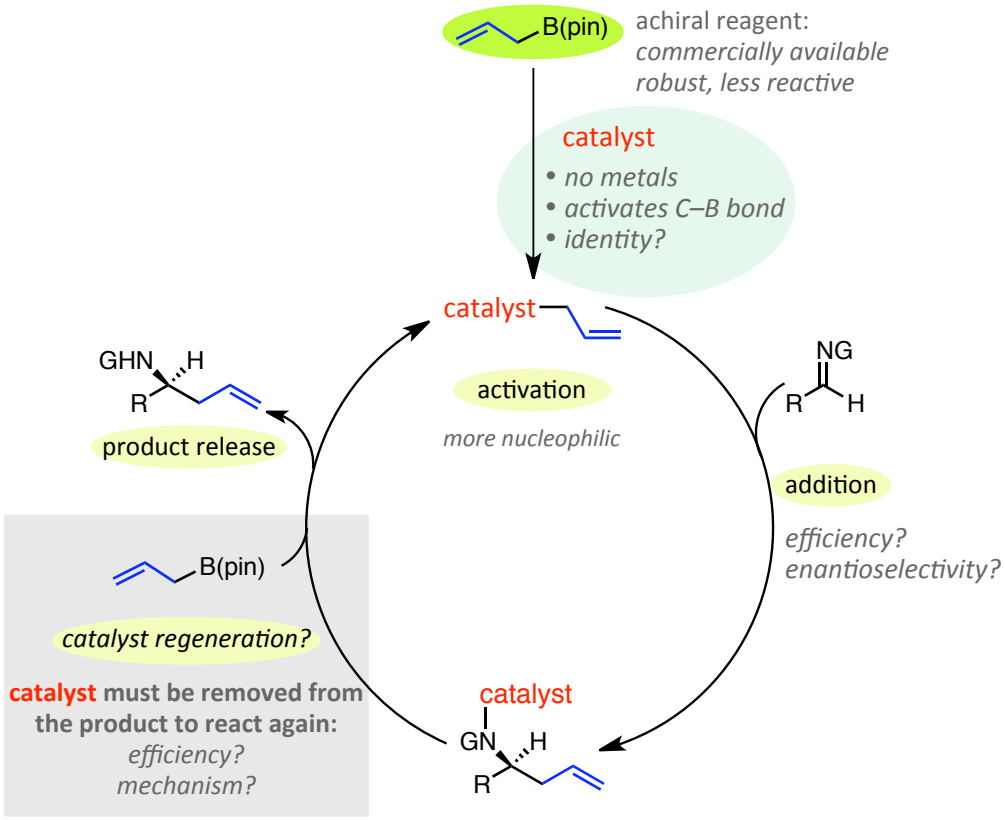

deficiencies: metal-based catalysts offered superior reactivity and rates of turnover, but are often sensitive, configurationally unstable, and require low temperatures; in contrast, metal-free catalysts are more robust and typically do not isomerize, but are plagued by inefficient turnover mechanisms and diminished nucleophilicities.[1] We set out to design a catalytic cycle, operated by a readily available metal-free catalyst, which could reach levels of efficiency typically reserved for metal-containing processes. The blueprint for such a cycle requires contending with several hurdles (Figure 4.1): 1) An organic molecule that reacts with allylboron in such a way to sufficiently increase its

[1] For a detailed discussion regarding selected metal and metal-free catalysts, refer to Section 2.2 of Chapter 2. The benefits and shortcomings to a number of strategies for enantioselective allyl additions to imine electrophiles are evaluated.

nucleophilicity must be identified. 2) This catalyst must react efficiently and the derived allyl adducts must be provided in excellent enantioselectivity. 3) The most crucial undertaking involves the identification of a mechanism for catalyst turnover. Metal-catalyzed transformations typically boast high turnover frequency numbers because of the favorable kinetics involved in transmetalation processes; in contrast, the turnover-limiting step for organic molecule catalysts is often regeneration of the active catalyst. A covalently bound catalyst-product intermediate must be decomplexed such that the product is released and the catalyst is freed to reenter the catalytic cycle. Typically, the mechanism for regeneration of the catalyst relies on energetically and entropically disfavored protolytic cleavage or hydrolysis events.

The small molecule allyl addition catalyst, to be described herein, incorporates a key proton into its design. This simple proton imbedded into the catalyst framework imparts enhanced nucleophilicity to the allyl group, lowers the energy for substrate coordination, is an organizing element in the transition state, and, perhaps most critically, serves as an *intramolecular* source of protolytic cleavage to rapidly release the product and regenerate the catalyst. The unique mechanism by which the allyl addition processes occur, their complementarity to the corresponding metal-catalyzed transformations, and application to new reaction methodologies will be discussed.

4.2 Background

Our interest in the development of catalysts that promote transformations of allylboron reagents was thoroughly reviewed in Chapter 2. These investigations led to the identification of three classes of catalysts with the capacity to activate the C–B bond of allylboron **4.2** towards allyl group transfer: 1) copper complexes of *N*-heterocyclic

carbene (NHC) ligands which proceed through thermodynamically favored transmetalation events,[2] 2) *N*-heterocyclic carbenes themselves engender activation through σ-donation into the empty p orbital on boron, and 3) sodium *tert*butoxide was also found to promote efficient allyl transfers in the presence of methanol, such that homoallylic amide **4.3a** is afforded in 72% conversion in 2 hours (equation 1), albeit through an unknown mechanism. We postulated that the alkoxide could serve as a Lewis basic activator of the boron center in an analogous fashion to the NHCs. Alternatively, the alkoxide could serve to decomplex the pinacol generating a more active boron-based nucleophile for an allylboration mechanism.

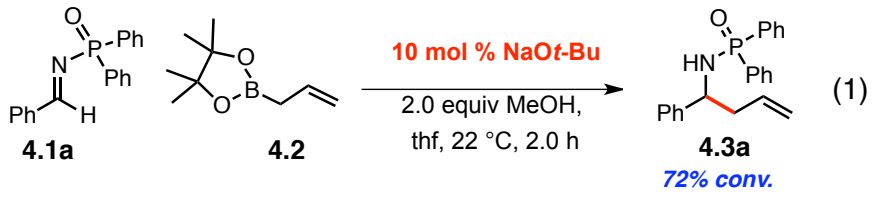

(1)

Further investigations targeted the capacity for deprotonated chiral alcohols to promote enantioinduction in the allyl transfer reactions to phosphinoyl aldimine **4.1a** (Scheme 4.1).[3] Unexpectedly, chiral phenoxides derived from BINOL derivatives, such as **4.4**, delivered appreciable facial selectivities (up to 83:17 e.r.). These results opposed earlier studies aimed at promoting facial discrimination with the supposedly mechanistically akin Lewis basic NHCs. The lack of enantioselectivity obtained with carbene catalysts led to the conclusion that activation through a σ-donation strategy positions the stereogenicity of the catalyst too remotely to influence the site of C–C bond

[2] The development of this class of catalysts is the main subject of Chapter 2. For a detailed account, see: "Enantioselective Synthesis of Homoallylic Amines through Reactions of (Pinacolato)allylborons with Aryl-, Heteroaryl-, Alkyl-, or Alkene-Substituted Aldimines Catalyzed by Chiral C_1-Symmetric NHC–Cu Complexes," Vieira, E. M.; Snapper, M. L.; Hoveyda, A. H. *J. Am. Chem. Soc.* **2011**, *133*, 3332–3335.
[3] Dr. Tatiana Pilyugina was instrumental in advancing the study of both NHCs and alkoxides as allyl transfer catalysts. Her extensive investigation, only very briefly summarized here, encompassed a wide range of chiral alcohols before the discovery of the aminophenols in Scheme 4.1.

Scheme 4.1 Catalytic Enantioselective Allyl Additions to Phosphinoylaldimines Promoted by Various Chiral Phenoxides

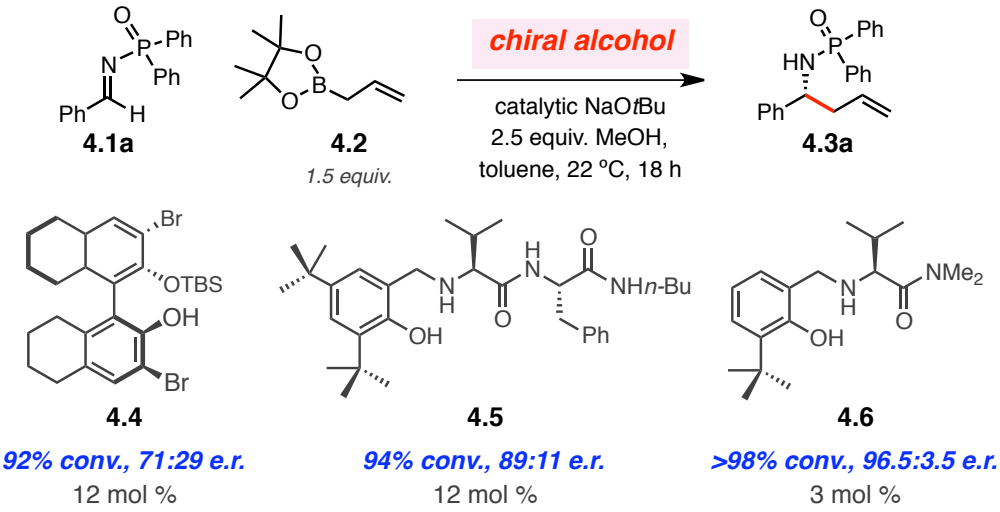

formation in the resultant acyclic transition state. Analogously, a coordinatively saturated chiral phenoxide-complexed boronate, activated for allyl transfer, is expected to react through an antiperiplanar or synclinal approach of the imine, and as such, is unlikely to be facially selective. However, unlike the carbene catalysts, the phenoxide may have an alternative mode of operation; the nucleophilic oxygen can displace a ligand on boron, releasing pinacol, to catalytically generate a chiral allylboron species. An ensuing allylboration mechanism would position the stereochemistry of the catalyst in close proximity through a cyclic Zimmerman Traxler-type transition state, a well-documented strategy for highly stereoselective synthesis of homoallyic alcohols and amines.

A seemingly similar strategy had been disclosed for catalytic enantioselective allyl additions promoted by a BINOL derivative, where the diol is proposed as the active species, rather than the phenoxide.[4] Ligand exchange is postulated between the chiral

[4] (a) "Asymmetric Allylboration of Acyl Imines Catalyzed by Chiral Diols," Lou, S.; Moquist, P. N.; Schaus, S. E. *J. Am. Chem. Soc.* **2007**, *129*, 15398–15404. For the catalysis of allyl additions to ketones, see: (b) "Asymmetric Allylboration of Ketones Catalyzed by Chiral Diols," Lou, S.; Moquist, P. N.;

alcohol and the more labile bis*iso*propoxy allylboron resulting in generation of a chiral allyl nucleophile, which reacts with *N*-benzoyl imines through an allylboration mechanism (Figure 4.2).[5] The complication in this approach lies in the subsequent

Figure 4.2 The Issue of Turnover for the Enantioselective Allylboration of Benzoyl Imines Catalyzed by Chiral BINOL Derivatives

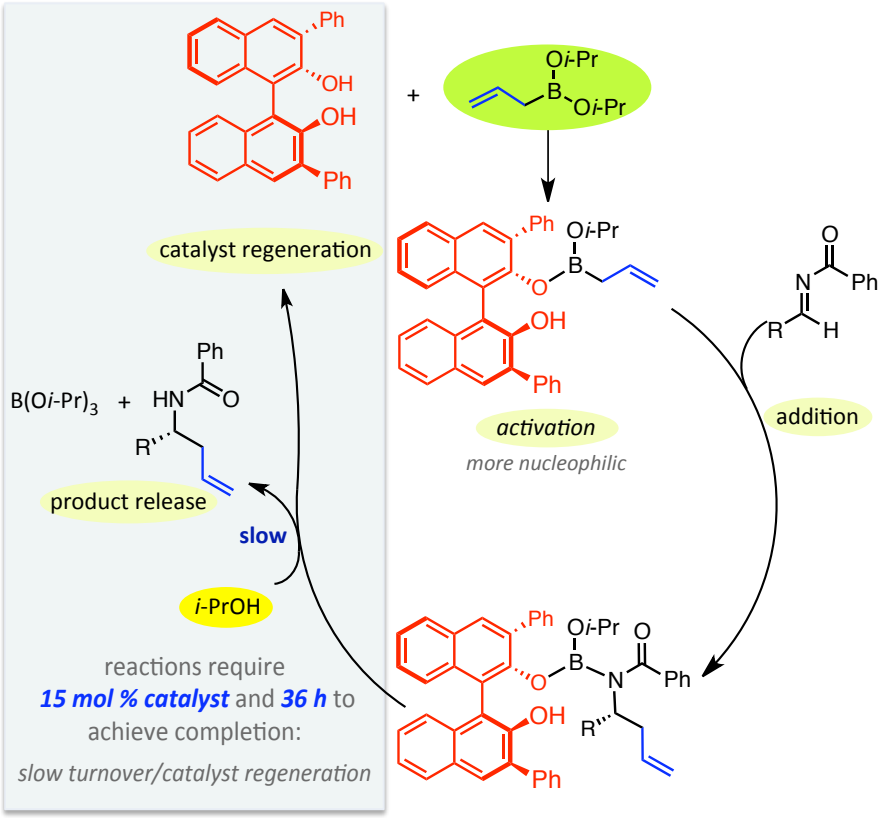

Schaus, S. E. *J. Am. Chem. Soc.* **2006**, *128*, 12660–12661. (c) "The Mechanism and an Improved Asymmetric Allylboration of Ketones Catalyzed by Chiral Biphenols," Barnett, D. S.; Moquist, P. N.; Schaus, S. E. *Angew. Chem., Int. Ed.* **2009**, *48*, 8679–8682. For catalyzed additions of other organoborons (besides allyl) to imines, see: (d) "Enantioselective Addition of Boronates to Acyl Imines Catalyzed by Chiral Biphenols," Bishop, J. A.; Lou, S.; Schaus, S. E. *Angew. Chem., Int. Ed.* **2009**, *48*, 4337–4340.

[5] Rather than mono-substitution of the bis-alkoxyallylboron species proposed by Schaus, theoretical studies suggest that binaphthols promote reactions by serving as cyclic bisphenoxy ligands for the boron atom, see: (a) "Asymmetric Conjugate Addition of Alkynylboronates to Enones: Rationale for the Intriguing Catalysis Exerted by Binaphthols," Pellegrinte, S. C.; Goodman, J. M. *J. Am. Chem. Soc.* **2006**, *128*, 3116–3117. (b) "Theoretical Study of the Asymmetric Conjugate Alkenylation of Enones Catalyzed by Binaphthols," Paton, R. S.; Goodman, J. M.; Pellegrinet, S. C. *J. Org. Chem.* **2008**, *73*, 5078–5089. (c) "Mechanistic Insights into the Catalytic Asymmetric Allylboration of Ketones: Bronsted or Lewis Acid Activation?" Paton, R. S.; Goodman, J. M.; Pellegrinet, S. C. *Org. Lett.* **2009**, *11*, 37–40.

product release from the chiral boron intermediate. The N–B bond must be protolytically removed by the intermolecular action of an *iso*propanol additive. Moreover, the diol catalyst must be regenerated, a process that involves intermolecular displacement of the chiral alcohol from the boron center with another molecule of *iso*propanol. Finally, the diol must reinitiate through ligand exchange to once again access the active chiral allylboron. This three-step mechanism for turnover represents a severe limitation to this approach; the presence of 15 mol % of the catalyst and 36 hours are used to compensate for the poor kinetics of each cycle.

The mechanism outlined in Figure 4.2 represents a plausible operative pathway to describe the action of the chiral phenoxides in Scheme 4.1 on allylboron **4.2**. The phenoxide-catalyzed reactions also require methanol as an additive, similar to the requirement for *iso*propanol for turnover in the system reported by Schaus. However, there are a few distinguishing features: 1) For the mechanism in Figure 4.2, the role of an alcohol additive is ascribed to facilitate turnover. However, when a stoichiometric quantity of phenoxide catalyst derived from **4.4** is employed to promote the allyl addition, *in the absence of methanol*, there is <2% conversion to product, suggestive of an alternative or additional role for the protic additive. 2) The pathway in Figure 4.2 hinges on the lability of the ligands on the allylboron employed; no reaction is observed with pinacol-complexed allylboron under the catalytic system developed by Schaus. 3) Reactions of phosphinoyl aldimines are promoted by 12 mol % of the chiral phenoxide to completion within 18 hours, suggesting a significantly more efficient system, particularly with the less activated reaction partners.

There appeared to be mechanistic implications triggered by the use of sodium phenoxide catalysts that were not yet understood. Further investigations focused on

elucidating the distinction in activity between phenol and phenoxide catalysts, alongside concomitant analysis of other classes of chiral phenols that could be employed as phenoxide precursors. Interestingly, the amino-acid based molecules (such as phenols **4.5** and **4.6** in Scheme 4.1), developed in these laboratories as ligands for metal-catalyzed transformations,[6] were found to provide promising levels of reactivity and selectivity.

The amino acid-derived molecules were originally designed to feature a benzylic amine or imine substituted at the *ortho* position with functionality capable of metal coordination, thus engendering a six-membered ring bidentate chelate with Lewis acidic metals. Substituents at the *ortho*-position ranged from alcohols, for oxophilic metals such as titanium, zirconium, or aluminum,[7] to softer ligands like phosphines for late transition metals such as copper and silver.[8] The amino acid-based molecules offer an easily accessible, highly modular, and sustainable platform for the generation of a vast array of structurally and electronically diverse ligands. It is this ability to readily modify the structural features and tune the electronic attributes of the molecules that has attributed to their successful implementation in numerous and varied catalytic transformations. In addition to serving as ligands for metal-catalyzed processes, the amino acid-derived

---

[6] Related phosphines were the optimal ligands for Ag-catalyzed Mannich reactions in Chapter 1, and were investigated for Ag-catalyzed allyl additions reactions as described in Section 2.3 in Chapter 2.

[7] For selected examples, see: (a) "Discovery of Chiral Catalysts through Ligand Diversity: Ti-Catalyzed Enantioselective Addition of TMSCN to *meso* Epoxides," Cole, B. M.; Shimizu, K. D.; Krueger, C. A.; Harrity, J. P. A.; Snapper, M. L.; Hoveyda, A. H. *Angew. Chem. Int. Ed. Engl.* **1996**, *35*, 1668–1671. (b) "Asymmetric Synthesis of Acyclic Amines through Zr- and Hf-Catalyzed Enantioselective Alkylzinc Reagents to Imines," Akullian, L. C.; Porter, J. R.; Traverse, J. F.; Snapper, M. L.; Hoveyda, A. H. *Adv. Synth. Catal.* **2005**, *347*, 417–425. (c) "Al-Catalyzed Enantioselective Alkylation of α-Ketoesters by Dialkylzinc Reagents. Enhancement of Enantioselectivity and Reactivity by an Achiral Lewis Base Additive," Wieland, L. C.; Deng, H.; Snapper, M. L.; Hoveyda, A. H. *J. Am. Chem. Soc.* **2005**, *127*, 15453–15456.

[8] For selected examples, see: (a) "Highly Enantioselective Cu-Catalyzed Conjugate Additions of Dialkylzinc Reagents to Unsaturated Furanones and Pyranones: Preparations of Air-Stable and Catalytically Active Cu–Peptide Complexes," Brown, M. K.; Degrado, S. J.; Hoveyda, A. H. *Angew. Chem., Int. Ed.* **2005**, *44*, 5306–5310. (b) "A Highly Efficient and Practical Method for Catalytic Asymmetric Vinylogous Mannich (AVM) Reactions," Carswell, E. L.; Snapper, M. L.; Hoveyda, A. H. *Angew. Chem., Int. Ed.* **2006**, *45*, 7230–7233.

molecules have been utilized as catalysts themselves.[9] Suiting the *N*-terminus of the amino acid with a potent silaphile, such as an *N*-oxide or an imidazole moiety, rather than a metal chelation site, has proven an efficacious strategy for the identification of chiral catalysts that promote reactions with silicon-based reagents. The 2-hydroxyl benzylic amines of **4.5** and **4.6**, in resemblance to their activity as ligands in metal-catalyzed transformations, may serve to complex with Lewis acidic boron-based reagents.

As demonstrated in Scheme 4.1, dipeptide **4.5,** carrying a 2-hydroxyl-substituted benzylic amine, promotes allyl transfer to afford homoallylic amide **4.3a** in 89:11 e.r. and 94% conversion. Catalyst optimization on this class of catalysts resulted in identification of a highly efficient and selective amine-bearing phenol **4.6** (>98% conversion, 96.5:3.5 e.r. within four hours with 3 mol % catalyst, Scheme 4.1). There are several features of the small organic molecule catalyst that became evident during these investigations: 1) A single stereogenic center arising from an amino acid residue, valine, was sufficient in providing excellent stereoselection in the allyl addition reaction. 2) The highest levels of efficiency were obtained when the *C*-terminus was fitted with a potent Lewis base; for example, when the dimethylamide of phenol **4.6** is instead modified to an ethyl ester, homoallylic amide **4.3a** is obtained in 83:17 e.r. but with only 14% conversion (data not shown). 3) A *tert*-butyl group positioned *ortho* to the hydroxyl group is deemed essential for both efficiency and facial selectivity of the allyl transfer

---

[9] (a) "Proline-Based *N*-Oxides as Readily Available and Modular Chiral Catalysts. Enantioselective Reactions of Allyltrichlorosilane with Aldehydes," Traverse, J. F.; Zhao, Y.; Hoveyda, A. H.; Snapper, M. L. *Org. Lett.* **2005**, *7*, 3151–3154. For examples that employ imidazole-containing amino acid-derived catalysts, see: (b) "Enantioselective Silyl Protection of Alcohols Catalysed by an Amino-Acid-Based Small Molecule," Zhao, Y.; Rodrigo, J.; Hoveyda, A. H.; Snapper, M. L. *Nature*, **2006**, *443*, 67–70. (c) "Kinetic Resolution of 1,2-Diols through Highly Site- and Enantioselective Catalytic Silylation," Zhao, Y.; Mitra, A. W.; Hoveyda, A. H.; Snapper, M. L. *Angew. Chem., Int. Ed.* **2007**, *46*, 8471–8474. (d) "Catalytic Enantioselective Silylation of Acyclic and Cyclic Triols: Application to Total Syntheses of Cleroindicins D, F, and C," You, Z.; Hoveyda, A. H.; Snapper, M. L. *Angew. Chem., Int. Ed.* **2009**, *48*, 547–550.

process; the derivative of phenol **4.6**, in which the *tert*-butyl substitution on the aryl ring has been eliminated, provides the allyl adduct **4.3a** in 88:12 e.r. and 82% conversion (data not shown).

Investigation of the scope of the enantioselective allyl addition processes promoted by amine-bearing phenol **4.6** revealed several critical attributes of the present catalytic system. A wide range of diphenylphosphinoylaldimines participate in enantioselective allyl transfers to provide **4.3a**–**4.3f** in 71–98% yield and >96.5:3.5 e.r. within four hours at ambient temperature (Scheme 4.2). Moreover, reaction of 2-substituted allylborons afforded equally efficient and enantioselective transformations such that 1,1-disubstituted alkene **4.7** is obtained in 97.5:2.5 e.r. and 98% yield.

Scheme 4.2 Catalytic Enantioselective Allyl Additions to Phosphinoyl Aldimines and Isatins in the Presence of Aminophenol **4.6**

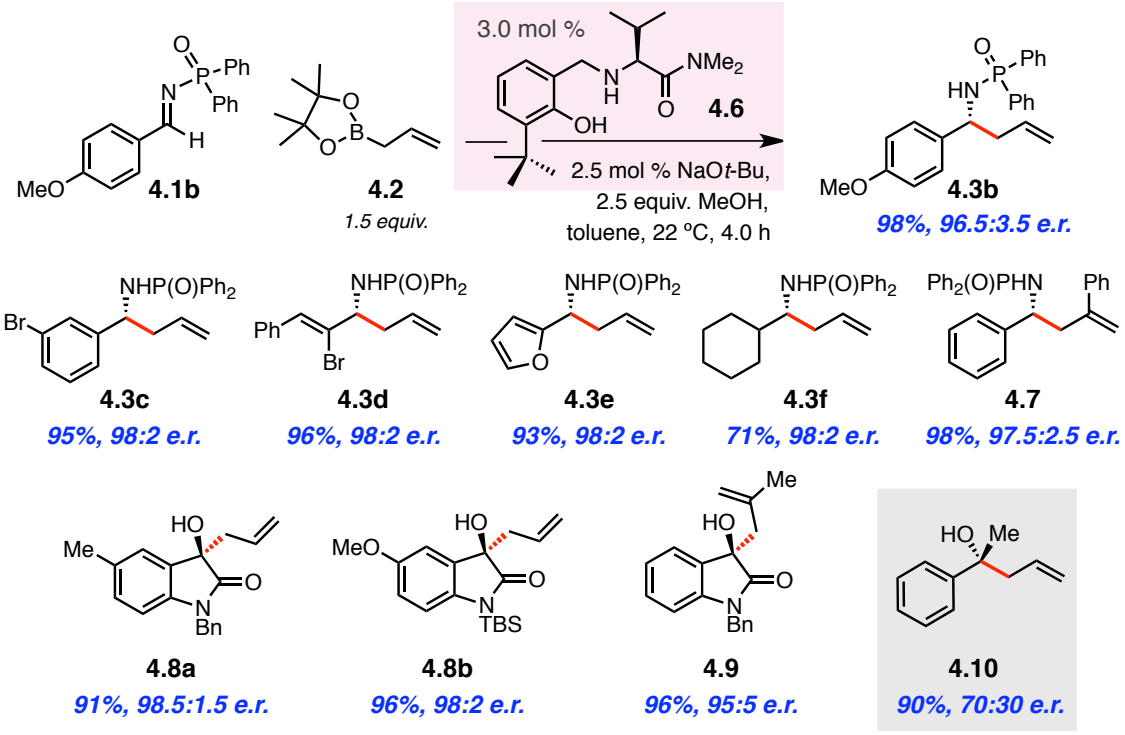

Reactions involving transfer of dissymmetric allyl groups, however, provided a mechanistic probe that will be discussed at length in the coming section. In addition to phosphinoyl imines, protected isatins proved competent reaction partners, yielding 3-hydroxy-2-oxindoles **4.8a**–**b** and **4.9** in >91% yield, and >95.5 e.r. (Scheme 4.2). Despite the facility with which transformations occurred in the presence of aminophenol **4.6** with both phosphinoyl imines and isatins, reactions of related classes of protected aldimines and ketones failed to provide sufficient stereoselectivity. For example, although homoallylic alcohol **4.10** can be obtained in 90% yield, the facial discrimination is substantially diminished (from typically >20:1) to a 2.3:1 preference (70:30 e.r.). Furthermore, there is <2% conversion in reactions of *N*-diphenylmethyl imines, a class of substrates differentiated from the phosphinoyl derivatives by the lack of a phosphoryl group. Together, these limitations of scope suggested the requirement of a secondary Lewis basic point of contact with the catalyst for high selectivity, whether by the phosphine oxide of the aldimines or the cyclic amide of the isatin substrates. Lack of an additional Lewis basic moiety on the electrophilic partner proved detrimental to the catalytic transformations, and as such, we pursued a mechanistic understanding that rationalized such a constraint for high efficiency and stereoinduction.

4.3 Mechanistic Implications of the Catalytic Cycle

Initial observations on the catalytic allyl additions promoted in the presence of chiral phenol **4.6** indicated a unique yet poorly understood operative mechanism. It was unclear how the amine-bearing phenol interacted with the boron-based reagents to impart activation to the allyl unit. Furthermore, the interactions involved between this activated

complex and the substrate were unknown, particularly given the requisite for electrophiles that could engage in two-point association. Finally, the mechanism of turnover of these simple organic molecule catalysts, whose rate rivaled those of analogous metal-catalyzed processes, needed to be established. Ensuing investigations were aimed at the elucidation of these mechanistic inquiries.[10]

One of the critical observations on this class of catalysts was revealed during the investigation of reactions involving the transfer of dissymmetric allyl units. Unexpectedly, reactions with isomerically pure *cis*- or *trans*-configured crotylboron reagents resulted in inefficient group transfer to phosphinoylaldimine **4.1a**, to afford only 40% conversion after 40 hours (data not shown). Moreover, there was a 3:1 preference for addition through the α-carbon of the allylic reagent, over the anticipated γ-addition (the cyclic transition states of allylborations are typically highly regio- and diastereoselective). This surprising outcome was further demonstrated through a deuterium-labeled experiment with allylboron **d_2–4.2**; the homoallylic amide **d_2–4.3a,** generated from α-addition of the allylic reagent, was obtained with >95% selectivity in

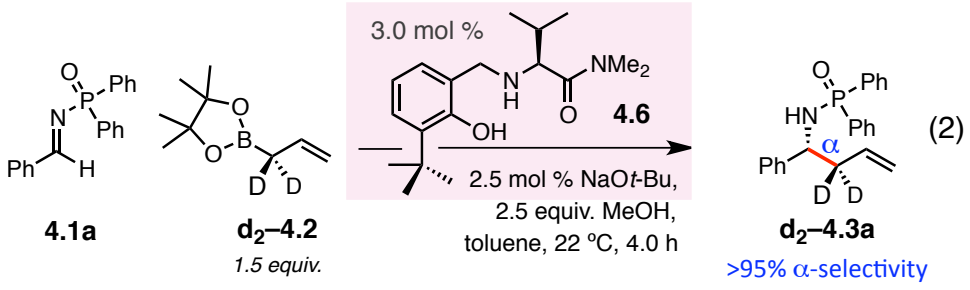

[10] Several colleagues were instrumental in executing the indispensable experimental and computational studies that provided the mechanistic understanding to be outlined in this Section. Only a very brief account of the observations made by Mr. Daniel Silverio, Dr. Tanya Pilyugina, Dr. Sebastian Torker, and Dr. Fredrik Haeffner will be discussed in relation to the concluding postulated catalytic cycle. For a more detailed account, see: "Simple Organic Molecules as Catalysts for Enantioselective Synthesis of Amines and Alcohols," Silverio, D. L.; Torker, S.; Pilyugina, T.; Vieira, E. M.; Snapper, M. L.; Haeffner, F.; Hoveyda, A. H. *Nature*, **2013**, *494*, 216–221.

the presence of aminophenol **4.6** (equation 2). There are two scenarios to consider to account for the unusual α-selectivity: either, 1) the HOMO coefficient of the alkylating species lies on the α-carbon and a Petasis-type mechanism, evoked for similar reactions with vinyl-, aryl-, and alkynyl-substituted borons, can be proposed,[4d] or, 2) the observed result is a product of *net α-addition*, arising from two stereoselective γ-additions.[11]

Subsequent experimental and computational data[10] supported the latter theory. The proposed catalytic cycle in Figure 4.3 describes the origin of the observed net α-addition and also provides a rationalization for the rapid kinetics for additions to imines and ketones. Aminophenol **4.6** could serve to decomplex the pinacol ester of allylboron **4.2** to generate chiral allylboron species ***i*** which, upon substrate coordination, can undergo a γ-selective allylboration reaction (***TS I***, Figure 4.3). Critical to the subsequent product release and the second γ-selective allyl transfer is the presence of a proton imbedded within the catalyst framework. The Brønsted acidity of the methanolic proton of allylboron–methanol complex ***ii*** is sufficiently raised (in respect to methanol)[12] to result in protonation of the boron-bound amine of ***i***. The protonated quaternized amine, which is stabilized through an intramolecular interaction with the Lewis basic amide terminus, leads to a significant increase of the Lewis acidity of boron. The electron-defficient boron center encourages substrate coordination and results in raising the energy of the HOMO of the allyl group, accelerating C–C bond fomation. Thus, the highly reactive protonated complex ***iii*** undergoes facile allyl transfer affording product–catalyst

---

[11] For an example employing allylboron reagents that proceeds through two γ-selective allyl transfers, (accomplished through a transmetalation to indium, followed by the addition of the allylindium to a hydrazone), see: "Indium(I)-Catalyzed Asymmetric Allylation, Crotylation, and a-Chloroallylation of Hydrazones with Rare Constitutional and High Configurational Selectivities," Chakrabarti, A.; Konishi, H.; Yamaguchi, M.; Schneider, U.; Kobayashi, S. *Angew. Chem., Int. Ed.* **2010**, *49*, 1838–1841.

[12] The acidity of the proton in Lewis base-Lewis acid complex ***ii*** is likely increased by several orders of magnitude. For example, the pK_a value (determined in H_2O) of methyloxonium ion is 17 orders of magnitude more acidic than methanol (pK_a = –2.2 vs. 15.5).

Figure 4.3 The Postulated Operative Catalytic Cycle for the Phenol Catalyst **4.6** Highlighting the Role of an Internally Imbedded Proton

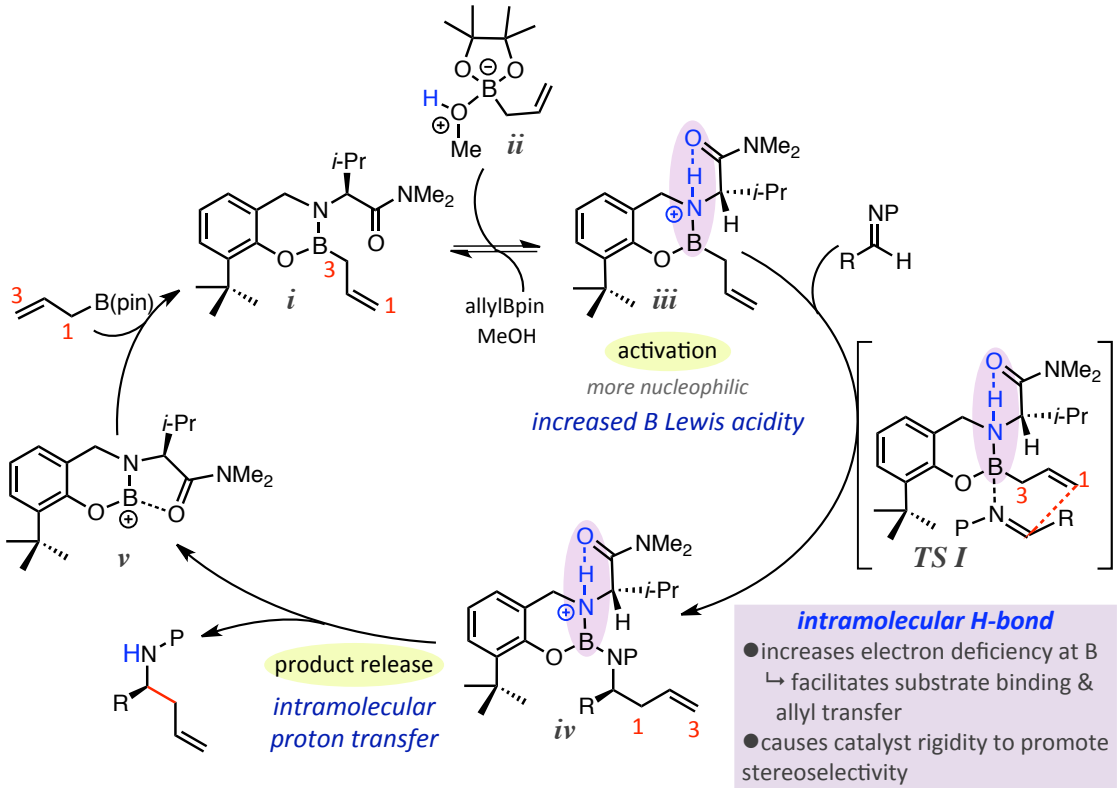

complex ***iv***. An ensuing intramolecular proton transfer releases the amine or alcohol product and results in the formation of amide-stabilized borenium cation ***v***. The highly electrophilic boron species ***v*** is susceptible to a γ-selective nucleophilic trap with a molecule of allylboron **4.2**, directly restoring the active catalytic species ***i***.

The mechanistic picture is further expounded in Figure 4.4. Beginning from protonated chiral allylboron complex ***iii***, coordination of the imine (or ketone) at the electron deficient boron center occurs with facility, affording ***TS I***. It is the strength of this coordination that is linked to the propensity for allylboron reagents to undergo allyl transfer through an allylboration mechanism. The degree of vacancy of the boron p-type

atomic orbital determines the potency of the boron–substrate association;[13] in the case of the allylboron derived from phenol **4.6**, protonation of the ordinarily donating amine ligand results in significant diminution in its ability to stabilize the electron deficiency on

Figure 4.4 The Detailed Mechanism Accounting for a Net α-Addition and the Role of the Implanted Proton

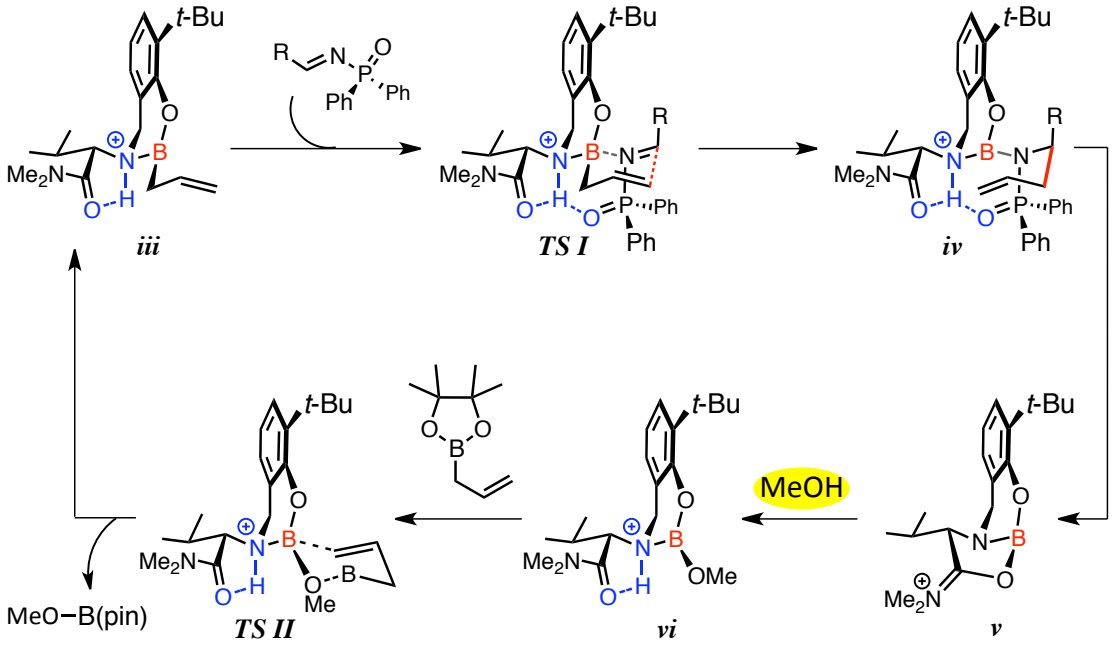

boron. The electron-accepting ability of the reacting orbital on boron is elevated, thus strengthening the Coulombic attraction between the boron center and the non-bonding electron pairs of the reacting imines or ketones.

An additional role for the aptly positioned proton, beyond inducing activation and facilitating catalyst regeneration, is depicted in ***TS I***: the approach of the substrate can be conformationally restricted through formation of a hydrogen-bond, i.e., the mode of

[13] It has been shown for various allylborons complexed with aminoalcohols, that those bearing amines with electron-withdrawing groups are more apt to accept electron density due to a higher degree of vacany at the LUMO on boron; for example, an allylboron containing an *N*-mesylated aminoalcohol vs. the corresponding *N*-methylated derivative is more prone to reaction with formaldehyde. For a computational study on allylboration that correlates reactivity of various allylboron reagents with the auxiliaries they bear, see: "Theoretical Study on the Effects of Structure and Substitutents on Reactivity in Allylboration," Omoto, K.; Fujimoto, H. *J. Org. Chem.* **1998**, *63*, 8331–8336.

approach of the phosphoryl group of the imine (or the adjacent amide group of an isatin) is dictated such that they are properly positioned to engage in intramolecular H-bonding. This additional Coulombic attraction results in further activation of the substrates, directs the favored mode of association, and lends rigidity to the transition state. A lower energy pathway to allyl transfer is thereby afforded by the advantageous interaction between the secondary electron-rich Lewis base of the substrate and the imbedded proton within the catalyst framework. In the catalyzed allyl additions to acetophenone, there is diminished enantioselectivity (**4.10** is obtained in 70:30 e.r., Scheme 4.2); the lack of a second point of contact frees the unhindered ketone to approach the boron-based catalyst through various coordination modes. The catalyst itself has few structural features to energetically bias the multitude of transition states that lead to allylboration, and therefore poor facial selectivity is obtained. However, with substrates that can engage in the electrostatic interaction with the catalyst proton, there is a single transition state that is lowest in energy due to the imparted stabilization of the complex (i.e., ***TS I***, Figure 4.4).

Allylboration results in the formation of a covalent catalyst-product complex, such as ***iv***. Intramolecular proton transfer releases the phosphinamide (or alcohol) and the resultant borenium cation is trapped with the Lewis basic amide, generating ***v***. Methanolysis provides protonated ***vi***, an electrophilic boron species that can react with (pinacolato)allylboron through a synclinal cyclic transition state ***TS II*** to regenerate chiral allylboron ***iii***. The mechanism that accounts for the γ-selective regeneration of the active chiral allylboron intermediate (***TS II***) was found to introduce stereochemical implications that are further expounded in Figure 4.5.

In the transformation of enantioenriched α-disubstituted allylboron **4.11**,[14] in the presence of 6.0 mol % aminophenol **4.6** and 2.5 mol % zinc(II) *tert*-butoxide, the contiguous *N*-substituted tertiary and all-carbon quaternary stereogenic centers of **4.12** are formed with 89:11 d.r. and 95:5 e.r.; the allyl transfer is completely α-selective and

Figure 4.5 Mechanistic Details of the Stereospecific Synthesis of Homoallylic Amides Bearing an α-Stereocenter

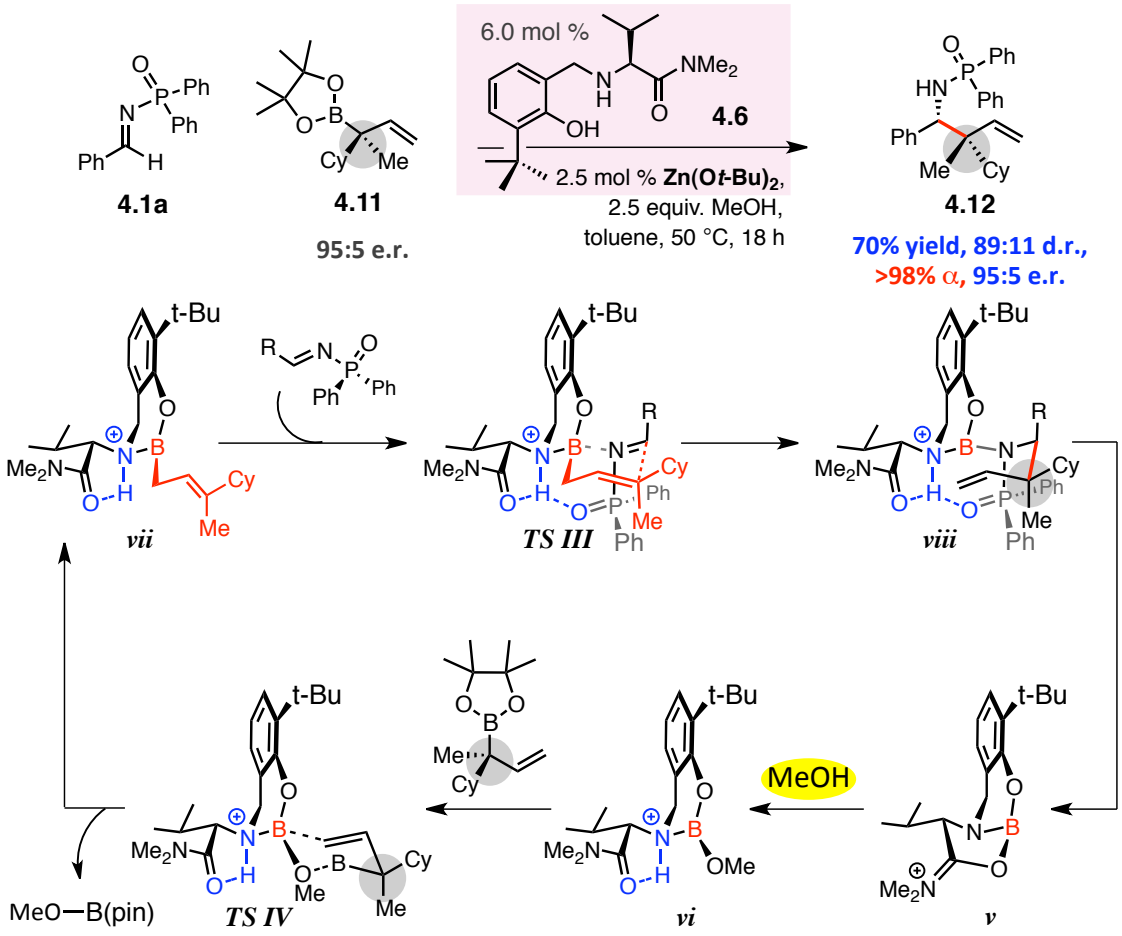

[14] Chiral allylic boron reagents, bearing tertiary or quaternary α-stereocenters, can be accessed through reported enantioselective NHC–Cu-catalyzed allylic substitution reactions developed in these laboratories. For details, see: "Enantioselective Synthesis of Allylboronates Bearing a Tertiary or Quaternary B-Substituted Stereogenic Carbon by NHC–Cu-catalyzed Substitution Reactions," Guzman-Martinez, A.; Hoveyda, A. H. *J. Am. Chem. Soc.* **2010**, *132*, 10634–10637.

the major diastereomer is obtained in 70% yield (Figure 4.5).[15] Moreover, the stereoselective synthesis of **4.12** revealed a unique attribute imparted by the mechanism of catalyst regeneration: *the stereochemistry defined in the starting allylboron species is inverted through allyl transfer*.[16] The synclinal γ-selective cyclic allyl transfer in ***TS IV*** results in the stereospecific formation of *E*-configured chiral allyl boron ***vii***, which, in turn reacts with an imine through a second γ-selective transfer in ***TS III*** (Figure 4.5). The reversed diastereoselectivity (reaction through the *Z* allylboron) or little stereochemical preference would be observed if acyclic mechanisms for allyl transfer were dominant. Moreover, the reversal of configuration observed in the reaction in Figure 4.5 diminishes the plausibility of an alternative reaction mechanism involving direct α-addition from the allylboron reagent, validating an operative catalytic cycle involving two γ- and stereoselective allyl additions.

The unique mechanism ascribed to the boron-based catalysts, particularly its divergence from that of catalytic cycles driven by NHC–Cu catalysts described in Chapter 2, warranted further evaluation. Specifically, we questioned whether the α-selectivity of the present class of catalysts could potentially allow access to allene addition adducts (from reactions with commercially available allenyl boronic acid pinacol esters). Furthermore, transformations of allenylboron promoted by copper-based catalysts exclusively provide propargyl additions (see Chapter 3 for details), thus, the development

---

[15] There is complete α selectivity (>98% by ^{1}H NMR analysis) in all instances. If the boron-based catalyst were to be generated by ligand exchange, between the allylboron reagent and the aminophenol, however, we would expect the initial catalytic cycle to produce a γ-selective addition. That none of the homoallylamine from overall γ-addition is detected suggests that the catalyst is either, derived from a minute fraction of the aminoalcohol in solution (producing an undetectable quantity of γ-addition), or, the active boron-based catalyst is formed by a pathway yet to be elucidated.

[16] The absolute stereochemical identity of the homoallylic amide **4.12** was ascertained through X-ray crystallography. Related transformations of enantioenriched allylborons bearing an α-tertiary stereocenter (not shown) also proceed with inversion with similar levels of diastereo- and enantiocontrol. For more information, see reference 9.

of allene addition protocols would serve to highlight the novelty and complementarity of the metal-free catalysts described herein.

4.4 Enantioselective Synthesis of Allenic Carbinols with a Catalyst Derived from a Valine-Based Aminophenol

Congruent to the mechanistic proposals described for allyl transfers promoted by an aminophenol in the previous section, we postulated that transformations of allenyl boronic acid pinacol ester **4.13** would proceed to provide allene-substituted amines and alcohols (Figure 4.6). Propargyl addition to electrophilic boron species ***vi*** through ***TS VI*** would result in chiral propargylboron ***ix***. Imine coordination followed by γ-selective addition through cyclic transition state ***TS V*** affords the product of net allenyl transfer. The catalytic activity outlined in Figure 4.6, however, substantially deviates from the

Figure 4.6 The Catalytic Activity Required for the Development of an Enantioselective Approach to α-Allenic Amines

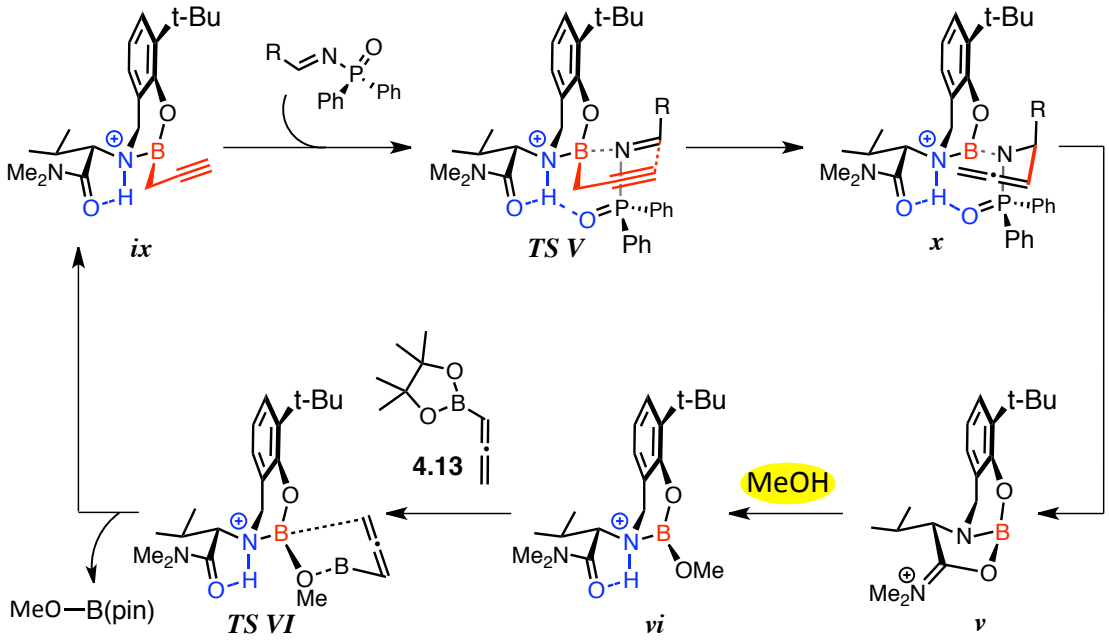

known allyl transfer activity ascribed to aminophenol **4.6** in the previous section. For example, the inclusion of an alkyne in the theoretical cyclic transition state for allenyl transfer, ***TS V***, results in a warped six-membered Zimmerman Traxler-type addition, conformationally distinct from the related complex that results in allylboration, ***TS I*** in Figure 4.4. The approximate 109º angles assumed in the six-membered allylboration reaction are not accessible to alkyne-bearing ***ix***. Consequentially, likely a result of the induced strain in ***TS V***, reaction of phosphinoyl aldimine **4.1a** and allenylboron **4.13** affords only 32% conversion to an approximate 3:1 ratio of allenyl adduct **4.14** to homopropargylic amide **4.15** (equation 3). The diminished activity and site selectivity, in

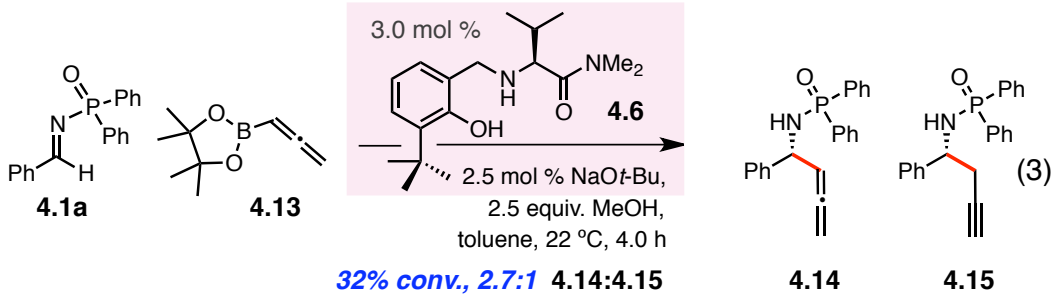

comparison to reactions with allylboron **4.2**, suggests that ***TS V*** is a higher energy structure. The desired mode of additions is conceivably inaccessible due to either, 1) poor alignment of the π-system with the π^* of the C=N bond, or, 2) represents a mode of association of the imine that weakens or disrupts the electrostatic interaction between the phosphoryl group and the proton within the catalyst structure.

We postulated that association of diphenylphosphinoylaldimine **4.1a** with the boron center of ***ix*** provides insufficient activation for the desired S_E2' reaction.[17]

[17] The inflexible six-membered association of phosphinoylaldimines with the boron-based catalyst, depicted in ***TS V*** of Figure 4.6, is a result of the simultaneous overlap of the lone pair on the imine nitrogen with the empty p atomic orbital of boron, and the interaction between the phosphoryl group and the

Therefore, the development of efficient allene transfers from chiral propargylboron ***ix*** would require substrates with a differing mode of coordination that could adjust to the geometry of the ensuing cyclic transition state. Two-point association of isatins to the boron-based catalyst occurs through a seven-membered ring (vs. six for phosphinoyl aldimines). Additionally, due to their planarity, there are fewer steric interactions that can

Scheme 4.3 Catalytic Enantioselective Allene Addition to *N*-Benzyl Isatin in the Presence of Aminophenol **4.6**

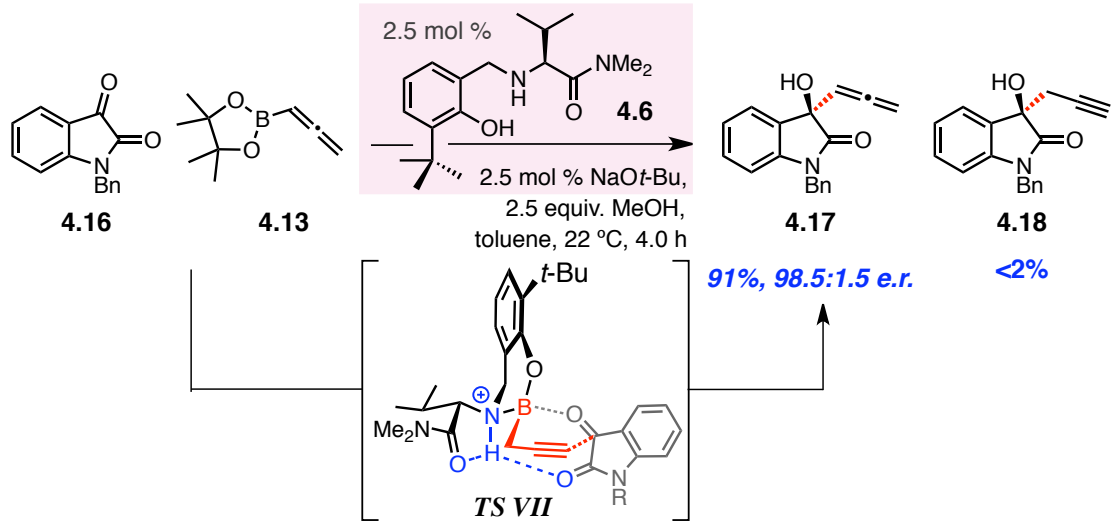

impede appropriate overlap. Gratifyingly, the postulated chiral propargylboron catalyst, derived *in situ* from phenol **4.6** and allenylboron **4.13**, provides exclusive allene transfer to *N*-benzyl isatin **4.16** to afford allenic carbinol **4.17** in 91% yield and 98.5:1.5 e.r. (Scheme 4.3). The cyclic S_E2' transition state ***TS VII*** is organized by the occurrence of an electrostatic interaction between the amide of the isatin and the protonated amine of the catalyst, a feature that facilitates the allene transfer. The two-pronged coordination mode exhibited by isatins allows for sufficient overlap of the HOMO on the alkyne with the π*

imbedded proton. Although perfectly aligned for allylboration (***TS I***), this coordination mode likely places the π* further from the alkyne. Steric demands imparted by the two-site binding may then impede productive allene additions.

of the ketone carbonyl. To further extend the scope of enantioselective additions of an allene unit we searched for electrophiles with parallel modes of association to the catalyst.

Ketones that bear an H_{BA} (H–bond acceptor) to engage the boron-based catalyst in a seven-membered cyclic two-point chelation were investigated as depicted in Scheme 4.4. Trifluoroacetophenone, whose electronegative α-fluorines may be able to stabilize

Scheme 4.4 Extending the Catalytic Enantioselective Allene Addition to Varied Classes of Electrophiles Bearing H-Bond Acceptors

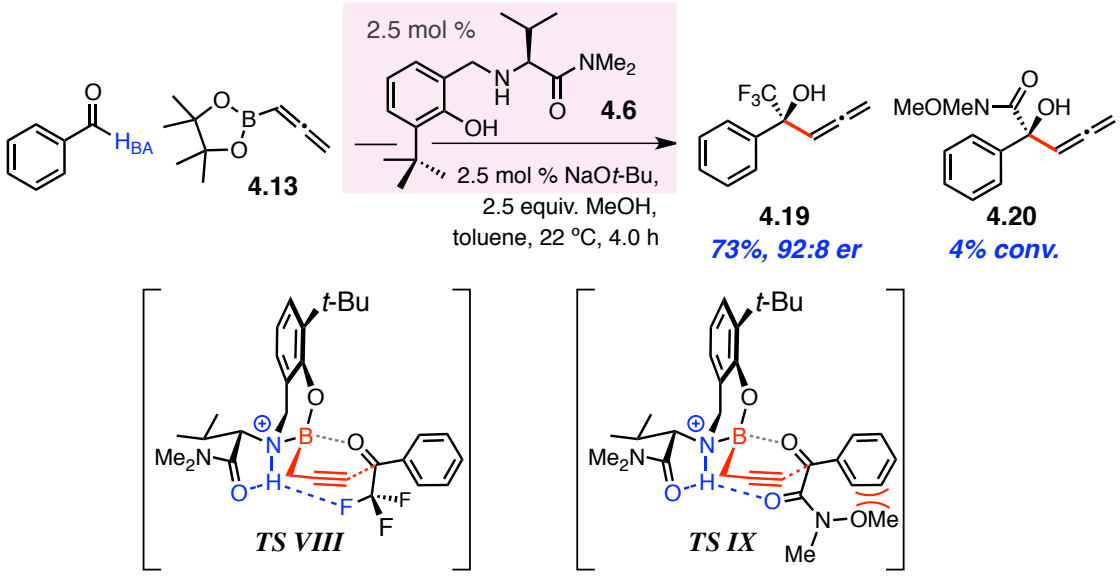

the electron deficiency of the neighboring protonated amine,[18] undergoes efficient allene addition to afford allenic carbinol **4.19** in 92:8 e.r. and 73% yield. The weak Coulombic attraction between the fluorine and the proton of the quaternized amine of the catalyst serves to sufficiently organize ***TS VIII*** and activate the ketone for allene transfer.

[18] For an in depth review on the controversy surrounding the existence of H–bonds with fluorine, see: (a) "Hydrogen Bonds with Fluorine. Studies in Solution, in Gas Phase and By Computations, Conflicting Conclusions from Crystallographic Analyses," Schneider, H-J. *Chem. Sci.* **2012**, *3*, 1381–1394. For a review that concerns the effect of fluorine substituted molecules, including their ability to H–bond, particularly as active pharmaceutical agents, see: (b) "Fluorine in Medicinal Chemistry," Purser, S.; Moore, P. R.; Swallow, S.; Gouverneur, V. *Chem. Soc. Rev.* **2008**, *37*, 320–330.

We expected additional classes of α-keto amides, besides the strained cyclic dicarbonyls of isatins, to also participate in enantioselective allene additions; these electrophilic ketones would be capable of a similar mode of association to the boron-based catalyst. However, there is only minimal conversion to Weinreb amide **4.20** (Scheme 4.4). A high energy conformer of the acyclic α-keto Weinreb amide would be required to participate in the two-point coordination to the catalyst (see ***TS IX***); such a conformation suffers both from steric clash of the ketone substituents, as well as electronic repulsion of the two adjoining carbonyls. Unlike their acyclic counterparts, isatins bear a strained five-membered ring that enforces the correct geometry of the two carbonyls, as such, the activation barrier to ***TS VII*** (Scheme 4.3) is likely considerably lower in energy to the energy required to arrive at ***TS IX***.

1.4a Enantioselective Synthesis of Allene-Substituted 3-Hydroxy-2-oxoindoles

Oxindoles (2-indolinones) are heterocyclic compounds with extraordinary potential for structural diversity and their incorporation in the structures of natural products and pharmaceutical agents is known to produce a spectrum of biological properties.[19] One of the commonly featured substitution patterns on the oxindole rings of naturally occurring molecules involves a tertiary alcohol at the 3-position; the medicinally relevant alkaloids in Figure 4.6 are representative.[20] As interest in the therapeutic potential of 3-hydroxyl oxindoles continues to intensify, the discovery of

[19] For reviews detailing the significance of natural products bearing a 3,3'-disubstituted oxindole moiety, see: (a) "Construction of Spiro[pyrrolidines-3,3'-oxindoles] – Recent Applications to the Synthesis of Oxindole Alkaloids," Marti, C.; Carreira, E. M. *Eur. J. Org. Chem.* **2003**, 2209–2219. (b) "Catalytic Asymmetric Synthesis of Oxindoles Bearing a Tetrasubstituted Stereocenter at the C-3 Position," Zhou, F.; Liu, Y-L.; Zhou, J. *Adv. Synth. Catal.* **2010**, *352*, 1381–1407.

[20] "3-Substituted-3-hydroxy-2-oxindole, an Emerging New Scaffold for Drug Discovery with Potential Anti-Cancer and Other Biological Activities, Peddibholtla, S. *Curr. Bioact. Cmpd.* **2009**, *5*, 20–38 and references cited therein for their isolation and bioactivities.

Figure 4.6 Biologically Relevant Molecules Bearing 3-Hydroxyl-3-alkyl Substituted 2-Oxindoles

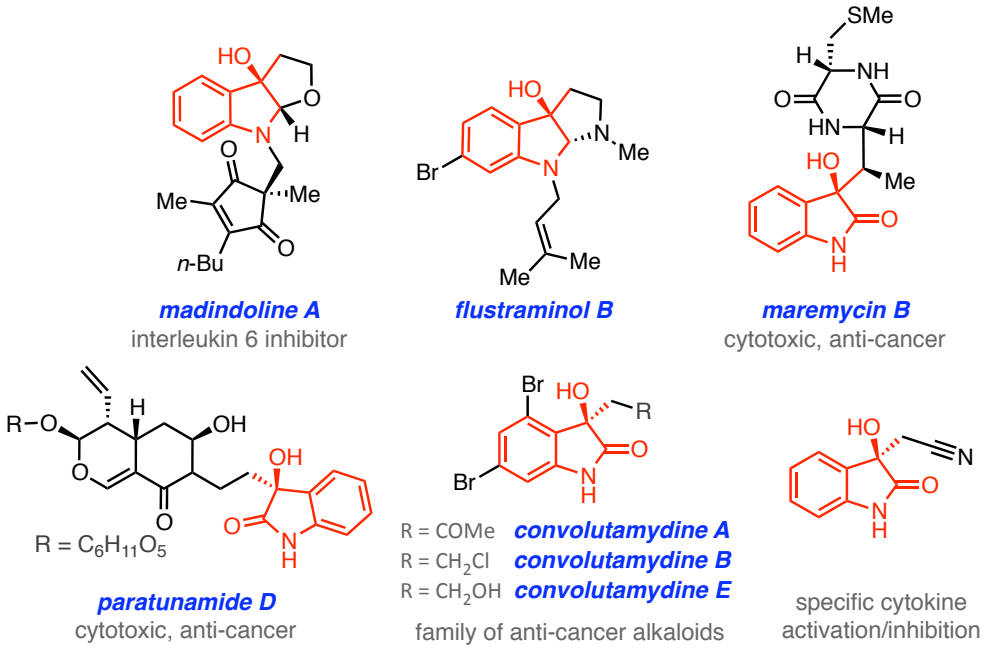

efficient synthetic methods for the preparation of the quaternary alcohol-substituted stereogenic center is of mounting significance. Although stereoselective hydroxylation of 2-oxindoles has been achieved,[21] the most widely used approach to access these structural motifs involves the enantioselective introduction of a carbon-based nucleophile to isatins (indole-2,3-diones). Catalysts that promote stereoselective 1,2-addition of enolates[22] and

[21] (a) "Catalytic Asymmetric Hydroxylation of Oxindoles by Molecular Oxygen Using a Phase-Transfer Catalyst," Sano, D.; Nagata, K.; Itoh, T. *Org. Lett.* **2008**, *10*, 1593–1595. (b) "Dimeric Quinidine-Catalyzed Enantioselective Aminooxygenation of Oxindoles: An Organocatalytic Approach to 3-Hyroxyoxindole Derivatives," Bui, T.; Candeias, N. R.; Barbas, C. F. III, *J. Am. Chem. Soc.* **2010**, *132*, 5574–5575.

[22] For enantioselective aldol additions to isatins and application to the synthesis of natural products, see: (a) "Enantioselective Synthesis of (*R*)–Convolutamydine A with New *N*-Heteroarylsulfonylprolinamides," Nakamura, S.; Hara, N.; Nakashima, H.; Kubo, K.; Shibara, N.; Toru, T. *Chem. Eur. J.* **2008**, *14*, 8079–8081. (b) "First Enantioselective Synthesis of (*R*)–Convolutamydine B and E with *N*-(Heteroarenesulfonyl) prolinamides," Hara, N.; Nakamura, S.; Shibata, N.; Toru, T. *Chem. Eur. J.* **2009**, *15*, 6790–6793. (c) "Asymmetric Aldol Reaction of Acetaldehyde and Isatin Derivatives for the Total Syntheses of *ent*-Convolutamydine E and CPC-1 and a Half Fragment of Madindoline A and B," Itoh, T.; Ishikawa, H.; Hayashi, Y. *Org. Lett.* **2009**, *11*, 3854–3857. (d) "Highly Enantioselective Aldol Reaction of Acetaldehyde and Isatins only with 4-Hydroxydiarylprolinol as Catalyst: Concise Stereoselective Synthesis of (*R*)–Convolutamydines B and E, (–)-Donaxaridine and (*R*)–Chimonamidine," Chen, W-B.; Du, X-L.; Cun, L-F.; Zhang, X-M.; Yuan, W-C. *Tetrahedron*, **2010**, *66*, 1441–1446. (e) "Direct Asymmetric Vinylogous

allyl groups,[23] or can append alkenes and arenes[24] to isatins to afford the derived tertiary alcohols have been disclosed. Although the preceding synthetic contributions have greatly advanced the breadth of 3-hydroxyl oxindoles that can be accessed, further developments are required to gain entry to the diversity of substitution patterns represented by the molecules in Figure 4.6.

The enantioselective addition of an allene unit to carbonyls is a highly desirable, yet remarkably underdeveloped strategy for the elaboration of carbon frameworks.[25] It is often the facile metallotropic rearrangement of the organometallic allenic or propargylic reagents employed that result in transformations with notoriously poor regio- and/or enantioselection.[26] The challenges regarding their synthesis notwithstanding, α-allenic carbinols have proven valuable and versatile synthetic intermediates due to the presence

---

Aldol Reaction of Allyl Ketones with Isatins: Divergent Synthesis of 3-Hydroxy-2-Oxindole Derivatives," Zhu, B.; Zhang, W.; Lee, R.; Han, Z.; Yang, W.; Tan, D.; Huang, K-W.; Jiang, Z. *Angew. Chem., Int. Ed.* **2013**, *52*, 6666–6670.

[23] (a) "Enantioselective Allylation, Crotylation, and Reverse Prenylation of Substituted Isatins: Iridium-Catalyzeed C–C Bond-Forming Transfer Hydrogenation," Itoh, J.; Han, S. B.; Krische, M. J. *Angew. Chem., Int. Ed.* **2009**, *48*, 6313–6316. (b) "Scandium(III)-Catalyzed Enantioselective Allylation of Isatins Using Allylsilanes," Hanhan, N. V.; Tang, Y. C.; Tran, N. T.; Franz, A. K. *Org. Lett.* **2012**, *14*, 2218–2221. (c) See Scheme 4.2 and reference 9 for allyl additions to isatins with the phenol **4.6** derived catalyst.

[24] For selected examples, see: (a) "Rhodium-Catalyzed Asymmetric Addition of Aryl- and Alkenylboronic Acids to Isatins," Shintani, R.; Inoue, M.; Hayashi, T. *Angew. Chem., Int. Ed.* **2006**, *45*, 3353–3356. (b) "Rhodium-Catalyzed Addition of Aryboronic Acids to Isatins: An Entry to Diversity in 3-Aryl-3-Hydroxyoxindoles," Toullec, P. Y.; Jagt, R. B. C.; de Vries, J. G.; Feringa, B. L.; Minnaard, A. J. *Org. Lett.* **2006**, *8*, 2715–2718. (c) "Enantioselective Synthesis of SM-130686 Based on the Development of Asymmetric Cu(I)F Catalysis to Access 2-Oxindoles Containing a Tetrasubstituted Carbon," Tomita, D.; Yamatsugu, K.; Kanai, M.; Shibasaki, M. *J. Am. Chem. Soc.* **2009**, *131*, 6946–6948. (d) "Catalytic Asymmetric Synthesis of Substituted 3-Hydroxy-2-Oxindoles," Hanhan, N. V.; Sahin, A. H.; Chang, T. W.; Fettinger J. C.; Franz, A. K. *Angew. Chem., Int. Ed.* **2010**, *49*, 744–747.

[25] There are no reported examples of catalytic enantioselective allene additions to ketones. For a diastereoselective method to afford the tertiary allenic carbinol, see: (a) "*B*-Allenyl- and *B*-(γ-Trimethylsilylpropargyl)-10-phenyl-9-borabicyclo[3.3.2]decanes: Asymmetric Synthesis of Propargyl and α-Allenyl 3º-Carbinols from Ketones," Hernandez, E.; Burgos, C. H.; Alicea, E.; Soderquist, J. A. *Org. Lett.* **2006**, *8*, 4089–4091. For catalytic enantioselective allene additions to aldehydes, see: (b) "Catalytic Enantioselective Allenylation Reactions of Aldehydes with Tethered Bis(8-quinolinolato) (TBOx) Chromium Complex," Xia, G.; Yamamoto, H. *J. Am. Chem. Soc.* **2007**, *129*, 496–497. (c) "Chiral Brønsted Acid Catalyzed Enantioselective Allenylation of Aldehyes," Reddy, L. R. *Chem. Commun.* **2012**, *48*, 9189–9191. (d) "Catalytic Enantioselective Addition of Allylic Organometallic Reagents to Aldehydes and Ketones," Denmark, S. E.; Fu, J. *Chem. Rev.* **2003**, *103*, 2763–2793 and references cited therein.

[26] For a discussion regarding the challenges associated with the use of allenic or propargylic organometallic reagents refer to Section 3.1 of Chapter 3.

of the reactive and orthogonal π-bonds.[27] For example, the alcohol can participate in cyclization reactions with the allene to afford substituted 2,5-dihydrofurans or furanones.[28] Moreover, the class of tertiary allenic carbinols derived from the present class of reactions can be transformed to various spircocyclic lactams through similar cyclization processes.[29] Additionally, recent investigations into the fundamental reactivity of allenes have led to the discovery of stereoselective metal-promoted additions to one of the π-bonds; arylpalladation[30] or borocupration[31] procedures are highly efficient methods for stereospecific elaboration to trisubstituted olefins or vinylborons, respectively.

The synthesis of α-allenol **4.17** depicted in Scheme 4.3 represents the first example of a catalytic enantioselective allene addition to a ketone, and, as a consequence

---

[27] For a review detailing the synthetic utility of allene-substituted molecules, particularly towards the preparation of natural products, see: "Allenes in Catalytic Asymmetric Synthesis and Natural Product Synthesis," Yu, S.; Ma. S. *Angew. Chem., Int. Ed.* **2012**, *51*, 3074–3122.

[28] For a silver-catalyzed cyclization, see: (a) "Chiral Silver Phosphate-Catalyzed Cycloisomeric Kinetic Resolution of *a*-Allenic Alcohols," Wang, Y.; Zheng, K.; Hong, R. *J. Am. Chem. Soc.* **2012**, *134*, 4096–4099. For examples of metal-catalyzed cyclocarbonylation procedures, see: (b) "Ruthenium-Catalyzed Cyclocarbonylation of Allenyl Alcohols and Amines: Selective Synthesis of Lactones and Lactams," Yoneda, E.; Zhang, S-W.; Zhou, D-Y.; Onitsuka, K.; Takahashi, S. *J. Org. Chem.* **2003**, *68*, 8571–8576. (c) "Carbometalation–Carboxylation of 2,3-Allenols with Carbon Dioxide: A Dramatic Effect of Halide Anion," Li. S.; Miao, B.; Yuan, W.; Ma, S. *Org. Lett.* **2013**, *15*, 977–979.

[29] (a) "Efficient Entry to Diversely Functionalized Spirocyclic Oxindoles from Isatins through Carbonyl-Addition/Cyclization Reaction Sequences," Alcaide, B.; Almendros, P.; Rodríguez-Acebes, R. *J. Org. Chem.* **2006**, *71*, 2346–2351. (b) "Synthesis of Spiroheterocycles by Palladium-Catalyzed Domino Cycloisomerization/Cross Coupling of α-Allenols and Baylis-Hillman Acetates," Alcaide, B.; Almendros, P.; Martínez del Campo, T.; Quirós, M. T. *Chem. Eur. J.* **2009**, *15*, 3344–3346.

[30] (a) "Total Syntheses of Enokipodins A and B Utilizing Palladium-Catalyzed Addition of an Arylboronic Acid to an Allene," Yoshia, M.; Shoji, Y.; Shishido, K. *Org. Lett.* **2009**, *11*, 1441–1443. (b) Enantioselective Formal Total Synthesis of Aplysin Utilizing a Palladium-Catalyzed Addition of an Arylboronic Acid to an Allenic Alcohol–Eschenmoser/Claisen Rearrangement," Yoshida, M.; Shoji, Y.; Shishido, K. *Tetrahedron*, **2010**, *66*, 5053–5058.

[31] In the case of borocupration of allenes, a 2-boron substituted allylcopper is generated which can *in situ* react with a proton, to afford the vinylborons, or, with carbonyls as electrophiles, to yield elaborated homoallylic alcohols. For details, see: (a) "Site- and Enantioselective Formation of Allene-Bearing Tertiary or Quaternary Carbon Stereogenic Centers through NHC–Cu-catalyzed Allylic Substitution," Jung, B.; Hoveyda, A. H. *J. Am. Chem. Soc.* **2012**, *134*, 1490–1493. (b) "NHC–Cu-Catalyzed Protoboration of Monosubstituted Allenes. Ligand-Controlled Site Selectivity, Application to Synthesis and Mechanism," Meng, F.; Jung, B.; Haeffner, F.; Hoveyda, A. H. *Org. Lett.* **2013**, *15*, 1414–1417. (c) "Cu-Catlayzed Chemoselective Preparation of 2-(Pinacolato)boron-Susbstituted Allylcopper Complexes and their In Situ Site-, Diastereo-, and Enantioselective Additions to Aldehydes and Ketones," Meng, F.; Jang, H.; Jung, B.; Hoveyda, A. H. *Angew. Chem., Int. Ed.* **2013**, *52*, 5046–5051.

of the unique reactivity of the allene, can serve as an intermediate in the preparation of a range of previously inaccessible 3-hydroxyl-2-oxindoles. The levels of unprecedented efficiency and group selectivity with which the boron-based catalyst derived from aminophenol **4.6** promotes allene additions were further investigated with a series of isatin derivatives (Scheme 4.5). *N*-Benzyl protected hydroxyindoles **4.17** and **4.21**–**4.23** can be prepared in >98:2 e.r. and in 88–>98% isolated yield within an hour with 1 mol %

Scheme 4.5 Isatin Derivatives that Participate in Highly Efficient and Stereoselective Allene Additions

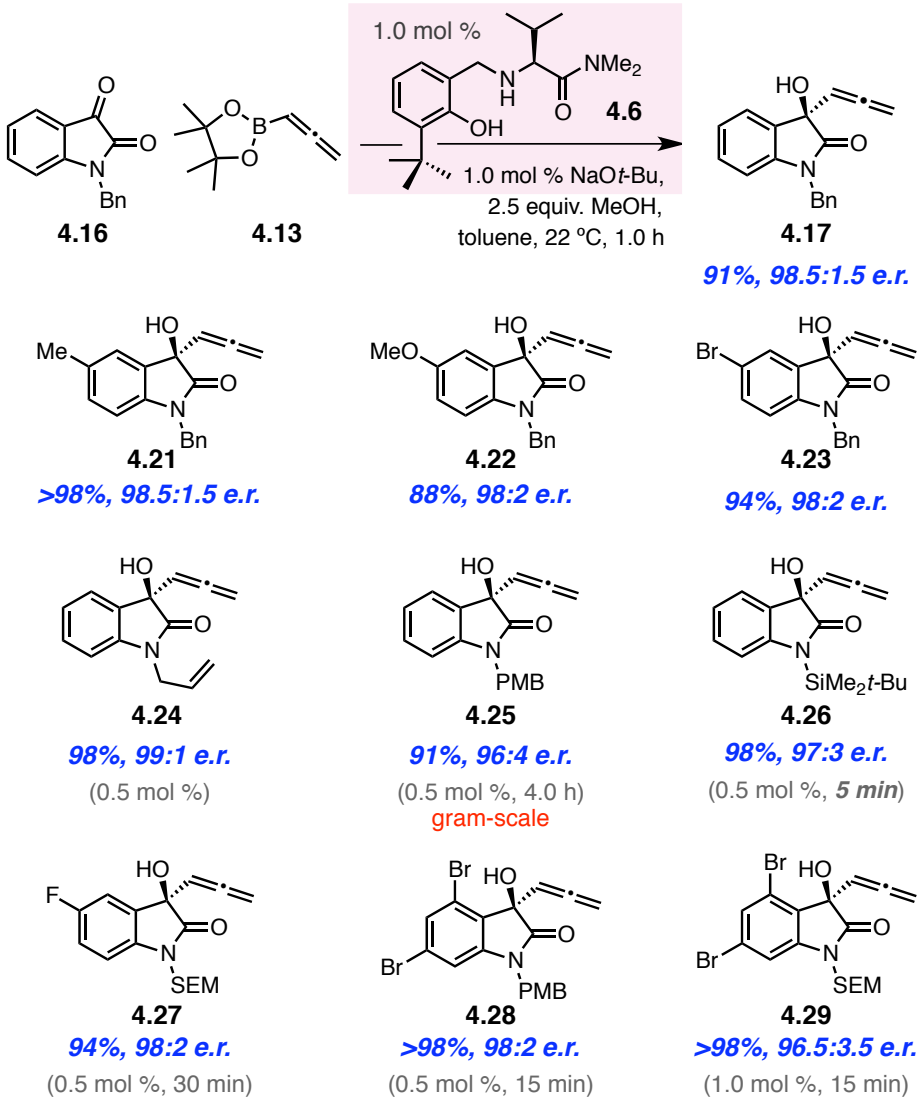

catalyst precursor. Electronic or steric modifications to the aryl ring of the indole, probed through the incorporation of substitution at the 5-position, did not have any effect on the catalytic process. A variety of *N*-protected isatin derivatives provide highly efficient transformations, such that allyl, *para*-methoxybenzyl, *tert*-butyldimethylsilyl, and trimethylsilylethoxymethyl containing allenic carbinols **4.24**–**4.27** are obtained in >96:4 e.r. and 91–98% yield. Although the nature of the protecting group on the amide does not significantly affect enantioselectivity, there is a notable influence on the rate of the allene addition process. The rate of reaction decreases in the order of isatins bearing *tert*-butyldimethylsilyl > trimethylsilylethoxymethyl > allyl > benzyl > and *para*-methoxybenzyl groups. The two important features that can lead to rate acceleration are the combined Lewis basicity of the two carbonyls of the dione. If the ketone oxygen is more Lewis basic, coordination to the boron center can be facilitated. Meanwhile, a more pronounced electrostatic interaction between the amide carbonyl and the proton in the catalyst structure results in increased activation of the ketone undergoing reaction.

The convolutamydines (Figure 4.6) are a related series of naturally-occurring alkaloids isolated from the Floridian marine bryozoan *Amathia convoluta*.[32] The 3-hydroxyl oxindole core of the natural products features a 4,6-dibrominated aryl ring. We postulated that access to the derived allene-substituted tertiary alcohols would provide a viable synthetic route to the bioactive targets and derivatives thereof. Although *N*-protected allene substituted hydroxyindoles **4.28** and **4.29** can readily be obtained in 98:2 and 96.5:3.5 e.r., respectively (Scheme 4.5), reaction of the unprotected 4,6-

[32] (a) "Convolutamydine A, a Novel Bioactive Hydroxyindole Alkaloid from Marine Bryozoan *Amathia convoluta*," Kamano, Y.; Zhang, H-p.; Ichihara, Y.; Kizu, H.; Komiyama, K.; Pettit, G. R. *Tetrahedron Lett*. **1995**, *36*, 2783–2784. (b) "Isolation and Structure of Convolutamydines B–D from Marine Bryozoan *Amathia convoluta*," Zhang, H-p.; Kamano, Y.; Ichihara, Y.; Kizu, H.; Komiyama, K.; Itokawa, H.; Pettit, G. R. *Tetrahedron* **1995**, *51*, 5523–5528.

dibromoisatin is sluggish (50% conversion in 24 hours) and provides a 1:1 mixture of the allenyl and propargyl adducts. Protection of the amide is likely required to ensure solubility of the dicarbonyl substrates in toluene. Furthermore, the acidity of the indole proton[33] can be detrimental to the proposed critical intermediates along the catalytic cycle; too acidic of a reaction medium would likely disfavor the formation of complexes whose interactions are electrostatic in nature.

Synthesis of convolutamydine A can be achieved from dibromoindoles **4.28** or **4.29** through a hydroboration/oxidation sequence of the allene to afford the *β*-hydroxy ketone,[34] followed by deprotection of the cyclic amide. However, the presence of a sensitive tertiary allylic and benzylic alcohol in the indole products prompted an initial study into the chemoselective deprotection of the amide group. All attempts, under acidic or oxidative conditions, to remove the *para*-methoxybenzyl group from **4.28** resulted only in complete decomposition. Alternative protecting group strategies were subsequently evaluated. Silylethoxymethyl (SEM) ethers or hemiaminals are known to undergo cleavage under mildly Lewis acidic conditions.[35] As demonstrated in equation 4, treatment of SEM-contaning allenic carbinol **4.27** with six equivalents of magnesium bromide ethyl etherate for 18 hours efficiently affords hydroxyindole **4.30** in 91% yield.

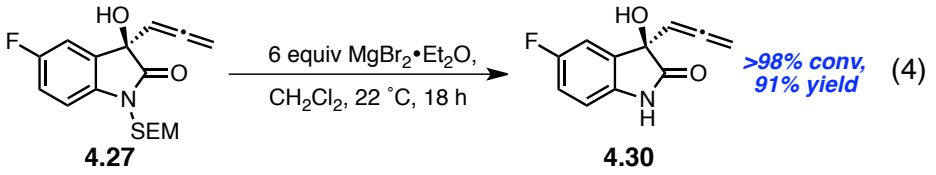

4.27 **4.30** (4)

[33] The pK_a is calculated to be 7.8 for 4,6-dibromoisatin while isatin itself is calculated to be 3 orders of magnitude less acidic at 10.3.

[34] Regioselective borocupration of the allene catalyzed by an NHC–Cu complex, followed by *in situ* protodemetallation affords a vinyl boron species, which, upon oxidation, affords the methyl ketone. For details see references 31a and b.

[35] "Novel Deprotection of SEM Ethers: A Very Mild and Selective Method Using Magnesium Bromide," Vakalopoulos, A.; Hoffmann, H. M. R. *Org. Lett.* **2000**, *2*, 1447–1450.

Scheme 4.6 Application of Enantioselective Allyl Additions to Isatins Towards the Synthesis of Bioactive Alkaloids

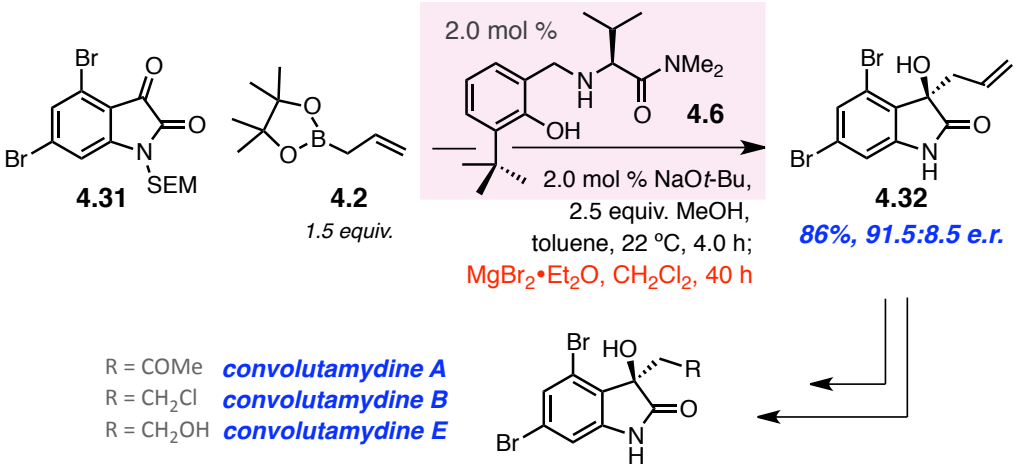

This approach was subsequently employed in the allylation/deprotection sequence of 4,6-dibromoisatin **4.31** to deliver the allyl-substituted oxindole **4.32** in 86% overall yield and 91.5:8.5 e.r. (Scheme 4.6). The allyl unit of hydroxyindole **4.32** can be converted to the *β*-hydroxy methyl ketone of convolutamydine A through a Wacker oxidation, an analogous strategy to the proposed synthesis from allene-containing **4.29**. Additionally, tertiary homoallylic alcohol **4.32** can serve as an intermediate for the syntheses of both convolutamydine B and E as well.

Manners in which to affect chemoselective removal of the *N*-protecting groups on the 3-hydroxyl-3-allenyl oxindoles, particularly in the presence of their unprotected allylic and benzylic tertiary alcohols, remained a significant challenge. Further studies focused on the identification of groups that could be appended to the cyclic amide to promote facile enantioselective additions, yet employed mild deprotection strategies to reveal the oxindole ring. An optimal protection strategy was discovered in the preparation of *N*-silyl amides, such as *tert*-butyldimethylsilyl-containing **4.33**. The weak N–Si bond can be readily cleaved with a mild acidic aqueous solution (1.0 M HCl), such that the

protonated oxindole is afforded quantitatively after two hours. The equation in Scheme 4.7 is illustrative to the features afforded by the silyl group: 1) A gram of silyl-containing isatin **4.33** can be converted to allenic carbinol in a matter of minutes in the presence

Scheme 4.7 Isatin Derivatives that Participate in Highly Efficient and Stereoselective Allene Additions

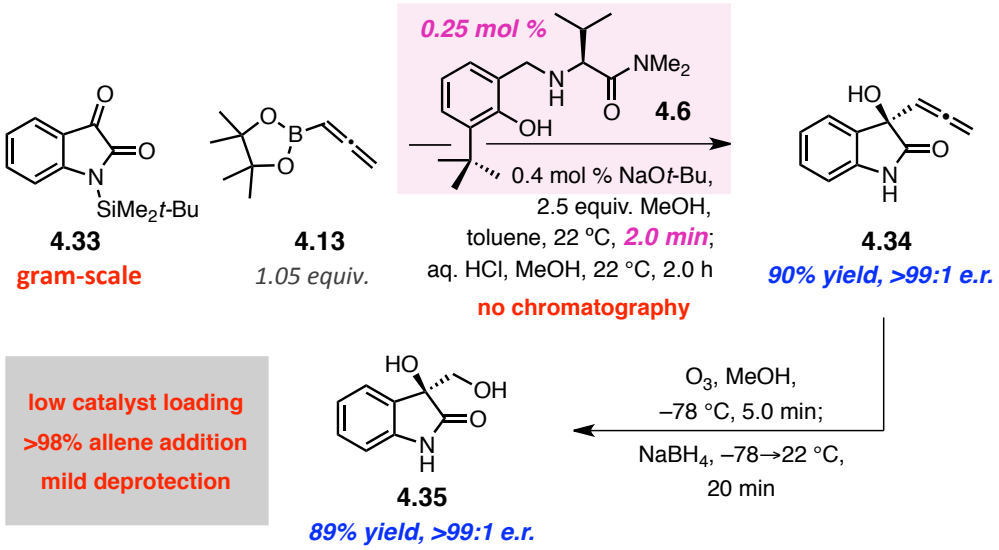

of only 0.25 mol % of the boron-based catalyst precursors. 2) The transformations are robust, scalable, procedurally simple, and are performed on benchtop with commercial-grade reagents. 3) The unpurified allenic silylated indole can be unmasked to the hydroxyindole **4.34** in a one-pot procedure in 90% overall yield and as a single enantiomer (Scheme 4.7). 4) Due to the crystallinity of the unprotected allenic carbinol **4.34**, the two-step protocol can be purified with a single recrystallization, avoiding the requirement of costly chromatographic procedures. Notably, although the silylated amide is readily protonated, it is sufficiently robust to be isolated and purified (see **4.26**, Scheme 4.5). However, this protection strategy was met with limitations; isatins bearing electron-deficient aryl rings could not be efficiently silylated. The *tert*-butyldimethylsilyl

amide derived from 4,6-dibromoisatin, carrying the requisite substitution for conversion to the convolutamydines, is protolytically unstable and cannot be isolated.

As detailed further in Scheme 4.7, the utility of the present class of allenic carbinols is demonstrated through the synthesis of 1,2-diol **4.35**. The allene moeity can be transformed to groups that are either, inaccessible or, difficult to obtain from the corresponding homoallylic alcohols. The ozonolytic cleavage/reduction sequence in Scheme 4.7 is representative; the 1,2-diol **4.35** (vs. the 1,3-diol from transformation of the allyl-containing derivative) is obtained in 89% yield. Ongoing investigations in these laboratories seek to emphasize the synthetic versatility uniquely afforded by allenyl groups, particularly in comparison to the more often-utilized allyl appendages, through application of the aforementioned protocols to the enantioselective synthesis of biologically significant molecules.

4.5 Future Studies

The catalytic enantioselective addition of allene groups presented exemplifies the first highly efficient and group selective transformation involving ketones. Further investigations were pursued to extend the scope of boron-based reagents and electrophilic partners that participate in transformations with similar efficiencies and selectivities. For example, studies to describe the enantioselective synthesis of various classes of α-chiral allenic amines and alcohols are ongoing.[36] Additionally, the capacity for the discovered boron-based catalysts to promote C–C bond formation of diverse "allylic" boron-containing molecules was explored. Introduction of propargylic borolane **4.36** is

[36] My colleagues Mr. Hao Wu and Dr. Daniel Robbins have been instrumental in the identification of new classes of electrophiles that bear a secondary Lewis basic site in order to engage in highly stereoselective allene additions.

exemplary; in the presence of 2.5 mol % aminophenol catalyst precursor, trifluoroacetophenone and *N*-benzyl isatin react to afford the derived tertiary homopropargylic alcohols with complete α-selectivity and >73% yield within four hours at ambient temperature (Scheme 4.8). Trifluorinated alcohol **4.37** is obtained in 73%

Scheme 4.8 Isatin Derivatives that Participate in Highly Efficient and Stereoselective Allene Additions

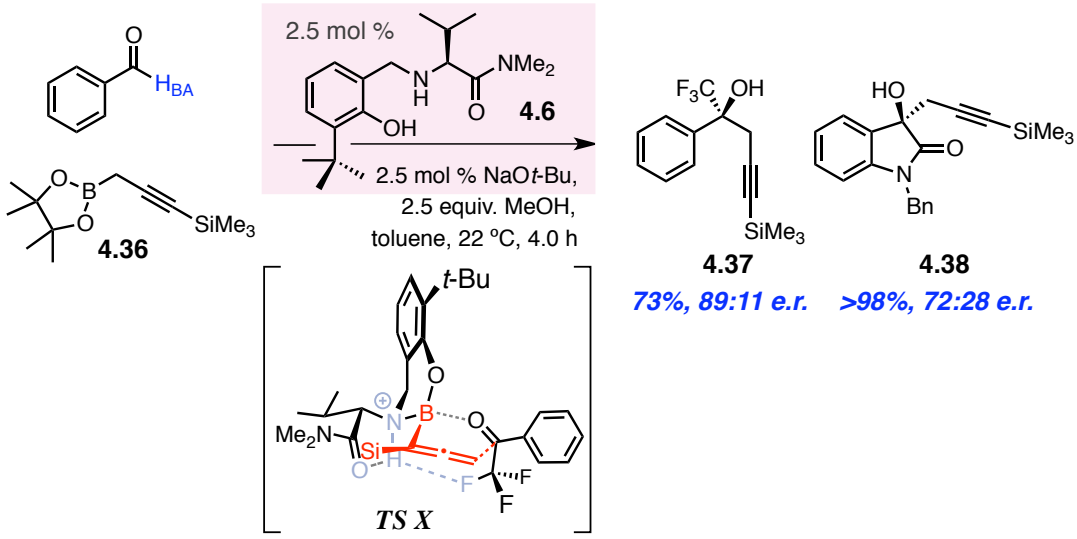

yield and 89:11 e.r. and alkylation likely proceeds through transition state ***TS X***. A similar mode of coordination of the fluorinated ketone to the boron-based catalyst to that proposed for allene addition of trifluoroacetophenone (***TS VIII***, Scheme 4.4) is likely operative. The α-fluorine atoms have an electrostatic attraction to the δ^+ charge on the proton of the catalyst engendering a seven-membered ring chelate. Substrate coordination to the chiral trimethylsilyl-substituted allenylboron leads to a distorted six-membered ring transition state for C–C bond formation. Although propargyl transfer through ***TS X*** remains relatively enantioselective (compared to 92:8 e.r. for corresponging allene adduct **4.19**, Scheme 4.4), the selectivity observed for the transformation with *N*-benzyl isatin is severly diminished (72:28 e.r. vs. 98.5:1.5 e.r. for allenic **4.17**). Whereas ***TS VII*** for

allene addition to isatins in Scheme 4.3 represents the lowest energy configuration for productive C–C bond formation, the silylated allenylboron intermediate can react with isatin through at least two energetically competitive pathways. Nevertheless, the propargyl additions depicted in Scheme 4.8 signify the ability of the boron-based catalyst to operate with alternative alkyl groups on boron.

4.6 Conclusions

The acknowledged shortcomings of the copper-based catalysts, designed and developed for enantioselective additions to aldimines and carbonyls described in Chapter 2, guided the effort for the identification of a metal-free catalyst with the capacity to activate the C–B bond of an allylboron for transfer. A small organic molecule derived from valine was developed and found to react with (pinacolato)organoborons *in situ* to generate highly active and selective chiral allyl and propargylboron intermediates. The derived boron-based catalysts exhibited unique mechanistic attributes, which enabled a metal-free catalytic process with turnover numbers typically reserved for metal-catalyzed processes. A proton, imbedded into the framework of the active catalyst, was deemed responsible for the high levels of reactivity. The protonated phenolic amine ligand scaffold serves to increase the Lewis acidity of the boron center, a feature which accelerates substrate coordination, facilitates allyl transfer, and lends rigidity to the transition state structure. The proton also organizes and directs substrate coordination; substrates bearing a secondary Lewis basic coordination site participate in highly stereoselective alkylations due to the advantageous Coulombic interaction in the transition state that leads to C–C bond formation. Moreover, facile product release/catalyst regeneration is induced by the intramolecularity of the requisite proton

transfer. The discovered metal-free catalyst can promote allyl additions to phosphinoyl aldimines and isatins with <5 mol % catalyst loading within four hours at ambient temperature. The transformations are characteristically completely α-selective, and highly diastereo- and enantioselective.

The development of catalytic additions of allenyl units was undertaken to highlight the distinct advantages of a uniquely α-selective catalyst. Methods for the enantioselective synthesis of allenic carbinols, the first of their kind, were demonstrated. The 3-allenyl-3-hydroxyl oxindoles, produced in >94% yield and >96:4 e.r., are synthetically versatile small molecules, which can be used in the preparation of a number of biologically relevant alkaloids bearing an oxindole core. The transformations described herein are scalable, procedurally simple, and require environmentally benign and inexpensive commercial reagents. The catalyst precursor, derived from valine, an inexpensive amino acid, can be prepared in multi-gram quantities through an uncomplicated sequence.

Further investigations are focused on the identification of new classes of both electrophiles and boron-based reagents that participate in highly efficient and enantioselective transformations. Moreover, we are designing and developing classes of catalysts that do not require electrophiles equipped with secondary Lewis basic sites to preserve the excellent levels of enantioinduction.

4.7 Experimentals

General. Infrared (IR) spectra were recorded on a Bruker FT–IR alpha (ATR mode) spectrophotometer, n_{max} in cm^{-1}. Bands are characterized as broad (br), strong (s),

medium (m), and weak (w). ^{1}H NMR spectra were recorded on a Varian Unity INOVA 400 (400 MHz) spectrometer. Chemical shifts are reported in ppm from tetramethylsilane with the solvent resonance as the internal standard ($CDCl_3$: δ 7.26 ppm). Data are reported as follows: chemical shift, integration, multiplicity (s = singlet, d = doublet, t = triplet, q = quartet, sept = septet, br = broad, m = multiplet), and coupling constants (Hz). ^{13}C NMR spectra were recorded on a Varian Unity INOVA 400 (100 MHz) spectrometer with complete proton decoupling. Chemical shifts are reported in ppm with the solvent resonance as the internal standard ($CDCl_3$: δ 77.16 ppm). High-resolution mass spectrometry was performed on a JEOL AccuTOF-DART (positive mode) at the Mass Spectrometry Facility, Boston College. Enantiomer ratio (e.r.) values were determined by analytical liquid chromatography (HPLC) analysis on a Shimadzu chromatograph (Chiral Technologies Chiralcel OD (4.6 x 250 mm), Chiral Technologies Chiralcel OD-H (4.6 x 250 mm), Chiral Technologies Chiralcel OJ-H (4.6 x 250 mm), Chiral Technologies Chiralpak AD-H (4.6 x 250 mm), Chiral Technologies Chiralpak AS-H (4.6 x 250 mm)). Specific rotations were measured on a Rudolph Research Analytical Autopol IV Polarimeter.

Unless otherwise noted, all reactions were carried out with distilled and degassed solvents under an atmosphere of dry N_2 in oven- (135 °C) or flame-dried glassware with standard dry box or vacuum-line techniques. All work-up and purification procedures were carried out with reagent grade solvents (purchased from Fisher) in air. Methanol (99.99% anhydrous) and trifluoroacetphenone were purchased from Acros and used as received. Sodium *tert*-butoxide was purchased from Strem and used as received. Protected isatin substrates were prepared from the commercially available indoline-2,3-

diones using known and modified procedures.[37] The aminophenol catalyst precursor **4.6** was prepared according to the published synthetic route.[10] Allenylboronic acid pinacol ester **4.13** was purchased (or received as a gift) from Fronteir Scientific and used as received. Propargylborolane **4.36** was prepared following known procedures.[38]

▪ ***Analytical Data for Isatins*** **4.31** and **4.33**:

4,6-Dibromo-1-((2-(trimethylsilyl)ethoxy)methyl)indoline-2,3-dione (**4.31**): yellow crystalline solid, mp = 142–143 °C. IR (neat): 3077 (w), 2896 (w), 1742 (m), 1595 (s), 1562 (m), 1419 (w), 1244 (m), 1073 (s), 1024 (m), 839 (s), 733 (m), 456 (m) cm^{-1}; ^1H NMR (400 MHz, $CDCl_3$): δ 7.51 (1H, d, *J* = 1.6 Hz), 7.28 (1H, d, *J* = 1.2 Hz), 5.16 (2H, s), 3.85 (2H, m), 0.94 (2H, m), –0.01 (9H, s); ^{13}C NMR (100 MHz, $CDCl_3$): δ 179.5, 157.2, 152.2, 133.5, 131.5, 122.1, 115.3, 114.3, 70.0, 67.1, 17.9, –1.3; HRMS Calcd for $C_{14}H_{21}Br_2N_2O_3Si$ $[M + NH_4]^+$: 450.96882; Found: 450.96873.

1-(*tert*-Butyldimethylsilyl)indoline-2,3-dione (**4.33**): orange crystalline solid, mp = 123–124 °C. IR (neat): 2929 (w), 2853 (w), 1731 (s), 1603 (m), 1589 (m), 1463 (m), 1325 (m), 1252 (m), 1170 (m), 1139 (m), 927 (m), 835 (s), 796 (m), 752 (s), 686 (m), 466 (m), 424 (m) cm^{-1}; ^1H NMR (400 MHz, $CDCl_3$): δ 7.63–7.61 (1H, m), 7.53–7.49 (1H, m), 7.10–7.03 (2H, m), 1.02 (9H, s), 0.56 (6H, s); ^{13}C NMR (100 MHz, $CDCl_3$): δ 184.2,

---

[37] Procedure for the synthesis of benzyl-protected isatins: "Novel Mono- and Bis(spiro-2-amino-4*H*-pyrans): Alum-Catalyzed Reaction of 4-Hydroxycoumarin and Malonitrile with Isatins, Quinones, or Ninhydrin," Karimi, A. R.; Sedaghatpour, F. *Synthesis*, **2010**, *10*, 1731–1735. Similar procedures were used employing instead *para*-methoxylbenzyl chloride, *tert*-butyldimethylsilyl chloride, or trimethylsilylethoxymethyl chloride.

[38] "Preparative Synthesis via Continuous Flow of 4,4,5,5-tetramethyl-2-(3-trimethylsilyl-2-propynyl)-1,3,2-dioxaborolane: A General Propargylation Reagent," Fandrick, D. R.; Roschangar, F.; Kim, C.; Hahm, B. J.; Cha, M. H.; Kim, H. Y.; Yoo, G.; Kim, T.; Reeves, J. T.; Song, J. J.; Tan, Z.; Qu, B.; Haddad, N.; Shen, S.; Grinberg, N.; Lee, H.; Yee, N.; Senanayake, C. H. *Org. Proc. Res. Dev.* **2012**, 16, 1131–1140.

164.9, 155.4, 138.3, 125.6, 123.4, 120.0, 115.1, 26.4, 19.7, –3.3; HRMS Calcd for $C_{14}H_{20}NO_2Si$ $[M + H]^+$: 262.12633; Found: 262.12608.

▪ **Representative Procedure for Aminophenol-Catalyzed Enantioselective Allene Group Additions to Isatins:** An oven-dried vial equipped with a stir bar was charged with aminophenol **4.6** (6.1 mg, 20 μmol) and NaO*t*-Bu (1.9 mg, 20. μmol) on benchtop. The vial was sealed with a septum and Teflon tape and purged with N_2. Anhydrous toluene (2.0 mL) was added and the mixture was allowed to stir for 10 min under N_2 at 22 °C. A separate oven-dried vial equipped with a stir bar was charged with isatin **4.16** (53.4 mg, 0.200 mmol). The vial was sealed with a septum and Teflon tape and purged with N_2. Toluene (600. μL) and MeOH (8.1 μL, 0.20 mmol) were then transferred by syringe to the vial containing isatin **4.16**. An appropriate portion of the stock solution of catalyst (100. μL) was transferred to the vial. Allenyl boron **4.13** (50.0 μL, 0.140 mmol) was added by syringe and the mixture was allowed to stir at 22 °C until the solution became colorless indicating complete consumption of the highly pigmented isatin. The reaction mixture was diluted with AcOEt and passed through a short column of silica gel. The unpurified residue obtained as a pale yellow oil was purified by silica gel chromatography (a gradient from 100% CH_2Cl_2 to 1:1 Et_2O:CH_2Cl_2 to 100 % Et_2O) to yield 56.0 mg (0.182 mmol, 91% yield) of pure **4.17** as a white crystalline solid in 98.5:1.5 e.r..

▪ ***Analytical Data for Allenic Carbinols*** **4.17**, **4.19**, and **4.21**–**4.29**:

(*R*)–1-Benzyl-3-hydroxy-3-(propa-1,2-dien-1-yl)indolin-2-one (4.17): mp = 133–134 °C.; ^{1}H NMR (400 MHz, $CDCl_3$): δ 7.43–7.41 (1H, m), 7.33–7.23 (5H, m), 7.21 (1H, dt,

J = 1.6, 7.6 Hz), 7.07 (1H, dt, J = 0.8, 7.2 Hz), 6.71 (1H, d, J = 8.0 Hz), 5.59 (1H, t, J = 6.8 Hz), 5.02–4.97 (3H, m), 4.86–4.76 (1H, m), 3.67 (1H, br s); ^{13}C NMR (100 MHz, $CDCl_3$): d 207.8, 176.7, 142.3, 135.4, 129.9, 129.6, 128.9, 127.8, 127.3, 124.9, 123.3, 109.7, 93.0, 80.2, 74.7, 44.0; HRMS Calcd for $C_{18}H_{16}NO_2$ [M + H]$^+$: 278.11810; Found: 278.11746. $[\alpha]^{25}_D$ = –21.3 (c = 1.00, $CHCl_3$) for a 97.5:2.5 e.r. sample. The enantiomeric purity of this compound was determined by HPLC analysis in comparison with authentic racemic material (Chiracel OD, 95:5 hexanes:*i*-PrOH, 0.8 mL/min, 220 nm): t_R of **4.17**: 22 min (minor) and 25 min (major).

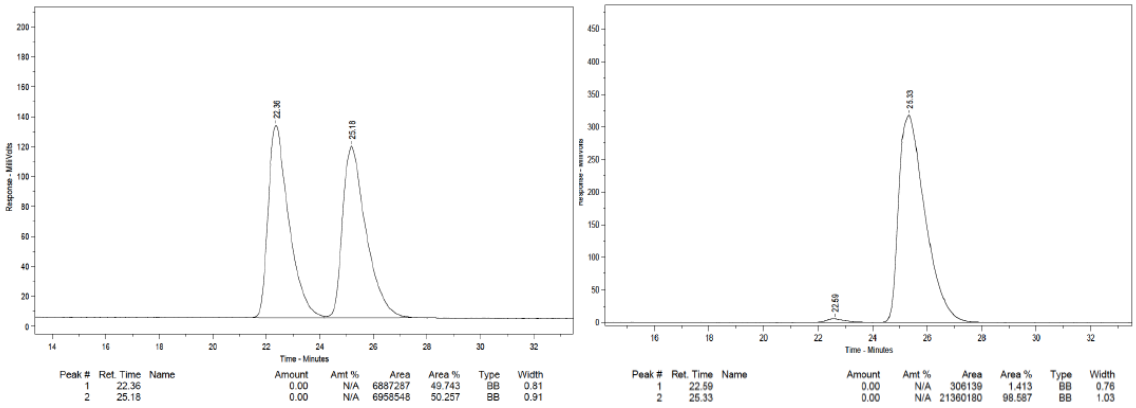

Peak #	Ret. Time	Area %	Peak #	Ret. Time	Area %
1	22.4 min	49.743	1	22.6 min	1.413
2	25.2 min	50.257	2	25.3 min	98.587

(*S*)–1,1,1-Trifluoro-2-phenylpenta-3,4-dien-2-ol (**4.19**): clear oil; ^{1}H NMR (400 MHz, $CDCl_3$): δ 7.65–7.62 (2H, m), 7.44–7.36 (3H, m), 5.86 (1H, t, J = 6.8 Hz), 5.23–5.12 (1H, m), 2.82 (1H, s). The enantiomeric purity of this compound was determined by HPLC analysis in comparison with authentic racemic material (Chirapak AS–H, 99:1 hexanes:*i*-PrOH, 0.6 mL/min, 220 nm): t_R of **4.19**: 25 min (minor) and 27 min major).

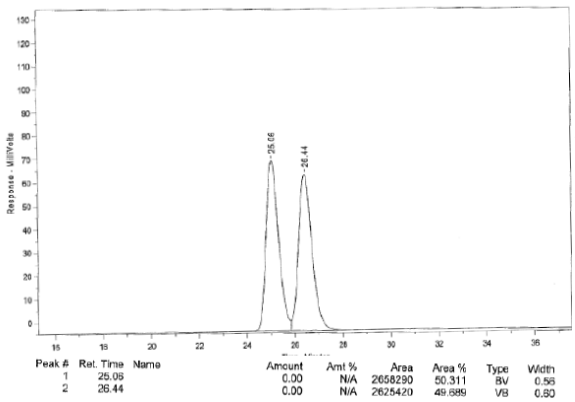

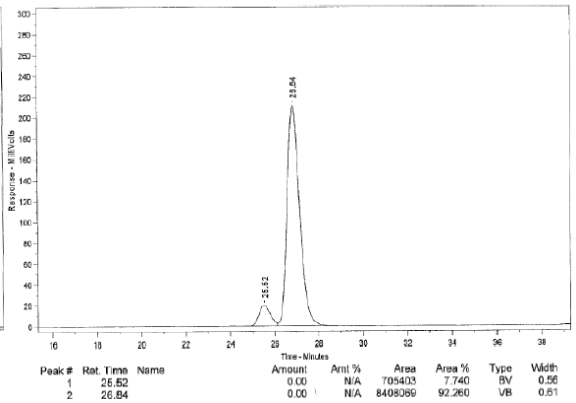

Peak #	Ret. Time	Area %	Peak #	Ret. Time	Area %
1	25.1 min	50.311	1	26.5 min	7.740
2	26.4 min	49.689	2	26.8 min	92.260

(*R*)–1-Benzyl-3-hydroxy-5-methyl-3-(propa-1,2-dien-1-yl)indolin-2-one (**4.21**): white crystalline solid, mp = 109–110 °C. IR (neat): 3368 (m, br), 1701 (s), 1604 (w), 1494 (m), 1371 (m), 1348 (m), 1154 (m), 809 (m), 698 (w) cm^{-1}; ^1H NMR (400 MHz, $CDCl_3$): δ 7.31–7.24 (6H, m), 7.01–6.99 (1H, m), 6.59 (1H, d, J = 8.0 Hz), 5.55 (1H, t, J = 6.4 Hz), 5.02–4.96 (3H, m), 4.76 (1H, d, J = 16.0 Hz), 3.39 (1H, br s), 2.31 (3H, s); ^{13}C NMR (100 MHz, $CDCl_3$): δ 207.6, 176.6, 139.9, 135.6, 133.0, 130.2, 129.6, 128.9, 127.8, 127.3, 125.5, 109.5, 93.2, 80.3, 74.8, 44.0, 21.2; HRMS Calcd for $C_{19}H_{18}NO_2$ $[M + H]^+$: 292.13375; Found: 292.13468. $[\alpha]^{25}_D$ = –32.3 (c = 1.00, $CHCl_3$) for a 99:1 e.r. sample. The enantiomeric purity of this compound was determined by HPLC analysis in comparison with authentic racemic material (Chiracel OD, 97:3 hexanes:*i*-PrOH, 0.8 mL/min, 220 nm): t_R of **4.21**: 26 min (major) and 33 min (minor), t_R of corresponding propargyl adduct: 31 min (major) and 37 min (minor).

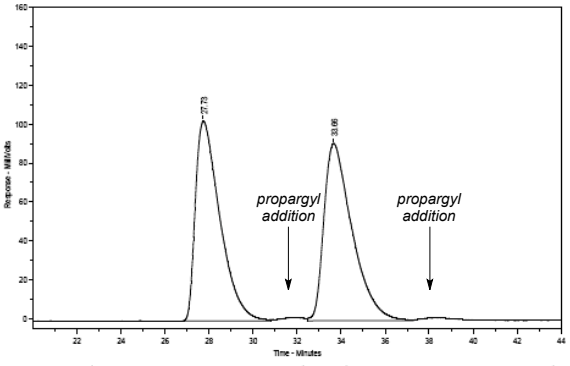

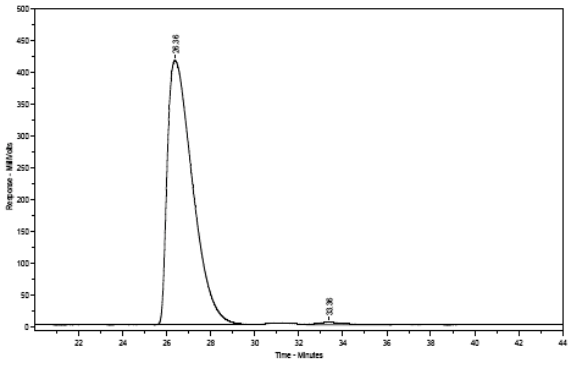

Peak #	Ret. Time	Area %	Peak #	Ret. Time	Area %
1	27.7 min	49.476	1	26.4 min	99.016
2	33.7 min	50.524	2	33.4 min	0.984

(*R*)–1-Benzyl-3-hydroxy-5-methoxy-3-(propa-1,2-dien-1-yl)indolin-2-one (**4.22**): white crystalline solid, mp = 117–119 °C. IR (neat): 3366 (m, br), 1697 (s), 1604 (w), 1490 (s), 1435 (m), 1346 (m), 1179 (m), 1017 (m), 853 (m), 730 (m), 697 (m) cm^{-1}; ^1H NMR (400 MHz, $CDCl_3$): δ 7.33–7.24 (5H, m), 7.03 (1H, d, *J* = 2.4 Hz), 6.73 (1H, dd, *J* = 8.4, 2.8 Hz), 6.60 (1H, d, *J* = 8.4 Hz), 5.55 (1H, t, *J* = 6.4 Hz), 5.02–4.95 (3H, m), 4.76 (1H, d, *J* = 16.0 Hz), 3.76 (3H, s), 3.36 (1H, br s); ^{13}C NMR (100 MHz, $CDCl_3$): δ 207.8, 176.6, 156.4, 135.5, 135.4, 130.9, 128.9, 127.8, 127.3, 114.7, 111.7, 110.3, 93.1, 80.2, 75.1, 55.9, 44.0; HRMS Calcd for $C_{19}H_{18}NO_3$ $[M + H]^+$: 308.12867; Found: 308.12935. $[\alpha]^{25}_D$ = –37.6 (*c* = 1.00, $CHCl_3$) for a 98.5:1.5 e.r. sample. The enantiomeric purity of this compound was determined by HPLC analysis in comparison with authentic racemic material (Chiracel OD, 92:8 hexanes:*i*-PrOH, 0.8 mL/min, 220 nm): t_R of **4.22**: 17 min (major) and 21 min (minor), t_R of corresponding propargyl adduct: 19 min (major) and 25 min (minor).

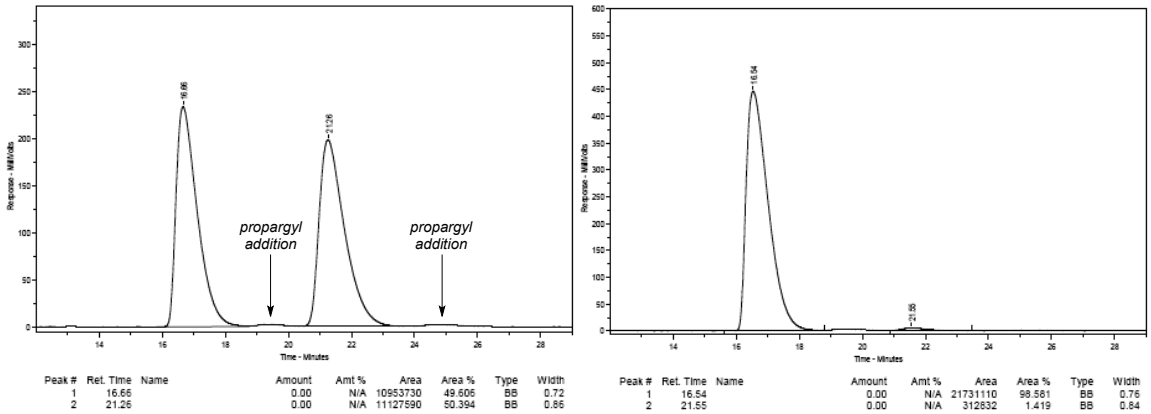

Peak #	Ret. Time	Area %	Peak #	Ret. Time	Area %
1	16.7 min	49.606	1	16.5 min	98.581
2	21.3 min	50.394	2	21.5 min	1.419

(*R*)–1-Benzyl-5-bromo-3-hydroxy-3-(propa-1,2-dien-1-yl)indolin-2-one (**4.23**): mp = 113–114 °C. IR (neat): 3371 (w, br), 1953 (w), 1705 (s), 1608 (m), 1481 (m), 1431 (m), 1344 (m), 1169 (m), 853 (w), 810 (w), 735 (w), 697 (s) cm^{-1}; ^1H NMR (400 MHz, $CDCl_3$): δ 7.52 (1H, d, J = 2.0 Hz), 7.33–7.27 (3H, m), 7.26–7.24 (2H, m), 6.57 (1H, d, J = 8.0 Hz), 5.52 (1H, t, J = 6.8 Hz), 5.04 (2H, d, J = 6.8 Hz), 4.87 (1H, ABq, $\Delta\delta_{AB}$ = 0.20, J = 15.6 Hz), 3.24 (1H, br s); ^{13}C NMR (100 MHz, $CDCl_3$): δ 207.7, 176.3, 141.2, 134.9, 132.7, 131.6, 129.0, 128.2, 128.1, 127.3, 116.1, 111.3, 92.7, 80.6, 74.7, 44.1; HRMS Calcd for $C_{18}H_{15}BrNO_2$ $[M + H]^+$: 356.02862; Found: 356.02791. $[\alpha]^{25}_D$ = –52.7 (*c* = 1.00, $CHCl_3$) for a 98:2 e.r. sample. The enantiomeric purity of this compound was determined by HPLC analysis in comparison with authentic racemic material (Chiracel OD, 92:8 hexanes:*i*-PrOH, 0.8 mL/min, 220 nm): t_R of **4.23**: 14 min (major) and 18 min (minor), t_R of corresponding propargyl adduct: 16 min (major) and 21 min (minor).

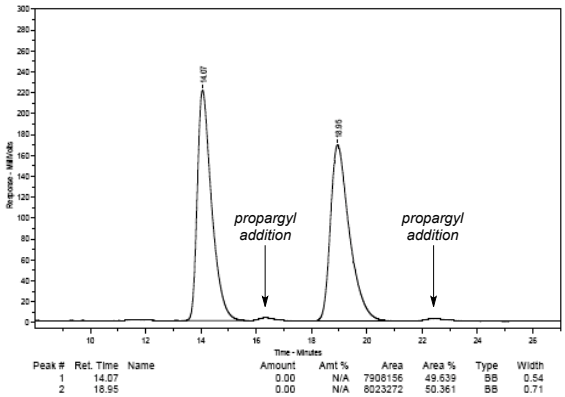

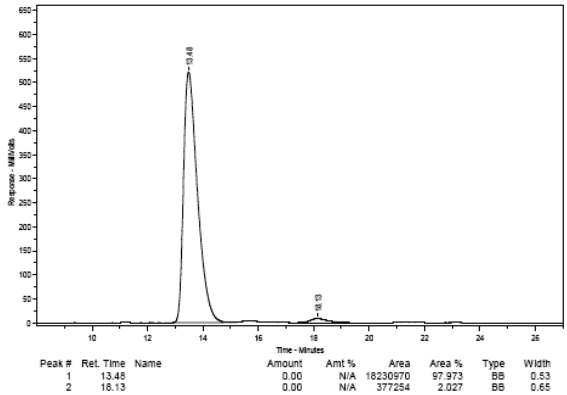

Peak #	Ret. Time	Area %
1	14.1 min	49.639
2	18.9 min	50.361

Peak #	Ret. Time	Area %
1	13.5 min	2.027
2	18.1 min	97.973

(*R*)–1-Allyl-3-hydroxy-3-(propa-1,2-dien-1-yl)indolin-2-one (**4.24**): clear oil. IR (neat): 3375 (m, br), 1955 (w), 1705 (s), 1615 (m), 1489 (m), 1468 (m), 1371 (m), 1180 (m), 1101 (m), 854 (m), 756 (m) cm^{-1}; ^1H NMR (400 MHz, $CDCl_3$): δ 7.42–7.40 (1H, m), 7.30 (1H, dt, *J* = 7.6, 1.2 Hz), 7.10 (1H, dt, *J* = 7.6, 1.2 Hz), 6.84 (1H, d, *J* = 8.0 Hz), 5.83 (1H, dddd, *J* = 17.2, 10.0, 10.0, 5.0 Hz), 5.51 (1H, t, *J* = 6.4 Hz), 5.25–5.20 (2H, m), 5.02–4.94 (2H, m), 4.39 (1H, dddd, *J* = Hz), 4.24 (1H, dddd, *J* = Hz), 3.19 (1H, br s); ^{13}C NMR (100 MHz, $CDCl_3$): δ 207.8, 176.4, 142.4, 131.1, 129.9, 129.5, 124.9, 123.2, 117.8, 109.6, 93.0, 80.2, 74.6, 42.5; HRMS Calcd for $C_{19}H_{18}NO_2$ $[M + H]^+$: 292.13375; Found: 292.13468. $[\alpha]^{25}_D$ = +11.4 (*c* = 1.00, $CHCl_3$) for a 97:3 e.r. sample. The enantiomeric purity of this compound was determined by HPLC analysis in comparison with authentic racemic material (Chiralpak AD–H, 95:5 hexanes:*i*-PrOH, 0.6 mL/min, 220 nm): t_R of **4.24**: 29 min (major) and 36 min (minor), t_R of corresponding propargyl adduct: 34 and 38 min.

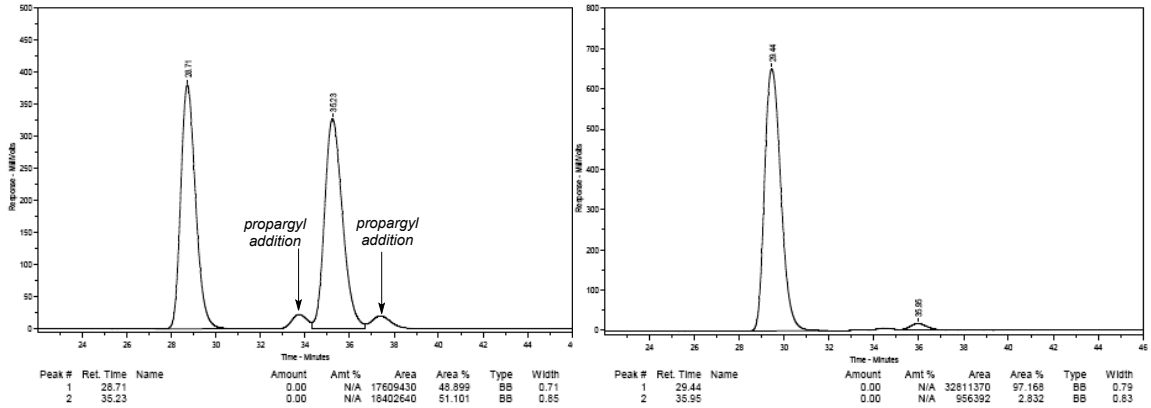

Peak #	Ret. Time	Area %	Peak #	Ret. Time	Area %
1	28.7 min	48.899	1	29.4 min	97.168
2	35.2 min	51.101	2	36.0 min	2.832

(*R*)–3-Hydroxy-1-(4-methoxybenzyl)-3-(propa-1,2-dien-1-yl)indolin-2-one (**4.25**): clear oil. IR (neat): 3367 (m, br), 1701 (s), 1612 (m), 1512 (m), 1467 (m), 1350 (m), 1246 (m), 1175 (m), 1031 (m), 810 (m), 749 (m) cm^{-1}; ^1H NMR (400 MHz, $CDCl_3$): δ 7.41–7.39 (1H, m), 7.23–7.19 (3H, m), 7.08–7.04 (1H, m), 6.85–6.81 (2H, m), 6.73 (1H, d, J = 7.6 Hz), 5.55 (1H, t, J = 6.4 Hz), 4.98 (2H, d, J = 6.8 Hz), 4.82 (1H, ABq, $\Delta\delta_{AB}$ = 0.19, J = 15.6 Hz), 3.76 (3H, s), 3.43 (1H, br s); ^{13}C NMR (100 MHz, $CDCl_3$): δ 207.8, 176.6, 159.3, 142.3, 129.9, 129.6, 128.7, 127.5, 124.8, 123.3, 114.3, 109.8, 93.0, 80.3, 74.7, 55.4, 43.5; HRMS Calcd for $C_{19}H_{18}NO_2$ $[M + H]^+$: 292.13375; Found: 292.13468. $[\alpha]^{25}_D$ = –2.92 (c = 1.00, $CHCl_3$) for a 96:4 e.r. sample. The enantiomeric purity of this compound was determined by HPLC analysis in comparison with authentic racemic material (Chiracel OD, 95:5 hexanes:*i*-PrOH, 0.8 mL/min, 220 nm): t_R of **4.25**: 31 min (minor) and 38 min (major), t_R of corresponding propargyl adduct: 36 min.

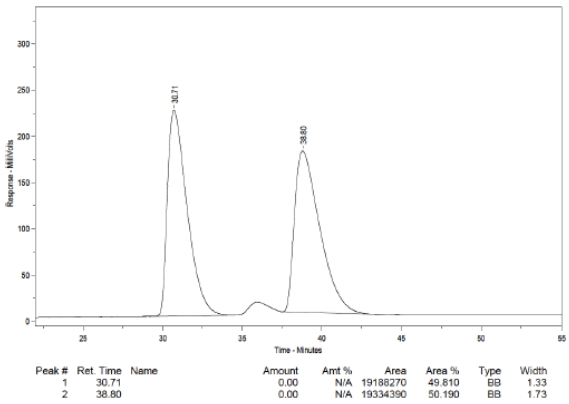

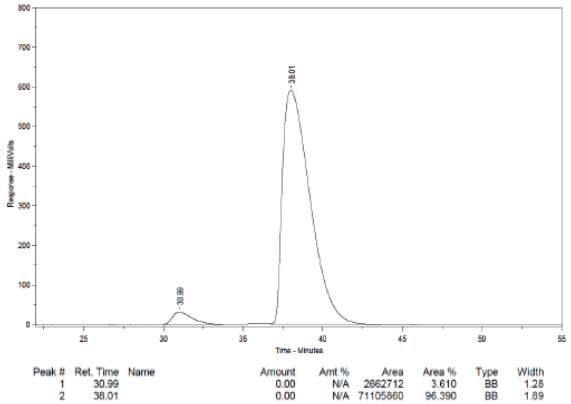

Peak #	Ret. Time	Area %	Peak #	Ret. Time	Area %
1	30.7 min	49.810	1	31.0 min	3.610
2	38.8 min	50.190	2	38.0 min	96.390

(*R*)–1-(*tert*-Butyldimethylsilyl)-3-hydroxy-3-(propa-1,2-dien-1-yl)indolin-2-one (**4.26**): pale yellow oil. IR (neat): 3398 (m, br), 2929 (w), 2858 (w), 1955 (w), 1703 (s), 1613 (m), 1464 (m), 1256 (m), 1172 (m), 1101 (m), 939 (m), 829 (s), 746 (m) cm^{-1}; ^1H NMR (400 MHz, $CDCl_3$): δ 7.38–7.36 (1H, m), 7.23–7.19 (1H, ddd, *J* = 7.6, 7.6, 1.6 Hz), 7.07–7.00 (2H, m), 5.44 (1H, t, *J* = 6.4 Hz), 4.96 (2H, d, *J* = 6.4 Hz), 3.13 (1H, br s), 1.00 (9H, s), 0.54 (3H, s), 0.52 (3H, s); ^{13}C NMR (100 MHz, $CDCl_3$): δ 207.6, 183.9, 145.6, 131.5, 129.6, 125.1, 122.7, 113.2, 93.7, 79.9, 74.9, 26.6, 19.8, –3.1, –3.2; HRMS Calcd for $C_{17}H_{24}NO_2Si$ $[M + H]^+$: 302.15763; Found: 302.15757. $[\alpha]^{25}_D$ = +25.9 (*c* = 1.00, $CHCl_3$) for a 98:2 e.r. sample. The enantiomeric purity of this compound was determined by HPLC analysis in comparison with authentic racemic material (Chiracel OD, 96:4 hexanes:*i*-PrOH, 0.6 mL/min, 220 nm): t_R of **4.26**: 10 min (minor) and 13 min (major), t_R of corresponding propargyl adduct: 12 and 18 min.

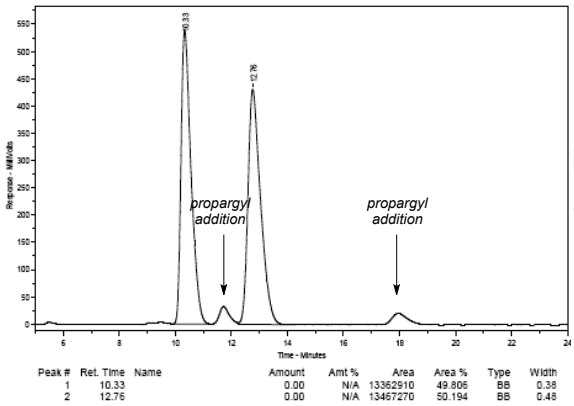

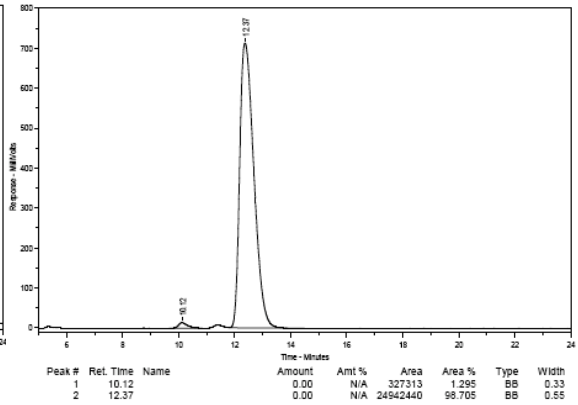

Peak #	Ret. Time	Area %	Peak #	Ret. Time	Area %
1	10.4 min	49.806	1	10.1 min	1.295
2	12.8 min	50.194	2	12.4 min	98.705

(*R*)–5-Fluoro-3-hydroxy-3-(propa-1,2-dien-1-yl)-1-((2-(trimethylsilyl)ethoxy)methyl)indolin-2-one (**4.27**): clear oil. IR (neat): 3367 (m, br), 1701 (s), 1612 (m), 1512 (m), 1467 (m), 1350 (m), 1246 (m), 1175 (m), 1031 (m), 810 (m), 749 (m) cm^{-1}; ^1H NMR (400 MHz, $CDCl_3$): δ 7.16–7.14 (1H, m), 7.06–6.98 (2H, m), 5.50 (1H, t, J = 6.4 Hz), 5.18–5.05 (2H, ABq, J = 11.2 Hz), 5.02–4.93 (2H, m), 3.57–3.52 (2H, m), 3.45 (1H, s), 0.92–0.88 (2H, s), 0.05 (9H, s); HRMS Calcd for $C_{17}H_{26}FN_2O_3Si$ $[M + NH_4]^+$: 353.16967; Found: 353.16821. The enantiomeric purity of this compound was determined by HPLC analysis in comparison with authentic racemic material (Chiralpak AD–H, 98:2 hexanes:*i*-PrOH, 0.65 mL/min, 220 nm): t_R of **4.27**: 30 min (minor) and 32 min (major), t_R of corresponding propargyl adduct: 33 and 34 min.

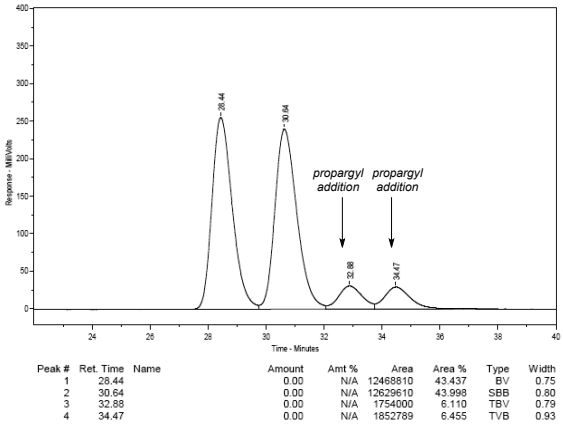

Peak #	Ret. Time	Name	Amount	Amt %	Area	Area %	Type	Width
1	28.44		0.00	N/A	12468810	43.437	BV	0.75
2	30.64		0.00	N/A	12629610	43.998	SBB	0.80
3	32.88		0.00	N/A	1754000	6.110	TBV	0.79
4	34.47		0.00	N/A	1852789	6.455	TVB	0.93

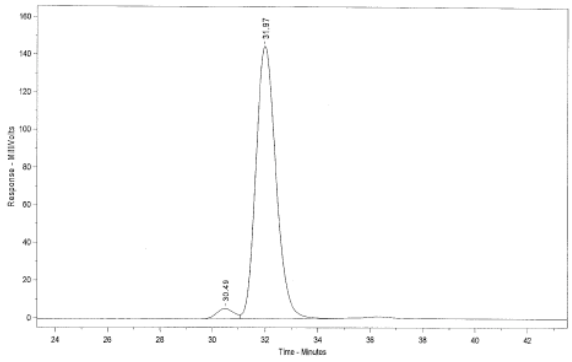

Peak #	Ret. Time	Name	Amount	Amt %	Area	Area %	Type	Width
1	30.49		0.00	N/A	252979	3.299	BV	0.76
2	31.97		0.00	N/A	7415754	96.701	VB	0.78

Peak #	Ret. Time	Area %
1	28.4 min	43.437
2	30.6 min	43.998

Peak #	Ret. Time	Area %
1	30.5 min	3.299
2	32.0 min	96.701

(*R*)–4,6-Dibromo-3-hydroxy-1-(4-methoxybenzyl)-3-(propa-1,2-dien-1-yl)indolin-2-one (**4.28**): clear oil. IR (neat): 3367 (m, br), 1701 (s), 1612 (m), 1512 (m), 1467 (m), 1350 (m), 1246 (m), 1175 (m), 1031 (m), 810 (m), 749 (m) cm^{-1}; ^{1}H NMR (400 MHz, $CDCl_3$): δ 7.41–7.39 (1H, m), 7.23–7.19 (3H, m), 7.08–7.04 (1H, m), 6.85–6.81 (2H, m), 6.73 (1H, d, J = 7.6 Hz), 5.55 (1H, t, J = 6.4 Hz), 4.98 (2H, d, J = 6.8 Hz), 4.82 (1H, ABq, $\Delta\delta_{AB}$ = 0.19, J = 15.6 Hz), 3.76 (3H, s), 3.43 (1H, br s); ^{13}C NMR (100 MHz, $CDCl_3$): δ 207.8, 176.6, 159.3, 142.3, 129.9, 129.6, 128.7, 127.5, 124.8, 123.3, 114.3, 109.8, 93.0, 80.3, 74.7, 55.4, 43.5; HRMS Calcd for $C_{19}H_{18}NO_2$ $[M + H]^+$: 292.13375; Found: 292.13468. The enantiomeric purity of this compound was determined by HPLC analysis in comparison with authentic racemic material (Chiracel OD, 95:5 hexanes:*i*-PrOH, 0.8 mL/min, 220 nm): t_R of **4.28**: 28 min (minor) and 32 min (major).

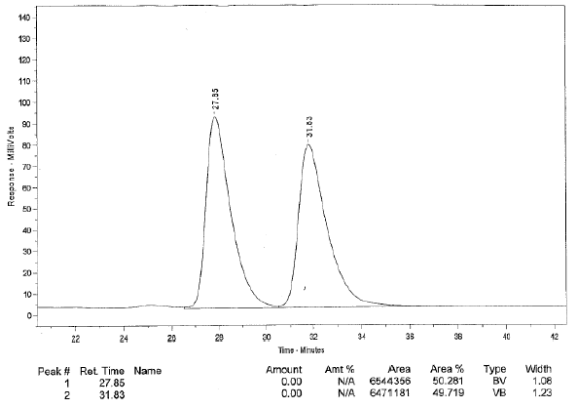

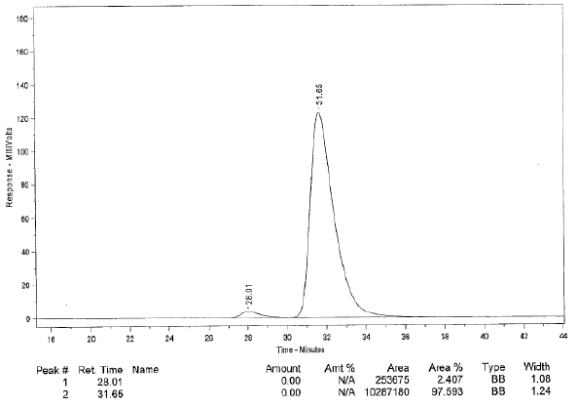

Peak #	Ret. Time	Area %
1	27.9 min	50.281
2	31.8 min	49.719

Peak #	Ret. Time	Area %
1	28.0 min	2.407
2	31.7 min	97.593

(*R*)–4,6-Dibromo-3-hydroxy-3-(propa-1,2-dien-1-yl)-1-((2-(trimethylsilyl)ethoxy)methyl)indolin-2-one (**4.29**): ^{1}H NMR (400 MHz, $CDCl_3$): δ 7.41 (1H, d, *J* = 1.6 Hz), 7.18 (1H, d, *J* = 1.6 Hz), 5.57 (1H, t, *J* = 6.4 Hz), 5.16–5.14 (1H, m), 5.06–4.98 (3H, m), 3.56–3.52 (2H, m), 3.24 (1H, br s), 0.98–0.85 (3H, m), 0.03 (9H, s); ^{13}C NMR (100 MHz, $CDCl_3$): δ 207.5, 175.4, 159.3, 144.3, 129.9, 126.8, 124.3, 120.4, 124.8, 113.0, 109.8, 90.8, 80.8, 76.2, 70.0, 66.6, 25.0, 24.7, 17.8, –1.3; HRMS Calcd for $C_{17}H_{25}Br_2N_2O_3Si$ $[M + H]^+$: 491.00012; Found: 491.00221. The enantiomeric purity of this compound was determined by HPLC analysis in comparison with authentic racemic material (Chiralpak AD–H, 96.5:3.5 hexanes:*i*-PrOH, 0.5 mL/min, 220 nm): t_R of **4.29**: 24 min (minor) and 27 min (major); t_R of corresponding propargyl adduct: 25 and 32 min.

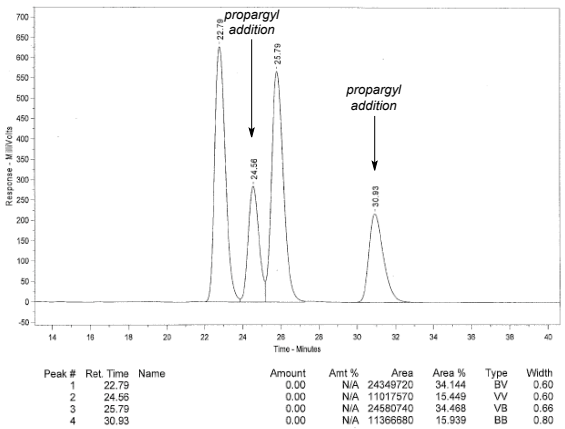

Peak #	Ret. Time	Name	Amount	Amt %	Area	Area %	Type	Width
1	22.79		0.00	N/A	24349720	34.144	BV	0.60
2	24.56		0.00	N/A	11017570	15.449	VV	0.60
3	25.79		0.00	N/A	24580740	34.468	VB	0.66
4	30.93		0.00	N/A	11366680	15.939	BB	0.80

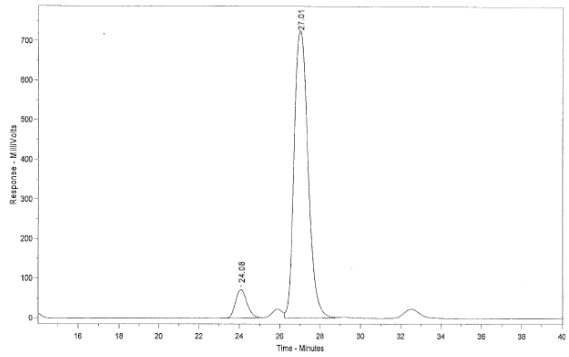

Peak #	Ret. Time	Name	Amount	Amt %	Area	Area %	Type	Width
1	24.08		0.00	N/A	2736148	7.345	BB	0.61
2	27.01		0.00	N/A	34517140	92.655	BB	0.73

Peak #	Ret. Time	Area %
1	22.8 min	34.144
2	25.8 min	34.468

Peak #	Ret. Time	Area %
1	24.1 min	7.345
2	27.0 min	92.655

■ **Representative Procedure for Aminophenol-Catalyzed Enantioselective Allene Group Additions to Isatins on Gram Scale:** An oven-dried vial equipped with a stir bar was charged with aminophenol **4.6** (11.6 mg, 38. μmol) and NaO*t*-Bu (3.6 mg, 38 μmol) on benchtop. The vial was sealed with a septum and Teflon tape and purged with N_2. Anhydrous toluene (2.0 mL) was added and the mixture was allowed to stir for 10 min under N_2 at 22 °C. A separate flame-dried 50 mL round bottom flask equipped with a stir bar was charged with *para*-methoxybenzyl-protected isatin (1.015 g, 3.800 mmol) on benchtop. The flask was sealed with a septum and Teflon tape and purged with N_2. Toluene (14.0 mL) and MeOH (307 μL, 7.60 mmol) were then transferred by syringe to the flask containing PMB-isatin. An appropriate portion of the stock solution of catalyst (1.00 mL) was transferred to the flask. Allenyl boron **4.13** (750. μL, 4.17 mmol) was added by syringe and the mixture was allowed to stir at 22 °C until the solution became colorless indicating complete consumption of the highly pigmented isatin (4.0 h). The reaction mixture was concentrated and the unpurified residue obtained as a pale yellow

oil was purified by silica gel chromatography (a gradient from 100% CH_2Cl_2 to 1:1 Et_2O:CH_2Cl_2 to 100 % Et_2O) to yield 1.056 g (3.43 mmol, 90% yield) of pure **4.25** in 96:4 e.r. and as a foamy white solid.

▪ **Procedure for One-Pot Aminophenol-Catalyzed Enantioselective Allene Group Addition/Desilylation of TBS-protected Isatin 4.33 on Gram Scale:** On benchtop, an oven-dried vial equipped with a stir bar was charged with aminophenol **4.6** (6.1 mg, 20. μmol) and NaO*t*-Bu (3.1 mg, 32 μmol). The vial was sealed with a septum and Teflon tape and purged with N_2. Anhydrous toluene (2.0 mL) was added and the mixture was allowed to stir for 10 min under N_2 at 22 °C. A separate flame-dried 50 mL round bottom flask equipped with a stir bar was charged with isatin **4.33** (1.045 g, 4.000 mmol). The flask was sealed with a septum and Teflon tape and purged with N_2. Toluene (9.0 mL) and MeOH (325 μL, 8.00 mmol) were then transferred by syringe to the flask containing TBS-protected isatin **4.33**. An appropriate portion of the stock solution of catalyst (1.00 mL) was transferred to the flask. Allenyl boron **4.13** (750. μL, 4.17 mmol) was added by syringe and the mixture was allowed to stir at 22 °C until the solution became colorless indicating complete consumption of the highly pigmented isatin (2.0 minutes). The reaction mixture was concentrated and the unpurified residue was redissolved in MeOH (20.0 mL) and treated with an aqueous 1.0 M solution of HCl (5.0 mL). The solution was allowed to stir at 22 °C until TLC analysis indicated complete consumption of the silylamide (typically 2.0 h). The solution was diluted with EtOAc (20 mL) and H_2O (20 mL) and the organic layer was separated. The aqueous layer was further washed with EtOAc (3 x 20 mL), the organic layers were combined and dried over Na_2SO_4. The volatiles were removed yielding a white solid, which was recrystallized from

EtOAc/hexanes (2 crops) to yield 675.8 mg of hydroxyindole **4.34** (3.61 mmol, 90% yield) as a white crystalline solid and as a single enantiomer.

(*R*)–3-Hydroxy-3-(propa-1,2-dien-1-yl)indolin-2-one (**4.34**): white crystalline solid, mp = 189–190 °C. IR (neat): 3316 (s, br), 1955 (w), 1691 (s), 1619 (m), 1469 (m), 1377 (m), 1355 (m), 1181 (m), 1103 (m), 1068 (m), 928 (m), 852 (m), 782 (m), 731 (m), 642 (s), 559 (m), 497 (m) cm^{-1}; ^{1}H NMR (400 MHz, CD_3OD): δ 7.33–7.31 (1H, m), 7.26–7.22 (1H, m), 7.05–7.01 (1H, m), 6.88–6.86 (1H, m), 5.51 (1H, t, J = 6.4 Hz), 4.90–4.75 (2H, m); ^{13}C NMR (100 MHz, CD_3OD): δ 209.5, 180.6, 142.5, 132.3, 130.8, 126.3, 123.7, 111.3, 93.5, 78.9, 76.3; HRMS Calcd for $C_{11}H_{10}NO_2$ $[M + H]^+$: 188.07115; Found: 188.07196. $[\alpha]^{25}_D$ = –35.2 (c = 1.00, MeOH) for a >99:1 e.r. sample. The enantiomeric purity of this compound was determined by HPLC analysis in comparison with authentic racemic material (Chiracel OD, 90:10 hexanes:*i*-PrOH, 0.6 mL/min, 220 nm): t_R of **4.34**: 21 min (minor) and 24 min (major).

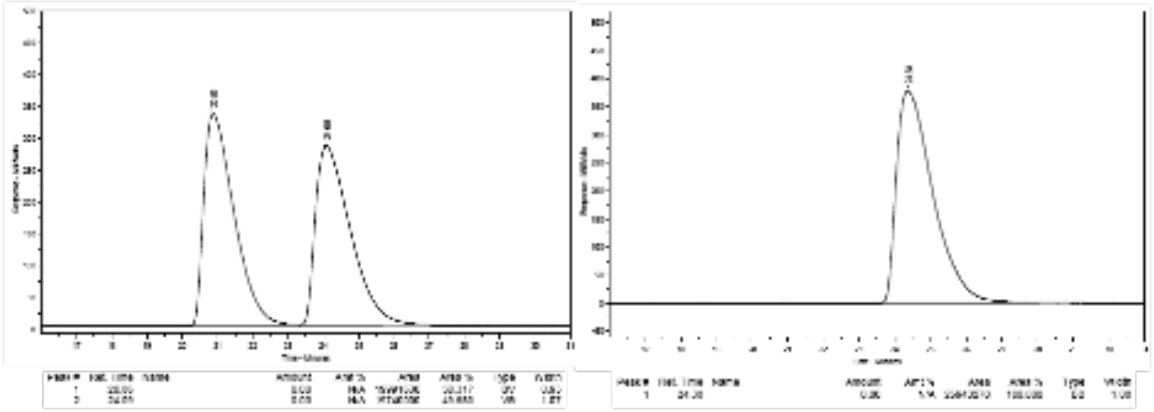

Peak #	Ret. Time	Area %	Peak #	Ret. Time	Area %
1	20.9 min	50.317	1	24.4 min	100.000
2	24.1 min	49.683			

▪ **Procedure for 2-step Conversion of Allenic Alcohol 4.34 to α–Hydroxy Alcohol 4.35:** A vial equipped with a stir bar was charged with allenyl carbinol **4.34** (37.4 mg, 0.200 mmol) to which was added enough MeOH to ensure complete dissolution of the solid (~2 mL). The solution was allowed to cool to –78 °C (acetone/dry ice bath), before a flow of O_3 (10 mL/min) was bubbled through the solution until TLC analysis indicated complete consumption of the allene (typically between 1 and 5 minutes). Upon complete oxidative cleavage, the solution was purged with O_2 before the addition of $NaBH_4$ (76.0 mg, 2.00 mmol) at –78 °C. The solution was allowed to warm to 22 °C and stir for 20 min during the reduction. A drop of acetyl chloride was added and the mixture was concentrated in vacuo. The residue was redissolved in MeOH and a drop of acetyl chloride was added and reconcentrated. This procedure was repeated twice more to ensure protonation to the diol with concomitant removal of $B(OMe)_3$. The maroon solids were purified by silica gel chromatography (gradient from 1:1 EtOAc:Et_2O to 100% EtOAc to 4:1 EtOAc:MeOH) to afford 31.8 mg of diol **4.35** (0.177 mmol, 89% yield) as a sticky pale yellow solid.

(*S*)–3-Hydroxy-3-(hydroxymethyl)indolin-2-one (**4.35**): sticky pale yellow solid. IR (neat): 3248 (s, br), 1701 (s), 1620 (m), 1470 (m), 1334 (w), 1184 (m), 1118 (m), 1052 (s), 810 (m), 749 (m), 670 (m), 489 (m) cm^{-1}; ^1H NMR (400 MHz, CD_3OD): δ 7.39 (1H, ddd, J = 7.6, 1.2, 0.8 Hz), 7.25 (1H, ddd, J = 7.6, 7.6, 1.2 Hz), 7.25 (1H, ddd, J = 7.6, 7.6, 1.2 Hz), 6.90–6.87 (1H, m), 3.81 (2H, ABq, $\Delta\delta_{AB}$ = 0.03, J = 10.8 Hz), 3.35 (1H, s); ^{13}C NMR (100 MHz, CD_3OD): δ 181.5, 143.7, 131.7, 130.7, 125.8, 123.7, 111.2, 78.1, 66.9; HRMS Calcd for $C_9H_{10}NO_3$ $[M + H]^+$: 180.06607; Found: 180.06614. $[\alpha]^{26}_D$ = +43.9 (*c* = 1.00, MeOH) for a >99:1 e.r. sample.

▪ **Representative Procedure for Aminophenol-Catalyzed Enantioselective Propargyl Group Additions:** An oven-dried vial equipped with a stir bar was charged with aminophenol **4.6** (6.1 mg, 20 μmol) and NaO*t*-Bu (1.9 mg, 20. μmol). The vial was sealed with a septum and Teflon tape and purged with N_2. Anhydrous toluene (2.0 mL) was added and the mixture was allowed to stir for 10 min under N_2 at 22 °C. A separate oven-dried vial equipped with a stir bar was charged with isatin **4.16** (53.4 mg, 0.200 mmol). The vial was sealed with a septum and Teflon tape and purged with N_2. Toluene (600. μL) and MeOH (8.1 μL, 0.20 mmol) were then transferred by syringe to the vial containing isatin **4.16**. An appropriate portion of the stock solution of catalyst (100. μL) was transferred to the vial. Propargyl borolane **4.36** (57.2 mg, 0.240 mmol) was added by syringe and the mixture was allowed to stir at 22 °C until the solution became colorless indicating complete consumption of the highly pigmented isatin. The reaction mixture was diluted with AcOEt and passed through a short column of silica gel. The unpurified residue obtained as a pale yellow oil was purified by silica gel chromatography.

▪ ***Analytical Data for Hompropargyic alcohols*** **4.37** and **4.38**:

(*S*)-1,1,1-Trifluoro-2-phenyl-5-(trimethylsilyl)pent-4-yn-2-ol (**4.37**): clear oil; ^{1}H NMR (400 MHz, $CDCl_3$): δ 7.58–7.56 (2H, m), 7.42–7.37 (3H, m), 3.19–3.02 (3H, m), 0.07 (9H, s). The enantiomeric purity of this compound was determined by HPLC analysis in comparison with authentic racemic material (Chirapak AS–H, 99:1 hexanes:*i*-PrOH, 0.6 mL/min, 220 nm): t_R of **4.37**: 25 min (minor) and 27 min major).

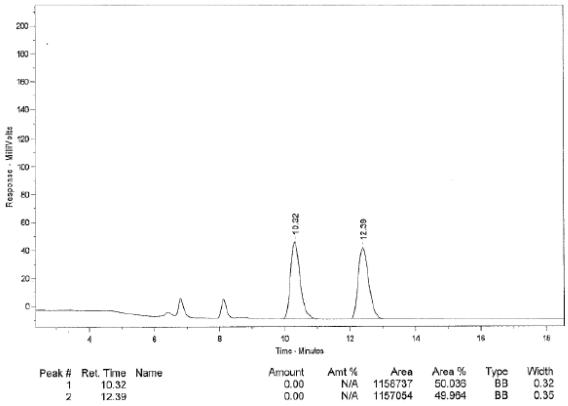

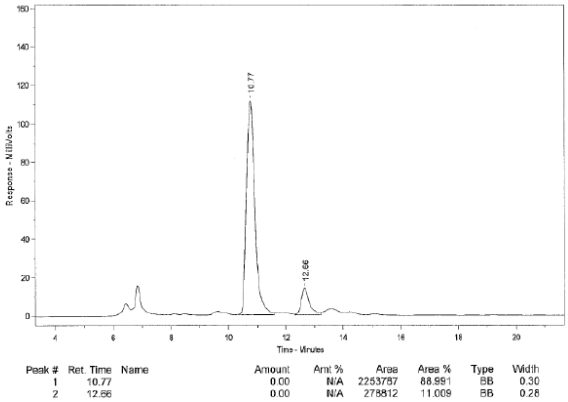

Peak #	Ret. Time	Area %	Peak #	Ret. Time	Area %
1	10.3 min	50.036	1	10.8 min	88.991
2	12.4 min	49.964	2	12.7 min	11.009

(*R*)–1-Benzyl-3-hydroxy-3-(3-(trimethylsilyl)prop-2-yn-1-yl)indolin-2-one (**4.38**): clear oil; ^{1}H NMR (400 MHz, $CDCl_3$): δ 7.56–7.54 (1H, m), 7.32–7.19 (6H, m), 7.08–7.04 (1H, m), 6.7 (1H, d, J = 8.0 Hz), 4.91–4.82 (2H, m), 3.34 (1H, br s), 3.03–2.77 (ABq, J = 16.4 Hz), 0.03 (9 H, s). The enantiomeric purity of this compound was determined by HPLC analysis in comparison with authentic racemic material (Chiralcel OD, 95:5 hexanes:*i*-PrOH, 0.8 mL/min, 220 nm): t_R of **4.38**: 12 min (minor) and 14 min (major).

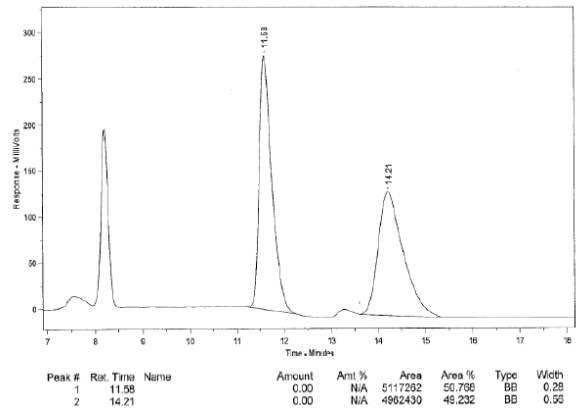

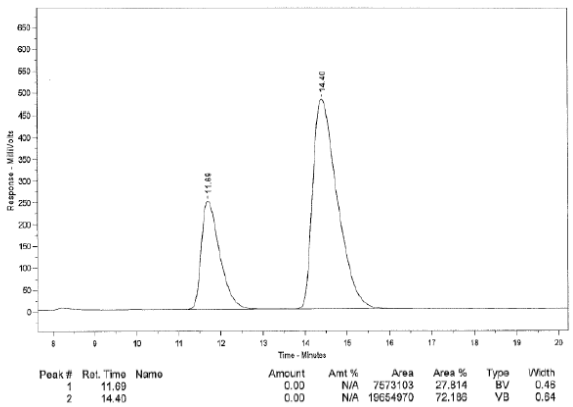

Peak #	Ret. Time	Area %	Peak #	Ret. Time	Area %
1	11.6 min	50.768	1	11.7 min	27.814
2	14.2 min	49.232	2	14.4 min	72.186

▪ **Absolute Configuration of 4.34:** ***X-ray Crystal Structure of Allenic Alcohol (R)–4.34:***

Proof of Absolute Stereochemistry: Please note that the absolute stereochemistry of the major product enantiomers are inferred from that obtained through the X-ray crystal structure of allenyl carbinol **4.34.** The enantiomeric purity of the obtained crystal was also verified by HPLC analysis in comparison with authentic racemic material (Chiracel OD, 90:10 hexanes:*i*-PrOH, 0.6 mL/min, 220 nm): t_R of **4.34**: 21 min (minor) and 24 min (major).

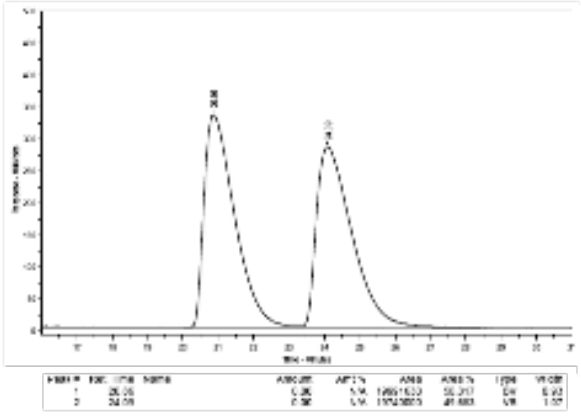

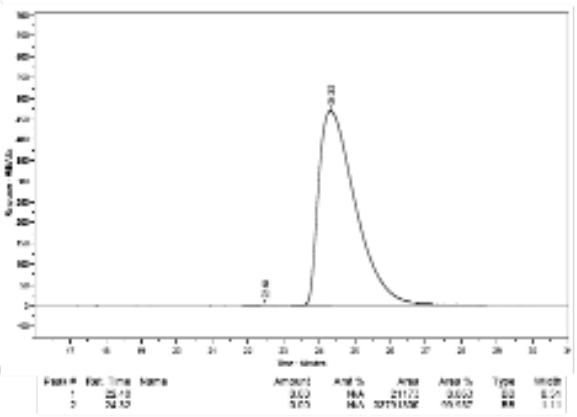

Peak #	Ret. Time	Area %
1	20.9 min	50.317
2	24.1 min	49.683

Peak #	Ret. Time	Area %
1	22.5 min	0.063
2	24.3 min	99.937

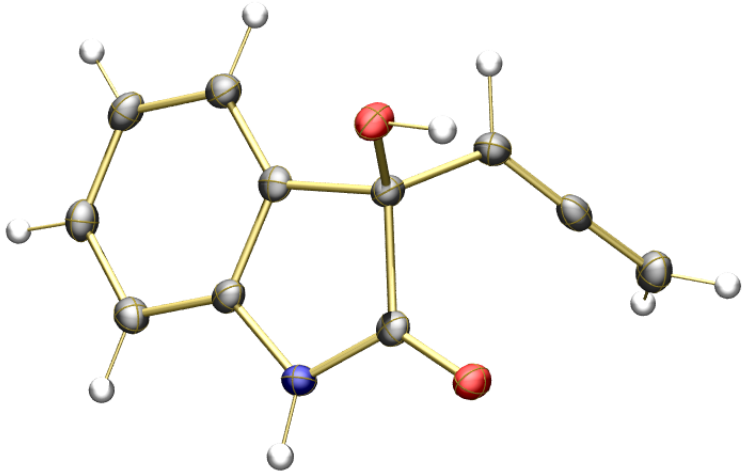

Table 1. Crystal data and structure refinement for (R)–4.34, $C_{11}H_9NO_2$

Identification code	$C_{11}H_9NO_2$	
Empirical formula	$C_{11}H_9NO_2$	
Formula weight	187.19	
Temperature	100(2) K	
Wavelength	1.54178 ≈	
Crystal system	Orthorhombic	
Space group	P2(1)2(1)2(1)	
Unit cell dimensions	a = 7.0851(7) ≈	a= 90∞.
	b = 7.1233(7) ≈	b= 90∞.
	c = 17.6028(16) ≈	g = 90∞.
Volume	888.40(15) $\approx^3$	
Z	4	
Density (calculated)	1.400 Mg/m^3	
Absorption coefficient	0.800 mm^{-1}	
F(000)	392	
Crystal size	0.15 x 0.12 x 0.06 mm^3	
Theta range for data collection	5.02 to 68.81∞.	
Index ranges	-8<=h<=8, -8<=k<=8, -21<=l<=18	

Reflections collected	10395
Independent reflections	1579 [R(int) = 0.0346]
Completeness to theta = 68.00∞	98.6 %
Absorption correction	Semi-empirical from equivalents
Max. and min. transmission	0.9536 and 0.8895
Refinement method	Full-matrix least-squares on F^2
Data / restraints / parameters	1579 / 0 / 142
Goodness-of-fit on F^2	1.088
Final R indices [I>2sigma(I)]	R1 = 0.0250, wR2 = 0.0641
R indices (all data)	R1 = 0.0260, wR2 = 0.0652
Absolute structure parameter	0.21(19)
Extinction coefficient	na
Largest diff. peak and hole	0.146 and -0.176 e.≈$^{-3}$

Table 2. Atomic coordinates (x 10^4) and equivalent isotropic displacement parameters (≈^{2}x 10^3) for $C_{11}H_9NO_2$. U(eq) is defined as one third of the trace of the orthogonalized U^{ij} tensor.

	x	y	z	U(eq)
O(1)	2374(1)	1954(1)	10038(1)	18(1)
O(2)	4912(1)	2864(1)	8733(1)	18(1)
N(1)	412(2)	1808(2)	9004(1)	16(1)
C(1)	2085(2)	1710(2)	9352(1)	15(1)
C(2)	3632(2)	1335(2)	8749(1)	15(1)
C(3)	2481(2)	1311(2)	8024(1)	15(1)
C(4)	3020(2)	1036(2)	7280(1)	18(1)
C(5)	1632(2)	1064(2)	6717(1)	20(1)
C(6)	-256(2)	1347(2)	6908(1)	20(1)

C(7)	-816(2)	1598(2)	7662(1)	19(1)
C(8)	584(2)	1576(2)	8207(1)	16(1)
C(9)	4648(2)	-509(2)	8866(1)	18(1)
C(10)	4259(2)	-1798(2)	9364(1)	18(1)
C(11)	3899(2)	-3140(2)	9842(1)	23(1)

Table 3. Selected Bond lengths [≈] and angles [∞] for $C_{11}H_9NO_2$.

O(1)-C(1)	1.2370(15)
O(2)-C(2)	1.4177(16)
C(9)-C(10)	1.299(2)
C(10)-C(11)	1.299(2)
C(11)-H(11A)	0.946(18)
C(11)-H(11B)	0.975(19)
C(10)-C(9)-C(2)	127.19(12)
C(10)-C(9)-H(9)	121.7(10)
C(11)-C(10)-C(9)	177.59(14)
C(10)-C(11)-H(11A)	120.1(11)
C(10)-C(11)-H(11B)	123.5(10)
H(11A)-C(11)-H(11B)	116.3(15)

Table 4. Hydrogen bonds for $C_{11}H_9NO_2$ [≈ and ∞].

D-H...A	d(D-H)	d(H...A)	d(D...A)	<(DHA)
O(2)-H(2O)...O(1)#1	0.858(19)	1.942(19)	2.7812(13)	165.6(17)
N(1)-H(1N)...O(1)#2	0.882(18)	2.003(18)	2.8729(15)	168.6(15)

Symmetry transformations used to generate equivalent atoms:

#1 x+1/2,-y+1/2,-z+2 #2 x-1/2,-y+1/2,-z+2

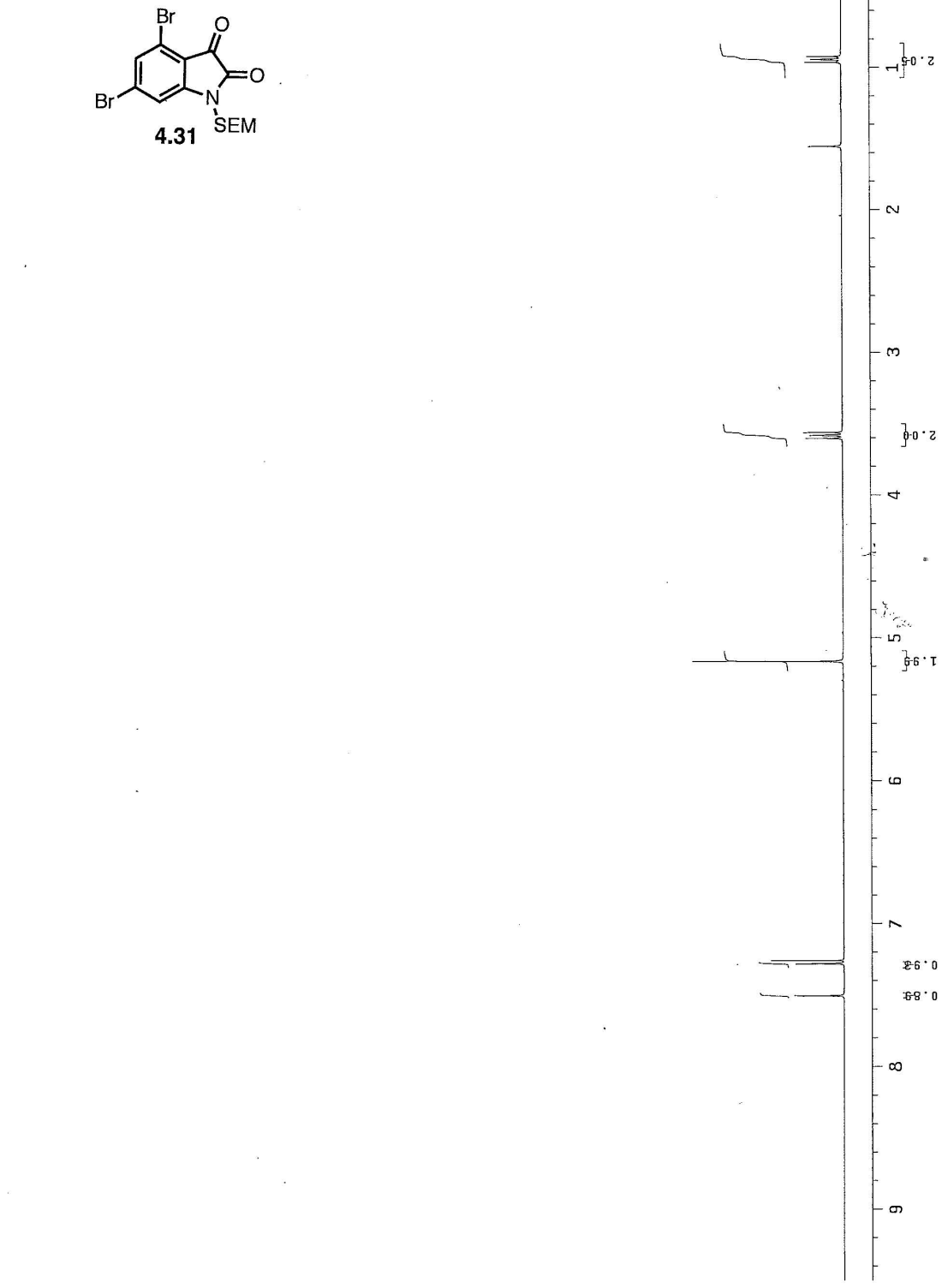
Br
O
O
Br
N
SEM
4.31
ppm
8.74
2.05
2.00
1.95
0.93
0.89

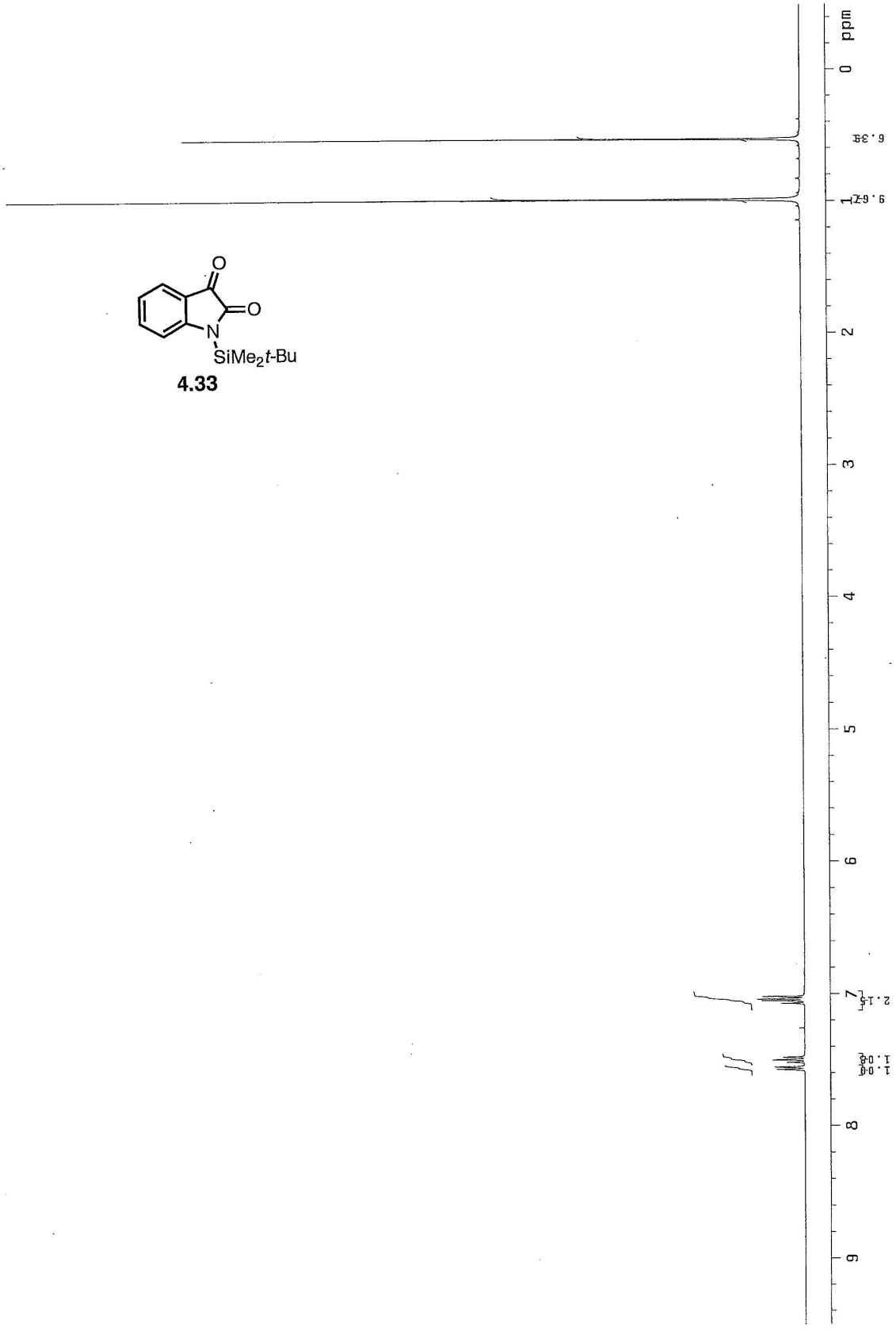

4.33

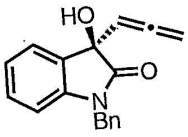

4.17

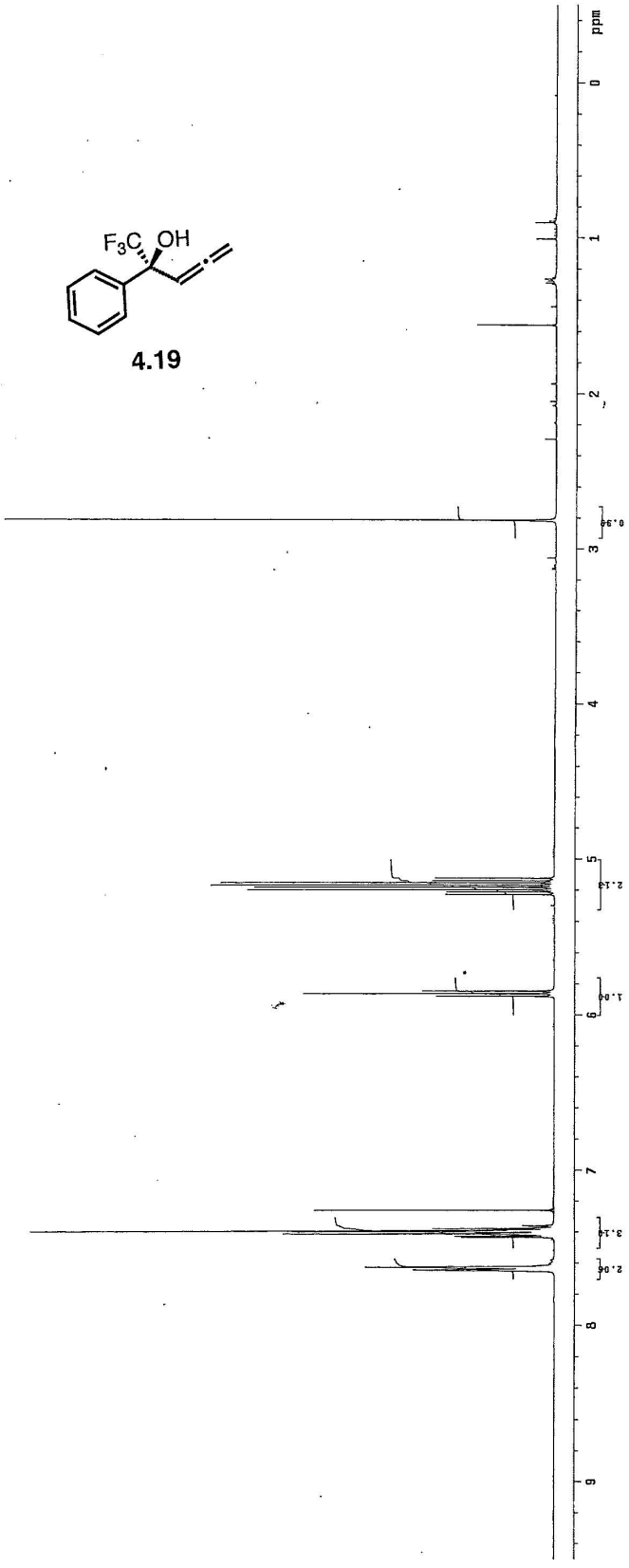

4.19

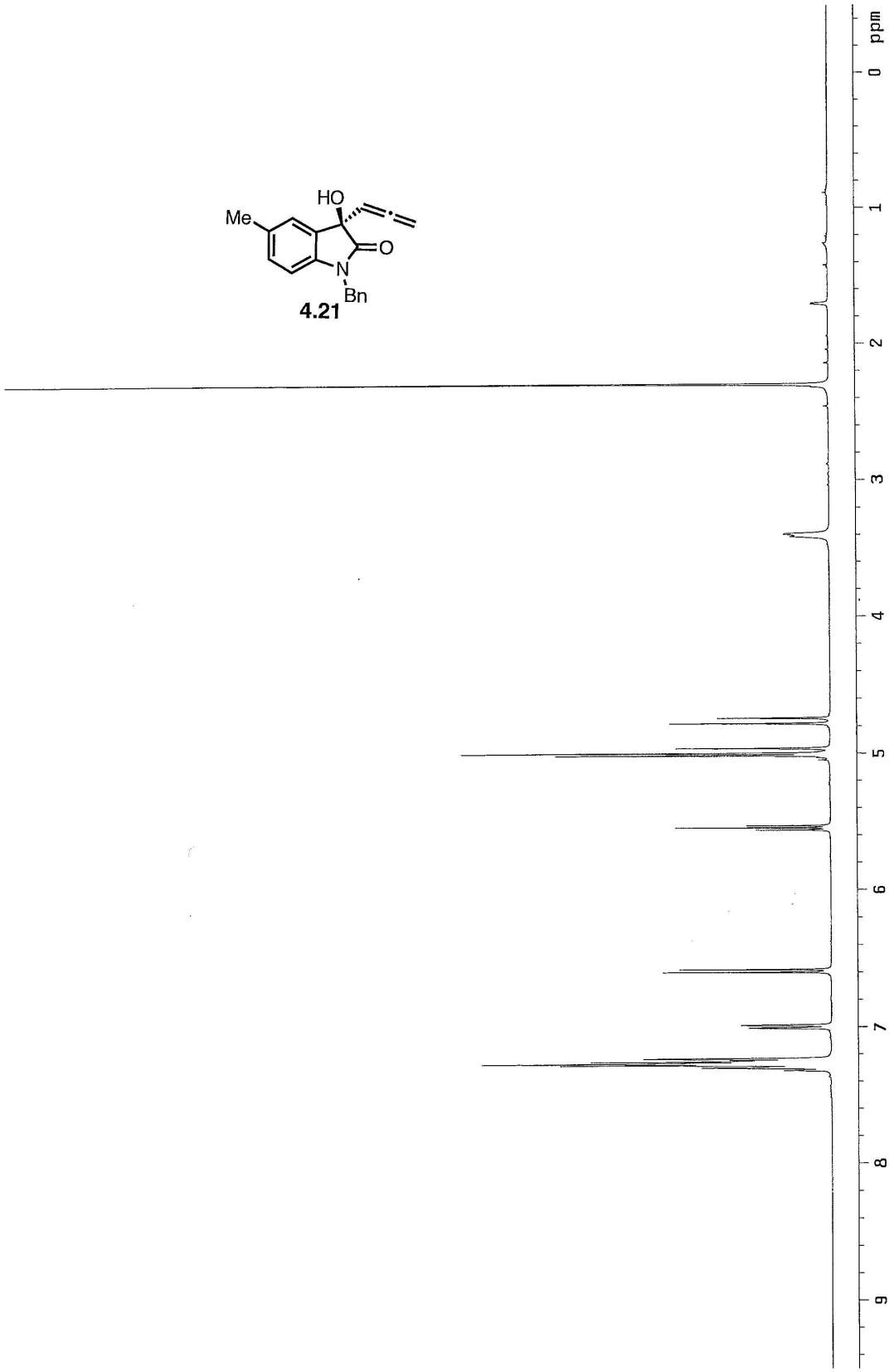
HO
Me
O
N
Bn
4.21
ppm
0
1
2
3
4
5
6
7
8
9

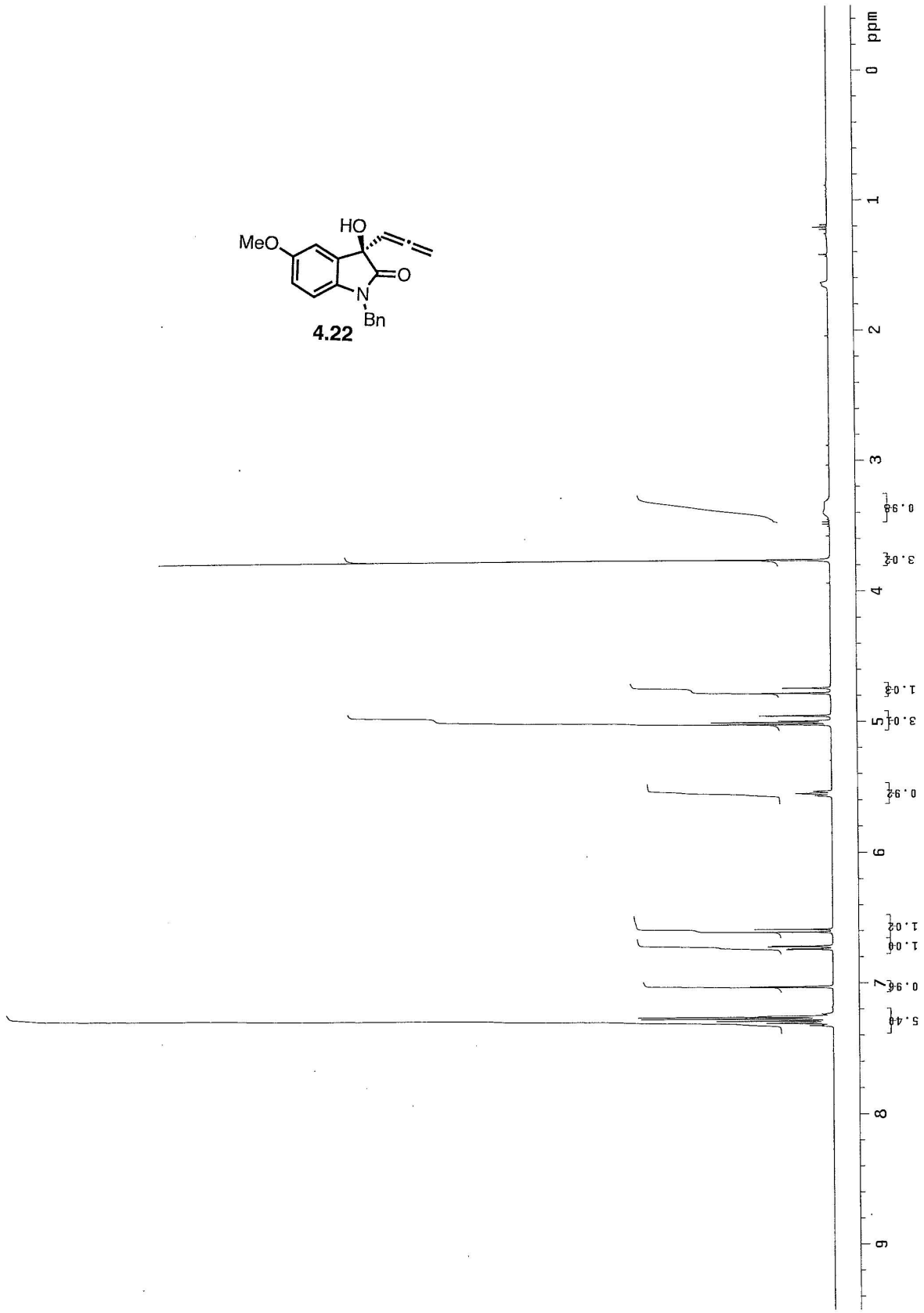
HO
MeO
O
N
Bn
4.22
ppm
0
1
2
3
4
5
6
7
8
9
0.98
3.04
1.04
3.01
0.92
1.02
1.00
0.96
5.40

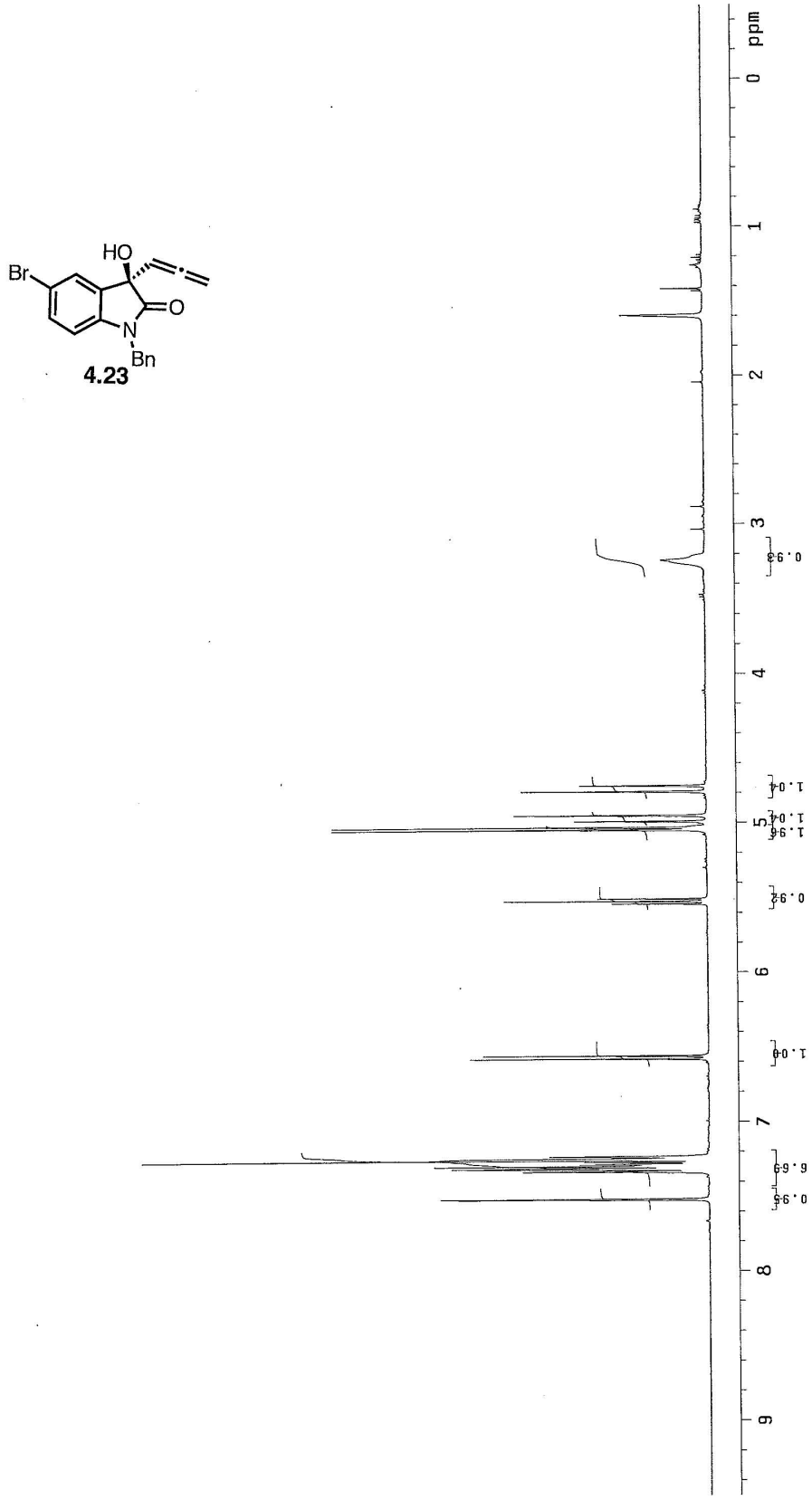
HO
Br
O
N
Bn
4.23
ppm
0
1
2
3
4
5
6
7
8
9
0.93
1.04
1.96
0.92
1.00
6.69
0.95

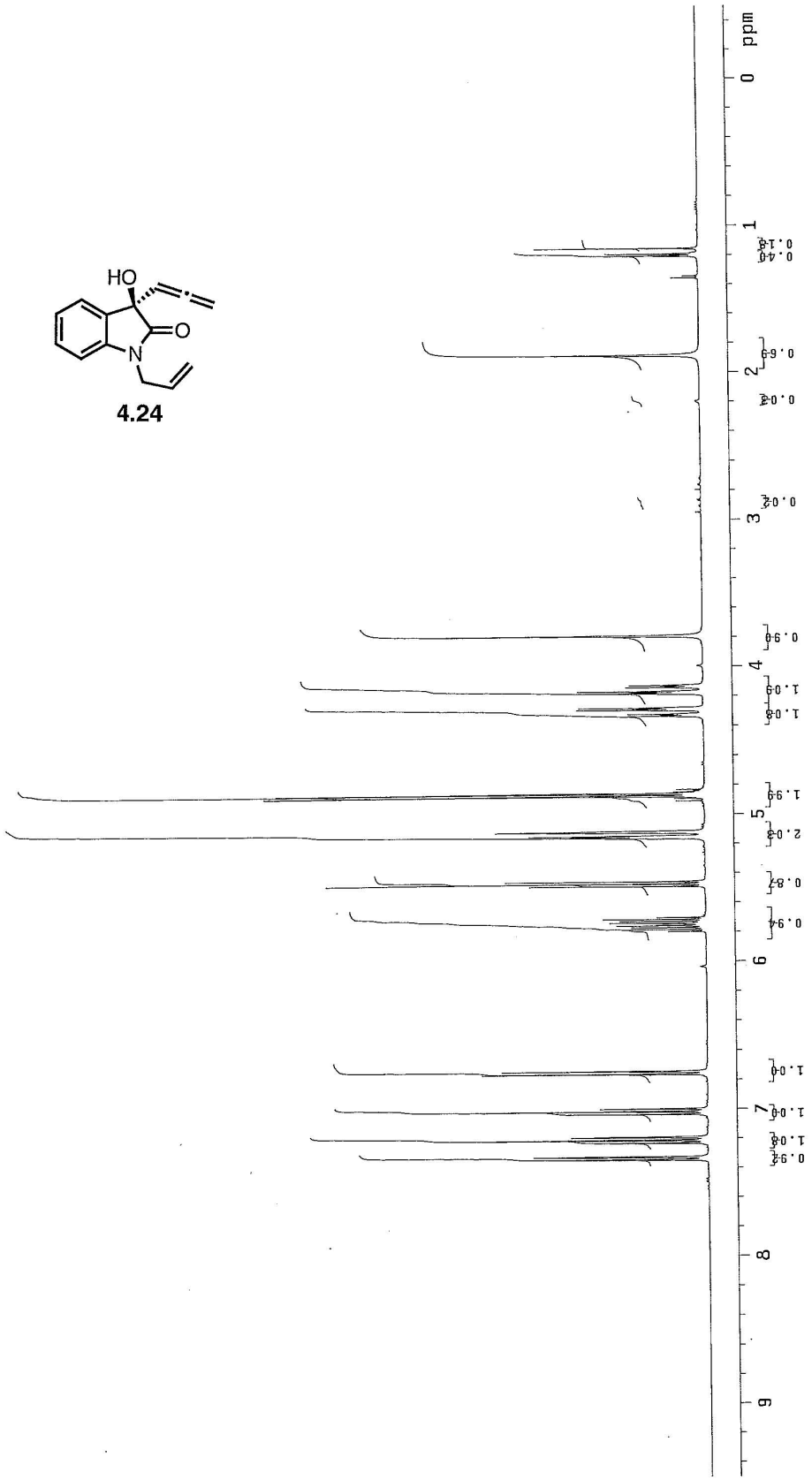
HO
O
N
4.24
ppm
0
1
2
3
4
5
6
7
8
9

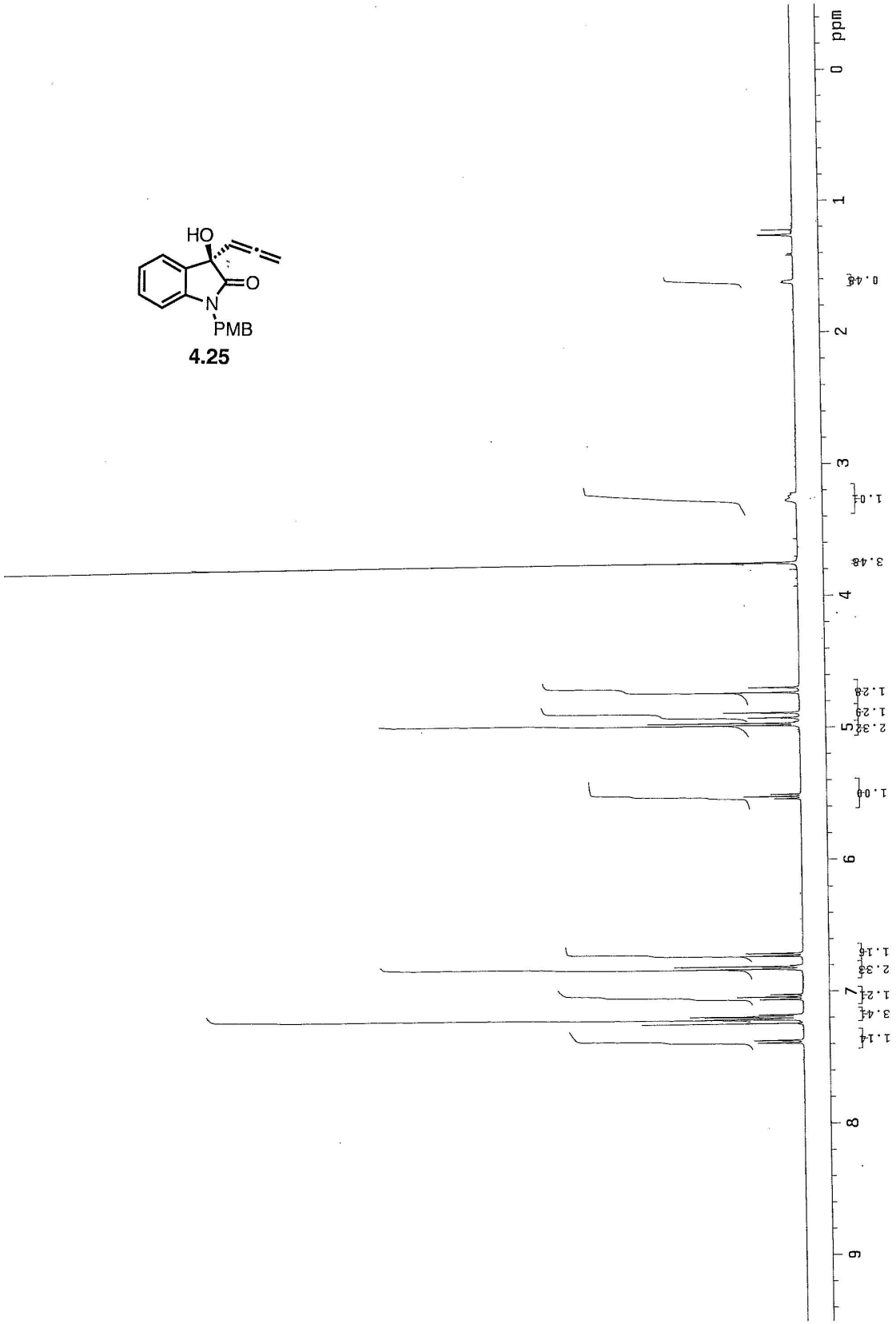
HO
O
N
PMB
4.25
ppm
0
1
2
3
4
5
6
7
8
9
0.48
1.01
3.48
1.28
1.29
2.32
1.00
1.16
2.33
1.24
3.44
1.14

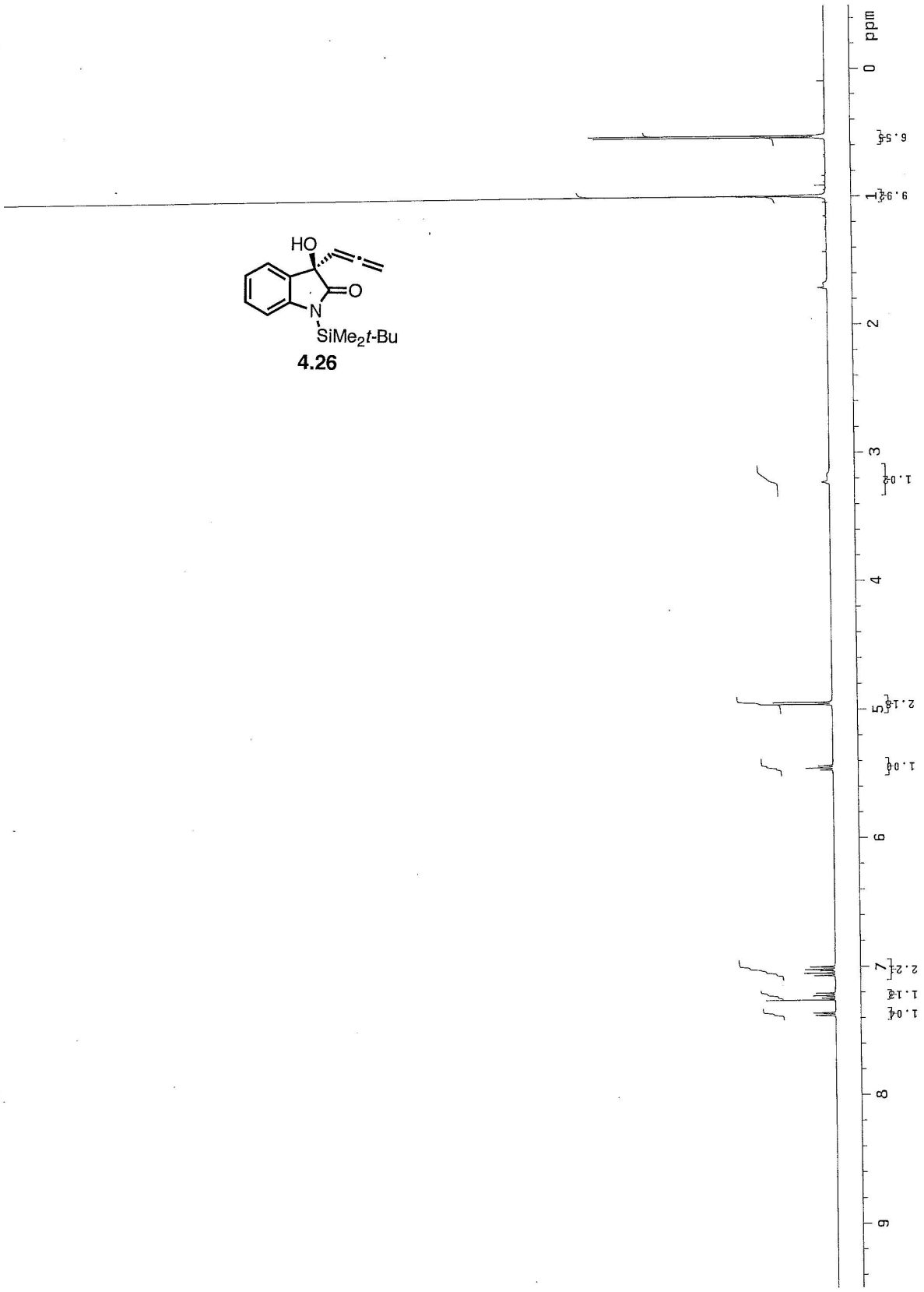

4.26

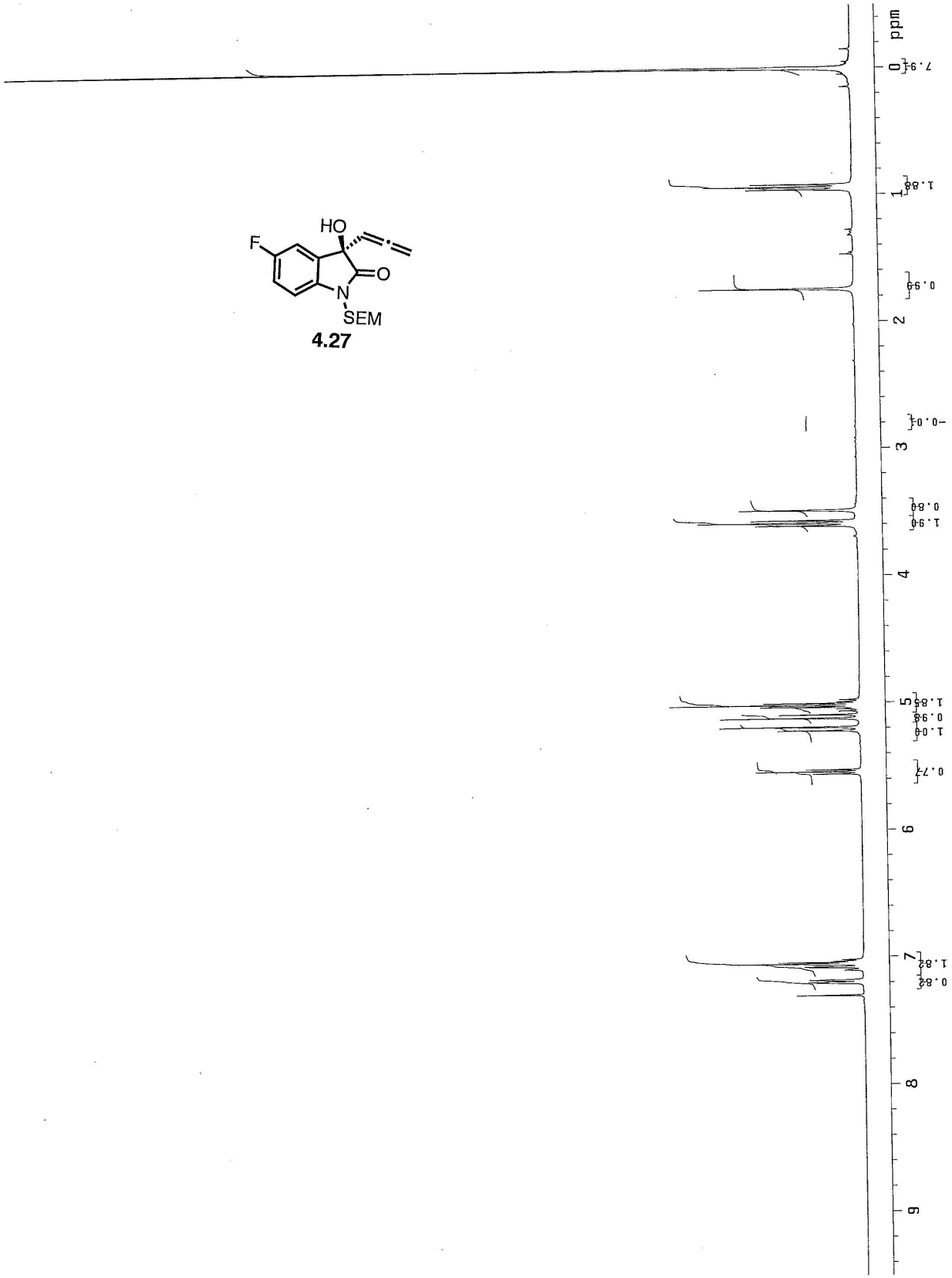

4.27

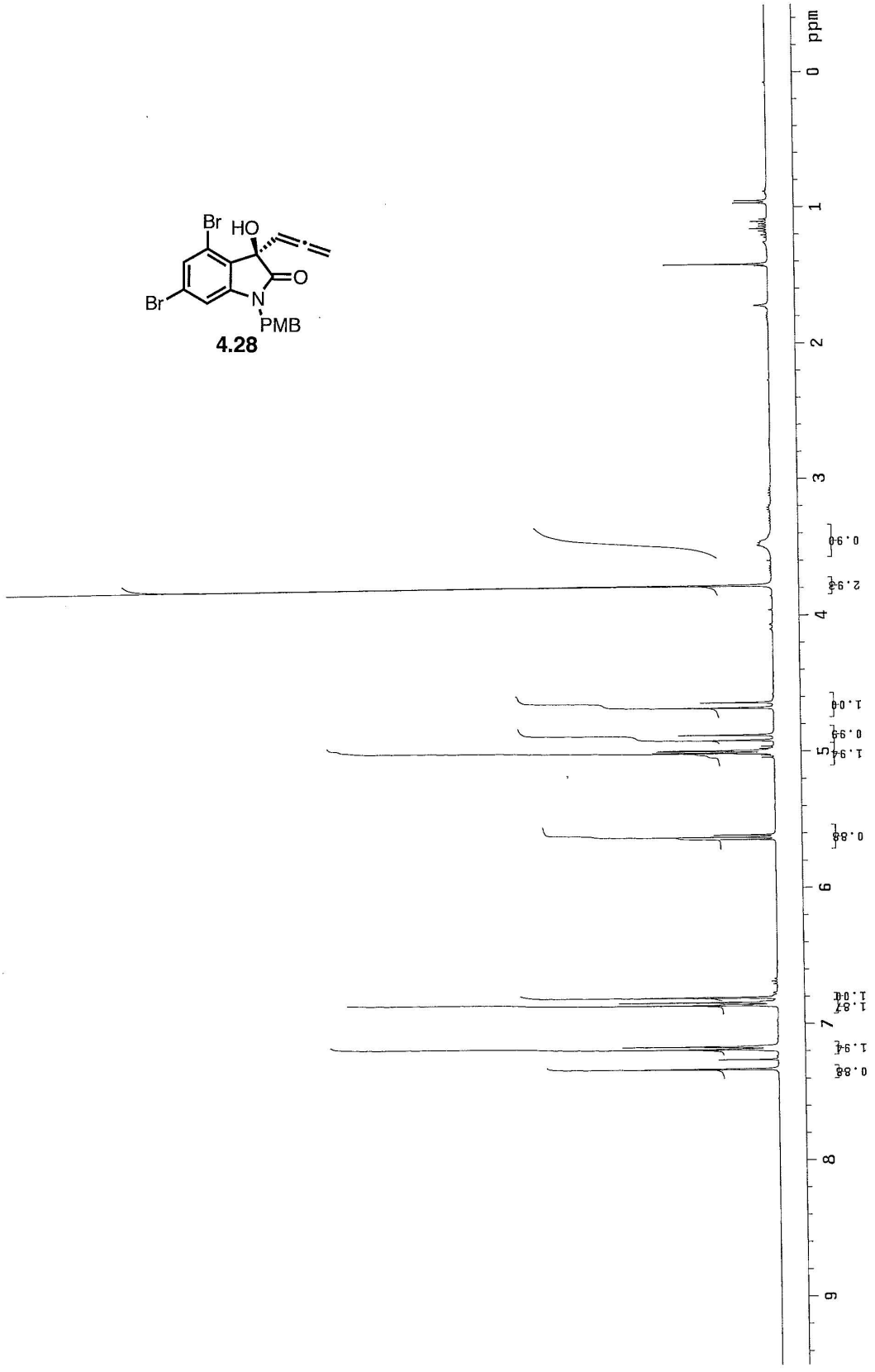
Br
HO
O
Br
N
PMB
4.28
ppm
0
1
2
3
4
5
6
7
8
9
0.90
2.93
1.04
0.93
1.94
0.88
1.87
1.00
1.94
0.88

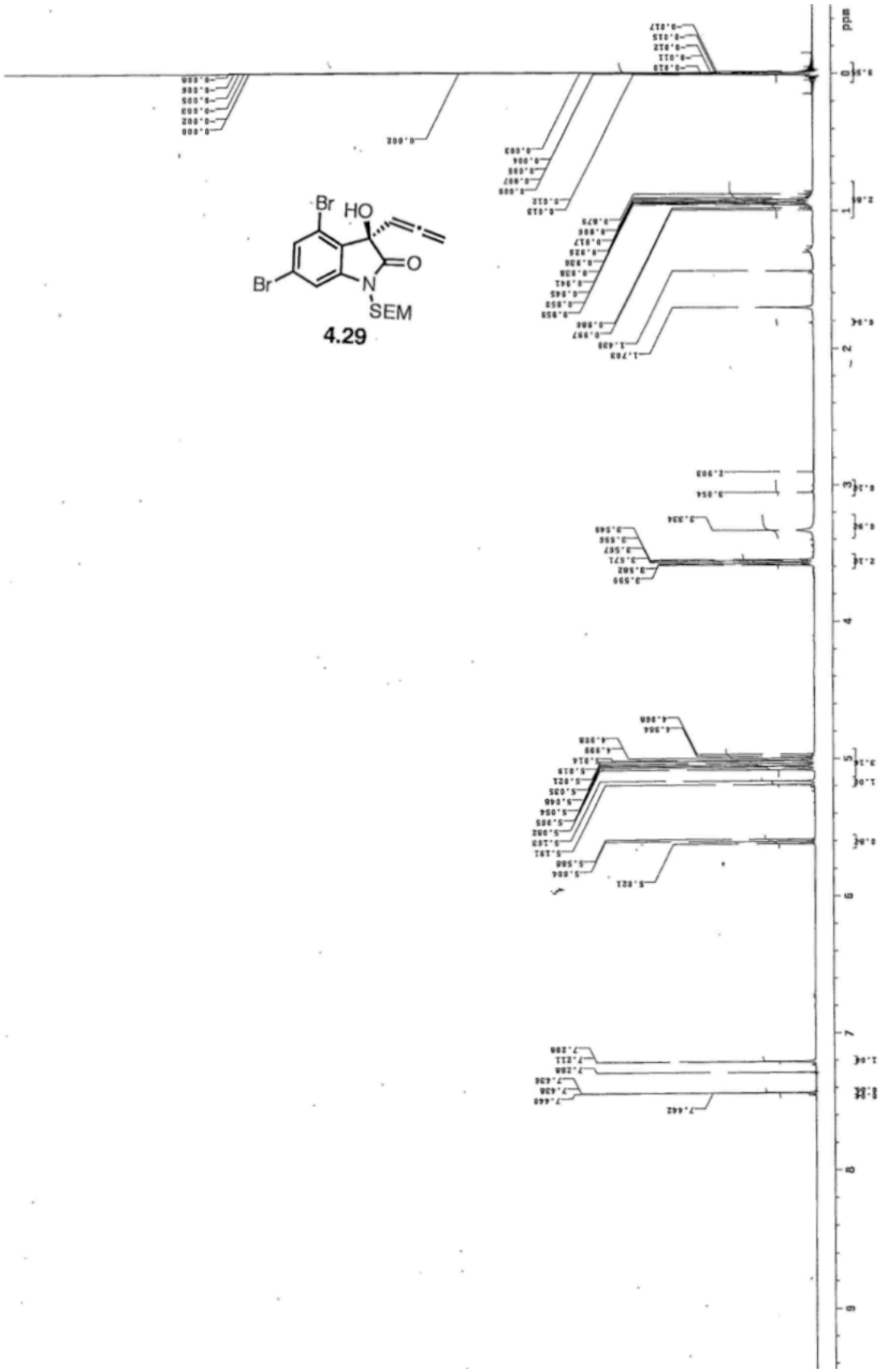
Br
HO
O
Br
N
SEM
4.29
ppm

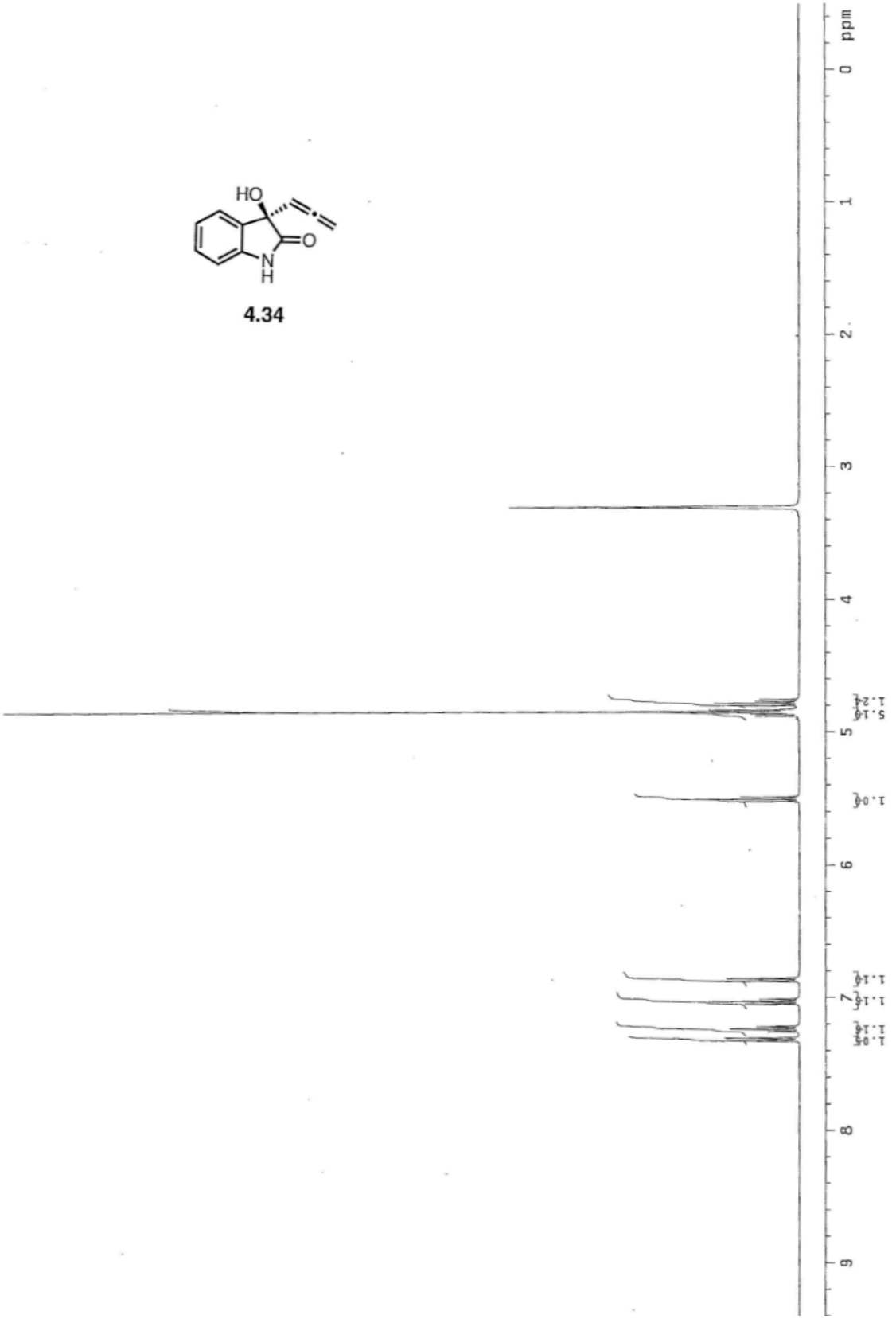
HO
O
N
H
4.34
ppm
0
1
2
3
4
5
6
7
8
9

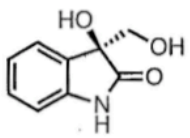

4.35

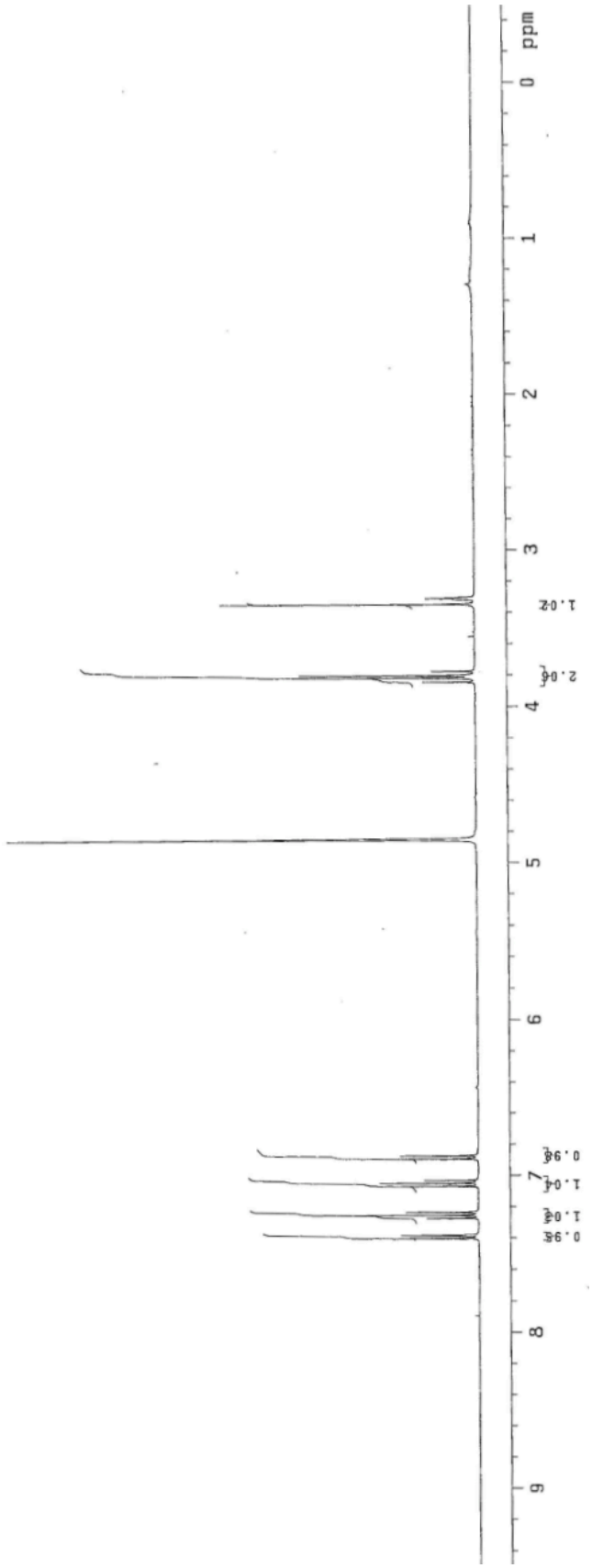

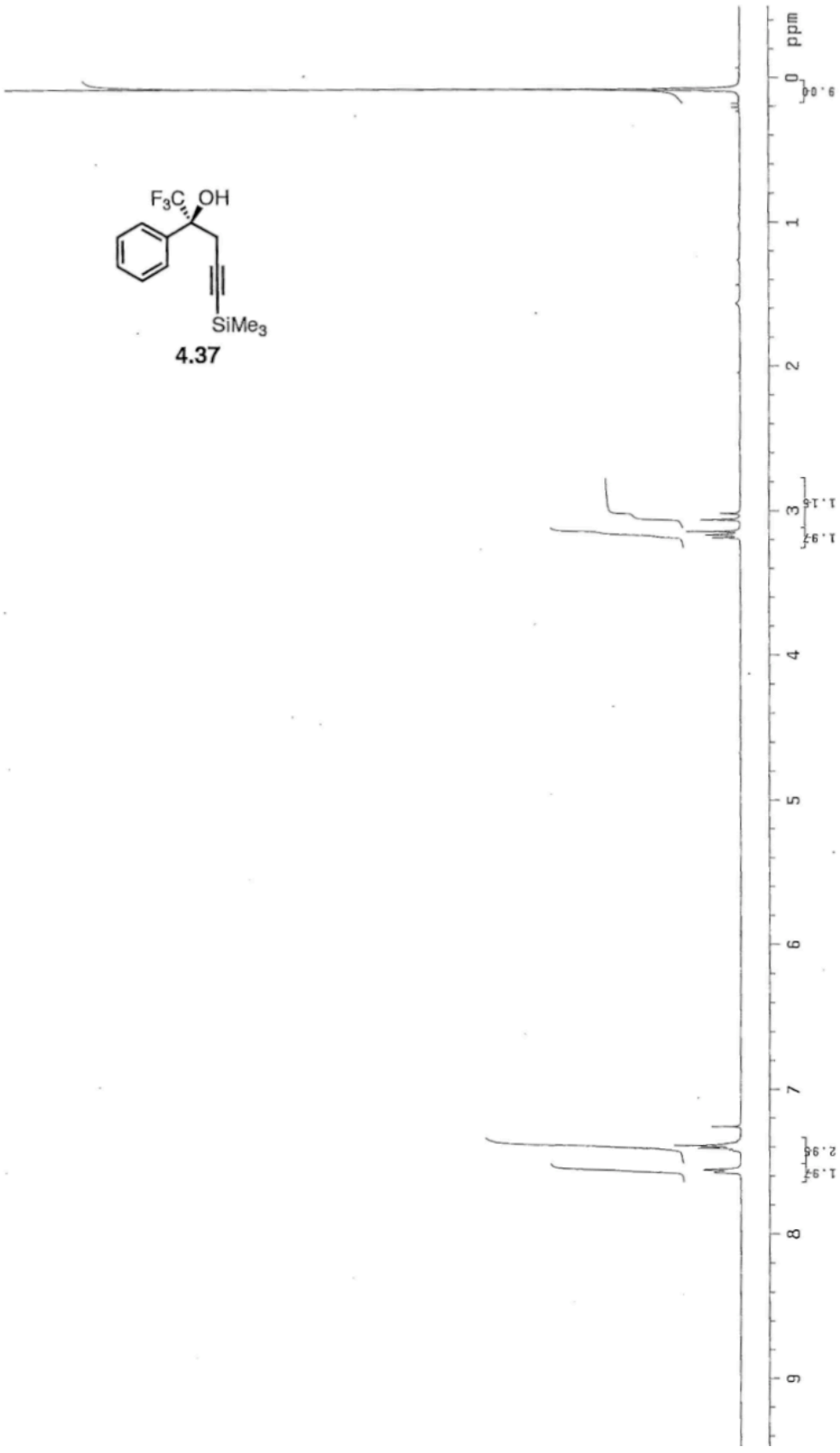

4.37

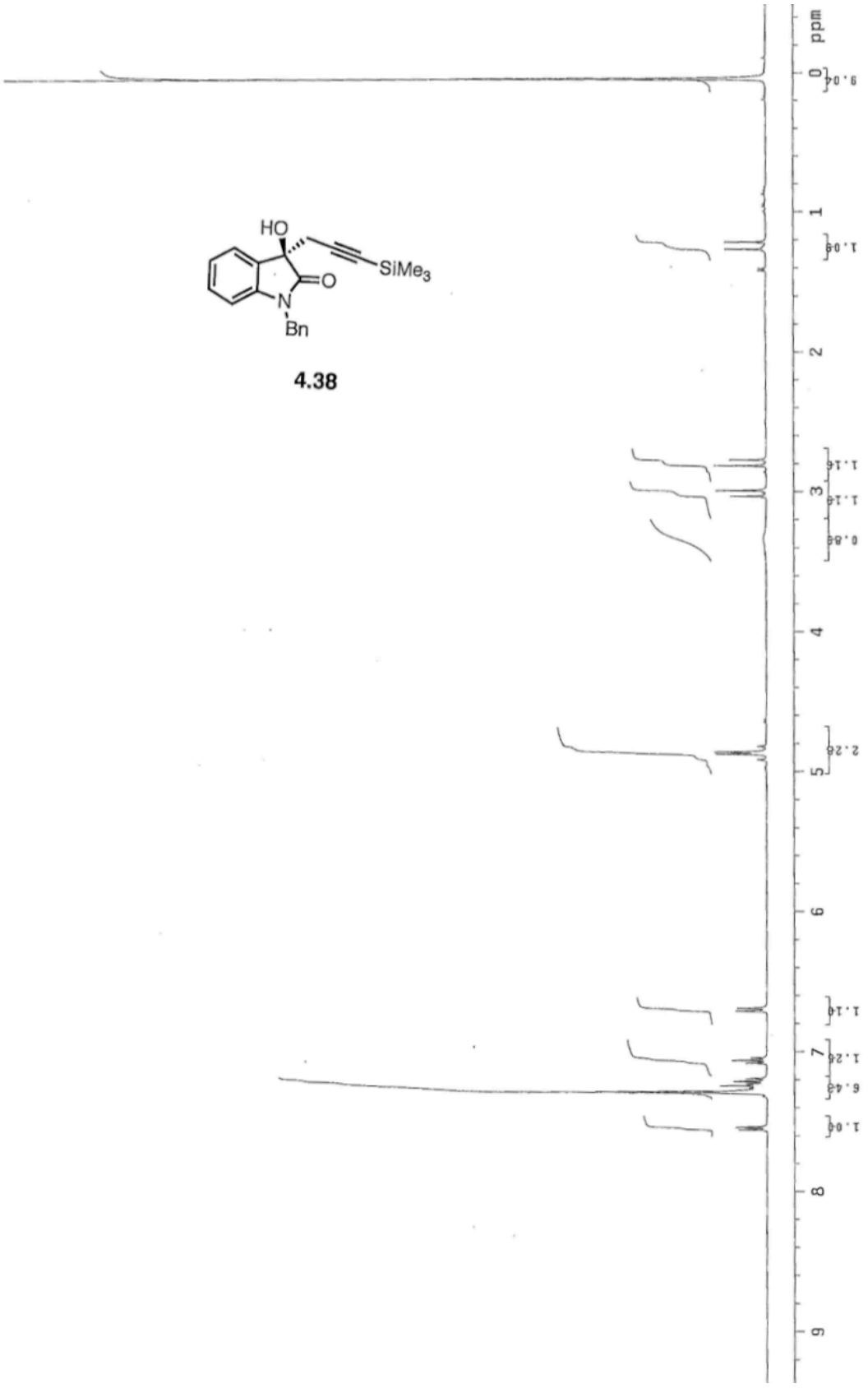
HO
SiMe3
O
N
Bn
ppm
0
1
2
3
4
5
6
7
8
9
9.04
1.08
1.16
1.16
0.88
2.26
1.16
1.26
6.46
1.00

4.38